Politechnika Śląska

WYDZIAŁ CHEMICZNY
KATEDRA CHEMII ORGANICZNEJ,
BIOORGANICZNEJ I BIOTECHNOLOGII

mgr inż. Monika Domińska

Załącznik do rozprawy doktorskiej

Glikokoniugacja *N*-heterocyklicznych związków biologicznie aktywnych oraz ocena ich aktywności przeciwnowotworowej

*Publikacje **P.1 - P.10***
stanowiące monotematyczny cykl

Promotor: dr hab. inż. Gabriela Pastuch-Gawołek, prof. PŚ

Gliwice 2023

Publikacja P.1

Synthesis of 8-Hydroxyquinoline Glycoconjugates
and Preliminary Assay of Their β1,4-GalT Inhibitory
and Anti-Cancer Properties

M. Krawczyk[*], G. Pastuch-Gawołek, A. Mrozek-Wilczkiewicz, M. Kuczak,
M. Skonieczna, R. Musioł

Materiały uzupełniające do publikacji znajdują się w dołączonej płycie CD

Synthesis of 8-hydroxyquinoline glycoconjugates and preliminary assay of their β1,4-GalT inhibitory and anti-cancer properties

Monika Krawczyk[a,b,*], Gabriela Pastuch-Gawolek[a,b], Anna Mrozek-Wilczkiewicz[c], Michal Kuczak[c,d], Magdalena Skonieczna[b,e], Robert Musiol[d]

[a] Department of Organic Chemistry, Bioorganic Chemistry and Biotechnology, Faculty of Chemistry, Silesian University of Technology, Krzywoustego 4, 44-100 Gliwice, Poland
[b] Biotechnology Centre, Silesian University of Technology, Krzywoustego 8, 44-100 Gliwice, Poland
[c] Institute of Physic and Silesian Center for Education and Interdisciplinary Research, University of Silesia in Katowice, 75 Pułku Piechoty 1A, 41-500 Chorzów, Poland
[d] Institute of Chemistry, University of Silesia, Szkolna 9, 40-006 Katowice, Poland
[e] Biosystems Group, Institute of Automatic Control, Silesian University of Technology, Akademicka 16, 44-100 Gliwice, Poland

ARTICLE INFO

ABSTRACT

8-Hydroxyquinoline scaffold is a privileged structure used in designing a new active agents with therapeutic potential. Its connections with the sugar unit is formed to improve the pharmacokinetic properties. The broad spectrum of activity of quinoline derivatives, especially glycoconjugates, is often associated with the ability to chelate metal ions or with the ability to intercalate into DNA. Simple and effective methods of synthesis glycoconjugates of 8-hydroxyquinoline and 8-hydroxyquinaldine derivatives, containing an *O*-glycosidic bond or a 1,2,3-triazole linker in their structure, have been developed. The obtained glycoconjugates were tested for their ability to inhibit β-1,4-Galactosyltransferase, as well as inhibit cancer cell proliferation. It was found that used glycoconjugation strategy influenced both improvement of activity and improvement of the bioavailability of 8-HQ derivatives. Their activity depends on type of attached sugar, presence of protecting groups in sugar moiety and presence of a linker between sugar and quinolone aglycone.

1. Introduction

The starting point in the search for new drugs of synthetic origin is the discovery of a privileged structure [1,2] such as 8-hydroxyquinoline **I** (8-HQ), which is a fragment of particular importance in the design of new active derivatives [3–6].

The 8-HQ scaffold can be found in many compounds having a therapeutic activity such as clioquinol **II**, intestopan **III**, nitroxoline **IV**, cloxiquine **V**, iodoquinol **VI**, chloroxine **VII** or chlorquinaldol **VIII** [7–12] (Scheme 1). In addition, some derivatives have been comprehensively tested for their anticancer activity, because of their abilities to chelate the metal ions that are necessary for cancer growth [13–16]. 8-HQ has at least two potential protonation sites: a nitrogen atom of the pyridine ring and an oxygen atom of phenol. Therefore, they form complexes with most of divalent transition metal ions, such as: Mn^{2+}, Cu^{2+}, Zn^{2+}, Co^{2+}, Ni^{2+}, Fe^{2+} which has been widely described in the literature. The ability of chelating metals through 8-HQ derivatives has become a promising therapeutic strategy in clinical practice [17–23].

On the other hand, design and synthesis of new molecules containing a sugar fragment is an increasingly active area of current chemical research [24–30]. The presence of a sugar unit improves the pharmacokinetic properties of potential drugs, including improved solubility, reduced toxicity and facilitated intermembrane transport and selectivity in targeting drugs for a specific purpose.

In 2012–2015 G. Vecchio and his co-workers, conducted a series of studies on the synthesis and anticancer properties of quinoline glycosides [31–33]. The whole range of glycosides of 8-HQ derivatives, containing the D-glucose and D-galactose units, were synthesized and evaluated. In these studies, the glycosidic bond was obtained by reaction a per-*O*-acetylated glucopyranosyl or galactopyranosyl bromides with 8-HQ derivatives, formed through an S_N2 type mechanism, in the two-phase system used TBABr as a phase transfer catalyst and K_2CO_3 as a base. Under the described conditions, mainly glycosides with a deprotected sugar part were obtained. These compounds were evaluated for their antiproliferative activity against cells of various types of cancer (A-2780, A-549, MDA-MB-231, Hep-G2), as well as the effect of

---

* Corresponding author at: Department of Organic Chemistry, Bioorganic Chemistry and Biotechnology, Silesian University of Technology, B. Krzywoustego 4, 44-100 Gliwice, Poland.
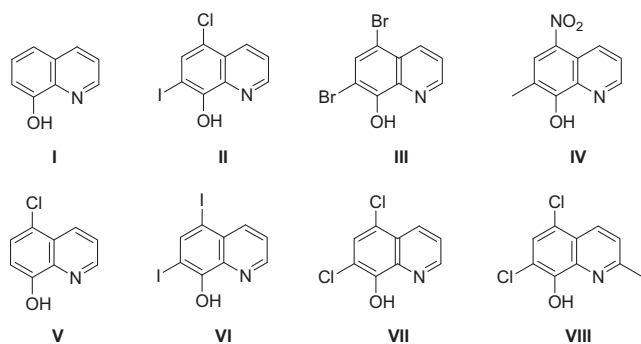*E-mail address:* monika.krawczyk@polsl.pl (M. Krawczyk).

Scheme 1. 8-Hydroxyquinoline derivatives having a biological activity.

addition of Cu^{2+} ions on their biological activity. The results showed that the average antiproliferative activity of glycosides without the addition of copper ions were lower compared to their parent compounds. However, after the addition of Cu^{2+} ions, similar activity to the starting derivatives was obtained. The authors suggest that the test compounds must be subject to hydrolysis by specific β-glycosidases, to release the active aglycone only in target cells, where aglycone was able to complex copper(II) ions.

The antiproliferative activity of 2-methyl-7-carboxy-8-hydroxyquinoline derivatives of glycoconjugates has recently been reported [34]. The obtained compounds were tested for anticancer activity in terms of colon cancer cells (HCT 116). Some of the combinations showed over 100 times higher activity than their parent compounds. It was observed that the glycoconjugates with unprotected sugar part lose their activity relative to their protected analogues. It has also been observed that the improvement of the activity occurs in the presence of an aromatic or heteroaromatic linkage between sugar and quinoline fragment.

As reported in the literature, 8-HQ derivatives containing in their structure a tetrazolium linker [35] or a triazole linker [36] and glucose units, show high antiproliferative activity against various cancer cell lines, comparable to the activity of anti-cancer drugs. It was also confirmed, that the presence of lone electron pairs on the nitrogen atoms in the triazole ring, improves the chelating properties of 8-HQ [37]. In addition, derivatives based on 1,2,3-triazoles play an important role in the preparation of inhibitors of various enzymes [38–42]. It is probably related to the ability to complex metal cations present in the active centers of many enzymes and thus to inhibit their activity.

Due to the more and more frequent relationships between tumor progression and the increase in the level of glycosyltransferases expression, a large number of quinoline derivatives have been tested for the ability to inhibit representatives of this class of enzymes. Glycosyltransferases (GTs) are characterized by a large variety of substrates and the prevalence of cells of eukaryotic organisms. Due to a number of important functions they perform, among others: post-translational protein modifications and the synthesis of oligosaccharide chains, they are an important object of research on potential anticancer drugs [43–45]. However, in spite of this, so far there are no effective

inhibitors capable of hampering their activity selectively.

One of the best-known GTs in biochemical terms is β-(1,4)-Galactosyltransferase (β-(1,4)-GalT). It catalyses the synthesis of glycosidic bonds by transferring the D-galactose fragment from UDP-Gal, which is the sugar donor, to specific acceptor molecules. Their classification is based mainly on the specificity of the donor and acceptor and the structure of the product being created [46]. The β-(1,4)-GalT inhibitors are very often designed based on the introduction, instead of the diphosphate group, of another, preferably non-charged, linker capable of coordinating the divalent metal ion bound at the active site of the enzyme. The presence of a metal ion binding moiety, seems to be necessary to inhibit GTs activity [43,46–48]. GT inhibitors have a large therapeutic potential due to the ability to regulate the biosynthesis of oligosaccharides that are involved in many disease processes. An effective inhibitor, in addition to demonstrating sufficient affinity and selectivity for the enzyme, should have the ability to penetrate into the organism and cross biological barriers to achieve its goal inside the cell [47].

Taking into account the above premises, it was decided to obtain heterocyclic sugar conjugates of rather low metabolic stability, i.e. 8-HQ derivatives glycoconjugates (acetals and hemiaminals), in which the sugar part will be connected to the quinoline fragment both by *O*-glycosidic linkage or via the linker containing the 1,2,3-triazole moiety (Scheme 2). The acylation of the sugar fragment, leading to increased hydrophobicity of the compounds, can be used to improve the bioavailability of the glycoconjugates. It seems that this modification may not only reduce the hydrophilicity of the compound, but also significantly affect the bioavailability and transport of the quinoline structures across the cell membrane in the biological environment compared to derivatives containing analogous sugar units with unprotected OH groups. In this work we present new, simple and effective methods of synthesis of designed connections and the results of the preliminary assessment of their biological activity. Considering the possibility of metal ions chelation by glycoconjugates derivatives of 8-HQ, the ability of obtained glycoconjugates to inhibition of commercially available, manganese ions dependent β-(1,4)-GalT and to inhibition of a cancer cell proliferation (in which overexpression of this enzyme was observed) was investigated. The addition of both the D-glucose and the D-galactose fragment to the 8-HQ derivatives was dictated by the overexpression of glucose transporters observed in the case of cancers, and in the case of the HCT 116 line by the additional overexpression of galactose transporters [49–52].

2. Results and discussion

2.1. Synthesis

8-Hydroxyquinoline or 8-hydroxyquinaldine fragment were connected with the sugar derivatives (D-glucose or D-galactose unit) by *O*-glycosidic linkage or via *O*-methylene 1,2,3-triazole linker. This treatment was aimed to improving the solubility and bioavailability of potential drugs. Based on this assumption, we obtained a whole range of
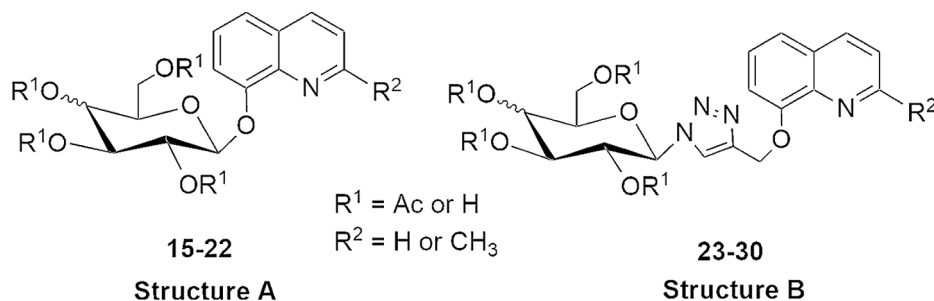
Scheme 2. General structure of the glycoconjugates **15–30**.
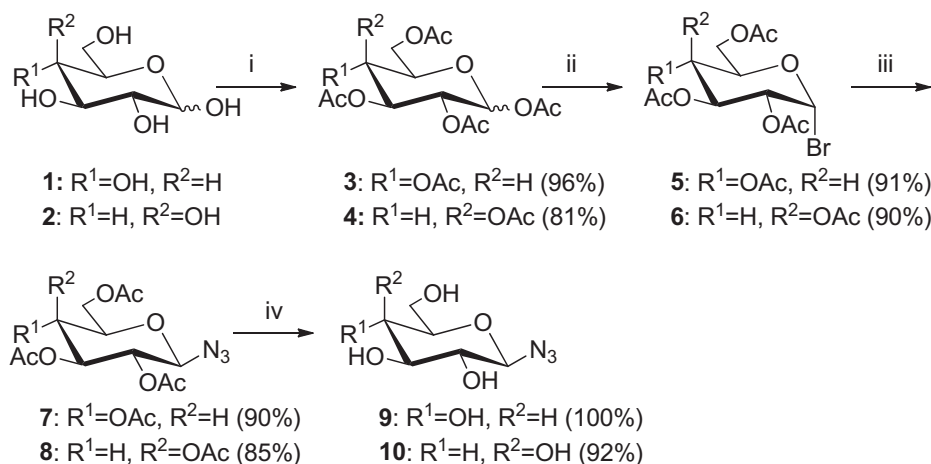
Scheme 3. Synthesis of sugar derivatives. *Reagents and Conditions:* (i) CH$_3$COONa, Ac$_2$O, b.p., 1 h; (ii) CH$_3$COOH, 33% HBr/AcOH, r.t. 1 h; (iii) NaN$_3$, TBASH, CHCl$_3$/ NaHCO$_3$, r.t. 2 h; (iv) 1. NaOMe, MeOH, r.t. 20 min; 2. Amberlyst-15.

quinoline glycoconjugates (Scheme 2).

In the first step of the synthesis, sugar derivatives **5–10** were prepared according to known procedures (Scheme 3) involving the acetylation of free sugars **1** or **2** and conversion of per-*O*-acetylated derivatives **3** or **4** into the corresponding glycosyl bromides **5** or **6** [53,54] The glycosyl bromides were used immediately for further reactions leading to obtain 2,3,4,6-tetra-*O*-acetyl-β-glycosyl azides **7** and **8** [54]. The last step was the removal of the acetyl groups under Zemplén conditions which allowed to get deprotected β-glycosyl azides **9** or **10**, which was sufficiently pure for a further reaction [55].

Per-*O*-acetylated glucopyranosyl or galactopyranosyl bromides **5** or **6** respectively were used as glycosyl donors in a *O*-glycosidic bond formation, while 8-hydroxyquinoline **11** and 8-hydroxyquinaldine **12** were used as glycosyl acceptors. Synthetic approach described earlier in the literature for glycosylation of 8-HQ in the phase transfer catalytic system, was compared to the several other known glycosylation methods for containing hydroxyl groups aromatic compounds. There are some problems in the case of phenols *O*-glycosylation. The first is associated with electron withdrawing character of phenol ring causes less nucleophilicity of phenols compared to alcohols, so phenols are difficult to glycosylate. Second, the glycosylation of phenols under acidic conditions can lead to obtaining significant amounts of *C*-glycosides, due to the electron-donating properties of the hydroxyl group [56]. Among methods of aromatic *O*-glycosylation can be mention those using donors such as glycosyl acetates [57,58], glycosyl halides-especially bromides [56,59] or fluorides [60], trichloroacetimidates [61,62], thioglycosides [63,64] under different catalytic systems. Other methods for aromatic *O*-glycosylation are the use of unprotected sugars in Mitsonobu reaction [65], nucleophilic aromatic substitution [66,67] as well as use of glycals [68], 2-nitroglycals [69], glycosyl phosphates [70] or glycosylidene carbenes [71].

The overview of the reactions used to obtaining of glycoconjugates **15–22** provides in Scheme 4.

The procedure A previously described in the literature [31], taking place according to S$_N$2 mechanism at anomeric carbon, performed in the classical two-phase system. The reaction conditions were selected for compounds **5** and **11** used as substrates. Synthesis with various molar ratio of sugar derivative **5** to quinoline **11** were performed (3:1, 2:1 and 1:1, Table 1). The obtained results indicated that gycosylation product could be isolated in the best yield, when three times the molar excess of the glycosyl donor relative to the quinoline acceptor was used. However, it is associated with significant amounts of by-products, difficult to separate from the post-reaction mixture. During the reaction carried out in a basic condition, acetyl protecting groups were removed and as a result, mainly glycoconjugate **19** with the deprotected sugar

part was obtained. The same regularity was observed during glyco-conjugation using the acceptor **12**, as well as in case of using of donor **6**. Taking into account earlier mentioned requirements for improving the bioavailability of drugs, it was necessary to obtain glycoconjugates with a protected sugar part, in order to carry out biological tests on cancer cell lines. Therefore, other phenols glycosylation methods were tested to obtain desired quinoline glycosides.

Procedure B is based on the *O*-glycosidation reaction of per-*O*-acetyl-α-glycosyl bromides **5** or **6** and quinoline derivatives **11** or **12** using an ionic liquid (BMIm·BF$_4$) [72]. In this case, the ionic liquid acted as a solvent and substrate in the generation of an activating agent in the glycosylation reaction. Silver *N*-heterocyclic carbene complexes (Ag-NHC) are formed *in situ* in ionic liquids. Reaction were performed in the presence of silver carbonate and various tetraalkylammonium salts. Treatment of imidazolium halide salts with silver carbonate generated Ag–NHC complexes that subsequently promoted *O*-glycosidation reactions. The reaction mechanism involved the dual role of Ag–NHC complexes as heavy metal ion sources and as bases, that were more effective in promoting the glycosidation reaction than silver carbonate. Four tetraalkylammonium salts (TBABr, Me$_4$NCl, Me$_4$NBF$_4$ and Et$_4$NClO$_4$) were tested for preparation of the compound **15**, to see which one is the best anion donor in the formation of the active Ag-NHC complex. The best salt turned out to be Me$_4$NCl, at which the product yield was 44%. Whereas, the worst catalyst for the reaction turned out to be Et$_4$NClO$_4$, where the product yield was only 24%. However, in the absence of tetraalkylammonium salts, the desired product was not found (Table 1).

Another effective way of forming the *O*-glycosidic linkage with phenol as glycosyl acceptor was published by Kur'yanov and co-workers [73]. In the next variant of the research (Procedure C) the glycosylation of quinoline catalyzed by polyethylene glycol (PEG 4000) was tested. The reaction was carried out in the phase transfer catalytic system, using anhydrous acetonitrile as a solvent at room temperature. We checked if it was necessary to conduct the reaction for 48 h. It turned out that shortening of the reaction time to 24 h does not significantly affect the yield of the obtained product. On the other hand, a further shortening of the reaction time to 2 h resulted in a decreased yield of product **15** from 22% to 16% (Table 1). After optimizing the conditions of individual glycosylation procedures, synthesis of the remaining quinoline glycosides was performed. The yields of the respective glycoconjugates are presented in Table 2**.**

During the glycosylation reaction performed according to procedures B and C, the formation of small amount of a product of 1,2-elimination of hydrogen bromide to give tetra-*O*-acetyl glycal was observed.
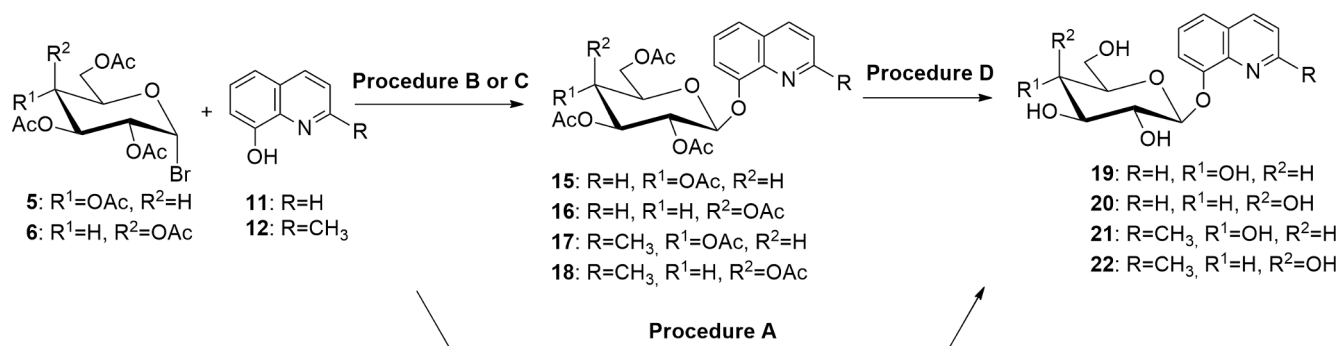
Scheme 4. Synthesis of glycoconjugates **15–22**. *Reagents and Conditions:* (Procedure A) K₂CO₃, Bu₄NBr, H₂O/CH₃OH/CH₂Cl₂, r.t., 72 h; (Procedure B) Ag₂CO₃, Me₄NCl, BMIm·BF₄, r.t., 24 h; (Procedure C) K₂CO₃, PEG 4000, CH₃CN, r.t., 48 h; (Procedure D) 1. NaOMe, MeOH, r.t. 0.5 h; 2. Amberlyst-15.

Part of the per-*O*-acetylated glycoconjugates **15–18** were deprotected under mild conditions using 1 M methanolic solution of sodium methoxide in methanol. The reaction was carried out at room temperature for only 25–30 min. The final step was to neutralize the reaction mixture with the use of Amberlyst-15 ion exchange resin, after which the mixture was filtered to give glycoconjugates **19–22** (Procedure D). This approach was slightly more efficient compared to Procedure A.

On the basis of literature reports and previously obtained results, it can be concluded that the presence in the glycoconjugate structure aromatic or heteroaromatic ring is important for their biological activity. Therefore, in subsequent syntheses quinoline derivatives were also combined with sugar units using copper(I)-catalyzed 1,3-dipolar azide-alkyne cycloaddition (CuAAC) [74]. The 1,2,3-triazole unit was introduced to investigate if such heteroaromatic system will affect the activity of the glycoconjugates.

The first essential structural element of the glycoconjugate are propargyl quinoline derivatives **13** or **14** which were obtained by reaction of quinoline derivatives **11** or **12** with propargyl bromide (Scheme 5) according to the previously published procedure [75].

New glycoconjugates were synthesized by the connection of 1-azido sugars, protected or unprotected derivatives of D-glucose **7, 9** or D-galactose **8, 10** with 8-(2-propyn-1-yloxy)quinoline **13** or 2-methyl-8-(2-propyn-1-yloxy)quinoline **14** (Scheme 6). For the above mentioned conjugation CuACC was applied. The reaction in an aqueous-alcoholic medium was carried out, using CuSO₄·5H₂O as a catalyst and sodium ascorbate (NaAsc) as a reducing agent, which was designed to reduce Cu(II) to Cu(I). The reaction was carried out for 24 h at room temperature. The crude products of these reactions were purified by column chromatography.

The main advantage of this approach is the capability of employing both protected or unprotected sugar derivatives. This solves the problem of the final deprotection of glycoconjugates by the action of 1 M
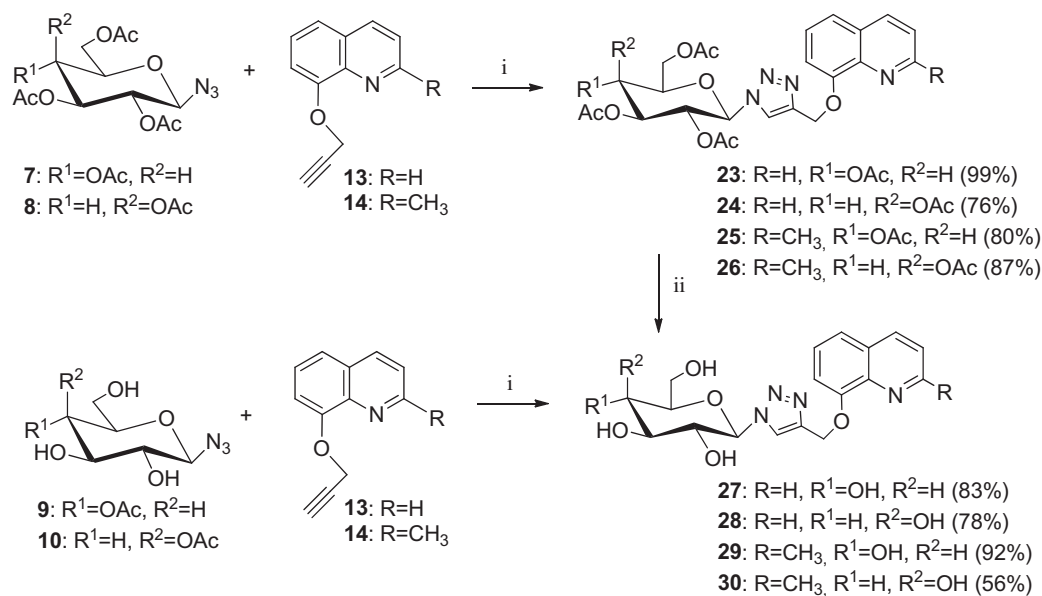
Table 2
Yields of glycoconjugates **15–22**.

Product	Procedure	Yield [%]
15	**B**	44
	C	22
16	**B**	37
	C	42
17	**B**	27
	C	29
18	**B**	45
	C	51
19	**A**	49
	D	41
20	**A**	34
	D	41
21	**A**	21
	D	68
22	**A**	29
	D	66
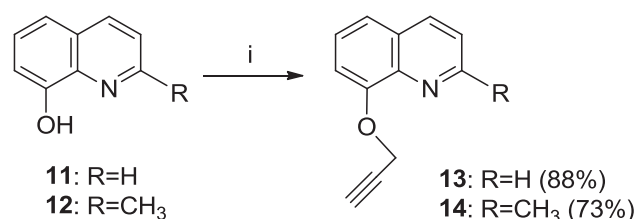
Scheme 5. Synthesis of quinoline derivatives **13–14**. *Reagents and Conditions:* (i) propargyl bromide, K₂CO₃, acetone, r.t., 24 h.

Table 1
Adjusting the glycosylation reaction conditions.

Procedure	Glycosyl donor	Glycosyl acceptor	Donor/acceptor molar ratio	Product	Reaction time [h]	Tetraalkylammonium salt	Yield [%]
A	**5**	**11**	3:1	**19**	72	Bu₄NBr	49
			2:1				23
			1:1				12
B	**5**	**11**	1:3	**15**	24	Bu₄NBr	34
						Me₄NCl	44
						Me₄NBF₄	28
						Et₄NClO₄	24
						–	–
C	**5**	**11**	1:1.15	**15**	48	–	22
					24		22
					2		16

Scheme 6. Synthesis of glycoconjugates **23–30**. *Reagents and Conditions:* (i) CuSO$_4$·5H$_2$O, NaAsc, *i*-PrOH, THF, H$_2$O, r.t., 24 h; (ii) 1. NaOMe, MeOH, r.t. 0.5 h; 2. Amberlyst-15.

NaOMe in methanol and avoided low yields of the desired products. In case of the trial of glycoconjugates **23** deprotection, full conversion of the starting material to the deprotected derivative **27** was unsuccessful despite an extended reaction time and the use of a larger amount of NaOMe.

Finally, both protected **23–26** and unprotected **27–30** glycoconjugates were obtained. The CuACC reaction proceeds with high yield and leading to the formation of only 1,4-disubstituted of 1,2,3-triazoles. The structures of all compounds were confirmed by means of NMR and MS spectra.

2.2. Biological studies

2.2.1. Inhibitory potential

The obtained glycoconjugates **15–30** have been evaluated for their inhibitory activity against commercially available β-1,4-GalT. To evaluate the activity of tested compounds, concentrations of substrate and product of enzymatic reaction in the reaction mixtures was determined by RP-HPLC method, which is a modification of the Vidal method [76]. This method uses UDP-Gal, a natural β-1,4-GalT substrate, as glycosyl donor and (6-esculetinyl) β–D–glucopyranoside (esculine) as glycosyl fluorescent acceptor. To accurately determine the activity of the compound, the amount of product formed in the reaction without the inhibitor (test reactions) is compared to the amount of product formed during the reaction with the addition of glycoconjugate as potential enzyme inhibitor carried out under the same conditions. All glycoconjugates were tested at 0.8 mM concentrations. Results presented in Table 3 indicate that none of the tested compounds **15–30** showed sufficient inhibitory activity against used in research β-1,4-GalT. However, it cannot be ruled out any mechanism of action at this step.

The results indicate that activity against β-1,4-GalT depends on the type of attached sugar and the presence of the protecting groups in the sugar moiety. However, the parent compounds **11** and **12** are not able to inhibit the enzyme, which may indicate that the sugar fragment is necessary for the proper acting of the compounds. Surprisingly we found that glycoconjugates derivatives of D-glucose (**19, 21, 27, 29**) are more active than analogs containing D-galactose unit. It is significant that ability of enzyme inhibition shows only glycoconjugates containing unprotected sugar part, while the derivatives with acetyl protection groups on the sugar unit show no activity. This is probably related to the fact that the hydroxy group protections cause that glycoconjugates

Table 3
Bovine milk β-1,4-Galactosyltransferase I assay results.

Compound	Percentage of inhibition at 0.8 mM [%]
11	2 ± 0.32
12	5 ± 0.04
13	0
14	0
15	0
16	0
17	0
18	0
19	14 ± 0.35
20	0
21	20 ± 0.86
22	0
23	0
24	0
25	0
26	0
27	43 ± 0.39
28	16 ± 0.36
29	33 ± 0.87
30	12 ± 0.48

to became too large to fit into the active site of enzyme.

Compounds **27–30** in which the sugar unit is connected to the quinoline moiety by the *O*-methylene 1,2,3-triazole linker showed slightly increased activity compared to compounds **19–22** in which sugar unit is connected directly by a glycosidic bond to 8-HQ derivative.

2.2.2. Cytotoxicity studies

The cytotoxic activity of quinoline derivatives **11–14** as well as obtained glycoconjugates **15–30** was conducted on seven cell lines: HeLa (cervical cancer cell line), HCT 116 (colorectal carcinoma cell line), MCF-7 (human breast adenocarcinoma cell line), U-251 and Hs683 (glioblastoma cell lines), PANC-1 and AsPC-1 (pancreatic cancer cell lines). In these lines, overexpression of the glucose and galactose transporters was observed [77,78]. First, screening tests were carried out for all compounds on three tumor lines (HeLa, HCT 116 and MCF-7) and additionally their selectivity was tested on Normal Human Dermal Fibroblasts-Neonatal (NHDF-Neo). Tests were conducted for

Table 4

Screening of cytotoxicity of glycoconjugates derivatives of 8-hydroxyquinoline.

Compound	Activity IC$_{50}$ [μM][*]			
	HeLa[**]	HCT 116[**]	MCF-7[***]	NHDF-Neo[**]
11	> 800	> 800	0.24 ± 0.01	> 800
12	> 800	> 800	43.18 ± 1.78	346.77 ± 2.23
13	> 800	> 800	95.95 ± 4.29	> 800
14	> 800	> 800	223.63 ± 8.06	> 800
15	> 800	> 800	> 800	–
16	> 800	> 800	> 800	–
17	732.80 ± 28.18	> 800	> 800	–
18	> 800	638.0 ± 5.26	> 800	–
19	> 800	> 800	> 800	–
20	> 800	> 800	> 800	–
21	> 800	> 800	> 800	–
22	> 800	> 800	> 800	–
23	59.48 ± 3.55	69.0 ± 2.53	57.69 ± 3.32	57.37 ± 3.19
24	30.98 ± 1.80	22.7 ± 1.58	4.12 ± 0.03	31.91 ± 1.63
25	> 800	750.9 ± 28.93	> 800	–
26	> 800	457.7 ± 15.3	> 800	–
27	> 800	212.0 ± 7.71	185.34 ± 2.21	247.24 ± 11.64
28	339.35 ± 6.96	265.5 ± 5.02	254.94 ± 8.81	703.45 ± 17.30
29	> 800	> 800	> 800	–
30	> 800	> 800	> 800	–
Doxorubicin	1.2 ± 0.03	5.59 ± 0.14	0.67 ± 0.01	> 20

[*] Cytotoxic was evaluated using the MTT assay.

[**] Incubation time 24 h.

[***] Incubation time 72 h.

Table 5

Cytotoxicity of glycoconjugates against selected cell lines.

Compound	Activity IC$_{50}$ [μM][*]			
	U-251[**]	Hs683[**]	PANC-1[**]	AsPC-1[**]
23	> 100	> 100	47.87 ± 2.97	> 100
24	37.37 ± 1.56	57.19 ± 0.84	30.31 ± 1.32	34.24 ± 0.43
25	> 100	> 100	> 100	> 100
26	> 100	> 100	> 100	> 100
27	> 100	> 100	> 100	> 100
28	> 100	> 100	> 100	> 100
29	> 100	> 100	> 100	93.28 ± 1.89
30	> 100	> 100	> 100	> 100
Doxorubicin	0.05 ± 0.01	0.04 ± 0.01	0.73 ± 0.09	0.86 ± 0.13

[*] Cytotoxic was evaluated using the MTS assay.

[**] Incubation time 72 h.

glycoconjugates solutions at concentrations range from 0.01 mM to 0.8 mM. For the most active compounds IC$_{50}$ value was designated (Tables 4 and 5). The dependence of cell proliferation on the concentration of the potential inhibitor was compared to the results obtained for the starting quinoline derivatives **11** and **12** and the results are presented in Figs. 1a–c.

The results of the cytotoxicity assay indicate that the tested glycosides **15–22** were not toxic to the tested cell lines. Low cytotoxic activity is probably due to the use of the quinoline OH group to form a glycosidic linkage and the formation of steric hindrance hampering the chelation of metal ions. Whereas, some derivatives containing 1,2,3-triazole fragment, appeared to be active on the tested cell lines. The presence of a triazole fragment improves the activity of glycoconjugates, probably by improving the metal chelation capacity found in many types of cancers. Within tested compounds, glycoconjugates **23** and **24** showed promising results.

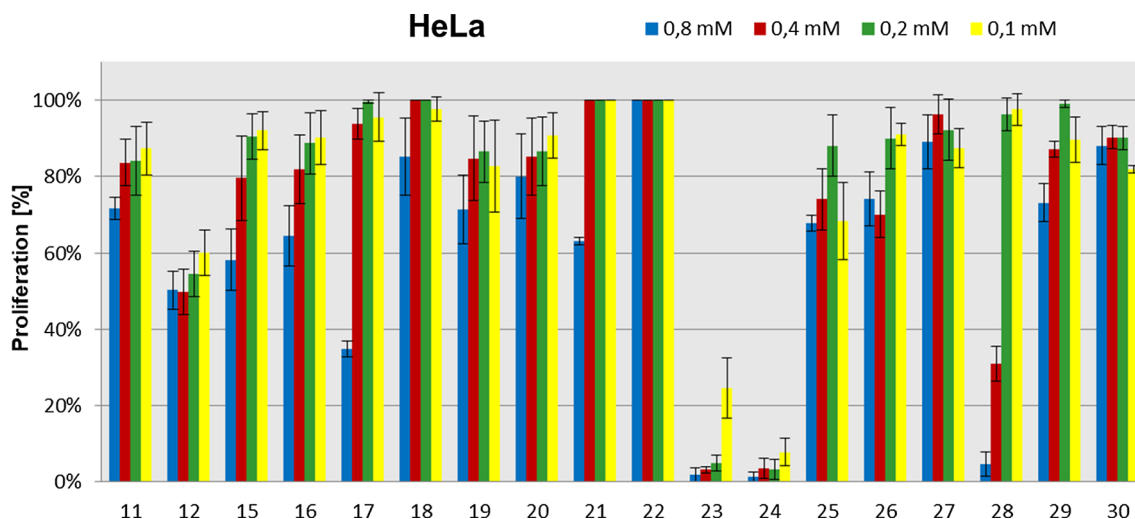The most active compounds were derivatives whose structure was

Fig. 1a. The dependence of HeLa cell proliferation on the concentration of the potential inhibitor.
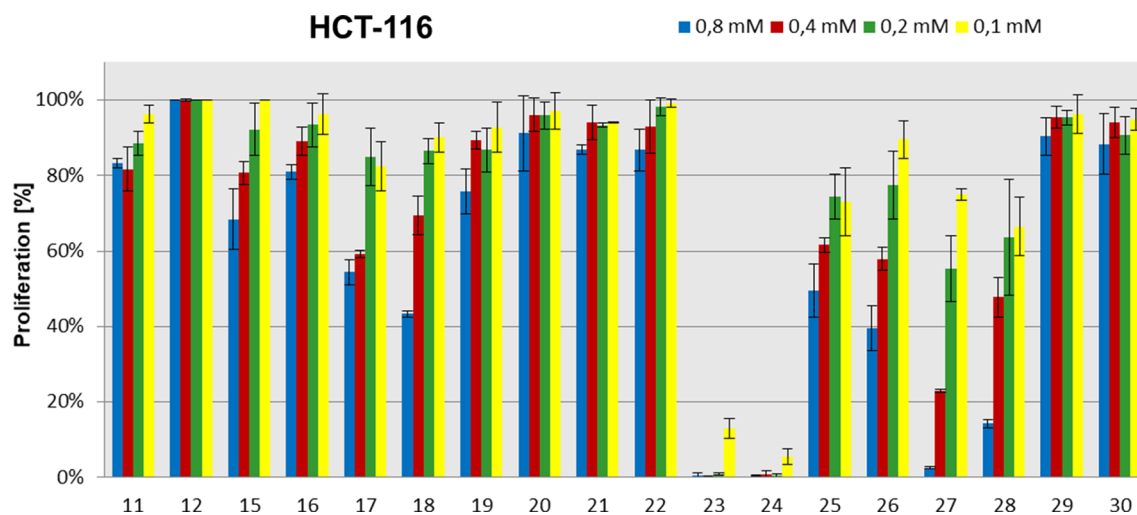
HCT-116

■ 0,8 mM ■ 0,4 mM ■ 0,2 mM □ 0,1 mM

Fig. 1b. The dependence of HCT 116 cell proliferation on the concentration of the potential inhibitor.
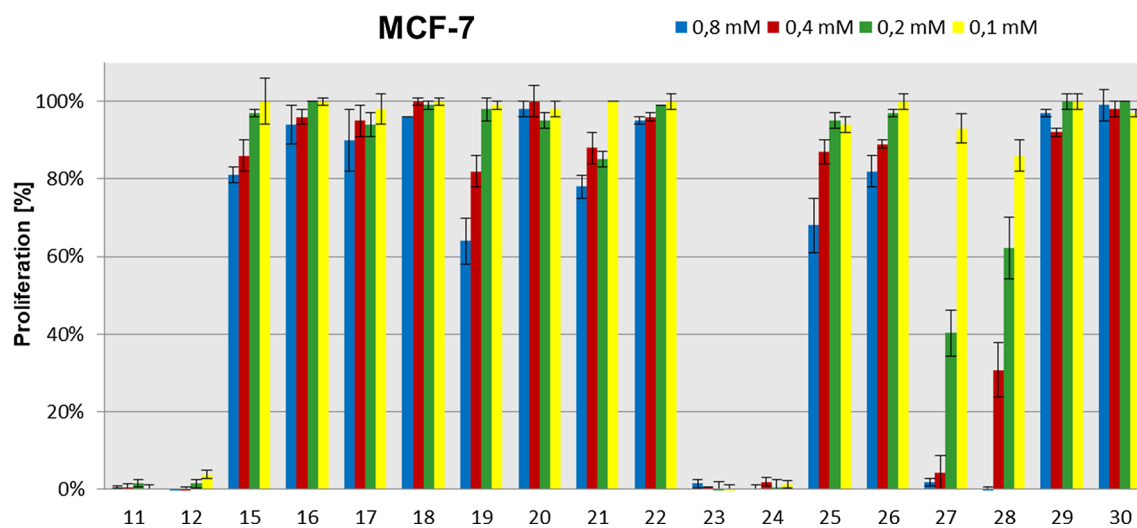
MCF-7

■ 0,8 mM ■ 0,4 mM ■ 0,2 mM □ 0,1 mM

Fig. 1c. The dependence of MCF-7 cell proliferation on the concentration of the potential inhibitor.

based on the 8-HQ fragment (**23, 24, 27, 28**). The same sugar derivatives but connected with 2-Me8-HQ units (**25, 26, 29, 30**) were not able to inhibit cancer cell proliferation so much. On the other hand, the type of sugar unit did not significantly affect to the glycoconjugate activity. It is only important that in these units hydroxyl group were protected with an acetyl moiety. The important issue is the penetration of the compound to the body and the crossing of all biological barriers. Therefore, for these studies it is necessary to use compounds with protected sugar units in order to improve the lipophilicity of the glycoconjugates so that they can freely penetrate inside the cell, whereupon the esterases are able to remove the acyl groups.

It should be noted that it was also checked whether the sugar substrates used for glycoconjugate synthesis are capable of inhibiting the cancer cells proliferation. All these substrates appeared to be inactive on tested cell lines. Additionally, the IC_{50} values obtained for quinoline derivatives for three of the four tested cell lines are mostly higher than for their glycoconjugates, which confirms the assumption that attached sugar unit increases the absorption and distribution of the compound.

The studies on HCT 116 and MCF-7 deliver information about quinoline derivatives selectivity against both cell lines, and indicate on the higher sensitivities of colorectal cancer cells, mostly followed by MTT viability assays [79,80]. The mode of action is mostly explained with Topoisomerase II activity and DNA damage assay, chromatin and histons modifications, what results with cell cycle arrest and apoptotic

cellular death induction, also in HeLa cells [81,82]. However, these findings do not precise how the active agents are downloaded into the cells. The chemical structure, most of tested compounds enable a transfer through the plasma membranes into the cytoplasm compartments. Although, the specific signaling pathway are usually activated, for quinoline derivatives the signal pathway of PI3K (phosphoinositide 3-kinase)-Akt (protein kinase B)-mTOR (rapamycin target protein) is one of the targets [80]. This specific transduction pathway regulates cell cycle and apoptosis, also processes, such as transcriptions, translations and proteins synthesis, influences general metabolisms [80]. Small quinoline derivatives are reported as inhibitors in PI3K-AKT-mTOR signaling pathway, what resulted with cell cycle arrest and apoptosis induction, with higher selectivity against MCF-7 than HCT 116 cells [80]. Glycoconjugates are more composite and structurally differ from quinoline precursors, so they probably cannot activate precise this specific cellular pathway, what resulted with lower cytotoxicity.

According to the idea that sugar-containing molecules may accumulate and act more effectively in cells that have high demand for sugars or relay on specific sugar metabolism we tested the glycoconjugates on additional cancer cell panel [83]. We selected cells that are known for their high demand for glucose as glioblastoma and pancreatic cancer [84]. Pancreatic cell's activity is regulated by glucose level. In pancreatic cancer the glucose metabolism determine morbidity

and malignancy of the tumor [85,86].

According to the results presented in the Table 5 compound **24** appeared most active among glycoconjugates that were tested against all additional cell lines, while **23** was active only against PANC-1.

3. Conclusion

In conclusion, a series of glycoconjugates derivatives of 8-HQ were obtained and their biological activity *in vitro* were tested. It turned out that the presence of both a sugar fragment and a 1,2,3-triazole linker in the structure was essential for biological activity. The *click-chemistry* approach in a simple, easily and inexpensive way leads to products with high yield, purity and selectivity. Obtained glycoconjugates were tested for their inhibitory potency against β-1,4-Galactosyltransferase as well as anticancer activity against wide bunch of cancer cell lines. Interestingly the conjugates designed on sugar moiety with free hydroxyl groups possessed some inhibitory potential contrary to their acetylated analogs. This result proves that only limited functionalization of the sugar core is allowed before final compound lost its recognition in biological system. On the other hand this activity do not correlate with antiproliferative activity of the compounds that were tested. Derivative of quinoline seemed to have better activity than quinaldines. Particularly acetylated sugar conjugates revealed interesting potential against breast cancer cells which appeared more vulnerable to quinoline derivatives. In other cell lines however several of the obtained compounds were at least ten times more active than the parent quinolines. As a result, these compounds could have valuable potential as therapeutic agents in the treatment of cancer diseases.

4. Experimental

4.1. General information

NMR spectra were recorded with an Agilent spectrometer at a frequency of 400 MHz using TMS as the internal standards and $CDCl_3$, CD_3OD or DMSO as the solvents. NMR solvents were purchased from ACROS Organics (Geel, Belgium). Chemical shifts (δ) are expressed in ppm and coupling constants (J) in Hz. Optical rotations were measured with a JASCO P-2000 polarimeter using a sodium lamp (589.3 nm) at room temperature. Melting point measurements were performed on OptiMelt (MPA 100) Stanford Research Systems. Mass spectra were recorded with a WATERS LCT Premier XE system using electrospray-ionization (ESI) technique. Reactions were monitored by TLC on pre-coated plates of silica gel 60 F254 (Merck Millipore). TLC plates were inspected under UV light (λ = 254 nm) or charring after spraying with 10% solution of sulfuric acid in ethanol. Crude products were purified using column chromatography performed on Silica Gel 60 (70–230 mesh, Fluka), developed using toluene/EtOAc or $CHCl_3$/MeOH solvent systems. All evaporations were performed on a rotary evaporator under diminished pressure at 40 °C. Reversed phase HPLC analyses were performed using JASCO LC 2000 apparatus equipped with a reverse phase column (Nucleosil 100 C18, 5 μm, 25 × 0.4 cm; mobile phase: H_2O/MeCN 90:10, flow rate 0.8 mL/min) with a fluorescence detector (FP). Fluorescence for substrate and product was read at 385 nm excitation/540 nm emission. The absorbance on MTT assay was measured spectrophotometrically at the 570 nm wave lenght using a plate reader (Epoch, BioTek, USA).

1,2,3,4,6-Penta-*O*-acetyl-β-D-glucopyranose **3** [53], 1,2,3,4,6-penta-*O*-acetyl-β-D-galactopyranose **4** [53], 2,3,4,6-tetra-*O*-acetyl-α-D-gluco-pyranosyl bromide **5** [54], 2,3,4,6-tetra-*O*-acetyl-α-D-galactopyranosyl bromide **6** [54], 2,3,4,6-tetra-*O*-acetyl-β-D-glucopyranosyl azide **7** [54], 2,3,4,6-tetra-*O*-acetyl-β-D-galactopyranosyl azide **8** [54], β-D-glucopyr-anosyl azide **9** [55], β-D-galactopyranosyl azide **10** [55], 8-(2-propyn-1-yloxy)quinoline **13** [75] and 2-methyl-8-(2-propyn-1-yloxy)quinoline **14** [75] were prepared according to the respective published procedures. D-Glucose, D-galactose, 8-hydroxyquinoline and 8-

hydroxyquinaldine are commercially available (Sigma-Aldrich). All used chemicals were purchased from Sigma-Aldrich, Fluka, Avantor and ACROS Organics and were used without purification. Bovine milk β-1,4-Galactosyltransferase I was purchased from Sigma-Aldrich.

4.2. Chemistry

4.2.1. Synthesis of glycoconjugates 15–22

Procedure A. 2,3,4,6-tetra-*O*-acetyl-α-D-glucopyranosyl bromide **5** or 2,3,4,6-tetra-*O*-acetyl-α-D-galactopyranosyl bromide **6** (0.9 mmol, 369.0 mg) and quinoline derivative **11** (0.3 mmol, 43.5 mg) or **12** (0.3 mmol, 47.7 mg) were dissolved in dichloromethane (22 mL). K_2CO_3 (2.9 mmol, 400.8 mg) and TBABr (0.3 mmol, 96.7 mg) were added to this mixture, followed by water (12 mL) and methanol (12 mL). The resulting mixture was stirred for 72 h at room temperature. The reaction progress was monitored on TLC in an eluents system $CHCl_3$:MeOH (2:1). Then the two-phase system was separated, and the aqueous phase was washed repeatedly with dichloromethane (18 mL). The aqueous phase was concentrated in vacuo. The crude products were purified using column chromatography ($CHCl_3$:MeOH, gradient: 12:1 to 2:1) to give products **19–22**.

Procedure B. Ag_2CO_3 (0.5 mmol, 137.9 mg), Me_4NCl (0.5 mmol, 54.8 mg) and $BMIm·BF_4$ (1.5 mL) were added to a round-bottom flask and stirred for 1 h at room temperature. Then the quinoline derivative **11** (0.6 mmol, 87.0 mg) or **12** (0.6 mmol, 95.4 mg) was added to this mixture, and after 20 min 2,3,4,6-tetra-*O*-acetyl-α-D-glucopyranosyl bromide **5** or 2,3,4,6-tetra-*O*-acetyl-α-D-galactopyranosyl bromide **6** (0.2 mmol, 82.0 mg) was added. The resulting mixture was stirred for 24 h at room temperature. The reaction progress was monitored on TLC in an eluents system toluene:AcOEt (2:1). Then CH_2Cl_2 (5 mL) and H_2O (5 mL) were added, the two-phase system was separated, and the organic phase was washed with dichloromethane (3x5 mL). The combined organic phases were dried with dry $MgSO_4$, filtered and the filtrate was evaporated in vacuo. The crude products were purified using column chromatography (toluene:AcOEt, gradient: 8:1 to 1:1) to give products **15–18**.

Procedure C. 2,3,4,6-Tetra-*O*-acetyl-α-D-glucopyranosyl bromide **5** or 2,3,4,6-tetra-*O*-acetyl-α-D-galactopyranosyl bromide **6** (1.2 mmol, 492.0 mg) and quinoline derivative **11** (1.4 mmol, 203.1 mg) or **12** (1.4 mmol, 222.7 mg) were dissolved in acetonitrile (15 mL), followed by addition of K_2CO_3 (5.5 mmol, 760.1 mg) and PEG 4000 (0.066 mmol, 264.0 mg). The resulting mixture was stirred for 48 h at room temperature. The reaction progress was monitored on TLC in an eluents system toluene:AcOEt (2:1 or 1:1). Then the reaction mixture was diluted with dichloromethane, filtered and the filtrate was evaporated in vacuo. The crude products were purified using column chromatography (toluene:AcOEt, gradient: 15:1 to 1:1) to give products **15–18**.

Procedure D. Per-*O*-acetylated glycosides **15–18** (0.375 mmol) was dissolved in methanol. Then 1 M solution of MeONa in MeOH (0.250 mmol, 250 μL) was added. Reaction was carried out for 0.5 h at room temperature. The reaction progress was monitored on TLC in an eluents system $CHCl_3$:MeOH (10:1). After the reaction was complete, the mixture was neutralized with Amberlyst-15, filtered and the filtrate was evaporated in vacuo. The crude products were purified using column chromatography (dry loading; $CHCl_3$:MeOH, gradient: 15:1 to 6:1) to give products **19–22**.

4.2.1.1. 8-Quinolinyl-2,3,4,6-tetra-O-acetyl-β-D-glucopyranoside

15. Starting from 2,3,4,6-tetra-*O*-acetyl-β-D-glucopyranosyl bromide **5** and 8-hydroxyquinoline **11** according to **Procedure B** yield: 44% (41.8 mg), according to **Procedure C** yield: 22% (125.4 mg), product was obtained as a solid; m.p.: 155–159 °C; $[\alpha]_D^{27}$ = −56.1 (c = 0.6, $CHCl_3$); HRMS (ESI-TOF): calcd for $C_{23}H_{26}NO_{10}$ ([M+H]$^+$): m/z 476.1557; found: m/z 476.1560; ^{1}H NMR (400 MHz, $CDCl_3$): δ 2.04, 2.05, 2.06, 2.10 (4 s, 12H, CH_3CO), 3.84 (ddd, 1H, J = 2.5 Hz,

$J = 5.0$ Hz, $J = 10.0$ Hz, H-5$_{Glu}$), 4.19 (dd, 1H, $J = 2.5$ Hz, $J = 12.2$ Hz, H-6a$_{Glu}$), 4.30 (dd, 1H, $J = 5.0$ Hz, $J = 12.2$ Hz, H-6b$_{Glu}$), 5.23 (dd, 1H, $J = 9.3$ Hz, $J = 10.0$ Hz, H-4$_{Glu}$), 5.33–5.50 (m, 3H, H-1$_{Glu}$, H-2$_{Glu}$, H-3$_{Glu}$), 7.40–7.48 (m, 3H, H-3$_{Chin}$, H-5$_{Chin}$, H-7$_{Chin}$), 7.57 (dd, 1H, $J = 2.4$ Hz, $J = 7.0$ Hz, H-6$_{Chin}$), 8.14 (dd, 1H, $J = 1.6$ Hz, $J = 8.4$ Hz, H-4$_{Chin}$), 8.90 (dd, 1H, $J = 1.7$ Hz, $J = 4.2$ Hz, H-2$_{Chin}$); ^{13}C NMR (100 MHz, CDCl$_3$): δ 20.70, 20.75, 20.77, 20.93, 62.09, 68.61, 71.54, 72.20, 72.81, 100.85, 117.30, 121.68, 123.58, 126.41, 129.63, 135.93, 141.13, 149.89, 152.63, 169.50, 169.73, 170.38, 170.65.

4.2.1.2. 8-Quinolinyl-2,3,4,6-tetra-O-acetyl-β-D-galactopyranoside

16. Starting from 2,3,4,6-tetra-O-acetyl-β-D-glucopyranosyl bromide **6** and 8-hydroxyquinoline **11** according to **Procedure B** yield: 37% (35.2 mg), according to **Procedure C** yield: 42% (239.5 mg), product was obtained as a solid; m.p.: 120–122 °C; $[\alpha]_D^{25} = -40.6$ (c = 1.7, CHCl$_3$); HRMS (ESI-TOF): calcd for C$_{23}$H$_{26}$NO$_{10}$ ([M + H]$^+$): m/z 476.1557; found: m/z 476.1559; ^{1}H NMR (400 MHz, CDCl$_3$): δ: 2.03, 2.04, 2.10, 2.19 (4 s, 12H, CH$_3$CO), 4.04 (ddd, 1H, $J = 1.1$ Hz, $J = 6.7$ Hz, $J = 7.0$ Hz, H-5$_{Gal}$), 4.18 (dd, 1H, $J = 6.7$ Hz, $J = 11.2$ Hz, H-6a$_{Gal}$), 4.25 (dd, 1H, $J = 7.0$ Hz, $J = 11.2$ Hz, H-6b$_{Gal}$), 5.18 (dd, 1H, $J = 3.4$ Hz, $J = 10.5$ Hz, H-3$_{Gal}$), 5.38 (d, 1H, $J = 8.0$ Hz, H-1$_{Gal}$), 5.47 (dd, 1H, $J = 1.1$ Hz, $J = 3.4$ Hz, H-4$_{Gal}$), 5.72 (dd, 1H, $J = 8.0$ Hz, $J = 10.5$ Hz, H-2$_{Gal}$), 7.40–7.49 (m, 3H, H-3$_{Chin}$, H-5$_{Chin}$, H-7$_{Chin}$), 7.57 (dd, 1H, $J = 3.2$ Hz, $J = 6.3$ Hz, H-6$_{Chin}$), 8.14 (dd, 1H, $J = 1.7$ Hz, $J = 8.3$ Hz, H-4$_{Chin}$), 8.91 (dd, 1H, $J = 1.7$ Hz, $J = 4.2$ Hz, H-2$_{Chin}$); ^{13}C NMR (100 MHz, CDCl$_3$): δ 20.80, 20.83, 21.08, 21.10, 61.47, 67.14, 68.96, 71.03, 71.20, 101.44, 117.07, 121.74, 123.48, 126.49, 129.69, 136.15, 144.70, 149.90, 152.77, 169.90, 170.37, 170.44, 170.49.

4.2.1.3. 2-Methyl-8-quinolinyl-2,3,4,6-tetra-O-acetyl-β-D-glucopyranoside

17. Starting from 2,3,4,6-tetra-O-acetyl-β-D-glucopyranosyl bromide **5** and 8-hydroxyquinoline **12** according to **Procedure B** yield: 27% (26.4 mg), according to **Procedure C** yield: 29% (170.2 mg), product was obtained as a solid; m.p.: 132–139 °C; $[\alpha]_D^{25} = -73.6$ (c = 1, CHCl$_3$); HRMS (ESI-TOF): calcd for C$_{24}$H$_{28}$NO$_{10}$ ([M + H]$^+$): m/z 490.1713; found: m/z 490.1707; ^{1}H NMR (400 MHz, CDCl$_3$): δ 2.05, 2.06, 2.07 (4 s, 12H, CH$_3$CO), 2.75 (s, 3H, CH$_3$), 3.85 (ddd, 1H, $J = 2.6$ Hz, $J = 5.0$ Hz, $J = 9.8$ Hz, H-5$_{Glu}$), 4.20 (dd, 1H, $J = 2.6$ Hz, $J = 12.2$ Hz, H-6a$_{Glu}$), 4.28 (dd, 1H, $J = 5.0$ Hz, $J = 12.2$ Hz, H-6b$_{Glu}$), 5.23 (dd, 1H, $J = 9.4$ Hz, $J = 9.8$ Hz, H-4$_{Glu}$), 5.35 (dd, 1H, $J = 9.3$ Hz, $J = 9.4$ Hz, H-3$_{Glu}$), 5.46–5.53 (m, 2H, H-1$_{Glu}$, H-2$_{Glu}$), 7.30 (d, 1H, $J = 8.4$ Hz, H-3$_{Chin}$), 7.34–7.41 (m, 2H, H-5$_{Chin}$, H-7$_{Chin}$), 7.52 (dd, 1H, $J = 2.6$ Hz, $J = 6.9$ Hz, H-6$_{Chin}$), 8.02 (d, 1H, $J = 8.4$ Hz, H-4$_{Chin}$); ^{13}C NMR (100 MHz, CDCl$_3$): δ 20.73, 20.79, 20.97, 25.67, 62.17, 68.71, 71.56, 72.15, 72.91, 100.89, 117.18, 122.51, 123.20, 125.47, 127.87, 136.06, 140.43, 152.18, 158.59, 169.56, 169.64, 170.47, 170.72.

4.2.1.4. 2-Methyl-8-quinolinyl-2,3,4,6-tetra-O-acetyl-β-D-galactopyranoside

18. Starting from 2,3,4,6-tetra-O-acetyl-β-D-glucopyranosyl bromide **6** and 8-hydroxyquinoline **12** according to **Procedure B** yield: 45% (44.0 mg), according to **Procedure C** yield: 51% (299.4 mg), product was obtained as a solid; m.p.: 134–138 °C; $[\alpha]_D^{25} = -57.0$ (c = 1, CHCl$_3$); HRMS (ESI-TOF): calcd for C$_{24}$H$_{28}$NO$_{10}$ ([M + H]$^+$): m/z 490.1713; found: m/z 490.1715; ^{1}H NMR (400 MHz, CDCl$_3$): δ 2.03, 2.04, 2.06, 2.18 (4 s, 12H, CH$_3$CO), 2.75 (s, 3H, CH$_3$), 4.06 (ddd, 1H, $J = 1.0$ Hz, $J = 6.6$ Hz, $J = 6.8$ Hz, H-5$_{Gal}$), 4.19 (dd, 1H, $J = 6.6$ Hz, $J = 11.2$ Hz, H-6a$_{Gal}$), 4.26 (dd, 1H, $J = 6.8$ Hz, $J = 11.2$ Hz, H-6b$_{Gal}$), 5.16 (dd, 1H, $J = 3.4$ Hz, $J = 10.5$ Hz, H-3$_{Gal}$), 5.39 (d, 1H, $J = 8.0$ Hz, H-1$_{Gal}$), 5.47 (dd, 1H, $J = 1.0$ Hz, $J = 3.4$ Hz, H-4$_{Gal}$), 5.75 (dd, 1H, $J = 8.0$ Hz, $J = 10.5$ Hz, H-2$_{Gal}$), 7.29 (d, 1H, $J = 8.4$ Hz, H-3$_{Chin}$), 7.34–7.41 (m, 2H, H-5$_{Chin}$, H-7$_{Chin}$), 7.51 (dd, 1H, $J = 2.1$ Hz, $J = 7.4$ Hz, H-6$_{Chin}$), 8.01 (d, 1H, $J = 8.4$ Hz, H-4$_{Chin}$); ^{13}C NMR (100 MHz, CDCl$_3$): δ 20.75, 20.77, 21.05, 25.66, 61.52, 67.16, 68.99, 71.03, 71.08, 101.51, 116.73, 122.49, 123.02, 125.45, 127.82, 135.99, 140.38, 152.42, 158.53, 169.74, 170.36, 170.40, 170.46.

4.2.1.5. 8-Quinolinyl-β-D-glucopyranoside

19. Starting from 2,3,4,6-tetra-O-acetyl-β-D-glucopyranosyl bromide **5** and 8-hydroxyquinoline **11** according to **Procedure A** yield: 49% (45.1 mg). Starting from 8-quinolinyl-tetra-O-acetyl-β-D-glucopyranoside **15** according to **Procedure D** yield: 41% (73.1 mg), product was obtained as a solid; m.p.: 193–196 °C; $[\alpha]_D^{25} = -99.0$ (c = 1.1, CH$_3$OH/CHCl$_3$ 9:1); HRMS (ESI-TOF): calcd for C$_{15}$H$_{18}$NO$_6$ ([M + H]$^+$): m/z 308.1134; found: m/z 308.1132; ^{1}H NMR (400 MHz, CD$_3$OD): δ 3.45 (dd, 1H, $J = 8.9$ Hz, $J = 9.6$ Hz, H-4$_{Glu}$), 3.56 (dd, 1H, $J = 8.9$ Hz, $J = 9.4$ Hz, H-3$_{Glu}$), 3.57 (ddd, 1H, $J = 2.2$ Hz, $J = 6.0$ Hz, $J = 9.6$ Hz, H-5$_{Glu}$), 3.72 (dd, 1H, $J = 7.8$ Hz, $J = 9.4$ Hz, H-2$_{Glu}$), 3.73 (dd, 1H, $J = 6.0$ Hz, $J = 12.0$ Hz, H-6b$_{Glu}$), 3.96 (dd, 1H, $J = 2.2$ Hz, $J = 12.0$ Hz, H-6a$_{Glu}$), 5.06 (d, 1H, $J = 7.8$ Hz, H-1$_{Glu}$), 7.49–7.60 (m, 4H, H-3$_{Chin}$, H-5$_{Chin}$, H-6$_{Chin}$, H-7$_{Chin}$), 8.34 (dd, 1H, $J = 1.7$ Hz, $J = 8.4$ Hz, H-4$_{Chin}$), 8.84 (dd, 1H, $J = 1.7$ Hz, $J = 4.3$ Hz, H-2$_{Chin}$); ^{13}C NMR (100 MHz, CD$_3$OD): δ 62.64, 71.58, 74.80, 77.26, 78.51, 103.17, 114.51, 122.60, 123.01, 128.46, 131.03, 138.47, 140.27, 150.24, 153.85.

4.2.1.6. 8-Quinolinyl-β-D-galactopyranoside

20. Starting from 2,3,4,6-tetra-O-acetyl-β-D-galactopyranosyl bromide **6** and 8-hydroxyquinoline **11** according to **Procedure A** yield: 34% (31.3 mg). Starting from 8-quinolinyl-tetra-O-acetyl-β-D-galactopyranoside **16** according to **Procedure D** yield: 41% (73.1 mg), product was obtained as a solid; m.p.: 200–205 °C; $[\alpha]_D^{25} = -43.8$ (c = 0.8, CH$_3$OH/CHCl$_3$ 9:1); HRMS (ESI-TOF): calcd for C$_{15}$H$_{18}$NO$_6$ ([M + H]$^+$): m/z 308.1134; found: m/z 308.1135; ^{1}H NMR (400 MHz, CD$_3$OD): δ 3.67 (dd, 1H, $J = 3.5$ Hz, $J = 9.9$ Hz, H-3$_{Gal}$), 3.77–3.89 (m, 3H, H-5$_{Gal}$, H-6a$_{Gal}$, H-6b$_{Gal}$), 3.95 (d, 1H, $J = 3.5$ Hz, H-4$_{Gal}$), 4.06 (dd, 1H, $J = 7.7$ Hz, $J = 9.9$ Hz, H-2$_{Gal}$), 5.01 (d, $J = 7.7$ Hz, H-1$_{Gal}$), 7.50–7.60 (m, 4H, H-3$_{Chin}$, H-5$_{Chin}$, H-6$_{Chin}$, H-7$_{Chin}$), 8.35 (dd, 1H, $J = 1.7$ Hz, $J = 8.4$ Hz, H-4$_{Chin}$), 8.85 (dd, 1H, $J = 1.6$ Hz, $J = 4.3$ Hz, H-2$_{Chin}$); ^{13}C NMR (100 MHz, CD$_3$OD): δ 62.57, 70.24, 72.12, 74.18, 77.40, 103.88, 114.59, 122.53, 122.97, 128.44, 130.98, 138.46, 140.24, 150.16, 153.88.

4.2.1.7. 2-Methyl-8-quinolinyl-β-D-glucopyranoside

21. Starting from 2,3,4,6-tetra-O-acetyl-β-D-glucopyranosyl bromide **5** and 8-hydroxyquinaldine **12** according to **Procedure A** yield: 21% (20.2 mg). Starting from 2-methyl-8-quinolinyl-tetra-O-acetyl-β-D-glucopyranoside **17** according to **Procedure D** yield: 68% (124.7 mg), product was obtained as a solid; m.p.: 206–210 °C; $[\alpha]_D^{24} = -109.4$ (c = 1, CH$_3$OH/CHCl$_3$ 9:1); HRMS (ESI-TOF): calcd for C$_{16}$H$_{20}$NO$_6$ ([M + H]$^+$): m/z 322.1291; found: m/z 322.1293; ^{1}H NMR (400 MHz, CD$_3$OD): δ 2.74 (s, 3H, CH$_3$), 3.45 (dd, 1H, $J = 8.8$ Hz, $J = 9.6$ Hz, H-4$_{Glu}$), 3.54 (ddd, 1H, $J = 2.3$ Hz, $J = 6.4$ Hz, $J = 9.6$ Hz, H-5$_{Glu}$), 3.56 (dd, 1H, $J = 8.8$ Hz, $J = 9.4$ Hz, H-3$_{Glu}$), 3.71 (dd, 1H, $J = 7.8$ Hz, $J = 9.4$ Hz, H-2$_{Glu}$), 3.72 (dd, 1H, $J = 6.4$ Hz, $J = 12.1$ Hz, H-6a$_{Glu}$), 3.95 (dd, 1H, $J = 2.3$ Hz, $J = 12.1$ Hz, H-6b$_{Glu}$), 5.03 (d, $J = 7.8$ Hz, H-1$_{Glu}$), 7.41–7.48 (m, 3H, H-3$_{Chin}$, H-5$_{Chin}$, H-7$_{Chin}$), 7.52 (dd, 1H, $J = 2.5$ Hz, $J = 7.0$ Hz, H-6$_{Chin}$), 8.19 (d, 1H, $J = 8.5$ Hz, H-4$_{Chin}$); ^{13}C NMR (100 MHz, CD$_3$OD): δ 24.56, 62.63, 71.54, 74.88, 77.41, 78.49, 103.39, 115.34, 122.74, 124.00, 127.37, 129.29, 138.55, 140.03, 153.24, 159.90.

4.2.1.8. 2-Methyl-8-quinolinyl-β-D-galactopyranoside

22. Starting from 2,3,4,6-tetra-O-acetyl-β-D-galactopyranosyl bromide **6** and 8-hydroxyquinaldine **12** according to **Procedure A** yield: 29% (27.9 mg). Starting from 2-methyl-8-quinolinyl-tetra-O-acetyl-β-D-galactopyranoside **18** according to **Procedure D** yield: 66% (121.1 mg), product was obtained as a solid; m.p.: 208–212 °C; $[\alpha]_D^{25} = -87.4$ (c = 1, CH$_3$OH/CHCl$_3$ 9:1); HRMS (ESI-TOF): calcd for C$_{16}$H$_{20}$NO$_6$ ([M + H]$^+$): m/z 322.1291; found: m/z 322.1292; ^{1}H NMR (400 MHz, CD$_3$OD): δ 2.72 (s, 3H, CH$_3$), 3.68 (dd, 1H, $J = 3.4$ Hz, $J = 9.8$ Hz, H-3$_{Gal}$), 3.75–3.88 (m, 3H, H-6a$_{Gal}$, H-5$_{Gal}$, H-6b$_{Gal}$), 3.94 (d, 1H, $J = 3.4$ Hz, H-4$_{Gal}$), 4.07 (dd, 1H, $J = 7.8$ Hz, $J = 9.8$ Hz, H-2$_{Gal}$), 4.97 (d, $J = 7.8$ Hz, H-1$_{Gal}$), 7.38–7.52 (m, 4H, H-3$_{Chin}$, H-5$_{Chin}$,

H-6$_{Chin}$, H-7$_{Chin}$), 8.17 (d, 1H, J = 8.5 Hz, H-4$_{Chin}$); ^{13}C NMR (100 MHz, CD$_3$OD): δ 24.55, 62.53, 70.20, 72.22, 74.34, 77.35, 104.09, 115.38, 122.69, 123.97, 127.35, 129.25, 138.52, 140.03, 153.31, 159.85.

4.2.2. Synthesis of glycoconjugates 23–30

To a solution of *O*-acetylated glycosyl azides **7** or **8** (0.5 mmol, 186.6 mg) or deprotected glycosyl azides **9** or **10** (0.5 mmol, 102.5 mg) and 8-(2-propyn-1-yloxy)quinoline **13** (0.5 mmol, 91.5 mg) or 2-methyl-8-(2-propyn-1-yloxy)quinoline **14** (0.5 mmol, 98.5 mg) in THF (5 mL) : *i*-PrOH (5 mL), CuSO$_4$·5H$_2$O (0.1 mmol, 25.0 mg) dissolved in H$_2$O (2.5 mL) and sodium ascorbate (0.2 mmol, 39.6 mg) dissolved in H$_2$O (2.5 mL) were added to this mixture. The reaction mixture was stirred for 24 h at room temperature. The reaction progress was monitored on TLC in an eluents system CHCl$_3$:MeOH (20:1 or 2:1). Mixture was concentrated in vacuo and purified using column chromatography (dry loading; toluene:AcOEt, 2:1 and CHCl$_3$:MeOH, 100:1 for fully protected glycoconjugates or CHCl$_3$:MeOH, gradient: 50:1 to 2:1 for glycoconjugates with unprotected sugar part) to give products **23–30**.

4.2.2.1. 8-((1-(2,3,4,6-Tetra-O-acetyl-β-D-glucopyranosyl)-1H-1,2,3-triazol-4-yl)methoxy)quinoline 23.

Starting from 2,3,4,6-tetra-*O*-acetyl-β-D-glucopyranosyl azide **7** and 8-(2-propyn-1-yloxy)quinoline **13**, product was obtained as a solid. Yield: 99% (275.3 mg); m.p.: 162–164 °C; [α]$_D^{25}$ = − 33.3 (c = 1.0, CHCl$_3$); HRMS (ESI-TOF): calcd for C$_{26}$H$_{29}$N$_4$O$_{10}$ ([M + H]$^+$): *m/z* 557.1884; found: *m/z* 557.1885; ^{1}H NMR (400 MHz, CDCl$_3$): δ 1.80, 2.00, 2.05, 2.06 (4 s, 12H, CH$_3$CO), 3.97 (ddd, 1H, J = 2.1 Hz, J = 5.0 Hz, J = 10.1 Hz, H-5$_{Glu}$), 4.12 (dd, 1H, J = 2.1 Hz, J = 12.7 Hz, H-6a$_{Glu}$), 4.23 (dd, 1H, J = 5.0 Hz, J = 12.7 Hz, H-6b$_{Glu}$), 5.21 (dd ~ t, 1H, J = 9.6 Hz, J = 10.1 Hz, H-4$_{Glu}$), 5.36–5.43 (m, 2H, H-3$_{Glu}$, H-2$_{Glu}$), 5.54 i 5.59 (qAB, 2H, J = 13.2 Hz, CH$_2$), 5.85 (d, 1H, J = 9.1 Hz, H-1$_{Glu}$), 7.25–7.27 (m, 1H, H-7$_{Chin}$), 7.39–7.48 (m, 3H, H-3$_{Chin}$, H-5$_{Chin}$, H-6$_{Chin}$), 7.98 (s, 1H, H-5$_{Triaz}$), 8.13 (dd, 1H, J = 1.5 Hz, J = 8.3 Hz, H-4$_{Chin}$), 8.95 (dd, 1H, J = 1.4 Hz, J = 4.0 Hz, H-2$_{Chin}$); ^{13}C NMR (100 MHz, CDCl$_3$): δ 20.11, 20.50, 20.52, 20.68, 61.51, 62.76, 67.68, 70.34, 72.68, 75.12, 85.78, 110.10, 120.43, 121.69, 121.92, 126.65, 129.54, 135.99, 140.37, 144.80, 149.43, 153.80, 168.73, 169.27, 169.92, 170.50.

4.2.2.2. 8-((1-(2,3,4,6-Tetra-O-acetyl-β-D-galactopyranosyl)-1H-1,2,3-triazol-4-yl)methoxy)quinolone 24.

Starting from 2,3,4,6-tetra-*O*-acetyl-β-D-galactopyranosyl azide **8** and 8-(2-propyn-1-yloxy)quinoline **13**, product was obtained as a solid. Yield: 76% (211.3 mg); m.p.: 165–170 °C; [α]$_D^{25}$ = − 24.0 (c = 1.0, CHCl$_3$); HRMS (ESI-TOF): calcd for C$_{26}$H$_{29}$N$_4$O$_{10}$ ([M + H]$^+$): *m/z* 557.1884; found: *m/z* 557.1884; ^{1}H NMR (400 MHz, CDCl$_3$): δ 1.83, 1.99, 2.03, 2.20 (4 s, 12H, CH$_3$CO), 4.11 (dd, 1H, J = 6.3 Hz, J 11.1 Hz, H-6a$_{Gal}$), 4.17 (dd, 1H, J = 5.9 Hz, J = 11.1 Hz, H-6b$_{Gal}$), 4.20 (m, 1H, H-5$_{Gal}$), 5.23 (dd, 1H, J = 3.3 Hz, J = 10.3 Hz, H-3$_{Gal}$), 5.50–5.62 (m, 4H, H-2$_{Gal}$, H-4$_{Gal}$, CH$_2$), 5.83 (d, 1H, J = 9.3 Hz, H-1$_{Gal}$), 7.27 (m, 1H, H-7$_{Chin}$), 7.40–7.48 (m, 3H, H-3$_{Chin}$, H-5$_{Chin}$, H-6$_{Chin}$), 8.06 (s, 1H, H-5$_{Triaz}$), 8.14 (d, 1H, J = 8.0 Hz, H-4$_{Chin}$), 8.96 (d, 1H, J = 2.8 Hz, H-2$_{Chin}$); ^{13}C NMR (100 MHz, CDCl$_3$): δ 20.19, 20.47, 20.64, 61.25, 62.87, 66.86, 67.89, 70.83, 74.01, 86.29, 110.12, 120.40, 121.68, 121.99, 126.68, 129.53, 136.00, 140.40, 144.74, 149.43, 153.86, 168.85, 169.79, 169.98, 170.31.

4.2.2.3. 2-Methyl-8-((1-(2,3,4,6-tetra-O-acetyl-β-D-glucopyranosyl)-1H-1,2,3-triazol-4-yl)methoxy)quinolone 25.

Starting from 2,3,4,6-tetra-*O*-acetyl-β-D-glucopyranosyl azide **7** and 2-methyl-8-(2-propyn-1-yloxy)quinoline **14**, product was obtained as a solid. Yield: 80% (228.1 mg); m.p.: 195–200 °C; [α]$_D^{25}$ = − 37.6 (c = 1.0, CHCl$_3$); HRMS (ESI-TOF): calcd for C$_{27}$H$_{31}$N$_4$O$_{10}$ ([M + H]$^+$): *m/z* 571.2040; found: *m/z* 571.2039; ^{1}H NMR (400 MHz, CDCl$_3$): δ 1.81, 2.01, 2.05, 2.07 (4 s, 12H, CH$_3$CO), 2.86 (s, 3H, CH$_3$), 3.98 (ddd, 1H, J = 2.1 Hz, J = 4.9 Hz, J = 10.1 Hz, H-5$_{Glu}$), 4.13 (dd, 1H, J = 2.1 Hz, J = 12.6 Hz, H-6a$_{Glu}$), 4.27 (dd, 1H, J = 4.9 Hz, J = 12.6 Hz, H-6b$_{Glu}$), 5.22 (dd ~ t, 1H,

J = 9.3 Hz, J = 10.1 Hz, H-4$_{Gal}$), 5.37–5.45 (m, 2H, H-3$_{Gal}$, H-2$_{Glu}$), 5.58 i 5.62 (qAB, 2H, J = 13.4 Hz, CH$_2$), 5.85 (d, 1H, J = 9.0 Hz, H-1$_{Glu}$), 7.23–7.28 (m, 1H, H-7$_{Chin}$), 7.34 (d, 1H, J = 8.4 Hz, H-3$_{Chin}$), 7.37–7.41 (m, 2H, H-5$_{Chin}$, H-6$_{Chin}$), 8.06 (s, 1H, H-5$_{Triaz}$), 8.07 (d, 1H, J = 8.4 Hz, H-4$_{Chin}$); ^{13}C NMR (100 MHz, CDCl$_3$): δ 20.11, 20.50, 20.52, 20.67, 25.39, 61.51, 63.18, 67.68, 70.33, 72.70, 75.11, 85.77, 111.15, 120.34, 122.06, 122.75, 125.98, 127.81, 136.86, 139.17, 145.02, 152.93, 158.31, 168.68, 169.28, 169.93, 170.51.

4.2.2.4. 2-Methyl-8-((1-(2,3,4,6-tetra-O-acetyl-β-D-galactopyranosyl)-1H-1,2,3-triazol-4-yl)methoxy)quinolone 26.

Starting from 2,3,4,6-tetra-*O*-acetyl-β-D-galactopyranosyl azide **8** and 2-methyl-8-(2-propyn-1-yloxy)quinoline **14**, product was obtained as a solid. Yield: 87% (248.0 mg); m.p.: 178–183 °C; [α]$_D^{25}$ = − 17.4 (c = 1.0, CHCl$_3$); HRMS (ESI-TOF): calcd for C$_{27}$H$_{31}$N$_4$O$_{10}$ ([M + H]$^+$): *m/z* 571.2040; found: *m/z* 571.2043; ^{1}H NMR (400 MHz, CDCl$_3$): δ 1.84, 1.99, 2.03, 2.20 (4 s, 12H, CH$_3$CO), 2.83 (s, 3H, CH$_3$), 4.10 (dd, 1H, J = 6.3 Hz, J = 10.6 Hz, H-6a$_{Gal}$), 4.17 (dd, 1H, J = 5.9 Hz, J = 10.6 Hz, H-6b$_{Gal}$), 4.20 (m, 1H, H-5$_{Gal}$), 5.23 (dd, 1H, J = 3.3 Hz, J = 10.3 Hz, H-3$_{Gal}$), 5.50–5.63 (m, 4H, H-2$_{Gal}$, H-4$_{Gal}$, CH$_2$), 5.82 (d, 1H, J = 9.3 Hz, H-1$_{Gal}$), 7.24 (dd, 1H, J = 2.4 Hz, J = 6.5 Hz, H-7$_{Chin}$), 7.33 (d, 1H, J = 8.2 Hz, H-3$_{Chin}$), 7.37–7.41 (m, 2H, H-5$_{Chin}$, H-6$_{Chin}$), 8.04 (d, 1H, J = 8.2 Hz, H-4$_{Chin}$), 8.08 (s, 1H, H-5$_{Triaz}$); ^{13}C NMR (100 MHz, CDCl$_3$): δ 20.21, 20.48, 20.63, 20.65, 25.62, 61.22, 63.36, 66.86, 67.90, 70.86, 74.00, 86.31, 111.02, 120.37, 121.97, 122.66, 125.82, 127.79, 136.49, 138.71, 145.08, 153.25, 158.29, 168.81, 169.80, 169.98, 170.30.

4.2.2.5. 8-((1-(β-D-Glucopyranosyl)-1H-1,2,3-triazol-4-yl)methoxy)quinoline 27.

Starting from β-D-glucopyranosyl azide **9** and 8-(2-propyn-1-yloxy)quinoline **13**, product was obtained as a solid. Yield: 83% (161.1 mg); m.p.: 213–218 °C; [α]$_D^{25}$ = − 9.6 (c = 1.0, DMSO); HRMS (ESI-TOF): calcd for C$_{18}$H$_{21}$N$_4$O$_6$ ([M + H]$^+$): *m/z* 389.1461; found: *m/z* 389.1461; ^{1}H NMR (400 MHz, DMSO): δ 3.26 (m, 1H, H-2$_{Glu}$), 3.37–3.50 (m, 3H, H-3$_{Glu}$, H-4$_{Glu}$, H-5$_{Glu}$), 3.70 (m, 1H, H-6a$_{Glu}$), 3.83 (m, 1H, H-6b$_{Glu}$), 4.71 (t, 1H, J = 5.9 Hz, 6-OH), 5.15 (d, 1H, J = 5.5 Hz, OH), 5.27 (d, 1H, J = 4.9 Hz, OH), 5.35 (s, 2H, CH$_2$) 5.43 (d, 1H, J = 6.0 Hz, OH), 5.61 (d, 1H, J = 9.3 Hz, H-1$_{Glu}$), 7.44 (dd, 1H, J = 4.7 Hz, J = 9.0 Hz, H-7$_{Chin}$), 7.51–7.58 (m, 3H, H-3$_{Chin}$, H-5$_{Chin}$, H-6$_{Chin}$), 8.32 (dd, 1H, J = 2.0 Hz, J = 8.2 Hz, H-4$_{Chin}$), 8.54 (s, 1H, H-5$_{Triaz}$), 8.82 (dd, 1H, J = 1.6 Hz, J = 4.3 Hz, H-2$_{Chin}$); ^{13}C NMR (100 MHz, DMSO): δ 60.70, 61.64, 69.56, 72.02, 76.98, 80.01, 87.53, 109.73, 119.97, 121.86, 124.25, 126.75, 129.03, 135.78, 139.63, 142.45, 148.96, 153.87.

4.2.2.6. 8-((1-(β-D-Galactopyranosyl)-1H-1,2,3-triazol-4-yl)methoxy)quinoline 28.

Starting from β-D-galactopyranosyl azide **10** and 8-(2-propyn-1-yloxy)quinoline **13**, product was obtained as a solid. Yield: 78% (151.4 mg); m.p.: 233–236 °C; [α]$_D^{25}$ = 6.0 (c = 1.0 DMSO); HRMS (ESI-TOF): calcd for C$_{18}$H$_{21}$N$_4$O$_6$ ([M + H]$^+$): *m/z* 389.1461; found: *m/z* 389.1459; ^{1}H NMR (400 MHz, DMSO): δ 3.49–3.61 (m, 3H, H-3$_{Gal}$, H-2$_{Gal}$, H-4$_{Gal}$), 3.71–3.80 (m, 2H, H-5$_{Gal}$, H-6a$_{Gal}$), 4.05–4.13 (m, 1H, H-6b$_{Gal}$), 4.64 (d, 1H, J = 5.5 Hz, OH), 4.75 (t, 1H, J = 5.9 Hz, 6-OH), 5.02 (d, 1H, J = 5.5 Hz, OH), 5.29 (d, 1H, J = 6.0 Hz, OH), 5.36 (s, 2H, CH$_2$), 5.55 (d, 1H, J = 9.2 Hz, H-1$_{Gal}$), 7.44 (dd, 1H, J = 4.4 Hz, J = 7.4 Hz, H-7$_{Chin}$), 7.51–7.58 (m, 3H, H-3$_{Chin}$, H-5$_{Chin}$, H-6$_{Chin}$), 8.32 (dd, 1H, J = 1.8 Hz, J = 8.3 Hz, H-4$_{Chin}$), 8.47 (s, 1H, H-5$_{Triaz}$), 8.83 (dd, 1H, J = 1.8 Hz, J = 4.1 Hz, H-2$_{Chin}$); ^{13}C NMR (100 MHz, DMSO): δ 60.51, 61.68, 68.54, 69.32, 73.69, 78.54, 88.15, 109.74, 119.96, 121.85, 123.76, 126.74, 129.03, 135.77, 139.64, 142.62, 148.97, 153.87.

4.2.2.7. 2-Methyl-8-((1-(β-D-glucopyranosyl)-1H-1,2,3-triazol-4-yl)methoxy)quinolone 29.

Starting from β-D-glucopyranosyl azide **9** and 2-methyl-8-(2-propyn-1-yloxy)quinoline **14**, product was obtained as a solid. Yield: 92% (185.0 mg); m.p.: 162–167 °C; [α]$_D^{25}$ = − 20.4 (c = 1.0, DMSO); HRMS (ESI-TOF): calcd for C$_{19}$H$_{23}$N$_4$O$_6$ ([M

+H]$^+$): m/z 403.1618; found: m/z 403.1618; ^{1}H NMR (400 MHz, DMSO): δ 2.62 (s, 3H, CH$_3$), 3.21–3.50 (m, 4H, H-2$_{Glu}$, H-3$_{Glu}$, H-4$_{Glu}$, H-5$_{Glu}$), 3.65–3.73 (m, 1H, H-6a$_{Glu}$), 3.78–3.85 (m, 1H, , H-6b$_{Glu}$), 4.67 (t, 1H, J = 5.5 Hz, 6-OH), 5.15 (d, 1H, J = 4.2 Hz, OH), 5.29 (bs, 1H, OH), 5.35 (s, 2H, CH$_2$), 5.43 (d, 1H, J = 5.8 Hz, OH), 5.60 (d, 1H, J = 9.3 Hz, H-1$_{Glu}$), 7.38–7.50 (m, 4H, H-3$_{Chin}$, H-5$_{Chin}$, H-6$_{Chin}$, H-7$_{Chin}$), 8.19 (d, 1H, J = 8.4 Hz, H-4$_{Chin}$), 8.54 (s, 1H, H-5$_{Triaz}$); ^{13}C NMR (100 MHz, DMSO): δ 24.91, 60.68, 61.48, 69.53, 72.03, 76.96, 79.98, 87.51, 110.01, 119.81, 122.47, 124.31, 125.66, 127.32, 135.96, 139.11, 142.51, 153.37, 157.28.

4.2.2.8. 2-Methyl-8-((1-(β-D-galactopyranosyl)-1H-1,2,3-triazol-4-yl) methoxy)quinoline 30.

Starting from β-D-galactopyranosyl azide **10** and 2-methyl-8-(2-propyn-1-yloxy)quinoline **14**, product was obtained as a solid. Yield: 56% (112.6 mg); m.p.: 206–211 °C; $[\alpha]_D^{25}$ = − 38.0 (c = 1.0, DMSO); HRMS (ESI-TOF): calcd for C$_{19}$H$_{23}$N$_4$O$_6$ ([M +H]$^+$): m/z 403.1618; found: m/z 403.1624; ^{1}H NMR (400 MHz, DMSO): δ 2.63 (s, 3H, CH$_3$), 3.47–3.60 (m, 3H, H-3$_{Gal}$, H-2$_{Gal}$, H-4$_{Gal}$), 3.70–3.79 (m, 2H, H-6a$_{Gal}$, H-5$_{Gal}$), 4.04–4.10 (m, 1H, H-6b$_{Gal}$), 4.63 (d, 1H, J = 5.4 Hz, OH), 4.72 (t, 1H, J = 5.8 Hz, 6-OH), 5.02 (d, 1H, J = 5.6 Hz, OH), 5.28 (d, 1H, J = 6.0 Hz, OH), 5.36 (s, 2H, CH$_2$), 5.54 (d, 1H, J = 9.2 Hz, H-1$_{Gal}$), 7.38–7.50 (m, 4H, H-3$_{Chin}$, H-5$_{Chin}$, H-6$_{Chin}$, H-7$_{Chin}$), 8.19 (d, 1H, J = 8.4 Hz, H-4$_{Chin}$), 8.46 (s, 1H, H-5$_{Triaz}$); ^{13}C NMR (100 MHz, DMSO): δ 24.90, 60.46, 61.50, 68.48, 69.29, 73.67, 78.49, 88.12, 110.02, 119.79, 122.45, 123.87, 125.63, 127.31, 135.94, 139.12, 142.63, 153.37, 157.26.

4.3. Biological assays

4.3.1. Bovine milk β-1,4-Galactosyltransferase I assay

β-1,4-GalT activity was assayed using UDP-Gal, a natural β-1,4-GalT glycosyl donor type substrate, and (6-esculetinyl) β-D-glucopyranoside (esculine) as glycosyl fluorescent acceptor. The reaction mixtures contained reagents in the following final concentrations: 50 mM citrate buffer (pH 5.4), 100 mM MnCl$_2$, 20 mg/mL BSA, 2 mM esculine, 0.4 mM UDP-Gal and 10 μL MeOH or methanolic solution of potential inhibitors **15–30** at 0.8 mM concentration. Assays were performed in a total volume of 200 μL. The enzymatic reactions were started by the addition of 8 mU β-1,4-GalT and incubated at 30 °C for 60 min. After that, the reaction mixture was diluted with water to a volume of 500 μL and then was placed in a thermoblock set at 90 °C for 3 min. After denaturation, the solutions were centrifuged at 10 °C for 30 min at 10,000 rpm. The supernatant was filtered using syringe filters (M.E. Cellulose filter, Teknokroma®, 0.2 μm × 13 mm). The filtrate was injected into RP-HPLC system. The percentage of inhibition was evaluated from the fluorescence intensity of the peaks referring to product (6-esculetinyl) 4′-O-β-D-galactopyranosyl-β-D-glucopyranoside).

4.3.2. Cell lines

The culture media were purchased from EuroClone, HyClone, MP Biomedicals and Pan Biotech. Fetal bovine serum (FBS) was delivered by Eurx, Poland and Antibiotic Antimycotic Solution (100×) by Sigma-Aldrich, Germany. The human cell line HeLa and MCF-7 were obtained from collections at the Maria Sklodowska-Curie Memorial Cancer Center and Institute of Oncology, branch in Gliwice, Poland, as kindly gift from dr Monika Pietrowska and prof. Wiesława Widłak. Normal Human Dermal Fibroblasts-Neonatal, NHDF-Neo were purchased from LONZA (Cat. No. CC-2509; NHDF-Neo, Dermal Fibroblasts, Neonatal; Lonza, Poland). HCT 116 and Hs683 were obtained from American Type Culture Collection (ATCC, Manassas, VA, USA). U-251, PANC-1, and AsPC-1 were bought from Sigma-Aldrich, Germany. The culture media consisted of RPMI 1640 or DMEM + F12 medium, supplemented with 10% or 12% fetal bovine serum and standard antibiotics.

4.3.3. MTT assay

A lifespan of the cells was assessed with an MTT (3-[4,5-dimethylthiazol-2-yl]-2,5-diphenyltetrazolium bromide) test (Sigma-Aldrich). The cells were seeded in the 96-well plates with concentration of 1×10^4 or 5×10^3 cells per well. The cells culture were incubated for 24 h at 37 °C in a humidified atmosphere of 5% CO$_2$. Then the culture medium was removed, replaced with solution of the tested compounds in medium and incubated for further 24 h or 72 h. After that, medium was removed and the MTT solution (50 μL, 0.5 mg/mL in RPMI 1640 without phenol red) was added. After 3 h of incubation, the MTT solution was removed and the acquired formazan was dissolved in isopropanol:HCl system. Finally, the absorbance at the 570 nm wave length was measured spectrophotometrically with the plate reader. The experiment was conducted in three independent iterations with four technical repetitions. Tests were conducted at concentrations tested compounds range from 0.01 mM to 0.8 mM solutions. For the most active compounds IC$_{50}$ values were calculated using CalcuSyn. The IC$_{50}$ parameter was defined as the compound concentration that was necessary to reduce the proliferation of cells to 50% of the untreated control.

4.3.4. MTS assay

The antiproliferative activity of selected compounds was tested on glioblastoma (U-251 and Hs683) and pancreatic cancer (PANC-1 and AsPC-1) cell lines with the MTS assay (Promega). The cells at concentration 5×10^3 per well were seeded into 96-well plates and cultured for 24 h under standard conditions (37 °C in a humidified atmosphere of 5% CO$_2$). After this time, medium was removed and supplied solutions of tested compounds with varying concentrations. The cell were incubated for 72 h. After this time the medium had been changed for 100 μL one without phenol red, 20 μL MTS dye [3-(4,5-dimethylthiazol-2-yl)-5-(3-carboxymethoxyphenyl)-2-(4-sulfophenyl)-2H-tetrazolium], and incubated for 1 h (in case of PANC-1 for 3 h). The optical product were qualitatively determined by measurement of the absorbance at 490 nm. The results were calculated as IC$_{50}$ values using GraphPad Prism 5. Each experiment in triplicate was repeated at least three times.

Conflict of interest

The authors declare no conflict of interest.

Acknowledgments

Appendix A. Supplementary material

Supplementary data to this article can be found online at https://doi.org/10.1016/j.bioorg.2018.11.047.

References

[1] L. Costantino, D. Barlocco, Privileged structures as leads in medicinal chemistry, Curr. Med. Chem. 13 (2006) 65–85, https://doi.org/10.2174/092986706775197999.

[2] C.D. Duarte, E.J. Barreiro, C.A.M. Fraga, Privileged structures: a useful concept for the rational design of new lead drug candidates, Mini Rev. Med. Chem. 7 (2007) 1108–1119, https://doi.org/10.2174/138955707782331722.

[3] Anjali, D. Pathak, D. Singh, Quinoline: a diverse therapeutic agent, IJPSR 7 (2016) 1–13, https://doi.org/10.13040/IJPSR.0975-8232.7(1).25-30.

[4] R. Musiol, An overview of quinoline as a privileged scaffold in cancer drug discovery, Exp. Op. Drug Disc. 12 (2017) 583–597, https://doi.org/10.1080/17460441.2017.1319357.

[5] Y. Song, H. Xu, W. Chen, P. Zhan, X. Liu, 8-Hydroxyquinoline: a privileged structure with a broad-ranging pharmacological potential, Med. Chem. Commun. 6 (2015) 61–74, https://doi.org/10.1039/C4MD00284A.

[6] V. Oliveri, G. Vecchio, 8-Hydroxyquinolines in medicinal chemistry: A structural perspective, Eur. J. Med. Chem. 120 (2016) 252–274, https://doi.org/10.1016/j.ejmech.2016.05.007.

[7] L. Cahoon, The curious case of clioquinol, Nat. Med. 15 (2009) 356–359, https://doi.org/10.1038/nm0409-356.

[8] B. Regland, W. Lehmann, I. Abedini, K. Blennow, M. Jonsson, I. Karlsson, M. Sjögren, A. Wallin, M. Xilinas, C.G. Gottfries, Treatment of Alzheimer's disease with clioquinol, Dement. Geriatr. Cogn. Disord. 12 (2001) 408–414, https://doi.org/10.1159/000051288.

[9] C.M. Darby, C.F. Nathan, Killing of non-replicating *Mycobacterium tuberculosis* by 8-hydroxyquinoline, J. Antimicrob. Chemother. 65 (2010) 1424–1427, https://doi.org/10.1093/jac/dkq145.

[10] P.A. Enquist, Å. Gylfe, U. Hägglund, P. Lindström, H. Norberg-Scherman, Ch. Sundin, M. Elofsson, Derivatives of 8-hydroxyquinoline—antibacterial agents that target intra- and extracellular Gram-negative pathogens, Bioorg. Med. Chem. Lett. 22 (2012) 3550–3553, https://doi.org/10.1016/j.bmcl.2012.03.096.

[11] J. Novakowa, E. Vlkova, B. Bonusova, V. Rada, L. Kokoska, *In vitro* selective inhibitory effect of 8-hydroxyquinoline against bifidobacteria and clostridia, Anaerobe 22 (2013) 134–136, https://doi.org/10.1016/j.anaerobe.2013.05.008.

[12] P. Hongmanee, K. Rukseree, B. Buabut, B. Somsri, P. Palittapongarnpim, In Vitro Activities of Cloxyquin (5-Chloroquinolin-8-ol) against *Mycobacterium tuberculosis*, Antimicrob. Agents Chemother. 51 (2007) 1105–1106, https://doi.org/10.1128/AAC.01310-06.

[13] H. Jiang, J.E. Taggart, X. Zhang, D.M. Benbrook, S.E. Lind, W.Q. Ding, Nitroxoline (8-hydroxy-5-nitroquinoline) is more a potent anti-cancer agent than clioquinol (5-chloro-7-iodo-8-quinoline), Cancer Lett. 312 (2011) 11–17, https://doi.org/10.1016/j.canlet.2011.06.032.

[14] W.Q. Ding, B. Liu, J.L. Vaught, H. Yamauchi, S.E. Lind, Anticancer activity of the antibiotic clioquinol, Cancer Res. 65 (2005) 3389–3395, https://doi.org/10.1158/0008-5472.CAN-04-3577.

[15] A.Y. Shen, S.N. Wu, C.T. Chiu, Synthesis and cytotoxicity evaluation of some 8-hydroxyquinoline derivatives, J. Pharm. Pharmacol. 51 (1999) 543–548, https://doi.org/10.1211/0022357991772826.

[16] S. Zhai, L. Yang, Q.C. Cui, Y. Sun, Q.P. Dou, B. Yan, Tumor cellular proteasome inhibition and growth suppression by 8-hydroxyquinoline and clioquinol requires their capabilities to bind copper and transport copper into cells, J. Biol. Inorg. Chem. 15 (2010) 259–269, https://doi.org/10.1007/s00775-009-0594-5.

[17] W.Q. Ding, S.E. Lind, metal ionophores – an emerging class of anticancer drugs, IUBMB Life 61 (2009) 1013–1018, https://doi.org/10.1002/iub.253.

[18] M.E. Helsel, K.J. Franz, Pharmacological activity of metal binding agents that alter copper bioavailability, Dalton Trans. 44 (2015) 8760–8770, https://doi.org/10.1039/c5dt00634a.

[19] V. Prachayasittikul, S. Prachayasittikul, S. Ruchirawat, V. Prachayasittikul, 8-Hydroxyquinolines: a review of their metal chelating properties and medicinal applications, Drug Des. Dev. Ther. 7 (2013) 1157–1178, https://doi.org/10.2147/DDDT.S49763.

[20] G.J. Brewer, Copper control as an antiangiogenic anticancer therapy: lessons from treating Wilson's disease, Exp. Biol. Med. 226 (2001) 665–673 https://www.ncbi.nlm.nih.gov/pubmed/11444102.

[21] A. Gupte, R.J. Mumper, Elevated copper and oxidative stress in cancer cells as a target for cancer treatment, Cancer Treat. Rev. 35 (2009) 32–46, https://doi.org/10.1016/j.ctrv.2008.07.004.

[22] V. Milacic, P. Jiao, B. Zhang, B. Yan, Q.P. Dou, Novel 8-hydroxylquinoline analogs induce copper-dependent proteasome inhibition and cell death in human breast cancer cells, Int. J. Oncol. 35 (2009) 1481–1491, https://doi.org/10.3892/ijo_00000467.

[23] A. Barilli, C. Atzeri, I. Bassanetti, F. Ingoglia, V. Dall'Asta, O. Bussolati, M. Maffini, C. Mucchino, L. Marchiò, Oxidative stress induced by copper and iron complexes with 8-hydroxyquinoline derivatives causes paraptotic death of HeLa cancer cells, Mol. Pharmaceut. 11 (2014) 1151–1163, https://doi.org/10.1021/mp400592n.

[24] E.C. Calvaresi, P.J. Hergenrother, Glucose conjugation for the specific targeting and treatment of cancer, Chem. Sci. 4 (2013) 2319–2333, https://doi.org/10.1039/C3SC22205E.

[25] G.J. Seifert, Nucleotide sugar interconversions and cell wall biosynthesis: how to bring the inside to the outside, Curr. Op. Plant Biol. 7 (2004) 277–284, https://doi.org/10.1016/j.pbi.2004.03.004.

[26] V. Oliveri, G. Vecchio, Glycoconjugates of quinolines: application in medicinal chemistry, Mini-Rev. Med. Chem. 16 (2016) 1185–1194, https://doi.org/10.2174/138955751666160505115634.

[27] V. Oliveri, G.I. Grasso, F. Bellia, F. Attanasio, M. Viale, G. Vecchio, Soluble sugar-based quinoline derivatives as new antioxidant modulators of metal-induced amyloid aggregation, Inorg. Chem. 54 (2015) 2591–2602, https://doi.org/10.1021/ic502713f.

[28] W. Li, Z.W. Zhang, S.X. Wang, S.M. Ren, T. Jiang, Synthesis and analysis of potential DNA intercalators containing quinoline-glucose hybrids, Chem. Biol. Drug. Des. 74 (2009) 80–86, https://doi.org/10.1111/j.1747-0285.2009.00831.x.

[29] T.A. Chupakhina, A.M. Katsev, V.O. Kur'yanov, Synthesis and investigation of antimicrobial activity of 8-hydroxyquinoline glucosaminides, Russ. J. Bioorg. Chem. 38 (2012) 422–427, https://doi.org/10.1134/S106816201204005X.

[30] V. Oliveri, A. Puglisi, M. Viale, C. Aiello, C. Sgarlata, G. Vecchio, J. Clarke, J. Milton, J. Spencer, New cyclodextrin-bearing 8-hydroxyquinoline ligands as multifunctional molecules, Chem. Eur. J. 19 (2013) 13946–13955, https://doi.org/10.1002/chem.201300237.

[31] V. Oliveri, M.L. Giuffrida, G. Vecchio, C. Aiello, M. Viale, Gluconjugates of 8-hydroxyquinolines as potential anti-cancer prodrugs, Dalton Trans. 41 (2012) 4530–4535, https://doi.org/10.1039/c2dt12371a.

[32] V. Oliveri, M. Viale, G. Caron, C. Aiello, R. Gangemi, G. Vecchio, Glycosylated copper(II) ionophores as prodrugs for β-glucosidase activation in targeted cancer therapy, Dalton Trans. 42 (2013) 2023–2034, https://doi.org/10.1039/c2dt32429f.

[33] V. Oliveri, M. Viale, C. Aiello, G. Vecchio, New 8-hydroxyquinoline galactosides. The role of the sugar in the antiproliferative activity of copper(II) ionophores, J., Inorg. Biochem. 142 (2015) 101–108, https://doi.org/10.1016/j.jinorgbio.2014.09.017.

[34] G. Pastuch-Gawołek, K. Malarz, A. Mrozek-Wilczkiewicz, M. Musioł, M. Serda, B. Czaplińska, R. Musioł, Small molecule glycoconjugates with anticancer activity, Eur. J. Med. Chem. 112 (2016) 130–144, https://doi.org/10.1016/j.ejmech.2016.01.061.

[35] A.E. Rashad, W.A. El-Sayed, A.M. Mohamed, M.M. Ali, Synthesis of new quinoline derivatives as inhibitors of human tumor cells growth, Arch. Pharm. Chem. Life Sci. 8 (2010) 440–448, https://doi.org/10.1002/ardp.201000002.

[36] L.B.de.O. Freitas, T.F. Borgati, R.P. de Freitas, A.L.T.G. Ruiz, G.M. Marchetti, J.E. de Carvalho, E.F.F. da Cunha, T.C. Ramalho, R.B. Alves, Synthesis and antiproliferative activity of 8-hydroxyquinoline derivatives containing a 1,2,3-triazole moiety, Eur. J. Med. Chem. 84 (2014) 595–604, https://doi.org/10.1016/j.ejmech.2014.07.061.

[37] S. Areti, S. Bandaru, Ch.P. Rao, Triazole-linked quinoline conjugate of glucopyranose: selectivity comparison among Zn^{2+}, Cd^{2+} and Hg^{2+} based on spectroscopy, thermodynamics, and microscopy, and reversible sensing of Zn^{2+} and the structure of the complex using DFT, ACS Omega 1 (2016) 626–635, https://doi.org/10.1021/acsomega.6b00277.

[38] D. Dheer, V. Sing, R. Shankar, Medicinal attributes of 1,2,3-triazoles: Current developments, Bioorg. Chem. 71 (2017) 30–54, https://doi.org/10.1016/j.bioorg.2017.01.010.

[39] M. Meldal, C.W. Tornøe, Cu-catalyzed azide-alkyne cycloaddition, Chem. Rev. 108 (2008) 2952–3015, https://doi.org/10.1021/cr0783479.

[40] P. Thirumurugan, D. Matosiuk, K. Jozwiak, Click chemistry for drug development and diverse chemical–biology applications, Chem. Rev. 113 (2013) 4905–4979, https://doi.org/10.1021/cr200409f.

[41] S.P. Mantoani, T.P.C. Chierrito, A.F.L. Vilela, C.L. Cardoso, A. Martínez, I. Carvalho, Novel triazole-quinoline derivatives as selective dual binding site acetylcholinesterase inhibitors, Molecules 21 (2016) 193–204, https://doi.org/10.3390/molecules21020193.

[42] H.C. Kolb, K.B. Sharpless, The growing impact of click chemistry on drug discovery, DDT 8 (2003) 1128–1137, https://doi.org/10.1016/S1359-6446(03)02933-7.

[43] C.A.G.M. Weijers, M.C.R. Franssen, G.M. Visser, Glycosyltransferase-catalyzed synthesis of bioactive oligosaccharides, Biotechnol. Adv. 26 (2008) 436–456, https://doi.org/10.1016/j.biotechadv.2008.05.001.

[44] Ch. Breton, S. Fournel-Gigleux, M.M. Palcic, Recent structures, evolution and mechanisms of glycosyltransferases, Curr. Opin. Struct. Biol. 22 (2012) 540–549, https://doi.org/10.1016/j.sbi.2012.06.007.

[45] L.L. Lairson, B. Henrissat, G.J. Davies, S.G. Withers, Glycosyltransferases: structures, functions, and mechanisms, Annu. Rev. Biochem. 77 (2008) 521–555, https://doi.org/10.1146/annurev.biochem.76.061005.092322.

[46] I. Brockhausen, M. Benn, S. Bhat, S. Marone, J.G. Riley, P. Montoya-Peleaz, J.Z. Vlahakis, H. Paulsen, J.S. Schutzbach, W.A. Szarek, UDP-Gal: GlcNAc-R β1,4-galactosyltransferase—a target enzyme for drug design. Acceptor specificity and inhibition of the enzyme, Glycoconj. J 23 (2006) 525–541, https://doi.org/10.1007/s10719-006-7153-x.

[47] X. Qian, M.M. Palcic, Glycosyltransferase inhibitors, Carbohydrates in Chemistry and Biology, WILEY-VCH Verlag GmbH, 2000, pp. 293–312, , https://doi.org/10.1002/9783527618255.ch56.

[48] S. Wang, J.A. Cuesta-Seijo, D. Lafont, M.M. Palcic, S. Vidal, Design of glycosyltransferase inhibitors: pyridine as a pyrophosphate surrogate, Chem. Eur. J. 19 (2013) 15346–15357, https://doi.org/10.1002/chem.201301871.

[49] K. Kumamoto, Y. Goto, K. Sekikawa, S. Takenoshita, N. Ishida, M. Kawakita, R. Kannagi, Increased expression of UDP-galactose transporter messenger RNA in human colon cancer tissues and its implication in synthesis of Thomsen-Friedenreich Antigen and Sialyl Lewis A/X determinants, Cancer Res. 61 (2001) 4620–4627 https://www.ncbi.nlm.nih.gov/pubmed/11389099.

[50] R.D. Murray, A. Ailabouni, L.A. Heitlinger, B.U.K. Li, H.J. McClung, P. Powers, J. Gutt, L. Kien, Galactose-containing carbohydrates are preferentially absorbed in the neonatal pig colon, Pediatr. Res. 39 (1996) 656–660, https://doi.org/10.1203/00006450-199604000-00016.

[51] R.C. Evans, S. Fear, D. Ashby, A. Hackett, E. Williams, M. van der Vliet, F.D.J. Dunstan, J.M. Rhodes, Diet and colorectal cancer: an investigation of the lectin/galactose hypothesis, Gastroenterology 122 (2002) 1784–1792, https://doi.org/10.1053/gast.2002.33659.

[52] R.S. Haber, A. Rathan, K.R. Weiser, A. Pritsker, S.H. Itzkowitz, C. Bodian, G. Slater, A. Weiss, D.E. Burstein, GLUT1 glucose transporter expression in colorectal carcinoma: a marker for poor prognosis, Cancer 83 (1998) 34–40, https://doi.org/10.1002/(SICI)1097-0142(19980701)83:1<34::AID-CNCR5>3.0.CO;2-E.

[53] Q.R. Yang, W.H. Qiao, S.M. Zhang, J.P. Qu, D.L. Liu, Synthesis and characterization of a new cationic galactolipid with carbamate for gene delivery, Tenside Surf. Det. 5 (2010) 294–299, https://doi.org/10.3139/113.110080.

[54] H. Rajaram, M.K. Palanivelu, T.V. Arumugam, V.M. Rao, P.N. Shaw, R.P. McGeary, B.P. Ross, 'Click' assembly of glycoclusters and discovery of a trehalose analogue that retards Aβ40 aggregation and inhibits Aβ40-induced neurotoxicity, Bioorg. Med. Chem. Lett. 24 (2014) 4523–4528, https://doi.org/10.1016/j.bmcl.2014.07.077.

[55] I. Shin, H. Jung, M. Lee, Chemoselective ligation of maleimidosugars to peptides/protein for the preparation of neoglycopeptides/neoglycoprotein, Tetrahedron Lett. 42 (2001) 1325–1328, https://doi.org/10.1016/S0040-4039(00)02286-3.

[56] M. Jacobsson, J. Malmberg, U. Ellervik, Aromatic *O*-glycosylation, Carbohydr. Res. 341 (2006) 1266–1281, https://doi.org/10.1016/j.carres.2006.04.004.

[57] U. Aich, D. Loganathan, Stereoselective single-step synthesis and X-ray crystallographic investigation of acetylated aryl 1,2-*trans* glycopyranosides and aryl 1,2-*cis* C2-hydroxy-glycopyranosides, Carbohydr. Res. 341 (2006) 19–28, https://doi.org/10.1016/j.carres.2005.10.010.

[58] Y.S. Lee, E.S. Rho, Y.K. Min, B.T. Kim, K.H. Kim, Practical β-stereoselective *O*-glycosylation of phenols with penta-*O*-acetyl-β-D-glucopyranose, Carbohydr. Chem. 20 (2001) 503–506, https://doi.org/10.1081/CAR-100106933.

[59] T. Zenkoh, H. Tanaka, H. Setoi, T. Takahashi, Solid-phase synthesis of aryl *O*-glycoside using aqueous base and phase transfer catalyst, Synlett 6 (2002) 867–870, https://doi.org/10.1055/s-2002-31926.

[60] T.J. Wadzinski, A. Steinauer, L. Hie, G. Pelletier, A. Schepartz, S.J. Miller, Rapid phenolic *O*-glycosylation of small molecules and complex unprotected peptides in aqueous solvent, Nat. Chem. 10 (2018) 644–652.

[61] Y. Li, H. Mo, G. Lian, B. Yu, Revisit of the phenol *O*-glycosylation with glycosyl imidates, BF₃·OEt₂ is a better catalyst than TMSOTf, Carbohydr. Res. 363 (2012) 14–22, https://doi.org/10.1016/j.carres.2012.09.025.

[62] M.J. Thompson, E.J. Hutchinson, T.H. Stratford, W.B. Bowlerb, G.M. Blackburna, Sugar conjugates of fulvestrant (ICI 182,780): efficient general procedures for glycosylation of the fulvestrant core, Tetrahedron Lett. 45 (2004) 1207–1210, https://doi.org/10.1016/j.tetlet.2003.11.140.

[63] Q. Qin, D.-C. Xiong, X.-S. Ye, Additive-controlled stereoselective glycosylations of 2,3-oxazolidinone protected glucosamine or galactosamine thioglycoside donors with phenols based on preactivation protocol, Carbohydr. Res. 403 (2015) 104–114, https://doi.org/10.1016/j.carres.2014.07.004.

[64] S.G. Duron, T. Polat, C.H. Wong, N-(Phenylthio)-ε-caprolactam: A new promoter for the activation of thioglycosides, Org. Lett. 6 (2004) 839–841, https://doi.org/10.1021/ol0400084.

[65] W.R. Roush, X.F. Lin, A highly stereoselective synthesis of aryl 2-deoxy-β-glycosides via the Mitsunobu reaction, J. Org. Chem. 56 (1991) 5740–5742, https://doi.org/10.1021/jo00020a003.

[66] N. Lucchetti, R. Glimour, Reengineering chemical glycosylation: direct, metal-free anomeric *O*-arylation of unactivated carbohydrates, Chem. Eur. J. 24 (2018) 16266–16270, https://doi.org/10.1002/chem.201804416.

[67] H. Ye, C. Xiao, Q.-Q. Zhou, P.G. Wang, W.-J. Xiao, Synthesis of phenolic glycosides: glycosylation of sugar lactols with aryl bromides via dual photoredox/Ni catalysis, J. Org. Chem. 83 (2018) 13325–13334, https://doi.org/10.1021/acs.joc.8b02129.

[68] R.A. Tromp, S.S.G.E. van Boom, C.M. Timmers, S. van Zutphen, G.A. van der Marel, H.S. Overkleeft, J.H. van Boom, J. Reedijk, The β-glucuronyl-based prodrug strategy allows for its application on β-glucuronyl-platinum conjugates, J. Bioorg. Med. Chem. Lett. 14 (2004) 4273–4276, https://doi.org/10.1016/j.bmcl.2004.06.015.

[69] K. Yoshida, Y. Kanoko, K. Takao, Kinetically controlled α-selective O-glycosylation of phenol derivatives using 2-nitroglycals by a bifunctional chiral thiourea catalyst, Asian J. Org. Chem. 5 (2016) 1230–1236, https://doi.org/10.1002/ajoc.201600307.

[70] E.R. Palmacci, P.H. Seeberger, Synthesis of *C*-aryl and *C*-alkyl glycosides using glycosyl phosphates, Org. Lett. 3 (2001) 1547–1550, https://doi.org/10.1021/ol0158462.

[71] A. Vasella, New reactions and intermediates involving the anomeric center, Pure Appl. Chem. 63 (1991) 507–518, https://doi.org/10.1351/pac199163040507.

[72] I.J. Talisman, V. Kumar, J. Razzaghy, S.V. Malhotra, *O*-Glycosidation reactions promoted by in situ generated silver *N*-heterocyclic carbenes in ionic liquids, Carbohydr. Res. 346 (2011) 883–890, https://doi.org/10.1016/j.carres.2011.03.007.

[73] V.O. Kur'yanov, U.S. Priskoka, T.A. Chupakhina, V.Y. Chirva, A phase-transfer glucosamination of phenols catalyzed by polyethylene glycol, Russ. J. Bioorg. Chem. 31 (2005) 335–336, https://doi.org/10.1007/s11171-005-0042-4.

[74] H.C. Kolb, M.G. Finn, K.B. Sharpless, Click chemistry: diverse chemical function from a few good reactions, Angew. Chem. Int. Ed. 40 (2001) 2004–2021, https://doi.org/10.1002/1521-3773(20010601)40:11<2004::AID-ANIE2004>3.0.CO;2-5.

[75] Y. Wu, M. Pan, Y. Dai, B. Liu, J. Cui, W. Shi, Q. Qiu, W. Huang, H. Qian, Design, synthesis and biological evaluation of LBM-A5 derivatives as potent P-glycoprotein-mediated multidrug resistance inhibitors, Bioorg. Med. Chem. 24 (2016) 2287–2297, https://doi.org/10.1016/j.bmc.2016.03.065.

[76] S. Vidal, I. Bruyère, A. Malleron, C. Augé, J.P. Praly, Non-isosteric C-glycosyl analogues of natural nucleotide diphosphate sugars as glycosyltransferase inhibitors, Bioorg. Med. Chem. 14 (2006) 7293–7301, https://doi.org/10.1016/j.bmc.2006.06.057.

[77] C.C. Barron, P.J. Bilan, T. Tsakiridis, E. Tsiani, Facilitative glucose transporters: Implications for cancer detection, prognosis and treatment, Metabolism 65 (2016) 124–139, https://doi.org/10.1016/j.metabol.2015.10.007.

[78] C. Granchi, F. Minutolo, Anticancer agents that counteract tumor glycolysis, Chem. Med. Chem. 7 (2012) 1318–1350, https://doi.org/10.1002/cmdc.201200176.

[79] N. Wang, M. Świtalska, M.Y. Wu, K. Imai, T.A. Ngoc, C.Q. Pang, L. Wang, J. Wietrzyk, T. Inokuchi, Synthesis and in vitro cytotoxic effect of 6-amino-substituted 11H- and 11Me-indolo[3,2-c]quinolines, Eur. J. Med. Chem. 78 (2014) 314–323, https://doi.org/10.1016/j.ejmech.2014.03.038.

[80] Z. Xiao, F. Lei, X. Chen, X. Wang, L. Cao, K. Ye, W. Zhu, S. Xu, Design, synthesis, and antitumor evaluation of quinoline-imidazole derivatives, Arch. Pharm. Chem. Life Sci. 351 (2018) 1–11, https://doi.org/10.1002/ardp.201700407.

[81] Y.L. Chen, Ch.H. Chung, I.L. Chen, P.H. Chen, H.Y. Jeng, Synthesis and cytotoxic activity evaluation of indolo-, pyrrolo-, and benzofuro-quinolin-2(1H)-ones and 6-anilinoindoloquinoline derivatives, Bioorg. Med. Chem. 10 (2002) 2705–2712, https://doi.org/10.1016/S0968-0896(02)00111-6.

[82] Ch. Chen, X. Hou, G. Wang, W. Pan, X. Yang, Y. Zhang, H. Fang, Design, synthesis and biological evaluation of quinoline derivatives as HDAC class I inhibitors, Eur. J. Med. Chem. 133 (2017) 11–23, https://doi.org/10.1016/j.ejmech.2017.03.064.

[83] J. Kim, C.V. Dang, Cancer's molecular sweet tooth and the Warburg effect, Cancer Res. 66 (2006) 8927–8930, https://doi.org/10.1158/0008-5472.CAN-06-1501.

[84] D.K. Podolsky, K.J. Isselbacher, Cancer-associated galactosyltransferase acceptor: inhibition of transformed cell and tumor growth, Cancer 45 (1980) 1212–1217 http://www.ncbi.nlm.nih.gov/pubmed/6766800.

[85] C.R. Dates, T. Fahmi, S.J. Pyrek, A. Yao-Borengasser, B. Borowa-Mazgaj, S.M. Bratton, S.A. Kadlubar, P.I. Mackenzie, R.S. Haun, A. Radominska-Pandya, Human UDP-Glucuronosyltransferases: Effects of altered expression in breast and pancreatic cancer cell lines. Cancer Biol. Ther. 16 (2015) 714–723, https://doi.org/10.1080/15384047.2015.1026480.

[86] L. Yilmaz, E. Borazan, T. Aytekin, I. Baskonus, A. Aytekin, S. Oztuzcu, Z. Bozdag, A. Balik, Increased UGT1A3 and UGT1A7 expression is associated with pancreatic cancer, Asian Pac. J. Cancer Prev. 16 (2015) 1651–1655, https://doi.org/10.7314/APJCP.2015.16.4.1651.

Publikacja P.2

8-Hydroxyquinoline Glycoconjugates: Modifications in the
Linker Structure and Their Effect on the Cytotoxicity
of the Obtained Compounds

M. Krawczyk[*], G. Pastuch-Gawołek, A. Pluta, K. Erfurt, A. Domiński, P. Kurcok

Materiały uzupełniające do publikacji znajdują się w dołączonej płycie CD

8-Hydroxyquinoline Glycoconjugates: Modifications in the Linker Structure and Their Effect on the Cytotoxicity of the Obtained Compounds

Monika Krawczyk [1,2,]*[iD], **Gabriela Pastuch-Gawołek** [1,2][iD], **Aleksandra Pluta** [1], **Karol Erfurt** [3], **Adrian Domiński** [4] **and Piotr Kurcok** [4][iD]

1   Department of Organic Chemistry, Bioorganic Chemistry and Biotechnology, Silesian University of Technology, B. Krzywoustego 4, 44-100 Gliwice, Poland; gabriela.pastuch@polsl.pl (G.P.-G.); aleksandrapluta93@o2.pl (A.P.)
2   Biotechnology Centre, Silesian University of Technology, B. Krzywoustego 8, 44-100 Gliwice, Poland
3   Department of Chemical Organic Technology and Petrochemistry, Silesian University of Technology, B. Krzywoustego 4, 44-100 Gliwice, Poland; karol.erfurt@polsl.pl
4   Centre of Polymer and Carbon Materials, Polish Academy of Sciences, M. Curie-Sklodowskiej 34, 41-819 Zabrze, Poland; adrian.dominski@cmpw-pan.edu.pl (A.D.); piotr.kurcok@cmpw-pan.edu.pl (P.K.)
*   Correspondence: monika.krawczyk@polsl.pl; Tel.: +48-32-237-1759

Abstract: Small molecule nitrogen heterocycles are very important structures, widely used in the design of potential pharmaceuticals. Particularly, derivatives of 8-hydroxyquinoline (8-HQ) are successfully used to design promising anti-cancer agents. Conjugating 8-HQ derivatives with sugar derivatives, molecules with better bioavailability, selectivity, and solubility are obtained. In this study, 8-HQ derivatives were functionalized at the 8-OH position and connected with sugar derivatives (D-glucose or D-galactose) substituted with different groups at the anomeric position, using copper(I)-catalyzed 1,3-dipolar azide-alkyne cycloaddition (CuAAC). Glycoconjugates were tested for inhibition of the proliferation of cancer cell lines (HCT 116 and MCF-7) and inhibition of β-1,4-galactosyltransferase activity, which overexpression is associated with cancer progression. All glycoconjugates in protected form have a cytotoxic effect on cancer cells in the tested concentration range. The presence of additional amide groups in the linker structure improves the activity of glycoconjugates, probably due to the ability to chelate metal ions present in many types of cancers. The study of metal complexing properties confirmed that the obtained glycoconjugates are capable of chelating copper ions, which increases their anti-cancer potential.

Keywords: quinoline; glycoconjugates; click reaction; 1,3-dipolar cycloaddition; chelators; anticancer properties

1. Introduction

Cancer is one of the biggest problems in modern medicine and one of the main causes of death in the world. The high toxicity of drugs and the growing resistance of cancer cells to a significant number of pharmaceuticals increasingly limit the possibility of obtaining successful results of anti-cancer therapy. Therefore, it is necessary to search for new, effective chemotherapeutics characterized by low toxicity and high selectivity profile. Analysis of the Food and Drug Administration (FDA) database revealed that of the novel approved drugs for oncology in 2018, 7 are biologicals and 13 are small-molecules drugs. Importantly, all of the newly reported chemotherapeutics contain an *N*-heterocyclic fragment in their structure [1]. Small molecule nitrogen heterocycles are very important structures, widely used

in the design of potential pharmaceuticals for several years [2]. Among them, the quinoline scaffold, which is present in many classes of biologically active compounds, deserves special attention [3–6]. The quinoline scaffold is often used as a privileged structure in the design of a large number of structurally diverse molecules that exhibit promising pharmacological effects. Particularly, derivatives of 8-hydroxyquinoline (8-HQ) are successfully applied to design chemotherapeutics used in the treatment of bacterial [7–9], fungal [10,11] and neurodegenerative diseases [12,13]. An important element of 8-HQ biological activity is the ability to chelate metal ions, which makes 8-HQ a promising anti-cancer agent [14–16].

Transition metal ions, including Fe^{2+}, Cu^{2+}, and Zn^{2+} play a significant role in the human organism. They affect the proper course of many key cellular processes. Therefore, it is important to maintain homeostasis. Incorrect metabolism of the above microelements may contribute to the development of many diseases [17,18]. There are several strategies for controlling the proper level of metals within cells and tissues. For this purpose, a common strategy is the use of chelators or ionophores. Chelating agents are successfully used to remove excess metal ions from the body. Whereas, ionophores are used to transport metal ions via cell membrane in both directions [18,19]. Copper is one of the transition metals which complex compounds have been intensively studied in recent years for anticancer applications. As is well known, copper is an essential cofactor for cancer growth and angiogenesis. Numerous studies have shown that an elevated level of copper is directly correlated with cancer progression. Additionally, copper concentration correlated with the age of patients and the stage of cancer [20–24]. Excess of copper ions was found in the serum and tissues of patients with, among others: breast [24,25], prostate [26,27], colorectal [28], lung [29] and brain [30] cancers, compared to healthy people. These observations suggest that copper ions may be one of the selective targets for cancer treatment [20,31–33].

Among the known copper chelators include tetrathiomolybdate, trientine, and D-penicillamine primarily used to treat Wilson's disease [34]. Clinical studies have shown that these compounds are effective in inhibiting the angiogenesis of some types of cancer [35–41]. The literature also reports on the use of 8-HQ derivatives as copper chelators. Due to the presence of free electron pairs on nitrogen and oxygen atoms of 8-HQ, they have the ability to complex Cu^{2+} ions, forming chelates, which are then removed from the body [14–16,42,43]. However, metal ions play an important role in many cellular processes, including those necessary for the proper functioning of the organism. Therefore, traditional chelators can cause a deficiency of copper in healthy tissues. The consequence of the lack of selectivity in directing drugs to a specific site of action may be undesirable side effects resulting from the implemented anticancer therapy. That is why the aim of many researchers is to develop more selective and safer drugs. Therefore, an ideal anti-cancer drug should be selective for cancer cells, thereby alleviating the undesirable toxic effects of chemotherapy.

During designing new drugs, it is very important to know and use the differences between cancer cells and healthy cells. One such difference is the specific metabolism of glucose in cancer cells. It has been proven that cancer cells have an increased demand for glucose compared to healthy cells, which metabolizes it to obtain the energy needed to increase proliferation. This provides the cells with a sufficient amount of nutrients and energy to carry out the processes taking place during the cell cycle. This phenomenon is known as the Warburg effect and arises from mitochondrial metabolic changes. It consists in the fact that cancer cells produce their energy through glycolysis followed by lactic acid fermentation, characteristic of hypoxic conditions, and its level is much higher (more than a hundred times) than in healthy cells, for which the main source of energy is mitochondrial oxidative phosphorylation [44,45]. Increased glycolysis process in cancer cells is associated with the overexpression of GLUT transporters. There are special proteins that mediate the transfer of sugars across cell membranes [46–48]. Therefore, sugars are an attractive system for transporting drugs directly to cancer cells. The strategy of conjugating sugar derivatives with biological active aglycons is widely used in research on the synthesis of new drugs, supporting the treatment against various diseases [49]. The chelating functions of glycoconjugates are masked by the presence of a sugar unit until the release of active aglycon in the target cells, occurring as a result of hydrolysis catalyzed by

specific β-glycosidases [50]. Consequently, drug interference in the glycolytic pathway should be effective and more selective for cancer cells.

As a result of conjugating 8-HQ derivatives with sugar derivatives, a molecule with better bioavailability, selectivity and solubility can be obtained [50–53]. Considering the potential therapeutic application of planned connections, this synthesis must be simple, fast, selective and efficient. An example of a reaction that meets these criteria is the reaction of 1,3-dipolar azide-alkyne cycloaddition, which leads to receiving the 1,2,3-triazole ring between joined compounds.

We have recently shown that the 1,2,3-triazole ring is an important element for glycoconjugate activity [54] (Figure 1). Except for the role of a connection between two active groups, it also has other interesting properties. The H-C(5) atom in the triazole ring is a donor for a hydrogen bond, while the free electron pair at the N(3) atom in the triazole can be used as an acceptor in the formation of a hydrogen bond. Their tendency to form hydrogen bonds increases the solubility of such molecules, which favor binding to biomolecular targets [55]. The aim of present work is to extend the library of such combinations. The general structure of the planned glycoconjugates is shown in Figure 2. It was decided to reverse the direction of linking reactive moieties compared to the previously reported glycoconjugates [54], consisting of sugar azides and propargyl derivatives of 8-HQ (Figure 1) and see how this will affect the activity of glycoconjugates. In addition, it was decided to check how the structure modification of the linker of the quinoline glycoconjugates affects their biological properties. It was assumed that an extension of the alkyl chain between the triazole ring and quinoline or sugar part should increase the "flexibility" of the obtained compounds, which may affect the cytotoxicity profile of the molecules. Moreover, insertion into a linker an additional amide or carbamate bonds, the presence of which is observed in many biologically active compounds should improve glycoconjugates chelating ability [56]. Therefore, it was decided to check whether the addition of this structural element to quinoline glycoconjugates will improve their activity compared to previously obtained derivatives.
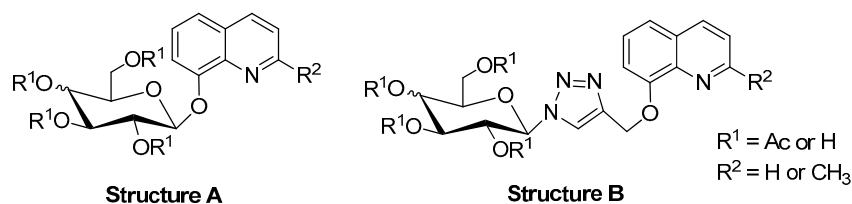
Figure 1. Structures of previously obtained glycoconjugates [54].
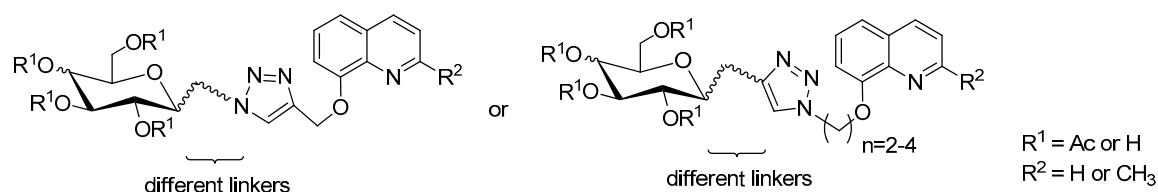
Figure 2. General structure of the glycoconjugates presented in this paper.

A multiplicity of structural modifications in building blocks for the synthesis of glycoconjugates and their combination in various configurations will allow determining the relationships between the chemical structure of this group of compounds and their biological activity. This will allow also identifying those specific structural elements that are responsible for demonstrating biological activity. This is important information from the point of view of the mechanisms of action of designed structures.

2. Results and Discussion

2.1. Synthesis

As mentioned above, the synthetic aim of this work was to create a large library of compounds based on the 8-HQ scaffold with a sugar fragment attached via an appropriate linker. Target glycoconjugates

were obtained by modifying commercially available 8-hydroxyquinoline **1** or 8-hydroxyquinaldine **2**, and then connecting them with derivatives of D-glucose or D-galactose substituted with different groups at the anomeric position. A common feature of all glycoconjugates is the presence of a 1,2,3-triazole ring in the linker structure. This improves their cytotoxic activity, probably by increasing the ability to metal ions chelation found in many types of cancers [54,55]. In addition, the used substrates have a relatively small size and are easy to modify, which makes them particularly interesting from the point of view of using them to design potential drugs.

The first part of the synthesis concerned the preparation of the corresponding quinoline derivatives functionalized in the 8-OH position with propargyl or azide groups, that are involved in the *click chemistry* reaction. The path of the syntheses is presented in Scheme 1.
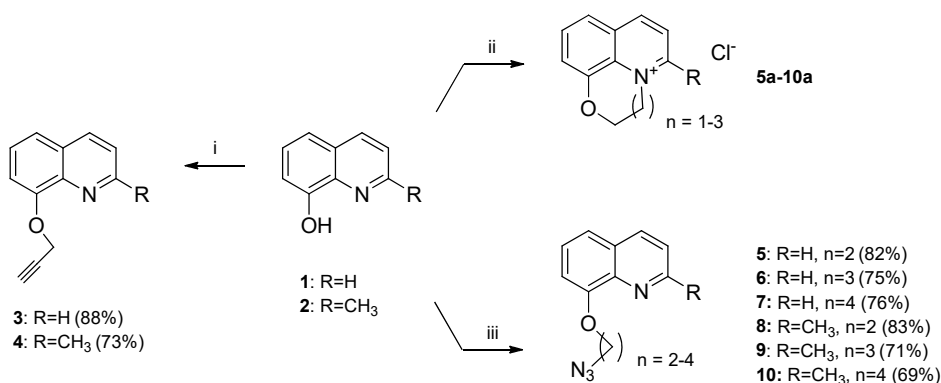
Scheme 1. Synthesis of 8-hydroxyquinoline derivatives **3–10**. *Reagents and Conditions:* (**i**) propargyl bromide, K_2CO_3, acetone, r.t., 24 h; (**ii**) 1. 2-bromoethanol or 3-bromo-1-propanol or 4-bromo-1-butanol, K_2CO_3, acetone, r.t., 24 h; 2. methanesulfonyl chloride or *p*-toluenesulfonyl chloride, Et_3N, CH_2Cl_2; r.t., 3h; 3. NaN_3, DMF, r.t., 24 h; (**iii**) 1-azido-2-bromoethane or 1-azido-3-bromopropane or 1-azido-4-bromobutane, K_2CO_3, acetone, 50 °C-r.t., 24 h.

Propargyl quinoline derivatives **3** or **4** were obtained in good yields (88% and 73% respectively), according to the previously published procedure [54,57]. The corresponding compound **1** or **2** was reacted with propargyl bromide in a reaction carried out under basic conditions. The first approach to the synthesis of 8-(2-azidoethoxy)quinolone **5** was the reaction of 8-HQ **1** with 2-bromoethanol to obtain 8-(2-hydroxyethoxy)quinoline. The obtained alcohol was treated with methanesulfonyl or *p*-toluenesulfonyl chloride in the presence of a non-nucleophilic base (TEA) followed by sodium azide in DMF. However, the formation of the expected product **5** was no observed. Also in case of lengthening the alkyl chain of the donor, the desired products **6–10** could not be obtained. Treatment of 8-(2-hydroxyethoxy)quinoline by azidotrimethylsilane ($TMSN_3$) in the presence of Lewis acid also did not give the expected products. The application of the Appel reaction conditions, in which the alcohol reacts with carbon tetrachloride in the presence of triphenylphosphine also not allowed to obtain the desired products. Instead, spectroscopic data (HRMS) confirmed the formation of a resonance-stabilized structure of the tricyclic oxazaquinolinium salts **5a–10a** [58]. Finally, to obtain compounds **5–10**, a reaction of quinoline derivatives **1** or **2** with 1-azido-2-bromoethane, 1-azido-3-bromopropane or 1-azido-4-bromobutane as donors of desired groups was carried out. These donors were previously obtained by monoazidation of the corresponding dibromoalkane with NaN_3 in DMF [59]. The optimal yield of the desired products was obtained by carrying out the reaction at 50 °C, using an equimolar ratio of substrates. Except for the monosubstituted derivatives (50% yields), diazidesubstituted derivatives (25% yield) were also obtained (the yield was estimated by ^{1}H NMR).

Sugar derivatives substituted at the anomeric position were a second necessary structural element for the synthesis of glycoconjugates. The synthesis route to the corresponding protected and deprotected derivatives of D-glucose and D-galactose are shown in Schemes 2–4. The choice of sugar units is dictated by the frequency of their occurrence and their importance for cell metabolism. The procedure

for obtaining 2,3,4,6-tetra-*O*-acetyl-β-ᴅ-glycopyranosyl amines **19** and **20** has been described in detail in earlier works [51,54,60] (Scheme 2).
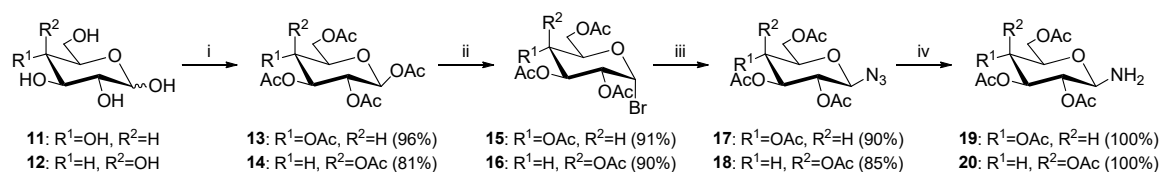
Scheme 2. Synthesis of sugar derivatives **13–20**. *Reagents and Conditions:* (**i**) CH₃COONa, Ac₂O, b.p., 1 h; (**ii**) CH₃COOH, 33% HBr/AcOH, r.t. 1 h; (**iii**) NaN₃, TBASH, CHCl₃/NaHCO₃, r.t. 2 h; (**iv**) 20% Pd(OH)₂/C, THF:EtOH (2:1, *v/v*), H₂, 1.5 bar, 2 h.
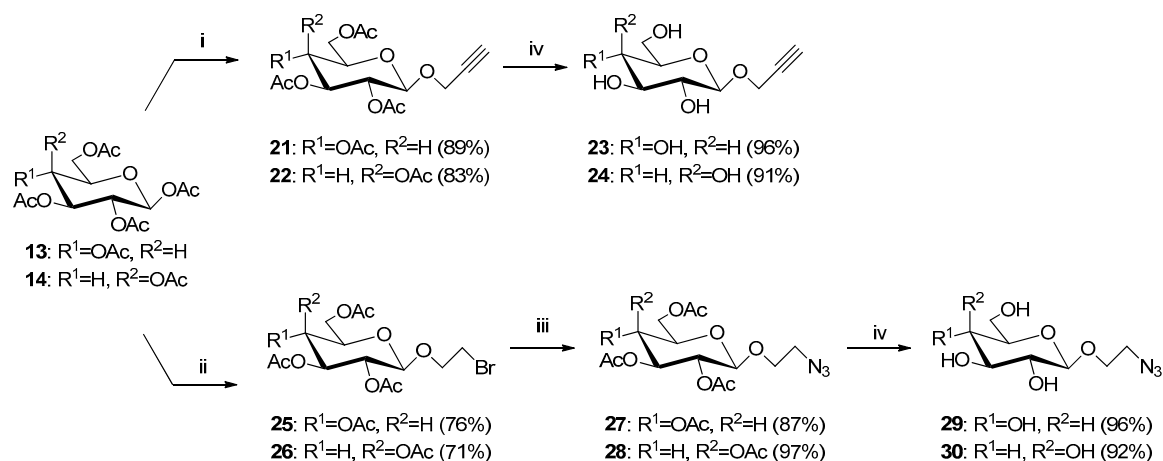
Scheme 3. Synthesis of sugar derivatives **21–30**. *Reagents and Conditions:* (**i**) propargyl alcohol, BF₃·Et₂O, DCM, r.t., 1 h; (**ii**) 2-bromoethanol, BF₃·Et₂O, DCM, r.t., 2 h; (**iii**) NaN₃, DMF, r.t. 24 h; (**iv**) 1. MeONa, MeOH, r.t. 20 min; 2. Amberlyst-15.
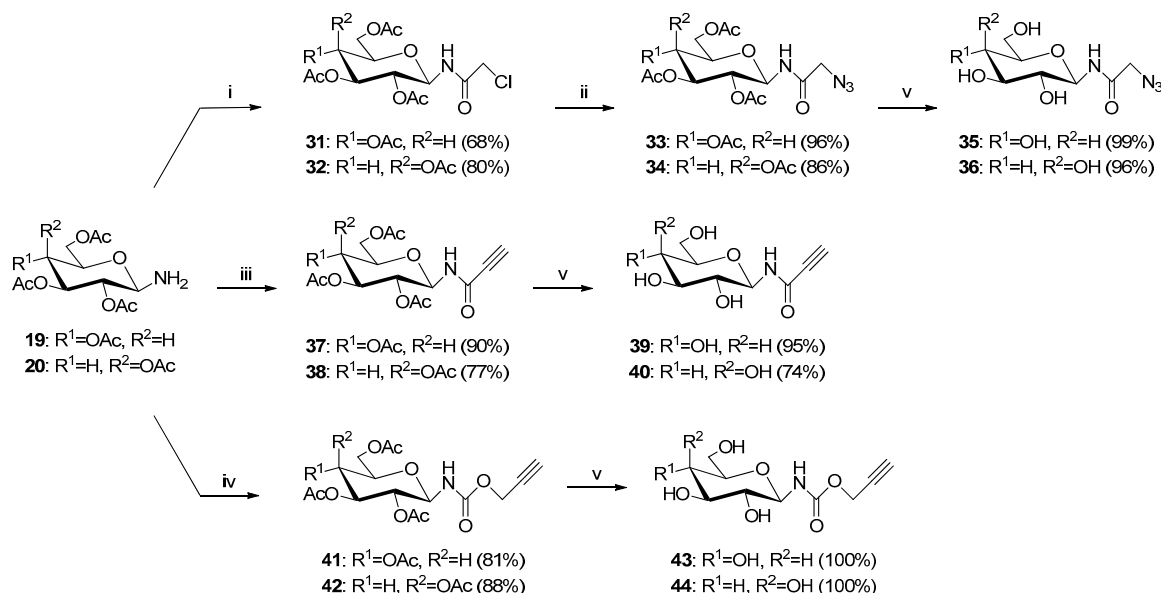
Scheme 4. Synthesis of sugar derivatives **31–44**. *Reagents and Conditions:* (**i**) chloroacetyl chloride, TEA, DCM, r.t., 1 h; (**ii**) NaN₃, DMF, r.t. 24 h; (**iii**) Propiolic acid, DCC, DCM, r.t. 2 h; (**iv**) propargyl chloroformate, Hünig's base, DCM, r.t. 2 h; (**v**) 1. MeONa, MeOH, r.t. 20 min; 2. Amberlyst-15.

Sugar derivatives in which the alkynyl or azide moiety was introduced by the formation of an *O*-glycosidic linkage were prepared by reacting per-*O*-acetylated D-glucose **13** or D-galactose **14** with

propargyl alcohol or 2-bromoethanol in the presence of a Lewis acid as a catalyst (Scheme 3) [61,62]. The reactions were carried out in an anhydrous DCM in the presence of boron trifluoride etherate until the complete conversion of the substrate, which was monitored by TLC. The reaction mixture was diluted with dichloromethane and extracted with $NaHCO_3$ and brine to wash off the acid. The acetyl neighboring-group participation at the C-2 position of the sugar ensured the formation of an intermediate acyloxonium ion, which for steric reasons could be "attacked" by a nucleophile only from the opposite side, resulting in only products of the β-configuration. This is confirmed by the large coupling constant from the H-1 proton equal J = 8.0 Hz observed in the ^{1}H NMR spectra for compounds **21**–**22** and **25**–**26**. As a result, propargyl 2,3,4,6-tetra-*O*-acetyl-β-D-glycopyranosides **21** and **22** were obtained in good yields (89% and 83% respectively), whereas 2-bromoethyl 2,3,4,6-tetra-*O*-acetyl-β-D-glycopyranosides **25** and **26** were obtained in slightly lower yields (76% and 71% respectively). 2-Azidoethyl 2,3,4,6-tetra-*O*-acetyl-β-D-glycopyranosides **27** and **28** were obtained by substituting bromine by sodium azide in the reaction carried out in DMF in almost quantitative yield. Confirmation of bromine exchange to the azide moiety was the appearance in the ^{13}C NMR spectra of the signal of CH_2N_3 carbon with a shift of about δ = 50.55 ppm for **27** and 50.60 ppm for **28**, while the signal of CH_2Br carbon was observed at about δ = 29.83 ppm for **25** and 29.91 ppm for **26**.

In the next step, sugar derivatives containing an amide or a carbamate moiety at the sugar anomeric position were obtained by several-step synthesis presented in Scheme 4.

Derivatives of 2,3,4,6-tetra-*O*-acetyl-*N*-(β-D-glycopyranosyl)azidoacetamide **33, 34** were obtained in two-steps procedure. 1-Aminosugars **19** or **20** were reacted with chloroacetyl chloride in the presence of TEA, which neutralized the formed of hydrogen chloride. This approach eliminates the use of toxic $SnCl_4$ and tin metal to reduce glycopyranosyl azides, which has been described as a method for the synthesis of *N*-glycopyranosyl chloroacetamides [63]. In the second step, the terminal chlorine atom in compounds **31** and **32** was exchanged with an azide group by a nucleophilic substitution reaction with sodium azide in dry DMF. The structures of the obtained products were confirmed on the basis of NMR spectra analysis. In this case, the characteristic carbon signal of CH_2N_3 located at δ = 52.59 ppm for **33** and 52.61 ppm for **34** in ^{13}C NMR spectra was shifted from δ = 42.25 ppm and 42.26 ppm corresponding to chloroacetamide derivatives **31** and **32**.

In turns, structures **37** and **38** were obtained in the reaction of 1-amino sugars **19** or **20** with propargylic acid. In these reactions activating the non-reactive carboxyl group seems to be necessary. Of the many ways to form an amide bond, initially, it was decided to use the method developed by Kaminski and co-workers [64]. This method involves creating so-called superactive ester 4-(4,6-dimethoxy-1,3,5-triazin-2-yl)-4-methylmorpholinium chloride (DMTMM) in situ in reaction between 2-chloro-4,6-disubstituted-1,3,5-triazines (CDMT) and *N*-methylmorpholine (NMM). It turned out that as a result of this reaction, only traces of expected products were formed. In the next approach, the carbodiimide method was used to the condensation reaction using DCC as a coupling agent [65]. The reaction was carried out in DCM in which the isolated DCU is insoluble and could be separated from the reaction mixture by filtration. As a result, 2,3,4,6-tetra-*O*-acetyl-*N*-(β-D-glycopyranosyl)propiolamides **37** and **38** were obtained in high yields (90% and 77% respectively).

In order to obtain sugar derivatives containing a carbamate group at the sugar anomeric position, reactions of 1-amino sugars **19** and **20** with propargyl chloroformate, which is a reactive acylating agent, were also carried out. This reaction requires the presence of a tertiary amine in the reaction medium to entrap the formed HCl and avoid conversion of the amine into its non-reactive hydrochloride salt [66]. However, the use of TEA gave only moderate yield, while the replacement of TEA with *N*,*N*-diisopropylethylamine allowed obtaining the desired products **41** and **42** in high yields (81% and 88% respectively).

The ester type protecting groups in the sugar part increase the lipophilicity of glycoconjugates and improved its passive transport inside the cell, where are enzymes capable of hydrolyzing them. However, for some biological studies, it is also necessary to use compounds with unprotected hydroxyl groups. The removal of the acetyl protecting groups from sugars was carried out according to the classic

Zemplén protocol under alkaline conditions using a solution of sodium methoxide in methanol (0.2 molar equiv.) [67]. The final step was to neutralize the reaction mixture with the use of Amberlyst-15 ion exchange resin, after which the mixture was filtered to give compounds **23, 24, 29, 30, 35, 36, 39, 40, 43, 44** sufficiently pure for further reactions.

For the preparation of glycoconjugates, the obtained protected or deprotected derivatives of D-glucose or D-galactose were combined with derivatives of 8-HQ using copper(I)-catalyzed 1,3-dipolar azide-alkyne cycloaddition (CuAAC) [68,69]. A general scheme for the synthesis of glycoconjugates is shown in Scheme 5. The reactants were combined in an equimolar ratio in a THF/*i*-PrOH/H$_2$O solvent system at room temperature. As the source of copper ions, CuSO$_4$·5H$_2$O was used. Whereas, sodium ascorbate (NaAsc) was a reducing agent for Cu ions from II for the I oxidation stage. Due to the using Cu(I) as a catalyst, the reaction was carried out at room temperature and only 1,4-disubstituted 1,2,3-triazoles were obtained. It is worth noting that both protected and deprotected sugar derivatives can be used for this reaction. This eliminates the need for a final deprotection of glycoconjugates, which could adversely affect the yields of the unprotected products. The crude products of these reactions were purified by column chromatography. As a result of the CuAAC reaction, glycoconjugates **45–108** were obtained with the yields shown in the Tables 1–5. The structure of substrates for CuAAC reactions and all obtained glycoconjugates were confirmed by ^{1}H and ^{13}C NMR spectroscopy. For glycoconjugates, HRMS analyses were also performed. All these data are included in the Supplementary Materials. The physicochemical properties, such as melting point and optical rotation, were also determined.
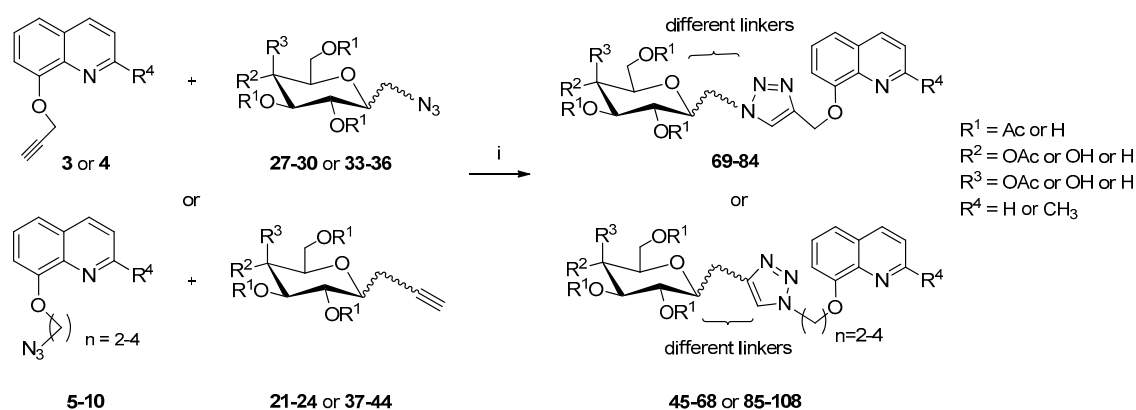
Scheme 5. General scheme for the synthesis of glycoconjugates **45–108**. *Reagents and Conditions:* (**i**) CuSO$_4$·5H$_2$O, NaAsc, *i*-PrOH, THF, H$_2$O, r.t., 24 h.

2.2. Biological Studies

2.2.1. Cytotoxicity Evaluation of Glycoconjugates

Glycoconjugates have been tested for their potential anticancer activity in vitro. For this purpose, the whole range of obtained glycoconjugates and substrates used for their synthesis were subjected to a cytotoxicity screening using MTT assay on cell lines: HCT 116 (colorectal carcinoma cell line) and MCF-7 (human breast adenocarcinoma cell line). In these lines, overexpression of the glucose and galactose transporters was observed [49,70–73]. For compounds presenting the highest antiproliferative activity within the cancer cell line, cytotoxicity tests on Normal Human Dermal Fibroblast-Neonatal cells (NHDF-Neo) were also be performed, to determine their selectivity index. Tests were conducted for glycoconjugates solutions at concentrations ranging from 0.01 mM to 0.8 mM. The determined IC$_{50}$ values, defined as 50% cell growth inhibition compared to the untreated control, are shown in Tables 6 and 7). The effect of the length and structure of the linker connecting quinoline with the sugar fragment for the activity of glycoconjugates was investigated.

Table 1. Yields of glycoconjugates **45–68**.

General Structure								

Product	R^1	R^2	R^3	R^4	n	8-HQ Derivative	Sugar Derivative	Yield [%]
45	Ac	OAc	H	H		**5**	**21**	73
46	Ac	H	OAc	H		**5**	**22**	74
47	Ac	OAc	H	CH$_3$		**8**	**21**	100
48	Ac	H	OAc	CH$_3$	2	**8**	**22**	71
49	H	OH	H	H		**5**	**23**	95
50	H	H	OH	H		**5**	**24**	67
51	H	OH	H	CH$_3$		**8**	**23**	88
52	H	H	OH	CH$_3$		**8**	**24**	78
53	Ac	OAc	H	H		**6**	**21**	100
54	Ac	H	OAc	H		**6**	**22**	100
55	Ac	OAc	H	CH$_3$		**9**	**21**	65
56	Ac	H	OAc	CH$_3$	3	**9**	**22**	77
57	H	OH	H	H		**6**	**23**	100
58	H	H	OH	H		**6**	**24**	76
59	H	OH	H	CH$_3$		**9**	**23**	87
60	H	H	OH	CH$_3$		**9**	**24**	65
61	Ac	OAc	H	H		**7**	**21**	96
62	Ac	H	OAc	H		**7**	**22**	93
63	Ac	OAc	H	CH$_3$		**10**	**21**	92
64	Ac	H	OAc	CH$_3$	4	**10**	**22**	100
65	H	OH	H	H		**7**	**23**	72
66	H	H	OH	H		**7**	**24**	90
67	H	OH	H	CH$_3$		**10**	**23**	76
68	H	H	OH	CH$_3$		**10**	**24**	66

Table 2. Yields of glycoconjugates **69–76**.

General Structure							

Product	R^1	R^2	R^3	R^4	8-HQ Derivative	Sugar Derivative	Yield [%]
69	Ac	OAc	H	H	**3**	**27**	78
70	Ac	H	OAc	H	**3**	**28**	62
71	Ac	OAc	H	CH$_3$	**4**	**27**	97
72	Ac	H	OAc	CH$_3$	**4**	**28**	77
73	H	OH	H	H	**3**	**29**	62
74	H	H	OH	H	**3**	**30**	55
75	H	OH	H	CH$_3$	**4**	**29**	58
76	H	H	OH	CH$_3$	**4**	**30**	59

Table 3. Yields of glycoconjugates **77–84**.

General Structure							

Product	R^1	R^2	R^3	R^4	8-HQ Derivative	Sugar Derivative	Yield [%]
77	Ac	OAc	H	H	3	33	67
78	Ac	H	OAc	H	3	34	74
79	Ac	OAc	H	CH$_3$	4	33	81
80	Ac	H	OAc	CH$_3$	4	34	78
81	H	OH	H	H	3	35	60
82	H	H	OH	H	3	36	58
83	H	OH	H	CH$_3$	4	35	61
84	H	H	OH	CH$_3$	4	36	78

Table 4. Yields of glycoconjugates **85–100**.

General Structure								

Product	R^1	R^2	R^3	R^4	n	8-HQ Derivative	Sugar Derivative	Yield [%]
85	Ac	OAc	H	H		5	37	85
86	Ac	H	OAc	H		5	38	86
87	Ac	OAc	H	CH$_3$		8	37	87
88	Ac	H	OAc	CH$_3$	2	8	38	88
89	H	OH	H	H		5	39	89
90	H	H	OH	H		5	40	90
91	H	OH	H	CH$_3$		8	39	91
92	H	H	OH	CH$_3$		8	40	92
93	Ac	OAc	H	H		6	37	93
94	Ac	H	OAc	H		6	38	94
95	Ac	OAc	H	CH$_3$		9	37	95
96	Ac	H	OAc	CH$_3$	3	9	38	96
97	H	OH	H	H		6	39	97
98	H	H	OH	H		6	40	98
99	H	OH	H	CH$_3$		9	39	99
100	H	H	OH	CH$_3$		9	40	100

Table 5. Yields of glycoconjugates **101–108**.

General Structure							

Product	R^1	R^2	R^3	R^4	8-HQ Derivative	Sugar Derivative	Yield [%]
101	Ac	OAc	H	H	6	41	94
102	Ac	H	OAc	H	6	42	90
103	Ac	OAc	H	CH$_3$	9	41	68
104	Ac	H	OAc	CH$_3$	9	42	64
105	H	OH	H	H	6	43	83
106	H	H	OH	H	6	44	82
107	H	OH	H	CH$_3$	9	43	80
108	H	H	OH	CH$_3$	9	44	78

Table 6. Screening of cytotoxicity of substrates **1–10** used for glycoconjugation.

Compound	Activity IC$_{50}$ [µM] [a]		
	HCT 116 [b]	MCF-7 [c]	NHDF-Neo [b]
1	>800	0.24 ± 0.01	>800
2	>800	43.18 ± 1.78	346.77 ± 2.23
3	>800	95.95 ± 4.29	>800
4	>800	223.63 ± 8.06	>800
5	83.02 ± 1.83	27.27 ± 0.06	26.60 ± 0.60
6	461.39 ± 1.34	244.44 ± 1.34	-
7	237.48 ± 2.11	67.18 ± 3.49	37.71 ± 0.94
8	>800	633.02 ± 6.39	-
9	295.51 ± 7.37	166.70 ± 7.15	188.14 ± 2.47
10	196.47 ± 7.38	114.72 ± 1.23	168.14 ± 1.13
Doxorubicin	5.60 ± 0.10	0.70 ± 0.01	>20

[a] Cytotoxic was evaluated using the MTT assay; [b] Incubation time 24 h; [c] Incubation time 72 h.

Table 7. Screening of cytotoxicity of glycoconjugates derivatives of 8-hydroxyquinoline **45–108**.

Compound	Activity IC$_{50}$ [µM] [a]			Compound	Activity IC$_{50}$ [µM] [a]		
	HCT 116 [b]	MCF-7 [c]	NHDF-Neo [b]		HCT 116 [b]	MCF-7 [c]	NHDF-Neo [b]
45	217.0 ± 4.7	196.5 ± 1.9	405.9 ± 5.7	**49**	>800	>800	-
46	248.8 ± 7.1	196.5 ± 3.1	262.4 ± 1.7	**50**	>800	>800	-
47	229.6 ± 2.6	375.6 ± 8.3	-	**51**	>800	>800	-
48	257.1 ± 7.2	231.8 ± 9.6	-	**52**	>800	>800	-
53	143.0 ± 2.3	200.6 ± 1.1	214.8 ± 6.4	**57**	>800	>800	-
54	168.9 ± 1.0	190.4 ± 3.0	213.1 ± 3.0	**58**	>800	>800	-
55	135.1 ± 7.0	221.1 ± 2.4	426.8 ± 3.8	**59**	>800	>800	-
56	244.8 ± 4.7	240.2 ± 3.8	-	**60**	>800	605.2 ± 1.3	-
61	328.8 ± 9.0	254.8 ± 3.6	-	**65**	382.4 ± 2.1	320.2 ± 4.9	-
62	389.5 ± 4.9	233.1 ± 5.8	-	**66**	>800	788.8 ± 7.5	-
63	294.7 ± 1.8	214.8 ± 1.7	>800	**67**	>800	>800	-
64	499.8 ± 2.7	241.9 ± 2.8	-	**68**	>800	>800	-
69	240.0 ± 2.3	105.9 ± 4.1	216.1 ± 9.7	**73**	>800	>800	-
70	280.9 ± 8.9	217.9 ± 5.2	220.0 ± 2.5	**74**	426.1 ± 1.3	>800	-
71	290.6 ± 7.0	136.0 ± 1.5	715.2 ± 9.6	**75**	>800	>800	-
72	763.3 ± 5.4	317.8 ± 8.5	-	**76**	>800	>800	-
77	246.2 ± 6.2	192.7 ± 3.7	219.1 ± 2.4	**81**	112.8 ± 1.6	87.9 ± 4.1	94.7 ± 0.5
78	119.1 ± 5.6	39.1 ± 0.9	103.6 ± 2.5	**82**	194.4 ± 0.6	384.7 ± 8.3	166.3 ± 5.8
79	142.9 ± 2.9	226.6 ± 4.0	480.8 ± 4.4	**83**	>800	>800	-
80	519.2 ± 7.2	301.0 ± 4.4	-	**84**	>800	>800	-
85	239.1 ± 3.0	203.8 ± 3.6	382.6 ± 2.4	**89**	>800	>800	-
86	270.6 ± 7.5	129.7 ± 1.8	>800	**90**	690.3 ± 4.0	629.0 ± 1.2	-
87	379.8 ± 1.4	211.9 ± 1.1	>800	**91**	>800	>800	-
88	272.3 ± 1.2	178.9 ± 6.8	>800	**92**	>800	>800	-
93	137.3 ± 2.1	95.7 ± 0.02	113.4 ± 0.9	**97**	677.9 ± 2.8	702.6 ± 1.9	-
94	229.8 ± 4.7	256.0 ± 9.6	-	**98**	>800	>800	-
95	217.1 ± 1.5	781.2 ± 3.5	163.1 ± 1.1	**99**	>800	595.9 ± 9.0	-
96	249.2 ± 5.5	297.9 ± 2.1	-	**100**	>800	>800	-
101	246.2 ± 1.3	176.4 ± 1.8	696,7 ± 1.6	**105**	>800	436.3 ± 3.1	-
102	369.0 ± 4.7	203.6 ± 4.9	-	**106**	>800	>800	-
103	295.2 ± 8.2	177.6 ± 2.6	586.0 ± 5.6	**107**	630.2 ± 2.7	>800	-
104	515.7 ± 4.3	223.4 ± 8.6	-	**108**	>800	>800	-

[a] Cytotoxic was evaluated using the MTT assay; [b] Incubation time 24 h; [c] Incubation time 72 h.

As part of the experiments, it was checked whether the building blocks necessary to obtain final glycoconjugates are able to limit the proliferation of cancer cells (Table 6). Sugar derivatives appeared to be inactive on the tested cell lines. However, the high toxicity of parent compounds **1** and **2** towards the MCF-7 cancer cell line was observed. A lower IC$_{50}$ value was determined for 8-HQ than for doxorubicin commonly used in cancer treatment. This observation indicates the huge sensitivity of this particular cancer cell line to 8-HQ and gives hope for even more effective therapeutics based on the 8-HQ scaffold. In addition, some of the derivatives of 8-HQ **5–10** were toxic to the tested

cell lines. However, further experiments have shown that they also cause the death of healthy cells. Therefore, the next studies checked whether the addition of the sugar moiety to aglycon would affect the selectivity of the obtained glycoconjugates.

The results of the cytotoxicity assay indicate that the glycoconjugates with a deprotected sugar unit (right part of Table 7) are mostly unable to inhibit cell proliferation in the tested concentration range. This is probably related to their hindered penetration into the cell through the lipid biological barriers, due to the high hydrophilicity of the compounds, compared to glycoconjugates having acetyl protecting groups. The exception is compound **81**, whose IC_{50} = 112.8 ± 1.6 µM for HCT 116 and 87.9 ± 4.1 µM for MCF-7. For its protected analog **77**, the IC_{50} value twice as high was determined for both tumor cell lines. Most likely, in this case, GLUT transporters had a more important role in transporting into the cell, and passive transport is less important. Unfortunately, this compound is also toxic to healthy cells, so it cannot be considered a selective drug.

All glycoconjugates containing ester protection of hydroxyl groups in the sugar part proved to be active on the tested cancer cell lines in the tested concentration range (left part of Table 7). Their non-polar nature should facilitate the process of crossing through phospholipid bilayer and penetrating into the cell, where then intracellular hydrolytic enzymes are able to remove the acetyl groups. In addition, as opposed to substrates, some of the obtained glycoconjugates showed low cytotoxicity to NHDF-Neo cells, especially glycoconjugates **45**, **46**, **85**, and **86** derived from quinoline **5**. Moreover, for the HCT 116 cell line, all protected glycoconjugates exhibit higher antiproliferative activity relative to aglycons **1** and **2**. This fact confirms the accuracy of the assumption that in this case, the presence of the sugar fragment improves the distribution and absorption of the compound, and thus its activity.

In the beginning, it was decided to check the effect of the length of the linker between the 1,2,3-triazole fragment and the derivative of 8-HQ for glycoconjugate activity (compounds **45–68**). The lowest IC_{50} values were obtained for glycoconjugates **53–56**, whose alkyl chain between triazole and 8-HQ consisted of 3 carbon atoms. However, further elongation of the alkyl chain in the compounds **61–64** resulted in a decrease in the cytotoxic activity of glyconjugates. Therefore, no further chain extension seems necessary. On the other hand, the alkyl chain extension between the 1,2,3-triazole ring and the sugar moiety in compounds **69–72** did not significantly affect the antiproliferative activity of glycoconjugates. Noteworthy is compound **71**, which turned out to be more active than the unconjugated quinoline derivative **4** and for which the selectivity index, calculated as the ratio of the IC_{50} value determined for healthy cells to the IC_{50} value determined for tumor cells, equal 5.3 for MCF-7 lines and 2.5 for HCT 116 lines. This observation makes it interesting in the aspect of further, more detailed studies involving different cell lines.

Glycoconjugates **77–100** containing an additional amide bond in the linker structure proved to be more active relative to the tested cancer cell lines. Among them, the most promising results were obtained for compounds **78** and **93**. For the MCF-7 cell line, the IC_{50} value equals 39.1 ± 0.9 µM and 95.7 ± 0.02 µM, respectively. However, for HCT 116 not much higher IC_{50} were noted: 119.1 ± 5.6 µM and 137.3 ± 2.1 µM, respectively. Unfortunately, these compounds were also toxic to healthy cells, so they cannot be considered selective drugs. It was noted that compound with 8-HQ fragment usually showed higher cytotoxicity compared to derivatives with 2Me8HQ unit, while the type of sugar moiety did not significantly affect to the glycoconjugate activity. Importantly, compounds **86–88** did not show any ability to inhibit the proliferation of healthy cells while having a moderate ability to inhibit cancer cells.

Recently, an important role in drug design has been played by compounds containing a carbamate moiety in the structure. Carbamates are usually more stable under enzymatic hydrolysis than the corresponding esters and are generally more susceptible to hydrolysis than amides. Carbamate prodrugs have been designed for selective hydrolysis by human carboxylesterases to release active drugs [56,74]. It appeared that glycoconjugates **101** and **103**, based on the D-glucose moiety, showed

low cytotoxicity to healthy cells while showing significant antiproliferative activity against cancer cells. For these compounds, a selectivity index for the MCF-7 cell line was 3.9 and 3.3 respectively.

2.2.2. Inhibitory Activity Against β-1,4-GalT

Tested cancer cell lines are characterized by overexpression of the β-1,4-galactosyltransferase (β-1,4-GalT) [75]. This enzyme belongs to the group of glycosyltransferases (GTs). Due to a number of important functions that GTs perform, among others: post-translational protein modifications and synthesis of oligosaccharide chains, they are an important object of research on potential anticancer drugs. A high rate of glycosylation is a common disorder of cancer cell metabolism, and the expression of GTs can be associated with cancer progression. GTs are a group of metal-dependent enzymes, therefore the presence of a species capable of binding divalent metal ions in the molecule of potential inhibitor appears to be necessary to inhibit the activity of these enzymes [75,76]. It seems appropriate to use glycoconjugates derivatives of 8-HQ to coordinate the metal ions present in the active centers of many enzymes, and thus to inhibit their activity.

It was decided to evaluate the obtained glycoconjugates for their inhibitory activity against enzyme from the glycosyltransferases group. Therefore, the experiments will be carried out using commercially available metal-dependent β-1,4-GalT I from bovine milk. To evaluate the activity of tested compounds, concentrations of substrate and product of the enzymatic reaction in the reaction mixtures was determined by RP-HPLC method, which is a modification of the Vidal method [77]. This method uses UDP-Gal, a natural β-1,4-GalT donor type substrate and (6-esculetinyl) β-D glucopyranoside (esculine) as glycosyl fluorescent acceptor. The number of products formed in the reaction with the addition of glycoconjugates as potential enzyme inhibitors was compared with the number of products in reactions carried out under the same conditions without the addition of inhibitors (test reactions). Analyzes were conducted in the linear range of the peak area from the product and substrate concentration. Experiments were conducted for glycoconjugates solutions at concentrations ranging from 0.1 mM to 0.8 mM. For the most active compounds, IC_{50} values were designated. The results are presented in Table 8.

Table 8. Bovine milk β-1,4-Galactosyltransferase I assay results.

Compound	Percentage of Inhibition at 0.8 mM [%]	IC_{50} [mM]
49	65 ± 0.27	0.57
50	10 ± 0.17	-
51	64 ± 0.23	0.60
52	8 ± 0.17	-
57	72 ± 0.03	0.40
58	2 ± 0.37	-
59	68 ± 0.25	0.40
60	6 ± 0.47	-
65	70 ± 0.19	0.46
66	8 ± 0.51	-
67	73 ± 0.03	0.35
68	4 ± 0.45	-
73	45 ± 0.17	-
74	14 ± 0.22	-
75	35 ± 0.06	-
76	7 ± 0.29	-
81	33 ± 0.29	-
82	17 ± 0.07	-
83	18 ± 0.25	-
84	14 ± 0.07	-

In this study, the influence of the alkyl chain length between the 1,2,3-triazole fragment and the 8-HQ derivative (**49–52, 57–60, 65–68**), as well as between the 1,2,3-triazole fragment and the sugar

unit (**73–76**) for enzyme inhibition was tested. In addition, the effect of the presence of an additional amide bond in the structure of the glycoconjugate linker (**81–84**) was analyzed. Based on previous experience [54], only glycoconjugates with an unprotected sugar part were tested.

　Experiments have shown that parent compounds **1**, **2** and substrates **3–10** are not able to inhibit the enzyme, which may indicate that the sugar fragment is necessary to obtain inhibitory activity. For glycoconjugates obtained as a result of CuAAC reactions between sugar derivatives containing a propargyl moiety and quinoline derivatives containing an azide moiety, the results indicate that all tested glycoconjugates derivatives of D-glucose showed higher activity compared to their analogs containing the D-galactose unit. However, the type of 8-HQ derivative did not matter in this case. Considering the effect of linker length between the 1,2,3-triazole fragment and the 8-HQ derivative, it can be clearly stated that the extension of the alkyl chain increases the inhibition of β-1,4-GalTI by glycoconjugates. In this group of compounds (**49–52, 57–60, 65–68**), all glycoconjugates based on D-glucose moiety showed the ability to inhibit the enzyme by over 50% compared to the test reaction. However, for compound **67**, having four carbon atoms in the alkyl linker, the lowest IC_{50} value was determined (0.35 mM). It is probable, that an extension of the alkyl chain length between the triazole ring and quinolone, increases the "flexibility" of the molecule, which may have a better fit into the active center of the enzyme. Much lower ability to inhibition of the model enzyme was observed for glycoconjugates that were obtained in the CuAAC reaction of sugar derivatives containing an azide group and quinoline derivatives containing the propargyl moiety. Glycoconjugates with an ethoxy fragment between the 1,2,3-triazole and sugar units (**73–76**) were not able to inhibit β-1,4-GalTI by 50%. However, they showed slightly increased activity compared to glycoconjugates **81–84**, containing an additional amide fragment in the structure. The amide fragment is in close distance to the aromatic moiety, which creates a high rigidity of the molecule and probably makes it difficult to fit into the active center of the enzyme. Therefore, the addition of an amide fragment is not a good idea for the design of β-1,4-GalT inhibitors.

2.3. Study of Metal Complexing Properties

　Previously it was mentioned that cancer cells exhibit an increased concentration of copper ions [20–24]. Moreover, it is broadly known that some quinoline derivatives possess metal ions complexing properties [18] what is essential for their anti-proliferative properties [51]. Bivalent metal ions are coordinated by phenol oxygen atom as well as nitrogen atom of 8-HQ ring with the formation of an 8HQ-metal ion complex with stoichiometry 2:1 [78]. In addition, 1,2,3-triazole ring also has a metal-complexation ability [79]. Therefore, it is interesting if the addition of linker containing such fragment having metal ions chelation ability into 8-HQ might significantly increase the metal ion complexation capability. The capability of complexes formation by investigated glycoconjugates and stoichiometry of such complexes was evaluated for compounds **101** and **93** with copper ions by spectroscopic titration experiments using UV-VIS. The UV-VIS spectrum of **101** is shown in Figure 3a. The addition of subsequent copper ion portions to glycoconjugate solution results in a gradual lowering of absorption bands at 242 nm and 310 nm. In addition, increase of the absorption band at 265 nm was observed. Importantly, during titration two well-defined isosbestic points around 250 nm and 286 nm were noted indicating the glycoconjugate-copper ion complex formation. The stoichiometry of obtained complexes was determined with Job's plot using the changes in absorption band at 265 nm. The plotted graph presenting the difference in absorbance, $\Delta A = A_x - A_0$ as a function of molar fraction [101]/[**101** + Cu^{2+}] was shown in Figure 3b. Maximum observed at molar fraction 0.5 in obtained curve indicates a formation of 1:1 complex of glycoconjugate:copper ion, regardless of the type of linker (see Supplementary Materials).

　ESI-MS spectra showed that copper ions are complexed by investigated glycoconjugates. The ESI-MS spectrum in positive ions mode of the investigated compound **101** (Figure 4a) revealed the presence of the ion at m/z = 658.35 (adduct [**101** + H]$^+$) corresponding to protonated glycoconjugate molecule and less intensive one corresponding to its sodium adduct, m/z = 680.36 [**101** + Na]$^+$. Additionally,

ions of 101_2 aggregate (dimer) adducts can be noticed, respectively at m/z = 1314.23 [101_2 + H]$^+$, 1337.26 [101_2 + Na]$^+$ and 1353.19 [101_2 + K]$^+$. In the ESI-MS of glycoconjugate partially titrated with copper ions (Figure 4b) the most abundant peak at m/z = 720.15 correspondings to [101 + Cu(I)]$^+$ is visible. The second intensive signal m/z = 658.2 is derived from glycoconjugate still present in the solution. Moreover the signals at m/z = 1377.17 and at m/z = 360.28 corresponding to dimer 101_2 complex with Cu [101_2 + Cu(I)]$^+$ and complex [101 + Cu(II)]$^{2+}$ were observed. The ESI-MS/MS fragmentation spectrum of the ion with m/z = 1377.17 (see Supplementary Data) reveals only one peak at m/z = 720 corresponding to complex [101 + Cu(I)]$^+$. It confirms that ion at m/z = 1377.17 corresponds to Cu$^+$-dimer complex (101_2 is present in the initial solution, see Figure 4a). Thus, complex with apparent 2:1 stoichiometry is observed, but in fact, the complex is formed probably only with one of the 101 molecules of the dimer. Moreover, in the signals ascribed to formed complexes characteristic two peaks with the difference of 2 Da are observed. Such spectrum is typical of copper complexes due to existence of copper in two basic isotopic forms (^{63}Cu (69,17%) and ^{65}Cu (30,83%)) [80]. It may seem surprising that copper(I) complexes are observed in the ESI-MS spectrum since copper(II) was used for titration. This phenomenon can be explained by a reduction reaction proceeding under the conditions of the analysis as a result of charge transfer between the metal complexes and the solvent molecules in the gas-phase [81–83].
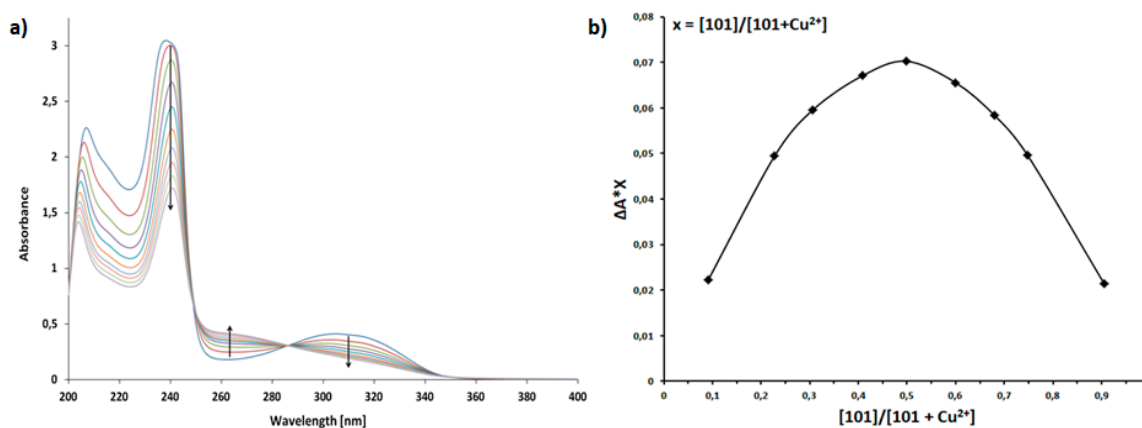
Figure 3. (**a**)—UV spectrum of compound **101** with the addition of copper sulfate pentahydrate in methanol; (**b**)—Job's plot of **101** with Cu^{2+}. The absorbance was monitored at 265 nm.
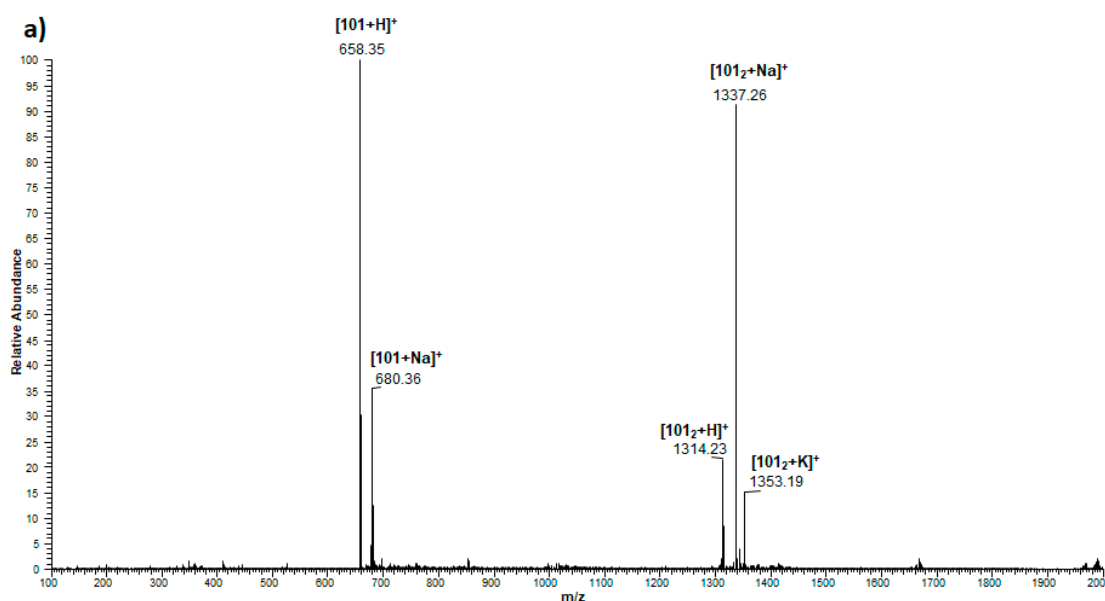
Figure 4. *Cont.*
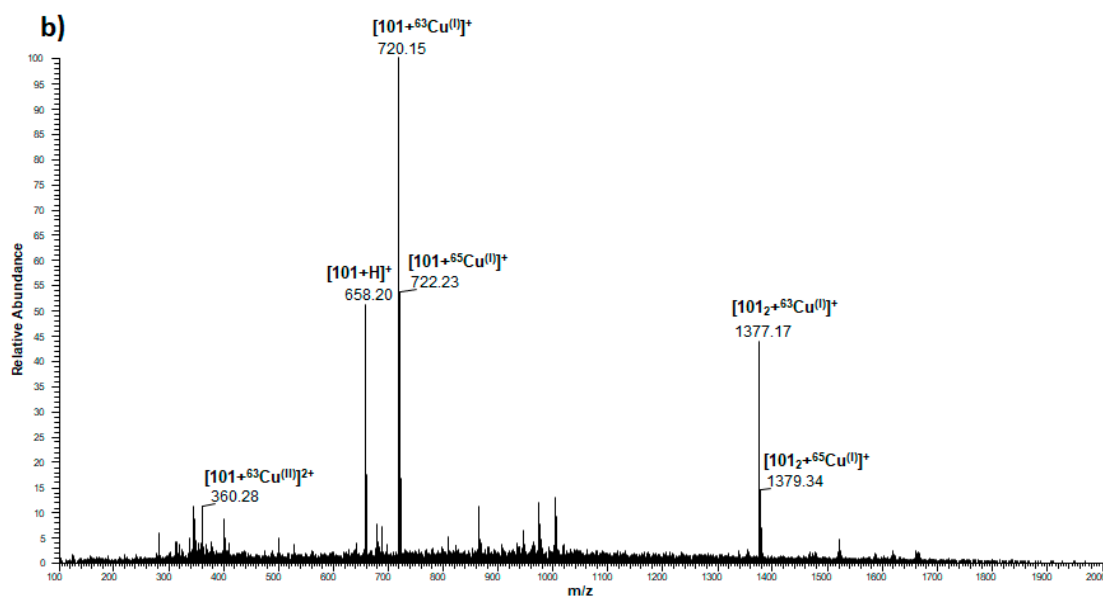
Figure 4. ESI-MS (positive-ion mode) spectrum of (**a**) **101** compound and (**b**) **101** compound after addition of Cu^{2+} ions into **101** solution.

3. Materials and Methods

3.1. General Information

NMR spectra were recorded with an Agilent spectrometer at a frequency of 400 MHz using TMS or DSS as the internal standards and $CDCl_3$, CD_3OD, DMSO-d6 or D_2O as the solvents. NMR solvents were purchased from ACROS Organics (Geel, Belgium). Chemical shifts (δ) are expressed in ppm and coupling constants (J) in Hz. The following abbreviations were used to explain the observed multiplicities: s: singlet, d: doublet, dd: doublet of doublets, ddd: doublet of doublet of doublets, t: triplet, dd-t: doublet of doublets resembling a triplet (with similar values of coupling constants), m: multiplet, p: pentet (quintet), b: broad. High-resolution mass spectra (HRMS) were recorded with a WATERS LCT Premier XE system using the electrospray-ionization (ESI) technique. Optical rotations were measured with a JASCO P-2000 polarimeter using a sodium lamp (589.3 nm) at room temperature. Melting point measurements were performed on OptiMelt (MPA 100) Stanford Research Systems. Reactions were monitored by thin-layer chromatography (TLC) on precoated plates of silica gel 60 F254 (Merck Millipore, Burlington, MA, USA). The TLC plates were visualized under UV light (λ = 254 nm) or by charring the plates after spraying with 10% solution of sulfuric acid in ethanol. Crude products were purified using column chromatography performed on Silica Gel 60 (70–230 mesh, Fluka, St. Louis, MI, USA), developed using toluene:EtOAc or $CHCl_3$:MeOH as solvent systems. All evaporations were performed on a rotary evaporator under diminished pressure at 40 °C. Reversed-phase HPLC analyses were performed using JASCO LC 2000 apparatus equipped with a reverse-phase column (Nucleosil 100 C18.5 μm, 25 × 0.4 cm; mobile phase: H_2O/MeCN 90:10, flow rate 0.8 mL/min) with a fluorescence detector (FP). Fluorescence for substrate and product was read at 385 nm excitation/540 nm emission. The absorbance on MTT assay was measured spectrophotometrically at the 570 nm wavelength using a plate reader (Epoch, BioTek, USA).

All of the chemicals used in the experiments were purchased from Sigma- Aldrich, ACROS Organics, Fluka and Avantor and were used without purification. 8- Hydroxyquinoline **1**, 8-hydroxyquinaldine **2**, D-glucose **11** and D-galactose **12** are commercially available (Sigma-Aldrich). 8-(2-Propyn-1-yloxy)quinoline **3** [57], 2-methyl-8-(2-propyn-1-yloxy)quinoline **4** [57], 1,2,3,4,6-penta-*O*-acetyl-β-D-glucopyranose **13** [54], 1,2,3,4,6-penta-*O*-acetyl-β-D-galactopyranose **14** [54], 2,3,4,6-tetra-*O*-acetyl-α-D-glucopyranosyl bromide **15** [54], 2,3,4,6-tetra-*O*-acetyl-α-D-galactopyranosyl bromide **16** [54], 2,3,4,6-tetra-*O*-acetyl-β-D-glucopyranosyl azide **17** [54], 2,3,4,6-tetra-*O*-acetyl-β-D-galactopyranosyl

azide **18** [54], 2,3,4,6-tetra-*O*-acetyl-β-D-glucopyranosyl amine **19** [60], 2,3,4,6-tetra-*O*-acetyl-β-D-galactopyranosyl amine **20** [60], propargyl 2,3,4,6-tetra-*O*-acetyl-β-D-glucopyranoside **21** [61], propargyl 2,3,4,6-tetra-*O*-acetyl-β-D-galactopyranoside **22** [61], 2-bromoethyl 2,3,4,6-tetra-*O*-acetyl-β-D-glucopyranoside **25** [62], 2-bromoethyl 2,3,4,6-tetra-*O*-acetyl-β-D-galactopyranoside **26** [62], 2-azidoethyl 2,3,4,6-tetra-*O*-acetyl-β-D-glucopyranoside **27** [62], 2-azidoethyl 2,3,4,6-tetra-*O*-acetyl-β-D-galactopyranoside **28** [62], 2,3,4,6-tetra-*O*-acetyl-*N*-(β-D-glucopyranosyl)propiolamide **37** [65], 2,3,4,6-tetra-*O*-acetyl-*N*-(β-D-galactopyranosyl)propiolamide **38** [65], 2,3,4,6-tetra-*O*-acetyl-*N*-(β-D-glucopyranosyl)-*O*-propargyl carbamate **41** [66] and 2,3,4,6-tetra-*O*-acetyl-*N*-(β-D-galactopyranosyl)-*O*-propargyl carbamate **42** [66] were prepared according to the respective published procedures. Propargyl β-D-glucopyranoside **23**, propargyl β-D-galactopyranoside **24**, 2-azidoethyl β-D-glucopyranoside **29**, 2-azidoethyl β-D-galactopyranoside **30**, *N*-(β-D-glucopyranosyl)azidoacetamide **35**, *N*-(β-D-galactopyranosyl)azidoacetamide **36**, *N*-(β-D-glucopyranosyl)propiolamide **39**, *N*-(β-D-galactopyranosyl)propiolamide **40** *N*- (β-D- glucopyranosyl)-*O*-propargyl carbamate **43**, *N*-(β-D-galactopyranosyl)-*O*-propargyl carbamate **44** were obtained by Zemplén protocol [67] by deacetylation of the corresponding sugar derivatives.

3.2. Chemistry

3.2.1. General Procedure for the Synthesis of Quinoline Derivatives **5–10**

To a solution of 1,2-dibromoethane or 1,3-dibromopropane or 1,4-dibromobutane (23.1 mmol) in dry DMF (10 mL), sodium azide (23.1 mmol, 1.5 g) was added. The reaction mixture was stirred overnight at 50 °C. Afterwards, the reaction mixture was diluted with ether and the organic layer was washed (three times) with H_2O (3 × 10 mL). The organic layer was dried over anhydrous magnesium sulfate ($MgSO_4$), concentrated under vacuum to afford the corresponding azide as a clear oil, which was used in the next reaction without further purification.

Obtained 1-azido-2-bromoethane or 1-azido-3-bromopropane or 1-azido-4-bromobutane (4.0 mmol), was added to a solution of 8-hydroxyquinoline **1** or 8-hydroxyquinaldine **2** (4.0 mmol) in acetone (20 mL), followed by addition of potassium carbonate (10.0 mmol, 1.38 g). The reaction mixture was heated under reflux for 4 h and then at room temperature overnight. After completion, the reaction mixture was filtered off and the filtrate was concentrated under vacuum and purified by column chromatography (toluene:AcOEt; gradient 20:1 to 2:1) to give products **5–10**.

8-(2-Azidoethoxy)quinolone **5**: Starting from 1-azido-2-bromoethane and 8-hydroxyquinoline **1**, product was obtained as a brown oil (702.7 mg, 82%); $[\alpha]^{24}_D = -0.6$ (c = 1.0, $CHCl_3$); ^1H NMR (400 MHz, $CDCl_3$): δ 3.87 (t, 2H, *J* = 5.6 Hz, CH_2N), 4.43 (t, 2H, *J* = 5.6 Hz, CH_2O), 7.12 (dd, 1H, *J* = 2.5 Hz, *J* = 6.5 Hz, H-7$_{chin}$), 7.41–7.50 (m, 3H, H-3$_{chin}$, H-5$_{chin}$, H-6$_{chin}$), 8.14 (dd, 1H, *J* = 1.7 Hz, *J* = 8.3 Hz, H-4$_{chin}$), 8.96 (dd, 1H, *J* = 1.7 Hz, *J* = 4.2 Hz, H-2$_{chin}$); ^{13}C NMR (100 MHz, $CDCl_3$): δ 50.06, 67.64, 109.77, 120.66, 121.70, 126.52, 129.61, 135.95, 140.39, 149.51, 154.19.

8-(3-Azidopropoxy)quinolone **6**: Starting from 1-azido-3-bromopropane and 8-hydroxyquinoline **1**, product was obtained as a brown oil (684.7 mg, 75%); $[\alpha]^{24}_D = -0.4$ (c = 1.0, $CHCl_3$); ^1H NMR (400 MHz, $CDCl_3$): δ 2.28 (p, 2H, *J* = 6.4 Hz, CH_2), 3.65 (t, 2H, *J* = 6.6 Hz, CH_2N), 4.33 (t, 2H, *J* = 6.2 Hz, CH_2O), 7.09 (dd, 1H, *J* = 1.4 Hz, *J* = 7.5 Hz, H-7$_{chin}$), 7.38–7.49 (m, 3H, H-3$_{chin}$, H-5$_{chin}$, H-6$_{chin}$), 8.13 (dd, 1H, *J* = 1.8 Hz, *J* = 8.3 Hz, H-4$_{chin}$), 8.95 (dd, 1H, *J* = 1.8 Hz, *J* = 4.2 Hz, H-2$_{chin}$); ^{13}C NMR (100 MHz, $CDCl_3$): δ 28.67, 48.44, 65.70, 109.08, 119.97, 121.62, 126.69, 129.55, 136.04, 140.28, 149.31, 154,50.

8-(4-Azidobutoxy)quinoline **7**: Starting from 1-azido-4-bromobutane and 8-hydroxyquinoline **1**, product was obtained as a brown oil (736.5 mg, 76%); $[\alpha]^{23}_D = -0.4$ (c = 1.0, $CHCl_3$); ^1H NMR (400 MHz, $CDCl_3$): δ 1.90 (p, 2H, *J* = 7.0 Hz, CH_2), 2.11 (p, 2H, *J* = 6.5 Hz, CH_2), 3.42 (t, 2H, *J* = 6.9 Hz, CH_2N), 4.29 (t, 2H, *J* = 6.5 Hz, CH_2O), 7.07 (dd, 1H, *J* = 1.2 Hz, *J* = 7.6 Hz, H-7$_{chin}$), 7.37–7.49 (m, 3H, H-3$_{chin}$, H-5$_{chin}$, H-6$_{chin}$), 8.14 (dd, 1H, *J* = 1.7 Hz, *J* = 8.3 Hz, H-4$_{chin}$), 8.95 (dd, 1H, *J* = 1.7 Hz, *J* = 4.2 Hz,

H-2$_{chin}$); ^{13}C NMR (100 MHz, CDCl$_3$): δ 25.86, 26.31, 51.29, 68.26, 108.90, 119.72, 121.58, 126.71, 129.56, 136.06, 140.26, 149.28, 154,59.

2-Methyl-8-(2-azidoethoxy)quinolone **8**: Starting from 1-azido-2-bromoethane and 2-methylo-8-hydroxyquinoline **2**, product was obtained as a brown oil (757.8 mg, 83%); [α]$^{23}_D$ = −0.4 (c = 1.0, CHCl$_3$); ^{1}H NMR (400 MHz, CDCl$_3$): δ 2.79 (s, 3H, CH$_3$), 3.83 (t, 2H, *J* = 5.5 Hz, CH$_2$N), 4.43 (t, 2H, *J* = 5.5 Hz, CH$_2$O), 7.10 (dd, 1H, *J* = 2.6 Hz, *J* = 6.4 Hz, H-7$_{chin}$), 7.31 (d, 1H, *J* = 8.4 Hz, H-3$_{chin}$), 7.35–7.44 (m, 2H, H-5$_{chin}$, H-6$_{chin}$), 8.03 (d, 1H, *J* = 8.4 Hz, H-4$_{chin}$); ^{13}C NMR (100 MHz, CDCl$_3$): δ 25.66, 50.19, 68.05, 110.41, 120.62, 122.57, 125.49, 127.82, 136.00, 140.06, 153.78, 158,36.

2-Methyl-8-(3-azidopropoxy)quinolone **9**: Starting from 1-azido-3-bromopropane and 2-methylo-8-hydroxyquinoline **2**, product was obtained as a brown oil (688.1 mg, 71%); [α]$^{24}_D$ = −0.6 (c = 1.0, CHCl$_3$); ^{1}H NMR (400 MHz, CDCl$_3$): δ 2.28 (p, 2H, *J* = 6.5 Hz, CH$_2$), 2.78 (s, 3H, CH$_3$), 3.65 (t, 2H, *J* = 6.6 Hz, CH$_2$N), 4.33 (t, 2H, *J* = 6.3 Hz, CH$_2$O), 7.07 (dd, 1H, *J* = 2.4 Hz, *J* = 6.5 Hz, H-7$_{chin}$), 7.30 (d, 1H, *J* = 8.4 Hz, H-3$_{chin}$), 7.33–7.42 (m, 2H, H-5$_{chin}$, H-6$_{chin}$), 8.01 (d, 1H, *J* = 8.4 Hz, H-4$_{chin}$); ^{13}C NMR (100 MHz, CDCl$_3$): δ 25.71, 28.64, 48.48, 66.03, 109.73, 119.95, 122.52, 125.65, 127.76, 136.11, 140.00, 154.01, 158,18.

2-Methyl-8-(4-azidobutoxy)quinoline **10**: Starting from 1-azido-4-bromobutane and 2-methylo-8-hydroxyquinoline **2**, product was obtained as a brown oil (707.4 mg, 69%); [α]$^{22}_D$ = −0.6 (c = 1.0, CHCl$_3$); ^{1}H NMR (400 MHz, CDCl$_3$): δ 1.89 (p, 2H, *J* = 7.0 Hz, CH$_2$), 2.10 (p, 2H, *J* = 6.7 Hz, CH$_2$), 2.78 (s, 3H, CH$_3$), 3.45 (t, 2H, *J* = 6.9 Hz, CH$_2$N), 4.27 (t, 2H, *J* = 6.5 Hz, CH$_2$O), 7.03 (dd, 1H, *J* = 1.8 Hz, *J* = 7.1 Hz, H-7$_{chin}$), 7.29 (d, 1H, *J* = 8.4 Hz, H-3$_{chin}$), 7.32–7.41 (m, 2H, H-5$_{chin}$, H-6$_{chin}$), 8.00 (d, 1H, *J* = 8.4 Hz, H-4$_{chin}$); ^{13}C NMR (100 MHz, CDCl$_3$): δ 25.71, 25.89, 26.24, 51.36, 68.46, 109.35, 119.66, 122.49, 125.64, 127.74, 136.08, 139.91, 154.13, 158,13.

3.2.2. General Procedure for the Synthesis of Sugar Derivatives **31** and **32**

To a solution of 2,3,4,6-tetra-*O*-acetyl-β-D-glucopyranosyl amine **19** or 2,3,4,6-tetra-*O*-acetyl-β-D-galactopyranosyl amine **20** (1.7 g, 4.9 mmol) in dry CH$_2$CL$_2$ (20 mL), triethylamine (2 mL) was added. The reaction mixture was cooled to 0 °C and chloroacetyl chloride was added dropwise (613 μL, 7.7 mmol) then stirring was continued at room temperature. After 1 h, the resulting mixture was diluted with dichloromethane (90 mL) and washed with brine (2 × 60 mL). The combined organic layer was dried over anhydrous MgSO$_4$, concentrated under vacuum and purified by column chromatography (toluene:AcOEt; gradient 8:1 to 2:1) to give products **31–32**.

2,3,4,6-Tetra-*O*-acetyl-*N*-(β-D-glucopyranosyl)chloroacetamide **31**: Starting from 2,3,4,6-tetra-*O*-acetyl-β-D-glucopyranosyl amine **19**, product was obtained as a white solid (1.41 g, 68%); m.p.: 160–163 °C; [α]$^{24}_D$ = 8.3 (c = 1.0, CHCl$_3$); ^{1}H NMR (400 MHz, CDCl$_3$): δ 2.03, 2.04, 2.06, 2.09 (4s, 12H, CH$_3$CO), 3.84 (ddd, 1H, *J* = 2.1 Hz, *J* = 4.4 Hz, *J* = 10.1 Hz, H-5$_{glu}$), 4.00 and 4.07 (qAB, 2H, *J* = 15.4 Hz, CH$_2$Cl), 4.10 (dd, 1H, *J* = 2.1 Hz, *J* = 12.5 Hz, H-6a$_{glu}$), 4.31 (dd, 1H, *J* = 4.4 Hz, *J* = 12.5 Hz, H-6b$_{glu}$), 5.01 (dd-t, 1H, *J* = 9.4 Hz, *J* = 10.0 Hz, H-1$_{glu}$), 5.09 (dd-t, 1H, *J* = 9.4 Hz, *J* = 10.1 Hz, H-4$_{glu}$), 5.21 (dd-t, 1H, *J* = 9.0 Hz, *J* = 9.4 Hz, H-3$_{glu}$), 5.33 (dd-t, 1H, *J* = 9.0 Hz, *J* = 9.4 Hz, H-2$_{glu}$), 7.29 (d, 1H, *J* = 9.0 Hz, CONH); ^{13}C NMR (100 MHz, CDCl$_3$): δ 20.57, 20.61, 20.72, 20.76, 42.25, 61.56, 68.09, 70.26, 72.55, 73.83, 78.54, 166.81, 169.49, 169.87, 170.58, 170.79; HRMS (ESI-TOF): calcd for C$_{16}$H$_{22}$ClNO$_{10}$Na ([M + Na]$^+$): *m/z* 446.0830; found: *m/z* 446.0834.

2,3,4,6-Tetra-*O*-acetyl-*N*-(β-D-galactopyranosyl)chloroacetamide **32**: Starting from 2,3,4,6-tetra-*O*-acetyl-β-D-galactopyranosyl amine **20**, product was obtained as a white solid (1.66 g, 80%); m.p.: 143-144 °C; [α]$^{25}_D$ = 21.3 (c = 1.0, CHCl$_3$); ^{1}H NMR (400 MHz, CDCl$_3$): δ 2.01, 2.04, 2.07, 2.16 (4s, 12H, CH$_3$CO), 4.01 and 4.08 (qAB, 2H, *J* = 15.5 Hz, CH$_2$Cl), 4.04-4.18 (m, 3H, H-5$_{gal}$, H-6a$_{gal}$, H-6b$_{gal}$), 5.11-5.24 (m, 3H, H-1$_{gal}$, H-2$_{gal}$, H-3$_{gal}$), 5.45 (dd, 1H, *J* = 0. 7 Hz, *J* = 3.0 Hz, H-4$_{gal}$), 7.32 (d, 1H, *J* = 6.9 Hz, CONH); ^{13}C NMR (100 MHz, CDCl$_3$): δ 20.54, 20.61, 20.67, 20.71, 42.26, 61.12, 67.10, 67.97,

70.72, 72.58, 78.84, 166.71, 169.76, 170.01, 170.34, 171.06; HRMS (ESI-TOF): calcd for $C_{16}H_{22}ClNO_{10}Na$ ([M + Na]$^+$): *m/z* 446.0830; found: *m/z* 446.0832.

3.2.3. General Procedure for the Synthesis of Sugar Derivatives **33** and **34**

To a solution of 2,3,4,6-tetra-*O*-acetyl-*N*-(β-D-glucopyranosyl)chloroacetamide **31** or 2,3,4,6-tetra-*O*-acetyl-*N*-(β-D-galactopyranosyl)chloroacetamide **32** (1.0 g, 2.36 mmol) in dry DMF (15 mL), sodium azide (753 mg, 11.59 mmol) was added. The reaction mixture was stirred at room temperature for 24 h. After completion reaction, the solvent was evaporated under reduced pressure, and the residue was diluted with ethyl acetate (50 mL) and extracted with water (30 mL), 0.25 M HCl (20 mL) and brine (20 mL). The combined organic layer was dried over anhydrous $MgSO_4$, concentrated under vacuum, to afford the corresponding azide **33** and **34**, which were used for the next reaction without further purification.

2,3,4,6-tetra-*O*-acetyl-*N*-(β-D-glucopyranosyl)azidoacetamide **33**: Starting from 2,3,4,6-tetra-*O*-acetyl-*N*-(β-D-glucopyranosyl)chloroacetamide **31**, product was obtained as a white solid (975.0 mg, 96%); m.p.: 150-153 °C; $[\alpha]^{24}_D$ = 12.4 (c = 1.0, CHCl$_3$); ^{1}H NMR (400 MHz, CDCl$_3$): δ 2.03, 2.04, 2.06, 2.09 (4s, 12H, CH$_3$CO), 3.83 (ddd, 1H, *J* = 2.1 Hz, *J* = 4.4 Hz, *J* = 10.1 Hz, H-5$_{glu}$), 3.95 and 4.00 (qAB, 2H, *J* = 16.9 Hz, CH$_2$N), 4.09 (dd, 1H, *J* = 2.1 Hz, *J* = 12.5 Hz, H-6a$_{glu}$), 4.30 (dd, 1H, *J* = 4.4 Hz, *J* = 12.5 Hz, H-6b$_{glu}$), 4.98 (dd-t, 1H, *J* = 9.4 Hz, *J* = 9.8 Hz, H-1$_{glu}$), 5.08 (dd-t, 1H, *J* = 9.4 Hz, *J* = 10.1 Hz, H-4$_{glu}$), 5.22 (dd-t, 1H, *J* = 9.0 Hz, *J* = 9.4 Hz, H-3$_{glu}$), 5.32 (dd-t, 1H, *J* = 9.0 Hz, *J* = 9.8 Hz, H-2$_{glu}$), 7.10 (d, 1H, *J* = 9.1 Hz, CONH); ^{13}C NMR (100 MHz, CDCl$_3$): δ 20.57, 20.61, 20.72, 20.75, 52.59, 61.56, 68.08, 70.45, 72.57, 73.78, 78.15, 167.41, 169.50, 169.86, 170.57, 170.88; HRMS (ESI-TOF): calcd for $C_{16}H_{22}N_4O_{10}Na$ ([M + Na]$^+$): *m/z* 453.1234; found: *m/z* 453.1236.

2,3,4,6-tetra-*O*-acetyl-*N*-(β-D-galactopyranosyl)azidoacetamide **34**: Starting from 2,3,4,6-tetra-*O*-acetyl-*N*-(β-D-galactopyranosyl)chloroacetamide **32**, product was obtained as a white solid (873.5 mg, 86%); m.p.: 60–63 °C; $[\alpha]^{24}_D$ = 25.4 (c = 1.0, CHCl$_3$); ^{1}H NMR (400 MHz, CDCl$_3$): δ 2.01, 2.04, 2.07, 2.16 (4s, 12H, CH$_3$CO), 3.96 and 4.01 (qAB, 2H, *J* = 16.8 Hz, CH$_2$N), 4.02–4.17 (m, 3H, H-5$_{gal}$, H-6a$_{gal}$, H-6b$_{gal}$), 5.11–5.25 (m, 3H, H-1$_{gal}$, H-2$_{gal}$, H-3$_{gal}$), 5.45 (dd, 1H, *J* = 1.1 Hz, *J* = 2.9 Hz, H-4$_{gal}$), 7.13 (d, 1H, *J* = 8.5 Hz, CONH); ^{13}C NMR (100 MHz, CDCl$_3$): δ 20.54, 20.60, 20.67, 20.70, 52.61, 61.14, 67.11, 68.17, 70.73, 72.52, 78.43, 167.31, 169.76, 170.00, 170.35, 171.15; HRMS (ESI-TOF): calcd for $C_{16}H_{22}N_4O_{10}Na$ ([M + Na]$^+$): *m/z* 453.1234; found: *m/z* 453.1227.

3.2.4. Synthesis of Glycoconjugates **45–108**

The appropriate derivatives of 8-hydroxyquinoline **3–10** (0.5 mmol) and sugar derivatives **21–24**, **27–30**, **33–44** (0.5 mmol) were dissolved in dry THF (5 mL) and *i*-PrOH (5 mL). To the obtained solution, CuSO$_4$·5H$_2$O (0.1 mmol, 25.0 mg) dissolved in H$_2$O (2.5 mL) and sodium ascorbate (0.2 mmol, 39.6 mg) dissolved in H$_2$O (2.5 mL) were added. The reaction mixture was stirred for 24 h at room temperature. The progress of the reaction was monitored on TLC in an CHCl$_3$:CH$_3$OH eluents system (20:1 for protected or 2:1 for unprotected compounds). After completion, the reaction mixture was concentrated in vacuo and purified using column chromatography (dry loading; toluene:AcOEt, 2:1 and CHCl$_3$:MeOH, 100:1 for fully protected glycoconjugates or CHCl$_3$:MeOH, gradient: 50:1 to 2:1 for glycoconjugates with unprotected sugar part) to give products **45–108**.

Glycoconjugate **45**: Starting from propargyl 2,3,4,6-tetra-*O*-acetyl-β-D-glucopyranoside **21** and 8-(2-azidoethoxy)quinoline **5**, product was obtained as a yellow solid (219.2 mg, 73%); m.p.: 130–133 °C; $[\alpha]^{24}_D$ = −36.0 (c = 1.0, CHCl$_3$); ^{1}H NMR (400 MHz, CDCl$_3$): δ 1.84, 1.97, 2.01, 2.07 (4s, 12H, CH$_3$CO), 3.66 (ddd, 1H, *J* = 2.3 Hz, *J* = 4.6 Hz, *J* = 9.8 Hz, H-5$_{glu}$), 4.10 (dd, 1H, *J* = 2.3 Hz, *J* = 12.3 Hz, H-6a$_{glu}$), 4.21 (dd, 1H, *J* = 4.6 Hz, *J* = 12.3 Hz, H-6b$_{glu}$), 4.63 (d, 1H, *J* = 8.0 Hz, H-1$_{glu}$), 4.59–4.70 (m, 2H, CH$_2$N), 4.80 and 4.88 (qAB, 2H, *J* = 12.7 Hz, CH$_2$C), 4.95 (dd, 1H, *J* = 8.0 Hz, *J* = 9.4 Hz H-2$_{glu}$), 5.01 (t, 2H, *J* = 5.2 Hz, CH$_2$O), 5.04 (dd-t, 1H, *J* = 9.4 Hz, *J* = 9.8 Hz, H-4$_{glu}$), 5.13 (dd-t, 1H, *J* = 9.4 Hz, *J* = 9.4 Hz, H-3$_{glu}$), 7.05 (dd, 1H, *J* = 2.1 Hz, *J* = 6.4 Hz, H-7$_{chin}$), 7.42–7.55 (m, 3H, H-3$_{chin}$, H-5$_{chin}$, H-6$_{chin}$), 8.21

(d, 1H, *J* = 8.1 Hz, H-4$_{chin}$), 8.27 (s, 1H, H-5$_{triaz}$), 8.99 (d, 1H, *J* = 2.9 Hz, H-2$_{chin}$); ^{13}C NMR (100 MHz, CDCl$_3$): δ 20.47, 20.48, 20.59, 20.75, 49.75, 61.84, 62.40, 67.89, 68.34, 71.17, 71.82, 72.86, 99.32, 110.31, 121.07, 121.95, 125.10, 126.87, 129.65, 136.68, 139.55, 143.93, 149.26, 153.45, 169.36, 169.40, 170.18, 170.66; HRMS (ESI-TOF): calcd for C$_{28}$H$_{33}$N$_4$O$_{11}$ ([M + H]$^+$): *m/z* 601.2146; found: *m/z* 601.2148.

Glycoconjugate 46: Starting from propargyl 2,3,4,6-tetra-*O*-acetyl-β-D-galactopyranoside **22** and 8-(2-azidoethoxy)quinoline **5**, product was obtained as a yellow solid (222.2 mg, 74%); m.p.: 69–72 °C; [α]$^{24}_D$ = −30.0 (c = 1.0, CHCl$_3$); ^{1}H NMR (400 MHz, CDCl$_3$): δ 1.85, 1.95, 2.05, 2.13 (4s, 12H, CH$_3$CO), 3.83-3.92 (m, 1H, H-5$_{gal}$), 4.10-4.16 (m, 2H, H-6a$_{gal}$, H-6b$_{gal}$), 4.60 (d, 1H, *J* = 8.0 Hz, H-1$_{gal}$), 4.62–4.69 (m, 2H, CH$_2$N), 4.79 and 4.90 (qAB, 2H, *J* = 12.6 Hz, CH$_2$C), 4.94 (dd, 1H, *J* = 3.4 Hz, *J* = 10.4 Hz H-3$_{gal}$), 4.97-5.05 (m, 2H, CH$_2$O), 5.17 (dd, 1H, *J* = 8.0 Hz, *J* = 10.4 Hz, H-2$_{gal}$), 5.35 (dd, 1H, *J* = 0.7 Hz, *J* = 3.4 Hz, H-4$_{gal}$), 6.99–7.12 (m, 1H, H-7$_{chin}$), 7.38–7.58 (m, 3H, H-3$_{chin}$, H-5$_{chin}$, H-6$_{chin}$), 8.12–8.34 (m, 2H, H-4$_{chin}$, H-5$_{triaz}$), 8.99 (bs, 1H, H-2$_{chin}$); ^{13}C NMR (100 MHz, DMSO-d6): δ 20.26, 20.28, 20.35, 20.47, 49.18, 61.17, 61.76, 67.25, 67.43, 68.53, 69.91, 70.19, 98.99, 110.74, 120.57, 121.98, 124.93, 126.84, 129.15, 136.26, 139.30, 143.07, 149.00, 153.50, 169.03, 169.41, 169.85, 169.88; HRMS (ESI-TOF): calcd for C$_{28}$H$_{33}$N$_4$O$_{11}$ ([M + H]$^+$): *m/z* 601.2146; found: *m/z* 601.2145.

Glycoconjugate 47: Starting from propargyl 2,3,4,6-tetra-*O*-acetyl-β-D-glucopyranoside **21** and 2-methyl-8-(2-azidoethoxy)quinoline **8**, product was obtained as a yellow solid (307.3 mg, 100%); m.p.: 119-123 °C; [α]$^{24}_D$ = −32.4 (c = 1.0, CHCl$_3$); ^{1}H NMR (400 MHz, DMSO-d6): δ 1.83, 1.91, 1.98, 2.02 (4s, 12H, CH$_3$CO), 2.69 (s, 3H, CH$_3$), 3.93 (ddd, 1H, *J* = 2.4 Hz, *J* = 4.9 Hz, *J* = 10.0 Hz, H-5$_{glu}$), 4.01 (dd, 1H, *J* = 2.4 Hz, *J* = 12.3 Hz, H-6a$_{glu}$), 4.15 (dd, 1H, *J* = 4.9 Hz, *J* = 12.3 Hz, H-6b$_{glu}$), 4.59 (t, 2H, *J* = 4.9 Hz, CH$_2$N), 4.65 and 4.81 (qAB, 2H, *J* = 12.3 Hz, CH$_2$C), 4.74 (dd, 1H, *J* = 8.0 Hz, *J* = 9.6 Hz H-2$_{glu}$), 4.87 (d, 1H, *J* = 8.0 Hz, H-1$_{glu}$), 4.86–4.95 (m, 3H, CH$_2$O, H-4$_{glu}$), 5.20 (dd-t, 1H, *J* = 9.6 Hz, *J* = 9.6 Hz, H-3$_{glu}$), 7.20 (dd, 1H, *J* = 1.2 Hz, *J* = 7.7 Hz, H-7$_{chin}$), 7.39-7.46 (m, 2H, H-3$_{chin}$, H-6$_{chin}$), 7.50 (dd, 1H, *J* = 1.2 Hz, *J* = 8.2 Hz, H-5$_{chin}$), 8.20 (d, 1H, *J* = 8.4 Hz, H-4$_{chin}$), 8.59 (s, 1H, H-5$_{triaz}$); ^{13}C NMR (100 MHz, DMSO-d6): δ 20.15, 20.22, 20.34, 20.46, 25.01, 49.18, 61.60, 61.90, 67.58, 68.04, 70.58, 70.80, 72.05, 98.51, 111.21, 120.48, 122.52, 125.45, 125.65, 127.35, 136.04, 139.29, 142.89, 153.20, 157.55, 168.88, 169.20, 169.45, 169.99; HRMS (ESI-TOF): calcd for C$_{29}$H$_{35}$N$_4$O$_{11}$ ([M + H]$^+$): *m/z* 615.2302; found: *m/z* 615.2304.

Glycoconjugate 48: Starting from propargyl 2,3,4,6-tetra-*O*-acetyl-β-D-galactopyranoside **22** and 2-methyl-8-(2-azidoethoxy)quinoline **8**, product was obtained as a yellow solid (218.2 mg, 71%); m.p.: 52–56 °C; [α]$^{23}_D$ = −20.8 (c = 1.0, CHCl$_3$); ^{1}H NMR (400 MHz, DMSO-d6): δ 1.83, 1.89, 2.01, 2.11 (4s, 12H, CH$_3$CO), 2.69 (s, 3H, CH$_3$), 3.99–4.10 (m, 2H, H-5$_{gal}$, H-6a$_{gal}$), 4.13–4.21 (m, 1H, H-6b$_{gal}$), 4.59 (t, 2H, *J* = 5.0 Hz, CH$_2$N), 4.64 and 4.81 (qAB, 2H, *J* = 12.3 Hz, CH$_2$C), 4.79 (d, 1H, *J* = 8.0 Hz, H-1$_{gal}$), 4.86–4.97 (m, 3H, CH$_2$O, H-2$_{gal}$), 5.11 (dd, 1H, *J* = 0.9 Hz, *J* = 10.3 Hz, H-4$_{gal}$), 5.24 (dd, 1H, *J* = 3.6 Hz, *J* = 10.3 Hz, H-3$_{gal}$), 7.20 (dd, 1H, *J* = 1.2 Hz, *J* = 7.7 Hz, H-7$_{chin}$), 7.38-7.47 (m, 2H, H-3$_{chin}$, H-6$_{chin}$), 7.50 (dd, 1H, *J* = 1.2 Hz, *J* = 8.2 Hz, H-5$_{chin}$), 8.21 (d, 1H, *J* = 8.4 Hz, H-4$_{chin}$), 8.60 (s, 1H, H-5$_{triaz}$); ^{13}C NMR (100 MHz, DMSO-d6): δ 20.25, 20.28, 20.35, 20.47, 25.01, 49.19, 61.19, 61.76, 67.26, 67.59, 68.53, 69.89, 70.20, 98.94, 111.22, 120.48, 122.52, 125.40, 125.66, 127.35, 136.04, 139.31, 142.97, 153.21, 157.56, 168.98, 169.40, 169.85, 169.89; HRMS (ESI-TOF): calcd for C$_{29}$H$_{35}$N$_4$O$_{11}$ ([M + H]$^+$): *m/z* 615.2302; found: *m/z* 615.2303.

Glycoconjugate 49: Starting from propargyl β-D-glucopyranoside **23** and 8-(2-azidoethoxy)quinoline **5**, product was obtained as a yellow solid (205.4 mg, 95%); m.p.: 42-45 °C; [α]$^{25}_D$ = −17.2 (c = 1.0, MeOH); ^{1}H NMR (400 MHz, DMSO-d6): δ 2.92-3.09 (m, 2H, H-2$_{glu}$, H-5$_{glu}$), 3.10-3.17 (m, 2H, H-3$_{glu}$, H-4$_{glu}$), 3.40–3.50 (m, 1H, H-6a$_{glu}$), 3.66–3.75 (m, 1H, H-6b$_{glu}$), 4.08 (bs, 1H, OH), 4.27 (d, 1H, *J* = 7.8 Hz, H-1$_{glu}$), 4.57 (bs, 1H, OH), 4.60–4.66 (m, 3H, CH$_2$N, CH$_2$C), 4.83–4.95 (m, 4H, CH$_2$O, CH$_2$C, OH), 5.02 (bs, 1H, OH), 7.25 (dd, 1H, *J* = 1.5 Hz, *J* = 7.5 Hz, H-7$_{chin}$), 7.47–7.58 (m, 3H, H-3$_{chin}$, H-5$_{chin}$, H-6$_{chin}$), 8.32 (dd, 1H, *J* = 1.7 Hz, *J* = 8.3 Hz, H-4$_{chin}$), 8.40 (s, 1H, H-5$_{triaz}$), 8.89 (dd, 1H, *J* = 1.7 Hz, *J* = 4.2 Hz, H-2$_{chin}$); ^{13}C NMR (100 MHz, DMSO-d6): δ 49.12, 61.15, 61.47, 67.36, 70.10, 73.37, 76.70, 76.94, 102.14,

110.57, 120.51, 121.91, 124.96, 126.71, 129.08, 135.85, 139.69, 143.78, 149.27, 153.68; HRMS (ESI-TOF): calcd for $C_{20}H_{25}N_4O_7$ ([M + H]$^+$): *m/z* 433.1723; found: *m/z* 433.1723.

Glycoconjugate **50**: Starting from propargyl β-D-galactopyranoside **24** and 8-(2-azidoethoxy)quinoline **5**, product was obtained as a yellow solid (144.9 mg, 67%); m.p.: 44–45 °C; [α]$^{23}_D$ = −12.9 (c = 1.0, MeOH); ^{1}H NMR (400 MHz, DMSO-d6): δ 3.21–3.39 (m, 3H, H-2$_{gal}$, H-3$_{gal}$, H-4$_{gal}$), 3.40–3.48 (m, 1H, H-5$_{gal}$), 3.50–3.57 (m, 1H, H-6a$_{gal}$), 3.59–3.66 (m, 1H, H-6b$_{gal}$), 4.21 (d, 1H, *J* = 7.4 Hz, H-1$_{gal}$), 4.61 and 4.83 (qAB, 2H, *J* = 12.2 Hz, CH$_2$C), 4.63 (t, 2H, *J* = 5.2 Hz, CH$_2$N), 4.90 (t, 2H, *J* = 5.2 Hz, CH$_2$O), 7.25 (dd, 1H, *J* = 1.5 Hz, *J* = 7.5 Hz, H-7$_{chin}$), 7.47–7.58 (m, 3H, H-3$_{chin}$, H-5$_{chin}$, H-6$_{chin}$), 8.32 (dd, 1H, *J* = 1.7 Hz, *J* = 8.3 Hz, H-4$_{chin}$), 8.40 (s, 1H, H-5$_{triaz}$), 8.89 (dd, 1H, *J* = 1.7 Hz, *J* = 4.2 Hz, H-2$_{chin}$); ^{13}C NMR (100 MHz, DMSO-d6): δ 49.11, 60.52, 61.31, 67.37, 68.18, 70.44, 73.40, 75.32, 102.69, 110.58, 120.51, 121.92, 124.91, 126.70, 129.07, 135.83, 139.70, 143.85, 149.30, 153.69; HRMS (ESI-TOF): calcd for $C_{20}H_{25}N_4O_7$ ([M + H]$^+$): *m/z* 433.1723; found: *m/z* 433.1725.

Glycoconjugate **51**: Starting from propargyl β-D-glucopyranoside **23** and 2-methyl-8-(2-azidoethoxy)quinoline **8**, product was obtained as a yellow solid (196.4 mg, 88%); m.p.: 120–121 °C; [α]$^{24}_D$ = −20.0 (c = 1.0, MeOH); ^{1}H NMR (400 MHz, DMSO-d6): δ 2.69 (s, 3H, CH$_3$), 2.92–3.08 (m, 2H, H-2$_{glu}$, H-5$_{glu}$), 3.09-3.19 (m, 2H, H-3$_{glu}$, H-4$_{glu}$), 3.40–3.49 (m, 1H, H-6a$_{glu}$), 3.66–3.73 (m, 1H, H-6b$_{glu}$), 4.09 (bs, 1H, OH), 4.27 (d, 1H, *J* = 7.8 Hz, H-1$_{glu}$), 4.33 (bs, 1H, OH), 4.53 (t, 1H, *J* = 5.6 Hz, OH), 4.60 (t, 2H, *J* = 5.2 Hz, CH$_2$N), 4.63 and 4.87 (qAB, 2H, *J* = 12.1 Hz, CH$_2$C), 4.89 (t, 2H, *J* = 5.2 Hz, CH$_2$O), 4.99 (d, 1H, *J* = 4.9 Hz, OH), 7.21 (dd, 1H, *J* = 1.3 Hz, *J* = 7.7 Hz, H-7$_{chin}$), 7.39–7.45 (m, 2H, H-3$_{chin}$, H-6$_{chin}$), 7.50 (dd, 1H, *J* = 1.2 Hz, *J* = 8.2 Hz, H-5$_{chin}$), 8.20 (d, 1H, *J* = 8.4 Hz, H-4$_{chin}$), 8.54 (s, 1H, H-5$_{triaz}$); ^{13}C NMR (100 MHz, DMSO-d6): δ 25.11, 49.11, 61.14, 61.48, 67.56, 70.08, 73.35, 76.70, 76.93, 102.19, 111.16, 120.45, 122.54, 125.21, 125.66, 127.35, 136.01, 139.28 143.77, 153.21, 157.61; HRMS (ESI-TOF): calcd for $C_{21}H_{27}N_4O_7$ ([M + H]$^+$): *m/z* 447.1880; found: *m/z* 447.1882.

Glycoconjugate **52**: Starting from propargyl β-D-galactopyranoside **24** and 2-methyl-8-(2-azidoethoxy)quinoline **8**, product was obtained as a yellow solid (174.1 mg, 78%); m.p.: 52–54 °C; [α]$^{24}_D$ = −15.0 (c = 1.0, MeOH); ^{1}H NMR (400 MHz, DMSO-d6): δ 2.69 (s, 3H, CH$_3$), 3.21–3.38 (m, 4H, H-2$_{gal}$, H-3$_{gal}$, H-4$_{gal}$, H-5$_{gal}$), 3.49–3.57 (m, 1H, H-6a$_{gal}$), 3.60–3.66 (m, 1H, H-6b$_{gal}$), 4.22 (d, 1H, *J* = 7.3 Hz, H-1$_{gal}$), 4.32 (d, 1H, *J* = 4.5 Hz, OH), 4.58 (t, 1H, *J* = 5.6 Hz, OH), 4.60 (t, 2H, *J* = 5.2 Hz, CH$_2$N), 4.60 and 4.87 (qAB, 2H, *J* = 12.0 Hz, CH$_2$C), 4.66 (d, 1H, *J* = 5.2 Hz, OH), 4.83 (t, 1H, *J* = 2.2 Hz, OH), 4.89 (t, 2H, *J* = 5.2 Hz, CH$_2$O), 7.21 (dd, 1H, *J* = 1.3 Hz, *J* = 7.7 Hz, H-7$_{chin}$), 7.38–7.46 (m, 2H, H-3$_{chin}$, H-6$_{chin}$), 7.50 (dd, 1H, *J* = 1.2 Hz, *J* = 8.2 Hz, H-5$_{chin}$), 8.20 (d, 1H, *J* = 8.4 Hz, H-4$_{chin}$), 8.54 (s, 1H, H-5$_{triaz}$); ^{13}C NMR (100 MHz, DMSO-d6): δ 25.10, 49.11, 60.45, 61.28, 67.57, 68.13, 70.41, 73.42, 75.28, 102.72, 111.18, 120.45, 122.53, 125.19, 125.66, 127.35, 136.01, 139.28, 143.79, 153.21, 157.62; HRMS (ESI-TOF): calcd for $C_{21}H_{27}N_4O_7$ ([M + H]$^+$): *m/z* 447.1880; found: *m/z* 447.1879.

Glycoconjugate **53**: Starting from propargyl 2,3,4,6-tetra-*O*-acetyl-β-D-glucopyranoside **21** and 8-(3-azidopropoxy)quinoline **6**, product was obtained as a yellow oil (307.3 mg, 100%); [α]$^{25}_D$ = −21.4 (c = 1.0, CHCl$_3$); ^{1}H NMR (400 MHz, DMSO-d6): δ 1.88, 1.92, 1.98, 2.03 (4s, 12H, CH$_3$CO), 2.43 (p, 2H, *J* = 6.5 Hz, CH$_2$), 3.99 (ddd, 1H, *J* = 2.4 Hz, *J* = 4.9 Hz, *J* = 10.0 Hz, H-5$_{glu}$), 4.10 (dd, 1H, *J* = 2.4 Hz, *J* = 12.3 Hz, H-6a$_{glu}$), 4.15–4.24 (m, 3H, CH$_2$N, H-6b$_{glu}$), 4.66 (t, 2H, *J* = 6.9 Hz, CH$_2$O), 4.65 and 4.80 (qAB, 2H, *J* = 12.1 Hz, CH$_2$C), 4.76 (dd, 1H, *J* = 8.0 Hz, *J* = 9.6 Hz H-2$_{glu}$), 4.88 (d, 1H, *J* = 8.0 Hz, H-1$_{glu}$), 4.91 (dd-t, 1H, *J* = 9.6 Hz, *J* = 9.7 Hz, H-4$_{glu}$), 5.25 (dd-t, 1H, *J* = 9.6 Hz, *J* = 9.6 Hz, H-3$_{glu}$), 7.19 (dd, 1H, *J* = 1.9 Hz, *J* = 7.1 Hz, H-7$_{chin}$), 7.47–7.53 (m, 2H, H-3$_{chin}$, H-6$_{chin}$), 7.56 (dd, 1H, *J* = 4.0 Hz, *J* = 8.2 Hz, H-5$_{chin}$), 8.24 (s, 1H, H-5$_{triaz}$), 8.33 (dd, 1H, *J* = 1.6 Hz, *J* = 8.2 Hz, H-4$_{chin}$), 8.89 (bs, 1H, H-2$_{chin}$); ^{13}C NMR (100 MHz, DMSO-d6): δ 20.23, 20.25, 20.35, 20.47, 29.57, 46.66, 61.64, 61.85, 65.39, 68.11, 70.61, 70.83, 72.03, 98.47, 109.82, 119.93, 121.85, 124.50, 126.77, 129.03, 135.78, 139.79, 142.94, 149.01, 154.20, 168.92, 169.22, 169.48, 170.01; HRMS (ESI-TOF): calcd for $C_{29}H_{35}N_4O_{11}$ ([M + H]$^+$): *m/z* 615.2302; found: *m/z* 615.2303.

Glycoconjugate 54: Starting from propargyl 2,3,4,6-tetra-*O*-acetyl-β-D-galactopyranoside **22** and 8-(3-azidopropoxy)quinoline **6**, product was obtained as a yellow oil (307.3 mg, 100%); $[\alpha]^{25}_{D} = -16.2$ (c = 1.0, CHCl$_3$); ^{1}H NMR (400 MHz, DMSO-d6): δ 1.89, 1.90, 2.01, 2.11 (4s, 12H, CH$_3$CO), 2.43 (p, 2H, *J* = 6.4 Hz, CH$_2$), 4.01–4.11 (m, 2H, H-5$_{gal}$, H-6a$_{gal}$), 4.15–4.24 (m, 3H, H-6b$_{gal}$, CH$_2$N), 4.64 and 4.79 (qAB, 2H, *J* = 12.4 Hz, CH$_2$C), 4.66 (t, 2H, *J* = 6.8 Hz, CH$_2$O), 4.79 (d, 1H, *J* = 8.0 Hz, H-1$_{gal}$), 4.92 (dd, 1H, *J* = 8.0 Hz, *J* = 10.3 Hz, H-2$_{gal}$), 5.15 (dd, 1H, *J* = 3.6 Hz, *J* = 10.3 Hz, H-3$_{gal}$), 5.25 (dd, 1H, *J* = 0.9 Hz, *J* = 3.6 Hz, H-4$_{gal}$), 7.20 (dd, 1H, *J* = 1.5 Hz, *J* = 7.4 Hz, H-7$_{chin}$), 7.46–7.61 (m, 3H, H-3$_{chin}$, H-5$_{chin}$, H-6$_{chin}$), 8.24 (s, 1H, H-5$_{triaz}$), 8.31–8.35 (m, 1H, H-4$_{chin}$), 8.90 (bs, 1H, H-2$_{chin}$); ^{13}C NMR (100 MHz, DMSO-d6): δ 20.28, 20.29, 20.35, 20.47, 29.58, 46.66, 61.22, 61.72, 65.39, 67.28, 68.57, 69.91, 70.19, 98.89, 109.81, 119.94, 124.47, 125.27, 126.76, 128.16, 128.86, 135.77, 143.00, 148.99, 154.22, 169.03, 169.42, 169.86, 169.89; HRMS (ESI-TOF): calcd for C$_{29}$H$_{35}$N$_4$O$_{11}$ ([M + H]$^+$): *m/z* 615.2302; found: *m/z* 615.2302.

Glycoconjugate 55: Starting from propargyl 2,3,4,6-tetra-*O*-acetyl-β-D-glucopyranoside **21** and 2-methyl-8-(3-azidopropoxy)quinoline **9**, product was obtained as a yellow oil (204.3 mg, 65%); $[\alpha]^{23}_{D} = -20.2$ (c = 1.0, CHCl$_3$); ^{1}H NMR (400 MHz, DMSO-d6): δ 1.88, 1.92, 1.98, 2.03 (4s, 12H, CH$_3$CO), 2.42 (p, 2H, *J* = 6.5 Hz, CH$_2$), 2.67 (s, 3H, CH$_3$), 3.98 (ddd, 1H, *J* = 2.4 Hz, *J* = 4.9 Hz, *J* = 10.0 Hz, H-5$_{glu}$), 4.04 (dd, 1H, *J* = 2.4 Hz, *J* = 12.4 Hz, H-6a$_{glu}$), 4.15–4.24 (m, 3H, CH$_2$N, H-6b$_{glu}$), 4.64 and 4.80 (qAB, 2H, *J* = 12.3 Hz, CH$_2$C), 4.65 (t, 2H, *J* = 6.9 Hz, CH$_2$O), 4.75 (dd, 1H, *J* = 8.0 Hz, *J* = 9.6 Hz H-2$_{glu}$), 4.87 (d, 1H, *J* = 8.0 Hz, H-1$_{glu}$), 4.91 (dd-t, 1H, *J* = 9.6 Hz, *J* = 9.8 Hz, H-4$_{glu}$), 5.24 (dd-t, 1H, *J* = 9.6 Hz, *J* = 9.6 Hz, H-3$_{glu}$), 7.16 (dd, 1H, *J* = 1.2 Hz, *J* = 7.6 Hz, H-7$_{chin}$), 7.38–7.50 (m, 3H, H-3$_{chin}$, H-5$_{chin}$, H-6$_{chin}$), 8.19 (d, 1H, *J* = 8.4 Hz, H-4$_{chin}$), 8.25 (s, 1H, H-5$_{triaz}$); ^{13}C NMR (100 MHz, DMSO-d6): δ 20.23, 20.24, 20.35, 20.48, 25.05, 29.52, 46.64, 61.64, 61.83, 65.57, 68.11, 70.60, 70.83, 72.03, 98.46, 110.37, 119.86, 122.44, 124.47, 125.70, 127.32, 135.98, 139.32, 142.93, 153.67, 157.30, 168.92, 169.23, 169.48, 170.01; HRMS (ESI-TOF): calcd for C$_{30}$H$_{37}$N$_4$O$_{11}$ ([M + H]$^+$): *m/z* 629.2459; found: *m/z* 629.2458.

Glycoconjugate 56: Starting from propargyl 2,3,4,6-tetra-*O*-acetyl-β-D-galactopyranoside **22** and 2-methyl-8-(3-azidopropoxy)quinoline **9**, product was obtained as a yellow oil (242.0 mg, 77%); $[\alpha]^{24}_{D}$ = −8.8 (c = 1.0, CHCl$_3$); ^{1}H NMR (400 MHz, DMSO-d6): δ 1.89, 1.90, 2.01, 2.11 (4s, 12H, CH$_3$CO), 2.42 (p, 2H, *J* = 6.3 Hz, CH$_2$), 2.67 (s, 3H, CH$_3$), 4.01–4.11 (m, 2H, H-5$_{gal}$, H-6a$_{gal}$), 4.15–4.24 (m, 3H, H-6a$_{gal}$, CH$_2$N), 4.64 and 4.79 (qAB, 2H, *J* = 12.6 Hz, CH$_2$C), 4.66 (t, 2H, *J* = 6.9 Hz, CH$_2$O), 4.78 (d, 1H, *J* = 8.0 Hz, H-1$_{gal}$), 4.92 (dd, 1H, *J* = 8.0 Hz, *J* = 10.4 Hz, H-2$_{gal}$), 5.14 (dd, 1H, *J* = 3.6 Hz, *J* = 10.4 Hz, H-3$_{gal}$), 5.25 (dd, 1H, *J* = 0.9 Hz, *J* = 3.6 Hz, H-4$_{gal}$), 7.16 (dd, 1H, *J* = 0.8 Hz, *J* = 7.5 Hz, H-7$_{chin}$), 7.37–7.51 (m, 3H, H-3$_{chin}$, H-5$_{chin}$, H-6$_{chin}$), 8.19 (d, 1H, *J* = 8.4 Hz, H-4$_{chin}$), 8.25 (s, 1H, H-5$_{triaz}$); ^{13}C NMR (100 MHz, DMSO-d6): δ18.53, 20.28, 20.29, 20.35, 20.48, 29.53, 46.64, 61.23, 61.70, 65.55, 68.57, 69.91, 70.19, 72.20, 98.88, 110.33, 119.87, 122.45, 124.46, 125.71, 127.31, 135.96, 139.32, 143.02, 153.26, 158.61, 169.03, 169.43, 169.87, 169.90; HRMS (ESI-TOF): calcd for C$_{30}$H$_{37}$N$_4$O$_{11}$ ([M + H]$^+$): *m/z* 629.2459; found: *m/z* 629.2455.

Glycoconjugate 57: Starting from propargyl β-D-glucopyranoside **23** and 8-(3-azidopropoxy)quinoline **6**, product was obtained as a white solid (223.2 mg, 100%); m.p.: 77–79 °C; $[\alpha]^{24}_{D} = -19.2$ (c = 1.0, MeOH); ^{1}H NMR (400 MHz, DMSO-d6): δ 2.42 (p, 2H, *J* = 6.4 Hz, CH$_2$), 2.94-3.09 (m, 2H, H-2$_{glu}$, H-5$_{glu}$), 3.10-3.17 (m, 2H, H-3$_{glu}$, H-4$_{glu}$), 3.40–3.50 (m, 1H, H-6a$_{glu}$), 3.67–3.75 (m, 1H, H-6b$_{glu}$), 4.05–4.11 (m, 1H, OH), 4.21 (t, 2H, *J* = 6.1 Hz, CH$_2$N), 4.27 (d, 1H, *J* = 7.8 Hz, H-1$_{glu}$), 4.34 (t, 1H, *J* = 5.1 Hz, OH), 4.57 (t, 1H, *J* = 5.9 Hz, OH), 4.64 (t, 1H, *J* = 7.1 Hz, CH$_2$O), 4.64 and 4.85 (qAB, 2H, *J* = 12.2 Hz, CH$_2$C), 5.01 (d, 1H, *J* = 4.9 Hz, OH), 7.20 (dd, 1H, *J* = 2.2 Hz, *J* = 6.8 Hz, H-7$_{chin}$), 7.47–7.58 (m, 3H, H-3$_{chin}$, H-5$_{chin}$, H-6$_{chin}$), 8.29 (s, 1H, H-5$_{triaz}$), 8.32 (dd, 1H, *J* = 1.7 Hz, *J* = 8.3 Hz, H-4$_{chin}$), 8.90 (dd, 1H, *J* = 1.6 Hz, *J* = 4.1 Hz, H-2$_{chin}$); ^{13}C NMR (100 MHz, DMSO-d6): δ 29.61, 46.61, 61.16, 61.57, 65.43, 70.11, 73.39, 76.69, 76.94, 102.14, 109.84, 119.92, 121.86, 124.42, 126.79, 129.04, 135.81, 139.76, 143.89, 149.07, 154.19; HRMS (ESI-TOF): calcd for C$_{21}$H$_{27}$N$_4$O$_7$ ([M + H]$^+$): *m/z* 447.1880; found: *m/z* 447.1880.

Glycoconjugate 58: Starting from propargyl β-D-galactopyranoside **24** and 8-(3-azidopropoxy) quinoline **6**, product was obtained as a yellow solid (169.7 mg, 76%); m.p.: 50–54 °C; $[\alpha]^{24}_{D}$ = −11.2 (c = 1.0, MeOH); ^{1}H NMR (400 MHz, DMSO-d6): δ 2.42 (p, 2H, *J* = 6.5 Hz, CH$_2$), 3.22-3.40 (m,

4H, H-2$_{gal}$, H-3$_{gal}$, H-4$_{gal}$, H-5$_{gal}$), 3.50-3.58 (m, 1H, H-6a$_{gal}$), 3.60–3.66 (m, 1H, H-6b$_{gal}$), 4.20 (t, 2H, *J* = 6.0 Hz, CH$_2$N), 4.21 (d, 1H, *J* = 6.3 Hz, H-1$_{gal}$), 4.34 (d, 1H, *J* = 4.4 Hz, OH), 4.57–4.71 (m, 2H, OH), 4.62 and 4.83 (qAB, 2H, *J* = 12.4 Hz, CH$_2$C), 4.64 (t, 2H, *J* = 7.0 Hz, CH$_2$O), 4.86 (d, 1H, *J* = 5.7 Hz, OH), 7.20 (dd, 1H, *J* = 2.1 Hz, *J* = 6.8 Hz, H-7$_{chin}$), 7.46–7.59 (m, 3H, H-3$_{chin}$, H-5$_{chin}$, H-6$_{chin}$), 8.28 (s, 1H, H-5$_{triaz}$), 8.32 (dd, 1H, *J* = 1.6 Hz, *J* = 8.4 Hz, H-4$_{chin}$), 8.90 (dd, 1H, *J* = 1.7 Hz, *J* = 4.1 Hz, H-2$_{chin}$); ^{13}C NMR (100 MHz, DMSO-d6): δ 29.62, 46.61, 60.53, 61.42, 65.44, 68.18, 70.47, 73.39, 75.32, 102.70, 109.85, 119.91, 121.85, 124.36, 126.79, 129.04, 135.79, 139.76, 143.96, 149.08, 154.19; HRMS (ESI-TOF): calcd for C$_{21}$H$_{27}$N$_4$O$_7$ ([M + H]$^+$): *m/z* 447.1880; found: *m/z* 447.1879.

Glycoconjugate **59:** Starting from propargyl β-D-glucopyranoside **23** and 2-methyl-8-(3-azidopropoxy) quinoline **9**, product was obtained as a yellow solid (200.3 mg, 87%); m.p.: 47-50 °C; [α]$^{23}_D$ = −16.6 (c = 1.0, MeOH); ^{1}H NMR (400 MHz, DMSO-d6): δ 2.42 (p, 2H, *J* = 6.5 Hz, CH$_2$), 2.68 (s, 3H, CH$_3$), 2.93–3.09 (m, 2H, H-2$_{glu}$, H-5$_{glu}$), 3.10–3.20 (m, 2H, H-3$_{glu}$, H-4$_{glu}$), 3.40–3.50 (m, 1H, H-6a$_{glu}$), 3.66–3.75 (m, 1H, H-6b$_{glu}$), 4.20 (t, 2H, *J* = 6.2 Hz, CH$_2$N), 4.26 (d, 1H, *J* = 7.8 Hz, H-1$_{glu}$), 4.34 (t, 2H, *J* = 5.0 Hz, OH), 4.56 (t, 1H, *J* = 5.8 Hz, OH), 4.63 and 4.84 (qAB, 2H, *J* = 12.2 Hz, CH$_2$C), 4.64 (t, 2H, *J* = 6.9 Hz, CH$_2$O), 5.00 (d, 1H, *J* = 4.9 Hz, OH), 7.16 (dd, 1H, *J* = 1.3 Hz, *J* = 7.6 Hz, H-7$_{chin}$), 7.38–7.49 (m, 3H, H-3$_{chin}$, H-5$_{chin}$, H-6$_{chin}$), 8.19 (d, 1H, *J* = 8.4 Hz, H-4$_{chin}$), 8.26 (s, 1H, H-5$_{triaz}$); ^{13}C NMR (100 MHz, DMSO-d6): δ 25.09, 29.57, 46.60, 61.16, 61.56, 65.57, 70.12, 73.40, 76.70, 76.95, 102.15, 110.35, 119.86, 122.48, 124.40, 125.75, 131.21, 136.01, 139.31, 143.15, 150.40, 153.68; HRMS (ESI-TOF): calcd for C$_{22}$H$_{29}$N$_4$O$_7$ ([M + H]$^+$): *m/z* 461.2036; found: *m/z* 461.2039.

Glycoconjugate **60:** Starting from propargyl β-D-galactopyranoside **24** and 2-methyl-8-(3-azidopropoxy) quinoline **9**, product was obtained as a brown solid (149.7 mg, 65%); m.p.: 50–54 °C; [α]$^{24}_D$ = −4.6 (c = 1.0, MeOH); ^{1}H NMR (400 MHz, DMSO-d6): δ 2.42 (p, 2H, *J* = 6.5 Hz, CH$_2$), 2.67 (s, 3H, CH$_3$), 3.22–3.42 (m, 4H, H-2$_{gal}$, H-3$_{gal}$, H-4$_{gal}$, H-5$_{gal}$), 3.49–3.57 (m, 1H, H-6a$_{gal}$), 3.60–3.66 (m, 1H, H-6b$_{gal}$), 4.20 (t, 2H, *J* = 5.9 Hz, CH$_2$N), 4.21 (d, 1H, *J* = 7.0 Hz, H-1$_{gal}$), 4.34 (bs, 1H, OH), 4.54-4.72 (m, 4H, CH$_2$O, CH$_2$C, OH), 4.77-4.89 (m, 2H, CH$_2$C, OH), 7.16 (dd, 1H, *J* = 1.2 Hz, *J* = 7.6 Hz, H-7$_{chin}$), 7.37-7.50 (m, 3H, H-3$_{chin}$, H-5$_{chin}$, H-6$_{chin}$), 8.19 (d, 1H, *J* = 8.4 Hz, H-4$_{chin}$), 8.26 (s, 1H, H-5$_{triaz}$); ^{13}C NMR (100 MHz, DMSO-d6): δ 25.00, 29.56, 46.58, 60.52, 61.40, 65.59, 68.18, 70.48, 73.40, 75.31, 102.71, 110.44, 119.85, 122.51, 124.32, 125.81, 127.34, 136.18, 139.12, 143.96, 153.58, 157.34; HRMS (ESI-TOF): calcd for C$_{22}$H$_{29}$N$_4$O$_7$ ([M + H]$^+$): *m/z* 461.2036; found: *m/z* 461.2038.

Glycoconjugate **61:** Starting from propargyl 2,3,4,6-tetra-*O*-acetyl-β-D-glucopyranoside **21** and 8-(4-azidobutoxy)quinoline **7**, product was obtained as a yellow oil (301.7 mg, 96%); [α]$^{23}_D$ = −17.8 (c = 1.0, CHCl$_3$); ^{1}H NMR (400 MHz, CDCl$_3$): δ 1.61 (bs, 2H, CH$_2$), 1.92, 1.98, 2.01, 2.08 (4s, 12H, CH$_3$CO), 2.26 (p, 2H, *J* = 7.1 Hz, CH$_2$), 3.69 (ddd, 1H, *J* = 2.4 Hz, *J* = 4.7 Hz, *J* = 9.9 Hz, H-5$_{glu}$), 4.12 (dd, 1H, *J* = 2.4 Hz, *J* = 12.3 Hz, H-6a$_{glu}$), 4.24 (dd, 1H, *J* = 4.7 Hz, *J* = 12.3 Hz, H-6a$_{glu}$), 4.28 (t, 2H, *J* = 6.1 Hz, CH$_2$N), 4.58 (t, 2H, *J* = 6.9 Hz, CH$_2$O), 4.68 (d, 1H, *J* = 8.0 Hz, H-1$_{glu}$), 4.81 and 4.93 (qAB, 2H, *J* = 12.6 Hz, CH$_2$C), 5.00 (dd, 1H, *J* = 8.0 Hz, *J* = 9.5 Hz H-2$_{glu}$), 5.08 (dd-t, 1H, *J* = 9.4 Hz, *J* = 9.8 Hz, H-4$_{glu}$), 5.17 (dd-t, 1H, *J* = 9.4 Hz, *J* = 9.4 Hz, H-3$_{glu}$), 7.05 (dd, 1H, *J* = 1.4 Hz, *J* = 7.5 Hz, H-7$_{chin}$), 7.38–7.49 (m, 3H, H-3$_{chin}$, H-5$_{chin}$, H-6$_{chin}$), 7.95 (s, 1H, H-5$_{triaz}$), 8.14 (dd, 1H, *J* = 1.7 Hz, *J* = 8.3 Hz, H-4$_{chin}$), 8.93 (dd, 1H, *J* = 1.7 Hz, *J* = 4.2 Hz, H-2$_{chin}$); ^{13}C NMR (100 MHz, CDCl$_3$): δ 20.60, 20.67, 20.75, 20.79, 25.61, 27.83, 49.93, 61.85, 62.86, 68.36, 71.24, 71.89, 72.86, 77.22, 99.66, 108.81, 119.91, 121.71, 123.74, 126.69, 129.54, 135.96, 140.35, 143.77, 149.32, 154.59, 169.35, 169.42, 170.19, 170.65; HRMS (ESI-TOF): calcd for C$_{29}$H$_{35}$N$_4$O$_{11}$ ([M + H]$^+$): *m/z* 629.2459; found: *m/z* 629.2458.

Glycoconjugate **62:** Starting from propargyl 2,3,4,6-tetra-*O*-acetyl-β-D-galactopyranoside **22** and 8-(4-azidobutoxy)quinoline **7**, product was obtained as a yellow oil (292.3 mg, 93%); [α]$^{25}_D$ = −12.8 (c = 1.0, CHCl$_3$); ^{1}H NMR (400 MHz, DMSO-d6): δ 1.78–1.87 (m, 2H, CH$_2$), 1.90, 1.90, 2.01, 2.10 (4s, 12H, CH$_3$CO), 2.05–2.10 (m, 2H, CH$_2$), 4.01-4.11 (m, 2H, H-5$_{gal}$, H-6a$_{gal}$), 4.16-4.25 (m, 3H, H-6b$_{gal}$, CH$_2$N), 4.54 (t, 2H, *J* = 7.0 Hz, CH$_2$O), 4.64 and 4.80 (qAB, 2H, *J* = 12.4 Hz, CH$_2$C), 4.81 (d, 1H, *J* = 8.0 Hz, H-1$_{gal}$), 4.92 (dd, 1H, *J* = 8.0 Hz, *J* = 10.3 Hz, H-2$_{gal}$), 5.15 (dd, 1H, *J* = 3.6 Hz, *J* = 10.3 Hz, H-3$_{gal}$), 5.25 (dd, 1H, *J*

= 0.9 Hz, *J* = 3.6 Hz, H-4$_{gal}$), 7.17–7.21 (m, 1H, H-7$_{chin}$), 7.47–7.57 (m, 3H, H-3$_{chin}$, H-5$_{chin}$, H-6$_{chin}$), 8.25 (s, 1H, H-5$_{triaz}$), 8.31 (dd, 1H, *J* = 1.7 Hz, *J* = 8.3 Hz, H-4$_{chin}$), 8.85 (bs, 1H, H-2$_{chin}$); ^{13}C NMR (100 MHz, DMSO-d6): δ 20.29, 20.32, 20.35, 20.48, 25.53, 27.04, 49.08, 61.21, 61.81, 67.28, 67.85, 68.58, 69.90, 70.19, 98.97, 109.37, 119.55, 121.79, 124.44, 126.80, 129.00, 135.76, 139.72, 142.87, 148.92, 154.38, 169.05, 169.42, 169.86, 169.89; HRMS (ESI-TOF): calcd for C$_{30}$H$_{37}$N$_4$O$_{11}$ ([M + H]$^+$): *m/z* 629.2459; found: *m/z* 629.2459.

Glycoconjugate 63: Starting from propargyl 2,3,4,6-tetra-*O*-acetyl-β-D-glucopyranoside **21** and 2-methyl-8-(4-azidobutoxy)quinoline **10**, product was obtained as a yellow oil (295.6 mg, 92%); [α]$^{23}_D$ = −18.8 (c = 1.0, CHCl$_3$); ^{1}H NMR (400 MHz, DMSO-d6): δ 1.80 (p, 2H, *J* = 6.6 Hz, CH$_2$), 1.88, 1.91, 1.97, 2.02 (4s, 12H, CH$_3$CO), 2.08 (p, 2H, *J* = 7.4 Hz, CH$_2$), 2.63 (s, 3H, CH$_3$), 3.97 (ddd, 1H, *J* = 2.4 Hz, *J* = 4.9 Hz, *J* = 10.0 Hz, H-5$_{glu}$), 4.03 (dd, 1H, *J* = 2.4 Hz, *J* = 12.4 Hz, H-6a$_{glu}$), 4.14–4.24 (m, 3H, CH$_2$N, H-6b$_{glu}$), 4.59 (t, 2H, *J* = 6.9 Hz, CH$_2$O), 4.64 and 4.80 (qAB, 2H, *J* = 12.4 Hz, CH$_2$C), 4.75 (dd, 1H, *J* = 8.0 Hz, *J* = 9.7 Hz H-2$_{glu}$), 4.90 (d, 1H, *J* = 8.0 Hz, H-1$_{glu}$), 4.91 (dd-t, 1H, *J* = 9.7 Hz, *J* = 9.7 Hz, H-4$_{glu}$), 5.24 (dd-t, 1H, *J* = 9.6 Hz, *J* = 9.6 Hz, H-3$_{glu}$), 7.15 (dd, 1H, *J* = 1.8 Hz, *J* = 7.2 Hz, H-7$_{chin}$), 7.38–7.47 (m, 3H, H-3$_{chin}$, H-5$_{chin}$, H-6$_{chin}$), 8.18 (d, 1H, *J* = 8.4 Hz, H-4$_{chin}$), 8.34 (s, 1H, H-5$_{triaz}$); ^{13}C NMR (100 MHz, DMSO-d6): δ 20.23, 20.30, 20.34, 20.47, 24.93, 25.25, 27.23, 49.08, 61.64, 61.92, 68.09, 68.14, 70.60, 70.82, 72.03, 98.53, 109.64, 119.42, 122.41, 124.62, 125.74, 127.26, 135.96, 139.19, 142.70, 153.89, 157.21, 168.92, 169.21, 169.46, 170.00; HRMS (ESI-TOF): calcd for C$_{31}$H$_{39}$N$_4$O$_{11}$ ([M + H]$^+$): *m/z* 643.2615; found: *m/z* 643.2618.

Glycoconjugate 64: Starting from propargyl 2,3,4,6-tetra-*O*-acetyl-β-D-galactopyranoside **22** and 2-methyl-8-(4-azidobutoxy)quinoline **10**, product was obtained as a yellow oil (321.3 mg, 100%); [α]$^{24}_D$ = −13.6 (c = 1.0, CHCl$_3$); ^{1}H NMR (400 MHz, DMSO-d6): δ 1.81 (p, 2H, *J* = 6.6 Hz, CH$_2$), 1.89, 1.89, 2.00, 2.10 (4s, 12H, CH$_3$CO), 2.03–2.10 (m, 2H, CH$_2$), 2.63 (s, 3H, CH$_3$), 4.01–4.11 (m, 2H, H-5$_{gal}$, H-6a$_{gal}$), 4.15–4.25 (m, 3H, H-6a$_{gal}$, CH$_2$N), 4.59 (t, 2H, *J* = 7.0 Hz, CH$_2$O), 4.64 and 4.80 (qAB, 2H, *J* = 12.9 Hz, CH$_2$C), 4.81 (d, 1H, *J* = 8.0 Hz, H-1$_{gal}$), 4.92 (dd, 1H, *J* = 8.0 Hz, *J* = 10.3 Hz, H-2$_{gal}$), 5.14 (dd, 1H, *J* = 3.6 Hz, *J* = 10.3 Hz, H-3$_{gal}$), 5.24 (dd, 1H, *J* = 0.9 Hz, *J* = 3.6 Hz, H-4$_{gal}$), 7.15 (dd, 1H, *J* = 1.8 Hz, *J* = 7.2 Hz, H-7$_{chin}$), 7.38–7.47 (m, 3H, H-3$_{chin}$, H-5$_{chin}$, H-6$_{chin}$), 8.18 (d, 1H, *J* = 8.4 Hz, H-4$_{chin}$), 8.33 (s, 1H, H-5$_{triaz}$); ^{13}C NMR (100 MHz, DMSO-d6): δ 20.22, 20.28, 20.34, 20.47, 24.93, 25.26, 27.25, 49.08, 61.20, 61.78, 67.28, 68.14, 68.57, 69.89, 70.19, 98.95, 109.64, 119.41, 122.40, 124.57, 125.74, 127.26, 135.96, 139.19, 142.78, 153.89, 157.21, 168.02, 169.41, 169.84, 169.88; HRMS (ESI-TOF): calcd for C$_{31}$H$_{39}$N$_4$O$_{11}$ ([M + H]$^+$): *m/z* 643.2615; found: *m/z* 643.2612.

Glycoconjugate 65: Starting from propargyl β-D-glucopyranoside **23** and 8-(4-azidobutoxy)quinoline **7**, product was obtained as a yellow solid (165.8 mg, 72%); m.p.: 49–51 °C; [α]$^{24}_D$ = −20.2 (c = 1.0, MeOH); ^{1}H NMR (400 MHz, DMSO-d6): δ 1.77-1.89 (m, 2H, CH$_2$), 2.03-2.15 (m, 2H, CH$_2$), 2.94–3.09 (m, 2H, H-2$_{glu}$, H-5$_{glu}$), 3.10–3.17 (m, 2H, H-3$_{glu}$, H-4$_{glu}$), 3.40–3.50 (m, 1H, H-6a$_{glu}$), 3.67–3.75 (m, 1H, H-6b$_{glu}$), 4.05–4.11 (m, 1H, OH), 4.21 (m, 2H, CH$_2$N), 4.27 (d, 1H, *J* = 7.8 Hz, H-1$_{glu}$), 4.34 (t, 1H, *J* = 5.1 Hz, OH), 4.52 (t, 1H, *J* = 6.8 Hz, CH$_2$O), 4.57 (t, 1H, *J* = 5.9 Hz, OH), 4.64 and 4.85 (qAB, 2H, *J* = 12.2 Hz, CH$_2$C), 5.01 (d, 1H, *J* = 4.9 Hz, OH), 7.17–7.22 (m, 1H, H-7$_{chin}$), 7.45–7.61 (m, 3H, H-3$_{chin}$, H-5$_{chin}$, H-6$_{chin}$), 8.28 (s, 1H, H-5$_{triaz}$), 8.31–8.35 (m, 1H, H-4$_{chin}$), 8.87 (bs, 1H, H-2$_{chin}$); ^{13}C NMR (100 MHz, DMSO-d6): δ 25.61, 26.96, 49.06, 61.16, 61.59, 67.84, 70.11, 73.38, 76.70, 76.95, 102.15, 109.35, 119.64, 121.85, 124.42, 126.84, 128.86, 135.68, 139.79, 143.73, 148.98, 154.35; HRMS (ESI-TOF): calcd for C$_{22}$H$_{29}$N$_4$O$_7$ ([M + H]$^+$): *m/z* 461.2036; found: *m/z* 461.2036.

Glycoconjugate 66: Starting from propargyl β-D-galactopyranoside **24** and 8-(4-azidobutoxy)quinoline **7**, product was obtained as a yellow solid (207.2 mg, 90%); m.p.: 62–64 °C; [α]$^{24}_D$ = −13.0 (c = 1.0, MeOH); ^{1}H NMR (400 MHz, DMSO-d6): δ 1.83 (p, 2H, *J* = 6.3 Hz, CH$_2$), 2.08 (p, 2H, *J* = 7.1 Hz, CH$_2$), 3.24–3.30 (m, 1H, H-2$_{gal}$), 3.33–3.48 (m, 3H, H-3$_{gal}$, H-4$_{gal}$, H-5$_{gal}$), 3.50–3.57 (m, 1H, H-6a$_{gal}$), 3.61–3.66 (m, 1H, H-6b$_{gal}$), 4.21 (t, 2H, *J* = 6.3 Hz, CH$_2$N), 4.22 (d, 1H, *J* = 7.5 Hz, H-1$_{gal}$), 4.31–4.36 (m, 2H, OH), 4.52 (t, 2H, *J* = 7.0 Hz, CH$_2$O), 4.62 and 4.83 (qAB, 2H, *J* = 12.1 Hz, CH$_2$C), 4.67 (d, 1H, *J* = 5.1 Hz, OH), 4.87 (d, 1H, *J* = 4.6 Hz, OH), 7.17–7.21 (m, 1H, H-7$_{chin}$), 7.46–7.57 (m, 3H, H-3$_{chin}$, H-5$_{chin}$, H-6$_{chin}$),

8.27 (s, 1H, H-5$_{triaz}$), 8.31 (dd, 1H, *J* = 1.7 Hz, *J* = 8.3 Hz, H-4$_{chin}$), 8.87 (dd, 1H, *J* = 1.7 Hz, *J* = 4.1 Hz, H-2$_{chin}$); ^{13}C NMR (100 MHz, DMSO-d6): δ 25.59, 26.98, 49.03, 60.52, 61.45, 67.82, 68.18, 70.47, 73.40, 75.32, 102.73, 109.39, 119.55, 121.80, 124.33, 126.80, 129.00, 135.75, 139.71, 143.77, 148.99, 154.38; HRMS (ESI-TOF): calcd for $C_{22}H_{29}N_4O_7$ ([M + H]$^+$): *m/z* 461.2036; found: *m/z* 461.2035.

Glycoconjugate 67: Starting from propargyl β-D-glucopyranoside **23** and 2-methyl-8-(4-azidobutoxy) quinoline **10**, product was obtained as an orange solid (180.3 mg, 76%); m.p.: 75–78 °C; [α]$^{24}_D$ = −17.6 (c = 1.0, MeOH); ^{1}H NMR (400 MHz, DMSO-d6): δ 1.82 (p, 2H, *J* = 6.5 Hz, CH$_2$), 2.08 (p, 2H, *J* = 7.0 Hz, CH$_2$), 2.64 (s, 3H, CH$_3$), 2.94–3.09 (m, 2H, H-2$_{glu}$, H-5$_{glu}$), 3.10–3.19 (m, 2H, H-3$_{glu}$, H-4$_{glu}$), 3.41–3.49 (m, 1H, H-6a$_{glu}$), 3.66–3.74 (m, 1H, H-6b$_{glu}$), 4.20 (t, 2H, *J* = 6.3 Hz, CH$_2$N), 4.27 (d, 1H, *J* = 7.8 Hz, H-1$_{glu}$), 4.55 (d, 1H, *J* = 5.9 Hz, OH), 4.56 (t, 2H, *J* = 6.9 Hz, CH$_2$O), 4.64 and 4.86 (qAB, 2H, *J* = 12.2 Hz, CH$_2$C), 4.89 (t, 2H, *J* = 5.2 Hz, OH), 4.91 (t, 1H, *J* = 4.7 Hz, OH), 5.01 (d, 1H, *J* = 4.9 Hz, OH), 7.15 (dd, 1H, *J* = 1.8 Hz, *J* = 7.1 Hz, H-7$_{chin}$), 7.38–7.47 (m, 3H, H-3$_{chin}$, H-5$_{chin}$, H-6$_{chin}$), 8.18 (d, 1H, *J* = 8.4 Hz, H-4$_{chin}$), 8.31 (s, 1H, H-5$_{triaz}$); ^{13}C NMR (100 MHz, DMSO-d6): δ 25.40, 25.44, 27.09, 49.07, 61.13, 61.55, 68.07, 70.09, 73.37, 76.69, 76.93, 102.13, 109.62, 119.44, 122.43, 124.51, 125.78, 127.28, 135.98, 139.16, 145.72, 148.08, 153.85; HRMS (ESI-TOF): calcd for $C_{23}H_{31}N_4O_7$ ([M + H]$^+$): *m/z* 475.2193; found: *m/z* 475.2194.

Glycoconjugate 68: Starting from propargyl β-D-galactopyranoside **24** and 2-methyl-8-(4-azidobutoxy) quinoline **10**, product was obtained as an orange solid (156.6 mg, 66%); m.p.: 38–41 °C; [α]$^{23}_D$ = −6.0 (c = 1.0, MeOH); ^{1}H NMR (400 MHz, DMSO-d6): δ 1.82 (m, 2H, CH$_2$), 2.08 (m, 2H, CH$_2$), 2.64 (s, 3H, CH$_3$), 3.23–3.43 (m, 4H, H-2$_{gal}$, H-3$_{gal}$, H-4$_{gal}$, H-5$_{gal}$), 3.49–3.58 (m, 1H, H-6a$_{gal}$), 3.61–3.66 (m, 1H, H-6b$_{gal}$), 4.15–4.25 (m 3H, H-1$_{gal}$, CH$_2$N), 4.56 (t, 2H, *J* = 6.8 Hz, CH$_2$O), 4.62 and 4.83 (qAB, 2H, *J* = 12.1 Hz, CH$_2$C), 7.16 (m, 1H, H-7$_{chin}$), 7.36–7.52 (m, 3H, H-3$_{chin}$, H-5$_{chin}$, H-6$_{chin}$), 8.19 (d, 1H, *J* = 8.2 Hz, H-4$_{chin}$), 8.29 (s, 1H, H-5$_{triaz}$); ^{13}C NMR (100 MHz, DMSO-d6): δ 24.94, 25.40, 27.10, 49.06, 60.50, 61.43, 68.08, 68.17, 70.47, 73.41, 75.31, 102.73, 109.74, 119.43, 122.45, 124.40, 125.81, 127.28, 136.09, 139.06, 143.74, 153.83, 157.26; HRMS (ESI-TOF): calcd for $C_{23}H_{31}N_4O_7$ ([M + H]$^+$): *m/z* 475.2193; found: *m/z* 475.2199.

Glycoconjugate 69: Starting from 2-azidoethyl 2,3,4,6-tetra-*O*-acetyl-β-D-glucopyranoside **27** and 8-(2-propyn-1-yloxy)quinoline **3**, product was obtained as a yellow solid (234.2 mg, 78%); m.p.: 52–55 °C; [α]$^{22}_D$ = −13.6 (c = 1.0, CHCl$_3$); ^{1}H NMR (400 MHz, CDCl$_3$): δ 1.92, 1.98, 2.02, 2.06 (4s, 12H, CH$_3$CO), 3.67 (ddd, 1H, *J* = 2.4 Hz, *J* = 4.7 Hz, *J* = 10.0 Hz, H-5$_{glu}$), 3.93–3.99 (m, 1H, CH$_2$O), 4.11 (dd, 1H, *J* = 2.4 Hz, *J* = 12.4 Hz, H-6a$_{glu}$), 4.19–4.24 (m, 2H, H-6b$_{glu}$, CH$_2$O), 4.48 (d, 1H, *J* = 7.9 Hz, H-1$_{glu}$), 4.49–4.62 (m, 2H, CH$_2$N), 4.95 (dd, 1H, *J* = 7.9 Hz, *J* = 9.5 Hz H-2$_{glu}$), 5.04 (dd, 1H, *J* = 9.4 Hz, *J* = 10.0 Hz, H-4$_{glu}$), 5.16 (dd-t, 1H, *J* = 9.4 Hz, *J* = 9.5 Hz, H-3$_{glu}$), 5.54 (s, 2H, CH$_2$O$_{chin}$), 7.32–7.50 (m, 4H, H-3$_{chin}$, H-5$_{chin}$, H-6$_{chin}$, H-7$_{chin}$), 7.84 (s, 1H, H-5$_{triaz}$), 8.14 (d, 1H, *J* = 8.0 Hz, H-4$_{chin}$), 8.94 (bs, 1H, H-2$_{chin}$); ^{13}C NMR (100 MHz, CDCl$_3$): δ 20.53, 20.55, 20.64, 20.70, 50.06, 61.74, 62.79, 67.58, 68.25, 70.90, 71.99, 72.52, 100.54, 110.09, 120.29, 121.63, 124.62, 126.77, 129.50, 136.05, 140.21, 143.85, 149.26, 153.90, 169.29, 169.35, 170.08, 170.54; HRMS (ESI-TOF): calcd for $C_{28}H_{33}N_4O_{11}$ ([M + H]$^+$): *m/z* 601.2146; found: *m/z* 601.2149.

Glycoconjugate 70: Starting from 2-azidoethyl 2,3,4,6-tetra-*O*-acetyl-β-D-galactopyranoside **28** and 8-(2-propyn-1-yloxy)quinoline **3**, product was obtained as a yellow solid (186.2 mg, 62%); m.p.: 55–58 °C; [α]$^{23}_D$ = −18.4 (c = 1.0, CHCl$_3$); ^{1}H NMR (400 MHz, DMSO-d6): δ 1.90, 2.00, 2.09, 2.10 (4s, 12H, CH$_3$CO), 3.91–3.99 (m, 1H, CH$_2$O), 4.00-4.22 (m, 4H, H-6a$_{gal}$, H-6b$_{gal}$, H-5$_{gal}$, CH$_2$O), 4.53–4.66 (m, 2H, CH$_2$N), 4.74 (d, 1H, *J* = 8.0 Hz, H-1$_{gal}$), 4.91 (dd, 1H, *J* = 8.0 Hz, *J* = 10.4, H-2$_{gal}$), 5.12 (dd, 1H, *J* = 3.6 Hz, *J* = 10.4 Hz, H-3$_{gal}$), 5.25 (dd, 1H, *J* = 0.8 Hz, *J* = 3.6 Hz, H-4$_{gal}$), 5.35 (s, 2H, CH$_2$O$_{chin}$), 7.41 (dd, 1H, *J* = 3.4 Hz, *J* = 5.6 Hz, H-7$_{chin}$), 7.50–7.57 (m, 3H, H-3$_{chin}$, H-5$_{chin}$, H-6$_{chin}$), 8.15 (s, 1H, H-5$_{triaz}$), 8.31 (dd, 1H, *J* = 1.6 Hz, *J* = 8.3 Hz, H-4$_{chin}$), 8.83 (bs, 1H, H-2$_{chin}$); ^{13}C NMR (100 MHz, DMSO-d6): δ 20.28, 20.32, 20.34, 20.47, 49.34, 61.21, 61.88, 67.26, 68.31, 69.98, 70.08, 79.14, 99.61, 110.10, 120.05,

121.82, 124.97, 126.72, 129.03, 135.75, 139.75, 142.46, 148.92, 153.85, 169.13, 169.43, 169.86, 169.88; HRMS (ESI-TOF): calcd for $C_{28}H_{33}N_4O_{11}$ ([M + H]$^+$): *m/z* 601.2146; found: *m/z* 601.2140.

Glycoconjugate **71**: Starting from 2-azidoethyl 2,3,4,6-tetra-*O*-acetyl-β-D-glucopyranoside **27** and 2-methyl-8-(2-propyn-1-yloxy)quinoline **4**, product was obtained as a pink solid (298.1 mg, 97%); m.p.: 50–53 °C; [α]$^{24}_D$ = −13.0 (c = 1.0, CHCl$_3$); ^{1}H NMR (400 MHz, DMSO-d6): δ 1.89, 1.92, 1.98, 2.01 (4s, 12H, CH$_3$CO), 2.63 (s, 3H, CH$_3$), 3.91–4.00 (m, 2H, H-5$_{glu}$, CH$_2$O), 4.04 (dd, 1H, *J* = 2.5 Hz, *J* = 12.4 Hz, H-6a$_{glu}$), 4.09–4.13 (m, 1H, CH$_2$O), 4.17 (dd, 1H, *J* = 5.0 Hz, *J* = 12.4 Hz, H-6b$_{glu}$), 4.52–4.66 (m, 2H, CH$_2$N), 4.75 (dd, 1H, *J* = 8.1 Hz, *J* = 9.7 Hz, H-2$_{glu}$), 4.85 (d, 1H, *J* = 8.1 Hz, H-1$_{glu}$), 4.90 (dd-t, 1H, *J* = 9.4 Hz, *J* = 9.8 Hz, H-4$_{glu}$), 5.23 (dd-t, 1H, *J* = 9.4 Hz, *J* = 9.7 Hz, H-3$_{glu}$), 5.34 (s, 2H, CH$_2$O$_{chin}$), 7.37 (dd, 1H, *J* = 1.7 Hz, *J* = 7.4 Hz, H-7$_{chin}$), 7.41 (d, 1H, *J* = 8.4 Hz, H-3$_{chin}$), 7.43 (dd, 1H, *J* = 7.4 Hz, *J* = 8.1 Hz, H-6$_{chin}$), 7.47 (dd, 1H, *J* = 1.7 Hz, *J* = 8.1 Hz, H-5$_{chin}$), 8.16 (s, 1H, H-5$_{triaz}$), 8.18 (d, 1H, *J* = 8.4 Hz, H-4$_{chin}$); ^{13}C NMR (100 MHz, DMSO-d6): δ 20.19, 20.20, 20.31, 20.43, 24.85, 49.27, 61.60, 61.71, 67.39, 68.07, 70.51, 71.87, 79.12, 99.12, 110.26, 119.83, 122.40, 125.05, 125.60, 127.29, 135.90, 139.17, 142.50, 153.34, 157.19, 168.98, 169.19, 169.44, 169.97; HRMS (ESI-TOF): calcd for $C_{29}H_{35}N_4O_{11}$ ([M + H]$^+$): *m/z* 615.2302; found: *m/z* 615.2303.

Glycoconjugate **72**: Starting from 2-azidoethyl 2,3,4,6-tetra-*O*-acetyl-β-D-galactopyranoside **28** and 2-methyl-8-(2-propyn-1-yloxy)quinoline **4**, product was obtained as a pink solid (236.6 mg, 77%); m.p.: 60–63 °C; [α]$^{24}_D$ = −13.6 (c = 1.0, CHCl$_3$); ^{1}H NMR (400 MHz, DMSO-d6): δ 1.89, 1.90, 2.00, 2.10 (4s, 12H, CH$_3$CO), 2.62 (s, 3H, CH$_3$), 3.95 (m, 1H, CH$_2$O), 4.00–4.08 (m, 2H, H-6a$_{gal}$, H-6b$_{gal}$), 4.08–4.21 (m, 2H, CH$_2$O, H-5$_{gal}$), 4.52–4.66 (m, 2H, CH$_2$N), 4.74 (d, 1H, *J* = 8.0 Hz, H-1$_{gal}$), 4.92 (dd, 1H, *J* = 8.0 Hz, *J* = 10.4, H-2$_{gal}$), 5.12 (dd, 1H, *J* = 3.6 Hz, *J* = 10.4 Hz H-3$_{gal}$), 5.25 (dd, 1H, *J* = 0.8 Hz, *J* = 3.6 Hz, H-4$_{gal}$), 5.34 (s, 2H, CH$_2$O$_{chin}$), 7.37 (dd, 1H, *J* = 1.6 Hz, *J* = 7.4 Hz, H-7$_{chin}$), 7.41 (d, 1H, *J* = 8.4 Hz, H-3$_{chin}$), 7.43 (dd, 1H, *J* = 7.4 Hz, *J* = 8.2 Hz, H-6$_{chin}$), 7.47 (dd, 1H, *J* = 1.6 Hz, *J* = 8.2 Hz, H-5$_{chin}$), 8.15 (s, 1H, H-5$_{triaz}$), 8.18 (d, 1H, *J* = 8.4 Hz, H-4$_{chin}$); ^{13}C NMR (100 MHz, DMSO-d6): δ 20.30, 20.37, 20.50, 21.05, 24.89, 49.36, 61.23, 61.79, 67.29, 68.31, 70.01, 70.11, 79.17, 99.65, 110.33, 119.90, 122.46, 125.05, 125.67, 127.35, 135.96, 139.23, 142.58, 153.40, 157.25, 169.18, 169.46, 169.89, 169.9k2; HRMS (ESI-TOF): calcd for $C_{29}H_{35}N_4O_{11}$ ([M + H]$^+$): *m/z* 615.2302; found: *m/z* 615.2305.

Glycoconjugate **73**: Starting from 2-azidoethyl β-D-glucopyranoside **29** and 8-(2-propyn-1-yloxy) quinoline **3**, product was obtained as a beige solid (134.1 mg, 62%); m.p.: 60–63 °C; [α]$^{23}_D$ = −9.6 (c = 1.0, MeOH); ^{1}H NMR (400 MHz, DMSO-d6): δ 2.95-3.08 (m, 1H, H-5$_{glu}$), 3.10–3.19 (m, 3H, H-2$_{glu}$, H-3$_{glu}$, H-4$_{glu}$), 3.40-3.48 (m, 1H, H-6a$_{glu}$), 3.65–3.72 (m, 1H, H-6b$_{glu}$), 3.91–3.98 (m, 1H, CH$_2$O), 4.07-4.14 (m, 1H, CH$_2$O), 4.26 (d, 1H, *J* = 7.8 Hz, H-1$_{glu}$), 4.52–4.56 (m, 1H, OH), 4.60–4.66 (m, 2H, CH$_2$N), 4.88–4.96 (m, 2H, OH), 5.10–5.14 (d, 1H, *J* = 4.7 Hz, OH), 5.34 (s, 2H, CH$_2$O$_{chin}$), 7.39–7.45 (m, 1H, H-7$_{chin}$), 7.50–7.57 (m, 3H, H-3$_{chin}$, H-5$_{chin}$, H-6$_{chin}$), 8.32 (dd, 1H, *J* = 1.8 Hz, *J* = 8.1 Hz, H-4$_{chin}$), 8.38 (s, 1H, H-5$_{triaz}$), 8.83 (dd, 1H, *J* = 1.8 Hz, *J* = 4.1 Hz, H-2$_{chin}$); ^{13}C NMR (100 MHz, DMSO-d6): δ 49.74, 61.06, 61.82 67.36, 70.01, 73.27, 76.59, 76.96, 102.95, 109.96, 119.95, 121.81, 125.69, 126.73, 129.03, 135.78, 139.67, 142.32, 148.96, 153.84; HRMS (ESI-TOF): calcd for $C_{20}H_{25}N_4O_7$ ([M + H]$^+$): *m/z* 433.1723; found: *m/z* 433.1719.

Glycoconjugate **74:** Starting from 2-azidoethyl β-D-galactopyranoside **30** and 8-(2-propyn-1-yloxy) quinoline **3**, product was obtained as a brown oil (118.9 mg, 55%); [α]$^{25}_D$ = 10.8 (c = 1.0, MeOH); ^{1}H NMR (400 MHz, D$_2$O): δ 3.44-3.54 (m, 1H, H-2$_{gal}$), 3.57–3.74 (m, 4H, H-3$_{gal}$, H-5$_{gal}$, H-6a$_{gal}$, H-6b$_{gal}$), 3.91 (d, 1H, *J* = 3.2 Hz, H-4$_{gal}$), 4.11-4.21 (m, 1H, CH$_2$O), 4.30–4.40 (m, 2H, CH$_2$O, H-1$_{gal}$), 4.72-4.78 (m, 2H, CH$_2$N$_{triaz}$), 5.66 (s, 2H, CH$_2$O$_{chin}$), 7.78 (dd, 1H, *J* = 2.3 Hz, *J* = 6.4 Hz, H-7$_{chin}$), 7.85-7.97 (m, 2H, H-3$_{chin}$, H-5$_{chin}$), 8.06–8.16 (m, 1H, H-6$_{chin}$), 8.35 (s, 1H, H-5$_{triaz}$), 9.05 (d, 1H, *J* = 4.7 Hz, H-2$_{chin}$), 9.14 (d, 1H, *J* = 8.1 Hz, H-4$_{chin}$); ^{13}C NMR (100 MHz, D$_2$O): δ 50.49, 60.83, 62.27, 67.96, 68.45, 70.52, 72.54, 75.05, 102.97, 114.63, 120.83, 122.17, 126.24, 129.37, 129.92, 130.37, 142.07, 143.05, 147.30, 147.5; HRMS (ESI-TOF): calcd for $C_{20}H_{25}N_4O_7$ ([M + H]$^+$): *m/z* 433.1723; found: *m/z* 433.1720.

Glycoconjugate **75**: Starting from 2-azidoethyl β-D-glucopyranoside **29** and 2-methyl-8-(2-propyn-1-yloxy)quinoline **4**, product was obtained as a brown oil (129.5 mg, 58%); $[\alpha]^{24}_D$ = 1.6 (c = 1.0, MeOH); ^{1}H NMR (400 MHz, D$_2$O): δ 3.01 (s, 3H, CH$_3$), 3.18 (dd-t, 1H, *J* = 8.2 Hz, *J* = 8.3 Hz, H-4$_{glu}$), 3.29 (dd-t, 1H, *J* = 8.6 Hz, *J* = 9.0 Hz, H-2$_{glu}$), 3.38–3.47 (m, 2H, H-3$_{glu}$, H-5$_{glu}$), 3.63 (dd, 1H, *J* = 4.7 Hz, *J* = 12.3 Hz, H-6a$_{glu}$), 3.81–3.90 (m, 1H, H-6b$_{glu}$), 4.10–4.22 (m, 1H, CH$_2$O), 4.27–4.37 (m, 1H, CH$_2$O), 4.41 (d, 1H, *J* = 7.8 Hz, H-1$_{glu}$), 4.68–4.77 (m, 2H, CH$_2$N), 5.64 (s, 2H, CH$_2$O$_{chin}$), 7.64–7.96 (m, 4H, H-3$_{chin}$, H-5$_{chin}$, H-6$_{chin}$, H-7$_{chin}$), 8.30 (s, 1H, H-5$_{triaz}$), 8.91 (d, 1H, *J* = 8.3 Hz, H-4$_{chin}$); ^{13}C NMR (100 MHz, D$_2$O): δ 19.99, 50.45, 60.60, 62.10, 67.96, 69.49, 72.88, 75.53, 75.82, 102.32, 114.65, 120.85, 124.20, 126.25, 128.08, 129.08, 129.44, 146.30, 146.98, 155.63, 157.49; HRMS (ESI-TOF): calcd for C$_{21}$H$_{27}$N$_4$O$_7$ ([M + H]$^+$): *m/z* 447.1880; found: *m/z* 447.1880.

Glycoconjugate **76**: Starting from 2-azidoethyl β-D-galactopyranoside **30** and 2-methyl-8-(2-propyn-1-yloxy)quinoline **4**, product was obtained as a pink solid (131.7 mg, 59%); m.p.: 102-105 °C; $[\alpha]^{23}_D$ = 4.8 (c = 1.0, MeOH); ^{1}H NMR (400 MHz, DMSO-d6): δ 2.63 (s, 3H, CH$_3$), 3.33–3.39 (m, 2H, H-2$_{gal}$, H-3$_{gal}$), 3.40–3.48 (m, 1H, H-5$_{gal}$), 3.49–3.55 (m, 2H, H-6a$_{gal}$, H-6b$_{gal}$), 3.63 (dd-t, 1H, *J* = 0.8 Hz, *J* = 3.6 Hz, H-4$_{gal}$), 3.88–3.96 (m, 1H, CH$_2$O), 4.06–4.14 (m, 1H, CH$_2$O), 4.19 (d, 1H, *J* = 7.3 Hz, H-1$_{gal}$), 4.35 (d, 1H, *J* = 4.6 Hz, OH), 4.53–4.64 (m, 3H, CH$_2$N, OH), 4.69 (d, 1H, *J* = 5.0 Hz, OH), 4.95 (d, 1H, *J* = 4.4 Hz, OH), 5.33 (s, 2H, CH$_2$O$_{chin}$), 7.38 (dd, 1H, *J* = 2.0 Hz, *J* = 7.2 Hz, H-7$_{chin}$), 7.41 (d, 1H, *J* = 8.4 Hz, H-3$_{chin}$), 7.44 (dd, 1H, *J* = 7.2 Hz, *J* = 7.8 Hz, H-6$_{chin}$), 7.47 (dd, 1H, *J* = 1.8 Hz, *J* = 7.8 Hz, H-5$_{chin}$), 8.18 (d, 1H, *J* = 8.4 Hz, H-4$_{chin}$), 8.37 (s, 1H, H-5$_{triaz}$); ^{13}C NMR (100 MHz, DMSO-d6): δ 24.89, 49.75, 60.46, 61.66, 67.16, 68.14, 70.35, 73.29, 75.39, 103.53, 110.20, 119.77, 122.42, 125.65, 125.69, 127.30, 135.93, 139.16, 142.39, 153.37, 157.23; HRMS (ESI-TOF): calcd for C$_{21}$H$_{27}$N$_4$O$_7$ ([M + H]$^+$): *m/z* 447.1880; found: *m/z* 447.1881.

Glycoconjugate **77**: Starting from 2,3,4,6-tetra-*O*-acetyl-*N*-(β-D-glucopyranosyl)azidoacetamide **33** and 8-(2-propyn-1-yloxy)quinoline **3**, product was obtained as a light yellow solid (205.5 mg, 67%); m.p.: 97–100 °C; $[\alpha]^{25}_D$ = 4.4 (c = 0.6, CHCl$_3$); ^{1}H NMR (400 MHz, DMSO-d6): δ 1.94, 1.97, 1.99, 2.00 (4s, 12H, CH$_3$CO), 3.99 (m, 1H, H-6a$_{glu}$), 4.10–4.18 (m, 2H, H-5$_{glu}$, H-6b$_{glu}$), 4.87 (dd-t, 1H, *J* = 9.4 Hz, *J* = 9.4 Hz, H-4$_{glu}$), 4.93 (dd-t, 1H, *J* = 9.7 Hz, *J* = 9.7 Hz, H-2$_{glu}$), 5.16 and 5.22 (qAB, 2H, *J* = 16.5 Hz, CH$_2$CO), 5.34–5.41 (m, 3H, H-1$_{glu}$, CH$_2$O$_{chin}$), 5.45 (dd-t, 1H, *J* = 9.4 Hz, *J* = 9.4 Hz, H-3$_{glu}$), 7.41 (dd, 1H, *J* = 3.6 Hz, *J* = 5.4 Hz, H-7$_{chin}$), 7.49–7.57 (m, 3H, H-3$_{chin}$, H-5$_{chin}$, H-6$_{chin}$), 8.24 (s, 1H, H-5$_{triaz}$), 8.32 (dd, 1H, *J* = 1.7 Hz, *J* = 8.3 Hz, H-4$_{chin}$), 8.83 (d, 1H, *J* = 2.7 Hz, H-2$_{chin}$), 9.25 (d, 1H, *J* = 9.3 Hz, CONH); ^{13}C NMR (100 MHz, DMSO-d6): δ 20.27, 20.30, 20.33, 20.48, 51.40, 61.73, 67.72, 70.58, 72.13, 72.64, 76.85, 79.12, 109.94, 119.95, 121.81, 126.38, 126.69, 129.02, 135.73, 139.70, 142.37, 148.94, 153.82, 166.17, 169.13, 169.25, 169.44, 169.94; HRMS (ESI-TOF): calcd for C$_{28}$H$_{32}$N$_5$O$_{11}$ ([M + H]$^+$): *m/z* 614.2098; found: *m/z* 614.2095.

Glycoconjugate **78**: Starting from 2,3,4,6-tetra-*O*-acetyl-*N*-(β-D-galactopyranosyl)azidoacetamide **34** and 8-(2-propyn-1-yloxy)quinoline **3**, product was obtained as a yellow solid (227.0 mg, 74%); m.p.: 100–103 °C; $[\alpha]^{22}_D$ = 14.8 (c = 1.0, CHCl$_3$); ^{1}H NMR (400 MHz, DMSO-d6): δ 1.92, 1.98, 1.99, 2.12 (4s, 12H, CH$_3$CO), 3.98 (dd, 1H, *J* = 6.7 Hz, *J* = 11.3 Hz, H-6a$_{gal}$), 4.05 (dd, 1H, *J* = 5.9 Hz, *J* = 11.3 Hz, H-6b$_{gal}$), 4.35 (m, 1H, H-5$_{gal}$), 5.08 (dd, 1H, *J* = 9.0 Hz, *J* = 9.4 Hz, H-2$_{gal}$), 5.13 and 5.21 (qAB, 2H, *J* = 16.5 Hz, CH$_2$CO), 5.27-5.44 (m, 5H, H-1$_{gal}$, H-3$_{gal}$, H-4$_{gal}$, CH$_2$O$_{chin}$), 7.42 (dd, 1H, *J* = 3.2 Hz, *J* = 5.8 Hz, H-7$_{chin}$), 7.50–7.58 (m, 3H, H-3$_{chin}$, H-5$_{chin}$, H-6$_{chin}$), 8.24 (s, 1H, H-5$_{triaz}$), 8.28–8.35 (m, 2H, H-4$_{chin}$, H-2$_{chin}$), 9.34 (d, 1H, *J* = 9.5 Hz, CONH); ^{13}C NMR (100 MHz, DMSO-d6): δ 20.33, 20.38, 20.48, 20.72, 51.37, 61.42, 61.75, 67.54, 68.24, 70.66, 71.43, 77.22, 109.95, 119.98, 121.88, 124.11, 126.39, 126.70, 135.73, 139.72, 142.38, 148.91, 153.85, 166.09, 169.31, 169.37, 169.78, 169.85; HRMS (ESI-TOF): calcd for C$_{28}$H$_{32}$N$_5$O$_{11}$ ([M + H]$^+$): *m/z* 614.2098; found: *m/z* 614.2091.

Glycoconjugate **79**: Starting from 2,3,4,6-tetra-*O*-acetyl-*N*-(β-D-glucopyranosyl)azidoacetamide **33** and 2-methyl-8-(2-propyn-1-yloxy)quinoline **4**, product was obtained as a pink solid (254.2 mg, 81%); m.p.: 93–96 °C; $[\alpha]^{27}_D$ = 5.2 (c = 1.0, CHCl$_3$); ^{1}H NMR (400 MHz, DMSO-d6): δ 1.94, 1.97, 1.99, 2.00 (4s, 12H, CH$_3$CO), 2.63 (s, 3H, CH$_3$), 3.94–4.03 (m, 1H, H-6a$_{glu}$), 4.06–4.18 (m, 2H, H-5$_{glu}$, H-6b$_{glu}$), 4.87 (dd-t,

J = 9.4 Hz, *J* = 10.4 Hz, H-4$_{glu}$), 4.92 (dd-t, *J* = 9.7 Hz, *J* = 9.8 Hz, H-2$_{glu}$), 5.15 and 5.21 (qAB, 2H, *J* = 16.5 Hz, CH$_2$CO), 5.33–5.48 (m, 4H, H-1$_{glu}$, H-3$_{glu}$, CH$_2$O$_{chin}$), 7.38 (dd, 1H, *J* = 1.6 Hz, *J* = 7.5 Hz, H-7$_{chin}$), 7.41 (d, 1H, *J* = 8.4 Hz, H-3$_{chin}$), 7.43 (dd, 1H, *J* = 7.5 Hz, *J* = 8.0 Hz, H-6$_{chin}$), 7.47 (dd, 1H, *J* = 1.6 Hz, *J* = 8.0 Hz, H-5$_{chin}$), 8.18 (d, 1H, *J* = 8.4 Hz, H-4$_{chin}$), 8.24 (s, 1H, H-5$_{triaz}$), 9.25 (d, 1H, *J* = 9.3 Hz, CONH); ^{13}C NMR (100 MHz, DMSO-d6): δ 20.21, 20.24, 20.27, 20.41, 24.85, 51.34, 61.53, 67.65, 70.51, 72.06, 72.57, 76.78, 79.06, 110.09, 119.72, 122.38, 125.54, 126.38, 127.27, 135.85, 139.11, 142.37, 153.27, 157.15, 166.10, 169.06, 169.19, 169.37, 169.87; HRMS (ESI-TOF): calcd for C$_{29}$H$_{34}$N$_5$O$_{11}$ ([M + H]$^+$): *m/z* 628.2255; found: *m/z* 628.2256.

Glycoconjugate 80: Starting from 2,3,4,6-tetra-*O*-acetyl-*N*-(β-D-galactopyranosyl)azidoacetamide **34** and 2-methyl-8-(2-propyn-1-yloxy)quinoline **4**, product was obtained as a pink solid (244.8 mg, 78%); m.p.: 98–101 °C; [α]^{27}$_D$ = 11.6 (c = 1.0, CHCl$_3$); ^{1}H NMR (400 MHz, DMSO-d6): δ 1.92, 1.98, 1.99, 2.12 (4s, 12H, CH$_3$CO), 2.63 (s, 3H, CH$_3$), 3.98 (dd, 1H, *J* = 6.6 Hz, *J* = 11.3 Hz, H-6a$_{gal}$), 4.06 (dd, 1H, *J* = 5.9 Hz, *J* = 11.3 Hz, H-6b$_{gal}$), 4.35 (m, 1H, H-5$_{gal}$,), 5.07 (dd-t, 1H, *J* = 9.4 Hz, *J* = 9.4 Hz, H-2$_{gal}$), 5.12 and 5.20 (qAB, 2H, *J* = 16.5 Hz, CH$_2$CO), 5.26–5.44 (m, 5H, H-1$_{gal}$, H-3$_{gal}$, H-4$_{gal}$, CH$_2$O$_{chin}$), 7.32–7.54 (m, 4H, H-3$_{chin}$, H-5$_{chin}$, H-6$_{chin}$, H-7$_{chin}$)8.21 (d, 1H, *J* = 7.9 Hz, H-4$_{chin}$), 8.24 (s, 1H, H-5$_{triaz}$), 9.33 (d, 1H, *J* = 9.5 Hz, CONH); ^{13}C NMR (100 MHz, DMSO-d6): δ 20.23, 20.26, 20.31, 20.40, 24.84, 51.30, 61.54, 67.47, 68.16, 70.59, 71.35, 77.14, 79.06, 110.10, 119.72, 122.36, 125.54, 126.38, 127.24, 135.85, 139.11, 142.36, 153.27, 157.15, 166.02, 169.23, 169.29, 169.71, 169.77; HRMS (ESI-TOF): calcd for C$_{29}$H$_{34}$N$_5$O$_{11}$ ([M + H]$^+$): *m/z* 628.2255; found: *m/z* 628.2253.

Glycoconjugate 81: Starting from *N*-(β-D-glucopyranosyl)azidoacetamide **35** and 8-(2-propyn-1-yloxy)quinoline **3**, product was obtained as a brown solid (133.6 mg, 60%); m.p.: 160-163 °C; [α]^{25}$_D$ = 16.7 (c = 2.0, DMSO); ^{1}H NMR (400 MHz, DMSO-d6): δ 3.04–3.15 (m, 3H, H-2$_{glu}$, H-4$_{glu}$, H-5$_{glu}$), 3.21 (dd-t, 1H, *J* = 8.4 Hz, *J* = 8.6 Hz, H-3$_{glu}$), 3.42 (m, 1H, H-6a$_{glu}$), 3.63 (m, 1H, H-6b$_{glu}$), 4.00–4.50 (m, 4H, OH), 4.71 (dd-t, 1H, *J* = 8.9 Hz, *J* = 9.0 Hz, H-1$_{glu}$), 5.17 and 5.22 (qAB, 2H, *J* = 16.5 Hz, CH$_2$CO), 5.57 (s, 2H, CH$_2$O$_{chin}$), 7.60–8.10 (m, 5H, H-3$_{chin}$, H-4$_{chin}$, H-5$_{chin}$, H-6$_{chin}$, H-7$_{chin}$), 8.39 (s, 1H, H-5$_{triaz}$), 8.96 (d, 1H, *J* = 7.4 Hz, H-2$_{chin}$), 9.04 (d, 1H, *J* = 8.8 Hz, CONH); ^{13}C NMR (100 MHz, DMSO-d6): δ 51.55, 60.72, 62.36, 69.74, 72.44, 77.18, 78.65, 79.63, 112.94, 120.36, 122.56, 126.79, 128.94, 132.86, 136.25, 136.88, 141.50, 146.25, 151.30, 165.67; HRMS (ESI-TOF): calcd for C$_{20}$H$_{24}$N$_5$O$_7$ ([M + H]$^+$): *m/z* 446.1676; found: *m/z* 446.1679.

Glycoconjugate 82: Starting from *N*-(β-D-galactopyranosyl)azidoacetamide **36** and 8-(2-propyn-1-yloxy)quinoline **3**, product was obtained as a brown solid (129.2 mg, 58%); m.p.: 170-173 °C; [α]^{25}$_D$ = 14.5 (c = 2.0, DMSO); ^{1}H NMR (400 MHz, DMSO-d6): δ 3.34 (dd, 1H, *J* = 3.2 Hz, *J* = 9.4 Hz, H-3$_{gal}$), 3.36–3.46 (m, 3H, H-2$_{gal}$, H-5$_{gal}$, H-6a$_{gal}$), 3.50 (dd, 1H, *J* = 5.8 Hz, *J* = 10.5 Hz, H-6b$_{gal}$), 3.69 (d, 1H, *J* = 3.0 Hz, H-4$_{gal}$), 4.09–4.42 (m, 4H, OH), 4.69 (dd-t, 1H *J* = 8.9 Hz, *J* = 9.0 Hz, H-1$_{gal}$), 5.18 (s, 2H, CH$_2$CO), 5.60 (s, 2H, CH$_2$O$_{chin}$), 7.56–8.16 (m, 4H, H-3$_{chin}$, H-5$_{chin}$, H-6$_{chin}$, H-7$_{chin}$), 8.41 (s, 1H, H-5$_{triaz}$), 8.85–9.20 (m, 3H, H-2$_{chin}$, H-4$_{chin}$, CONH); ^{13}C NMR (100 MHz, DMSO-d6): δ 51.62, 60.31, 68.02, 69.66, 73.85, 76.75, 79.08, 80.07, 112.53, 120.38, 126.83, 126.96, 129.01, 130.10, 141.66, 142.90, 146.07, 150.24, 152.06, 165.58; HRMS (ESI-TOF): calcd for C$_{20}$H$_{24}$N$_5$O$_7$ ([M + H]$^+$): *m/z* 446.1676; found: *m/z* 446.1670.

Glycoconjugate 83: Starting from *N*-(β-D-glucopyranosyl)azidoacetamide **35** and 2-methyl-8-(2-propyn-1-yloxy)quinoline **4**, product was obtained as a brown solid (140.1 mg, 61%); m.p.: 135–138 °C; [α]^{26}$_D$ = −2.8 (c = 1.0, MeOH); ^{1}H NMR (400 MHz, DMSO-d6): δ 2.92 (s, 3H, CH$_3$), 3.04–3.24 (m, 3H, H-2$_{glu}$, H-4$_{glu}$, H-5$_{glu}$), 3.39–3.47 (m, 2H, H-3$_{glu}$, H-6a$_{glu}$,), 3.62 (dd, 1H, *J* = 1.6 Hz, *J* = 12.1 Hz, H-6b$_{glu}$), 4.69 (dd-t, 1H, *J* = 8.9 Hz, *J* = 9.0 Hz, H-1$_{glu}$), 5.15 and 5.20 (qAB, 2H, *J* = 16.5 Hz, CH$_2$CO), 5.60 (s, 2H, CH$_2$O$_{chin}$), 7.73–7.93 (m, 4H, H-3$_{chin}$, H-5$_{chin}$, H-6$_{chin}$, H-7$_{chin}$), 8.34 (s, 1H, H-5$_{triaz}$), 8.89 (d, 1H, *J* = 8.3 Hz, H-4$_{chin}$), 9.04 (d, 1H, *J* = 8.8 Hz, CONH); ^{13}C NMR (100 MHz, DMSO-d6): δ 18.45, 51.52, 60.71, 62.31, 69.74, 72.42, 77.18, 78.65, 79.62, 113.85, 120.30, 124.31, 126.87, 127.70, 128.48, 141.31, 143.79,

148.61, 158.29, 163.67, 165.65; HRMS (ESI-TOF): calcd for $C_{21}H_{26}N_5O_7$ ([M + H]$^+$): *m/z* 460.1832; found: *m/z* 460.1830.

Glycoconjugate **84**: Starting from *N*-(β-D-galactopyranosyl)azidoacetamide **36** and 2-methyl-8-(2-propyn-1-yloxy)quinoline **4**, product was obtained as a brown solid (179.2 mg, 78%); m.p.: 145–148 °C; $[\alpha]^{24}_D$ = 5.0 (c = 1.0, MeOH); ^{1}H NMR (400 MHz, DMSO-d6): δ 2.88 (s, 3H, CH$_3$), 3.34 (dd, 1H, *J* = 3.2 Hz, *J* = 9.4 Hz, H-3$_{gal}$), 3.37-3.54 (m, 4H, H-2$_{gal}$, H-5$_{gal}$, H-6a$_{gal}$, H-6b$_{gal}$), 3.69 (d, 1H, *J* = 3.0 Hz, H-4$_{gal}$), 3.95–4.31 (m, 4H, OH), 4.67 (dd-t, 1H, *J* = 8.9 Hz, *J* = 9.0 Hz, H-1$_{gal}$), 5.17 (s, 2H, CH$_2$CO), 5.59 (s, 2H, CH$_2$O$_{chin}$), 7.62–7.98 (m, 4H, H-3$_{chin}$, H-5$_{chin}$, H-6$_{chin}$, H-7$_{chin}$), 8.34 (s, 1H, H-5$_{triaz}$), 8.84 (bs, 1H, H-4$_{chin}$), 9.01 (d, 1H, *J* = 9.0 Hz, CONH); ^{13}C NMR (100 MHz, DMSO-d6): δ 18.45, 51.55, 60.30, 62.27, 68.01, 69.65, 73.85, 76.74, 80.06, 113.46, 120.27, 124.12, 126.87, 128.23, 131.53, 141.40, 142.91, 149.12, 158.22, 162.36, 165.59; HRMS (ESI-TOF): calcd for $C_{21}H_{26}N_5O_7$ ([M + H]$^+$): *m/z* 460.1832; found: *m/z* 460.1831.

Glycoconjugate **85**: Starting from 2,3,4,6-tetra-*O*-acetyl-*N*-(β-D-glucopyranosyl)propiolamide **37** and 8-(2-azidoethoxy)quinoline **5**, product was obtained as a yellow solid (220.9 mg, 72%); m.p.: 89–94 °C; $[\alpha]^{23}_D$ = −18.0 (c = 1.0, CHCl$_3$); ^{1}H NMR (400 MHz, DMSO-d6): δ 1.86, 1.94, 1.98, 2.00 (4s, 12H, CH$_3$CO), 3.98 (dd, 1H, *J* = 3.9 Hz, *J* = 14.0 Hz, H-6a$_{glu}$), 4.07–4.18 (m, 2H, H-5$_{glu}$, H-6b$_{glu}$), 4.66 (t, 2H, *J* = 5.1 Hz, CH$_2$N), 4.90 (dd-t, 1H, *J* = 9.6 Hz, *J* = 9.6 Hz, H-4$_{glu}$), 4.98 (t, 2H, *J* = 5.1 Hz, CH$_2$O), 5.20 (dd-t, 1H, *J* = 9.3 Hz, *J* = 9.4 Hz, H-2$_{glu}$), 5.38 (dd-t, 1H, *J* = 9.5 Hz, *J* = 9.5 Hz, H-1$_{glu}$), 5.59 (dd-t, 1H, *J* = 9.3 Hz, *J* = 9.4 Hz, H-3$_{glu}$), 7.25 (dd, 1H, *J* = 1.4 Hz, *J* = 7.5 Hz, H-7$_{chin}$), 7.47–7.59 (m, 3H, H-3$_{chin}$, H-5$_{chin}$, H-6$_{chin}$), 8.32 (dd, 1H, *J* = 1.7 Hz, *J* = 8.4 Hz, H-4$_{chin}$), 8.87 (dd, 1H, *J* = 1.5 Hz, *J* = 4.1 Hz, H-2$_{chin}$), 8.98 (s, 1H, H-5$_{triaz}$), 9.20 (d, 1H, *J* = 9.5 Hz, NHCO); ^{13}C NMR (100 MHz, DMSO-d6): δ 20.30, 20.31, 20.37, 20.50, 49.56, 61.85, 67.07, 67.85, 70.49, 72.04, 73.03, 76.79, 110.69, 120.60, 121.93, 126.69, 128.20, 129.08, 135.86, 139.71, 141.83, 149.25, 153.60, 160.03, 169.02, 169.32, 169.54, 169.97; HRMS (ESI-TOF): calcd for $C_{28}H_{32}N_5O_{11}$ ([M + H]$^+$): *m/z* 614.2098; found: *m/z* 614.2097.

Glycoconjugate **86**: Starting from 2,3,4,6-tetra-*O*-acetyl-*N*-(β-D-galactopyranosyl)propiolamide **38** and 8-(2-azidoethoxy)quinoline **5**, product was obtained as a white solid (285.3 mg, 93%); m.p.: 187–189 °C; $[\alpha]^{24}_D$ = −6.8 (c = 1.0, CHCl$_3$); ^{1}H NMR (400 MHz, CDCl$_3$): δ 1.96, 2.00, 2.01, 2.17 (4s, 12H, CH$_3$CO), 4.03–4.17 (m, 3H, H-5$_{gal}$, H-6a$_{gal}$, H-6b$_{gal}$), 4.63 (t, 2H, *J* = 4.9 Hz, CH$_2$N), 5.02 (t, 2H, *J* = 4.9 Hz, CH$_2$O), 5.15 (dd, 1H, *J* = 3.3 Hz, *J* = 10.1 Hz, H-3$_{gal}$), 5.30 (dd-t, 1H, *J* = 9.3 Hz, *J* = 10.1 Hz, H-2$_{gal}$), 5.41 (dd-t, 1H, *J* = 9.3 Hz, *J* = 9.5 Hz, H-1$_{gal}$), 5.45 (dd, 1H, *J* = 0.6 Hz, *J* = 3.3 Hz, H-4$_{gal}$), 7.04 (dd, 1H, *J* = 1.7 Hz, *J* = 7.2 Hz, H-7$_{chin}$), 7.40–7.50 (m, 3H, H-3$_{chin}$, H-5$_{chin}$, H-6$_{chin}$), 7.83 (d, 1H, *J* = 9.5 Hz, NHCO); 8.14 (dd, 1H, *J* = 1.7 Hz, *J* = 8.3 Hz, H-4$_{chin}$), 8.95 (s, 1H, H-5$_{triaz}$), 9.00 (dd, 1H, *J* = 1.7 Hz, *J* = 4.2 Hz. H-2$_{chin}$); ^{13}C NMR (100 MHz, CDCl$_3$): δ 20.57, 20.63, 20.64, 20.67, 50.14, 61.27, 67.24, 67.53, 68.08, 71.17, 72.32, 78.15, 110.28, 121.34, 122.02, 126.42, 128.22, 129.64, 135.98, 140.36, 142.35, 149.81, 153.67, 160.32, 169.90, 170.15, 170.35, 170.46; HRMS (ESI-TOF): calcd for $C_{28}H_{32}N_5O_{11}$ ([M + H]$^+$): *m/z* 614.2098; found: *m/z* 614.2095.

Glycoconjugate **87**: Starting from 2,3,4,6-tetra-*O*-acetyl-*N*-(β-D-glucopyranosyl)propiolamide **37** and 2-methyl-8-(2-azidoethoxy)quinoline **8**, product was obtained as a yellow solid (207.1 mg, 66%); m.p.: 167–172 °C; $[\alpha]^{24}_D$ = −14.8 (c = 1.0, CHCl$_3$); ^{1}H NMR (400 MHz, DMSO-d6): δ 1.85, 1.93, 1.98, 2.00 (4s, 12H, CH$_3$CO), 2.72 (s, 3H, CH$_3$), 3.98 (dd, 1H, *J* = 4.5 Hz, *J* = 14.3 Hz, H-6a$_{glu}$), 4.07–4.18 (m, 2H, H-5$_{glu}$, H-6b$_{glu}$), 4.54–4.67 (m, 2H, CH$_2$N), 4.90 (dd-t, 1H, *J* = 9.4 Hz, *J* = 9.5 Hz, H-4$_{glu}$), 4.98 (t, 2H, *J* = 5.0 Hz, CH$_2$O), 5.21 (dd-t, 1H, *J* = 9.3 Hz, *J* = 9.4 Hz, H-2$_{glu}$), 5.38 (dd-t, 1H, *J* = 9.5 Hz, *J* = 9.5 Hz, H-1$_{glu}$), 5.60 (dd-t, 1H, *J* = 9.3 Hz, *J* = 9.4 Hz, H-3$_{glu}$), 7.21 (dd, 1H, *J* = 1.2 Hz, *J* = 7.7 Hz, H-7$_{chin}$), 7.38–7.46 (m, 2H, H-3$_{chin}$, H-6$_{chin}$), 7.50 (dd, 1H, *J* = 1.1 Hz, *J* = 8.2 Hz, H-5$_{chin}$), 8.20 (d, 1H, *J* = 8.5, H-4$_{chin}$), 9.17 (d, 1H, *J* = 9.5 Hz, NHCO), 9.20 (s, 1H, H-5$_{triaz}$); ^{13}C NMR (100 MHz, DMSO-d6): δ 20.29, 20.31, 20.37, 20.50, 25.00, 49.59, 61.86, 67.17, 67.85, 70.52, 72.01, 73.01, 76.75, 111.06, 120.46, 122.58, 125.63, 127.30, 128.62, 136.02, 139.28, 141.93, 153.06, 157.80, 160.08, 169.01, 169.32, 169.53, 169.97; HRMS (ESI-TOF): calcd for $C_{29}H_{33}N_5O_{11}$ ([M + H]$^+$): *m/z* 628.2255; found: *m/z* 628.2252.

Glycoconjugate **88**: Starting from 2,3,4,6-tetra-*O*-acetyl-*N*-(β-D-galactopyranosyl)propiolamide **38** and 2-methyl-8-(2-azidoethoxy)quinoline **8**, product was obtained as a white solid (257.3 mg, 82%); m.p.: 107–109 °C; $[\alpha]^{25}_D$ = −7.2 (c = 1.0, CHCl$_3$); ^{1}H NMR (400 MHz, CDCl$_3$): δ 1.95, 2.00, 2.02, 2.17 (4s, 12H, CH$_3$CO), 2.88 (s, 3H, CH$_3$), 4.03–4.17 (m, 3H, H-5$_{gal}$, H-6a$_{gal}$, H-6b$_{gal}$), 4.59 (t, 2H, *J* = 4.9 Hz, CH$_2$N), 5.00 (t, 2H, *J* = 4.8 Hz, CH$_2$O), 5.15 (dd, 1H, *J* = 3.4 Hz, *J* = 10.2 Hz, H-3$_{gal}$), 5.30 (dd-t, 1H, *J* = 9.4 Hz, *J* = 10.2 Hz, H-2$_{gal}$), 5.42 (dd-t, 1H, *J* = 9.4 Hz, *J* = 9.5 Hz, H-1$_{gal}$), 5.45 (dd, 1H, *J* = 0.7 Hz, *J* = 3.4 Hz, H-4$_{gal}$), 7.02 (dd, 1H, *J* = 1.3 Hz, *J* = 7.5 Hz, H-7$_{chin}$), 7.32–7.39 (m, 2H, H-3$_{chin}$, H-6$_{chin}$), 7.42 (dd, 1H, *J* = 1.3 Hz, *J* = 8.2 Hz, H-5$_{chin}$), 7.84 (d, 1H, *J* = 9.6 Hz, NHCO), 8.02 (d, 1H, *J* = 8.4 Hz, H-4$_{chin}$), 9.26 (s, 1H, H-5$_{triaz}$); ^{13}C NMR (100 MHz, CDCl$_3$): δ 20.57, 20.61, 20.64, 20.66, 25.62, 50.18, 61.23, 67.23, 67.45, 68.08, 71.18, 72.25, 78.11, 110.54, 121.14, 122.90, 125.38, 127.79, 128.65, 136.04, 139.94, 142.40, 153.15, 159.03, 160.36, 169.90, 170.15, 170.34, 170.41; HRMS (ESI-TOF): calcd for C$_{29}$H$_{34}$N$_5$O$_{11}$ ([M + H]$^+$): *m/z* 628.2255; found: *m/z* 628.2254.

Glycoconjugate **89**: Starting from *N*-(β-D-glucopyranosyl)propiolamide **39** and 8-(2-azidoethoxy) quinoline **5**, product was obtained as a white solid (133.6 mg, 60%); m.p.: 169–171 °C; $[\alpha]^{28}_D$ = 5.0 (c = 1.0, DMSO); ^{1}H NMR (400 MHz, DMSO-d6): δ 3.05-3.11 (m, 1H, H-5$_{glu}$), 3.13–3.18 (m, 2H, H-2$_{glu}$, H-4$_{glu}$), 3.33–3.37 (m, 1H, H-3$_{glu}$), 3.38–3.44 (m, 1H, H-6a$_{glu}$), 3.60–3.67 (m, 1H, H-6b$_{glu}$), 4.48 (t, 1H, *J* = 5.9 Hz, 6-OH), 4.66 (t, 2H, *J* = 4.6 Hz, CH$_2$N), 4.83–4.93 (m, 3H, H-1$_{glu}$, OH), 4.95–5.01 (m, 3H, CH$_2$O, OH), 7.25 (d, 1H, *J* = 7.5 Hz, H-7$_{chin}$), 7.47–7.62 (m, 3H, H-3$_{chin}$, H-5$_{chin}$, H-6$_{chin}$), 8.32 (d, 1H, *J* = 10.4 Hz, H-4$_{chin}$), 8.68 (d, 1H, *J* = 9.1 Hz, NHCO), 8.88 (bs, 1H, H-2$_{chin}$), 8.94 (s, 1H, H-5$_{triaz}$); ^{13}C NMR (100 MHz, DMSO-d6): δ 49.52, 60.97, 67.11, 69.97, 71.83, 77.44, 78.70, 79.51, 110.64, 120.60, 121.96, 126.69, 127.68, 129.08, 135.84, 139.71, 142.53, 149.29, 153.63, 160.08; HRMS (ESI-TOF): calcd for C$_{20}$H$_{24}$N$_5$O$_7$ ([M + H]$^+$): *m/z* 446.1676; found: *m/z* 446.1678.

Glycoconjugate **90**: Starting from *N*-(β-D-galactopyranosyl)propiolamide **40** and 8-(2-azidoethoxy) quinoline **5**, product was obtained as a white solid (189.3 mg, 85%); m.p.: 162–164 °C; $[\alpha]^{25}_D$ = 24.8 (c = 1.0, MeOH); ^{1}H NMR (400 MHz, DMSO-d6): δ 3.34-3.54 (m, 4H, H-2$_{gal}$, H-3$_{gal}$, H-4$_{gal}$ H-5$_{gal}$), 3.57–3.65 (m, 1H, H-6a$_{gal}$), 3.66–3.72 (m, 1H, H-6b$_{gal}$), 4.29 (d, 1H, *J* = 4.9 Hz, OH), 4.56 (t, 1H, *J* = 5.4, 6-OH), 4.66 (t, 2H, *J* = 5.1 Hz, CH$_2$N), 4.74 (d, 1H, *J* = 5.5 Hz, OH), 4.79 (d, 1H, *J* = 5.5 Hz, OH), 4.87 (dd-t, 1H, *J* = 9.0 Hz, *J* = 9.1 Hz, H-1$_{gal}$), 4.98 (t, 2H, *J* = 5.0 Hz, CH$_2$O), 7.26 (dd, 1H, *J* = 1.4 Hz, *J* = 7.5 Hz, H-7$_{chin}$), 7.47–7.59 (m, 3H, H-3$_{chin}$, H-5$_{chin}$, H-6$_{chin}$), 8.32 (dd, 1H, *J* = 1.5 Hz, *J* = 8.2 Hz, H-4$_{chin}$), 8.48 (d, 1H, *J* = 9.1 Hz, NHCO), 8.88 (dd, 1H, *J* = 1.7 Hz, *J* = 4.1 Hz, H-2$_{chin}$), 8.95 (s, 1H, H-5$_{triaz}$); ^{13}C NMR (100 MHz, DMSO-d6): δ 49.52, 60.42, 67.13, 68.37, 69.33, 74.03, 76.82, 79.93, 110.69, 120.60, 121.93, 126.68, 127.61, 129.07, 135.84, 139.72, 142.47, 149.29, 153.62, 159.97; HRMS (ESI-TOF): calcd for C$_{20}$H$_{24}$N$_5$O$_7$ ([M + H]$^+$): *m/z* 446.1676; found: *m/z* 446.1675.

Glycoconjugate **91**: Starting from *N*-(β-D-glucopyranosyl)propiolamide **39** and 2-methyl-8-(2-azidoethoxy)quinoline **8**, product was obtained as a white solid (144.7 mg, 63%); m.p.: 159–161 °C; $[\alpha]^{25}_D$ = −3.6 (c = 1.0, MeOH); ^{1}H NMR (400 MHz, DMSO-d6): δ 2.72 (s, 3H, CH$_3$), 3.03–3.12 (m, 1H, H-5$_{glu}$), 3.13–3.27 (m, 2H, H-2$_{glu}$, H-4$_{glu}$), 3.34–3.46 (m, 2H, H-3$_{glu}$, H-6a$_{glu}$), 3.60–3.68 (m, 1H, H-6b$_{glu}$), 4.47 (t, 1H, *J* = 5.9 Hz, 6-OH), 4.55–4.67 (m, 2H, CH$_2$N), 4.86–4.93 (m, 3H, H-1$_{glu}$, OH), 4.94–5.02 (m, 3H, CH$_2$O, OH), 7.21 (dd, 1H, *J* = 1.2 Hz, *J* = 7.7 Hz, H-7$_{chin}$), 7.39–7.47 (m, 2H, H-3$_{chin}$, H-6$_{chin}$), 7.50 (dd, 1H, *J* = 1.1 Hz, *J* = 8.2 Hz, H-5$_{chin}$), 8.20 (d, 1H, *J* = 8.4 Hz, H-4$_{chin}$), 8.63 (d, 1H, *J* = 9.1 Hz, NHCO), 9.15 (s, 1H, H-5$_{triaz}$); ^{13}C NMR (100 MHz, DMSO-d6): δ 25.07, 49.57, 60.99, 67.27, 69.97, 71.85, 77.42, 78.68, 79.47, 111.02, 120.47, 122.62, 125.64, 127.31, 128.11, 136.02, 139.28, 142.63, 153.11, 157.85, 160.12; HRMS (ESI-TOF): calcd for C$_{20}$H$_{24}$N$_5$O$_7$ ([M + H]$^+$): *m/z* 460.1832; found: *m/z* 460.1830.

Glycoconjugate **92**: Starting from *N*-(β-D-galactopyranosyl)propiolamide **40** and 2-methyl-8-(2-azidoethoxy)quinoline **8**, product was obtained as a white solid (186.1 mg, 81%); m.p.: 148–151 °C; $[\alpha]^{28}_D$ = 23.0 (c = 1.0, DMSO); ^{1}H NMR (400 MHz, DMSO-d6): δ 2.72 (s, 3H, CH$_3$), 3.34–3.55 (m, 4H, H-2$_{gal}$, H-3$_{gal}$, H-4$_{gal}$ H-5$_{gal}$), 3.57–3.66 (m, 1H, H-6a$_{gal}$), 3.66–3.72 (m, 1H, H-6b$_{gal}$), 4.28 (d, 1H, *J* = 5.0 Hz, OH), 4.52–4.67 (m, 3H, CH$_2$N, 6-OH), 4.73 (d, 1H, *J* = 5.5 Hz, OH), 4.79 (d, 1H, *J* = 5.5 Hz, OH),

4.88 (dd-t, 1H, J = 9.0 Hz, J = 9.1 Hz, H-1$_{gal}$), 4.98 (t, 2H, J = 5.0 Hz, CH$_2$O), 7.21 (dd, 1H, J = 1.2 Hz, J = 7.7 Hz, H-7$_{chin}$), 7.39–7.46 (m, 2H, H-3$_{chin}$, H-6$_{chin}$), 7.50 (dd, 1H, J = 1.1 Hz, J = 8.2 Hz, H-5$_{chin}$), 8.20 (d, 1H, J = 8.4 Hz, H-4$_{chin}$), 8.43 (d, 1H, J = 9.1 Hz, NHCO), 9.16 (s, 1H, H-5$_{triaz}$); ^{13}C NMR (100 MHz, DMSO-d6): δ 25.04, 49.56, 60.40, 67.28, 68.37, 69.36, 74.02, 76.78, 79.89, 111.08, 120.47, 122.59, 125.62, 127.30, 128.04, 136.00, 139.29, 142.57, 153.11, 157.83, 160.00; HRMS (ESI-TOF): calcd for C$_{21}$H$_{26}$N$_5$O$_7$ ([M + H]$^+$): *m/z* 460.1832; found: *m/z* 460.1836.

Glycoconjugate **93:** Starting from 2,3,4,6-tetra-*O*-acetyl-*N*-(β-D-glucopyranosyl)propiolamide **37** and 8-(3-azidopropoxy)quinoline **6**, product was obtained as a yellow solid (210.2 mg, 67%); m.p.: 178–180 °C; [α]^{24}$_D$ = −18.6 (c = 1.0, CHCl$_3$); ^{1}H NMR (400 MHz, DMSO-d6): δ 1.89, 1.94, 1.99, 2.00 (4s, 12H, CH$_3$CO), 2.40–2.50 (m, 2H, CH$_2$), 4.00 (dd, 1H, J = 4.4 Hz, J = 14.2 Hz, H-6a$_{glu}$), 4.06–4.18 (m, 2H, H-5$_{glu}$, H-6b$_{glu}$), 4.21 (t, 2H, J = 6.0 Hz, CH$_2$N), 4.72 (t, 2H, J = 6.8 Hz, CH$_2$O), 4.91 (dd-t, 1H, J = 9.5 Hz, J = 9.5 Hz, H-4$_{glu}$), 5.21 (dd-t, 1H, J = 9.3 Hz, J = 9.4 Hz, H-2$_{glu}$), 5.39 (dd-t, 1H, J = 9.5 Hz, J = 9.5 Hz, H-1$_{glu}$), 5.61 (dd-t, 1H, J = 9.3 Hz, J = 9.4 Hz, H-3$_{glu}$), 7.20 (dd, 1H, J = 1.8 Hz, J = 7.1 Hz, H-7$_{chin}$), 7.46–7.59 (m, 3H, H-3$_{chin}$, H-5$_{chin}$, H-6$_{chin}$), 8.32 (dd, 1H, J = 1.5 Hz, J = 8.1 Hz, H-4$_{chin}$), 8.90 (dd, 1H, J = 1.7 Hz, J = 4.0 Hz, H-2$_{chin}$), 8.90 (s, 1H, H-5$_{triaz}$), 9.17 (d, 1H, J = 9.5 Hz, NHCO); ^{13}C NMR (100 MHz, DMSO-d6): δ 20.32, 20.33, 20.38, 20.52, 29.36, 47.24, 61.85, 65.52, 67.84, 70.52, 72.04, 73.02, 76.80, 109.92, 119.97, 121.84, 126.77, 127.67, 129.03, 135.79, 139.77, 141.83, 149.07, 154.18, 160.10, 169.04, 169.32, 169.54, 169.98; HRMS (ESI-TOF): calcd for C$_{29}$H$_{34}$N$_5$O$_{11}$ ([M + H]$^+$): *m/z* 628.2255; found: *m/z* 628.2252.

Glycoconjugate **94:** Starting from 2,3,4,6-tetra-*O*-acetyl-*N*-(β-D-galactopyranosyl)propiolamide **38** and 8-(3-azidopropoxy)quinoline **6**, product was obtained as a white solid (263.6 mg, 84%); m.p.: 98–100 °C; [α]^{25}$_D$ = −5.6 (c = 1.0, CHCl$_3$); ^{1}H NMR (400 MHz, CDCl$_3$): δ 1.99, 2.00, 2.03, 2.17 (4s, 12H, CH$_3$CO), 2.62 (p, 2H, J = 6.2 Hz, CH$_2$), 4.04–4.18 (m, 3H, H-5$_{gal}$, H-6a$_{gal}$, H-6b$_{gal}$), 4.24 (t, 2H, J = 5.8 Hz, CH$_2$N), 4.81 (t, 2H, J = 6.6 Hz, CH$_2$O), 5.17 (dd, 1H, J = 3.3 Hz, J = 10.2 Hz, H-3$_{gal}$), 5.31 (dd-t, 1H, J = 9.4 Hz, J = 10.2 Hz, H-2$_{gal}$), 5.42 (dd-t, 1H, J = 9.4 Hz, J = 9.5 Hz, H-1$_{gal}$), 5.46 (dd, 1H, J = 0.6 Hz, J = 3.3 Hz, H-4$_{gal}$), 7.06 (dd, 1H, J = 1.7 Hz, J = 7.2 Hz, H-7$_{chin}$), 7.41–7.50 (m, 3H, H-3$_{chin}$, H-5$_{chin}$, H-6$_{chin}$), 7.85 (d, 1H, J = 9.5 Hz, NHCO), 8.16 (dd, 1H, J = 1.7 Hz, J = 8.3 Hz, H-4$_{chin}$), 8.52 (s, 1H, H-5$_{triaz}$), 9.01 (dd, 1H, J = 1.7 Hz, J = 4.2 Hz. H-2$_{chin}$); ^{13}C NMR (100 MHz, CDCl$_3$): δ 20.53, 20.57, 20.64, 20.68, 29.67, 47.73, 61.28, 65.36, 67.24, 68.11, 71.16, 72.33, 78.16, 109.94, 120.67, 121.82, 126.62, 127.18, 129.61, 136.09, 140.39, 142.04, 149.55, 154.23, 160.36, 169.90, 170.15, 170.36, 170.45; HRMS (ESI-TOF): calcd for C$_{29}$H$_{34}$N$_5$O$_{11}$ ([M + H]$^+$): *m/z* 628.2255; found: *m/z* 628.2253.

Glycoconjugate **95:** Starting from 2,3,4,6-tetra-*O*-acetyl-*N*-(β-D-glucopyranosyl)propiolamide **37** and 2-methyl-8-(3-azidopropoxy)quinoline **9**, product was obtained as a beige solid (195.7 mg, 61%); m.p.: 197–198 °C; [α]^{24}$_D$ = −18.0 (c = 1.0, CHCl$_3$); ^{1}H NMR (400 MHz, DMSO-d6): δ 1.88, 1.94, 1.99, 2.00 (4s, 12H, CH$_3$CO), 2.41–2.49 (m, 2H, CH$_2$), 2.67 (s, 3H, CH$_3$), 3.96–4.02 (m, 1H, H-6a$_{glu}$), 4.05–4.17 (m, 2H, H-5$_{glu}$, H-6b$_{glu}$), 4.20 (t, 2H, J = 6.2 Hz, CH$_2$N), 4.71 (t, 2H, J = 6.9 Hz, CH$_2$O), 4.91 (dd-t, 1H, J = 9.5 Hz, J = 9.5 Hz, H-4$_{glu}$), 5.20 (dd-t, 1H, J = 9.3 Hz, J = 9.4 Hz, H-2$_{glu}$), 5.38 (dd-t, 1H, J = 9.5 Hz, J = 9.5 Hz, H-1$_{glu}$), 5.59 (dd-t, 1H, J = 9.3 Hz, J = 9.4 Hz, H-3$_{glu}$), 7.17 (dd, 1H, J = 1.3 Hz, J = 7.6 Hz, H-7$_{chin}$), 7.36–7.44 (m, 2H, H-3$_{chin}$, H-6$_{chin}$), 7.47 (dd, 1H, J = 1.2 Hz, J = 8.2 Hz, H-5$_{chin}$), 8.19 (d, 1H, J = 8.4 Hz, H-4$_{chin}$), 8.83 (s, 1H, H-5$_{triaz}$), 9.17 (d, 1H, J = 9.5 Hz, NHCO); ^{13}C NMR (100 MHz, DMSO-d6): δ 20.31, 20.37, 20.51, 20.74, 25.03, 29.25, 47.14, 61.84, 65.56, 67.83, 70.51, 72.02, 73.01, 76.78, 110.54, 119.91, 122.44, 125.68, 127.32, 127.58, 135.97, 139.34, 141.77, 153.64, 157.35, 160.06, 169.02, 169.31, 169.53, 169.97; HRMS (ESI-TOF): calcd for C$_{30}$H$_{36}$N$_5$O$_{11}$ ([M + H]$^+$): *m/z* 642.2411; found: *m/z* 642.2408.

Glycoconjugate **96:** Starting from 2,3,4,6-tetra-*O*-acetyl-*N*-(β-D-galactopyranosyl)propiolamide **38** and 2-methyl-8-(3-azidopropoxy)quinoline **9**, product was obtained as a white solid (202.1 mg, 63%); m.p.: 121–123 °C; [α]^{25}$_D$ = −4.6 (c = 1.0, CHCl$_3$); ^{1}H NMR (400 MHz, CDCl$_3$): δ 1.98, 2.00, 2.03, 2.17 (4s, 12H, CH$_3$CO), 2.60 (p, 2H, J = 6.4 Hz, CH$_2$), 2.80 (s, 3H, CH$_3$), 4.04–4.17 (m, 3H, H-5$_{gal}$, H-6a$_{gal}$, H-6b$_{gal}$), 4.24 (t, 2H, J = 5.9 Hz, CH$_2$N), 4.82 (t, 2H, J = 6.7 Hz, CH$_2$O), 5.16 (dd, 1H, J = 3.4 Hz, J = 10.2 Hz, H-3$_{gal}$), 5.30 (dd-t, 1H, J = 9.4 Hz, J = 10.1 Hz, H-2$_{gal}$), 5.40 (dd-t, 1H, J = 9.4 Hz, J = 9.5 Hz, H-1$_{gal}$), 5.46

(dd, 1H, J = 0.6 Hz, J = 3.3 Hz, H-4$_{gal}$), 7.04 (dd, 1H, J = 1.8 Hz, J = 7.1 Hz, H-7$_{chin}$), 7.31–7.42 (m, 3H, H-3$_{chin}$, H-5$_{chin}$, H-6$_{chin}$), 7.84 (d, 1H, J = 9.5 Hz, NHCO), 8.03 (d, 1H, J = 8.4 Hz, H-4$_{chin}$), 8.38 (s, 1H, H-5$_{triaz}$); ^{13}C NMR (100 MHz, CDCl$_3$): δ 20.57, 20.63, 20.64, 20.68, 25.65, 29.58, 47.58, 61.27, 65.24, 67.23, 68.10, 71.15, 72.32, 78.14, 110.56, 120.60, 122.68, 125.58, 127.06, 127.85, 136.19, 140.02, 141.93, 153.59, 158.44, 160.30, 169.90, 170.14, 170.36, 170.44; HRMS (ESI-TOF): calcd for C$_{30}$H$_{36}$N$_5$O$_{11}$ ([M + H]$^+$): *m/z* 642.2411; found: *m/z* 642.2409.

Glycoconjugate **97**: Starting from *N*-(β-D-glucopyranosyl)propiolamide **39** and 8-(3-azidopropoxy) quinoline **6**, product was obtained as a white solid (158.5 mg, 69%); m.p.: 185–189 °C; [α]$^{28}_D$ = 6.0 (c = 1.0, DMSO); ^{1}H NMR (400 MHz, DMSO-d6): δ 2.46 (p, 2H, J = 6.5 Hz, CH$_2$), 3.06–3.11 (m, 1H, H-5$_{glu}$), 3.15-3.19 (m, 1H, H-2$_{glu}$), 3.20–3.25 (m, 1H, H-4$_{glu}$), 3.33–3.37 (m, 1H, H-3$_{glu}$), 3.39–3.45 (m, 1H, H-6a$_{glu}$), 3.63–3.68 (m, 1H, H-6b$_{glu}$), 4.19 (t, 2H, J = 6.0 Hz, OH), 4.49 (t, 1H, J = 5.9 Hz, 6-OH), 4.72 (t, 2H, J = 6.3 Hz, CH$_2$N), 4.84–4.94 (m, 3H, H-1$_{glu}$, CH$_2$O), 5.00 (d, 1H, J = 4.6 Hz, OH), 7.20 (dd, 1H, J = 1.5 Hz, J = 7.4 Hz, H-7$_{chin}$), 7.47-7.62 (m, 3H, H-3$_{chin}$, H-5$_{chin}$, H-6$_{chin}$), 8.32 (dd, 1H, J = 1.5 Hz, J = 8.0 Hz, H-4$_{chin}$), 8.66 (d, 1H, J = 9.1 Hz, NHCO), 8.86 (s, 1H, H-5$_{triaz}$), 8.91 (dd, 1H, J = 1.6 Hz, J = 4.1 Hz, H-2$_{chin}$); ^{13}C NMR (100 MHz, DMSO-d6): δ 26.42, 44.13, 58.00, 62.40, 66.98, 68.88, 74.44, 75.69, 76.48, 106.91, 116.97, 118.88, 123.77, 124.17, 132.78, 136.66, 139.53, 142.49, 145.37, 146.13, 157.11; HRMS (ESI-TOF): calcd for C$_{21}$H$_{26}$N$_5$O$_7$ ([M + H]$^+$): *m/z* 460.1832; found: *m/z* 460.1832.

Glycoconjugate **98**: Starting from *N*-(β-D-galactopyranosyl)propiolamide **40** and 8-(3-azidopropoxy) quinoline **6**, product was obtained as a white solid (170.0 mg, 74%); m.p.: 129–132 °C; [α]$^{28}_D$ = 22.0 (c = 1.0, DMSO); ^{1}H NMR (400 MHz, DMSO-d6): δ 2.41–2.49 (m, 2H, CH$_2$), 3.35–3.56 (m, 4H, H-2$_{gal}$, H-3$_{gal}$, H-4$_{gal}$ H-5$_{gal}$), 3.58–3.66 (m, 1H, H-6a$_{gal}$), 3.68–3.75 (m, 1H, H-6b$_{gal}$), 4.20 (t, 2H, J = 6.0 Hz, OH), 4.30 (d, 1H, J = 4.9 Hz, OH), 4.58 (t, 1H, J = 5.4 Hz, 6-OH), 4.68–4.77 (m, 3H, CH$_2$N, CH$_2$O), 4.81 (d, 1H, J = 5.5 Hz, CH$_2$O), 4.89 (dd-t, 1H, J = 9.0 Hz, J = 9.1 Hz, H-1$_{gal}$), 7.20 (dd, 1H, J = 1.8 Hz, J = 7.1 Hz, H-7$_{chin}$), 7.46–7.60 (m, 3H, H-3$_{chin}$, H-5$_{chin}$, H-6$_{chin}$), 8.32 (dd, 1H, J = 1.6 Hz, J = 8.3 Hz, H-4$_{chin}$), 8.47 (d, 1H, J = 9.1 Hz, NHCO), 8.87 (s, 1H, H-5$_{triaz}$), 8.91 (bs, 1H, H-2$_{chin}$); ^{13}C NMR (100 MHz, DMSO-d6): δ 29.41, 47.14, 60.43, 65.43, 68.38, 69.37, 74.04, 76.80, 79.92, 109.90, 119.97, 121.86, 126.77, 127.09, 129.03, 135.78, 139.77, 142.48, 149.12, 154.18, 160.01; HRMS (ESI-TOF): calcd for C$_{21}$H$_{26}$N$_5$O$_7$ ([M + H]$^+$): *m/z* 460.1832; found: *m/z* 460.1835.

Glycoconjugate **99**: Starting from *N*-(β-D-glucopyranosyl)propiolamide **39** and 2-methyl-8-(3-azidopropoxy)quinoline **9**, product was obtained as a brown solid (137.3 mg, 58%); m.p.: 167–169 °C; [α]$^{27}_D$ = −7.0 (c = 1.0, MeOH); ^{1}H NMR (400 MHz, DMSO-d6): δ 2.46 (p, 2H, J = 6.5 Hz, CH$_2$), 2.68 (s, 3H, CH$_3$), 3.05–3.12 (m, 1H, H-5$_{glu}$), 3.14–3.19 (m, 1H, H-2$_{glu}$), 3.20–3.25 (m, 1H, H-4$_{glu}$), 3.34–3.38 (m, 1H, H-3$_{glu}$), 3.39–3.46 (m, 1H, H-6a$_{glu}$), 3.61–3.68 (m, 1H, H-6b$_{glu}$), 4.18 (t, 2H, J = 6.1 Hz, OH), 4.49 (m, 1H, 6-OH), 4.72 (t, 2H, J = 6.9 Hz, CH$_2$N), 4.87–4.94 (m, 3H, H-1$_{glu}$, CH$_2$O), 5.00 (bs, 1H, OH), 7.17 (d, 1H, J = 7.5 Hz, H-7$_{chin}$), 7.38–7.50 (m, 3H, H-3$_{chin}$, H-5$_{chin}$, H-6$_{chin}$), 8.19 (d, 1H, J = 8.4 Hz, H-4$_{chin}$), 8.66 (d, 1H, J = 9.1 Hz, NHCO), 8.80 (s, 1H, H-5$_{triaz}$); ^{13}C NMR (100 MHz, DMSO-d6): δ 25.06, 29.32, 47.02, 60.99, 65.43, 69.98, 71.87, 77.44, 78.69, 79.49, 110.51, 119.92, 122.48, 125.71, 127.10, 127.33, 136.01, 142.48, 146.29, 153.63, 157.39, 160.08; HRMS (ESI-TOF): calcd for C$_{22}$H$_{28}$N$_5$O$_7$ ([M + H]$^+$): *m/z* 474.1989; found: *m/z* 474.1987.

Glycoconjugate **100**: Starting from *N*-(β-D-galactopyranosyl)propiolamide **40** and 2-methyl-8-(3-azidopropoxy)quinoline **9**, product was obtained as a brown solid (175.2 mg, 74%); m.p.: 77–80 °C; [α]$^{26}_D$ = 8.0 (c = 1.0, MeOH); ^{1}H NMR (400 MHz, DMSO-d6): δ 2.41–2.49 (m, 2H, CH$_2$), 2.67 (s, 3H, CH$_3$), 3.35–3.54 (m, 4H, H-2$_{gal}$, H-3$_{gal}$, H-4$_{gal}$ H-5$_{gal}$), 3.57–3.64 (m, 1H, H-6a$_{gal}$), 3.66–3.72 (m, 1H, H-6b$_{gal}$), 4.15–4.22 (m, 2H, OH), 4.30 (d, 1H, J = 4.9 Hz, OH), 4.37–4.44 (m, 1H, OH), 4.52–4.60 (m, 2H, CH$_2$N), 4.66–4.78 (m, 3H, CH$_2$N, CH$_2$O), 4.81 (d, 1H, J = 5.5 Hz, CH$_2$O), 4.87 (dd-t, 1H, J = 9.0 Hz, J = 9.1 Hz, H-1$_{gal}$), 7.17 (dd, 1H, J = 1.2 Hz, J = 7.6 Hz, H-7$_{chin}$), 7.37–7.50 (m, 3H, H-3$_{chin}$, H-5$_{chin}$, H-6$_{chin}$), 8.19 (d, 1H, J = 8.4 Hz, H-4$_{chin}$), 8.46 (d, 1H, J = 9.1 Hz, NHCO), 8.80 (s, 1H, H-5$_{triaz}$); ^{13}C NMR (100 MHz, DMSO-d6): δ 24.96, 29.23, 46.95, 60.33, 65.36, 68.28, 69.28, 73.94, 76.71, 79.83, 110.43,

119.82, 122.38, 125.62, 126.92, 127.24, 135.92, 139.22, 142.34, 153.54, 157.29, 159.88; HRMS (ESI-TOF): calcd for $C_{22}H_{28}N_5O_7$ ([M + H]$^+$): *m/z* 474.1989; found: *m/z* 474.1987.

Glycoconjugate **101:** Starting from 2,3,4,6-tetra-*O*-acetyl-*N*-(β-D-glucopyranosyl)-*O*-propargyl carbamate **41** and 8-(3-azidopropoxy)quinoline **6**, product was obtained as a white solid (309.1 mg, 94%); m.p.: 60–65 °C; [α]$^{25}_D$ = −2.6 (c = 1.0, CHCl$_3$); ^{1}H NMR (400 MHz, CDCl$_3$): δ 2.00, 2.01, 2.02, 2.07 (4s, 12H, CH$_3$CO), 2.62 (p, 2H, *J* = 6.4 Hz, CH$_2$), 3.73–3.83 (m, 1H, H-5$_{glu}$), 4.03–4.13 (m, 1H, H-6a$_{glu}$), 4.24 (t, 2H, *J* = 5.9 Hz, CH$_2$N), 4.26–4.34 (m, 1H, H-6b$_{glu}$), 4.74 (t, 2H, *J* = 6.7 Hz, CH$_2$O), 4.90 (dd-t, 1H, *J* = 9.5 Hz, *J* = 9.5 Hz, H-4$_{glu}$), 5.00 (dd-t, 1H, *J* = 9.5 Hz, *J* = 9.6 Hz, H-3$_{glu}$), 5.06 (dd-t, 1H, *J* = 9.7 Hz, *J* = 9.7 Hz, H-2$_{glu}$), 5.16 and 5.20 (qAB, 2H, *J* = 12.7 Hz, CH$_2$OCO), 5.59 (d, 1H, *J* = 9.5 Hz, H-1$_{glu}$), 7.04 (dd, 1H, *J* = 2.6 Hz, *J* = 6.3 Hz, H-7$_{chin}$), 7.40–7.50 (m, 3H, H-3$_{chin}$, H-5$_{chin}$, H-6$_{chin}$), 7.78 (s, 1H, H-5$_{triaz}$), 8.16 (dd, 1H, *J* = 1.7 Hz, *J* = 8.3 Hz, H-4$_{chin}$), 8.96 (dd, 1H, *J* = 1.7 Hz, *J* = 4.2 Hz, H-2$_{chin}$); ^{13}C NMR (100 MHz, CDCl$_3$): δ 20.56, 20.57, 20.63, 20.72, 29.66, 47.32, 58.81, 61.58, 65.26, 68.08, 70.11, 72.80, 73.36, 80.82, 109.52, 120.38, 121.74, 124.61, 126.68, 129.58, 136.07, 140.35, 142.38, 149.42, 154.23, 155.23, 169.48, 169.90, 170.55, 170.59; HRMS (ESI-TOF): calcd for $C_{30}H_{36}N_5O_{12}$ ([M + H]$^+$): *m/z* 658.2360; found: *m/z* 658.2360.

Glycoconjugate **102:** Starting from 2,3,4,6-tetra-*O*-acetyl-*N*-(β-D-galactopyranosyl)-*O*-propargyl carbamate **42** and 8-(3-azidopropoxy)quinoline **6**, product was obtained as a white solid (295.9 mg, 90%); m.p.: 66–69 °C; [α]$^{25}_D$ = −7.0 (c = 1.0, CHCl$_3$); ^{1}H NMR (400 MHz, CDCl$_3$): δ 1.98, 2.02, 2.03, 2.13 (4s, 12H, CH$_3$CO), 2.62 (p, 2H, *J* = 6.4 Hz, CH$_2$), 3.96–4.03 (m, 1H, H-6a$_{gal}$), 4.04–4.16 (m, 2H, H-5$_{gal}$, H-6a$_{gal}$), 4.25 (t, 2H, *J* = 5.9 Hz, CH$_2$N), 4.74 (t, 2H, *J* = 6.7 Hz, CH$_2$O), 4.97 (dd-t, 1H, *J* = 8.3 Hz, *J* = 8.8 Hz, H-2$_{gal}$), 5.03–5.13 (m, 2H, H-3$_{gal}$, H-4$_{gal}$), 5.16 and 5.20 (qAB, 2H, *J* = 12.8 Hz, CH$_2$OCO), 5.58 (d, 1H, *J* = 9.5 Hz, H-1$_{gal}$), 7.05 (dd, 1H, *J* = 2.5 Hz, *J* = 6.4 Hz, H-7$_{chin}$), 7.41–7.49 (m, 3H, H-3$_{chin}$, H-5$_{chin}$, H-6$_{chin}$), 7.78 (s, 1H, H-5$_{triaz}$), 8.16 (dd, 1H, *J* = 1.7 Hz, *J* = 8.3 Hz, H-4$_{chin}$), 8.96 (dd, 1H, *J* = 1.7 Hz, *J* = 4.2 Hz, H-2$_{chin}$); ^{13}C NMR (100 MHz, CDCl$_3$): δ 20.52, 20.60, 20.67, 20.71, 29.67, 47.33, 58.79, 61.07, 65.29, 67.10, 67.87, 70.92, 72.08, 81.16, 109.56, 120.39, 121.75, 124.57, 126.68, 129.59, 136.07, 140.37, 142.48, 149.43, 154.25, 155.25, 169.79, 170.04, 170.33, 170.83; HRMS (ESI-TOF): calcd for $C_{30}H_{36}N_5O_{12}$ ([M + H]$^+$): *m/z* 658.2360; found: *m/z* 658.2360.

Glycoconjugate **103:** Starting from 2,3,4,6-tetra-*O*-acetyl-*N*-(β-D-glucopyranosyl)-*O*-propargyl carbamate **41** and 2-methyl-8-(3-azidopropoxy)quinoline **9**, product was obtained as a white solid (228.4 mg, 68%); m.p.: 56–59 °C; [α]$^{26}_D$ = −3.0 (c = 1.0, CHCl$_3$); ^{1}H NMR (400 MHz, CDCl$_3$): δ 2.01, 2.01, 2.03, 2.07 (4s, 12H, CH$_3$CO), 2.59 (p, 2H, *J* = 6.4 Hz, CH$_2$), 2.79 (s, 3H, CH$_3$), 3.73–3.83 (m, 1H, H-5$_{glu}$), 4.01–4.13 (m, 1H, H-6a$_{glul}$), 4.23 (t, 2H, *J* = 5.9 Hz, CH$_2$N), 4.26–4.34 (m, 1H, H-6b$_{glu}$), 4.75 (t, 2H, *J* = 6.7 Hz, CH$_2$O), 4.89 (dd-t, 1H, *J* = 9.4 Hz, *J* = 9.5 Hz, H-4$_{glu}$), 4.99 (dd-t, 1H, *J* = 9.5 Hz, *J* = 9.7 Hz, H-3$_{glu}$), 5.06 (dd-t, 1H, *J* = 9.7 Hz, *J* = 9.8 Hz, H-2$_{glu}$), 5.13–5.23 (m, 2H, *J* = 12.7 Hz, CH$_2$OCO), 5.53 (d, 1H, *J* = 9.5 Hz, H-1$_{glu}$), 7.03 (dd, 1H, *J* = 2.3 Hz, *J* = 6.6 Hz, H-7$_{chin}$), 7.30–7.43 (m, 3H, H-3$_{chin}$, H-5$_{chin}$, H-6$_{chin}$), 7.83 (s, 1H, H-5$_{triaz}$), 8.04 (dd, 1H, *J* = 1.7 Hz, *J* = 8.4 Hz, H-4$_{chin}$); ^{13}C NMR (100 MHz, CDCl$_3$): δ 20.58, 20.59, 20.66, 20.74, 25.69, 29.62, 47.25, 58.79, 61.54, 65.32, 68.01, 70.03, 72.75, 73.30, 80.78, 110.04, 120.31, 122.64, 124.70, 125.66, 127.78, 136.21, 139.88, 142.28, 153.62, 155.20, 158.27, 169.50, 169.93, 170.58, 170.63; HRMS (ESI-TOF): calcd for $C_{31}H_{38}N_5O_{12}$ ([M + H]$^+$): *m/z* 672.2517; found: *m/z* 672.2516.

Glycoconjugate **104:** Starting from 2,3,4,6-tetra-*O*-acetyl-*N*-(β-D-galactopyranosyl)-*O*-propargyl carbamate **42** and 2-methyl-8-(3-azidopropoxy)quinoline **9**, product was obtained as a white solid (214.9 mg, 64%); m.p.: 62–65 °C; [α]$^{26}_D$ = 6.8 (c = 1.0, CHCl$_3$); ^{1}H NMR (400 MHz, CDCl$_3$): δ 1.98, 2.02, 2.03, 2.14 (4s, 12H, CH$_3$CO), 2.59 (p, 2H, *J* = 6.4 Hz, CH$_2$), 2.79 (s, 3H, CH$_3$), 3.96–4.03 (m, 1H, H-6a$_{gal}$), 4.04–4.16 (m, 2H, H-5$_{gal}$, H-6a$_{gal}$), 4.23 (t, 2H, *J* = 5.9 Hz, CH$_2$N), 4.76 (t, 2H, *J* = 6.7 Hz, CH$_2$O), 4.96 (dd-t, 1H, *J* = 8.3 Hz, *J* = 8.8 Hz, H-2$_{gal}$), 5.03–5.13 (m, 2H, H-3$_{gal}$, H-4$_{gal}$), 5.14–5.23 (m, 2H, CH$_2$OCO), 5.53 (d, 1H, *J* = 9.3 Hz, H-1$_{gal}$), 7.03 (dd, 1H, *J* = 2.5 Hz, *J* = 6.5 Hz, H-7$_{chin}$), 7.31–7.43 (m, 3H, H-3$_{chin}$, H-5$_{chin}$, H-6$_{chin}$), 7.83 (s, 1H, H-5$_{triaz}$), 8.04 (d, 1H, *J* = 8.4 Hz, H-4$_{chin}$); ^{13}C NMR (100 MHz, CDCl$_3$): δ 20.53, 20.61, 20.67, 20.72, 25.69, 29.68, 47.28, 58.80, 61.07, 65.45, 67.10, 67.85, 70.93, 72.08, 81.15, 110.24,

120.37, 122.63, 124.62, 125.67, 127.82, 136.19, 139.99, 142.36, 153.71, 155.23, 158.28, 169.80, 170.05, 170.34, 170.83; HRMS (ESI-TOF): calcd for $C_{31}H_{38}N_5O_{12}$ ([M + H]$^+$): *m/z* 672.2517; found: *m/z* 672.2518.

Glycoconjugate **105:** Starting from *N*-(β-D-glucopyranosyl)-*O*-propargyl carbamate **43** and 8-(3-azidopropoxy)quinoline **6**, product was obtained as a white solid (203.1 mg, 83%); m.p.: 73–75 °C; $[\alpha]^{27}_D = 0.2$ (c = 1.0, MeOH); ^{1}H NMR (400 MHz, DMSO-d6): δ 2.42 (p, 2H, *J* = 6.4 Hz, CH$_2$), 2.96–3.11 (m, 3H, H-2$_{glu}$, H-4$_{glu}$, H-5$_{glu}$), 3.15–3.20 (m, 1H, H-3$_{glu}$), 3.36–3.44 (m, 1H, H-6a$_{glu}$), 3.58–3.68 (m, 1H, H-6b$_{glu}$), 4.09 (d, 1H, *J* = 5.1 Hz, OH), 4.20 (t, 2H, *J* = 6.0 Hz, CH$_2$N), 4.45–4.54 (m, 2H, OH), 4.65 (t, 2H, *J* = 6.9 Hz, CH$_2$O), 4.86 (m, 2H, CH$_2$OCO), 4.95 (m, 1H, H-1$_{glu}$), 5.07 (s, 1H, OH), 7.20 (dd, 1H, *J* = 2.2 Hz, *J* = 6.8 Hz, H-7$_{chin}$), 7.47–7.59 (m, 3H, H-3$_{chin}$, H-5$_{chin}$, H-6$_{chin}$), 7.89 (d, 1H, *J* = 9.2 Hz, NHCO), 8.31 (s, 1H, H-5$_{triaz}$), 8.33 (dd, 1H, *J* = 1.7 Hz, *J* = 8.3 Hz, H-4$_{chin}$), 8.89 (dd, 1H, *J* = 1.7 Hz, *J* = 4.1 Hz, H-2$_{chin}$); ^{13}C NMR (100 MHz, DMSO-d6): δ 29.64, 46.70, 57.07, 60.95, 65.43, 69.92, 72.02, 77.56, 78.38, 82.44, 109.85, 119.94, 121.89, 124.98, 126.82, 129.06, 135.84, 139.77, 142.42, 149.09, 154.19, 155.71; HRMS (ESI-TOF): calcd for $C_{22}H_{28}N_5O_8$ ([M + H]$^+$): *m/z* 490.1938; found: *m/z* 490.1937.

Glycoconjugate **106:** Starting from *N*-(β-D-galactopyranosyl)-*O*-propargyl carbamate **44** and 8-(3-azidopropoxy)quinoline **6**, product was obtained as a white solid (200.7 mg, 82%); m.p.: 119–121 °C; $[\alpha]^{28}_D = 19.0$ (c = 1.0, DMSO); ^{1}H NMR (400 MHz, DMSO-d6): δ 2.42 (p, 2H, *J* = 6.5 Hz, CH$_2$), 3.33–3.53 (m, 4H, H-2$_{gal}$, H-3$_{gal}$, H-4$_{gal}$ H-5$_{gal}$), 3.63-3.69 (m, 1H, H-6a$_{gal}$), 4.08 (dd, 1H, *J* = 5.3 Hz, *J* = 10.5 Hz, H-6b$_{gal}$), 4.20 (t, 2H, *J* = 6.1 Hz, CH$_2$N), 4.32 (d, 1H, *J* = 3.8 Hz, OH), 4.46 (dd-t, 1H, *J* = 9.0 Hz, *J* = 9.0 Hz, H-1$_{gal}$), 4.55 (t, 1H, *J* = 5.6 Hz, OH), 4.61–4.72 (m, 4H, CH$_2$O, CH$_2$OCO), 5.06 (s, 2H, OH), 7.20 (dd, 1H, *J* = 2.2 Hz, *J* = 6.8 Hz, H-7$_{chin}$), 7.47–7.59 (m, 3H, H-3$_{chin}$, H-5$_{chin}$, H-6$_{chin}$), 7.84 (d, 1H, *J* = 9.2 Hz, NHCO), 8.29 (s, 1H, H-5$_{triaz}$), 8.32 (dd, 1H, *J* = 1.7 Hz, *J* = 8.2 Hz, H-4$_{chin}$), 8.89 (dd, 1H, *J* = 1.7 Hz, *J* = 4.1 Hz, H-2$_{chin}$); ^{13}C NMR (100 MHz, DMSO-d6): δ 29.62, 46.68, 57.03, 60.47, 65.44, 68.19, 69.27, 74.21, 76.53, 82.92, 109.86, 119.93, 121.86, 124.92, 126.80, 129.04, 135.80, 139.77, 142.47, 149.06, 154.18, 155.76; HRMS (ESI-TOF): calcd for $C_{22}H_{28}N_5O_8$ ([M + H]$^+$): *m/z* 490.1938; found: *m/z* 490.1935.

Glycoconjugate **107:** Starting from *N*-(β-D-glucopyranosyl)-*O*-propargyl carbamate **43** and 2-methyl-8-(3-azidopropoxy)quinoline **9**, product was obtained as a white solid (201.4 mg, 80%); m.p.: 57–60 °C; $[\alpha]^{27}_D = -0.2$ (c = 1.0, MeOH); ^{1}H NMR (400 MHz, DMSO-d6): δ 2.41 (p, 2H, *J* = 6.5 Hz, CH$_2$), 2.67 (s, 3H, CH$_3$), 2.96–3.11 (m, 3H, H-2$_{glu}$, H-4$_{glu}$, H-5$_{glu}$), 3.12–3.20 (m, 1H, H-3$_{glu}$), 3.36–3.44 (m, 1H, H-6a$_{glu}$), 3.59–3.68 (m, 1H, H-6b$_{glu}$), 4.09 (d, 1H, *J* = 5.3 Hz, OH), 4.19 (t, 2H, *J* = 6.2 Hz, CH$_2$N), 4.44–4.53 (m, 2H, OH), 4.61–4.69 (m, 2H, CH$_2$O), 4.86 (m, 2H, CH$_2$OCO), 4.94 (d, 1H, *J* = 4.7 Hz, H-1$_{glu}$), 5.06 (s, 1H, OH), 7.16 (dd, 1H, *J* = 1.1 Hz, *J* = 7.5 Hz, H-7$_{chin}$), 7.38–7.50 (m, 3H, H-3$_{chin}$, H-5$_{chin}$, H-6$_{chin}$), 7.88 (d, 1H, *J* = 9.2 Hz, NHCO), 8.02 (d, 1H, *J* = 9.2 Hz, H-2$_{chin}$), 8.19 (d, 1H, *J* = 8.4 Hz, H-4$_{chin}$), 8.30 (s, 1H, H-5$_{triaz}$); ^{13}C NMR (100 MHz, DMSO-d6): δ 25.08, 29.57, 46.68, 57.06, 60.94, 65.58, 69.92, 72.02, 77.54, 78.37, 82.43, 110.36, 119.86, 122.48, 124.94, 125.75, 127.34, 136.01, 139.32, 142.39, 153.68, 155.70, 157.35; HRMS (ESI-TOF): calcd for $C_{23}H_{30}N_5O_8$ ([M + H]$^+$): *m/z* 504.2094; found: *m/z* 504.2090.

Glycoconjugate **108:** Starting from *N*-(β-D-galactopyranosyl)-*O*-propargyl carbamate **44** and 2-methyl-8-(3-azidopropoxy)quinoline **9**, product was obtained as a white solid (196.4 mg, 78%); m.p.: 94–98 °C; $[\alpha]^{26}_D = 3.0$ (c = 1.0, H$_2$O); ^{1}H NMR (400 MHz, DMSO-d6): δ 2.41 (p, 2H, *J* = 6.6 Hz, CH$_2$), 2.67 (s, 3H, CH$_3$), 3.33–3.53 (m, 4H, H-2$_{gal}$, H-3$_{gal}$, H-4$_{gal}$ H-5$_{gal}$), 3.63–3.69 (m, 1H, H-6a$_{gal}$), 4.08 (dd, 1H, *J* = 5.3 Hz, *J* = 10.5 Hz, H-6b$_{gal}$), 4.19 (t, 2H, *J* = 6.2 Hz, CH$_2$N), 4.32 (d, 1H, *J* = 3.8 Hz, OH), 4.46 (m, 1H, H-1$_{gal}$), 4.55 (t, 1H, *J* = 5.6 Hz, OH), 4.61–4.73 (m, 4H, CH$_2$O, CH$_2$OCO), 5.06 (s, 2H, OH), 7.16 (dd, 1H, *J* = 1.3 Hz, *J* = 7.6 Hz, H-7$_{chin}$), 7.38–7.49 (m, 3H, H-3$_{chin}$, H-5$_{chin}$, H-6$_{chin}$), 7.83 (d, 1H, *J* = 9.2 Hz, NHCO), 8.19 (d, 1H, *J* = 8.4 Hz, H-4$_{chin}$), 8.29 (s, 1H, H-5$_{triaz}$), ^{13}C NMR (100 MHz, DMSO-d6): δ 25.07, 29.56, 46.66, 57.03, 60.47, 65.60, 68.18, 69.27, 74.21, 76.52, 82.92, 110.39, 119.86, 122.46, 124.88, 125.73, 127.33, 135.98, 139.33, 142.45, 153.68, 155.76, 157.32; HRMS (ESI-TOF): calcd for $C_{23}H_{30}N_5O_8$ ([M + H]$^+$): *m/z* 504.2094; found: *m/z* 504.2097.

3.3. Biological Assays

3.3.1. Cell Lines

The culture media were purchased from EuroClone, HyClone and Pan Biotech. Fetal bovine serum (FBS) was delivered by Eurx, Poland and Antibiotic Antimycotic Solution (100×) by Sigma-Aldrich, Germany. The human colon adenocarcinoma cell line HCT 116 was obtained from American Type Culture Collection (ATCC, Manassas, VA, USA). The human cell line MCF-7 was obtained from collections at the Maria Sklodowska-Curie Memorial Cancer Center and Institute of Oncology, branch in Gliwice, Poland, as kindly gift from Monika Pietrowska and prof. Wiesława Widłak. The Normal Human Dermal Fibroblasts-Neonatal, NHDF-Neo were purchased from LONZA (Cat. No. CC-2509, NHDF-Neo, Dermal Fibroblasts, Neonatal, Lonza, Poland). The culture media consisted of RPMI 1640 or DMEM+F12 medium, supplemented with 10% fetal bovine serum and standard antibiotics.

3.3.2. MTT Assay

A lifespan of the cells was assessed with an MTT (3-[4–dimethylthiazol-2-yl]-2,5-diphenyltetrazolium bromide) test (Sigma-Aldrich). The cells at concentration 1×10^4 (HCT 116, NHDF-Neo) or 5×10^3 (MCF-7) per well were seeded into 96-well plates. The cell cultures were incubated for 24 h at 37 °C in a humidified atmosphere of 5% CO_2. After this time, the culture medium was removed, replaced with solution of the tested compounds in medium and incubated for further 24 h or 72 h. After that, medium was removed and the MTT solution (50 μL, 0.5 mg/mL in PBS) was added. After 3 h of incubation, the MTT solution was removed and the acquired formazan was dissolved in DMSO. Finally, the absorbance at the 570 nm wavelength was measured spectrophotometrically with the plate reader. The experiment was conducted in three independent iterations with four technical repetitions. Tests were conducted at concentrations tested compounds range from 0.01 mM to 0.8 mM solutions. For the most active compounds IC_{50} values were calculated using CalcuSyn.

3.3.3. Bovine Milk β-1,4-Galactosyltransferase I Assay

Bovine milk β-1,4-Galactosyltransferase I was purchased from Sigma-Aldrich. The β-1,4-GalT activity was assayed using UDP-Gal, a natural β-1,4-GalT glycosyl donor type substrate, and (6-esculetinyl) β-D-glucopyranoside (esculine) as glycosyl fluorescent acceptor. The reaction mixtures contained reagents in the following final concentrations: 50 mM citrate buffer (pH 5.4), 100 mM $MnCl_2$, 20 mg/mL BSA, 2 mM esculine, 0.4 mM UDP-Gal and 10 μL MeOH or methanolic solution of potential inhibitors **49–52**, **57–60**, **65–68**, **73–76**, **81–84** at 0.8 mM concentration. Assays were performed in a total volume of 200 μL. The enzymatic reactions were started by the addition of 8 mU β-1,4-GalT and incubated at 30 °C for 60 min. After that, the reaction mixture was diluted with water to a volume of 500 μL and then was placed in a thermoblock set at 90 °C for 3 min. After protein denaturation, the solutions were centrifuged at 10 °C for 30 min at 10 000 rpm. The supernatant was filtered using syringe filters (M.E. Cellulose filter, Teknokroma®, 0.2 μm × 13 mm). The filtrate was injected into RP-HPLC system. The percentage of inhibition was evaluated from the fluorescence intensity of the peaks referring to product (6-esculetinyl) 4′-*O*-β-D-galactopyranosyl-β-D-glucopyranoside). For the most active compounds, IC_{50} values were determined by the same procedure using the reaction mixtures containing inhibitor in the concentrations of 0.1, 0.2, 0.4, and 0.8 mM and calculated using CalcuSyn software.

3.4. Metal Complexing Studies

Absorption measurements were carried out at room temperature, using a UV/VIS/NIR spectrophotometer JASCO V-570 (Tokyo, Japan) with the software Spectra Manager Program. Absorption spectra of selected compounds, in the presence of copper (II) sulfate pentahydrate in HPLC grade methanol, were recorded in spectra range of 200–450 nm. The stoichiometry of complexes were determined using Job's method, by titrating the particular compound methanol

solution with increasing concentrations of copper salt. The graph was plotted as the difference in absorbance of the absorption band at 265 nm, $\Delta A = A_x - A_0$ as a function of molar fraction of glycoconjugate. The maximum in the plot corresponds to the stoichiometry of complex formed.

Electrospray mass spectrometry (ESI-MS^n) was performed using a Thermo Scientific LCQ Fleet ion trap spectrometer (Thermo Fisher Scientific Inc., CA, USA). All analyses were performed in methanol. The solutions were introduced into the ESI source by continuous infusion at 4 μL·min^{-1} using the syringe pump. The ESI source was set to an operating voltage of 4 kV and the capillary heater was set to 160 °C. Nitrogen was used as the nebulizing gas and helium was used as the collision and damping gas in the ion trap.

4. Conclusions

In summary, a wide range of new glycoconjugates derivatives of 8-HQ, in which the sugar part was connected to the quinoline derivative via linker containing a 1,2,3-triazole fragment was obtained and characterized. The effect of modifying the structure of the mentioned linker on the biological activity in vitro exhibited by glycoconjugates was investigated. These modifications concerned the extension of the alkyl chain between 1,2,3-triazole ring and quinoline or sugar moiety, as well as the introduction of an additional amide or carbamate group into the linker structure. The obtained glycoconjugates contained the sugar unit with a binding of the β-configuration at the anomeric center since such orientation is preferred for binding to the GLUT transporters [84]. The new glycoconjugates structures have been designed in such a way to take advantage of some unique features of cancer cells, such as the high concentration of Cu^{2+} ions and overexpression of some proteins, such as β-1,4-galactosyltransferase or GLUT transporters to improving their selectivity and minimizing side effects of their application on healthy tissues.

Glycoconjugates were tested for inhibition of the proliferation of selected cancer cell lines and inhibition of β-1,4-Gal activity, in which overexpression is associated with cancer progression. All glycoconjugates in protected form have a cytotoxic effect on cancer cells in the tested concentration range. Tested glycoconjugates were more active on the HCT 116 cell line than parent quinolines. Therefore, it can be assumed that the presence of a sugar unit and an additional metal ion binding motif improves the cytotoxic activity of glycoconjugates. MCF-7 cell line appears to be more sensitive to quinoline derivatives. Most of the glycoconjugates showed lower activity than their parent compounds against the breast cancer cell line, however the addition of a sugar unit allowed to improve their selectivity (as can be seen from the example of compounds **63**, **85** and **86**). Glycoconjugates containing an additional amide bond in the linker structure proved to be more active relative to the cell lines tested. Among them, derivatives whose structure was based on the 8-HQ fragment showed better cytotoxicity compared to derivatives with 2Me8HQ unit. In turn, the type of sugar unit did not significantly affect the activity of synthesized glycoconjugates. It can be concluded that the presence of amide groups improves the activity of glycoconjugates, probably through the improvement of metal ions chelation. Interestingly, glycoconjugates with an amide moiety in the structure did not affect the inhibition of β-1,4-Gal activity. On the other hand, it was noted, that extension the alkyl chain between triazole and quinoline part increases the ability of glycoconjugates to inhibit enzyme activity, which is probably associated with increased "flexibility" of the molecule. However, it cannot be ruled out any mechanism of action at this step.

Although the IC_{50} values determined do not predestine the use of the obtained compounds as potential drugs, it is possible to notice some regularities in their structure that improve the activity of the obtained molecules. In the course of the research, it was found that the activity of the obtained glycoconjugates depends on the presence of the sugar moiety, the presence of protecting groups in the sugar unit as well as the type and length of the linker connecting the sugar parts and quinoline moiety. Sugar improves the solubility, bioavailability, and selectivity of potential drugs, whereas the heteroaromatic fragment improves the activity of glycoconjugate, probably due to the ability to chelate metals ions present in many types of cancer cells. The study of metal complexing properties confirmed

that the obtained glycoconjugates are capable of chelating copper ions. Moreover, the addition of the 1,2,3-triazole fragment improved the ability to form such complexes. The determined stoichiometry of the glycoconjugate complex indicates that the tested compounds chelate copper ions in a 1:1 molar ratio, while 8-HQ forms chelates in a 2:1 ratio.

One of the important strategies for improving the therapeutic efficacy of anticancer drugs is the synthesis of new derivatives with a modified structure. The obtained results encourage further structural optimization of quinoline glycoconjugates. A huge library of compounds will allow the identification of those specific structural elements that are responsible for demonstrating biological activity.

References

1. Mullard, A. FDA drug approvals. *Nat. Rev. Drug Discov.* **2019**, *18*, 85–89. [CrossRef]
2. Vitaku, E.; Smith, D.T.; Njardarson, J.T. Analysis of the structural diversity, substitution patterns, and frequency of nitrogen heterocycles among U.S. FDA approved pharmaceuticals. *J. Med. Chem.* **2014**, *57*, 10257–10274. [CrossRef] [PubMed]
3. Afzal, O.; Kumar, S.; Haider, R.; Ali, R.; Kumar, R.; Jaggi, M.; Bawa, S. A review on anticancer potential of bioactive heterocycle quinoline. *Eur. J. Med. Chem.* **2015**, *97*, 871–910. [CrossRef] [PubMed]
4. Sissi, C.; Palumbo, M. The quinolone family: From antibacterial to anticancer agents. *Curr. Med. Chem. Anticancer Agents* **2003**, *3*, 439–450. [CrossRef] [PubMed]
5. Musiol, R. An overview of quinoline as a privileged scaffold in cancer drug discovery. *Exp. Op. Drug Disc.* **2017**, *12*, 583–597. [CrossRef] [PubMed]
6. Keri, R.S.; Patil, S.A. Quinoline: A promising antitubercular target. *Biomed. Pharmacother.* **2014**, *68*, 1161–1175. [CrossRef]
7. Novakowa, J.; Vlkova, E.; Bonusova, B.; Rada, V.; Kokoska, L. In vitro selective inhibitory effect of 8-hydroxyquinoline against bifidobacteria and clostridia. *Anaerobe* **2013**, *22*, 134–136. [CrossRef]
8. Enquist, P.A.; Gylfe, A.; Hägglund, U.; Lindström, P.; Norberg-Scherman, H.; Sundin, C.; Elofsson, M. Derivatives of 8-hydroxyquinoline—Antibacterial agents that target intra- and extracellular Gram-negative pathogens. *Bioorg. Med. Chem. Lett.* **2012**, *22*, 3550–3553. [CrossRef]
9. Darby, C.M.; Nathan, C.F. Killing of non-replicating Mycobacterium tuberculosis by 8-hydroxyquinoline. *J. Antimicrob. Chemother.* **2010**, *65*, 1424–1427. [CrossRef]
10. Pippi, B.; Reginatto, P.; Machado, G.R.M.; Bergamo, V.Z.; Lana, D.F.D.; Teixeira, M.L.; Franco, L.L.; Alves, R.J.; Andrade, S.F.; Fuentefria, A.M. Evaluation of 8-Hydroxyquinoline Derivatives as Hits for Antifungal Drug Design. *Med. Mycol.* **2017**, *55*, 763–773. [CrossRef]
11. Musiol, R.; Jampilek, J.; Buchta, V.; Silva, L.; Niedbala, H.; Podeszwa, B.; Palka, A.; Majerz-Maniecka, K.; Oleksyn, B.; Polanski, J. Antifungal properties of new series of quinoline derivatives. *Bioorg. Med. Chem.* **2006**, *14*, 3592–3598. [CrossRef] [PubMed]

12. Regland, B.; Lehmann, W.; Abedini, I.; Blennow, K.; Jonsson, M.; Karlsson, I.; Sjögren, M.; Wallin, A.; Xilinas, M.; Gottfries, C.G. Treatment of Alzheimer's Disease with Clioquinol. *Dement. Geriatr. Cogn. Disord.* **2001**, *12*, 408–414. [CrossRef] [PubMed]

13. Bareggi, S.R.; Cornelli, U. Clioquinol: Review of its mechanisms of action and clinical uses in neurodegenerative disorders. *CNS Neurosci. Ther.* **2012**, *18*, 41–46. [CrossRef] [PubMed]

14. Prachayasittikul, V.; Prachayasittikul, S.; Ruchirawat, S.; Prachayasittikul, V. 8-Hydroxyquinolines: A review of their metal chelating properties and medicinal applications. *Drug Des. Dev. Ther.* **2013**, *7*, 1157–1178. [CrossRef]

15. Oliveri, V.; Vecchio, G. 8-Hydroxyquinolines in medicinal chemistry: A structural perspective. *Eur. J. Med. Chem.* **2016**, *120*, 252–274. [CrossRef]

16. Song, Y.; Xu, H.; Chen, W.; Zhan, P.; Liu, X. 8-Hydroxyquinoline: A privileged structure with a broad-ranging pharmacological potential. *Med. Chem. Commun.* **2015**, *6*, 61–74. [CrossRef]

17. Helsel, M.E.; Franz, K.J. Pharmacological activity of metal binding agents that alter copper bioavailability. *Dalton Trans.* **2015**, *44*, 8760–8770. [CrossRef]

18. Ding, W.Q.; Lind, S.E. Metal Ionophores—An Emerging Class of Anticancer Drugs. *IUBMB Life* **2009**, *61*, 1013–1018. [CrossRef]

19. Tripathi, L.; Kumar, P.; Singhai, A.K. Role of chelates in treatment of cancer. *Indian J. Cancer* **2007**, *44*, 62–71. [CrossRef]

20. Gupte, A.; Mumper, R.J. Elevated copper and oxidative stress in cancer cells as a target for cancer treatment. *Cancer Treat. Rev.* **2009**, *35*, 32–46. [CrossRef]

21. Harris, E.D. A Requirement for Copper in Angiogenesis. *Nutr. Rev.* **2004**, *62*, 60–64. [CrossRef] [PubMed]

22. Theophanides, T.; Anastassopoulou, J. Copper and carcinogenesis. *Crit. Rev. Oncol. Hematol.* **2002**, *42*, 57–64. [CrossRef]

23. Grubman, A.; White, A.R. Copper as a key regulator of cell signalling pathways. *Expert. Rev. Mol. Med.* **2014**, *16*. [CrossRef] [PubMed]

24. Kuo, H.W.; Chen, S.F.; Wu, C.C.; Chen, D.R.; Lee, J.H. Serum and tissue trace elements in patients with breast cancer in Taiwan. *Biol. Trace. Elem. Res.* **2002**, *89*, 1–11. [CrossRef]

25. Geraki, K.; Farquharson, M.J.; Bradley, D.A. Concentrations of Fe, Cu and Zn in breast tissue: A synchrotron XRF study. *Phys. Med. Biol.* **2002**, *47*, 2327–2339. [CrossRef]

26. Chen, D.; Cui, Q.C.; Yang, H.; Barrea, R.A.; Sarkar, F.H.; Sheng, S.; Yan, B.; Reddy, G.P.; Dou, Q.P. Clioquinol, a therapeutic agent for Alzheimer's disease, has proteasome-inhibitory, androgen receptor-suppressing, apoptosis-inducing, and antitumor activities in human prostate cancer cells and xenografts. *Cancer Res.* **2007**, *67*, 1636–1644. [CrossRef]

27. Chen, D.; Peng, F.; Cui, Q.C.; Daniel, K.G.; Orlu, S.; Liu, J.; Dou, Q.P. Inhibition of prostate cancer cellular proteasome activity by a pyrrolidine dithiocarbamate-copper complex is associated with suppression of proliferation and induction of apoptosis. *Front. Biosci.* **2005**, *10*, 2932–2939. [CrossRef]

28. Gupta, S.K.; Shukla, V.K.; Vaidya, M.P.; Roy, S.K.; Gupta, S. Serum and tissue trace elements in colorectal cancer. *J. Surg. Oncol.* **1993**, *52*, 172–175. [CrossRef]

29. Díez, M.; Arroyo, M.; Cerdàn, F.J.; Muñoz, M.; Martin, M.A.; Balibrea, J.L. Serum and tissue trace metal levels in lung cancer. *Oncology* **1989**, *46*, 230–234. [CrossRef]

30. Yoshida, D.; Ikeda, Y.; Nakazawa, S. Quantitative analysis of copper, zinc and copper/zinc ratio in selected human brain tumors. *J. Neurooncol.* **1993**, *16*, 109–115. [CrossRef]

31. Gaur, K.; Vázquez-Salgado, A.M.; Duran-Camacho, G.; Dominguez-Martinez, I.; Benjamín-Rivera, J.A.; Fernández-Vega, L.; Carmona Sarabia, L.; Cruz García, A.; Pérez-Deliz, F.; Méndez Román, J.A.; et al. Iron and Copper Intracellular Chelation as an Anticancer Drug Strategy. *Inorganics* **2018**, *6*, 126. [CrossRef]

32. Denoyer, D.; Masaldan, S.; La Fontaine, S.; Cater, M.A. Targeting copper in cancer therapy: 'Copper That Cancer'. *Metallomics* **2015**, *7*, 1459–1476. [CrossRef] [PubMed]

33. Tapiero, H.; Townsend, D.M.; Tew, K.D. Trace elements in human physiology and pathology. Copper. *Biomed. Pharmacother.* **2003**, *57*, 386–398. [CrossRef]

34. Brewer, G.J. Copper control as an antiangiogenic anticancer therapy: Lessons from treating Wilson's disease. *Exp. Biol. Med.* **2001**, *226*, 665–673. [CrossRef]

35. Brewer, G.J.; Dick, R.D.; Grover, D.K.; LeClaire, V.; Tseng, M.; Wicha, M.; Pienta, K.; Redman, B.G.; Jahan, T.; Sondak, V.K.; et al. Treatment of metastatic cancer with tetrathiomolybdate, an anticopper, antiangiogenic agent: Phase I study. *Clin. Cancer Res.* **2000**, *6*, 1–10.

36. Redman, B.G.; Esper, P.; Pan, Q.; Dunn, R.L.; Hussain, H.K.; Chenevert, T.; Brewer, G.J.; Merajver, S.D. Phase II trial of tetrathiomolybdate in patients with advanced kidney cancer. *Clin. Cancer Res.* **2003**, *9*, 1666–1672.

37. Pass, H.I.; Brewer, G.J.; Dick, R.; Carbone, M.; Merajver, S. A phase II trial of tetrathiomolybdate after surgery for malignant mesothelioma: Final results. *Ann. Thorac. Surg.* **2008**, *86*, 383–390. [CrossRef]

38. Jain, S.; Cohen, J.; Ward, M.M.; Kornhauser, N.; Chuang, E.; Cigler, T.; Moore, A.; Donovan, D.; Lam, C.; Cobham, M.V.; et al. Tetrathiomolybdate-associated copper depletion decreases circulating endothelial progenitor cells in women with breast cancer at high risk of relapse. *Ann. Oncol.* **2013**, *24*, 1491–1498. [CrossRef]

39. Schneider, B.J.; Lee, J.S.; Hayman, J.A.; Chang, A.C.; Orringer, M.B.; Pickens, A.; Pan, C.C.; Merajver, S.D.; Urba, S.G. Pre-operative chemoradiation followed by post-operative adjuvant therapy with tetrathiomolybdate, a novel copper chelator, for patients with resectable esophageal cancer. *Invest. New Drugs.* **2013**, *31*, 435–442. [CrossRef]

40. Yin, J.M.; Sun, L.B.; Zheng, J.S.; Wang, X.X.; Chen, D.X.; Li, N. Copper chelation by trientine dihydrochloride inhibits liver RFA-induced inflammatory responses in vivo. *Inflamm. Res.* **2016**, *65*, 1009–1020. [CrossRef]

41. Brem, S.; Grossman, S.A.; Carson, K.A.; New, P.; Phuphanich, S.; Alavi, J.B.; Mikkelsen, T.; Fisher, J.D. Phase 2 trial of copper depletion and penicillamine as antiangiogenesis therapy of glioblastoma. *Neuro. Oncol.* **2005**, *7*, 246–253. [CrossRef] [PubMed]

42. Tardito, S.; Barilli, A.; Bassanetti, I.; Tegoni, M.; Bussolati, O.; Franchi-Gazzola, R.; Mucchino, C.; Marchiò, L. Copper-Dependent Cytotoxicity of 8-Hydroxyquinoline Derivatives Correlates with Their Hydrophobicity and Does Not Require Caspase Activation. *J. Med. Chem.* **2012**, *55*, 10448–10459. [CrossRef] [PubMed]

43. Santini, C.; Pellei, M.; Gandin, V.; Porchia, M.; Tisato, F.; Marzano, C. Advances in copper complexes as anticancer agents. *Chem. Rev.* **2014**, *114*, 815–862. [CrossRef] [PubMed]

44. Warburg, O. On the origin of cancer cells. *Science* **1956**, *123*, 309–314. [CrossRef]

45. Vander Heiden, M.G.; Cantley, L.C.; Thompson, C. Understanding the Warburg effect: The metabolic requirements of cell proliferation. *Science.* **2009**, *324*, 1029–1033. [CrossRef]

46. Calvaresi, E.C.; Hergenrother, P.J. Glucose conjugation for the specific targeting and treatment of cancer. *Chem. Sci.* **2013**, *4*, 2319–2333. [CrossRef]

47. Szablewski, L. Expression of glucose transporters in cancers. *Biochim. Biophys. Acta.* **2013**, *1835*, 164–169. [CrossRef]

48. Adekola, K.; Rosen, S.T.; Shanmugam, M. Glucose transporters in cancer metabolism. *Curr. Opin. Oncol.* **2012**, *24*, 650–654. [CrossRef]

49. Barron, C.C.; Bilan, P.J.; Tsakiridis, T.; Tsiani, E. Facilitative glucose transporters: Implications for cancer detection, prognosis and treatment. *Metabolism* **2016**, *65*, 124–139. [CrossRef]

50. Oliveri, V.; Giuffrida, M.L.; Vecchio, G.; Aiello, C.; Viale, M. Gluconjugates of 8-hydroxyquinolines as potential anti-cancer prodrugs. *Dalton Trans.* **2012**, *41*, 4530–4535. [CrossRef]

51. Pastuch-Gawołek, G.; Malarz, K.; Mrozek-Wilczkiewicz, A.; Musioł, M.; Serda, M.; Czaplińska, B.; Musioł, R. Small molecule glycoconjugates with anticancer activity. *Eur. J. Med. Chem.* **2016**, *112*, 130–144. [CrossRef] [PubMed]

52. Freitas, L.B.O.; Borgati, T.F.; Freitas, R.P.; Ruiz, A.L.T.G.; Marchetti, G.M.; Carvalho, J.E.; Cunha, E.F.F.; Ramalho, T.C.; Alves, R.B. Synthesis and antiproliferative activity of 8-hydroxyquinoline derivatives containing a 1,2,3-triazole moiety. *Eur. J. Med. Chem.* **2014**, *84*, 595–604. [CrossRef]

53. Oliveri, V.; Vecchio, G. Glycoconjugates of Quinolines: Application in Medicinal Chemistry. *Mini-Rev. Med. Chem.* **2016**, *16*, 1185–1194. [CrossRef] [PubMed]

54. Krawczyk, M.; Pastuch-Gawolek, G.; Mrozek-Wilczkiewicz, A.; Kuczak, M.; Skonieczna, M.; Musiol, R. Synthesis of 8-hydroxyquinoline glycoconjugates and preliminary assay of their β1,4-GalT inhibitory and anti-cancer properties. *Bioorg. Chem.* **2019**, *84*, 326–338. [CrossRef] [PubMed]

55. Dheer, D.; Sing, V.; Shankar, R. Medicinal attributes of 1,2,3-triazoles: Current developments. *Bioorg. Chem.* **2017**, *71*, 30–54. [CrossRef] [PubMed]

56. Ghosh, A.K.; Brindisi, M. Organic Carbamates in Drug Design and Medicinal Chemistry. *J. Med. Chem.* **2015**, *58*, 2895–2940. [CrossRef]

57.	Wu, Y.; Pan, M.; Dai, Y.; Liu, B.; Cui, J.; Shi, W.; Qiu, Q.; Huang, W.; Qian, H. Design, synthesis and biological evaluation of LBM-A5 derivatives as potent P-glycoprotein-mediated multidrug resistance inhibitors. *Bioorg. Med. Chem.* **2016**, *24*, 2287–2297. [CrossRef]

58.	Kovel'man, I.R.; Tochilkin, A.I.; Volkova, O.A.; Dubinskii, V.Z. Synthesis of 2,3-dihidropyrido[1,2,3-de]-1,4-benzoxazinium chloride and some of its derivatives substitute in the carbocyclic ring. *Pharm. Chem. J.* **1995**, *29*, 350–352. [CrossRef]

59.	Agnew, H.D.; Rohde, R.D.; Millward, S.W.; Nag, A.; Yeo, W.S.; Hein, J.E.; Pitram, S.M.; Tariq, A.A.; Burns, V.M.; Krom, R.J.; et al. Iterative In Situ Click Chemistry Creates Antibody-like Protein-Capture Agents. *Angew. Chem. Int. Ed.* **2009**, *48*, 4944–4948. [CrossRef]

60.	Pastuch-Gawolek, G.; Plesniak, M.; Komor, R.; Byczek-Wyrostek, A.; Erfurt, K.; Szeja, W. Synthesis and preliminary biological assay of uridine glycoconjugate derivatives containing amide and/or 1,2,3-triazole linkers. *Bioorg. Chem.* **2017**, *72*, 80–88. [CrossRef]

61.	Lancuski, A.; Bossard, F.; Fort, S. Carbohydrate-Decorated PCL Fibers for Specific Protein Adhesion. *Biomacromol.* **2013**, *14*, 1877–1884. [CrossRef]

62.	Le Roux, A.; Meunier, S.; Le Gall, T.; Denis, J.M.; Bischoff, P.; Wagner, A. Synthesis and Radioprotective Properties of Pulvinic Acid Derivatives. *Chem. Med. Chem.* **2011**, *6*, 561–569. [CrossRef] [PubMed]

63.	Sahoo, L.; Singhamahapatra, A.; Paul, K.J.V.; Loganathan, D. SnCl₄/Sn catalyzed chemoselective reduction of glycopyranosyl azides for the synthesis of diversely functionalized glycopyranosyl chloroacetamides. *Tetrahedron Lett.* **2013**, *54*, 2361–5365. [CrossRef]

64.	Kamiński, Z.; Paneth, P.; Rudziński, J. A Study on the Activation of Carboxylic Acids by Means of 2-Chloro-4,6-dimethoxy-1,3,5-triazine and 2-Chloro-4,6-diphenoxy-1,3,5-triazine. *J. Org. Chem.* **1998**, *63*, 4248–4255. [CrossRef]

65.	Kónya, B.; Docsa, T.; Gergely, P.; Somsák, L. Synthesis of heterocyclic N-(β-D-glucopyranosyl)carboxamides for inhibition of glycogen phosphorylase. *Carbohydr. Res.* **2012**, *351*, 56–63. [CrossRef] [PubMed]

66.	Hemantha, H.P.; Lamani, R.S.; Sureshbabu, V.V. Synthesis of Hybrid Peptidomimetics and Neoglycoconjugates Employing Click Protocol: Dual Utility of Poc-Group for Inserting Carbamate-Triazole Units into Peptide Backbone. *Int. J. Pept. Res. Ther.* **2010**, *16*, 267–275. [CrossRef]

67.	Zemplén, G.; Pacsu, E. Über die Verseifung acetylierter Zucker und verwandter Substanzen. *Ber. Dtsch. Chem. Ges.* **1929**, *62*, 1613–1614. [CrossRef]

68.	Kolb, H.C.; Finn, M.G.; Sharpless, K.B. Click Chemistry: Diverse Chemical Function from a Few Good Reactions. *Angew. Chem. Int. Ed.* **2001**, *40*, 2004–2021. [CrossRef]

69.	Liang, L.; Astruc, D. The copper(I)-catalyzed alkyne-azide cycloaddition (CuAAC) "click" reaction and its applications. An overview. *Coord. Chem. Rev.* **2011**, *255*, 2933–2945. [CrossRef]

70.	Haber, R.S.; Rathan, A.; Weiser, K.R.; Pritsker, A.; Itzkowitz, S.H.; Bodian, C.; Slater, G.; Weiss, A.; Burstein, D.E. GLUT1 Glucose Transporter Expression in Colorectal Carcinoma: A marker for poor prognosis. *Cancer* **1998**, *83*, 34–40. [CrossRef]

71.	Kumamoto, K.; Goto, Y.; Sekikawa, K.; Takenoshita, S.; Ishida, N.; Kawakita, M.; Kannagi, R. Increased Expression of UDP-Galactose Transporter Messenger RNA in Human Colon Cancer Tissues and Its Implication in Synthesis of Thomsen-Friedenreich Antigen and Sialyl Lewis A/X Determinants. *Cancer Res.* **2001**, *61*, 4620–4627. [PubMed]

72.	Melisi, D.; Curcio, A.; Luongo, E.; Morelli, E.; Rimoli, M.G. D-galactose as a vector for prodrug design. *Curr. Top. Med. Chem.* **2011**, *11*, 2288–2298. [CrossRef] [PubMed]

73.	Brown, R.S.; Wahl, R.L. Overexpression of Glut-1 Glucose Transporter in Human Breast Cancer. *Cancer* **1993**, *72*, 2979–2985. [CrossRef]

74.	Wang, D.; Zou, L.; Jin, Q.; Hou, J.; Ge, G.; Yang, L. Human carboxylesterases: A comprehensive review. *Acta Pharm. Sin. B* **2018**, *8*, 699–712. [CrossRef] [PubMed]

75.	Christiansen, M.N.; Chik, J.; Lee, L.; Anugraham, M.; Abrahams, J.L.; Packer, N.H. Cell surface protein glycosylation in cancer. *Proteomics* **2014**, *14*, 525–546. [CrossRef] [PubMed]

76.	Weijers, C.A.G.M.; Franssen, M.C.R.; Visser, G.M. Glycosyltransferase-catalyzed synthesis of bioactive oligosaccharides. *Biotechnol. Adv.* **2008**, *26*, 436–456. [CrossRef]

77.	Vidal, S.; Bruyère, I.; Malleron, A.; Augé, C.; Praly, J.P. Non-isosteric C-glycosyl analogues of natural nucleotide diphosphate sugars as glycosyltransferase inhibitors. *Bioorg. Med. Chem.* **2006**, *14*, 7293–7301. [CrossRef] [PubMed]

78.   Ismael, M.; Tondre, C. Transition Metal Complexes with 8-Hydroxyquinoline and Kelex 100 in Micellar Systems. Stoichiometry of the Complexes and Kinetics of Dissociation in Acid Media. *J. Sep. Sci. Technol.* **1994**, *29*, 651–662. [CrossRef]

79.   Ghosh, D.; Rhodes, S.; Winder, D.; Atkinson, A.; Gibson, J.; Ming, W.; Padgett, C.; Landge, S.; Aiken, K. Spectroscopic investigation of bis-appended 1,2,3-triazole probe for the detection of Cu(II) ion. *J. Mol. Struct.* **2017**, *1134*, 638–648. [CrossRef]

80.   Maréchal, C.N.; Télouk, P.; Albarède, F. Precise analysis of copper and zinc isotopic compositions by plasma-source mass spectrometry. *Chem. Geol.* **1999**, *156*, 251–273. [CrossRef]

81.   Gianelli, L.; Amendola, V.; Fabbrizzi, L.; Pallavicini, P.; Mellerio, G.G. Investigation of reduction of Cu(II) complexes in positive-ion mode electrospray mass spectrometry. *Rapid Commun. Mass Spectrom.* **2001**, *15*, 2347–2352. [CrossRef]

82.   Tsybizova, A.; Tarábek, J.; Buchta, M.; Holý, P.; Schröder, D. Electrospray ionization mass spectrometric investigations of the complexation behavior of macrocyclic thiacrown ethers with bivalent transitional metals (Cu, Co, Ni and Zn). *Rapid Commun. Mass Spectrom.* **2012**, *26*, 2287–2294. [CrossRef] [PubMed]

83.   Keller, B.O.; Esbata, A.A.; Buncel, E.; van Loon, G.W. Rapidly formed quinalphos complexes with transition metal ions characterized by electrospray ionization mass spectrometry. *Rapid Commun. Mass Spectrom.* **2013**, *27*, 1319–1328. [CrossRef] [PubMed]

84.   Barnett, J.E.G.; Holman, G.D.; Munday, K.A. Structural Requirements for Binding to the Sugar-Transport. *Biochem. J.* **1973**, *131*, 211–221. [CrossRef] [PubMed]

Sample Availability: Samples of the compounds **45–108** are available from the authors.

Publikacja P.3

8-Hydroxyquinoline Glycoconjugates Containing Sulfur at the Sugar Anomeric Position — Synthesis and Preliminary Evaluation of Their Cytotoxicity

M. Krawczyk[*], G. Pastuch-Gawołek, A. Hadasik, K. Erfurt

Materiały uzupełniające do publikacji znajdują się w dołączonej płycie CD

8-Hydroxyquinoline Glycoconjugates Containing Sulfur at the Sugar Anomeric Position—Synthesis and Preliminary Evaluation of Their Cytotoxicity

Monika Krawczyk [1,2,*] ⓘ**, Gabriela Pastuch-Gawołek** [1,2] ⓘ**, Agnieszka Hadasik** [1] **and Karol Erfurt** [3] ⓘ

1   Department of Organic Chemistry, Bioorganic Chemistry and Biotechnology,
    Silesian University of Technology, B. Krzywoustego 4, 44-100 Gliwice, Poland;
    gabriela.pastuch@polsl.pl (G.P.-G.); agnieszkahadasik@gmail.com (A.H.)
2   Biotechnology Centre, Silesian University of Technology, B. Krzywoustego 8, 44-100 Gliwice, Poland
3   Department of Chemical Organic Technology and Petrochemistry, Silesian University of Technology,
    B. Krzywoustego 4, 44-100 Gliwice, Poland; karol.erfurt@polsl.pl
*   Correspondence: monika.krawczyk@polsl.pl; Tel.: +48-32-237-1759

Abstract: One of the main factors limiting the effectiveness of many drugs is the difficulty of their delivery to their target site in the cell and achieving the desired therapeutic dose. Moreover, the accumulation of the drug in healthy tissue can lead to serious side effects. The way to improve the selectivity of a drug to the cancer cells seems to be its conjugation with a sugar molecule, which should facilitate its selective transport through GLUT transporters (glucose transporters), whose overexpression is seen in some types of cancer. This was the idea behind the synthesis of 8-hydroxyquinoline (8-HQ) derivative glycoconjugates, for which 1-thiosugar derivatives were used as sugar moiety donors. It was expected that the introduction of a sulfur atom instead of an oxygen atom into the anomeric position of the sugar would increase the stability of the obtained glycoconjugates against untimely hydrolytic cleavage. The anticancer activity of new compounds was determined based on the results of the MTT cytotoxicity tests. Because of the assumption that the activity of this type of compounds was based on metal ion chelation, the effect of the addition of copper ions on cell proliferation was tested for some of them. It turned out that cancer cells treated with glycoconjugates in the presence of Cu^{2+} had a much slower growth rate compared to cells treated with free glycoconjugates in the absence of copper. The highest cytotoxic activity of the compounds was observed against the MCF-7 cell line.

Keywords: quinoline; glycoconjugates; 1-thiosugars; click reaction; anticancer activity; targeted drug delivery

1. Introduction

Despite significant progress in the treatment of various types of diseases, cancer is still one of the most considerable clinical problems. Anticancer therapies introduced so far are not effective enough. This is due to the low selectivity profile of approved chemotherapeutics, the use of which leads to numerous undesirable side effects. Moreover, the resistance of cancer cells to available pharmaceuticals results in their rapid proliferation and metastasis [1]. Therefore, it is necessary to develop new safe drugs that target cancer cells directly without damaging healthy cells.

One of the main factors limiting the effectiveness of many drugs is the difficulty of their delivery to their target site in the cell across the phospholipid cell membranes. A better understanding of

the processes ruling the delivery of substances to cancer cells can be helpful during planning new treatment strategies. There are several ways to transport into the cell [2,3]. The vast majority of available chemotherapeutics penetrate cell membranes by passive diffusion. This is due to the presence of specific gaps in the blood vessels of cancer cells resulting from chaotic neoangiogenesis. This is commonly known as the effect of enhanced permeability and retention (EPR) [3–5]. On the other hand, a variety of membrane proteins are anchored in the structure of lipid bilayer, which can act as carrier proteins or channel proteins (facilitated diffusion). An attractive alternative to transporting chemotherapeutics across a biological membrane may be their modification, which will increase affinity for binding to the appropriate receptor [2–5].

One of the strategies developed for delivering anticancer drugs is the use of glucose transporting proteins [6,7]. Compared to healthy cells, rapidly proliferating cancer cells have a different energy metabolism, characterized by a high rate of glycolysis process, known as the Warburg effect [8,9]. To ensure a sufficient amount of nutrients up to this process, cancer cells have an increased demand for glucose. The phospholipid membrane surrounding the cells is impermeable to hydrophilic glucose molecules by simple diffusion. Therefore, sugar to the cytosol is transferred by transmembrane proteins-GLUTs or SGLTs (sodium-glucose linked transporters) [10]. In most tumor cells, these transporters are overexpressed, especially GLUT1 [11]. Thanks to these transporters, it has been proven that they even receive over 30 times more glucose than normal cells [12]. GLUT1 transport substrates also include other sugars, such as galactose, mannose, and glucosamine [11]. Therefore, an attractive system for targeted drug delivery directly to cancer cells is their conjugation with sugar derivatives. The sugar fragment can be used as a drug carrier across the cell membrane by adapting to the structure of the GLUT transporter [6]. The crucial question to be answered in the case of such conjugates is whether the sugar-conjugated compound will be transported to the cancer cells by the sugar transporters. The results of research on structural requirements for binding variously substituted sugars to the sugar transporters indicate that β-configuration at the anomeric center of the sugar derivatives is preferred for binding to the GLUT transporters [13–15].

Our research focuses on the use of small quinoline molecules as metal ion chelators and potential anticancer agents [16,17]. The presence of copper ions is important in many biological processes and is essential for cellular physiology [18]. Copper is a co-factor of many enzymes and takes part in a variety of cellular processes in mammals [18]. Changes in the homeostasis of copper ions play an important role in different types of diseases, such as inflammation, neurodegeneration, as well as in carcinogenesis (copper is an essential cofactor for cancer growth and angiogenesis) [18–21]. Therefore, the use of metal chelating agents seems to be an ideal way to control the level of copper in the organism [21–23]. The concept of using metal chelators is shown in Figure 1. The formation of metal complexes by 8-hydroxyquinoline (8-HQ) derivatives has been widely described in the literature and has become a promising therapeutic strategy in clinical practice. Numerous 8-HQ derivatives have been shown to have cytotoxic activity on many cancer cells [16,24,25]. However, a significant limitation of their use is the lack of selectivity for healthy cells. We assumed that the therapeutic effectiveness of 8-HQ derivatives could be improved by attaching a sugar moiety, which should increase the selectivity of the obtained connections by targeting their transport to cancer cells through GLUT transporters. 8-Hydroxyquinoline glycoconjugates are of particular interest due to their simple synthesis procedures, as well as facilitated intermembrane transport and improved solubility.

Our recent studies on the cytotoxic activity of 8-HQ derivatives connected via various linkers with D-glucose or D-galactose derivatives containing an oxygen or nitrogen atom at the sugar anomeric position indicated that some of them were able to inhibit the proliferation of tested cell lines [26,27]. Their biological activity depended on the structure of the linker connecting the sugar parts and the quinoline moiety, as well as the type of protective groups in the attached sugar unit. The study of metal complexing properties confirmed that the obtained glycoconjugates were capable of chelating copper ions [27]. In the current research, 1-thiosugars derivatives were used for the synthesis of quinoline glycoconjugates. It was expected that the introduction of a sulfur atom into the anomeric position

of the sugar would increase the stability of the obtained glycoconjugates against hydrolytic cleavage. Compared to *O*-glycosyl derivatives, compounds with the *S*-glycosidic binding are less susceptible to enzymatic degradation, especially under the action of glycosylhydrolases [28,29]. 1-Thiosugars, due to their enzymatic stability, exhibit great therapeutic potential [30–32]. The thiosugar moiety can be found in many naturally occurring compounds, such as bacteriostatic antibiotics from the group of lincosamides (lincomycin) or ᴅ-glucosinolates (sinigrin, gluconasturcin), which have chemopreventive properties [30]. Synthetic thiosugars are effective inhibitors of numerous cellular enzyme pathways. Besides, numerous studies have shown their significant antimicrobial, antiviral, antithrombotic, and anticancer potential [33–36]. Therefore, increasingly sulfur derivatives of carbohydrates are used for the synthesis of new pharmaceuticals. An example of a 1-thiosugar glycoconjugate that exhibits antiproliferative effects in vivo is a gold-based compound 1-phenyl-bis(2-pyridyl)phosphole gold chloride thio-β-ᴅ-glucose tetraacetate (GOPI-sugar). It inhibits the proliferation of glioblastoma cell lines (NCH82, NCH89) to a much better extent than the drug used so far-carmustine, making it a promising candidate in cancer therapy. Attachment of a sugar unit to the complex GOPI has improved the solubility and bioavailability of this compound [37]. Previously reported quinolinecarboxylic acid glycoconjugates containing in their structure a fragment derived from 1-thioglycosides have shown a particularly interesting activity profile against colorectal cancer cells (HCT-116) more than 100 times exceeding the activity of the initial quinoline derivatives [38]. Considering the number of reports devoted to the use of thiosugars in the treatment of a wide range of human diseases, it is worth using this potential. In addition, compounds containing a sulfur atom have the ability to complex metal ions, with sulfur preferring the so-called "soft" metals, such as gold, silver, or copper [39,40]. The introduction of sulfur to the designed glycoconjugates may improve their ability to complex copper ions in relation to the previously obtained derivatives. In this article, we presented the results of carried out cytotoxicity tests of new 8-HQ derivatives, allowing us to determine their potential usefulness in anticancer therapy.
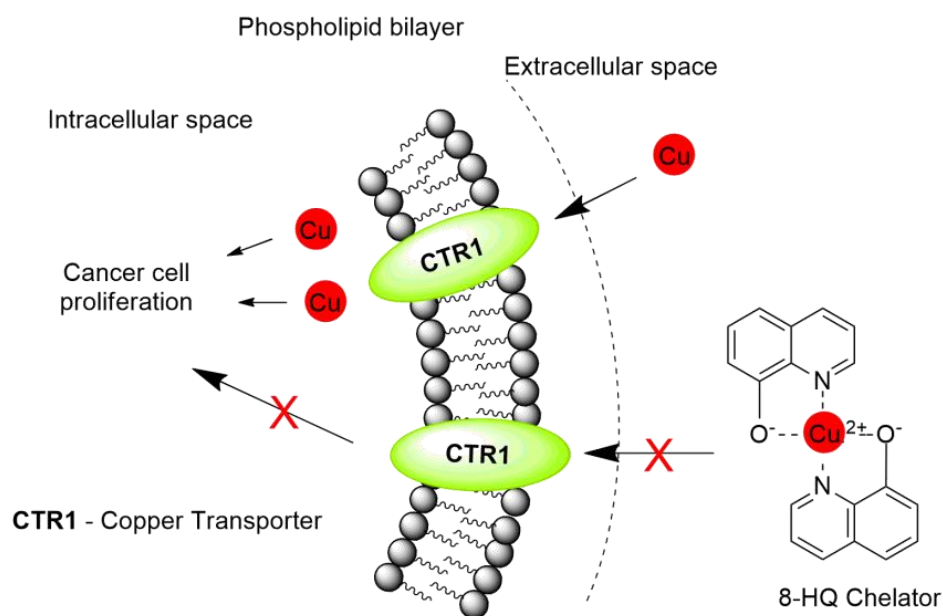
Figure 1. The concept of using metal chelators.

2. Results and Discussion

2.1. Synthesis

The structural modification of sugars used in this research concerned the introduction of a sulfur atom into the anomeric position of the sugar, followed by its functionalization by chemical groups

involved in the copper(I)-catalyzed alkyne-azide cycloaddition (CuAAC). The synthetic pathways leading to the formation of sugar derivatives are presented in Schemes 1–3. All substrates were prepared according to the previously published procedures thoroughly or making minor improvements.
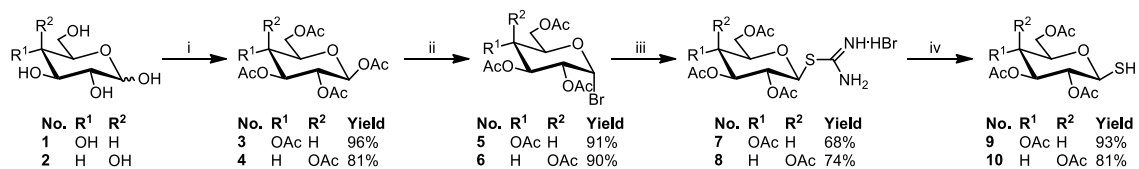
Scheme 1. Synthesis of sugar derivatives **3–10**. Reagents and Conditions: (**i**) CH_3COONa, Ac_2O, b.p., 1 h; (**ii**) CH_3COOH, 33% HBr/AcOH, 0 °C-r.t., 1 h; (**iii**) thiourea, acetone, b.p., 3 h; (**iv**) $K_2S_2O_5$, $CHCl_3$, H_2O, b.p., 1 h.
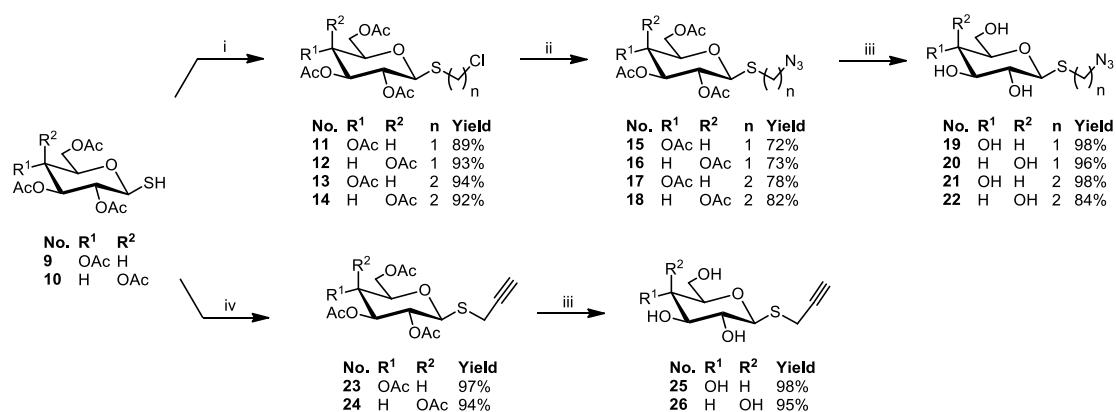
Scheme 2. Synthesis of 1-thiosugar derivatives **11–26**. Reagents and Conditions: (**i**) DBU, CH_2Cl_2 or $(CH_2)_2Cl_2$, r.t., 1 h; (**ii**) NaN_3, DMF, r.t., 24 h (**15** and **16**) or 60 °C, 72 h (**17** and **18**); (**iii**) 1. MeONa, MeOH, r.t., 50 min; 2. Amberlyst-15; (**iv**) propargyl bromide, K_2CO_3, acetone, r.t., 24 h.
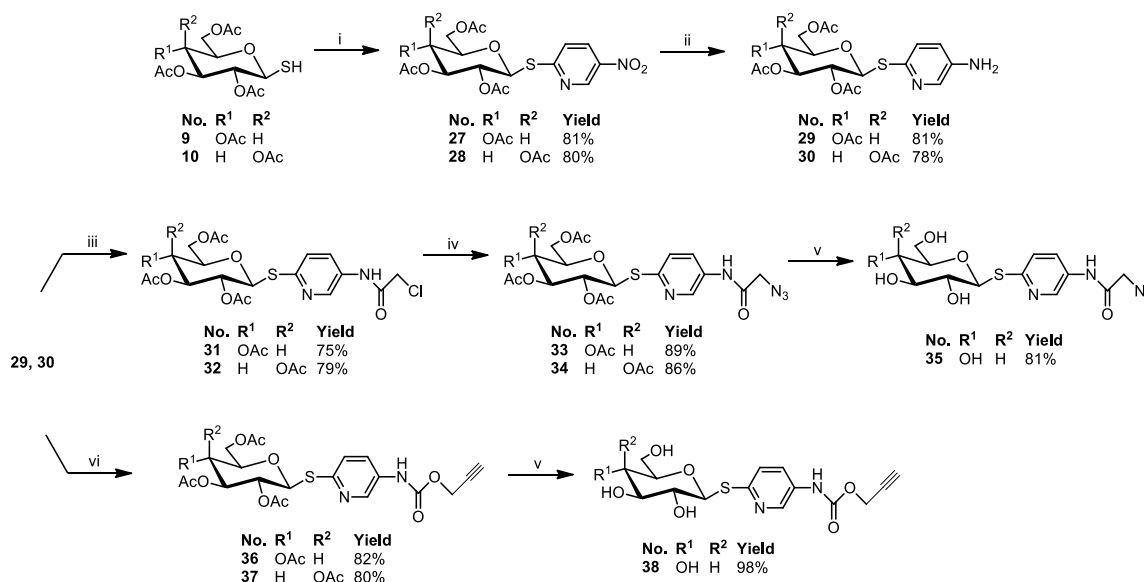
Scheme 3. Synthesis of 1-thiosugar derivatives **27–38**. Reagents and Conditions: (**i**) 2-chloro-5-nitropyridine, K_2CO_3, acetone, r.t., 2 h; (**ii**) Zn, AcOH, CH_2Cl_2, r.t., 1 h; (**iii**) chloroacetyl chloride, TEA, DCM, r.t., 1 h; (**iv**) NaN_3, DMF, r.t., 24 h; (**v**) 1. MeONa, MeOH, r.t., 1 h; 2. Amberlyst-15; (**vi**) propargyl chloroformate, Hünig's base, DCM, r.t., 2 h.

2,3,4,6-Tetra-*O*-acetyl-1-thio-β-ᴅ-glycopyranoses **9** and **10** were synthesized by carrying out a sequence of reactions in which first glycosyl bromides **5** or **6** reacted with thiourea in acetone, and then such prepared isothiouronium salts **7** and **8** were decomposed in the presence of potassium metabisulfite in a two-phase water/chloroform system [41] (Scheme 1).

1-Thiosugars **9** or **10** were substrates for the preparation of compounds used in the synthesis of final glycoconjugates. Due to the susceptibility of these compounds to oxidation to symmetrical disulfides, they were used immediately after purification by column chromatography for the next stages of synthesis. For the glycoconjugates synthesis, the CuAAC reaction was used, in which the substrates must possess an azide moiety or triple bond. Accordingly, it was necessary to receive different 1-thiosugar derivatives substituted at the anomeric position with a substituent containing either the azide moiety or triple bond.

In the beginning, chloromethyl 2,3,4,6-tetra-*O*-acetyl-1-thio-β-ᴅ-glycopyranosides **11** or **12** were obtained in the S_N2 reaction between corresponding glycosyl thiols **9** or **10** and dichloromethane, in the presence of a strong base, such as DBU (1,8-diazabicyclo[5.4.0]undec-7-ene) [42]. To lengthen the alkyl chain in the structure of chloroalkyl 1-thioglycosides, an analogous reaction of 1-thiosugars **9** or **10** with 1,2-dichloroethane was carried out to obtain 2-chloroethyl 2,3,4,6-tetra-*O*-acetyl-1-thio-β-ᴅ-glycopyranosides **13** or **14**. In these reactions, both dichloromethane and dichloroethane acted as a reactant and solvent at the same time. As a result, products **11**–**14** were obtained in a short time and with high yield. In the next step, the substitution of a chlorine atom with an azide moiety was carried out using sodium azide and DMF (*N*,*N*-dimethylformamide) as a solvent, which resulted in azidomethyl **15**, **16** and 2-azidoethyl 2,3,4,6-tetra-*O*-acetyl-1-thio-β-ᴅ-glycopyranosides **17**, **18**. Confirmation of chlorine exchange to the azide moiety was the appearance in the ^{13}C NMR spectra of the signal of CH_2N_3 carbon with a shift of δ = 51.03–51.72 ppm for products **15**–**18**, while the signal of CH_2Cl carbon was observed at δ = 43.31–45.45 ppm for substrates **11**–**14**.

Propargyl 2,3,4,6-tetra-*O*-acetyl-1-thio-β-ᴅ-glycopyranosides **23** and **24** were prepared by the alkylation of 1-thiosugars **9** or **10** with propargyl bromide. Minor modifications of the reaction conditions, compared to the previously reported synthesis method [43], consisting of replacing diisopropylethylamine (base) and dichloromethane (originally used as a solvent) with potassium carbonate and acetone, allowed obtaining the appropriate propargyl 1-thioglycosides **23** and **24** with high yields (97 and 94%, respectively, in comparison to 76 and 83% in cited position).

Removal of the acetyl protecting groups from compounds **15**–**18** and **23**–**24** was performed using a standard Zemplén procedure, involving the use of catalytic amounts of a methanolic solution of sodium methoxide [44]. The reactions were carried out until the complete conversion of the substrate, which was monitored by TLC (thin-layer chromatography). Crude products **19**–**22** and **25**–**26** were obtained with high yields (84–98%), sufficiently pure to be used in the next step.

Another direction of synthesis concerned the introduction of an additional aminopyridyl fragment in the sugar part of the final structure. A simple and efficient synthesis of (5-nitro-2-pyridyl) 2,3,4,6-tetra-*O*-acetyl-1-thio-β-ᴅ-glycopyranosides **27** and **28**, followed by reduction to (5-amino-2-pyridyl) 2,3,4,6-tetra-*O*-acetyl-1-thio-β-ᴅ-glycopyranoside **29** and **30,** was described a few years ago [45]. The presence of an amino group in the aglycone of 1-thioglycosides **29** and **30** allowed the addition of a fragment containing an azide or propargyl moiety. This was possible as a result of the reaction leading to the formation of an amide or carbamate bond. It is worth emphasizing that the introduction of an amide bond additionally enhanced linker stability. Compounds **29** or **30** were reacted with chloroacetyl chloride or propargyl chloroformate in anhydrous DCM (dichloromethane) (Scheme 3). The hydrogen chloride produced during these reactions was neutralized by the addition to the reaction mixture of a tertiary amine, such as triethylamine or *N*,*N*-diisopropylethylamine. Substitution of the chlorine atom in compounds **31** and **32,** leading to obtaining compounds **33** and **34**, as well as the removal of the acetyl protecting groups in the sugar part in order to obtain compounds **35** or **38**, was carried out under the same conditions as described above. Structures of sugar derivatives, obtained with high

yields, were confirmed by NMR spectra analysis. The spectroscopic data of obtained compounds are presented in the experimental section.

For the synthesis of glycoconjugates, derivatives of 1-thioglycosides were used both with the protected and deprotected hydroxyl groups in the sugar part. As the second structural element of the glycoconjugates, corresponding derivatives of 8-hydroxyquinoline **39–42** functionalized in the 8-OH position with propargyl or azide groups were used, obtained according to previously published procedures [27,46]. Target glycoconjugates were prepared using the copper(I)-catalyzed 1,3-dipolar azide-alkyne cycloaddition, described by Sharpless [47,48]. In these reactions, equimolar amounts of sugar derivatives and 8-HQ derivatives were combined in the configuration shown in Scheme 4. The use of $CuSO_4 \cdot 5H_2O$ as a catalyst allowed the carrying out of the reaction at room temperature and led to obtaining only 1,4-disubstituted 1,2,3-triazoles. Sodium ascorbate (NaAsc), used as a reducing agent of Cu(II) to Cu(I), avoided the formation of oxidation byproducts. All of the reagents were dissolved in the THF:*i*-PrOH:H$_2$O solvent system (tetrahydrofuran:isopropyl alcohol:water). The progress of the reaction was controlled by TLC analysis so that the moment of the total conversion of the substrates could be estimated. After purification of the crude products by column chromatography, in the result, pure glycoconjugates **43–72** with high yields were obtained (Figure 2). The structures of all prepared glycoconjugates were confirmed using NMR and HRMS spectroscopy methods. The formation of the glycoconjugate was evidenced by the presence of a singlet at about $\delta = 7.9$ ppm from the H-C(5) proton triazole ring in ^{1}H NMR spectra and two characteristic carbon signals at about 123 ppm and 144 ppm for C(4) and C(5) from triazole ring in the ^{13}C NMR spectra, as well as the presence of signals characteristic of the sugar and quinoline fragments. The obtained glycoconjugates contained the sugar unit with a binding of the β-configuration at the anomeric center since such orientation is preferred for binding to the GLUT transporters overexpressed in the cancer cells [13]. Such a structure was confirmed by the large coupling constant from the H-1 proton, equal to about $J = 9.0$ Hz, observed in the ^{1}H NMR spectra. The NMR spectra of all the synthesized glycoconjugates are presented in the supporting information. Their physicochemical properties, such as melting point and optical rotation, were also determined.
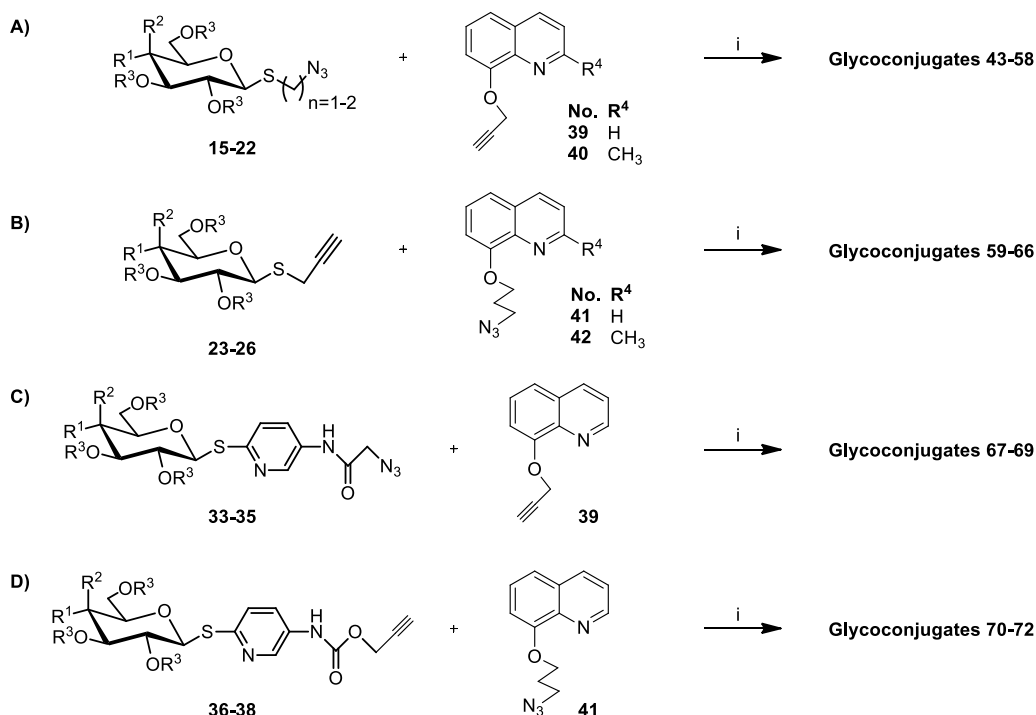
Scheme 4. Synthesis of glycoconjugates **43–58** (**A**), **59–66** (**B**), **67–69** (**C**), and **70–72** (**D**). Reagents and Conditions: (**i**) $CuSO_4 \cdot 5H_2O$, NaAsc, i-PrOH, THF, H$_2$O, r.t., 24 h.

Structure A

Structure B

No.	R^1	R^2	R^3	R^4	n	Yield		No.	R^1	R^2	R^3	R^4	n	Yield
43	OAc	H	Ac	H	1	79%		51	OAc	H	Ac	H	2	79%
44	H	OAc	Ac	H	1	93%		52	H	OAc	Ac	H	2	82%
45	OAc	H	Ac	CH$_3$	1	87%		53	OAc	H	Ac	CH$_3$	2	77%
46	H	OAc	Ac	CH$_3$	1	92%		54	H	OAc	Ac	CH$_3$	2	70%
47	OH	H	H	H	1	71%		55	OH	H	H	H	2	99%
48	H	OH	H	H	1	79%		56	H	OH	H	H	2	77%
49	OH	H	H	CH$_3$	1	83%		57	OH	H	H	CH$_3$	2	87%
50	H	OH	H	CH$_3$	1	92%		58	H	OH	H	CH$_3$	2	88%

No.	R^1	R^2	R^3	R^4	Yield
59	OAc	H	Ac	H	94%
60	H	OAc	Ac	H	79%
61	OAc	H	Ac	CH$_3$	77%
62	H	OAc	Ac	CH$_3$	80%
63	OH	H	H	H	81%
64	H	OH	H	H	89%
65	OH	H	H	CH$_3$	91%
66	H	OH	H	CH$_3$	90%

Structure C

Structure D

No.	R^1	R^2	R^3	Yield
67	OAc	H	Ac	84%
68	H	OAc	Ac	83%
69	OH	H	H	77%

No.	R^1	R^2	R^3	Yield
70	OAc	H	Ac	72%
71	H	OAc	Ac	73%
72	OH	H	H	78%

Figure 2. Structures and yields of obtained glycoconjugates **43–72**.

2.2. Cytotoxicity Studies

In vitro cytotoxicity studies of the obtained building blocks and glycoconjugates were carried out on cell lines characterized by the high expression of GLUT transporters and the strongly changed glucose metabolism (strong Warburg effect) [10,49–51]. Based on this, colon cancer cell line (HCT-116) and breast cancer cell line (MCF-7) were selected for the research. Compounds with a high ability to inhibit the proliferation of tumor cells were also tested against the Normal Human Dermal Fibroblast-Neonatal cells (NHDF-Neo) to assess the safety of their use. Cytotoxicity was evaluated using the MTT assay. The results of the screening tests were used to determine the IC$_{50}$ values (the half maximal inhibitory concentration), which are summarized in Tables 1 and 2. These values represented 50% inhibition of cell growth concerning the control system, which were the cells suspended in the medium supplemented with DMSO in the amount used to dissolve the tested compounds.

Table 1. Summary of cytotoxicity of substrates used for glycoconjugation.

Compound	Activity IC$_{50}$ [µM] [a]		
	HCT-116 [b]	MCF-7 [c]	NHDF-Neo [b]
15–26	>800	>800	-
33	13.39 ± 0.10	6.39 ± 0.07	11.20 ± 0.31
34	541.37 ± 3.73	382.69 ± 4.23	-
35	>800	>800	-
36	124.79 ± 8.98	38.33 ± 2.44	41.69 ± 3.40
37	456.70 ± 3.85	392.41 ± 5.29	-
38	>800	>800	-
8HQ	>800	0.24 ± 0.01	>800
2Me8HQ	>800	43.18 ± 1.78	346.77 ± 2.23
Doxorubicin	5.59 ± 0.14	0.67 ± 0.01	>20

[a] Cytotoxicity was evaluated using the MTT assay; [b] Incubation time 24 h; [c] Incubation time 72 h. Data are presented as the mean ± standard deviation (*n* = 3).

Table 2. Summary of cytotoxicity of tested glycoconjugates **43–72**.

Compound	Activity IC$_{50}$ [μM] [a]		
	HCT-116 [b]	MCF-7 [c]	NHDF-Neo [b]
43	106.71 ± 4.10	59.12 ± 1.46	54.62 ± 0.74
44	162.34 ± 1.35	85.65 ± 3.28	140.41 ± 7.25
45	268.54 ± 5.55	218.40 ± 6.24	-
46	789.98 ± 2.33	235.24 ± 6.77	-
47	791.73 ± 2.30	428.16 ± 8.84	-
48	376.07 ± 7.16	204.88 ± 5.85	-
49	>800	>800	-
50	>800	>800	-
51	127.05 ± 1.75	76.30 ± 1.33	105.32 ± 3.40
52	144.59 ± 4.84	93.97 ± 1.66	111.08 ± 1.24
53	338.97 ± 4.61	135.55 ± 1.58	-
54	519.18 ± 0.90	204.79 ± 2.53	-
55	394.77 ± 6.44	315.93 ± 1.66	-
56	431.84 ± 5.10	172.46 ± 5.43	-
57	>800	>800	-
58	>800	332.85 ± 1.39	-
59	172.83 ± 3.48	153.34 ± 0.25	229.12 ± 2.06
60	304.80 ± 1.34	212.15 ± 3.46	421.20 ± 0.14
61	107.68 ± 1.62	130.45 ± 0.20	260.43 ± 7.65
62	324.00 ± 1.61	243.65 ± 3.04	667.65 ± 6.43
63	>800	>800	-
64	>800	>800	-
65	>800	>800	-
66	>800	>800	-
67	146.16 ± 3.49	69.72 ± 3.50	71.81 ± 6.70
67 + Cu^{2+} [d]	74.50 ± 0.16	28.94 ± 1.52	71.43 ± 1.35
68	130.31 ± 1.31	96.32 ± 5.99	110.60 ± 2.78
68 + Cu^{2+} [d]	96.01 ± 0.59	23.77 ± 0.48	83.60 ± 3.03
69	210.39 ± 0.55	144.42 ± 2.68	163.81 ± 0.01
70	63.49 ± 2.37	67.50 ± 1.58	64.00 ± 5.34
70 + Cu^{2+} [d]	73.87 ± 2.99	25.90 ± 1.76	68.43 ± 1.11
71	90.68 ± 0.52	68.32 ± 3.68	75.26 ± 0.38
71 + Cu^{2+} [d]	82.99 ± 1.37	20.51 ± 1.55	69.31 ± 2.90
72	>800	739.20 ± 3.79	>800

[a] Cytotoxicity was evaluated using the MTT assay; [b] Incubation time 24 h; [c] Incubation time 72 h; [d] Addition of cooper acetate at 100 μM. Data are presented as the mean ± standard deviation (*n* = 3).

The screening tests of sugar substrates used for glycoconjugation indicated no toxicity of compounds **15–26** and significant cytotoxicity of compounds **33** and **36** (Table 1). Probably due to the small size, compounds **33** and **36** were able to penetrate through phospholipid membranes into cells by passive diffusion. On the other hand, the presence of additional fragments in their structure capable of coordinating divalent metal ions (an amidopyridyl part), compared to substrates **15–26**, affected their ability to inhibit cancer cell growth. As it turned out, these compounds were also highly toxic to healthy cells. Interestingly, the D-galactose derivatives **34** and **37,** as well as the compounds **35** and **38,** without the acetyl protection of the hydroxyl groups were much less toxic and showed no anti-proliferative activity. In the case of the deprotected derivatives **35** and **38**, this result could be explained by the fact that they are too little lipophilic to enter the cell by passive transport and simultaneously, apparently, do not have sufficient affinity for GLUT transporters. However, the results obtained for per-*O*-acetylated galactoconjugates **34** and **37** were surprising. The significant difference in glycoconjugates cytotoxic activity observed with a simple replacement of the D-glucose residue with D-galactose might indicate a significant influence of the type of sugar residue on the biological activity of the whole compound. Cytotoxicity studies of 8-HQ and 2Me8HQ, the second building blocks of

glycoconjugates, showed that both compounds were non-toxic to HCT-116 cells and toxic to MCF-7 cells. 8-HQ appeared to be of particular interest as it exhibited high toxicity against the breast cancer cell line, while not being toxic against the NHDF normal cell line. Thus, this compound is a good starting point for structural modifications that should further improve its activity.

Taking into account the obtained results, it seemed necessary to develop a prodrug that would improve the selectivity of a given compound. By starting to design prodrugs by functionalizing the biologically active compound, we focused on differences in the properties of cancer and normal cells. In this case, we paid attention to factors that increase the affinity of the prodrug for the interphase space. It is known that there is a mildly acidic environment in cancer tissues that results from excessive glycolysis in tumors (Warburg effect) [52,53]. In the case of healthy cells, this acidic environment does not exist. Therefore, the presence of the 1,2,3-triazole ring having base properties should increase the concentration of the prodrug at the interphase space of the cancer cells.

Dose-dependent cytotoxicity was observed for glycoconjugates derivatives of 8-HQ containing a 1,2,3-triazole fragment in the structure. The summary of cytotoxicity of tested glycoconjugates **43–72** is shown in Table 2. In order to approximate the mechanism of glycoconjugate transport into the cell, the influence of the presence of acetyl protecting groups in the sugar part of the glycoconjugate on the activity was examined. High IC_{50} values of glycoconjugates with a deprotected sugar fragment (**47–50**, **55–58**, **63–66**) indicated that these compounds were not able to bind to glucose transporters and be transported by them across biological membranes. Glycoconjugates with acetyl protecting groups in the sugar part (**43–46**, **51–54**, **59–62**) turned out to be more active. This suggested that due to their higher lipophilicity, they could cross the phospholipid bilayer by passive transport. Derivatives **43**, **44**, and **51**, **52** revealed interesting antiproliferative properties against the tested tumor cell lines. Unfortunately, at the same time, they also turned out to be toxic to healthy cells (NHDF-Neo). This was probably because this type of transport is not preferred in the case of the designed prodrugs, as it does not guarantee selectivity, and, as a result, the tested compounds damage both cancer cells as well as healthy cells.

As part of the research, the effect of introducing a sulfur atom into the anomeric position of sugar was assessed. Glycoconjugates **51–54** derivatives of azidoalkyl 1-thioglycosides showed higher cytotoxic activity than the analogous glycoconjugates obtained earlier containing oxygen atom at the sugar anomeric position [27]. This was particularly evident for the 8-HQ derivatives **51** and **52**, for which the cytotoxic activity was about twice as high as that of their structural counterparts with an anomeric oxygen atom (Figure 3). Unfortunately, an increase in cytotoxicity for glycoconjugates containing anomeric sulfur was observed, both to neoplastic cells and to healthy cells. So, it can be assumed that their stability in the presence of hydrolytic enzymes affects their activity and may suggest that they were not prematurely degraded before entering the cell. In order to verify this assumption, two galactoconjugates **56** and **64** (being the deprotected counterparts of galactoconjugates **52** and **60**) and their two analogs with anomeric oxygen were chosen and subjected to hydrolysis reactions using β-galactosidase from *Aspergillus oryzae* [54]. The conducted experiments, for which the description of the procedure is attached to Supplementary Materials, showed that glycoconjugates **56** and **64**, containing the sulfur atom in the anomeric position, did not undergo hydrolysis in the presence of the enzyme even after 24 h of the reaction, while their counterparts with the anomeric oxygen had completely undergone hydrolysis after just 60 min of the enzymatic reaction.

In the case of glycoconjugates **59–62**, their higher cytotoxicity, compared to the oxygen counterparts, was not observed, despite the fact that also for a representative of these compounds, the positive influence of the anomeric sulfur on the hydrolytic stability was confirmed experimentally. For glycoconjugates **59–62**, to form a 1,2,3-triazole system in their structure, acetylated derivatives of 1-thiosugars with an anomeric propargyl moiety were used. In this reaction, an "inverted" 1,2,3-triazole system was formed in relation to the one that was in the glycoconjugates **51–54**. It can be assumed that for the cytotoxicity of glycoconjugates, not only their hydrolytic stability is important but also the mutual spatial orientation of the atom in the anomeric position of the sugar (sulfur or oxygen) and the 1,2,3-triazole ring, but confirmation of this thesis requires further research.
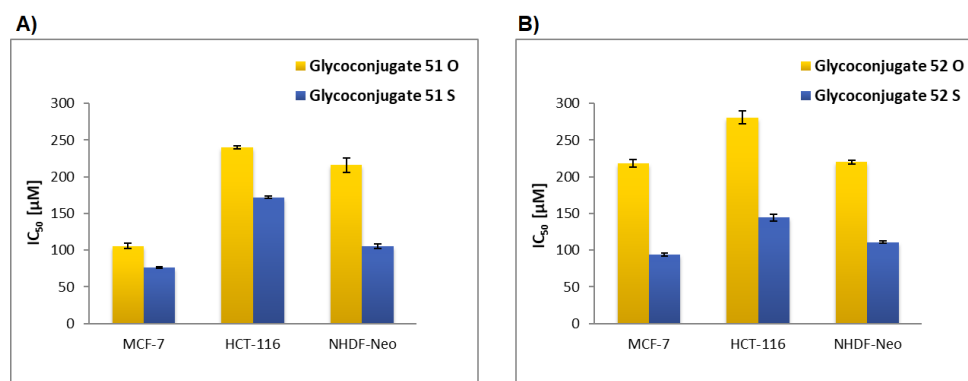
Figure 3. Comparison of IC$_{50}$ activity glycoconjugates **51** (**A**) and **52** (**B**) containing sulfur or oxygen atom at the sugar anomeric position.

The length of the aliphatic chain between the sugar and the 1,2,3-triazole ring did not significantly affect the activity of glycoconjugates. It was found that D-glucose derivatives, in most cases, were more active than D-galactose derivatives. Among them, greater cytotoxicity was demonstrated by derivatives whose structure was based on the 8-HQ fragment, compared to derivatives with 2Me8-HQ units. Higher antiproliferative activity of the tested compounds was found against the breast cancer cell line (MCF-7). In this case, high toxicity to the cells of this line was observed for the quinoline aglycones themselves. This indicated the huge sensitivity of the cells of this particular tumor line to 8-HQ.

Previously, we showed that 8-HQ derivative glycoconjugates containing 1,2,3-triazole fragment in the linker structure were able to form complexes with copper ions and potentially inhibit the multiplication of neoplastic cells by eliminating an important factor for their growth [27]. In the current study, we decided to enhance this effect by creating new analogs, with an additional heteroaromatic fragment in the structure **67–72**. The presence of sulfur, a pyridine ring, and an additional amide bond in the structure of glycoconjugate should improve their cytotoxic activity as their method of action may be related to metal ion chelation. The protected glycoconjugates **67**, **68**, and **70**, **71** showed good antiproliferative activity against HCT-116 and MCF-7 cancer cells. The unprotected glucose derivative **69** showed moderate activity. Whereas, unprotected glucoconjugate **72** was not active in the concentration range studied. Unfortunately, active compounds showed toxic activity also to the NHDF-Neo cell line. Interestingly, the discussed compounds were created by connecting exhibiting cytotoxic activity substrates **33** and **36** with quinoline derivatives **39** or **41**. The cytotoxicity of the resulting glycoconjugates was expected to increase relative to the substrates themselves, but this did not happen. Perhaps the large size of the resulting glycoconjugates is one of the possible explanations for the observed activity decrease.

Cultured cancer cells, in contrast to in vivo environment, are characterized by a low copper level [55,56]. Therefore, additional experiments were carried out for compounds whose expected mechanism of action is based on the chelation of metal ions. The antiproliferative activities of glycoconjugates **67**, **68**, **70**, and **71** were tested in the presence of Cu^{2+} ions. The effect of the interaction of glycoconjugate complexes with metal ions on cell proliferation was measured by adding a copper salt solution to the growth medium and observing the rate of cell growth compared to copper-untreated cells.

First, measurements were made of the effect of different concentrations of copper on the proliferation of cancer and non-cancer cells. Cell cultures under standard conditions were treated for 24 h or 72 h with copper solutions of various concentrations, and their effect on cell proliferation was verified by the MTT assay. Cells with the non-supplemented medium were used as controls. For further experiments, a 100 μM copper acetate solution was used, as it did not affect the viability of any of the tested cell lines in any way.

During the appropriate experiments, the cells (MCF-7, HCT-116, and NHDF-Neo) were treated with solutions of glycoconjugate **67**, **68**, **70**, or **71** in medium culture, supplemented with 100 μM copper acetate, and then their proliferation was measured by the MTT assay. The control system

was cells suspended in medium supplemented with DMSO in the amount used to dissolve the compounds and the addition of the same amount of copper. It turned out that cancer cells treated with glycoconjugates in the presence of Cu^{2+} had a much slower growth rate compared to cells treated with free glycoconjugates in the absence of copper. The highest cytotoxic activity of the compounds was observed against the MCF-7 cell line. Their IC_{50} values ranged from 20.51 ± 1.55 μM to 28.94 ± 1.52 μM (Table 2). This confirmed the strong sensitivity of breast cancer cells to 8-HQ derivatives.

Figure 4 shows the cell viability treated with free glycoconjugate at 50 μM and glycoconjugates with the addition of Cu^{2+} at 100 μM for MCF-7, HCT-116, and NHDF-Neo cells after 24 h (HCT-116 and NHDF-Neo) or 72 h (MCF-7) of incubation. It can be seen that the greatest differences in cell survival occurred in the case of MCF-7 cell lines. The detailed dependence of MCF-7 cells' proliferation on the concentration of a potential inhibitor is shown in Figure 5. A significant decrease in the proliferation of MCF-7 cells was observed after treatment with glycoconjugates at a concentration of 50 μM in the presence of Cu^{2+} (cell viability 10–28%), compared to experiments with glycoconjugates alone. In this case, the cytotoxicity of glycoconjugates increased about three-fold in the presence of Cu(II) ions. Lower concentrations of glycoconjugates also improved antiproliferative activity in the presence of Cu(II), while concentrations above 50 μM led to complete inhibition of tumor cell growth. For HCT-116 and NHDF-Neo cell lines, only slight differences in cell viability were observed after treatment with free compounds and when Cu(II)(II) ions were added. This suggested that the cells' viability of these lines was not affected by the concentration of copper ions to the same extent as it was for the breast cancer cell line.
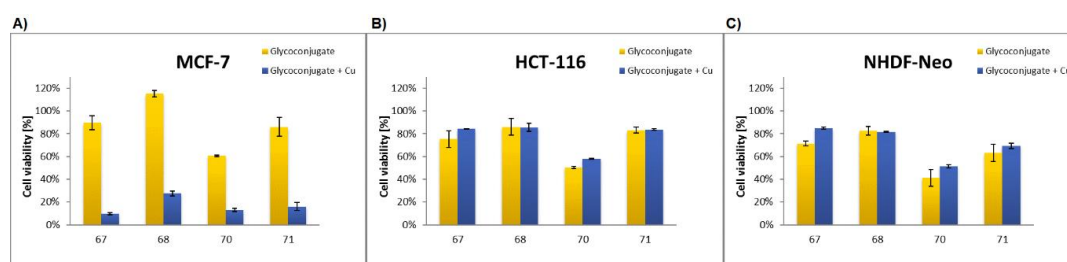
Figure 4. The cell viability treated with free glycoconjugate at 50 μM and glycoconjugates with the addition of Cu^{2+} at 100 μM for MCF-7 (**A**), HCT-116 (**B**), and NHDF-Neo (**C**) cells after 24 h (HCT-116 and NHDF-Neo) or 72 h (MCF-7) incubation. Data are presented as the mean ± standard deviation (*n* = 3).
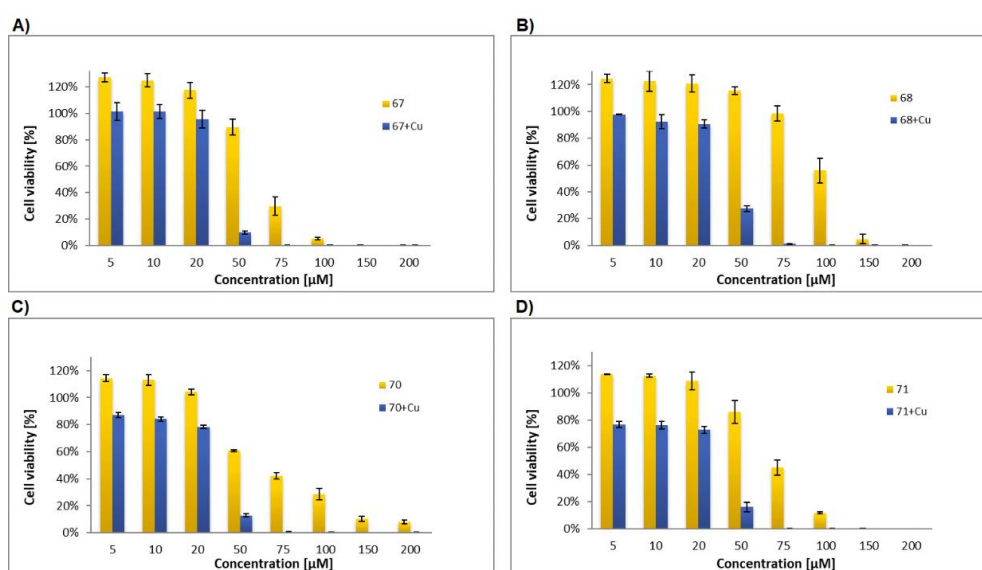
Figure 5. The dependence of MCF-7 cell proliferation on the concentration of the potential inhibitor **67** (**A**), **68** (**B**), **70** (**C**) or **71** (**D**) in the absence and presence of Cu^{2+}.

3. Materials and Methods

3.1. General Information

NMR spectra were recorded with an Agilent spectrometer at a frequency of 400 MHz using TMS (tetramethylsilane) as the internal standards and CDCl$_3$, CD$_3$OD, or DMSO-d6 as the solvents. NMR solvents were purchased from ACROS Organics (Geel, Belgium). Chemical shifts (δ) were expressed in ppm and the coupling constants (*J*) in Hz. The following abbreviations were used to explain the observed multiplicities: s: singlet, d: doublet, dd: doublet of doublets, ddd: doublet of doublet of doublets, t: triplet, dd~t: doublet of doublets resembling a triplet (with similar values of coupling constants), m: multiplet, p: pentet (quintet), b: broad. High-resolution mass spectra (HRMS) were recorded with a WATERS LCT Premier XE system using the electrospray-ionization (ESI) technique. Optical rotations were measured with a JASCO P-2000 polarimeter using a sodium lamp (589.3 nm) at room temperature. Melting point measurements were performed on OptiMelt (MPA 100) Stanford Research Systems. Reactions were monitored by thin-layer chromatography (TLC) on precoated plates of silica gel 60 F254 (Merck Millipore, Burlington, MA, USA). The TLC plates were visualized under UV light (λ = 254 nm) or by charring the plates after spraying with a 10% solution of sulfuric acid in ethanol. Crude products were purified using column chromatography performed on Silica Gel 60 (70–230 mesh, Fluka, St. Louis, MI, USA), developed using toluene:EtOAc or CHCl$_3$:MeOH as solvent systems. All evaporations were performed on a rotary evaporator under diminished pressure at 40 °C. The absorbance on MTT assay was measured spectrophotometrically at the 570 nm wavelength using a plate reader (Epoch, BioTek, Winooski, VT, USA).

All used chemicals were purchased from Sigma-Aldrich (Saint Louis, MO, USA, ACROS Organics (Geel, Belgium), and Avantor (Gliwice, Poland) and were used without purification. D-Glucose, D-galactose, 8-hydroxyquinoline, and 8-hydroxyquinaldine are commercially available (Sigma-Aldrich). 2,3,4,6-Tetra-*O*-acetyl-1-thio-β-D-glycopyranoses **9**, **10** [41], chloromethyl- **11, 12** and azidomethyl 2,3,4,6-tetra-*O*-acetyl-1-thio-β-D-glycopyranosides **15, 16** [42], 2-chloroethyl- **13, 14** and 2-azidoethyl 2,3,4,6-tetra-*O*-acetyl-1-thio-β-D-glycopyranosides **17, 18** [42], propargyl 2,3,4,6-tetra-*O*-acetyl-1-thio-β-D-glycopyranosides **23, 24** [43], (5-amino-2-pyridyl) 2,3,4,6-tetra-*O*-acetyl-1-thio-β-D-glycopyranosides **29, 30** [45], 8-(2-propyn-1-yloxy)quinoline **39** [46], 2-methyl-8-(2-propyn-1-yloxy) quinoline **40** [46], 8-(3-azidopropoxy)quinolone **41** [27], and 2-methyl-8-(3-azidopropoxy)quinolone **42** [27] were prepared according to the respective published procedures.

3.2. Chemistry

3.2.1. General Procedure for the Synthesis of Sugar Derivatives **31** and **32**

To a solution of (5-amino-2-pyridyl) 2,3,4,6-tetra-*O*-acetyl-1-thio-β-D-glucopyranoside **29** or (5-amino-2-pyridyl) 2,3,4,6-tetra-*O*-acetyl-1-thio-β-D-galactopyranoside **30** (685 mg, 1.5 mmol) in dry CH$_2$Cl$_2$ (30 mL), triethylamine (625 μL, 4.5 mmol) was added. The reaction mixture was cooled to 0 °C, and chloroacetyl chloride was added dropwise (175 μL, 2.2 mmol), then stirring was continued at room temperature. After 1 h, the resulting mixture was diluted with dichloromethane (50 mL) and washed with brine (2 × 50 mL). The combined organic phases were dried over anhydrous MgSO$_4$, filtered, and concentrated in vacuo. The crude products were purified by column chromatography (toluene:AcOEt; 2:1) to give products **31**–**32**.

(5-chloroacetamide-2-pyridyl) 2,3,4,6-tetra-O-acetyl-1-thio-β-D-glucopyranoside **31***: Starting from (5-amino-2 -pyridyl) 2,3,4,6-tetra-O-acetyl-1-thio-β-D-glucopyranoside* **29***, the product was obtained as an orange solid (600 mg, 75%)*, m.p.: 145–146 °C; [α]$^{25}_D$ = 0.4 (c = 1.0, CHCl$_3$); ^{1}H NMR (400 MHz, CDCl$_3$): δ 2.02, 2.02, 2,04, 2.05 (4s, 12H, CH$_3$CO), 3.86 (ddd, 1H, *J* = 2.3 Hz, *J* = 4.6 Hz, *J* = 10.1 Hz, H-5$_{Glu}$), 4.10 (dd, 1H, *J* = 2.3 Hz, *J* = 12.4 Hz, H-6a$_{Glu}$), 4.22 (s, 2H, CH$_2$Cl), 4.27 (dd, 1H, *J* = 4.6 Hz, *J* = 12.4 Hz, H-6b$_{Glu}$), 5.15 (dd~t, 1H, *J* = 9.4 Hz, *J* = 10.4 Hz, H-2$_{Glu}$), 5.20 (dd~t, 1H, *J* = 9.3 Hz, *J* = 10.1 Hz, H-4$_{Glu}$), 5.34 (dd~t, 1H, *J* = 9.3 Hz, *J* = 9.4 Hz, H-3$_{Glu}$), 5.72 (d, 1H, *J* = 10.4 Hz, H-1$_{Glu}$), 7.26 (d, 1H, *J* = 8.6 Hz, H-3$_{Pyr}$), 7.97

(dd, 1H, J = 2.6 Hz, J = 8.6 Hz, H-4$_{Pyr}$), 8.29 (bs, 1H, NH), 8.59 (d, 1H, J = 2.6 Hz, H-6$_{Pyr}$); ^{13}C NMR (100 MHz, CDCl$_3$): δ 20.60, 20.62, 20.69, 20.75 (CH$_3$CO), 42.72 (CH$_2$Cl), 61.94 (C-6$_{Glu}$), 68.24, 69.47, 74.09, 75.97 (C-2$_{Glu}$, C-3$_{Glu}$, C-4$_{Glu}$, C-5$_{Glu}$), 82.11 (C-1$_{Glu}$), 123.65, 128.60, 131.53, 141.37, 151.09 (C$_{Pyr}$), 164.29 (C=O) 169.42, 169.50, 170.15, 170.66 (CH$_3$CO); HRMS (ESI-TOF): calcd for C$_{21}$H$_{26}$N$_2$O$_{10}$SCl ([M + H]$^+$): *m/z* 533.0997; found: *m/z* 533.0997.

*(5-chloroacetamide-2-pyridyl) 2,3,4,6-tetra-O-acetyl-1-thio-β-*D*-galactopyranoside* **32**: *Starting from (5-amino-2-pyridyl) 2,3,4,6-tetra-O-acetyl-1-thio-β-*D*-galactopyranoside* **30**, *the product was obtained as a beige solid (632 mg, 79%)*, m.p.: 49–51 °C; [α]^{25}$_D$ = 13.6 (c = 1.0, CHCl$_3$); ^{1}H NMR (400 MHz, CDCl$_3$): δ 2.00, 2.01, 2,03, 2.17 (4s, 12H, CH$_3$CO), 4.00–4.16 (m, 3H, H-5$_{Gal}$, H-6a$_{Gal}$, H-6b$_{Gal}$), 4.22 (s, 2H, CH$_2$Cl), 5.18 (dd, 1H, J = 3.4 Hz, J = 9.9 Hz, H-3$_{Gal}$), 5.40 (dd~t, 1H, J = 9.9 Hz, J = 10.4 Hz, H-2$_{Gal}$), 5.49 (dd, 1H, J = 0.7 Hz, J = 3.4 Hz, H-4$_{Gal}$), 5.69 (d, 1H, J = 10.4 Hz, H-1$_{Gal}$), 7.28 (d, 1H, J = 8.6 Hz, H-3$_{Pyr}$), 7.97 (dd, 1H, J = 2.6 Hz, J = 8.6 Hz, H-4$_{Pyr}$), 8.27 (s, 1H, NH), 8.57 (d, 1H, J = 2.6 Hz, H-6$_{Pyr}$); ^{13}C NMR (100 MHz, CDCl$_3$): δ 20.60, 20.68, 20.70, 20.78 (CH$_3$CO), 42.72 (CH$_2$Cl), 61.29 (C-6$_{Gal}$), 66.82, 67.30, 72.07, 74.58 (C-2$_{Gal}$, C-3$_{Gal}$, C-4$_{Gal}$, C-5$_{Gal}$), 82.67 (C-1$_{Gal}$), 123.59, 128.54, 131.47, 141.47, 151.36 (C$_{Pyr}$), 164.30 (C=O) 169.70, 170.02, 170.26, 170.36 (CH$_3$CO); HRMS (ESI-TOF): calcd for C$_{21}$H$_{26}$N$_2$O$_{10}$SCl ([M + H]$^+$): *m/z* 533.0997; found: *m/z* 533.1002.

3.2.2. General Procedure for the Synthesis of Sugar Derivatives **33** and **34**

To a solution of compounds **31** or **32** (320 mg, 0.6 mmol) in dry DMF (10 mL), sodium azide (214 mg, 3.3 mmol) was added. The reaction mixture was stirred at room temperature for 24 h. After completion of the reaction, the solvent was evaporated under reduced pressure, and the residue was dissolved in ethyl acetate (50 mL) and extracted with water (2 × 30 mL) and brine (30 mL). The combined organic phases were dried over anhydrous MgSO$_4$, filtered, and concentrated in vacuo to afford the corresponding azide **33** and **34**, which were used for the next reaction without further purification.

*(5-azidoacetamide-2-pyridyl) 2,3,4,6-tetra-O-acetyl-1-thio-β-*D*-glucopyranoside* **33**: *Starting from (5-chloroacetamide-2-pyridyl) 2,3,4,6-tetra-O-acetyl-1-thio-β-*D*-glucopyranoside* **31**, *the product was obtained as an orange solid (288 mg, 89%)*, m.p.: 75–78 °C; [α]^{25}$_D$ = 11.4 (c = 1.0, CHCl$_3$); ^{1}H NMR (400 MHz, CDCl$_3$): δ 2.02, 2.04, 2,04, 2.05 (4s, 12H, CH$_3$CO), 3.86 (ddd, 1H, J = 2.3 Hz, J = 4.6 Hz, J = 10.1 Hz, H-5$_{Glu}$), 4.10 (dd, 1H, J = 2.3 Hz, J = 12.4 Hz, H-6a$_{Glu}$), 4.19 (s, 2H, CH$_2$N$_3$), 4.27 (dd, 1H, J = 4.6 Hz, J = 12.4 Hz, H-6b$_{Glu}$), 5.15 (dd~t, 1H, J = 9.3 Hz, J = 10.4 Hz, H-2$_{Glu}$), 5.20 (dd~t, 1H, J = 9.3 Hz, J = 10.1 Hz, H-4$_{Glu}$), 5.34 (dd~t, 1H, J = 9.3 Hz, J = 9.3 Hz, H-3$_{Glu}$), 5.71 (d, 1H, J = 10.4 Hz, H-1$_{Glu}$), 7.25 (d, 1H, J = 8.6 Hz, H-3$_{Pyr}$), 7.97 (dd, 1H, J = 2.6 Hz, J = 8.6 Hz, H-4$_{Pyr}$), 8.07 (bs, 1H, NH), 8.57 (d, 1H, J = 2.6 Hz, H-6$_{Pyr}$); ^{13}C NMR (100 MHz, CDCl$_3$): δ20.60, 20.63, 20.69, 20.75 (CH$_3$CO), 52.85 (CH$_2$N$_3$), 61.95 (C-6$_{Glu}$), 68.26, 69.49, 74.10, 75.96 (C-2$_{Glu}$, C-3$_{Glu}$, C-4$_{Glu}$, C-5$_{Glu}$), 82.15 (C-1$_{Glu}$), 123.59, 128.41, 131.53, 141.33, 150.91 (C$_{Pyr}$), 164.88 (C=O) 169.42, 169.50, 170.15, 170.66 (CH$_3$CO); HRMS (ESI-TOF): calcd for C$_{21}$H$_{26}$N$_5$O$_{10}$S ([M + H]$^+$): *m/z* 540.1400; found: *m/z* 540.1396.

*(5-azidoacetamide-2-pyridyl) 2,3,4,6-tetra-O-acetyl-1-thio-β-*D*-galactopyranoside* **34**: *Starting from (5-chloroacetamide -2-pyridyl) 2,3,4,6-tetra-O-acetyl-1-thio-β-*D*-galactopyranoside* **32**, *the product was obtained as a beige solid (278 mg, 86%)*, m.p.: 57–59 °C; [α]^{25}$_D$ = 17.0 (c = 0.4, CHCl$_3$); ^{1}H NMR (400 MHz, CDCl$_3$): δ 2.00, 2.01, 2,03, 2.17 (4s, 12H, CH$_3$CO), 4.04–4.16 (m, 3H, H-5$_{Gal}$, H-6a$_{Gal}$, H-6b$_{Gal}$), 4.19 (s, 2H, CH$_2$N$_3$), 5.18 (dd, 1H, J = 3.4 Hz, J = 9.9 Hz, H-3$_{Gal}$), 5.40 (dd~t, 1H, J = 9.9 Hz, J = 10.2 Hz, H-2$_{Gal}$), 5.48 (dd, 1H, J = 0.7 Hz, J = 3.4 Hz, H-4$_{Gal}$), 5.68 (d, 1H, J = 10.4 Hz, H-1$_{Gal}$), 7.27 (d, 1H, J = 8.6 Hz, H-3$_{Pyr}$), 7.98 (dd, 1H, J = 2.7 Hz, J = 8.6 Hz, H-4$_{Pyr}$), 8.08 (bs, 1H, NH), 8.57 (dd, 1H, J = 0.6 Hz, J = 2.7 Hz, H-6$_{Pyr}$); ^{13}C NMR (100 MHz, CDCl$_3$): δ 20.60, 20.68, 20.70, 20.78 (CH$_3$CO), 52.84 (CH$_2$N$_3$), 61.29 (C-6$_{Gal}$), 66.83, 67.30, 72.07, 74.57 (C-2$_{Gal}$, C-3$_{Gal}$, C-4$_{Gal}$, C-5$_{Gal}$), 82.71 (C-1$_{Gal}$), 123.62, 128.43, 131.56, 141.35, 151.05 (C$_{Pyr}$), 164.94 (C=O) 169.69, 170.02, 170.25, 170.35 (CH$_3$CO); HRMS (ESI-TOF): calcd for C$_{21}$H$_{26}$N$_5$O$_{10}$S ([M + H]$^+$): *m/z* 540.1400; found: *m/z* 540.1403.

3.2.3. General Procedure for the Synthesis of Sugar Derivatives **36** and **37**

To a solution of (5-amino-2-pyridyl) 2,3,4,6-tetra-*O*-acetyl-1-thio-β-ᴅ-glucopyranoside **29** or (5-amino-2-pyridyl) 2,3,4,6-tetra-*O*-acetyl-1-thio-β-ᴅ-galactopyranoside **30** (274 mg, 0.6 mmol) in dry CH₂CL₂ (20 mL), *N*,*N*-diisopropylethylamine (347 μL, 2.1 mM) was added. The reaction mixture was cooled to 0 °C, and propargyl chloroformate was added dropwise (117 μL, 1.2 mmol), then stirring was continued at room temperature. After 2 h, the resulting mixture was diluted with dichloromethane (60 mL) and washed with 1M HCl (40 mL), saturated NaHCO₃ (40 mL), and brine (40 mL). The combined organic phases were dried over anhydrous MgSO₄, filtered, and concentrated in vacuo. The crude products were purified by column chromatography (toluene:AcOEt; 5:1) to give products **36–37**.

(5-(((prop-2-yn-1-yloxy)carbonyl)amino)-2-pyridyl) 2,3,4,6-tetra-O-acetyl-1-thio-β-ᴅ-glucopyranoside **36**: *Starting from (5-amino-2-pyridyl) 2,3,4,6-tetra-O-acetyl-1-thio-β-ᴅ-glucopyranoside* **29**, *the product was obtained as an orange solid (265 mg, 82%)*, m.p.: 162–165 °C; $[\alpha]^{26}_D = 0.9$ (c = 0.46, CHCl₃); ^{1}H NMR (400 MHz, CDCl₃): δ 2.02, 2.02, 2,03, 2.05 (4s, 12H, CH₃CO), 2.54 (t, 1H, *J* = 2.5 Hz, CH), 3.85 (ddd, 1H, *J* = 2.3 Hz, *J* = 4.6 Hz, *J* = 10.1 Hz, H-5$_{Glu}$), 4.10 (dd, 1H, *J* = 2.3 Hz, *J* = 12.4 Hz, H-6a$_{Glu}$), 4.26 (dd, 1H, *J* = 4.6 Hz, *J* = 12.4 Hz, H-6b$_{Glu}$), 4.80 (d, 2H, *J* = 2.5 Hz, CH₂), 5.15 (dd~t, 1H, *J* = 9.3 Hz, *J* = 10.4 Hz, H-2$_{Glu}$), 5.19 (dd~t, 1H, *J* = 9.3 Hz, *J* = 10.1 Hz, H-4$_{Glu}$), 5.33 (dd~t, 1H, *J* = 9.3 Hz, *J* = 9.3 Hz, H-3$_{Glu}$), 5.67 (d, 1H, *J* = 10.4 Hz, H-1$_{Glu}$), 6.86 (bs, 1H, NH), 7.23 (d, 1H, *J* = 8.2 Hz, H-4$_{Pyr}$), 7.84 (d, 1H, *J* = 8.2 Hz, H-3$_{Pyr}$), 8.43 (d, 1H, *J* = 2.5 Hz, H-6$_{Pyr}$); ^{13}C NMR (100 MHz, CDCl₃): δ 20.61, 20.63, 20.70, 20.75 (CH₃CO), 53.20 (CH₂), 61.96 (C-6$_{Glu}$), 68.27, 69.55, 74.11, 75.44 (C-2$_{Glu}$, C-3$_{Glu}$, C-4$_{Glu}$, C-5$_{Glu}$), 75.92, 77.40 (C≡CH), 82.37 (C-1$_{Glu}$), 123.95, 127.24, 132.48, 140.31, 149.35 (C$_{Pyr}$), 152.39 (C=O) 169.44, 169.52, 170.17, 170.68 (CH₃CO); HRMS (ESI-TOF): calcd for C₂₃H₂₇N₂O₁₁S ([M + H]⁺): *m/z* 539.1336; found: *m/z* 539.1337.

(5-(((prop-2-yn-1-yloxy)carbonyl)amino)-2-pyridyl 2,3,4,6-tetra-O-acetyl-1-thio-β-ᴅ-galactopyranoside **37**: *Starting from (5-amino-2-pyridyl) 2,3,4,6-tetra-O-acetyl-1-thio-β-ᴅ-galactopyranoside* **30**, *the product was obtained as a beige solid (258 mg, 80%)*, m.p.: 53–55 °C; $[\alpha]^{26}_D = 14.2$ (c = 1.0, CHCl₃); ^{1}H NMR (400 MHz, CDCl₃): δ 2.00, 2.00, 2,03, 2.17 (4s, 12H, CH₃CO), 2.54 (t, 1H, *J* = 2.4 Hz, CH), 4.03–4.16 (m, 3H, H-5$_{Gal}$, H-6a$_{Gal}$, H-6b$_{Gal}$), 4.80 (d, 2H, *J* = 2.4 Hz, CH₂), 5.17 (dd, 1H, *J* = 3.4 Hz, *J* = 9.9 Hz, H-3$_{Gal}$), 5.39 (dd~t, 1H, *J* = 9.9 Hz, *J* = 10.4 Hz, H-2$_{Gal}$), 5.48 (dd, 1H, *J* = 0.9 Hz, *J* = 3.4 Hz, H-4$_{Gal}$), 5.64 (d, 1H, *J* = 10.4 Hz, H-1$_{Gal}$), 6.91 (bs, 1H, NH), 7.27 (d, 1H, *J* = 8.6 Hz, H-4$_{Pyr}$), 7.85 (d, 1H, *J* = 8.6 Hz, H-3$_{Pyr}$), 8.43 (d, 1H, *J* = 2.6 Hz, H-6$_{Pyr}$); ^{13}C NMR (100 MHz, CDCl₃): δ 20.60, 20.67, 20.70, 20.79 (CH₃CO), 53.19 (CH₂), 61.31 (C-6$_{Gal}$), 66.90, 67.31, 72.08, 74.54 (C-2$_{Gal}$, C-3$_{Gal}$, C-4$_{Gal}$, C-5$_{Gal}$), 75.44, 77.41 (C≡CH), 82.93 (C-1$_{Gal}$), 123.98, 127.22, 132.49, 140.30, 149.52 (C$_{Pyr}$), 152.42 (C=O) 169.71, 170.04, 170.28, 170.37 (CH₃CO); HRMS (ESI-TOF): calcd for C₂₃H₂₇N₂O₁₁S ([M + H]⁺): *m/z* 539.1336; found: *m/z* 539.1340.

3.2.4. General Procedure for the Synthesis of Sugar Derivatives **35** and **38**

(5-azidoacetamide-2-pyridyl) 2,3,4,6-tetra-*O*-acetyl-1-thio-β-ᴅ-glucopyranoside **33** or (5-(((prop-2-yn-1-yloxy)carbonyl)amino)-2-pyridyl 2,3,4,6-tetra-*O*-acetyl-1-thio-β-ᴅ-glucopyranoside **36** (0.5 mmol) was dissolved in MeOH (20 mL), and then 1 M solution of NaOMe in MeOH (200 μL, 0.2 mmol) was added. The reaction mixture was stirred for 1 h at room temperature. After the reaction mixture was neutralized with Amberlyst-15 ion exchange resin, the mixture was filtered off, and the filtrate was concentrated in vacuo to give compounds **35** and **38**, pure enough for further reactions.

(5-azidoacetamide-2-pyridyl) 1-thio-β-ᴅ-glucopyranoside **35**: *Starting from (5-azidoacetamide-2-pyridyl) 2,3,4,6-tetra-O-acetyl-1-thio-β-ᴅ-glucopyranoside* **33**, *the product was obtained as an orange solid (150 mg, 81%)*, m.p.: 74–75 °C; $[\alpha]^{26}_D = -59.6$ (c = 0.45, CH₃OH); ^{1}H NMR (400 MHz, CD₃OD): δ 3.32–3.42 (m, 3H, H-2$_{Glu}$, H-4$_{Glu}$, H-5$_{Glu}$), 3.44 (dd~t, 1H, *J* = 8.6 Hz, *J* = 8.7 Hz, H-3$_{Glu}$), 3.66 (dd, 1H, *J* = 5.6 Hz, *J* = 12.1 Hz, H-6a$_{Glu}$), 3.85 (dd, 1H, *J* = 2.2 Hz, *J* = 12.1 Hz, H-6b$_{Glu}$), 4.05 (s, 2H, CH₂N₃), 5.11 (d, 1H, *J* = 9.9 Hz, H-1$_{Glu}$), 7.48 (dd, 1H, *J* = 0.6 Hz, *J* = 8.7 Hz, H-3$_{Pyr}$), 8.00 (dd, 1H, *J* = 2.6 Hz, *J* = 8.7 Hz, H-4$_{Pyr}$), 8.63 (d, 1H, *J* = 2.6 Hz, H-6$_{Pyr}$); ^{13}C NMR (100 MHz, CD₃OD): δ 53.21 (CH₂N₃), 62.81 (C-6$_{Glu}$), 71.35, 73.92,

79.77, 82.23 (C-2$_{Glu}$, C-3$_{Glu}$, C-4$_{Glu}$, C-5$_{Glu}$), 86.83 (C-1$_{Glu}$), 125.20, 130.13, 134.33, 142.20, 153.64 (C$_{Pyr}$), 168.90 (C=O); HRMS (ESI-TOF): calcd for C$_{13}$H$_{18}$N$_5$O$_6$S ([M + H]$^+$): *m/z* 372.0978; found: *m/z* 372.0979.

(5-(((prop-2-yn-1-yloxy)carbonyl)amino)-2-pyridyl 1-thio-β-D-glucopyranoside **38**: *Starting from (5-(((prop-2-yn-1-yloxy)carbonyl)amino)-2-pyridyl 2,3,4,6-tetra-O-acetyl-1-thio-β-D-glucopyranoside* **36**, *the product was obtained as an orange solid (181 mg, 98%),* m.p.: 69–71 °C; [α]^{26}$_D$ = −52.8 (c = 1.0, CH$_3$OH); ^{1}H NMR (400 MHz, CD$_3$OD): δ 2.94 (t, 1H, *J* = 2.5 Hz, CH), 3.31–3.35 (m, 2H, H-2$_{Glu}$, H-4$_{Glu}$), 3.39 (ddd, 1H, *J* = 2.3 Hz, *J* = 5.7 Hz, *J* = 9.7 Hz, H-5$_{Glu}$), 3.43 (dd~t, 1H, *J* = 8.8 Hz, *J* = 8.8 Hz, H-3$_{Glu}$), 3.66 (dd, 1H, *J* = 5.7 Hz, *J* = 12.2 Hz, H-6a$_{Glu}$), 3.85 (dd, 1H, *J* = 2.3 Hz, *J* = 12.2 Hz, H-6b$_{Glu}$), 4.78 (d, 2H, *J* = 2.5 Hz, CH$_2$), 5.03 (d, 1H, *J* = 9.9 Hz, H-1$_{Glu}$), 7.48 (d, 1H, *J* = 8.6 Hz, H-4$_{Pyr}$), 7.89 (d, 1H, *J* = 8.6 Hz, H-3$_{Pyr}$), 8.50 (d, 1H, *J* = 2.3 Hz, H-6$_{Pyr}$); ^{13}C NMR (100 MHz, CD$_3$OD): δ 53.63 (CH$_2$), 62.83 (C-6$_{Glu}$), 71.36, 73.94, 76.32, 79.03 (C-2$_{Glu}$, C-3$_{Glu}$, C-4$_{Glu}$, C-5$_{Glu}$), 79.74, 82.22 (C≡CH), 87.15 (C-1$_{Glu}$), 125.86, 128.62, 135.43, 140.94, 151.80 (C$_{Pyr}$), 154.82 (C=O); HRMS (ESI-TOF): calcd for C$_{15}$H$_{19}$N$_2$O$_7$S ([M + H]$^+$): *m/z* 371.0913; found: *m/z* 371.0911.

3.2.5. General Procedure for the Synthesis of Glycoconjugates **43**–**72**

The appropriate sugar derivatives **15**–**26**, **33**–**38** (1 eq.) and 8-hydroxyquinoline derivatives **39**–**41** (1 eq.) were dissolved in a dry solvent system: THF (2 mL) and *i*-PrOH (2 mL). The catalyst systems were prepared: sodium ascorbate (0.4 eq.) dissolved in H$_2$O (1 mL) and CuSO$_4$·5H$_2$O (0.2 eq.) dissolved in H$_2$O (1 mL), mixed, and immediately added to the reaction mixture. The reaction mixture was stirred for 24 h at room temperature. Then, the solvents were evaporated in vacuo, and the crude products were purified by column chromatography (dry loading; toluene:AcOEt, 2:1 and CHCl$_3$:MeOH, 100:1 for fully protected glycoconjugates or CHCl$_3$:MeOH, gradient: 50:1 to 2:1 for glycoconjugates with unprotected sugar part) to give products **43**–**72**.

Glycoconjugate **43**: *Starting from sugar derivative* **15** *and 8-HQ derivative* **39**, *the product was obtained as a beige solid (79% yield),* m.p.: 191–196 °C; [α]^{23}$_D$ = −70.4 (c = 1.0, CHCl$_3$); ^{1}H NMR (400 MHz, CDCl$_3$): δ 1.94, 1.99, 2.02, 2.05 (4s, 12H, CH$_3$CO), 3.61 (ddd, 1H, *J* = 2.2 Hz, *J* = 4.8 Hz, *J* = 10.0 Hz, H-5$_{Glu}$), 4.05 (dd, 1H, *J* = 2.2 Hz, *J* = 12.5 Hz, H-6a$_{Glu}$), 4.17 (dd, 1H, *J* = 4.8 Hz, *J* = 12.5 Hz, H-6b$_{Glu}$), 4.55 (d, 1H, *J* = 10.1 Hz, H-1$_{Glu}$), 5.02 (dd~t, 1H, *J* = 9.2 Hz, *J* = 10.0 Hz, H-4$_{Glu}$), 5.06 (dd~t, 1H, *J* = 9.4 Hz, *J* = 10.1 Hz, H-2$_{Glu}$), 5.15 (dd~t, 1H, *J* = 9.2 Hz, *J* = 9.4 Hz, H-3$_{Glu}$), 5.29 i 5.71 (qAB, 2H, *J* = 14.5 Hz, CH$_2$N$_3$), 5.58 (s, 2H, CH$_2$O), 7.29 (dd, 1H, *J* = 1.9 Hz, *J* = 6.9 Hz, H-7$_{Quin}$), 7.40–7.49 (m, 3H, H-3$_{Quin}$, H-5$_{Quin}$, H-6$_{Quin}$), 7.94 (s, 1H, H-5$_{Triaz}$), 8.14 (dd, 1H, *J* = 1.6 Hz, *J* = 8.3 Hz, H-4$_{Quin}$), 8.93 (dd, 1H, *J* = 1.6 Hz, 4.1 Hz, H-2$_{Quin}$); ^{13}C NMR (100 MHz, CDCl$_3$): δ 20.51, 20.55, 20.57, 20.74 (CH$_3$CO), 48.05 (CH$_2$N$_3$), 61.58, 62.85 (C-6$_{Glu}$, CH$_2$O), 67.91, 69.77, 73.56, 76.20 (C-2$_{Glu}$, C-3$_{Glu}$, C-4$_{Glu}$, C-5$_{Glu}$), 81.48 (C-1$_{Glu}$), 109.93 (C-7$_{Quin}$), 120.44 (C-5$_{Quin}$), 121.71 (C-3$_{Quin}$), 123.20 (C-5$_{Triaz}$), 126.68 (C-6$_{Quin}$), 129.52 (C-4a$_{Quin}$), 136.00 (C-4$_{Quin}$), 140.32 (C-8a$_{Quin}$), 145.12 (C-4$_{Triaz}$), 149.42 (C-2$_{Quin}$), 155.63 (C-8$_{Quin}$), 169.35, 169.40, 169.98, 170.54 (CH$_3$C̲O); HRMS (ESI-TOF): calcd for C$_{27}$H$_{31}$N$_4$O$_{10}$S ([M + H]$^+$): *m/z* 603.1761; found: *m/z* 603.1766.

Glycoconjugate **44**: *Starting from sugar derivative* **16** *and 8-HQ derivative* **39**, *the product was obtained as a beige solid (93% yield),* m.p.: 92–96 °C; [α]^{23}$_D$ = −55.8 (c = 1.0, CHCl$_3$); ^{1}H NMR (400 MHz, CDCl$_3$): δ 1.95, 1.97, 2.03, 2.15 (4s, 12H, CH$_3$CO), 3.67 (ddd, 1H, *J* = 0.8 Hz, *J* = 6.0 Hz, *J* = 6.9 Hz, H-5$_{Gal}$), 3.93 (dd, 1H, *J* = 6.0 Hz, *J* = 11.4 Hz, H-6a$_{Gal}$), 3.98 (dd, 1H, *J* = 6.9 Hz, *J* = 11.4 Hz, H-6b$_{Gal}$), 4.46 (d, 1H, *J* = 10.0 Hz, H-1$_{Gal}$), 4.95 (dd, 1H, *J* = 3.4 Hz, *J* = 10.0 Hz, H-3$_{Gal}$), 5.21 (dd~t, 1H, *J* = 10.0 Hz, *J* = 10.0 Hz, H-2$_{Gal}$), 5.31 and 5.71 (qAB, 2H, *J* = 14.6 Hz, CH$_2$N$_3$), 5.33 (dd, 1H, *J* = 0.8 Hz, *J* = 3.4 Hz, H-4$_{Gal}$), 5.60 (s, 2H, CH$_2$O), 7.28 (dd, 1H, *J* = 2.7 Hz, *J* = 6.4 Hz, H-7$_{Quin}$), 7.41–7.48 (m, 3H, H-3$_{Quin}$, H-5$_{Quin}$, H-6$_{Quin}$), 7.94 (s, 1H, H-5$_{Triaz}$), 8.15 (dd, 1H, *J* = 1.6 Hz, *J* = 8.3 Hz, H-4$_{Quin}$), 8.93 (dd, 1H, *J* = 1.6 Hz, 4.1 Hz, H-2$_{Quin}$); ^{13}C NMR (100 MHz, CDCl$_3$): δ20.52, 20.60, 20.65, 20.69 (CH$_3$CO), 47.93 (CH$_2$N$_3$), 61.36, 62.85 (C-6$_{Gal}$, CH$_2$O), 66.98, 67.13, 71.54, 74.92 (C-2$_{Gal}$, C-3$_{Gal}$, C-4$_{Gal}$, C-5$_{Gal}$), 81.81 (C-1$_{Gal}$), 109.96 (C-7$_{Quin}$), 120.40 (C-5$_{Quin}$), 121.74 (C-3$_{Quin}$), 123.25 (C-5$_{Triaz}$), 126.69 (C-6$_{Quin}$), 129.53 (C-4a$_{Quin}$), 135.98 (C-4$_{Quin}$), 140.34 (C-8a$_{Quin}$), 144.99 (C-4$_{Triaz}$), 149.45 (C-2$_{Quin}$), 153.71 (C-8$_{Quin}$), 169.60, 169.81, 170.12, 170.26 (CH$_3$C̲O); HRMS (ESI-TOF): calcd for C$_{27}$H$_{31}$N$_4$O$_{10}$S ([M + H]$^+$): *m/z* 603.1761; found: *m/z* 603.1760.

Glycoconjugate **45***: Starting from sugar derivative* **15** *and 8-HQ derivative* **40***, the product was obtained as a white solid (87% yield)*, m.p.: 159–163 °C; $[\alpha]^{23}_D = -84.8$ (c = 1.0, CHCl$_3$); ^{1}H NMR (400 MHz, CDCl$_3$): δ 1.94, 1.99, 2.02, 2.07 (4s, 12H, CH$_3$CO), 2.78 (s, 3H, CH$_3$), 3.55 (ddd, 1H, *J* = 1.9 Hz, *J* = 4.8 Hz, *J* = 10.1 Hz, H-5$_{Glu}$), 4.01 (dd, 1H, *J* = 1.9 Hz, *J* = 12.5 Hz, H-6a$_{Glu}$), 4.15 (dd, 1H, *J* = 4.8 Hz, *J* = 12.5 Hz, H-6b$_{Glu}$), 4.52 (d, 1H, *J* = 10.1 Hz, H-1$_{Glu}$), 5.01 (dd~t, 1H, *J* = 9.3 Hz, *J* = 10.1 Hz, H-4$_{Glu}$), 5.04 (dd~t, 1H, *J* = 9.3 Hz, *J* = 10.1 Hz, H-2$_{Glu}$), 5.14 (dd~t, 1H, *J* = 9.3 Hz, *J* = 9.3 Hz, H-3$_{Glu}$), 5.28 i 5.71 (qAB, 2H, *J* = 14.6 Hz, CH$_2$N$_3$), 5.59 i 5.62 (qAB, 2H, *J* = 13.4 Hz, CH$_2$O), 7.22 (dd, 1H, *J* = 1.4 Hz, *J* = 7.2 Hz, H-7$_{Quin}$), 7.31 (d, 1H, *J* = 8.4 Hz, H-3$_{Quin}$), 7.34–7.40 (m, 2H, H-5$_{Quin}$, H-6$_{Quin}$), 7.92 (s, 1H, H-5$_{Triaz}$), 8.01 (d, 1H, *J* = 8.4 Hz, H-4$_{Quin}$); ^{13}C NMR (100 MHz, CDCl$_3$): δ 20.51, 20.55, 20,57, 20.74 ($\underline{C}$H$_3$CO), 25.74 (CH$_3$), 47.97 (CH$_2$N), 61.57, 63.21 (C-6$_{Glu}$, CH$_2$O), 67.90, 69.79, 73.55, 76.17 (C-2$_{Glu}$, C-3$_{Glu}$, C-4$_{Glu}$, C-5$_{Glu}$), 81.33 (C-1$_{Glu}$), 110.48 (C-7$_{Quin}$), 120.41 (C-5$_{Quin}$), 122.62 (C-3$_{Quin}$), 123.04 (C-5$_{Triaz}$), 125.61 (C-6$_{Quin}$), 127.76 (C-4a$_{Quin}$), 136.17 (C-4$_{Quin}$), 139.89 (C-8a$_{Quin}$), 145.46 (C-4$_{Triaz}$), 153.23 (C-2$_{Quin}$), 158.29 (C-8$_{Quin}$), 169.33, 169.40, 169.96, 170.51 (CH$_3$$\underline{C}$O); HRMS (ESI-TOF): calcd for C$_{28}$H$_{33}$N$_4$O$_{10}$S ([M + H]$^+$): *m/z* 617.1917; found: *m/z* 617.1915.

Glycoconjugate **46***: Starting from sugar derivative* **16** *and 8-HQ derivative* **40***, the product was obtained as a beige solid (92% yield)*, m.p.: 65–68 °C; $[\alpha]^{23}_D = -34.8$ (c = 1.0, CHCl$_3$); ^{1}H NMR (400 MHz, CDCl$_3$): δ 1.95, 1.97, 2.06, 2.14 (4s, 12H, CH$_3$CO), 2.78 (s, 3H, CH$_3$), 3.49 (ddd, 1H, *J* = 0.8 Hz, *J* = 5.7 Hz, *J* = 7.1 Hz, H-5$_{Gal}$), 3.83 (dd, 1H, *J* = 5.7 Hz, *J* = 11.5 Hz, H-6a$_{Gal}$), 3.93 (dd, 1H, *J* = 7.1 Hz, *J* = 11.5 Hz, H-6b$_{Gal}$), 4.38 (d, 1H, *J* = 10.0 Hz, H-1$_{Gal}$), 4.93 (dd, 1H, *J* = 3.4 Hz, *J* = 10.0 Hz, H-3$_{Gal}$), 5.19 (dd~t, 1H, *J* = 10.0 Hz, *J* = 10.0 Hz, H-2$_{Gal}$), 5.28 (dd, 1H, *J* = 0.8 Hz, *J* = 3.4 Hz, H-4$_{Gal}$), 5.30 and 5.70 (qAB, 2H, *J* = 14.5 Hz, CH$_2$N$_3$), 5.61 (dd, 2H, *J* = 2.5 Hz, *J* = 16.5 Hz, CH$_2$O), 7.20 (dd, 1H, *J* = 1.4 Hz, *J* = 7.4 Hz, H-7$_{Quin}$), 7.31 (d, 1H, *J* = 8.4 Hz, H-3$_{Quin}$), 7.34–7.43 (m, 2H, H-5$_{Quin}$, H-6$_{Quin}$), 7.91 (s, 1H, H-5$_{Triaz}$), 8.02 (d, 1H, *J* = 8.4 Hz, H-4$_{Quin}$); ^{13}C NMR (100 MHz, CDCl$_3$): δ 20.52, 20.60, 20.63, 20.69 ($\underline{C}$H$_3$CO), 25.71 (CH$_3$) 47.77 (CH$_2$N$_3$), 61.49, 63.13 (C-6$_{Gal}$, CH$_2$O), 67.03, 67.16, 71.51, 74.85 (C-2$_{Gal}$, C-3$_{Gal}$, C-4$_{Gal}$, C-5$_{Gal}$), 81.51 (C-1$_{Gal}$), 110.47 (C-7$_{Quin}$), 120.38 (C-5$_{Quin}$), 122.70 (C-3$_{Quin}$), 123.20 (C-5$_{Triaz}$), 125.62 (C-6$_{Quin}$), 127.77 (C-4a$_{Quin}$), 136.15 (C-4$_{Quin}$), 139.90 (C-8a$_{Quin}$), 145.27 (C-4$_{Triaz}$), 153.14 (C-2$_{Quin}$), 158.37 (C-8$_{Quin}$), 169.60, 169.80, 170.10, 170.24 (CH$_3$$\underline{C}$O); HRMS (ESI-TOF): calcd for C$_{28}$H$_{33}$N$_4$O$_{10}$S ([M + H]$^+$): *m/z* 617.1917; found: *m/z* 617.1917.

Glycoconjugate **47**: *Starting from sugar derivative* **19** *and 8-HQ derivative* **39***, the product was obtained as a white solid (71% yield)*, m.p.: 123–126 °C; $[\alpha]^{23}_D = -127.0$ (c = 1.0, DMSO); ^{1}H NMR (400 MHz, DMSO): δ 3.02–3.10 (m, 2H, H-2$_{Glu}$, H-4$_{Glu}$), 3.16 (m, 1H, H-5$_{Glu}$), 3.26 (m, 1H, H-3$_{Glu}$), 3.48 (m, 1H, H-6a$_{Glu}$), 3.78 (m, 1H, H-6b$_{Glu}$), 4.47 (d, 1H, *J* = 9.7 Hz, H-1$_{Glu}$), 4.96 (t, 1H, *J* = 5.4 Hz, 6-OH), 5.02 (d, 1H, *J* = 5.5 Hz, OH), 5.10 (d, 1H, *J* = 4.9 Hz, OH), 5.29 (d, 1H, *J* = 6.2 Hz, OH), 5.36 (s, 2H, CH$_2$O), 5.65 and 5.82 (qAB, 2H, *J* = 14.5 Hz, CH$_2$N$_3$), 7.42 (dd, 1H, *J* = 3.4 Hz, *J* = 5.4 Hz, H-7$_{Quin}$), 7.51–7.58 (m, 3H, H-3$_{Quin}$, H-5$_{Quin}$, H-6$_{Quin}$), 8.34 (dd, 1H, *J* = 1.4 Hz, *J* = 8.3 Hz, H-4$_{Quin}$), 8.56 (s, 1H, H-5$_{Triaz}$), 8.83 (d, 1H, *J* = 2.4 Hz, H-2$_{Quin}$); ^{13}C NMR (100 MHz, DMSO): δ 47.81 (CH$_2$N$_3$), 61.39, 61.97 (C-6$_{Glu}$, CH$_2$O), 70.16, 73.25, 78.05, 81.25 (C-2$_{Glu}$, C-3$_{Glu}$, C-4$_{Glu}$, C-5$_{Glu}$), 83.88 (C-1$_{Glu}$), 110.01 (C-7$_{Quin}$), 120.04 (C-5$_{Quin}$), 121.88 (C-3$_{Quin}$), 125.28 (C-5$_{Triaz}$), 126.79 (C-6$_{Quin}$), 129.08 (C-4a$_{Quin}$), 135.97 (C-4$_{Quin}$), 139.55 (C-8a$_{Quin}$), 142.95 (C-4$_{Triaz}$), 148.96 (C-2$_{Quin}$), 153.74 (C-8$_{Quin}$); HRMS (ESI-TOF): calcd for C$_{19}$H$_{23}$N$_4$O$_6$S ([M + H]$^+$): *m/z* 435.1338; found: *m/z* 435.1339.

Glycoconjugate **48**: *Starting from sugar derivative* **20** *and 8-HQ derivative* **39***, the product was obtained as a beige solid (79% yield)*, m.p.: 142–145 °C; $[\alpha]^{23}_D = -58.7$ (c = 1.0, DMSO); ^{1}H NMR (400 MHz, DMSO): δ 3.29 (m, 1H, H-3$_{Gal}$), 3.39 (m, 1H, H-5$_{Gal}$), 3.45 (m, 1H, H-2$_{Gal}$), 3.53 (m, 1H, H-6a$_{Gal}$), 3.60 (m, 1H, H-6b$_{Gal}$), 3.69 (m, 1H, H-4$_{Gal}$), 4.40 (d, 1H, *J* = 9.6 Hz, H-1$_{Gal}$), 4.52 (d, 1H, *J* = 4.5 Hz, OH), 4.84 (d, 1H, *J* = 5.2 Hz, OH), 4.91 (t, 1H, *J* = 5.2 Hz, 6-OH), 5.12 (d, 1H, *J* = 6.1 Hz, OH), 5.36 (s, 2H, CH$_2$O), 5.63 and 5.79 (qAB, 2H, *J* = 14.5 Hz, CH$_2$N$_3$), 7.41 (dd, 1H, *J* = 3.6, *J* = 5.4 Hz, H-7$_{Quin}$), 7.50–7.58 (m, 3H, H-3$_{Quin}$, H-5$_{Quin}$, H-6$_{Quin}$), 8.33 (dd, 1H, *J* = 1.7 Hz, *J* = 8.3 Hz, H-4$_{Quin}$), 8.52 (s, 1H, H-5$_{Triaz}$), 8.83 (dd, 1H, *J* = 1.7 Hz, *J* = 4.1 Hz, H-2$_{Quin}$); ^{13}C NMR (100 MHz, DMSO): δ 47.88 (CH$_2$N), 60.89, 61.98 (C-6$_{Gal}$, CH$_2$O), 68.61, 70.01, 74.55, 79.68 (C-2$_{Gal}$, C-3$_{Gal}$, C-4$_{Gal}$, C-5$_{Gal}$), 84.39 (C-1$_{Gal}$), 110.03

(C-7$_{\text{Quin}}$), 120.04 (C-5$_{\text{Quin}}$), 121.88 (C-3$_{\text{Quin}}$), 125.20 (C-5$_{\text{Triaz}}$), 126.79 (C-6$_{\text{Quin}}$), 129.08 (C-4a$_{\text{Quin}}$), 135.95 (C-4$_{\text{Quin}}$), 139.57 (C-8a$_{\text{Quin}}$), 142.91 (C-4$_{\text{Triaz}}$), 148.96 (C-2$_{\text{Quin}}$), 153.72 (C-8$_{\text{Quin}}$); HRMS (ESI-TOF): calcd for $C_{19}H_{23}N_4O_6S$ ([M + H]$^+$): *m/z* 435.1338; found: *m/z* 435.1333.

Glycoconjugate **49**: *Starting from sugar derivative* **19** *and 8-HQ derivative* **40**, *the product was obtained as a white solid (83% yield)*, m.p.: 140–144 °C; $[\alpha]^{23}_D = -64.0$ (c = 1.0, DMSO); ^{1}H NMR (400 MHz, DMSO): δ 2.64 (s, 3H, CH$_3$), 3.02–3.10 (m, 2H, H-2$_{\text{Glu}}$, H-4$_{\text{Glu}}$), 3.15 (m, 1H, H-5$_{\text{Glu}}$), 3.24 (m, 1H, H-3$_{\text{Glu}}$), 3.45 (m, 1H, H-6a$_{\text{Glu}}$), 3.75 (m, 1H, H-6b$_{\text{Glu}}$), 4.46 (d, 1H, *J* = 9.7 Hz, H-1$_{\text{Glu}}$), 4.77 (t, 1H, *J* = 5.5 Hz, 6-OH), 5.01 (d, 1H, *J* = 5.4 Hz, OH), 5.10 (d, 1H, *J* = 4.8 Hz, OH), 5.28 (d, 1H, *J* = 6.2 Hz, OH), 5.35 (s, 2H, CH$_2$O), 5.64 and 5.81 (qAB, 2H, *J* = 14.5 Hz, CH$_2$N$_3$), 7.37 (dd, 1H, *J* = 1.4 Hz, *J* = 7.6, H-7$_{\text{Quin}}$), 7.42 (d, 1H, *J* = 8.3 Hz, H-3$_{\text{Quin}}$), 7.44 (dd~t, 1H, *J* = 7.3 Hz, *J* = 7.6 Hz, H-6$_{\text{Quin}}$), 7.47 (dd, 1H, *J* = 1.2 Hz, *J* = 8.1 Hz, H-5$_{\text{Quin}}$), 8.19 (d, 1H, *J* = 8.4 Hz, H-4$_{\text{Quin}}$), 8.49 (s, 1H, H-5$_{\text{Triaz}}$); ^{13}C NMR (100 MHz, DMSO): δ 24.88 (CH$_3$), 47.69 (CH$_2$N$_3$), 61.31, 61.65 (C-6$_{\text{Glu}}$, CH$_2$O), 70.10, 73.24, 78.04, 81.27 (C-2$_{\text{Glu}}$, C-3$_{\text{Glu}}$, C-4$_{\text{Glu}}$, C-5$_{\text{Glu}}$), 83.74 (C-1$_{\text{Glu}}$), 110.22 (C-7$_{\text{Quin}}$), 119.85 (C-5$_{\text{Quin}}$), 122.49 (C-3$_{\text{Quin}}$), 125.40, 125.66 (C-5$_{\text{Triaz}}$, C-6$_{\text{Quin}}$), 127.35 (C-4a$_{\text{Quin}}$), 136.03 (C-4$_{\text{Quin}}$), 139.14 (C-8a$_{\text{Quin}}$), 142.91 (C-4$_{\text{Triaz}}$), 153.29 (C-2$_{\text{Quin}}$), 157.33 (C-8$_{\text{Quin}}$); HRMS (ESI-TOF): calcd for $C_{20}H_{25}N_4O_6S$ ([M + H]$^+$): *m/z* 449.1495; found: *m/z* 449.1494.

Glycoconjugate **50**: *Starting from sugar derivative* **20** *and 8-HQ derivative* **40**, *the product was obtained as a beige solid (92% yield)*, m.p.: 134–138 °C; $[\alpha]^{23}_D = -90.0$ (c = 1.0, DMSO); ^{1}H NMR (400 MHz, DMSO): δ 2.64 (s, 3H, CH$_3$), 3.27 (m, 1H, H-3$_{\text{Gal}}$), 3.34–3.44 (m, 2H, H-2$_{\text{Gal}}$, H-5$_{\text{Gal}}$), 3.49 (m, 1H, H-6a$_{\text{Gal}}$), 3.55 (m, 1H, H-6b$_{\text{Gal}}$), 3.67 (m, 1H, H-4$_{\text{Gal}}$), 4.37 (d, 1H, *J* = 9.6 Hz, H-1$_{\text{Gal}}$), 4.48 (d, 1H, *J* = 4.6 Hz, OH), 4.74 (t, 1H, *J* = 5.4 Hz, 6-OH), 4.84 (d, 1H, *J* = 4.9 Hz, OH), 5.11 (d, 1H, *J* = 6.1 Hz, OH), 5.36 (s, 2H, CH$_2$O), 5.62 and 5.78 (qAB, 2H, *J* = 14.5 Hz, CH$_2$N$_3$), 7.36 (dd, 1H, *J* = 1.7 Hz, *J* = 7.4 Hz, H-7$_{\text{Quin}}$), 7.39–7.44 (m, 2H, H-3$_{\text{Quin}}$, H-6$_{\text{Quin}}$), 7.47 (dd, 1H, *J* = 1.6 Hz, *J* = 8.1 Hz, H-5$_{\text{Quin}}$), 8.19 (d, 1H, *J* = 8.4 Hz, H-4$_{\text{Quin}}$), 8.44 (s, 1H, H-5$_{\text{Triaz}}$); ^{13}C NMR (100 MHz, DMSO): δ 24.89 (CH$_3$), 47.73 (CH$_2$N$_3$), 60.77, 61.65 (C-6$_{\text{Gal}}$, CH$_2$O), 68.53, 70.01, 74.54, 79.66 (C-2$_{\text{Gal}}$, C-3$_{\text{Gal}}$, C-4$_{\text{Gal}}$, C-5$_{\text{Gal}}$), 84.21 (C-1$_{\text{Gal}}$), 110.26 (C-7$_{\text{Quin}}$), 119.84 (C-5$_{\text{Quin}}$), 122.49 (C-3$_{\text{Quin}}$), 125.32, 125.66 (C-5$_{\text{Triaz}}$, C-6$_{\text{Quin}}$), 127.35 (C-4a$_{\text{Quin}}$), 136.01 (C-4$_{\text{Quin}}$), 139.17 (C-8a$_{\text{Quin}}$), 142.87 (C-4$_{\text{Triaz}}$), 153.25 (C-2$_{\text{Quin}}$), 157.33 (C-8$_{\text{Quin}}$); HRMS (ESI-TOF): calcd for $C_{20}H_{25}N_4O_6S$ ([M + H]$^+$): *m/z* 449.1495; found: *m/z* 449.1496.

Glycoconjugate **51**: *Starting from sugar derivative* **17** *and 8-HQ derivative* **39**, *the product was obtained as a brown solid (79% yield)*, m.p.: 150–152 °C; $[\alpha]^{23}_D = -31.2$ (c = 1.0, CHCl$_3$); ^{1}H NMR (400 MHz, CDCl$_3$): δ 2.00, 2.01, 2.03, 2.03 (4s, 12H, CH$_3$CO), 3.05 (m, 1H, CHS), 3.25 (m, 1H, CHS), 3.70 (ddd, 1H, *J* = 2.8 Hz, *J* = 4.6 Hz, *J* = 10.1 Hz, H-5$_{\text{Glu}}$), 4.13 (dd, 1H, *J* = 2.8 Hz, *J* = 12.5 Hz, H-6a$_{\text{Glu}}$), 4.19 (dd, 1H, *J* = 4.6 Hz, *J* = 12.5 Hz, H-6b$_{\text{Glu}}$), 4.47 (d, 1H, *J* = 10.0 Hz, H-1$_{\text{Glu}}$), 4.50–4.67 (m, 2H, CH$_2$N$_3$), 5.02 (dd~t, 1H, *J* = 9.4 Hz, *J* = 10.1 Hz, H-4$_{\text{Glu}}$), 5.04 (dd~t, 1H, *J* = 9.4 Hz, *J* = 10.0 Hz, H-2$_{\text{Glu}}$), 5.21 (dd~t, 1H, *J* = 9.4 Hz, *J* = 9.4 Hz, H-3$_{\text{Glu}}$), 5.58 (s, 2H, CH$_2$O), 7.32 (dd, 1H, *J* = 1.3 Hz, *J* = 7.2 Hz, H-7$_{\text{Quin}}$), 7.38–7.49 (m, 3H, H-3$_{\text{Quin}}$, H-5$_{\text{Quin}}$, H-6$_{\text{Quin}}$), 7.85 (s, 1H, H-5$_{\text{Triaz}}$), 8.13 (dd, 1H, *J* = 1.4 Hz, *J* = 8.3 Hz, H-4$_{\text{Quin}}$), 8.93 (d, 1H, *J* = 2.7 Hz, H-2$_{\text{Quin}}$); ^{13}C NMR (100 MHz, CDCl$_3$): δ 20.56, 20.57, 20.63, 20.66 ($\underline{C}$H$_3$CO), 30.28 (CH$_2$S) 50.61 (CH$_2$N$_3$), 61.85, 62.97 (C-6$_{\text{Glu}}$, CH$_2$O), 68.11, 69.50, 73.56, 76.25 (C-2$_{\text{Glu}}$, C-3$_{\text{Glu}}$, C-4$_{\text{Glu}}$, C-5$_{\text{Glu}}$), 83.73 (C-1$_{\text{Glu}}$), 110.07 (C-7$_{\text{Quin}}$), 120.27 (C-5$_{\text{Quin}}$), 121.65 (C-3$_{\text{Quin}}$), 124.05 (C-5$_{\text{Triaz}}$), 126.74 (C-6$_{\text{Quin}}$), 129.51 (C-4a$_{\text{Quin}}$), 135.98 (C-4$_{\text{Quin}}$), 140.37 (C-8a$_{\text{Quin}}$), 144.03 (C-4$_{\text{Triaz}}$), 149.37 (C-2$_{\text{Quin}}$), 153.87 (C-8$_{\text{Quin}}$), 169.35, 169.38, 170.04, 170.49 (CH$_3\underline{C}$O); HRMS (ESI-TOF): calcd for $C_{28}H_{33}N_4O_{10}S$ ([M + H]$^+$): *m/z* 617.1917; found: *m/z* 617.1918.

Glycoconjugate **52**: *Starting from sugar derivative* **18** *and 8-HQ derivative* **39**, *the product was obtained as a yellow solid (82% yield)*, m.p.: 90–95 °C; $[\alpha]^{23}_D = -9.4$ (c = 1.0, CHCl$_3$); ^{1}H NMR (400 MHz, CDCl$_3$): δ 1.98, 1.99, 2.04, 2.15 (4s, 12H, CH$_3$CO), 3.06 (m, 1H, CHS), 3.28 (m, 1H, CHS), 3.92 (ddd, 1H, *J* = 0.8 Hz, *J* = 6.0 Hz, *J* = 6.9 Hz, H-5$_{\text{Gal}}$), 4.08 (dd, 1H, *J* = 6.0 Hz, *J* = 11.7 Hz, H-6a$_{\text{Gal}}$), 4.12 (dd, 1H, *J* = 6.9 Hz, *J* = 11.7 Hz, H-6b$_{\text{Gal}}$), 4.46 (d, 1H, *J* = 9.9 Hz, H-1$_{\text{Gal}}$), 4.53–4.69 (m, 2H, CH$_2$N$_3$), 5.03 (dd, 1H, *J* = 3.3 Hz, *J* = 10.0 Hz, H-3$_{\text{Gal}}$), 5.24 (dd~t, 1H, *J* = 9.9 Hz, *J* = 10.0 Hz, H-2$_{\text{Gal}}$), 5.43 (dd, 1H, *J* = 0.8 Hz, *J* = 3.3 Hz, H-4$_{\text{Gal}}$), 5.58 (s, 2H, CH$_2$O), 7.34 (d, 1H, *J* = 7.1 Hz, H-7$_{\text{Quin}}$), 7.38–7.49 (m, 3H, H-3$_{\text{Quin}}$, H-5$_{\text{Quin}}$, H-6$_{\text{Quin}}$),

7.85 (s, 1H, H-5$_{Triaz}$), 8.13 (d, 1H, J = 8.0 Hz, H-4$_{Quin}$), 8.94 (d, 1H, J = 1.9 Hz, H-2$_{Quin}$); ^{13}C NMR (100 MHz, CDCl$_3$): δ 20.56, 20.63, 20.68, 20.74 (C̱H$_3$CO), 30.29 (CH$_2$S) 50.66 (CH$_2$N), 61.61, 62.93 (C-6$_{Gal}$, CH$_2$O), 66.76, 67.24, 71.64, 74.90 (C-2$_{Gal}$, C-3$_{Gal}$, C-4$_{Gal}$, C-5$_{Gal}$), 84.17 (C-1$_{Gal}$), 109.99 (C-7$_{Quin}$), 120.27 (C-5$_{Quin}$), 121.66 (C-3$_{Quin}$), 123.86 (C-5$_{Triaz}$), 126.74 (C-6$_{Quin}$), 129.51 (C-4a$_{Quin}$), 135.96 (C-4$_{Quin}$), 140.36 (C-8a$_{Quin}$), 144.09 (C-4$_{Triaz}$), 149.37 (C-2$_{Quin}$), 153.89 (C-8$_{Quin}$), 169.61, 169.94, 170.13, 170.33 (CH$_3$C̱O); HRMS (ESI-TOF): calcd for C$_{28}$H$_{33}$N$_4$O$_{10}$S ([M + H]$^+$): *m/z* 617.1917; found: *m/z* 617.1920.

Glycoconjugate **53**: *Starting from sugar derivative* **17** *and 8-HQ derivative* **40**, *the product was obtained as a beige solid (77% yield)*, m.p.: 139–142 °C; [α]$^{23}_D$ = −29.8 (c = 1.0, CHCl$_3$); ^{1}H NMR (400 MHz, CDCl$_3$): δ 2.00, 2.01, 2.02, 2.03 (4s, 12H, CH$_3$CO), 2.79 (s, 3H, CH$_3$), 3.05 (m, 1H, CHS), 3.25 (m, 1H, CHS), 3.70 (ddd, 1H, J = 2.9 Hz, J = 4.5 Hz, J = 10.1 Hz, H-5$_{Glu}$), 4.12 (dd, 1H, J = 2.9 Hz, J = 12.5 Hz, H-6a$_{Glu}$), 4.18 (dd, 1H, J = 4.5 Hz, J = 12.5 Hz, H-6b$_{Glu}$), 4.47 (d, 1H, J = 10.0 Hz, H-1$_{Glu}$), 4.50–4.67 (m, 2H, CH$_2$N$_3$), 5.01 (dd~t, 1H, J = 9.4 Hz, J = 10.1 Hz, H-4$_{Glu}$), 5.04 (dd~t, 1H, J = 9.4 Hz, J = 10.0 Hz, H-2$_{Glu}$), 5.20 (dd~t, 1H, J = 9.4 Hz, J = 9.4 Hz, H-3$_{Glu}$), 5.59 (s, 2H, CH$_2$O), 7.26 (dd, 1H, J = 3.3 Hz, J = 5.6 Hz, H-7$_{Quin}$), 7.31 (d, 1H, J = 8.4 Hz, H-3$_{Quin}$), 7.33–7.39 (m, 2H, H5$_{Quin}$, H-6$_{Quin}$), 7.83 (s, 1H, H-5$_{Triaz}$), 8.01 (d, 1H, J = 8.4 Hz, H-4$_{Quin}$); ^{13}C NMR (100 MHz, CDCl$_3$): δ 20.56, 20.57, 20.63, 20.66 (C̱H$_3$CO), 25.73 (CH$_3$), 30.33 (CH$_2$S) 50.60 (CH$_2$N$_3$), 61.86, 63.33 (C-6$_{Glu}$, CH$_2$O), 68.12, 69.50, 73.57, 76.24 (C-2$_{Glu}$, C-3$_{Glu}$, C-4$_{Glu}$, C-5$_{Glu}$), 83.74 (C-1$_{Glu}$), 110.65 (C-7$_{Quin}$), 120.26 (C-5$_{Quin}$), 122.59 (C-3$_{Quin}$), 123.91 (C-5$_{Triaz}$), 125.70 (C-6$_{Quin}$), 127.76 (C-4a$_{Quin}$), 136.17 (C-4$_{Quin}$), 139.93 (C-8a$_{Quin}$), 144.37 (C-4$_{Triaz}$), 153.37 (C-2$_{Quin}$), 158.19 (C-8$_{Quin}$), 169.36, 169.40, 170.04, 170.50 (CH$_3$C̱O); HRMS (ESI-TOF): calcd for C$_{29}$H$_{35}$N$_4$O$_{10}$S ([M + H]$^+$): *m/z* 631.2074; found: *m/z* 631.2075.

Glycoconjugate **54**: *Starting from sugar derivative* **18** *and 8-HQ derivative* **40**, *the product was obtained as a white solid (70% yield)*, m.p.: 56–61 °C; [α]$^{23}_D$ = −9.3 (c = 1.0, CHCl$_3$); ^{1}H NMR (400 MHz, CDCl$_3$): δ 1.98, 1.99, 2.04, 2.15 (4s, 12H, CH$_3$CO), 2.79 (s, 3H, CH$_3$), 3.06 (m, 1H, CHS), 3.28 (m, 1H, CHS), 3.90 (ddd, 1H, J = 0.7 Hz, J = 6.0 Hz, J = 7.0 Hz, H-5$_{Gal}$), 4.07 (dd, 1H, J = 6.0 Hz, J = 11.9 Hz, H-6a$_{Gal}$), 4.11 (dd, 1H, J = 7.0 Hz, J = 11.9 Hz, H-6b$_{Gal}$), 4.45 (d, 1H, J = 9.9 Hz, H-1$_{Gal}$), 4.53–4.69 (m, 2H, CH$_2$N$_3$), 5.02 (dd, 1H, J = 3.3 Hz, J = 10.0 Hz, H-3$_{Gal}$), 5.24 (dd~t, 1H, J = 9.9 Hz, J = 10.0 Hz, H-2$_{Gal}$), 5.42 (dd, 1H, J = 0.7 Hz, J = 3.3 Hz, H-4$_{Gal}$), 5.60 (s, 2H, CH$_2$O), 7.28 (m, 1H, H-7$_{Quin}$), 7.31 (d, 1H, J = 8.4 Hz, H-3$_{Quin}$), 7.33–7.39 (m, 2H, H-5$_{Quin}$, H-6$_{Quin}$), 7.83 (s, 1H, H-5$_{Triaz}$), 8.01 (d, 1H, J = 8.4 Hz, H-4$_{Quin}$); ^{13}C NMR (100 MHz, CDCl$_3$): δ 20.56, 20.63, 20.67, 20.74 (C̱H$_3$CO), 25.79 (CH$_3$), 30.30 (CH$_2$S) 50.65 (CH$_2$N), 61.62, 63.33 (C-6$_{Gal}$, CH$_2$O), 66.75, 67.24, 71.64, 74.89 (C-2$_{Gal}$, C-3$_{Gal}$, C-4$_{Gal}$, C-5$_{Gal}$), 84.15 (C-1$_{Gal}$), 110.59 (C-7$_{Quin}$), 120.25 (C-5$_{Quin}$), 122.58 (C-3$_{Quin}$), 123.69 (C-5$_{Triaz}$), 125.70 (C-6$_{Quin}$), 127.75 (C-4a$_{Quin}$), 136.17 (C-4$_{Quin}$), 139.90 (C-8a$_{Quin}$), 144.44 (C-4$_{Triaz}$), 153.36 (C-2$_{Quin}$), 158.20 (C-8$_{Quin}$), 169.61, 169.93, 170.12, 170.33 (CH$_3$C̱O); HRMS (ESI-TOF): calcd for C$_{29}$H$_{35}$N$_4$O$_{10}$S ([M + H]$^+$): *m/z* 631.2074; found: *m/z* 631.2070.

Glycoconjugate **55**: *Starting from sugar derivative* **21** *and 8-HQ derivative* **39**, *the product was obtained as a brown solid (99% yield)*, m.p.: 65–69 °C; [α]$^{23}_D$ = −4.0 (c = 1.0, CH$_3$OH); ^{1}H NMR (400 MHz, DMSO): δ 2.97–3.24 (m, 6H, H-2$_{Glu}$, H-3$_{Glu}$, H-4$_{Glu}$ H-5$_{Glu}$, CH$_2$S), 3.45 (m, 1H, 6a$_{Glu}$), 3.72 (m, 1H, 6b$_{Glu}$), 4.37 (d, 1H, J = 9.6 Hz, H-1$_{Glu}$), 4.57–4.73 (m, 3H, CH$_2$N$_3$, 6-OH), 4.95 (d, 1H, J = 5.3 Hz, OH), 5.03 (d, 1H, J = 4.8 Hz, OH), 5.21 (d, 1H, J = 5.8 Hz, OH), 5.35 (s, 2H, CH$_2$O), 7.41 (dd, 1H, J = 3.8 Hz, J = 5.3 Hz, H-7$_{Quin}$), 7.50–7.57 (m, 3H, H-3$_{Quin}$, H-5$_{Quin}$, H-6$_{Quin}$), 8.32 (dd, 1H, J = 1.8 Hz, J = 8.3 Hz, H-4$_{Quin}$), 8.34 (s, 1H, H-5$_{Triaz}$), 8.83 (dd, 1H, J = 1.8 Hz, J = 4.1 Hz, H-2$_{Quin}$); ^{13}C NMR (100 MHz, DMSO): δ 29.78 (CH$_2$S), 49.91 (CH$_2$N$_3$), 61.28, 61.91 (C-6$_{Glu}$, CH$_2$O), 70.06, 72.95, 78.10, 81.00 (C-2$_{Glu}$, C-3$_{Glu}$, C-4$_{Glu}$, C-5$_{Glu}$), 85.36 (C-1$_{Glu}$), 110.06 (C-7$_{Quin}$), 120.01 (C-5$_{Quin}$), 121.84 (C-3$_{Quin}$), 125.39 (C-5$_{Triaz}$), 126.75 (C-6$_{Quin}$), 129.06 (C-4a$_{Quin}$), 135.81 (C-4$_{Quin}$), 139.70 (C-8a$_{Quin}$), 142.21 (C-4$_{Triaz}$), 148.95 (C-2$_{Quin}$), 153.86 (C-8$_{Quin}$); HRMS (ESI-TOF): calcd for C$_{20}$H$_{25}$N$_4$O$_6$S ([M + H]$^+$): *m/z* 449.1495; found: *m/z* 449.1492.

Glycoconjugate **56**: *Starting from sugar derivative* **22** *and 8-HQ derivative* **39**, *the product was obtained as a beige solid (77% yield)*, m.p.: 125–128 °C; [α]$^{23}_D$ = 6.2 (c = 1.0, CH$_3$OH); ^{1}H NMR (400 MHz, DMSO): δ 3.06 (m, 1H, CHS), 3.19 (m, 1H, CHS), 3.28 (m, 1H, H-3$_{Gal}$), 3.36–3.46 (m, 2H, 2$_{Gal}$, 5$_{Gal}$),

3.47–3.58 (m, 2H, 6a$_{Gal}$, 6b$_{Gal}$), 3.69 (m, 1H, H-4$_{Gal}$), 4.30 (d, 1H, *J* = 9.4 Hz Hz, H-1$_{Gal}$), 4.45 (d, 1H, *J* = 4.5 Hz, OH), 4.58–4.73 (m, 3H, CH$_2$N$_3$, 6-OH), 4.82 (d, 1H, *J* = 5.4 Hz, OH), 5.06 (d, 1H, *J* = 5.7 Hz, OH), 5.35 (s, 2H, CH$_2$O), 7.42 (dd, 1H, *J* = 4.2 Hz, *J* = 4.9 Hz, H-7$_{Quin}$), 7.50–7.57 (m, 3H, H-3$_{Quin}$, H-5$_{Quin}$, H-6$_{Quin}$), 8.32 (dd, 1H, *J* = 1.8 Hz, *J* = 8.3 Hz, H-4$_{Quin}$), 8.34 (s, 1H, H-5$_{Triaz}$), 8.83 (dd, 1H, *J* = 1.8 Hz, *J* = 4.1 Hz, H-2$_{Quin}$); ^{13}C NMR (100 MHz, DMSO): δ 29.66 (CH$_2$S), 50.04 (CH$_2$N$_3$), 60.82, 61.91 (C-6$_{Gal}$, CH$_2$O), 68.57, 69.65, 74.64, 79.36 (C-2$_{Gal}$, C-3$_{Gal}$, C-4$_{Gal}$, C-5$_{Gal}$), 85.80 (C-1$_{Gal}$), 110.07 (C-7$_{Quin}$), 120.06 (C-5$_{Quin}$), 121.92 (C-3$_{Quin}$), 125.37 (C-5$_{Triaz}$), 126.83 (C-6$_{Quin}$), 129.11 (C-4a$_{Quin}$), 135.89 (C-4$_{Quin}$), 139.71 (C-8a$_{Quin}$), 142.31 (C-4$_{Triaz}$), 149.03 (C-2$_{Quin}$), 153.88 (C-8$_{Quin}$); HRMS (ESI-TOF): calcd for C$_{20}$H$_{25}$N$_4$O$_6$S ([M + H]$^+$): *m/z* 449.1495; found: *m/z* 449.1494.

Glycoconjugate **57**: *Starting from sugar derivative* **21** *and 8-HQ derivative* **40**, *the product was obtained as a brown solid (87% yield)*, m.p.: 91–95 °C; [α]^{23}$_D$ = 5.0 (c = 1.0, CH$_3$OH); ^{1}H NMR (400 MHz, DMSO): δ 2.63 (s, 3H, CH$_3$), 2.98–3.23 (m, 6H, H-2$_{Glu}$, H-3$_{Glu}$, H-4$_{Glu}$ H-5$_{Glu}$, CH$_2$S), 3.44 (m, 1H, 6a$_{Glu}$), 3.72 (m, 1H, 6b$_{Glu}$), 4.38 (d, 1H, *J* = 9.6 Hz, H-1$_{Glu}$), 4.55–4.73 (m, 3H, CH$_2$N$_3$, 6-OH), 4.95 (d, 1H, *J* = 5.3 Hz, OH), 5.03 (d, 1H, *J* = 4.8 Hz, OH), 5.20 (d, 1H, *J* = 5.8 Hz, OH), 5.35 (s, 2H, CH$_2$O), 7.37 (dd, 1H, *J* = 1.7 Hz, *J* = 8.1 Hz, H-7$_{Quin}$), 7.39–7.44 (m, 2H, H-3$_{Quin}$, H-6$_{Quin}$), 7.47 (dd, 1H, *J* = 1.7 Hz, *J* = 7.4 Hz, H-5$_{Quin}$), 8.19 (d, 1H, *J* = 8.4 Hz, H-4$_{Quin}$), 8.33 (s, 1H, H-5$_{Triaz}$); ^{13}C NMR (100 MHz, DMSO): δ 24.83 (CH$_3$), 29.70 (CH$_2$S), 49.82 (CH$_2$N), 61.19, 61.68 (C-6$_{Glu}$, CH$_2$O), 69.96, 72.85, 78.01, 80.91 (C-2$_{Glu}$, C-3$_{Glu}$, C-4$_{Glu}$, C-5$_{Glu}$), 85.30 (C-1$_{Glu}$), 110.21 (C-7$_{Quin}$), 119.74 (C-5$_{Quin}$), 122.36 (C-3$_{Quin}$), 125.34 (C-5$_{Triaz}$), 125.57 (C-6$_{Quin}$), 127.24 (C-4a$_{Quin}$), 135.88 (C-4$_{Quin}$), 139.10 (C-8a$_{Quin}$), 142.21 (C-4$_{Triaz}$), 153.28 (C-2$_{Quin}$), 157.16 (C-8$_{Quin}$); HRMS (ESI-TOF): calcd for C$_{21}$H$_{27}$N$_4$O$_6$S ([M + H]$^+$): *m/z* 463.1651; found: *m/z* 463.1651.

Glycoconjugate **58**: *Starting from sugar derivative* **22** *and 8-HQ derivative* **40**, *the product was obtained as a brown solid (88% yield)*, m.p.: 83–87 °C; [α]^{23}$_D$ = 10.2 (c = 1.0, CH$_3$OH); ^{1}H NMR (400 MHz, DMSO): δ 2.63 (s, 3H, CH$_3$), 3.05 (m, 1H, CHS), 3.18 (m, 1H, CHS), 3.28 (m, 1H, H-3$_{Gal}$), 3.36–3.46 (m, 2H, H-2$_{Gal}$, H-5$_{Gal}$), 3.48–3.58 (m, 2H, 6a$_{Gal}$, 6b$_{Gal}$), 3.68 (m, 1H, H-4$_{Gal}$), 4.30 (d, 1H, *J* = 9.5 Hz, H-1$_{Gal}$), 4.47 (d, 1H, *J* = 4.6 Hz, OH), 4.57–4.72 (m, 3H, CH$_2$N$_3$, 6-OH), 4.86 (d, 1H, *J* = 5.6 Hz, OH), 5.09 (d, 1H, *J* = 5.8 Hz, OH), 5.34 (s, 2H, CH$_2$O), 7.37 (dd, 1H, *J* = 1.8 Hz, *J* = 7.4 Hz, H-7$_{Quin}$), 7.40–7.46 (m, 2H, H-3$_{Quin}$, H-6$_{Quin}$), 7.47 (dd, 1H, *J* = 1.8 Hz, *J* = 8.1 Hz, H-5$_{Quin}$), 8.19 (d, 1H, *J* = 8.4 Hz, H-4$_{Quin}$), 8.33 (s, 1H, H-5$_{Triaz}$); ^{13}C NMR (100 MHz, DMSO): δ 24.97 (CH$_3$), 29.67 (CH$_2$S), 50.01 (CH$_2$N$_3$), 60.77, 61.71 (C-6$_{Gal}$, CH$_2$O), 68.52, 69.60, 74.63, 79.36 (C-2$_{Gal}$, C-3$_{Gal}$, C-4$_{Gal}$, C-5$_{Gal}$), 85.84 (C-1$_{Gal}$), 110.23 (C-7$_{Quin}$), 119.85 (C-5$_{Quin}$), 122.52 (C-3$_{Quin}$), 125.43, 125.72 (C-5$_{Triaz}$, C-6$_{Quin}$), 127.36 (C-4a$_{Quin}$), 136.03 (C-4$_{Quin}$), 139.19 (C-8a$_{Quin}$), 142.34 (C-4$_{Triaz}$), 153.39 (C-2$_{Quin}$), 157.32 (C-8$_{Quin}$); HRMS (ESI-TOF): calcd for C$_{21}$H$_{27}$N$_4$O$_6$S ([M + H]$^+$): *m/z* 463.1651; found: *m/z* 463.1654.

Glycoconjugate **59**: *Starting from sugar derivative* **23** *and 8-HQ derivative* **41**, *the product was obtained as a brown oil (94% yield)*, [α]^{23}$_D$ = 36.8 (c = 1.0, CHCl$_3$); ^{1}H NMR (400 MHz, CDCl$_3$): δ 1.98, 2.00, 2.02, 2.06 (4s, 12H, CH$_3$CO), 2.63 (p, 2H, *J* = 6.3 Hz, CH$_2$), 3.67 (ddd, 1H, *J* = 2.2 Hz, *J* = 4.6 Hz, *J* = 10.0 Hz, H-5$_{Glu}$), 3.85 and 4.05 (qAB, 2H, *J* = 14.3 Hz, CH$_2$S), 4.07 (dd, 1H, *J* = 2.2 Hz, *J* = 12.4 Hz, H-6a$_{Glu}$), 4.20 (dd, 1H, *J* = 4.6 Hz, *J* = 12.4 Hz, H-6b$_{Glu}$), 4.24 (t, 2H, *J* = 5.9 Hz, CH$_2$O), 4.60 (d, 1H, *J* = 10.1 Hz, H-1$_{Glu}$), 4.73 (t, 2H, *J* = 6.7 Hz, CH$_2$N), 5.02 (dd~t, 1H, *J* = 9.3 Hz, *J* = 10.1 Hz, H-2$_{Glu}$), 5.08 (dd~t, 1H, *J* = 9.4 Hz, *J* = 10.0 Hz, H-4$_{Glu}$), 5.19 (dd~t, 1H, *J* = 9.3 Hz, *J* = 9.4 Hz, H-3$_{Glu}$), 7.05 (dd, 1H, *J* = 2.1 Hz, *J* = 6.7 Hz, H-7$_{Quin}$), 7.39–7.52 (m, 3H, H-3$_{Quin}$, H-5$_{Quin}$, H-6$_{Quin}$), 7.67 (s, 1H, H-5$_{Triaz}$), 8.17 (dd, 1H, *J* = 1.6 Hz, *J* = 8.3 Hz, H-4$_{Quin}$), 8.96 (dd, 1H, *J* = 1.6 Hz, *J* = 4.0 Hz, H-2$_{Quin}$); ^{13}C NMR (100 MHz, CDCl$_3$): δ 20.60, 20.62, 20.66, 20.77 (C̲H$_3$CO), 24.39 (CH$_2$), 29.61 (CH$_2$S) 47.28 (CH$_2$N), 61.85 (C-6$_{Glu}$), 65.19 (CH$_2$O), 68.15, 69.89, 73.82, 75.76 (C-2$_{Glu}$, C-3$_{Glu}$, C-4$_{Glu}$, C-5$_{Glu}$), 82.75 (C-1$_{Glu}$), 109.40 (C-7$_{Quin}$), 120.34 (C-5$_{Quin}$), 121.74 (C-3$_{Quin}$), 123.03 (C-5$_{Triaz}$), 126.71 (C-6$_{Quin}$), 129.56 (C-4a$_{Quin}$), 136.08 (C-4$_{Quin}$), 140.30 (C-8a$_{Quin}$), 144.53 (C-4$_{Triaz}$), 149.41 (C-2$_{Quin}$), 154.20 (C-8$_{Quin}$), 169.40, 169.81, 170.14, 170.65 (CH$_3$C̲O); HRMS (ESI-TOF): calcd for C$_{29}$H$_{35}$N$_4$O$_{10}$S ([M + H]$^+$): *m/z* 631.2074; found: *m/z* 631.2070.

Glycoconjugate **60**: *Starting from sugar derivative* **24** *and 8-HQ derivative* **41**, *the product was obtained as a beige solid (79% yield)*, m.p.: 56–58 °C; $[\alpha]^{25}_{D}$ = −27.0 (c = 1.0, CHCl$_3$); ^{1}H NMR (400 MHz, CDCl$_3$): δ 1.97, 1.99, 2.02, 2.14 (4s, 12H, CH$_3$CO), 2.63 (p, 2H, *J* = 6.3 Hz, CH$_2$), 3.80 (m, 1H, H-5$_{Gal}$), 3.88 and 4.07 (qAB, 2H, *J* = 14.2 Hz, CH$_2$S), 3.96–4.07 (m, 2H, CH$_2$O), 4.16–4.31 (m, 2H, H-6a$_{Gal}$, H-6b$_{Gal}$), 4.55 (d, 1H, *J* = 10.0 Hz, H-1$_{Gal}$), 4.73 (t, 2H, *J* = 6.7 Hz, CH$_2$N), 5.00 (dd~t, 1H, *J* = 3.4 Hz, *J* = 10.0 Hz, H-3$_{Gal}$), 5.22 (dd~t, 1H, *J* = 10.0 Hz, *J* = 10.0 Hz, H-2$_{Gal}$), 5.38 (d, 1H, *J* = 2.9 Hz, H-4$_{Gal}$), 7.06 (dd, 1H, *J* = 1.6 Hz, *J* = 7.0 Hz, H-7$_{Quin}$), 7.40–7.51 (m, 3H, H-3$_{Quin}$, H-5$_{Quin}$, H-6$_{Quin}$), 7.66 (s, 1H, H-5$_{Triaz}$), 8.16 (dd, 1H, *J* = 1.5 Hz, *J* = 8.3 Hz, H-4$_{Quin}$), 8.96 (dd, 1H, *J* = 1.4 Hz, *J* = 4.0 Hz, H-2$_{Quin}$); ^{13}C NMR (100 MHz, CDCl$_3$): δ 20.58, 20.67, 20.69, 20.74 (CH$_3$CO), 24.24 (CH$_2$), 29.65 (CH$_2$S) 47.25 (CH$_2$N), 61.42 (C-6$_{Gal}$), 65.19 (CH$_2$O), 67.30, 71.78, 74.45, 77.23 (C-2$_{Gal}$, C-3$_{Gal}$, C-4$_{Gal}$, C-5$_{Gal}$), 83.04 (C-1$_{Gal}$), 109.44 (C-7$_{Quin}$), 120.38 (C-5$_{Quin}$), 121.77 (C-3$_{Quin}$), 123.04 (C-5$_{Triaz}$), 126.74 (C-6$_{Quin}$), 129.59 (C-4a$_{Quin}$), 136.06 (C-4$_{Quin}$), 140.35 (C-8a$_{Quin}$), 144.38 (C-4$_{Triaz}$), 149.43 (C-2$_{Quin}$), 154.26 (C-8$_{Quin}$), 169.58, 169.97, 170.21, 170.31 (CH$_3$CO); HRMS (ESI-TOF): calcd for C$_{29}$H$_{35}$N$_4$O$_{10}$S ([M + H]$^+$): *m/z* 631.2074; found: *m/z* 631.2076.

Glycoconjugate **61**: *Starting from sugar derivative* **23** *and 8-HQ derivative* **42**, *the product was obtained as a brown solid (77% yield)*, m.p.: 48–49 °C; $[\alpha]^{23}_{D}$ = 36.0 (c = 1.0, CHCl$_3$); ^{1}H NMR (400 MHz, CDCl$_3$): δ 1.97, 2.00, 2.02, 2.06 (4s, 12H, CH$_3$CO), 2.56 (p, 2H, *J* = 6.3 Hz, CH$_2$), 2.79 (s, 3H, CH$_3$), 3.65 (ddd, 1H, *J* = 2.1 Hz, *J* = 4.5 Hz, *J* = 10.0 Hz, H-5$_{Glu}$), 3.85 and 4.05 (qAB, 2H, *J* = 14.3 Hz, CH$_2$S), 4.06 (dd, 1H, *J* = 2.1 Hz, *J* = 12.4 Hz, H-6a$_{Glu}$), 4.19 (dd, 1H, *J* = 4.5 Hz, *J* = 12.4 Hz, H-6b$_{Glu}$), 4.24 (t, 2H, *J* = 5.4 Hz, CH$_2$O), 4.60 (d, 1H, *J* = 10.1 Hz, H-1$_{Glu}$), 4.74 (t, 2H, *J* = 6.7 Hz, CH$_2$N), 5.01 (dd~t, 1H, *J* = 9.3 Hz, *J* = 10.1 Hz, H-2$_{Glu}$), 5.08 (dd~t, 1H, *J* = 9.4 Hz, *J* = 10.0 Hz, H-4$_{Glu}$), 5.18 (dd~t, 1H, *J* = 9.3 Hz, *J* = 9.4 Hz, H-3$_{Glu}$), 7.04 (dd, 1H, *J* = 2.8 Hz, *J* = 6.1 Hz, H-7$_{Quin}$), 7.30–7.43 (m, 3H, H-3$_{Quin}$, H-5$_{Quin}$, H-6$_{Quin}$), 7.74 (s, 1H, H-5$_{Triaz}$), 8.04 (d, 1H, *J* = 8.4 Hz, H-4$_{Quin}$); ^{13}C NMR (100 MHz, CDCl$_3$): δ 20.60, 20.61, 20.65, 20.77 (CH$_3$CO), 24.42 (CH$_2$), 25.75 (CH$_3$), 29.63 (CH$_2$S) 47.20 (CH$_2$N), 61.84 (C-6$_{Glu}$), 65.34 (CH$_2$O), 68.14, 69.91, 73.83, 75.72 (C-2$_{Glu}$, C-3$_{Glu}$, C-4$_{Glu}$, C-5$_{Glu}$), 82.74 (C-1$_{Glu}$), 110.06 (C-7$_{Quin}$), 120.32 (C-5$_{Quin}$), 122.63 (C-3$_{Quin}$), 123.08 (C-5$_{Triaz}$), 125.70 (C-6$_{Quin}$), 127.76 (C-4a$_{Quin}$), 136.19 (C-4$_{Quin}$), 139.91 (C-8a$_{Quin}$), 144.47 (C-4$_{Triaz}$), 153.64 (C-2$_{Quin}$), 158.23 (C-8$_{Quin}$), 169.40, 169.77, 170.14, 170.65 (CH$_3$CO); HRMS (ESI-TOF): calcd for C$_{30}$H$_{37}$N$_4$O$_{10}$S ([M + H]$^+$): *m/z* 645.2230; found: *m/z* 645.2233.

Glycoconjugate **62**: *Starting from sugar derivative* **24** *and 8-HQ derivative* **42**, *the product was obtained as a beige solid (80% yield)*, m.p.: 56–58 °C; $[\alpha]^{24}_{D}$ = −26.0 (c = 1.0, CHCl$_3$); ^{1}H NMR (400 MHz, CDCl$_3$): δ 1.97, 1.98, 2.02, 2.14 (4s, 12H, CH$_3$CO), 2.60 (p, 2H, *J* = 6.3 Hz, CH$_2$), 2.79 (s, 3H, CH$_3$), 3.78 (m, 1H, H-5$_{Gal}$), 3.88 and 4.07 (qAB, 2H, *J* = 14.1 Hz, CH$_2$S), 3.96–4.10 (m, 2H, CH$_2$O), 4.15–4.31 (m, 2H, H-6a$_{Gal}$, H-6b$_{Gal}$), 4.54 (d, 1H, *J* = 10.0 Hz, H-1$_{Gal}$), 4.75 (t, 2H, *J* = 6.7 Hz, CH$_2$N), 5.00 (dd~t, 1H, *J* = 3.2 Hz, *J* = 10.0 Hz, H-3$_{Gal}$), 5.22 (dd~t, 1H, *J* = 10.0 Hz, *J* = 10.0 Hz, H-2$_{Gal}$), 5.37 (d, 1H, *J* = 3.2 Hz, H-4$_{Gal}$), 7.04 (m, 1H, H-7$_{Quin}$), 7.33 (d, 1H, *J* = 8.4 Hz, H-3$_{Quin}$), 7.36–7.43 (m, 2H, H-5$_{Quin}$, H-6$_{Quin}$), 7.72 (s, 1H, H-5$_{Triaz}$), 8.04 (d, 1H, *J* = 8.4 Hz, H-4$_{Quin}$); ^{13}C NMR (100 MHz, CDCl$_3$): δ 20.58, 20.62, 20.68, 20.74 (CH$_3$CO), 24.26 (CH$_2$), 25.70 (CH$_3$), 29.67 (CH$_2$S) 47.18 (CH$_2$N), 61.41 (C-6$_{Gal}$), 65.32 (CH$_2$O), 67.30, 67.32, 71.78, 74.42 (C-2$_{Gal}$, C-3$_{Gal}$, C-4$_{Gal}$, C-5$_{Gal}$), 83.02 (C-1$_{Gal}$), 110.07 (C-7$_{Quin}$), 120.34 (C-5$_{Quin}$), 122.65 (C-3$_{Quin}$), 123.07 (C-5$_{Triaz}$), 125.73 (C-6$_{Quin}$), 127.80 (C-4a$_{Quin}$), 136.20 (C-4$_{Quin}$), 139.93 (C-8a$_{Quin}$), 144.31 (C-4$_{Triaz}$), 153.70 (C-2$_{Quin}$), 158.25 (C-8$_{Quin}$), 169.58, 169.97, 170.22, 170.30 (CH$_3$CO); HRMS (ESI-TOF): calcd for C$_{30}$H$_{37}$N$_4$O$_{10}$S ([M + H]$^+$): *m/z* 645.2230; found: *m/z* 645.2233.

Glycoconjugate **63**: *Starting from sugar derivative* **25** *and 8-HQ derivative* **41**, *the product was obtained as a beige solid (81% yield)*, m.p.: 59–62 °C; $[\alpha]^{25}_{D}$ = −51.0 (c = 1.0, CH$_3$OH); ^{1}H NMR (400 MHz, DMSO): δ 2.41 (p, 2H, *J* = 6.5 Hz, CH$_2$), 3.02–3.10 (m, 2H, H-3$_{Glu}$, H-5$_{Glu}$), 3.11–3.19 (m, 2H, H-2$_{Glu}$, H-6a$_{Glu}$), 3.45 (m, 1H, H-6b$_{Glu}$), 3.73 (m, 1H, H-4$_{Glu}$), 3.85 and 3.98 (qAB, 2H, *J* = 14.2, CH$_2$S), 4.19 (t, 2H, *J* = 6.1 Hz CH$_2$O), 4.27 (d, 1H, *J* = 9.6 Hz, H-1$_{Glu}$), 4.61 (t, 2H, *J* = 7.0 Hz, CH$_2$N), 4.75 (t, 1H, *J* = 5.7 Hz, 6-OH), 4.97 (d, 1H, *J* = 5.3 Hz, OH), 5.00 (d, 1H, *J* = 4.9 Hz, OH), 5.17 (d, 1H, *J* = 5.9 Hz, OH), 7.20 (dd, 1H, *J* = 1.8 Hz, *J* = 7.1 Hz, H-7$_{Quin}$), 7.48–7.54 (m, 2H, H-5$_{Quin}$, H-6$_{Quin}$), 7.59 (dd, 1H, *J* = 4.1 Hz, *J* = 8.3 Hz, H-3$_{Quin}$), 8.20 (s, 1H, H-5$_{Triaz}$), 8.33 (dd, 1H, *J* = 1.7 Hz, *J* = 8.3 Hz, H-4$_{Quin}$), 8.90 (dd, 1H, *J* = 1.7 Hz, *J* = 4.1 Hz, H-2$_{Quin}$); ^{13}C NMR (100 MHz, DMSO): δ 23.16 (CH$_2$), 29.61 (CH$_2$S),

46.59 (CH$_2$N), 61.35 (C-6$_{Glu}$), 65.38 (CH$_2$O), 70.14, 73.08, 78.16, 81.06 (C-2$_{Glu}$, C-3$_{Glu}$, C-4$_{Glu}$, C-5$_{Glu}$), 84.26 (C-1$_{Glu}$), 109.80 (C-7$_{Quin}$), 119.89 (C-5$_{Quin}$), 121.86 (C-3$_{Quin}$), 123.52 (C-5$_{Triaz}$), 126.82 (C-6$_{Quin}$), 129.05 (C-4a$_{Quin}$), 135.85 (C-4$_{Quin}$), 139.72 (C-8a$_{Quin}$), 144.39 (C-4$_{Triaz}$), 149.07 (C-2$_{Quin}$), 154.15 (C-8$_{Quin}$); HRMS (ESI-TOF): calcd for C$_{21}$H$_{27}$N$_4$O$_6$S ([M + H]$^+$): *m/z* 463.1651; found: *m/z* 463.1653.

Glycoconjugate **64**: *Starting from sugar derivative* **26** *and 8-HQ derivative* **41**, *the product was obtained as a white solid (89% yield)*, m.p.: 150–153 °C; [α]^{26}$_D$ = −30.0 (c = 1.0, DMSO); ^{1}H NMR (400 MHz, DMSO): δ 2.42 (p, 2H, *J* = 6.5 Hz, CH$_2$), 3.25 (m, 1H, H-3$_{Gal}$), 3.34–3.46 (m, 2H, H-2$_{Gal}$, H-5$_{Gal}$), 3.45–3.58 (m, 2H, H-6a$_{Gal}$, H-6b$_{Gal}$), 3.65 (m, 1H, H-4$_{Gal}$), 3.84 and 3.96 (qAB, 2H, *J* = 14.1 Hz, CH$_2$S), 4.13–4.24 (m, 2H, CH$_2$O), 4.20 (d, 1H, *J* = 9.5 Hz, H-1$_{Gal}$), 4.42 (d, 1H, *J* = 3.8 Hz, OH), 4.61 (t, 2H, *J* = 7.0 Hz, CH$_2$N), 4.72 (bs, 1H, 6-OH), 4.78 (d, 1H, *J* = 4.4 Hz, OH), 5.00 (d, 1H, *J* = 5.5 Hz, OH), 7.19 (dd, 1H, *J* = 2.2 Hz, *J* = 6.8 Hz, H-7$_{Quin}$), 7.47–7.54 (m, 2H, H-5$_{Quin}$, H-6$_{Quin}$), 7.59 (dd, 1H, *J* = 4.2 Hz, *J* = 8.3 Hz, H-3$_{Quin}$), 8.18 (s, 1H, H-5$_{Triaz}$), 8.32 (dd, 1H, *J* = 1.7 Hz, *J* = 8.3 Hz, H-4$_{Quin}$), 8.90 (dd, 1H, *J* = 1.7 Hz, *J* = 4.2 Hz, H-2$_{Quin}$); ^{13}C NMR (100 MHz, DMSO): δ 23.08 (CH$_2$), 29.59 (CH$_2$S), 46.58 (CH$_2$N), 60.86 (C-6$_{Gal}$), 65.34 (CH$_2$O), 68.60, 69.84, 74.64, 79.38 (C-2$_{Gal}$, C-3$_{Gal}$, C-4$_{Gal}$, C-5$_{Gal}$), 84.70 (C-1$_{Gal}$), 109.78 (C-7$_{Quin}$), 119.90 (C-5$_{Quin}$), 121.87 (C-3$_{Quin}$), 123.53 (C-5$_{Triaz}$), 126.82 (C-6$_{Quin}$), 129.05 (C-4a$_{Quin}$), 135.85 (C-4$_{Quin}$), 139.73 (C-8a$_{Quin}$), 144.41 (C-4$_{Triaz}$), 149.09 (C-2$_{Quin}$), 154.16 (C-8$_{Quin}$); HRMS (ESI-TOF): calcd for C$_{21}$H$_{27}$N$_4$O$_6$S ([M + H]$^+$): *m/z* 463.1651; found: *m/z* 463.1651.

Glycoconjugate **65**: *Starting from sugar derivative* **25** *and 8-HQ derivative* **42**, *the product was obtained as a brown solid (91% yield)*, m.p.: 55–58 °C; [α]^{26}$_D$ = −40.0 (c = 1.0, DMSO); ^{1}H NMR (400 MHz, DMSO): δ 2.40 (p, 2H, *J* = 6.6 Hz, CH$_2$), 2.67 (s, 3H, CH$_3$), 2.99–3.19 (m, 4H, H-2$_{Glu}$, H-3$_{Glu}$, H-4$_{Glu}$, H-5$_{Glu}$), 3.43 (m, 1H, H-6a$_{Glu}$), 3.71 (m, 1H, H-6b$_{Glu}$), 3.84 and 3.98 (qAB, 2H, *J* = 14.1 Hz, CH$_2$S), 4.19 (t, 2H, *J* = 6.2 Hz, CH$_2$O), 4.26 (d, 1H, *J* = 9.6 Hz, H-1$_{Glu}$), 4.61 (t, 2H, *J* = 7.0 Hz, CH$_2$N), 4.69 (t, 1H, *J* = 5.8 Hz, 6-OH), 4.94 (d, 1H, *J* = 5.1 Hz, OH), 5.01 (d, 1H, *J* = 4.7 Hz, OH), 5.15 (d, 1H, *J* = 5.8 Hz, OH), 7.15 (dd, 1H, *J* = 1.3 Hz, *J* = 7.5 Hz, H-7$_{Quin}$), 7.38–7.49 (m, 3H, H-3$_{Quin}$, H-5$_{Quin}$, H-6$_{Quin}$), 8.17 (s, 1H, H-5$_{Triaz}$), 8.19 (d, 1H, *J* = 8.4 Hz, H-4$_{Quin}$); ^{13}C NMR (100 MHz, DMSO): δ 23.10 (CH$_2$), 25.07 (CH$_3$), 29.54 (CH$_2$S), 46.58 (CH$_2$N), 61.31 (C-6$_{Glu}$), 65.54 (CH$_2$O), 70.13, 73.09, 78.16, 81.06 (C-2$_{Glu}$, C-3$_{Glu}$, C-4$_{Glu}$, C-5$_{Glu}$), 84.21 (C-1$_{Glu}$), 110.33 (C-7$_{Quin}$), 119.83 (C-5$_{Quin}$), 122.47 (C-3$_{Quin}$), 123.45 (C-5$_{Triaz}$), 125.75 (C-6$_{Quin}$), 127.33 (C-4a$_{Quin}$), 136.00 (C-4$_{Quin}$), 139.31 (C-8a$_{Quin}$), 144.36 (C-4$_{Triaz}$), 153.67 (C-2$_{Quin}$), 157.32 (C-8$_{Quin}$); HRMS (ESI-TOF): calcd for C$_{22}$H$_{29}$N$_4$O$_6$S ([M + H]$^+$): *m/z* 477.1808; found: *m/z* 477.1806.

Glycoconjugate **66**: *Starting from sugar derivative* **26** *and 8-HQ derivative* **42**, *the product was obtained as a beige solid (90% yield)*, m.p.: 83–87 °C; [α]^{23}$_D$ = 10.2 (c = 1.0, DMSO); ^{1}H NMR (400 MHz, DMSO): δ 2.41 (p, 2H, *J* = 6.3 Hz, CH$_2$), 3.43 (s, 3H, CH$_3$), 3.23 (m, 1H, H-3$_{Gal}$), 3.34–3.42 (m, 2H, H-2$_{Gal}$, H-5$_{Gal}$), 3.43–3.58 (m, 2H, H-6a$_{Gal}$, H-6b$_{Gal}$), 3.65 (m, 1H, H-4$_{Gal}$), 3.83 and 3.96 (qAB, 2H, *J* = 14.1 Hz, CH$_2$S), 4.12–4.24 (m, 2H, CH$_2$O), 4.19 (d, 1H, *J* = 9.4 Hz, H-1$_{Gal}$), 4.41 (d, 1H, *J* = 4.0 Hz, OH), 4.61 (t, 2H, *J* = 7.0 Hz, CH$_2$N), 4.68 (bs, 1H, 6-OH), 4.77 (d, 1H, *J* = 4.7 Hz, OH), 4.99 (d, 1H, *J* = 5.6 Hz, OH), 7.16 (dd, 1H, *J* = 1.3 Hz, *J* = 7.6 Hz, H-7$_{Quin}$), 7.38–7.45 (m, 2H, H-3$_{Quin}$, H-6$_{Quin}$), 7.47 (dd, 1H, *J* = 1.4 Hz, *J* = 8.2 Hz, H-5$_{Quin}$), 8.16 (s, 1H, H-5$_{Triaz}$), 8.19 (d, 1H, *J* = 8.4 Hz, H-4$_{Quin}$); ^{13}C NMR (100 MHz, DMSO): δ 23.02 (CH$_2$), 25.08 (CH$_3$), 29.52 (CH$_2$S), 46.56 (CH$_2$N), 60.81 (C-6$_{Gal}$), 65.50 (CH$_2$O), 68.57, 69.83, 74.64, 79.36 (C-2$_{Gal}$, C-3$_{Gal}$, C-4$_{Gal}$, C-5$_{Gal}$), 84.65 (C-1$_{Gal}$), 110.31 (C-7$_{Quin}$), 119.83 (C-5$_{Quin}$), 122.47 (C-3$_{Quin}$), 123.43 (C-5$_{Triaz}$), 125.73 (C-6$_{Quin}$), 127.33 (C-4a$_{Quin}$), 135.99 (C-4$_{Quin}$), 139.31 (C-8a$_{Quin}$), 144.37 (C-4$_{Triaz}$), 153.67 (C-2$_{Quin}$), 157.33 (C-8$_{Quin}$); HRMS (ESI-TOF): calcd for C$_{22}$H$_{29}$N$_4$O$_6$S ([M + H]$^+$): *m/z* 477.1808; found: *m/z* 477.1807.

Glycoconjugate **67**: *Starting from sugar derivative* **33** *and 8-HQ derivative* **39**, *the product was obtained as a brown solid (84% yield)*, m.p.: 114–115 °C; [α]^{20}$_D$ = −2.2 (c = 1.0, CHCl$_3$); ^{1}H NMR (400 MHz, CDCl$_3$): δ 1.97, 2.00, 2.00, 2.02 (4s, 12H, CH$_3$CO), 3.80 (ddd, 1H, *J* = 2.2 Hz, *J* = 4.4 Hz, *J* = 10.1 Hz, H-5$_{Glu}$), 4.07 (dd, 1H, *J* = 2.2 Hz, *J* = 12.4 Hz, H-6a$_{Glu}$), 4.22 (dd, 1H, *J* = 4.4 Hz, *J* = 12.4 Hz, H-6b$_{Glu}$), 5.05–5.20 (m, 4H, H-2$_{Glu}$, H-4$_{Glu}$, CH$_2$O), 5.29 (dd~t, 1H, *J* = 9.3 Hz, *J* = 9.3 Hz, H-3$_{Glu}$), 5.40 (s, 2H, CH$_2$O), 5.59 (d, 1H, *J* = 10.4 Hz, H-1$_{Glu}$), 6.89 (d, 1H, *J* = 8.4 Hz, H-3$_{Pyr}$), 7.34 (d, 1H, *J* = 6.6 Hz, H-7$_{Quin}$), 7.44–7.59

(m, 3H, H-3$_{Quin}$, H-5$_{Quin}$, H-6$_{Quin}$), 7.76 (d, 1H, *J* = 8.4 Hz, H-4$_{Pyr}$), 7.97 (s, 1H, H-5$_{Triaz}$), 8.25 (d, 1H, *J* = 7.7 Hz, H-4$_{Quin}$), 8.41 (s, 1H, H-6$_{Pyr}$), 8.84 (bs, 1H, H-2$_{Quin}$), 10.84 (bs, 1H, NH); ^{13}C NMR (100 MHz, CDCl$_3$): δ 20.60, 20.62, 20.71, 20.71 (C̲H$_3$CO), 52.80 (CH$_2$N), 61. 87, 62.04 (CH$_2$O, C-6$_{Glu}$), 68.20, 69.47, 74.11, 75.83 (C-2$_{Glu}$, C-3$_{Glu}$, C-4$_{Glu}$, C-5$_{Glu}$), 82.22 (C-1$_{Glu}$), 109.56 (C-7$_{Quin}$), 120.45 (C-5$_{Quin}$), 122.10 (C-3$_{Quin}$), 123.27 (C-5$_{Triaz}$), 125.92 (C$_{Pyr}$), 127.29 (C$_{Pyr}$), 128.09 (C-6$_{Quin}$), 129.73 (C-4a$_{Quin}$), 132.80 (C-7$_{Quin}$), 136.99 (C-4$_{Quin}$), 139.54 (C-7$_{Quin}$), 141.30 (C-8a$_{Quin}$), 142.92 (C-4$_{Triaz}$), 148.63 (C-7$_{Quin}$), 149.61 (C-2$_{Quin}$), 153.69 (C-8$_{Quin}$), 163.96 (C=O), 169.44, 169.53, 170.11, 170.65 (CH$_3$C̲O); HRMS (ESI-TOF): calcd for C$_{33}$H$_{35}$N$_6$O$_{11}$S ([M + H]$^+$): *m/z* 732.2085; found: *m/z* 732.2084.

*Glycoconjugate **68***: *Starting from sugar derivative **34** and 8-HQ derivative **39**, the product was obtained as a beige solid (83% yield)*, m.p.: 128–129 °C; [α]^{21}$_D$ = 9.6 (c = 1.0, CHCl$_3$); ^{1}H NMR (400 MHz, CDCl$_3$): δ 1.94, 1.98, 2,01, 2.15 (4s, 12H, CH$_3$CO), 4.01 (m, 1H, H-5$_{Gal}$), 4.05–4.10 (m, 2H, H-6a$_{Gal}$, H-6b$_{Gal}$), 5.11 (s, 2H, CH$_2$O), 5.14 (dd, 1H, *J* = 3.4 Hz, *J* = 10.1 Hz, H-3$_{Gal}$), 5.36 (dd~t, 1H, *J* = 10.1 Hz, *J* = 10.2 Hz, H-2$_{Gal}$), 5.40 (s, 2H, CH$_2$N), 5.45 (dd, 1H, *J* = 0.7 Hz, *J* = 3.4 Hz, H-4$_{Gal}$), 5.58 (d, 1H, *J* = 10.2 Hz, H-1$_{Gal}$), 7.00 (d, 1H, *J* = 8.7 Hz, H-3$_{Pyr}$), 7.33 (d, 1H, *J* = 7.4 Hz, H-7$_{Quin}$), 7.44–7.58 (m, 3H, H-3$_{Quin}$, H-5$_{Quin}$, H-6$_{Quin}$), 7.81 (dd, 1H, *J* = 2.3 Hz, *J* = 8.7 Hz, H-4$_{Pyr}$), 7.97 (s, 1H, H-5$_{Triaz}$), 8.24 (d, 1H, *J* = 8.3 Hz, H-4$_{Quin}$), 8.43 (d, 1H, *J* = 1.9 Hz, H-6$_{Pyr}$), 8.32 (d, 1H, *J* = 3.0 Hz, H-2$_{Quin}$), 10.77 (bs, 1H, NH); ^{13}C NMR (100 MHz, CDCl$_3$): δ 20.60, 20.64, 20.68, 20.80 (C̲H$_3$CO), 52.83 (CH$_2$N), 61. 23, 62.07 (CH$_2$O, C-6$_{Gal}$), 66.84, 67.29, 72.04, 74.46 (C-2$_{Gal}$, C-3$_{Gal}$, C-4$_{Gal}$, C-5$_{Gal}$), 82.75 (C-1$_{Gal}$), 109.57 (C-7$_{Quin}$), 120.49 (C-5$_{Quin}$), 122.08 (C-3$_{Quin}$), 123.29 (C-5$_{Triaz}$), 125.85 (C$_{Pyr}$), 127.24 (C$_{Pyr}$), 128.21 (C-6$_{Quin}$), 129.73 (C-4a$_{Quin}$), 132.76 (C-7$_{Quin}$), 136.96 (C-4$_{Quin}$), 139.55 (C-7$_{Quin}$), 141.36 (C-8a$_{Quin}$), 143.02 (C-4$_{Triaz}$), 148.65 (C-7$_{Quin}$), 149.93 (C-2$_{Quin}$), 153.67 (C-8$_{Quin}$), 163.91 (C=O), 169.72, 169.98, 170.24, 170.33 (CH$_3$C̲O); HRMS (ESI-TOF): calcd for C$_{33}$H$_{35}$N$_6$O$_{11}$S ([M + H]$^+$): *m/z* 723.2085; found: *m/z* 723.2086.

*Glycoconjugate **69***: *Starting from sugar derivative **35** and 8-HQ derivative **39**, the product was obtained as a brown solid (77% yield)*, m.p.: 143–144 °C; [α]^{22}$_D$ = −24.0 (c = 0.5, H$_2$O); ^{1}H NMR (400 MHz, DMSO): δ 3.13 (m, 1H, H-2$_{Glu}$), 3.21–3.29 (m, 2H, H-3$_{Glu}$, H-4$_{Glu}$), 3.37–3.50 (m, 2H, H-6a$_{Glu}$, H-6b$_{Glu}$), 3.66 (m, 1H, H-5$_{Glu}$), 4.51 (t, 1H, *J* = 5.7 Hz, 6-OH), 5.00 (d, 1H, *J* = 5.3 Hz, OH), 5.07 (d, 1H, *J* = 9.9 Hz, H-1$_{Glu}$), 5.13 (d, 1H, *J* = 4.9 Hz, OH), 5.36 (d, 1H, *J* = 6.1 Hz, OH), 5.39 (t, 2H, *J* = 6.0 Hz, CH$_2$O), 5.42 (t, 2H, *J* = 6.9 Hz, CH$_2$N), 7.40 (d, 1H, *J* = 8.6 Hz, H-3$_{Pyr}$), 7.44 (dd, 1H, *J* = 4.4 Hz, *J* = 8.9 Hz, H-7$_{Quin}$), 7.50–7.58 (m, 3H, H-3$_{Quin}$, H-5$_{Quin}$, H-6$_{Quin}$), 7.92 (dd, 1H, *J* = 2.6 Hz, *J* = 8.6 Hz, H-4$_{Pyr}$), 8.32 (dd, 1H, *J* = 1.8 Hz, *J* = 8.3 Hz, H-4$_{Quin}$), 8.35 (s, 1H, H-5$_{Triaz}$), 8.63 (d, 1H, *J* = 2.6 Hz, H-6$_{Pyr}$), 8.84 (dd, 1H, *J* = 1.7 Hz, *J* = 4.1 Hz, H-2$_{Quin}$), 10.73 (s, 1H, NH); ^{13}C NMR (100 MHz, DMSO): δ 52.10 (CH$_2$N), 60. 83, 61.77 (CH$_2$O, C-6$_{Glu}$), 69.71, 72.39, 78.28, 81.05 (C-2$_{Glu}$, C-3$_{Glu}$, C-4$_{Glu}$, C-5$_{Glu}$), 84.60 (C-1$_{Glu}$), 109.94 (C-7$_{Quin}$), 119.98 (C-5$_{Quin}$), 121.85 (C-3$_{Quin}$), 122.17 (C-5$_{Triaz}$), 126.51 (C$_{Pyr}$), 126.74 (C$_{Pyr}$), 127.76 (C-6$_{Quin}$), 129.06 (C-4a$_{Quin}$), 132.35 (C-7$_{Quin}$), 135.77 (C-4$_{Quin}$), 139.73 (C-7$_{Quin}$), 140.29 (C-8a$_{Quin}$), 142.49 (C-4$_{Triaz}$), 148.98 (C-7$_{Quin}$), 152.52 (C-2$_{Quin}$), 153.87 (C-8$_{Quin}$), 164.69 (C=O); HRMS (ESI-TOF): calcd for C$_{25}$H$_{27}$N$_6$O$_7$S ([M + H]$^+$): *m/z* 555.1662; found: *m/z* 555.1667.

*Glycoconjugate **70***: *Starting from sugar derivative **36** and 8-HQ derivative **41**, the product was obtained as a white solid (72% yield)*, m.p.: 93–95 °C; [α]^{21}$_D$ = −3.0 (c = 1, CHCl$_3$); ^{1}H NMR (400 MHz, DMSO): δ 1.96, 1.97, 1.98, 2.00 (4s, 12H, CH$_3$CO), 2.43 (bs, 2H, CH$_2$), 4.02 (m, 1H, H-5$_{Glu}$), 4.10–4.17 (m, 2H, H-6a$_{Glu}$, H-6b$_{Glu}$), 4.21 (bs, 2H, CH$_2$O), 4.67 (t, 2H, *J* = 6.0 Hz, CH$_2$N), 4.93–5.02 (m, 2H, H-2$_{Glu}$, H-4$_{Glu}$), 5.22 (s, 2H, CH$_2$OCO), 5.41 (dd~t, 1H, *J* = 9.4 Hz, *J* = 9.4 Hz, H-3$_{Glu}$), 5.69 (d, 1H, *J* = 10.3 Hz, H-1$_{Glu}$), 7.21 (d, 1H, *J* = 8.0 Hz, H-7$_{Quin}$), 7.37 (d, 1H, *J* = 8.7 Hz, H-3$_{Pyr}$), 7.50 (dd~t, 1H, *J* = 7.5 Hz, *J* = 8.0 Hz, H-3$_{Quin}$), 7.47–7.64 (m, 2H, H-5$_{Quin}$, H-6$_{Quin}$), 7.83 (dd, 1H, *J* = 2.4 Hz, *J* = 8.7 Hz, H-4$_{Pyr}$), 8.32–8.40 (m, 2H, H-4$_{Quin}$, H-6$_{Pyr}$), 8.54 (s, 1H, H-5$_{Triaz}$), 8.91 (bs, 1H, H-2$_{Quin}$), 10.00 (s, 1H, NH); ^{13}C NMR (100 MHz, DMSO): δ 20.19, 20.24, 20.28, 20.24 (C̲H$_3$CO), 29.51 (CH$_2$), 46.63 (CH$_2$N), 57.63 (C̲H$_2$OCO), 61.73 (C-6$_{Glu}$), 65.36 (CH$_2$O), 67.94, 69.33, 72.91, 74.41 (C-2$_{Glu}$, C-3$_{Glu}$, C-4$_{Glu}$, C-5$_{Glu}$), 81.26 (C-1$_{Glu}$), 109.82 (C-7$_{Quin}$), 119.92 (C-5$_{Quin}$), 121.81 (C-3$_{Quin}$), 123.05 (C-5$_{Triaz}$), 125.00 (C$_{Pyr}$), 126.60 (C$_{Pyr}$), 126.78 (C-6$_{Quin}$), 128.98 (C-4a$_{Quin}$), 133.84 (C$_{Pyr}$), 135.92 (C-4$_{Quin}$), 139.43 (C$_{Pyr}$), 139.68 (C-8a$_{Quin}$), 141.91

(C-4$_{Triaz}$), 148.01 (C$_{Pyr}$), 148.84 (C-2$_{Quin}$), 153.10 (C-8$_{Quin}$), 153.99 (C=O), 168.99, 169.18, 169.38, 169.80 (CH$_3$$\underline{C}$O); HRMS (ESI-TOF): calcd for C$_{35}$H$_{39}$N$_6$O$_{12}$S ([M + H]$^+$): *m/z* 767.2347; found: *m/z* 767.2344.

Glycoconjugate **71***: Starting from sugar derivative* **37** *and 8-HQ derivative* **41***, the product was obtained as a white solid (73% yield),* m.p.: 97–99 °C; [α]$^{21}_D$ = 9.8 (c = 1.0, CHCl$_3$); ^{1}H NMR (400 MHz, DMSO): δ 1.94, 1.95, 2.00, 2.14 (4s, 12H, CH$_3$CO), 2.43 (bs, 2H, CH$_2$), 3.97–4.07 (m, 2H, H-6a$_{Gal}$, H-6b$_{Gal}$), 4.21 (bs, 2H, CH$_2$O), 4.35 (m, 1H, H-5$_{Gal}$), 4.67 (t, 2H, *J* = 6.5 Hz, CH$_2$N), 5.13 (dd~t, 1H, *J* = 9.9 Hz, *J* = 10.2 Hz, H-2$_{Gal}$), 5.22 (s, 2H, CH$_2$OCO), 5.30–5.38 (m, 2H, H-3$_{Gal}$, H-4$_{Gal}$), 5.65 (d, 1H, *J* = 10.2 Hz, H-1$_{Gal}$), 7.21 (d, 1H, *J* = 8.4 Hz, H-7$_{Quin}$), 7.38 (d, 1H, *J* = 8.7 Hz, H-3$_{Pyr}$), 7.50 (dd~t, 1H, *J* = 7.5 Hz, *J* = 8.1 Hz, H-3$_{Quin}$), 7.50–7.65 (m, 2H, H-5$_{Quin}$, H-6$_{Quin}$), 7.84 (dd, 1H, *J* = 2.4 Hz, *J* = 8.7 Hz, H-4$_{Pyr}$), 8.32–8.40 (m, 2H, H-4$_{Quin}$, H-6$_{Pyr}$), 8.54 (s, 1H, H-5$_{Triaz}$), 8.90 (bs, 1H, H-2$_{Quin}$), 10.00 (s, 1H, NH); ^{13}C NMR (100 MHz, DMSO): δ 20.33, 20.39, 20.41, 20.43 ($\underline{C}$H$_3$CO), 29.60 (CH$_2$), 46.72 (CH$_2$N), 57.72 ($\underline{C}$H$_2$OCO), 61.51 (C-6$_{Gal}$), 65.44 (CH$_2$O), 66.80, 67.55, 71.01, 73.66 (C-2$_{Gal}$, C-3$_{Gal}$, C-4$_{Gal}$, C-5$_{Gal}$), 81.77 (C-1$_{Gal}$), 109.89 (C-7$_{Quin}$), 120.00 (C-5$_{Quin}$), 121.91 (C-3$_{Quin}$), 123.04 (C-5$_{Triaz}$), 125.08 (C$_{Pyr}$), 126.67 (C$_{Pyr}$), 126.85 (C-6$_{Quin}$), 129.08 (C-4a$_{Quin}$), 133.87 (C$_{Pyr}$), 135.95 (C-4$_{Quin}$), 139.36 (C$_{Pyr}$), 139.78 (C-8a$_{Quin}$), 142.00 (C-4$_{Triaz}$), 148.29 (C$_{Pyr}$), 148.90 (C-2$_{Quin}$), 153.19 (C-8$_{Quin}$), 154.18 (C=O), 169.31, 169.39, 169.75, 169.94 (CH$_3$$\underline{C}$O); HRMS (ESI-TOF): calcd for C$_{35}$H$_{39}$N$_6$O$_{12}$S ([M + H]$^+$): *m/z* 767.2347; found: *m/z* 767.2345.

Glycoconjugate **72***: Starting from sugar derivative* **38** *and 8-HQ derivative* **41***, the product was obtained as a white solid (78% yield),* m.p.: 152–154 °C; [α]$^{22}_D$ = −36.0 (c = 1.0, CH$_3$OH); ^{1}H NMR (400 MHz, DMSO): δ 2.43 (p, 2H, *J* = 6.3 Hz, CH$_2$),3.09–3.19 (m, 2H, H-2$_{Glu}$, H-4$_{Glu}$), 3.21–3.29 (m, 2H, H-3$_{Glu}$, H-5$_{Glu}$), 3.44 (m, 1H, H-6a$_{Glu}$), 3.66 (m, 1H, H-6b$_{Glu}$), 4.19 (t, 2H, *J* = 6.0 Hz, CH$_2$O), 4.51 (t, 1H, *J* = 5.7 Hz, 6-OH), 4.67 (t, 2H, *J* = 6.9 Hz, CH$_2$N), 4.99 (d, 1H, *J* = 5.3 Hz, OH), 5.03 (d, 1H, *J* = 9.9 Hz, H-1$_{Glu}$), 5.11 (d, 1H, *J* = 4.8 Hz, OH), 5.21 (s, 2H, CH$_2$OCO), 5.34 (d, 1H, *J* = 6.1 Hz, OH), 7.19 (dd, 1H, *J* = 1.7 Hz, *J* = 7.1 Hz, H-7$_{Quin}$), 7.36 (d, 1H, *J* = 8.7 Hz, H-3$_{Pyr}$), 7.45–7.60 (m, 2H, H-5$_{Quin}$, H-6$_{Quin}$), 7.56 (dd, 1H, *J* = 4.0 Hz, *J* = 8.3 Hz, H-3$_{Quin}$), 7.76 (dd, 1H, *J* = 2.1 Hz, *J* = 8.7 Hz, H-4$_{Pyr}$), 8.32 (dd, 1H, *J* = 1.3 Hz, *J* = 7.0 Hz, H-4$_{Quin}$), 8.37 (s, 1H, H-5$_{Triaz}$), 8.49 (d, 1H, *J* = 2.1 Hz, H-6$_{Pyr}$), 8.89 (bs, 1H, H-2$_{Quin}$), 9.92 (bs, 1H, NH); ^{13}C NMR (100 MHz, DMSO): δ 29.51 (CH$_2$), 46.62 (CH$_2$N), 57.56 ($\underline{C}$H$_2$OCO), 60.76 (C-6$_{Glu}$), 65.32 (CH$_2$O), 69.65, 72.30, 78.20, 80.97 (C-2$_{Glu}$, C-3$_{Glu}$, C-4$_{Glu}$, C-5$_{Glu}$), 84.71 (C-1$_{Glu}$), 109.75 (C-7$_{Quin}$), 119.86 (C-5$_{Quin}$), 121.77 (C-3$_{Quin}$), 122.19 (C-5$_{Triaz}$), 124.99 (C$_{Pyr}$), 126.58 (C$_{Pyr}$), 126.68 (C-6$_{Quin}$), 128.96 (C-4a$_{Quin}$), 132.91 (C-7$_{Quin}$), 135.71 (C-4$_{Quin}$), 139.38 (C-7$_{Quin}$), 139.68 (C-8a$_{Quin}$), 141.96 (C-4$_{Triaz}$), 148.95 (C-7$_{Quin}$), 150.91 (C-2$_{Quin}$), 153.12 (C-8$_{Quin}$), 154.09 (C=O); HRMS (ESI-TOF): calcd for C$_{27}$H$_{31}$N$_6$O$_8$S ([M + H]$^+$): *m/z* 599.1924; found: *m/z* 599.1919.

3.3. Biological Assays

3.3.1. Cell Lines

The human colon adenocarcinoma cell line HCT-116 was obtained from American Type Culture Collection (ATCC, Manassas, VA, USA). The human cell line MCF-7 was obtained from collections at the Maria Sklodowska-Curie Memorial Cancer Center and Institute of Oncology, branch in Gliwice, Poland. The Normal Human Dermal Fibroblasts-Neonatal (NHDF-Neo) was purchased from LONZA (Cat. No. CC-2509, NHDF-Neo, Dermal Fibroblasts, Neonatal, Lonza, Poland). The culture media consisted of RPMI 1640 or DMEM+F12 medium, supplemented with 10% fetal bovine serum and 1% of standard antibiotics (penicillin and streptomycin). The culture media were purchased from EuroClone and HyClone. Fetal bovine serum (FBS) was delivered by EURx, Poland, and Antibiotic Antimycotic Solution (100×) by Sigma-Aldrich, Germany. The cells were cultured under standard conditions at 37 °C in a humidified atmosphere at 5% CO$_2$.

3.3.2. MTT Assay

The viability of the cells was determined using an MTT (3-[4,5–dimethylthiazol-2-yl]-2,5-diphenyltetrazolium bromide) test (Sigma-Aldrich). Stock solutions of tested compounds were prepared

in DMSO and diluted with the appropriate volumes of the growth medium directly before the experiment. The cells were seeded into 96-well plates at concentration 1×10^4 (HCT 116, NHDF-Neo) or 5×10^3 (MCF-7) per well. The cell cultures were incubated for 24 h at 37 °C in a humidified atmosphere of 5% CO_2. Then, the culture medium was removed, replaced with the solution of the tested compounds in medium with varying concentrations, and incubated for further 24 h or 72 h. After that, the medium was removed, and the MTT solution (50 µL, 0.5 mg/mL in PBS) was added. After 3 h of incubation, the MTT solution was removed, and the precipitated formazan was dissolved in DMSO. Finally, the absorbance at the 570 nm wavelength was measured spectrophotometrically with the plate reader. The experiment was conducted in at least three independent iterations with four technical repetitions. The IC_{50} values were calculated using CalcuSyn software (version 2.0, Biosoft, Cambridge, UK).

3.3.3. Influence of Metal Ions on Cellular Proliferation

The cells were seeded into 96-well plates at concentration 1×10^4 (HCT 116, NHDF-Neo) or 5×10^3 (MCF-7) per well. The cell cultures were incubated for 24 h at 37 °C in a humidified atmosphere of 5% CO_2. Then, the culture medium was removed, replaced with the solution of the tested compounds in medium with varying concentrations. Additionally, 100 µM solution of $Cu(CH_3COO)_2$ was added into wells with tested compounds. After 24 h or 72 h incubation, the MTT assay was performed.

4. Conclusions

Glycoconjugation of quinoline derivatives with appropriately functionalized 1-sugar derivatives was supposed to increase the selectivity of such obtained prodrugs in relation to the cancer cells, thanks to the facilitation of its transport through GLUT transporters, whose overexpression is seen in some types of cancer. The cytotoxic activity *in vitro* of the new quinoline glycoconjugates was tested against the MCF-7, HCT-116, and NHDF-Neo cell lines. In order to approximate the mechanism of glycoconjugates transport into the cell, both types of glycoconjugates: Protected in the sugar part and their unprotected counterparts were investigated. Based on the obtained results, it can be stated that only compounds with acetyl protection of hydroxyl groups in the sugar part have the ability to inhibit the proliferation of tumor cells. Thus, lipophilicity has a significant influence on the biological activity of the tested compounds, which can be explained by the facilitation of passive transport through biological membranes into the cells. Derivatives with an unprotected sugar fragment showed low activity, probably due to their high hydrophilicity and low affinity for the cell membrane, as well as the inability to bind to GLUT transporters. It is likely that the functionalization of the anomeric position in sugar and the use of the compounds thus obtained to binding with 8-HQ derivatives reduces the affinity of the sugar residue for GLUT transporters. In this situation, the improvement of the hydrolytic stability of the obtained glycoconjugates by introducing a sulfur atom into the anomeric position of the sugar did not affect their selectivity, but only in some cases (compounds **51**–**54**), increased cytotoxicity compared to their oxygen counterparts. This can be explained by the fact that they were not prematurely degraded before entering the cell, and, as a consequence of facilitated passive transport, their concentration in the cells was higher.

Among the tested compounds, the glycoconjugates **67**–**71** containing an additional heteroaromatic (5-amine-2-pyridyl) moiety in the linker structure turned out to be the most active. For these compounds, the additional experiments of antiproliferative activity in the presence of Cu^{2+} ions were carried out. It was observed that the activity of glycoconjugates increased significantly in the presence of copper compared to cells treated with alone glycoconjugates in the absence of Cu^{2+}. The highest cytotoxicity of the compounds was observed against the MCF-7 cell line. This confirmed the strong sensitivity of breast cancer cells to the presence of copper ions as well as their sensitivity to compounds capable of complexing these ions, such as 8-HQ or sugar derivatives containing 2-thio-5-amino-pyridine moiety. Unfortunately, in the case of the latter, cytotoxicity to non-cancer cells was also observed. In such a case, the research on the dependence of glycoconjugates' cytotoxic activity on their structure should be extended in the direction that allows better matching of glycoconjugates to GLUT transporters, which should improve their selectivity. According to

some literature reports, the 6-OH group is the position in the sugar that is least involved in binding to the GLUT transporter. Perhaps the use of this position for binding with quinoline derivatives will prove effective and allow to increase the selectivity of the obtained glycoconjugates.

References

1. Krishna, R.; Mayer, L.D. Multidrug resistance (MDR) in cancer: Mechanisms, reversal using modulators of MDR and the role of MDR modulators in influencing the pharmacokinetics of anticancer drugs. *Eur. J. Pharm. Sci.* **2000**, *11*, 265–283. [CrossRef]

2. Szachowicz-Petelska, B.; Figaszewski, Z.; Lewandowski, W. Mechanisms of transport across cell membranes of complexes contained in antitumour drugs. *Int. J. Pharm.* **2001**, *222*, 169–182. [CrossRef]

3. Kratz, F.; Müller, I.A.; Ryppa, C.; Warnecke, A. Prodrug Strategies in Anticancer Chemotherapy. *Chem. Med. Chem.* **2008**, *3*, 20–53. [CrossRef] [PubMed]

4. Jang, S.H.; Wientjes, M.G.; Lu, D.; Au, J.L.-S. Drug Delivery and Transport to Solid Tumors. *Pharm. Res.* **2003**, *20*, 1337–1350. [CrossRef]

5. Das, M.; Mohanty, C.; Sahoo, S.K. Ligand-based targeted therapy for cancer tissue. *Expert Opin. Drug Deliv.* **2009**, *6*, 285–304. [CrossRef]

6. Calvaresi, E.C.; Hergenrother, P.J. Glucose conjugation for the specific targeting and treatment of cancer. *Chem. Sci.* **2013**, *4*, 2319–2333. [CrossRef]

7. Tanasova, M.; Fedie, J.R. Molecular Tools for Facilitative Carbohydrate Transporters (Gluts). *ChemBioChem* **2017**, *18*, 1774–1788. [CrossRef]

8. Warburg, O. On the origin of cancer cells. *Science* **1956**, *123*, 309–314. [CrossRef]

9. Vander Heiden, M.G.; Cantley, L.C.; Thompson, C. Understanding the Warburg effect: The metabolic requirements of cell proliferation. *Science* **2009**, *324*, 1029–1033. [CrossRef]

10. Barron, C.C.; Bilan, P.J.; Tsakiridis, T.; Tsiani, E. Facilitative glucose transporters: Implications for cancer detection, prognosis and treatment. *Metabolism* **2016**, *65*, 124–139. [CrossRef]

11. Zhao, F.Q.; Keating, A.F. Functional Properties and Genomics of Glucose Transporters. *Curr. Genom.* **2007**, *8*, 113–128. [CrossRef]

12. Ganapathy, V.; Thangaraju, M.; Prasad, P.D. Nutrient transporters in cancer: Relevance to Warburg hypothesis and beyond. *Pharmacol. Ther.* **2009**, *121*, 29–40. [CrossRef]

13. Barnett, J.E.G.; Holman, G.D.; Munday, K.A. Structural Requirements for Binding to the Sugar-Transport. *Biochem. J.* **1973**, *131*, 211–221. [CrossRef]

14. Ma, J.; Liu, H.; Xi, Z.; Hou, J.; Li, Y.; Niu, J.; Liu, T.; Bi, S.; Wang, X.; Wang, C.; et al. Protected and De-protected Platinum(IV) Glycoconjugates With GLUT1 and OCT2-Mediated Selective Cancer Targeting: Demonstrated Enhanced Transporter-Mediated Cytotoxic Properties in vitro and in vivo. *Front. Chem.* **2018**, *6*, 386. [CrossRef]

15. Zou, T.B.; Feng, D.; Song, G.; Li, H.W.; Tang, H.W.; Ling, W.H. The Role of Sodium-Dependent Glucose Transporter 1 and Glucose Transporter 2 in the Absorption of Cyanidin-3-*O*-β-Glucoside in Caco-2 Cells. *Nutrients* **2014**, *6*, 4165–4177. [CrossRef]

16. Prachayasittikul, V.; Prachayasittikul, S.; Ruchirawat, S.; Prachayasittikul, V. 8-Hydroxyquinolines: A review of their metal chelating properties and medicinal applications. *Drug Des. Dev. Ther.* **2013**, *7*, 1157–1178. [CrossRef]

17. Savić-Gajić, I.M.; Savić, I.M. Drug design strategies with metal-hydroxyquinoline complexes. *Expert Opin. Drug Deliv.* **2020**, *15*, 383–390. [CrossRef]

18. Chen, J.; Jiang, Y.; Shi, H.; Peng, Y.; Fan, X.; Li, C. The molecular mechanisms of copper metabolism and its roles in human diseases. *Pflüg. Arch. Eur. J. Phy.* **2020**. [CrossRef]

19. Denoyer, D.; Masaldan, S.; La Fontaine, S.; Cater, M.A. Targeting copper in cancer therapy: 'Copper That Cancer'. *Metallomics* **2015**, *7*, 1459–1476. [CrossRef]

20. Grubman, A.; White, A.R. Copper as a key regulator of cell signalling pathways. *Expert Rev. Mol. Med.* **2014**, *16*. [CrossRef]

21. Gaur, K.; Vázquez-Salgado, A.M.; Duran-Camacho, G.; Dominguez-Martinez, I.; Benjamín-Rivera, J.A.; Fernández-Vega, L.; Carmona Sarabia, L.; Cruz García, A.; Pérez-Deliz, F.; Méndez Román, J.A.; et al. Iron and Copper Intracellular Chelation as an Anticancer Drug Strategy. *Inorganics* **2018**, *6*, 126. [CrossRef]

22. Gupte, A.; Mumper, R.J. Elevated copper and oxidative stress in cancer cells as a target for cancer treatment. *Cancer Treat. Rev.* **2009**, *35*, 32–46. [CrossRef] [PubMed]

23. Santini, C.; Pellei, M.; Gandin, V.; Porchia, M.; Tisato, F.; Marzano, C. Advances in copper complexes as anticancer agents. *Chem. Rev.* **2014**, *114*, 815–862. [CrossRef]

24. Song, Y.; Xu, H.; Chen, W.; Zhan, P.; Liu, X. 8-Hydroxyquinoline: A privileged structure with a broad-ranging pharmacological potential. *Med. Chem. Commun.* **2015**, *6*, 61–74. [CrossRef]

25. Oliveri, V.; Vecchio, G. 8-Hydroxyquinolines in medicinal chemistry: A structural perspective. *Eur. J. Med. Chem.* **2016**, *120*, 252–274. [CrossRef]

26. Krawczyk, M.; Pastuch-Gawolek, G.; Mrozek-Wilczkiewicz, A.; Kuczak, M.; Skonieczna, M.; Musiol, R. Synthesis of 8-hydroxyquinoline glycoconjugates and preliminary assay of their β1,4-GalT inhibitory and anti-cancer properties. *Bioorg. Chem.* **2019**, *84*, 326–338. [CrossRef]

27. Krawczyk, M.; Pastuch-Gawołek, G.; Pluta, A.; Erfurt, K.; Domiński, A.; Kurcok, P. 8-Hydroxyquinoline glycoconjugates: Modifications in the linker structure and their effect on the cytotoxicity of the obtained compounds. *Molecules* **2019**, *24*, 4181. [CrossRef]

28. De Leon, C.A.; Levine, P.M.; Craven, T.W.; Pratt, M.R. The sulfur-linked analog of *O*-GlcNAc (S-GlcNAc) is an enzymatically stable and a reasonable structural surrogate for *O*-GlcNAc at the peptide and protein levels. *Biochemistry* **2017**, *56*, 3507–3517. [CrossRef]

29. Cagnoni, A.J.; Kovensky, J.; Uhrig, M.L. Design and Synthesis of Hydrolytically Stable Multivalent Ligands Bearing Thiodigalactoside Analogues for Peanut Lectin and Human Galectin-3 Binding. *J. Org. Chem.* **2014**, *79*, 6456–6467. [CrossRef]

30. Witczak, Z.J.; Culhane, J.M. Thiosugars: New perspectives regarding availability and potential biochemical and medicinal applications. *Appl. Microbiol. Biotechnol.* **2005**, *69*, 237–244. [CrossRef]

31. Ibrahim, N.; Alami, M.; Messaoudi, S. Recent Advances in Transition–Metal–Catalyzed Functionalization of 1–Thiosugars. *Asian J. Org. Chem.* **2018**, *7*, 2026–2038. [CrossRef]

32. Driguez, H. Thiooligosaccharides as Tools for Structural Biology. *ChemBioChem* **2001**, *2*, 311–318. [CrossRef]

33. Castaneda, F.; Burse, A.; Boland, W.; Kinne, R.K.-H. Thioglycosides as inhibitors of hSGLT1 and hSGLT2: Potential therapeutic agents for the control of hyperglycemia in diabetes. *Int. J. Med. Sci.* **2007**, *4*, 131–139. [CrossRef] [PubMed]

34. Korycka-Machała, M.; Brzostek, A.; Dziadek, B.; Kawka, M.; Popławski, T.; Witczak, Z.J.; Dziadek, J. Evaluation of the Mycobactericidal Effect of Thio-functionalized Carbohydrate Derivatives. *Molecules* **2017**, *22*, 812. [CrossRef] [PubMed]

35. Aouad, M.R. Synthesis and Antimicrobial Screening of Novel Thioglycosides and Acyclonucleoside Analogs Carrying 1,2,3-Triazole and 1,3,4-Oxadiazole Moieties. *Nucleos. Nucleot. Nucl.* **2016**, *35*, 1–15. [CrossRef] [PubMed]

36. Metaferia, B.B.; Fetterolf, B.J.; Shazad-ul-Hussan, S.; Moravec, M.; Smith, J.A.; Ray, S.; Gutierrez-Lugo, M.T.; Bewley, C.A. Synthesis of Natural Product-Inspired Inhibitors of Mycobacterium tuberculosis Mycothiol-Associated Enzymes: The First Inhibitors of GlcNAc-Ins Deacetylase. *J. Med. Chem.* **2007**, *50*, 6326–6336. [CrossRef] [PubMed]

37. Jortzik, E.; Farhadi, M.; Ahmadi, R.; Tóth, K.; Lohr, J.; Helmke, B.M.; Kehr, S.; Unterberg, A.; Ott, I.; Gust, R.; et al. Antiglioma activity of GoPI-sugar, a novel gold(I)–phospholeinhibitor: Chemical synthesis, mechanistic studies, and effectiveness in vivo. *Biochim. Biophys. Acta* **2014**, *1844*, 1415–1426. [CrossRef] [PubMed]

38. Pastuch-Gawołek, G.; Malarz, K.; Mrozek-Wilczkiewicz, A.; Musioł, M.; Serda, M.; Czaplińska, B.; Musioł, R. Small molecule glycoconjugates with anticancer activity. *Eur. J. Med. Chem.* **2016**, *112*, 130–144. [CrossRef]

39. Sugai, Y.; Fujii, S.; Fujimoto, T.; Yano, S.; Mikata, Y. Asymmetric sulfur atom coordination in a copper(II) dipicolylamine (DPA) complex with a thioglycoside ligand. *Dalton Trans.* **2007**, 3705–3709. [CrossRef]

40. Yamauchi, O.; Seki, H.; Shoda, T. Copper(II)-sulfur interactions in pyridine- and imidazole-containing disulfide complexes. Syntheses, spectra and solution equilibria. *Bull. Chem. Soc. Jpn.* **1983**, *56*, 3258–3267. [CrossRef]

41. Fulton, D.A.; Stoddart, J.F. Synthesis of Cyclodextrin-Based Carbohydrate Clusters by Photoaddition Reactions. *J. Org. Chem.* **2001**, *66*, 8309–8319. [CrossRef] [PubMed]

42. Zhu, X.; Schmidt, R.R. Glycosylthiomethyl Chloride: A New Species for S-Neoglycoconjugate Synthesis. Synthesis of 1-*N*-Glycosylthiomethyl-1,2,3-triazoles. *J. Org. Chem.* **2004**, *69*, 1081–1085. [CrossRef] [PubMed]

43. Pietrzik, N.; Schips, C.; Ziegler, T. Efficient Synthesis of Glycosylated Asparaginic Acid Building Blocks via Click Chemistry. *Synthesis* **2008**, *4*, 519–526. [CrossRef]

44. Zemplén, G.; Pacsu, E. Über die Verseifung acetylierter Zucker und verwandter Substanzen. *Ber. Dtsch. Chem. Ges.* **1929**, *62*, 1613–1614. [CrossRef]

45. Pastuch-Gawołek, G.; Szeja, W. A facile and efficient synthesis of *S*-glycosylated derivatives of 5-nitropyridine. *Carbohydr. Lett.* **1997**, *2*, 281–286.

46. Wu, Y.; Pan, M.; Dai, Y.; Liu, B.; Cui, J.; Shi, W.; Qiu, Q.; Huang, W.; Qian, H. Design, synthesis and biological evaluation of LBM-A5 derivatives as potent P-glycoprotein-mediated multidrug resistance inhibitors. *Bioorg. Med. Chem.* **2016**, *24*, 2287–2297. [CrossRef]

47. Kolb, H.C.; Finn, M.G.; Sharpless, K.B. Click Chemistry: Diverse Chemical Function from a Few Good Reactions. *Angew. Chem. Int. Ed.* **2001**, *40*, 2004–2021. [CrossRef]

48. Liang, L.; Astruc, D. The copper(I)-catalyzed alkyne-azide cycloaddition (CuAAC) "click" reaction and its applications. An overview. *Coord. Chem. Rev.* **2011**, *255*, 2933–2945. [CrossRef]

49. Haber, R.S.; Rathan, A.; Weiser, K.R.; Pritsker, A.; Itzkowitz, S.H.; Bodian, C.; Slater, G.; Weiss, A.; Burstein, D.E. GLUT1 Glucose Transporter Expression in Colorectal Carcinoma: A marker for poor prognosis. *Cancer* **1998**, *83*, 34–40. [CrossRef]

50. Brown, R.S.; Wahl, R.L. Overexpression of Glut-1 Glucose Transporter in Human Breast Cancer. *Cancer* **1993**, *72*, 2979–2985. [CrossRef]

51. Barbosa, A.M.; Martel, F. Targeting Glucose Transporters for Breast Cancer Therapy: The Effect of Natural and Synthetic Compounds. *Cancers* **2020**, *12*, 154. [CrossRef] [PubMed]

52. Kato, Y.; Ozawa, S.; Miyamoto, C.; Maehata, Y.; Suzuki, A.; Maeda, T.; Baba, Y. Acidic Extracellular Microenvironment and Cancer. *Cancer Cell Int.* **2013**, *13*, 89. [CrossRef] [PubMed]

53. Swietach, P.; Vaughan-Jones, R.D.; Harris, A.L.; Hulikova, A. The chemistry, physiology and pathology of pH in cancer. *Phil. Trans. R. Soc.* **2014**, *369*. [CrossRef] [PubMed]

54. β-Galactosidase from Aspergillus oryzae (G5160)-Enzyme Assay. Available online: https://www.sigmaaldrich.com/content/dam/sigma-aldrich/docs/Sigma/Enzyme_Assay/g5160enz.pdf (accessed on 30 August 2020).

55. Daniel, K.G.; Gupta, P.; Harbach, R.H.; Guida, W.C.; Dou, Q.P. Organic copper complexes as a new class of proteasome inhibitors and apoptosis inducers in human cancer cells. *Biochem. Pharmacol.* **2004**, *67*, 1139–1151. [CrossRef]

56. Milacic, V.; Jiao, P.; Zhang, B.; Yan, B.; Dou, Q.P. Novel 8-hydroxylquinoline analogs induce copper-dependent proteasome inhibition and cell death in human breast cancer cells. *Int. J. Oncol.* **2009**, *35*, 1481–1491. [CrossRef]

Sample Availability: Samples of the compounds **43**–**72** are available from the authors.

Publikacja P.4

Glycoconjugation of Quinoline Derivatives Using the C-6 Position in Sugars as a Strategy for Improving the Selectivity and Cytotoxicity of Functionalized Compounds

M. Domińska[*], G. Pastuch-Gawołek, M. Skonieczna, W. Szeja, A. Domiński, P. Kurcok

Materiały uzupełniające do publikacji znajdują się w dołączonej płycie CD

Article

Glycoconjugation of Quinoline Derivatives Using the C-6 Position in Sugars as a Strategy for Improving the Selectivity and Cytotoxicity of Functionalized Compounds

Monika Domińska [1,2,*], **Gabriela Pastuch-Gawołek** [1,2], **Magdalena Skonieczna** [2,3], **Wiesław Szeja** [1], **Adrian Domiński** [4] **and Piotr Kurcok** [4]

[1] Department of Organic Chemistry, Bioorganic Chemistry and Biotechnology, Silesian University of Technology, B. Krzywoustego 4, 44-100 Gliwice, Poland

[2] Biotechnology Centre, Silesian University of Technology, B. Krzywoustego 8, 44-100 Gliwice, Poland

[3] Department of Systems Biology and Engineering, Faculty of Automatic Control, Electronics and Computer Science, Silesian University of Technology, Akademicka 16, 44-100 Gliwice, Poland

[4] Centre of Polymer and Carbon Materials, Polish Academy of Sciences, M. Curie-Skłodowskiej 34, 41-819 Zabrze, Poland

[*] Correspondence: monika.dominska@polsl.pl; Tel.: +48-32-237-1759

Abstract: Based on the Warburg effect and the increased demand for glucose by tumor cells, a targeted drug delivery strategy was developed. A series of new glycoconjugates with increased ability to interact with GLUT transporters, responsible for the transport of sugars to cancer cells, were synthesized. Glycoconjugation was performed using the C-6 position in the sugar unit, as the least involved in the formation of hydrogen bonds with various aminoacids residues of the transporter. The carbohydrate moiety was connected with the 8-hydroxyquinoline scaffold via a 1,2,3-triazole linker. For the obtained compounds, several in vitro biological tests were performed using HCT-116 and MCF-7 cancer cells as well as NHDF-Neo healthy cells. The highest cytotoxicity of both cancer cell lines in the MTT test was noted for glycoconjugates in which the triazole-quinoline was attached through the triazole nitrogen atom to the D-glucose unit directly to the carbon at the C-6 position. These compounds were more selective than the analogous glycoconjugates formed by the C-1 anomeric position of D-glucose. Experiments with an EDG inhibitor have shown that GLUTs can be involved in the transport of glycoconjugates. The results of apoptosis and cell cycle analyses by flow cytometry confirmed that the new type of glycoconjugates shows pro-apoptotic properties, without significantly affecting changes in the distribution of the cell cycle. Moreover, glycoconjugates were able to decrease the clonogenic potential of cancer cells, inhibit the migration capacity of cells and intercalate with DNA.

Keywords: quinoline glycoconjugates; 1,2,3-triazole; click chemistry; anticancer activity; drug targeting; GLUT transporter; Warburg effect

1. Introduction

Efficacy, as well as safety, are the main criteria influencing the approval of any new drug by regulatory agencies. The latest medicine aims for treatment that is precise and personalized with the needs of each patient, in which drugs will be delivered specifically to diseased cells, but not healthy ones. One of the attractive strategies to increase the efficacy and safety of the treatment is the use of a proven therapeutic agent with the addition of a targeting ligand, which should exhibit low affinity for healthy cells, but high for pathological cells. The efficacy of the formed conjugate is primarily determined by the activity of the drug, while the safety of the conjugate is dependent on the specificity of the targeting ligand to diseased cells. By separating the selectivity and therapeutic activity into two separate parts of the conjugate, it is possible to optimize drug action by avoiding side

damage to healthy tissues [1–5]. The safety profile of a targeted drug is mainly dependent on the expression of a given receptor, and precisely its ratio in diseased and normal tissues. It has been found that at least 3-fold overexpression of the receptors in pathological tissues is usually sufficient to avoid high toxicity for healthy tissues. Receptors in pathological cells can be overexpressed both intracellularly and on the cell surface [1,6–8]. It is preferable, that the ligand targets receptors found mainly on the surface of the diseased cell where they are overexpressed relative to normal cells with low receptor expression, whereas conjugates targeting intracellular receptors must first be well permeable through the cell membrane, which may be associated with low selectivity and systemic toxicity of the drug.

New strategies for the rational design of anticancer drug candidates relate to the improvement of the transport of the active molecule directly into the cancer cell. This is achieved by binding potential drugs to appropriate ligands (sugars, peptides, vitamins, proteins, or antibodies) specific to a given receptor. The ligand-based prodrug then binds to its receptor, which should be present only in the cancer cell or be overexpressed in it. In particular, in recent years, there has been a lot of interest in research involving liposomes, polymer micelles, nanoparticles, dendrimers, monoclonal antibodies, or specialized transmembrane proteins characteristic of the target cells [9–11]. In the design of ligand-targeting drugs in cancer therapy, the focus is on differences in the metabolism of healthy cells and cancer cells. An important difference is the carbohydrate metabolism mechanism described by Warburg [12,13]. Compared to healthy cells, rapidly proliferating tumor cells are characterized by a high rate of the glycolysis process. To provide enough nutrients for this process and to meet their energy demand, cancer cells have an increased need for glucose. Glucose, as the basic source of energy, is actively transported inside the cells by specialized proteins, the so-called GLUT transporters [14,15]. Increased glucose consumption requires overexpression of the GLUT transporters in cancer cells as compared to normal cells [16]. This observation has become an attractive strategy for the controlled delivery of prodrugs obtained by coupling biologically active compounds with sugar derivatives. Due to the high affinity of glycoconjugates for GLUT protein, glycoconjugation can be seen as a system for the selective delivery of anti-cancer drugs [17–19].

The oldest example of a drug actively transported by GLUT proteins is glufosfamide, discovered in 1995 [20]. Since then, numerous clinical trials have been conducted with glufosfamide in the treatment of various types of cancer. It turned out that the glycoconjugate is safer and more selective than its aglycon, and its antiproliferative activity is similar to the original aglycone. Its mechanism of action favors cancers with overexpression of GLUT transporters [21,22]. Following the success of glufosfamide, the glycoconjugation strategy gained popularity. In targeted cancer therapy using GLUT, various glycoconjugates based on molecules such as oxaliplatin [23], chlorambucil [24], paclitaxel [25], adriamycin [26], azomycin [27], methotrexate [28], as well as derivatives of thiosemicarbazone [29] have been designed. Numerous glycoconjugates showed better cancer specificity, reduced systemic toxicity, and increased anticancer activity both in vitro and in vivo.

GLUT1 is one of the most common glucose transporters in the vicinity of neoplastic cells. Encoded by SLC2A1, it can bind to glucose, galactose, mannose, or ascorbic acid and then transport these molecules across membranes into the cell. It has been shown that increased GLUT1 expression appears to be strongly correlated with poor prognosis in many neoplastic diseases [19,30]. However, the ability of GLUT to transport a substrate may be influenced by factors such as the structure of the carbohydrate, the position of its substitution, the type of linkers, and the properties of the aglycons themselves. Recently, the crystalline structure of human GLUT1 has been published [31]. This structure revealed that all hydroxyl groups of D-glucose, except for this at the C-6 position, are involved in the formation of hydrogen bonds with various residues of aminoacids of the transporter. Therefore, modification at the C-6 position of D-glucose should not affect the binding of the receptor to the transporter. The Fernandez group synthesized several glycosyl derivatives of dopamine and tested the affinity of the resulting prodrugs for GLUT1 in human erythrocytes. Dopamine was connected with C-1, C-3, or C-6 positions of D-glucose

using various linkages. The glucose absorption inhibition results showed that derivatives of glucose conjugated at the C-6 position had the best affinity for GLUT1 [32]. It was also found that C-6-glucose conjugates of 4-nitrobenzofurazane, ketoprofen, and indomethacin connect to GLUT1 with even better affinity than unmodified D-glucose. Patra et al. designed glucose-platinum conjugates in which the chelator was connected via the C-6 position of the sugar. They found that the obtained glycoconjugates show a high level of cytotoxicity against a panel of cancer cells, and GLUT transporters are involved in their transport [33].

So far, as part of the research cycle, our team has developed methods of connecting biologically active compounds with derivatives of D-glucose and D-galactose differently functionalized at the anomeric position. Our research focuses on the use of small quinoline derivative molecules as aglycones in potential anti-cancer agents [34–36]. The cytotoxic potential of derivatives of 8-hydroxyquinoline (8HQ) is related to its ability to complex many metal ions [37–39]. It is well known that cancer cells have an increased need for metal ions such as iron, copper, zinc, calcium, etc. As these microelements are involved in major cellular processes, the use of chelators appears to be an ideal way to control the level of metals in the body and is important in developing new treatment strategies [40–42]. However, to be effective, the glycoconjugate must meet several conditions on its way from blood vessels to a molecular target in cancer tissue. It is necessary that attaching the cytotoxic compound to the sugar does not interfere with its receptor binding specificity. Moreover, the linker between the drug and the carrier must be stable in the extracellular space and be easily degraded in target cells after uptake by receptors. Cleavage of the linker should release the unmodified drug inside the neoplastic cells. Additionally, to observe the desired cytotoxicity, sufficient intracellular drug concentration must be achieved. In the project on the targeted transport of prodrugs, we used a fragment of 1,2,3-triazole in the linker structure, a base which, due to the low extracellular pH in cancer cells, will allow for the selective placement of the prodrug in the tumor microenvironment. On the other hand, after protonation, the created cation due to the delocalization of the charge should not constitute a barrier preventing the penetration of the prodrug into the neoplastic cell [43–45].

Based on literature reports and insights gained during the research on the targeted introduction of prodrugs into cancer cells, we designed a series of new compounds to better match GLUT transporters. As part of the structural modification, new glycoconjugates will be formed via the C-6 position in the sugar unit. This approach should allow increasing the selectivity in targeting glycoconjugates to tumor cells, where the units released from the prodrug will be able to induce cytotoxicity. The functionalized at the C-6 position sugar structures planned to be obtained and connected through this position to the 8HQ derivative, the fragment responsible for inducing the cytotoxic effect, are shown in Figure 1. The research includes both the synthesis of glycoconjugates and the assessment of their biological activity in vitro against selected cancer cell lines and healthy cells.
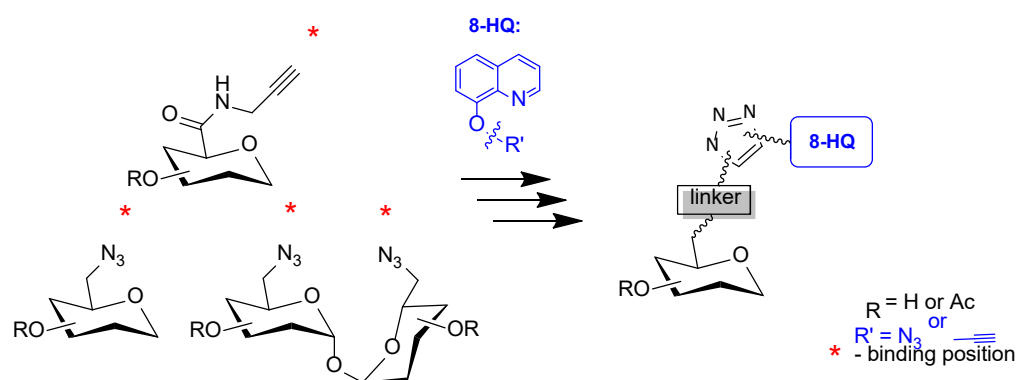
Figure 1. Strategies for the synthesis of quinoline glycoconjugates.

2. Results and Discussion

2.1. Synthesis

As mentioned above, the structure of the molecules presented in this work was designed based on the recently published crystal structure of the human GLUT1 transporter, according to which the least significant group for binding to the receptor is the 6-OH group. Therefore, the group at the C-6 position seems to be the best functional group to which a molecule of the drug could be attached to maintain the affinity of the glucose conjugate for the transporter. Based on assumption that the glycoconjugate will be selectively transferred to the neoplastic cell by GLUT transporters, in the first place, synthetic pathways of several sugar derivatives substituted with different groups at the C-6 position were developed. To accurately determine the route of drug absorption, both compounds with free hydroxyl groups as substrates for binding to GLUT transporters as well as compounds with acetyl protection of hydroxyl groups in the sugar unit were designed. The comparison of the effect of these two groups of compounds will allow determining whether a given compound enters the cell using passive transport (diffusion of the lipophilic compound through cell membranes) or active transport (by GLUT transporters).

In order to obtain 6-azido-6-deoxy-D-glucopyranose, in the first approach reaction of D-glucose with *p*-toluenesulfonyl chloride in pyridine was performed [46]. The reaction was to selectively introduce into the C-6 position the tosyl as a good leaving group. The obtained product can be first treated with an acetylating agent to protect the remaining hydroxyl groups or the tosyl substitution reaction with an azide moiety can be performed right away. Unfortunately, in both approaches, a complicated, difficult to separate product mixture was obtained. Therefore, the synthesis of sugar derivatives functionalized only at the C-6 position requires other, multi-step sequences of reactions shown in Scheme 1. First, the primary hydroxyl group of D-glucose **1** at the C-6 position was selectively protected with a sterically large triphenylmethyl (trityl, Tr) group which was introduced using triphenylmethyl chloride in the presence of a catalytic amount of DMAP [47]. The reaction was carried out in pyridine until the substrate was completely converted to the product as monitored by TLC. The remaining secondary sugar hydroxyl groups were then protected with an acetyl moiety by adding acetyl chloride to the reaction mixture, resulting in the formation of fully protected 1,2,3,4-tetra-*O*-acetyl-6-*O*-triphenylmethyl-D-glucopyranose **2** with 84% yield. In the next step, the trityl protection at C-6 carbon was removed under acidic conditions with 33% HBr in acetic acid, receiving 1,2,3,4-tetra-*O*-acetyl-D-glucopyranose **3** [47]. Then, an easily leaving *p*-toluenesulfonyl group (tosyl, Ts) was introduced into the 6-OH position using *p*-toluenesulfonyl chloride [48]. This group was substituted with an azide moiety in the reaction with sodium azide in DMF to give 1,2,3,4-tetra-*O*-acetyl-6-azido-6-deoxy-D-glucopyranose **5** [46]. The introduction of the azide group required heating of the reaction mixture at 80 °C for 2 h. The lower reaction temperature did not allow the substrate to react completely even despite the significant increase in reaction time. The presence of the CH_2N_3 carbon signal with a shift of about 50 ppm in the ^{13}C NMR spectra confirms obtaining the product with an azide moiety. Removal of acetyl protecting groups from product **5** was performed according to the classic Zemplén protocol under alkaline conditions using a solution of sodium methoxide in methanol to give the desired product 6-azido-6-deoxy-D-glucopyranose **6** with 83% yield [49]. The structures of all intermediates were confirmed by analysis of ^1H and ^{13}C NMR spectra. As a result of individual reactions, the formation of products in the form of a mixture of α and β anomers was observed.

The derivative of D-galactose containing the azide moiety at position C-6 was obtained according to the sequence shown in Scheme 2. For one-step protection of the galactose hydroxyl groups at C1–C4 positions, isopropylidene groups were applied. For this purpose, di-*O*-isopropylideneation of D-galactose was carried out using acetone both as a solvent and as a reagent. The reaction was performed in the presence of catalytic amounts of iodine at room temperature giving product **8** with a very good yield [50]. As in the case of D-glucose derivatives, activation of the hydroxyl group at the C-6 position was carried

out by introducing a good leaving group using *p*-toluenesulfonyl chloride in pyridine in the presence of a catalytic amount of DMAP to give product **9**, which participated in the nucleophilic substitution reaction with sodium azide in DMF carried out at an increased temperature of 120 °C [48]. Removal of the isopropylidene groups from **10** was performed in an acidic environment with 80% trifluoroacetic acid [50] to obtain the desired 6-azido-6-deoxy-D-galactopyranose **11**. Acetylation of the latter one with acetic anhydride in the presence of sodium acetate allowed to obtain 1,2,3,4-tetra-*O*-acetyl-6-azido-6-deoxy-D-galactopyranose **12**. Product structures were confirmed by analysis of the NMR spectra. Products **11** and **12** were obtained as a mixture of α and β anomers.
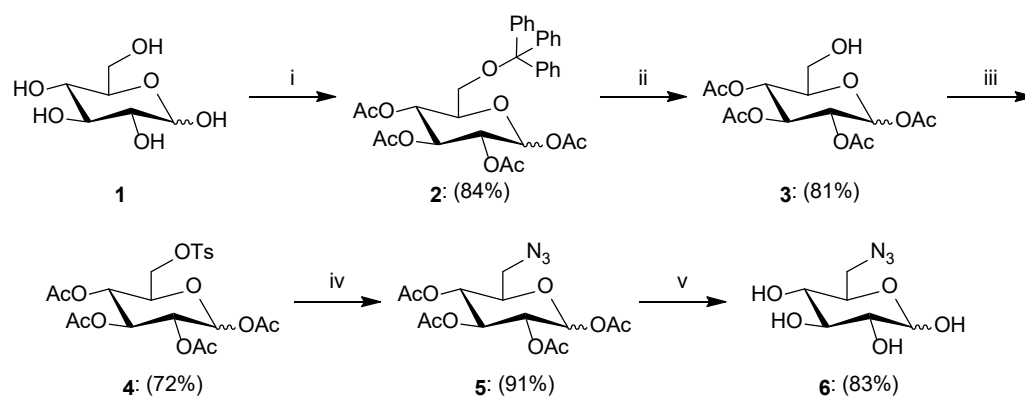
Scheme 1. Synthesis of sugar derivatives **2–6**. Reagents and conditions: (**i**) 1. trityl chloride, DMAP, pyridine, r.t., 24 h; 2. CH₃COCl, pyridine, r.t., 1 h; (**ii**) CH₃COOH, 33% HBr/AcOH, 0 °C-r.t., 1 h; (**iii**) *p*-TsCl, DMAP, pyridine, r.t., 24 h; (**iv**) NaN₃, DMF, 80 °C, 2 h; (**v**) 1. MeONa, MeOH, r.t., 0.5 h; 2. Amberlyst-15.
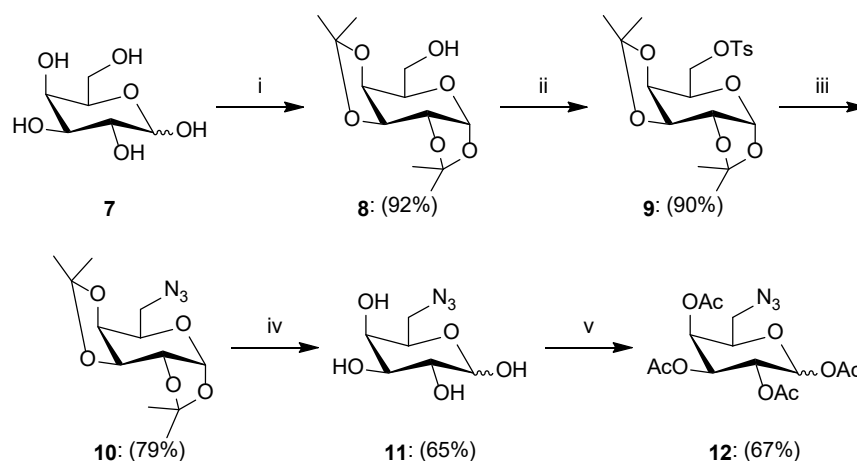
Scheme 2. Synthesis of sugar derivatives **8–12**. Reagents and Conditions: (**i**) I₂, acetone, r.t., 24 h; (**ii**) *p*-TsCl, DMAP, pyridine, r.t., 24 h; (**iii**) NaN₃, DMF, 120 °C, 24 h; (**iv**) 80% CF₃COOH, 0 °C-r.t., 2 h; (**v**) CH₃COONa, Ac₂O, reflux, 1 h.

Having glucuronic acid, i.e., a monosaccharide in which the C-6 position is oxidized to the carboxyl group, we decided to obtain derivatives containing an amide bond in the structure. The propargyl sugar derivative was prepared as shown in Scheme 3, according to the previously described procedure [51]. The synthesis started with the acetylation of commercially available D-glucuronic acid **13** using acetic anhydride in the presence of a catalytic amount of iodine as the acetyl transfer reagent. The obtained mixed anhydride **14** was treated with propargylamine in dichloromethane to give the protected amide **15** with 44% yield after column chromatographic purification. From the NMR spectra, it can be seen that compounds **14** and **15** were obtained only as a β-anomer. This is confirmed by

the high coupling constant from proton H-1 equal to about *J* = 8.0 Hz observed in the ^{1}H NMR spectra. In the last step, the protective groups were removed under basic conditions by the Zemplén method, giving the expected *N*-(prop-2-yn-1-yl)-D-glucopyranuronic acid amide **16** as a mixture of anomers, as confirmed by NMR analysis.
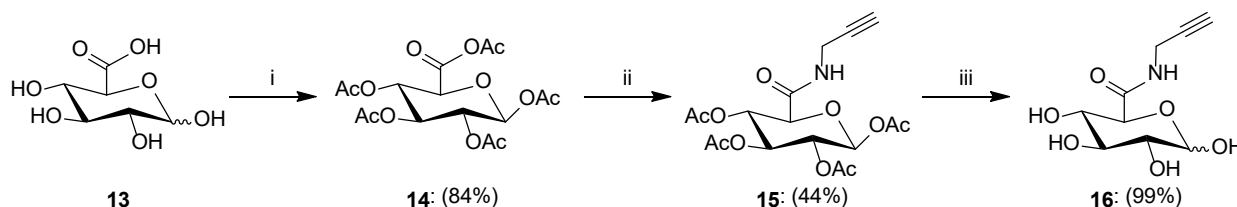
Scheme 3. Synthesis of sugar derivatives **14–16**. Reagents and Conditions: (**i**) Ac$_2$O, I$_2$, 0 °C-r.t., 3 h; (**ii**) propargyl amine, CH$_2$Cl$_2$, r.t., 24 h; (**iii**) 1. MeONa, MeOH, r.t., 0.5 h; 2. Amberlyst-15.

Next, structures based on trehalose were designed. Trehalose is a disaccharide composed of two D-glucose molecules linked by α,α-1,1′-*O*-glycosidic bond. For this reason, it is quite easy to modify the C-6 position in this molecule. This disaccharide was selected because, as a result of the hydrolysis of the glycosidic bond in trehalose, two C-6 substituted glucoconjugate molecules will be released, preferred as ligands of the GLUT1 transmembrane protein responsible for glucose transport to pathological cells, where the units released from the prodrug will be able to induce cytotoxicity. The synthesis was started according to the previously described procedure, which involved tosylation of the substrate followed by displacement with azide [52]. Unexpectedly, the tosylation of trehalose led to a mixture of products. After the purification of the reaction mixture by crystallization and column chromatography, only traces of the expected product are isolated. Therefore, the reaction sequence shown in Scheme 4 was performed to obtain 6,6′-diazido-6,6′-dideoxy-D-trehalose [53,54]. Trehalose **17** was first dissolved in DMF and then brominated with NBS or iodinated with I$_2$ in the presence of triphenylphosphine. As a result of these reactions, the corresponding halide derivatives **18** or **19** with high yields were obtained. Then, two synthesis variants were tested. The first was the substitution of halogen atoms in 6,6′-dibromo-6,6′-dideoxy-D-trehalose **18** with sodium azide in DMF (Procedure A). Product **20**, after purification from the multi-component reaction mixture, was isolated with a moderate yield of 55%. Modification of the temperature and reaction time also did not help in this case. The second method (Procedure B) assumes acetylation of compounds **18** or **19** with acetic anhydride in pyridine, isolation of acetylation products **21** or **22** by column chromatography, and then substitution of bromine or iodine from such protected compounds with an azide moiety using sodium azide. Nucleophilic substitution of the protected sugars **21** and **22** with sodium azide proceeds with a much better yield (98%) than in the case of the reaction with the unprotected molecule. De-*O*-acetylation of compound **23** under Zemplén conditions gave 6,6′-diazido-6,6′-dideoxy-D-trehalose **20** with 87% yield.

The glycoconjugates described in this paper have been divided into 4 types and their synthesis is presented in Schemes 5–8. The designed constructs contain sugar derivatives functionalized at the C-6 position linked via a linker containing a 1,2,3-triazole moiety to 8-hydroxyquinoline derivatives. The synthesis of 8-(2-propyn-1-yloxy)quinoline **24**, 8-(2-azidoethoxy)quinoline **25**, and 8-(3-azidopropoxy)quinoline **26** were described in the earlier works [34,35]. Glycoconjugates were prepared by the copper(I)-catalyzed 1,3-dipolar azide-alkyne cycloaddition, in a variant developed by Sharples [55,56]. The synthesis procedure consists of mixing the terminal alkyne and the terminal azide in an equimolar ratio in the solvent system of tetrahydrofuran and isopropanol and then adding to the mixture an aqueous catalyst system consisting of copper sulfate and sodium ascorbate. The last one is used to reduce Cu(II) to Cu(I), needed for accelerates the reaction and guarantee control over its regioselectivity. The use of such reaction conditions leads to the target products being obtained with high yields. This reaction does not generate any byproducts, only the

1,4-disubstituted isomers of 1,2,3-triazole are obtained. Already after a few hours at room temperature, TLC analysis of the reaction mixture showed almost complete conversion of the starting materials to the target product. In order to purify the crude product, it is sufficient to filter the precipitate of inorganic salts from the reaction mixture, remove the solvent in vacuo, and load onto a chromatographic column.
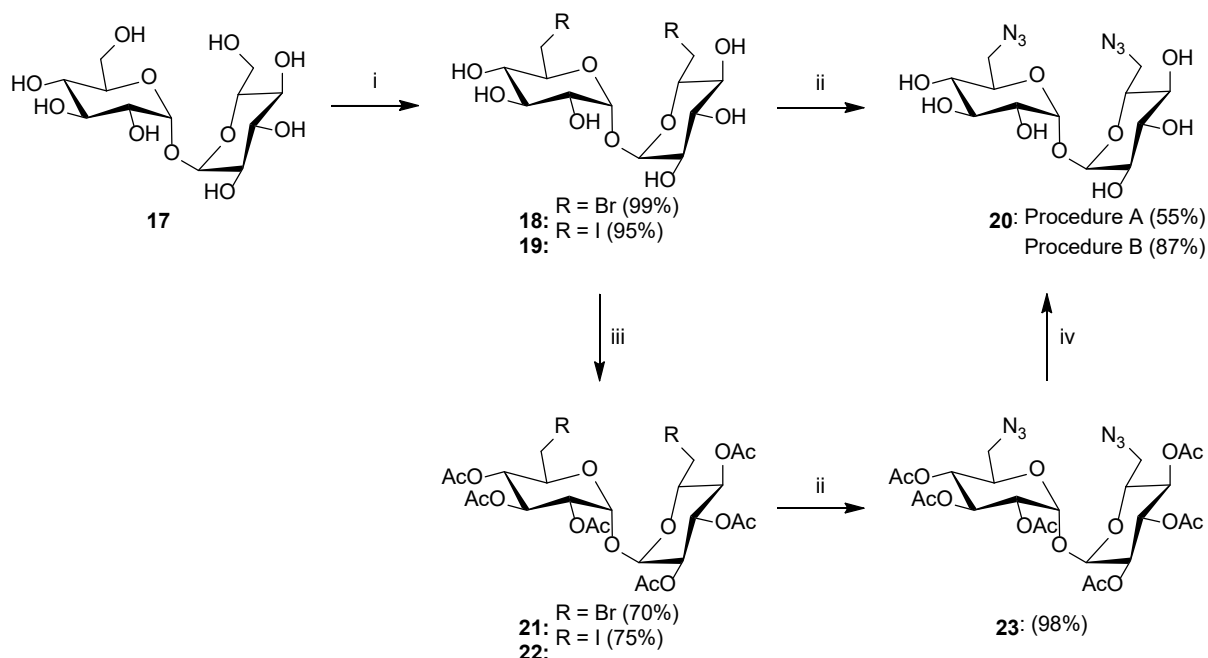
Scheme 4. Synthesis of sugar derivatives **18–23**. Reagents and Conditions: (**i**) PPh$_3$, NBS, DMF, 0 °C-r.t., 72 h (**18**) or PPh$_3$, I$_2$, DMF, 0 °C-r.t., 72 h (**19**); (**ii**) NaN$_3$, DMF, 60 °C, 24 h; (**iii**) Ac$_2$O, pyridine, 0 °C-r.t., 24 h; (**iv**) 1. MeONa, MeOH, r.t., 1 h; 2. Amberlyst-15.

Glycoconjugates type A
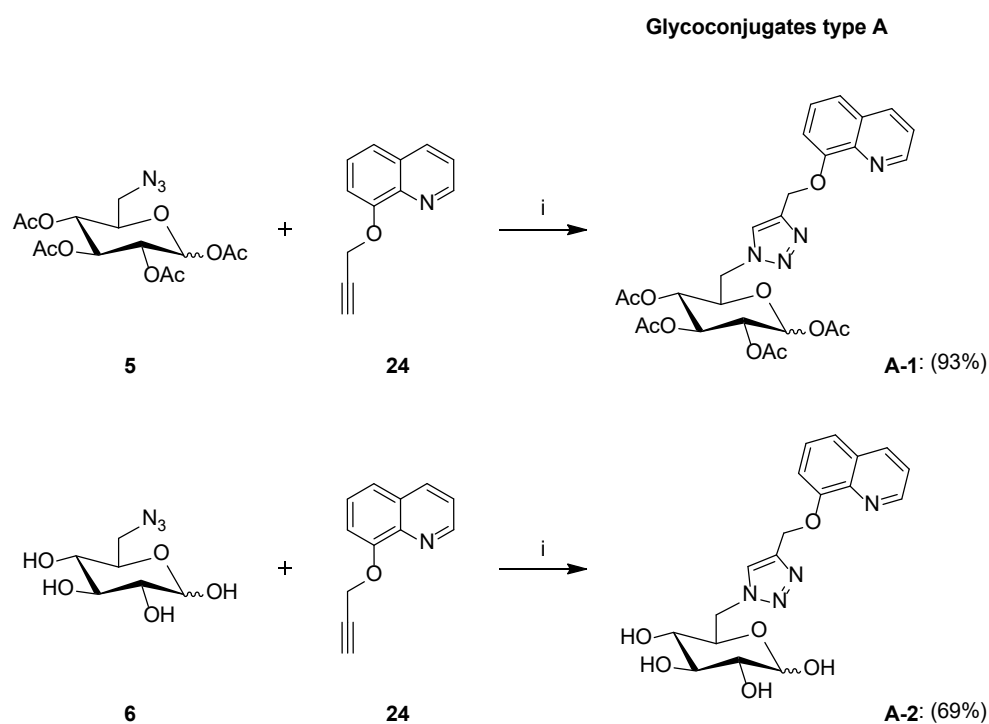
Scheme 5. Synthesis of *type A* glycoconjugates. Reagents and Conditions: (**i**) CuSO$_4$·5H$_2$O, NaAsc, *i*-PrOH/THF/H$_2$O (1:1:1, *v:v:v*), r.t., 24 h.

Glycoconjugates type B
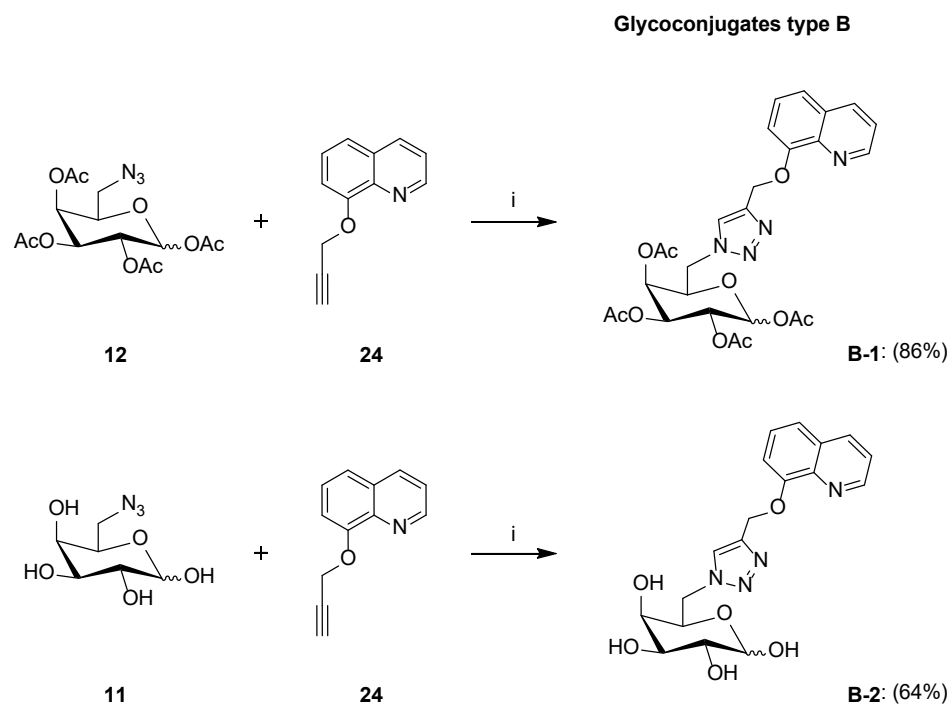
Scheme 6. Synthesis of *type B* glycoconjugates. Reagents and Conditions: (**i**) $CuSO_4 \cdot 5H_2O$, NaAsc, *i*-PrOH/THF/H_2O (1:1:1, *v:v:v*), r.t., 24 h.

Glycoconjugates type C
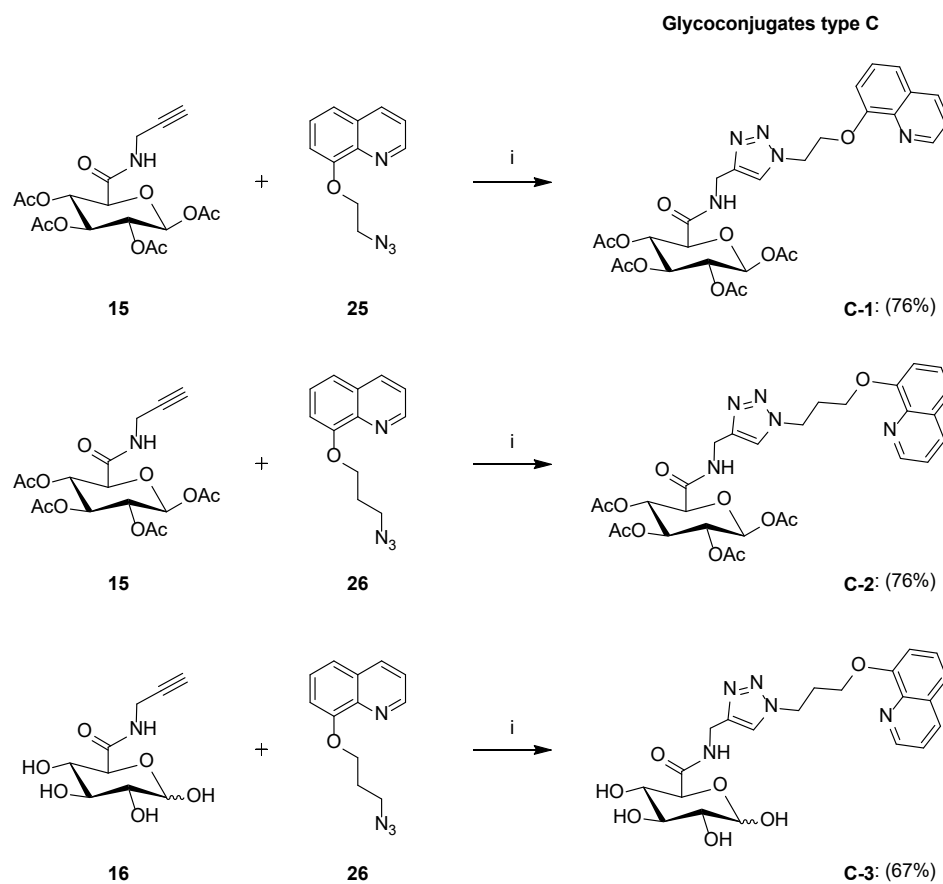
Scheme 7. Synthesis of *type C* glycoconjugates. Reagents and Conditions: (**i**) $CuSO_4 \cdot 5H_2O$, NaAsc, *i*-PrOH/THF/H_2O (1:1:1, *v:v:v*), r.t., 24 h.

Glycoconjugates type D
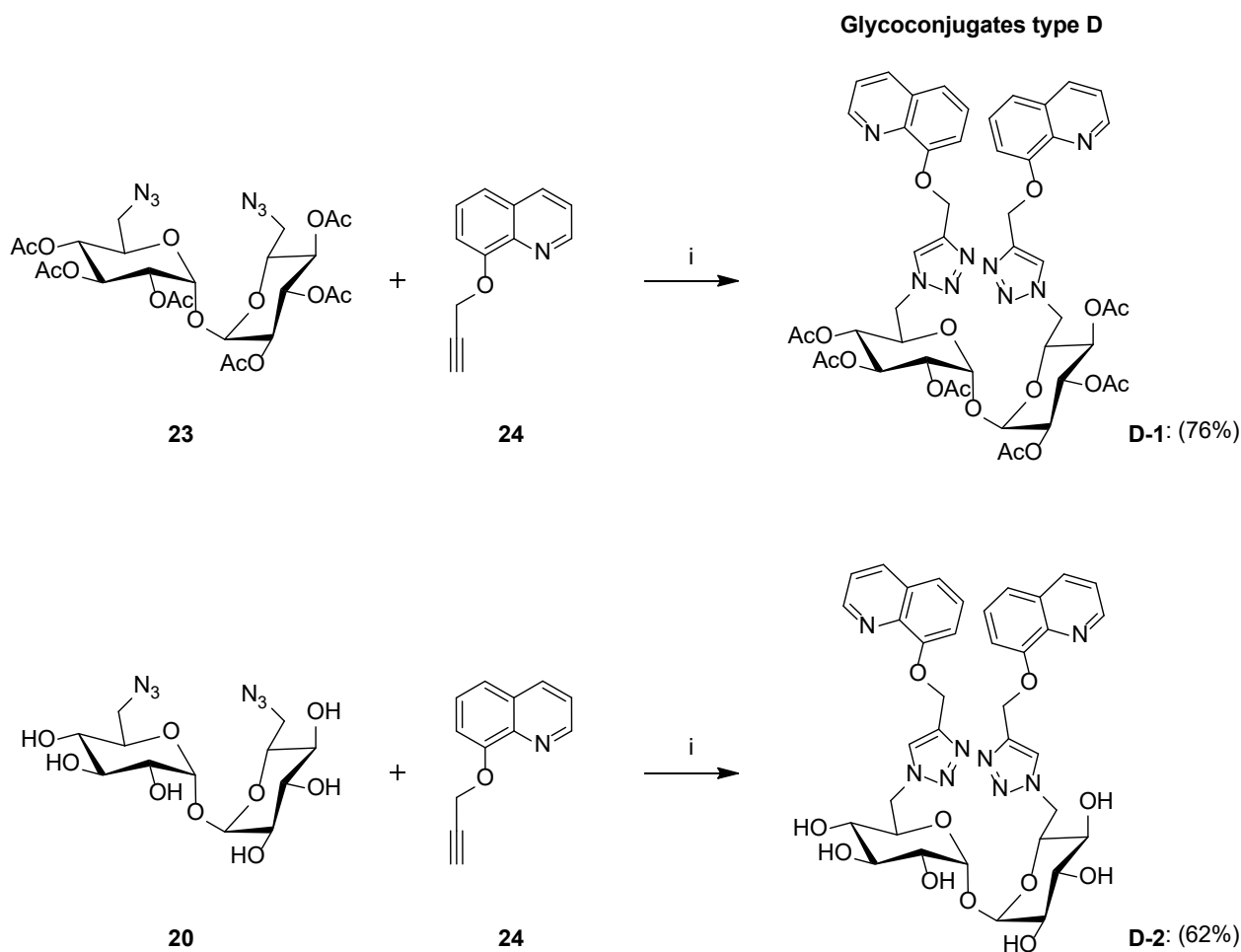
Scheme 8. Synthesis of *type D* glycoconjugates. Reagents and Conditions: (**i**) CuSO$_4$·5H$_2$O, NaAsc, *i*-PrOH/THF/H$_2$O (1:1:1, *v:v:v*), r.t., 24 h.

The resulting glycoconjugates were designed as prodrugs that could be metabolized in the cell by hydrolytic enzymes into simpler compounds. Therefore, except for the assessment of the cytotoxicity of the glycoconjugates themselves, it is also worth determining the activity of potential products of their degradation [57]. For this purpose, the potential sugar metabolites **29–36** presented in Scheme 9 were designed and prepared. The obtained sugar derivatives were reacted with propargyl alcohol **27** or 2-azidoethanol **28**, under the same reaction conditions as described for glycoconjugates synthesis.

The structures of all newly created products were confirmed using nuclear magnetic resonance spectroscopy (^{1}H NMR and ^{13}C NMR) and high-resolution mass spectrometry (HRMS). The formation of the desired products was indicated by the presence of characteristic signals from the 1,2,3-triazole ring in the NMR spectra. These are the singlet signal observed at about δ = 8.0 ppm from the H-C(5) proton of triazole ring in ^{1}H NMR spectra and two characteristic carbon signals at about 124 ppm and 144 ppm for C(4) and C(5) in the ^{13}C NMR spectra. The double signals for the sugar part observed in the NMR spectra and the characteristic coupling constants from the H-1 protons (*J* = 8.2 Hz for the β anomer and *J* = 3.7 Hz for the α anomer) indicate the formation of glycoconjugates as a mixture of anomers. The NMR spectra of all synthesized products are presented in the Supplementary Materials.
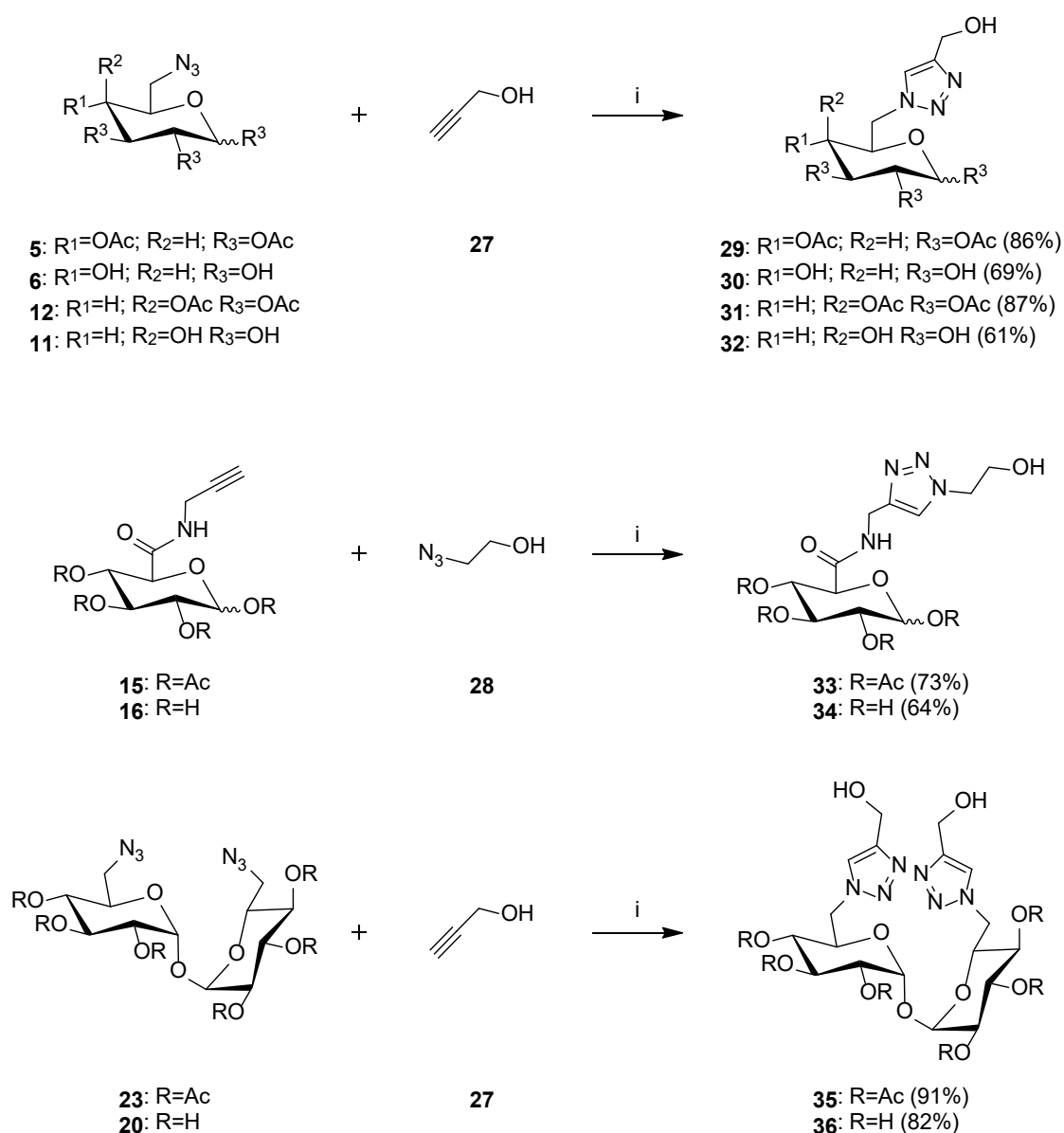
Scheme 9. Synthesis of metabolites of sugar derivatives. Reagents and Conditions: (**i**) CuSO$_4$·5H$_2$O, NaAsc, *i*-PrOH/THF/H$_2$O (1:1:1, *v:v:v*), r.t., 24 h.

2.2. Biological Evaluation

2.2.1. Antiproliferative Studies

An in vitro biological test package was performed for the obtained derivatives. All newly synthesized compounds were assessed for their cytotoxic activity against human cell lines with increased GLUT expression: the colon cancer cell line (HCT-116) and the breast cancer cell line (MCF-7), as well as on normal human dermal fibroblasts cells (NHDF-Neo), using the MTT assay (3-(4,5-dimethylthiazol-2-yl)-2,5-diphenyltetrazolium bromide). The MTT test is a colorimetric method for detecting proliferating cells. It is based on the ability of the enzyme mitochondrial dehydrogenase to convert yellow tetrazole salt (MTT) into purple formazan. The amount of the product formed in the reaction, determined spectrophotometrically, is proportional to the number of living cells [58]. The antiproliferative activity was expressed as the concentration that caused 50% inhibition of the growth of the population of cells treated with the test compounds relative to the control cells (inhibitory concentration activity—IC$_{50}$). Tables 1 and 2 summarize the IC$_{50}$ values calculated for all tested compounds.

Table 1. Summary of cytotoxicity of substrates used for glycoconjugation and metabolites of sugar derivatives.

Compound	Activity IC$_{50}$ [µM] [a]	
	HCT-116 [b]	MCF-7 [c]
5	>800	201.12 ± 2.09
6	>800	>800
11	>800	>800
12	>800	641.24 ± 1.79
15	584.30 ± 9.39	713.59 ± 15.69
16	>800	>800
20	>800	>800
23	>800	>800
24	>800	95.95 ± 4.29
25	83.02 ± 1.83	27.27 ± 0.06
26	461.39 ± 1.34	244.44 ± 1.34
29	>800	>800
30	>800	>800
31	>800	>800
32	>800	>800
33	>800	>800
34	>800	>800
35	>800	>800
36	>800	>800

[a] Cytotoxicity was evaluated using the MTT assay; [b] Incubation time 24 h; [c] Incubation time 72 h. Data are presented as the mean ± standard deviation (*n* = 3).

Table 2. Cytotoxicity of quinoline glycoconjugates evaluated by the MTT test.

Compound	Activity IC$_{50}$ [µM] [a]			
	HCT-116 [b]	HCT-116 [c]	MCF-7 [c]	NHDF-Neo [c]
A-1	83.51 ± 1.91	11.98 ± 0.90	52.84 ± 0.75	129.73 ± 1.49
A-2	191.15 ± 2.46	22.32 ± 0.70	54.92 ± 8.71	317.22 ± 9.46
B-1	75.08 ± 1.30	-	36.67 ± 0.03	81.42 ± 0.52
B-2	293.19 ± 8.00	-	155.73 ± 7.40	271.60 ± 0.35
C-1	173.40 ± 6.68	81.49 ± 3.36	223.67 ± 7.34	215.24 ± 3.10
C-2	94.24 ± 1.48	62.35 ± 0.32	157.15 ± 7.86	318.53 ± 3.09
C-3	>800	767.00 ± 2.39	706.60 ± 2.87	>800
D-1	46.26 ± 3.12	26.33 ± 0.72	30.71 ± 0.99	34.48 ± 0.39
D-2	53.44 ± 5.14	21.28 ± 0.94	34.04 ± 0.95	70.66 ± 0.75
E-1	69.00 ± 2.53	45.73 ± 1.81	57.69 ± 3.32	55.28 ± 5.08
E-2	212.00 ± 7.71	162.47 ± 5.97	185.34 ± 2.21	232.75 ± 9.44

[a] Cytotoxicity was evaluated using the MTT assay; [b] Incubation time 24 h; [c] Incubation time 72 h. Data are presented as the mean ± standard deviation (*n* = 3).

The conducted cytotoxicity studies show that both sugar substrates and possible potential glycoconjugate metabolites did not show significant growth inhibitory activity on the tested cells (Table 1). This means that for the obtained constructs to show the expected activity, they should reach the interior of the cell in an unchanged form, without any degradation. The tested glycoconjugates inhibited cell growth in a dose-dependent manner, which allowed the expression of their activity through IC$_{50}$ values (Table 2). 24 h treatment with candidate drugs of the HCT-116 cell line showed moderate cytotoxic potency of the tested glycoconjugates. After increasing the incubation time to 72 h, the HCT-116 cell line was more sensitive to the presence of the tested derivatives. Experiments for MCF-7 and NHDF-Neo cell lines were carried out for 72 h due to longer times of cell division of this line. Owing to the tests performed on healthy cells, it was possible to assess the selectivity of the tested compounds in relation to neoplastic cells, which is crucial in the design and synthesis of antiproliferative compounds. It is worth noting that most of the

tested compounds showed lower cytotoxicity on normal human NHDF-Neo cells than on cancer cells. The selectivity index (SI) was calculated as a ratio of the IC_{50} value for healthy cells (NHDF-Neo) and the IC_{50} value for cancer cells (HCT-116 or MCF-7) and is presented in Table 3.

Table 3. Selectivity index (SI) of tested compounds after 72 h incubation time.

Compound	Selectivity Index (SI) [a]	
	HCT-116	**MCF-7**
A-1	10.83	2.46
A-2	14.21	5.78
B-1	1.08 [b]	2.22
B-2	0.93 [b]	1.74
C-1	2.64	0.96
C-2	5.11	2.03
C-3	-	-
D-1	1.31	1.12
D-2	3.32	2.08
E-1	1.21	0.96
E-2	1.43	1.26

[a] Selectivity index (SI) was calculated as a ratio of the IC_{50} value for healthy cells (NHDF-Neo) and the IC_{50} value for cancer cells (HCT-116 or MCF-7); [b] Incubation time 24 h.

The highest growth inhibitory activity of both cancer cell lines was noted for glycoconjugates *type A* and *type D*. In these derivatives, the triazole-quinoline was attached through the triazolic nitrogen atom to the D-glucose unit directly to the carbon at the C-6 position. In the case of compounds **A-1** and **A-2**, the calculated IC_{50} values after 72 h of incubation for HCT-116 were equal to 11.98 ± 0.90 μM and 22.32 ± 0.70 μM, respectively, while for MCF-7 were equal to 52.84 ± 0.75 μM and 54.92 ± 8.71 μM. For compounds **D-1** and **D-2**, IC_{50} values were recorded of 26.33 ± 0.72 μM and 21.28 ± 0.94 μM for HCT-116 and 30.71 ± 0.99 and 34.04 ± 0.95 μM for MCF-7, whereas glycoconjugates *type A* were characterized by a higher selectivity index (SI = 10.83, 14.21 for HCT-116 and 2.46, 5.78 for MCF-7), in contrast to trehalose derivatives *type D*, which showed a similar level of antiproliferative activity against healthy NHDF-Neo cells (SI = 1.31, 3.32 for HCT-116 and 1.12, 2.08 for MCF-7). The HCT-116 cell line was characterized by higher sensitivity to the tested compounds. The selectivity indexes for this line were also more favorable. It is also worth emphasizing that the **A-2** derivative shows comparable antiproliferative activity to the **A-1** derivative against cancer cell lines. However, the selectivity of **A-2**, i.e., a conjugate containing an unprotected glucose residue and thus having an increased affinity for GLUT1, was higher compared to derivative **A-1** with acetylated sugar part. GLUT transporters are not overexpressed in NHDF-Neo cells, therefore in the case of deprotected derivatives, it was expected to observe lower cytotoxicity than in the case of acetylated derivatives, where passive transport of compounds across the cell membrane is not selective. Similarly, due to the lack of selectivity, the involvement of GLUT proteins in the transport of trehalose derivatives should be excluded. Probably in the case of *D-type* glycoconjugates, the disaccharide was not hydrolyzed to two glucose units, which made the binding to the GLUT transporter much more difficult.

Type B glycoconjugates derived from D-galactose cannot be considered compatible with the GLUT transporter. The deprotected **B-2** derivative was shown to be less cytotoxic than its acetylated counterpart **B-1** and had one of the highest IC_{50} values among all compounds tested. The higher anticancer activity of the **B-1** derivative with acetyl protection in the sugar part indicates that this type of compound prefers passive transport across the cell membrane. At the same time, this derivative is also cytotoxic to healthy cells, because this transport is not selective.

Tests show that glycoconjugates *type C* are also not good substrates for GLUT transporter proteins. After 72 h of incubation time, the **C-3** derivative remained inactive against

the cancer cell lines tested. Probably a rigid amide fragment in the structure between the sugar moiety and the triazole ring limits the flexibility of the molecule and its possibility to fit into the GLUT transporter. The presence of the amide bond also did not improve the activity of glycoconjugates with acetyl protections, as compounds **C-1** and **C-2** did not show significant ability to inhibit cell growth and are characterized by quite high IC_{50} values. This suggests that a too stable linker is unable to release the cytotoxic charge. It was noted that the **C-2** derivative was slightly more active than the **C-1** derivative. This is due to the difference in linker length between the quinoline and triazole parts. Such regularity has already been observed during the cytotoxicity testing of previously prepared glycoconjugates [35]. Interestingly, compound **C-2** was not highly toxic to normal human skin cells (SI = 5.11 for HCT-116 and 2.03 for MCF-7). Because of these observations, it is advisable to test these structures on a different panel of tumor cell lines in the future. Additionally, for these derivatives, the reverse orientation of the 1,2,3-triazole system in the linker structure was designed compared to the other tested glycoconjugates. Perhaps this treatment also has a negative impact on the biological activity of these connections.

Several additional experiments were performed to evaluate the effect of the substitution position of a given hydroxyl group of a sugar unit on the activity of glycoconjugates. The cytotoxicity of the most active derivatives described for the first time in this paper was compared with the previously obtained analogous glycoconjugates formed through the C-1 anomeric position of D-glucose [34]. Figure 2 shows the structures of analogous quinoline glycoconjugates functionalized at the C-6 position (**A-1**, **A-2**) and the anomeric position (**E-1**, **E-2**), and Figure 3 compares their cytotoxic activity as well as calculated and predicted IC_{50} values and selectivity indexes.

Glycoconjugates type A   **Glycoconjugates type E**
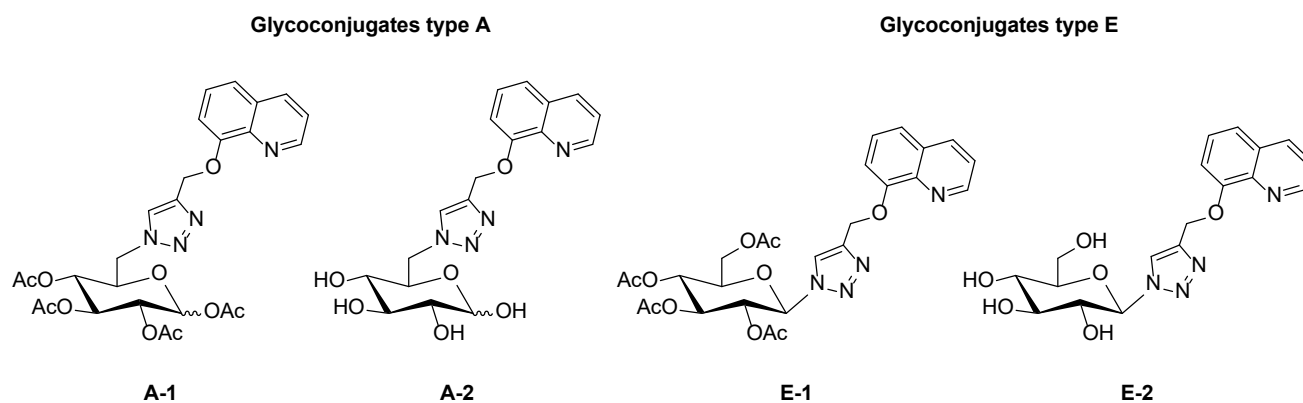
Figure 2. Structures of analogous quinoline glycoconjugates functionalized at the C-6 position (**A-1**, **A-2**) or the anomeric position (**E-1**, **E-2**).

The presented data show that the C-6 functionalized glycoconjugates show some differences in activity compared to the analogous structures of the C-1 functionalized glycoconjugates. Namely, after 72 h of incubation of cells with tested compounds, *type A* glycoconjugates compared to *type E* glycoconjugates, show increased toxicity against HCT-116 and MCF-7 cancer cells. For both tumor cell lines, 100% inhibition of cell growth was recorded at the highest doses of **A-1**, **A-2**, and **E-1**. It should be noted that in both cell lines it is the deprotected **A-2** derivative that is characterized by much better cytotoxicity than the analogous **E-2** derivative, which practically did not affect the cell viability. This suggests an increased permeability of the cell membrane, possibly through the involvement of GLUT proteins to transport a new type of glycoconjugate across the cell membrane. In addition, both the **A-1** and **A-2** derivatives exhibit reduced toxicity to normal cells as compared to previously reported glycoconjugates modified in an anomeric position which were characterized by rather a low SI. These results indicate that the C-6 substitution of D-glucose is preferable to the C-1 substitution for cellular uptake of quinoline glycoconjugates

in neoplastic cells. These properties suggest that the newly designed glycoconjugates show great potential for further research.
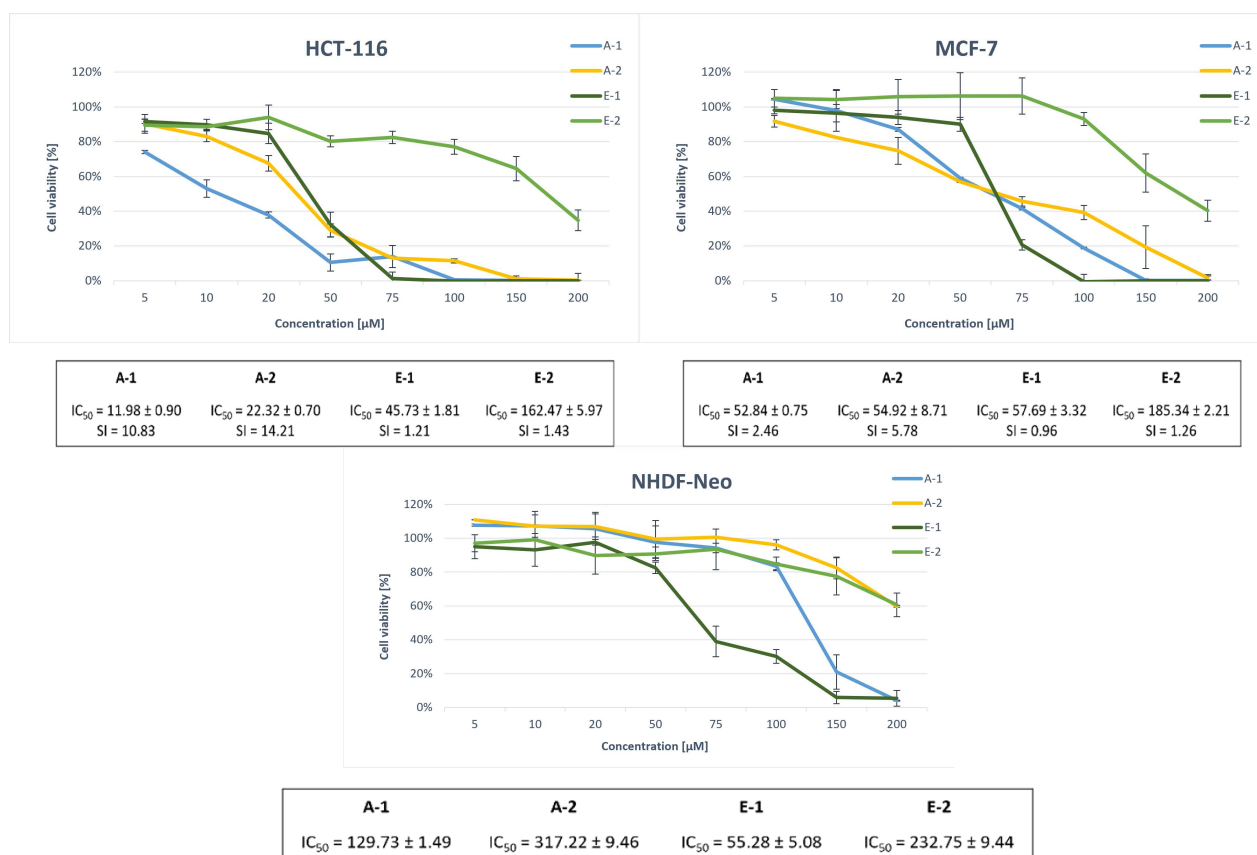
Figure 3. Comparison of the viability of HCT-116, MCF-7, and NHDF-Neo cells treated with different concentrations of the tested glucoconjugates: **A-1**, **A-2**, **E-1**, and **E-2**. Cell viability was measured by the MTT test. Data are presented as the mean ± standard deviation (*n* = 3).

2.2.2. Effect of the GLUT1 Inhibitor

To investigate the possible interaction of the tested compounds with glucose receptors and thus to check whether they target the Warburg effect, tests of the influence of the presence of the GLUT inhibitor on the effectiveness of the glycoconjugates were carried out. For this, cells were treated each time with the test compounds in the presence of 100 μM of the GLUT1 inhibitor 4,6-*O*-ethylidene-α-D-glucose (EDG). After 72 h of incubation with test compounds, cell viability was measured and presented in Figure 4.

The obtained results confirmed that GLUT transporters are involved in the transport of *type A* glycoconjugates to the cell. Following the use of an EDG inhibitor and partial inhibition of GLUT activity, probably decreased compound uptake occurred, which resulted in less accumulation in cells and less anti-cancer activity. For the HCT-116 cell line, a 13–25% increase in cell viability was observed in the concentration range tested for compound **A-2** and by 3–19% for compound **A-1**. While MCF-7 cell viability was increased by 6–15% in the concentration range tested for compound **A-2** and 2–10% for compound **A-1**. In the case of the NHDF cell line, even a slight decrease in cell viability was observed in the presence of EDG as compared to cells without the inhibitor. The increase in cytotoxicity in the presence of a GLUT inhibitor is due to the restriction of glucose transport, which is the main nutrient entry for proliferating cells. The observations for the **A-2** glycoconjugate are as expected as its structure allows for a fit with GLUT transporters. In contrast, compound **A-1** is a hydrophobic molecule, so it is unlikely that in this form it undergoes a different transport than passive diffusion through the lipid cell membrane. The possible explanation for the

partial uptake of **A-1** by GLUT transporters may be the possibility of partial hydrolysis of acetyl protections by hydrolytic enzymes in the extracellular space. To determine how the position of the substitution in D-glucose influences the specific uptake of the resulting conjugates, glycoconjugates *type E* were also used for the tests. It turned out that in both tumor cell lines there was little or no significant change in cell viability in the presence of the EDG inhibitor. This result supports the hypothesis that the position of the sugar substitution is an important parameter in determining the GLUT1 specificity of the glycoconjugates. As expected, it was also found that the use of an EDG inhibitor did not have any effect on the cellular uptake of *D-type* glycoconjugates and the 8HQ aglycone.
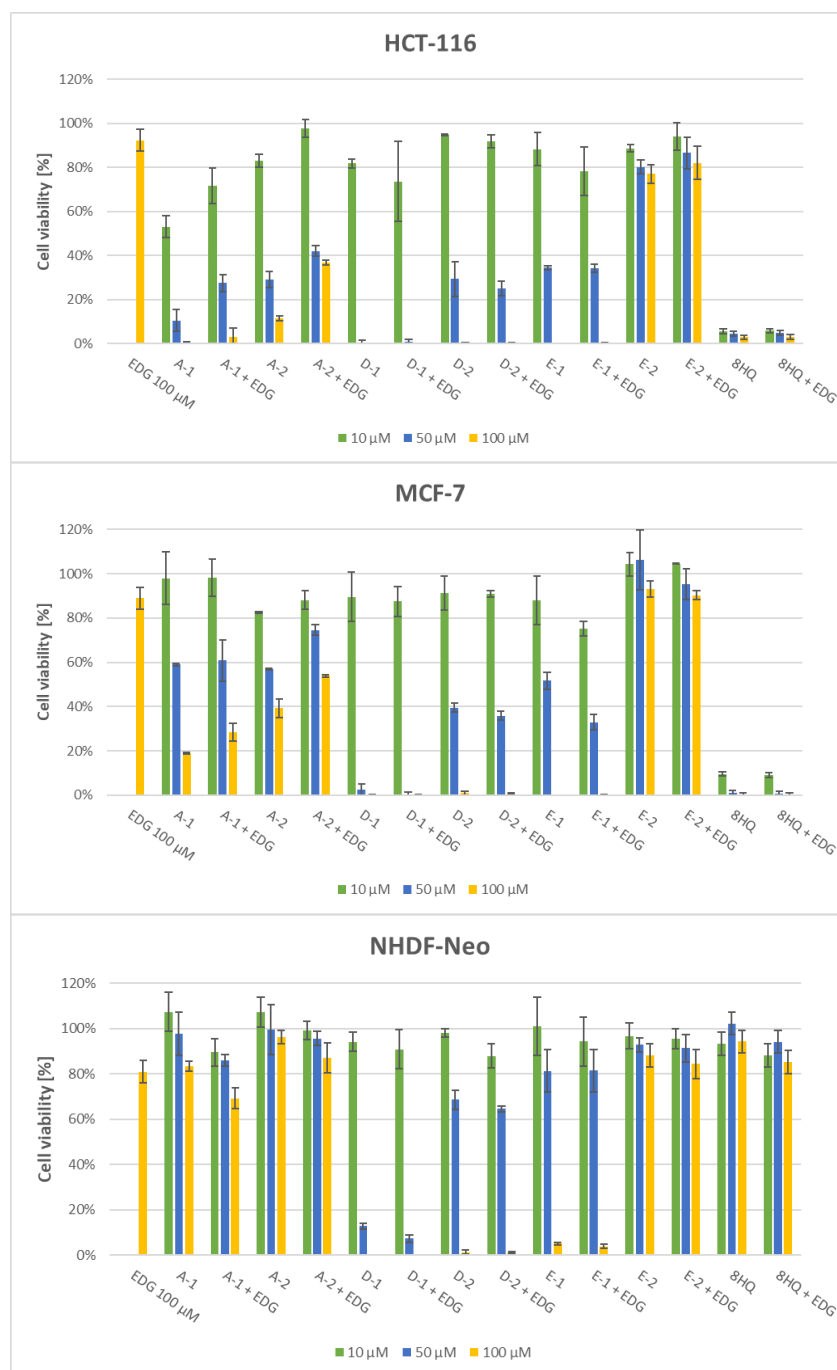
Figure 4. Effect of glucose transporter GLUT1 inhibitor EDG on the activity of compounds **A-1**, **A-2**, **D-1**, **D-2**, **E-1**, **E-2**, and 8HQ for 72 h incubation with HCT-116, MCF-7, and NHDF-Neo cells. Cell viability was measured by the MTT test. Data are presented as the mean $\pm$ standard deviation ($n = 2$).

GLUTs are the most common transporters that facilitate the recognition and uptake of glycoconjugates. As mentioned, the use of an EDG inhibitor had the effect of changing the survival of cells treated with glycoconjugates *A-type*. However, it cannot be clearly stated that the cellular uptake of the newly designed **A-2** glycoconjugate depends only on GLUT. Perhaps the dose of the inhibitor turned out to be too low and increasing its concentration would result in greater inhibition of uptake. It should also be noted that the transport of sugars is mediated not only by GLUT but also by other receptors, such as SGLT, SWEET, OCT2, or ASGPR [19,59].

2.2.3. Clonogenic Assay

Then, the clonogenic potential of cells exposed to the tested compounds was investigated [60]. The ability of a cell to form colonies is one of the defining features of cancer and determines its ability to metastasize. Thus, the test is used to evaluate the efficacy of anticancer therapy in vitro by observing the ability of the treated cell to divide.

MCF-7 and HCT-116 cells were treated with *type A* glycoconjugates and their ability to proliferate was observed. Cells were incubated with compounds at IC_{50} concentrations for 72 h, and then the cells were collected, seeded again, and incubated for 10 days in a fresh medium. The formed colonies were stained with crystal violet (Figure 5). The control shows the ability of a single cell to grow back into a large colony that can be seen with the naked eye. The results indicate that **A-1** and **A-2** derivatives were able to decrease the clonogenic potential of HCT-116 and MCF-7 cells under the experimental conditions. Similar effects were observed for both compounds.
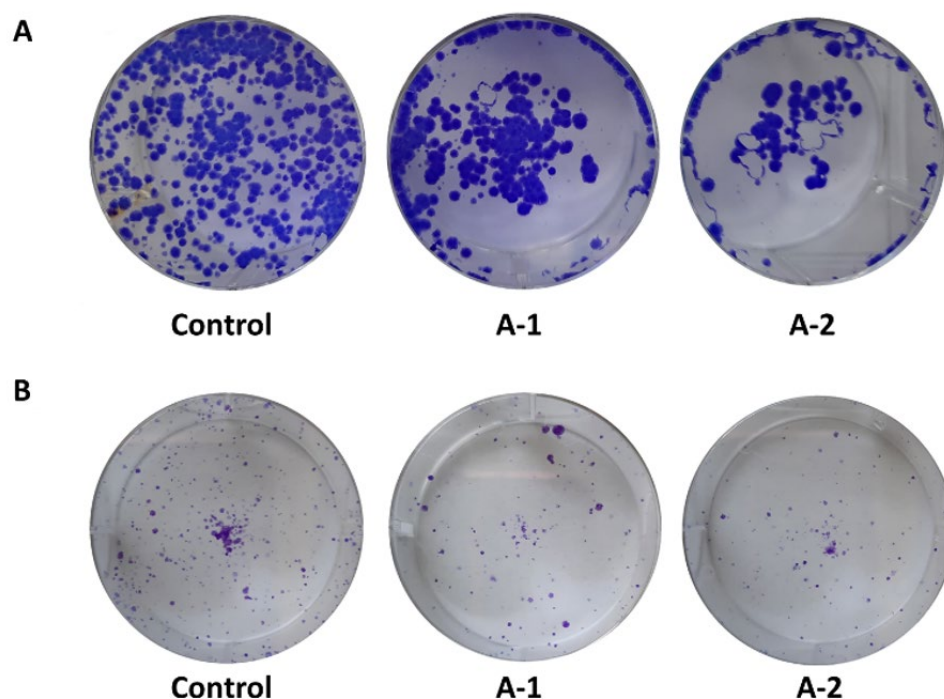
Figure 5. Representative colony formation images of: (**A**) HCT-116 cancer cells and (**B**) MCF-7 cancer cells, after 72 h treatment with compounds **A-1** and **A-2**.

2.2.4. Wound Healing Assay

Cell migration is a hallmark of many physiological and pathological processes such as wound healing, cancer invasion, and metastasis. To investigate the migration capacity of cells after exposure to test compounds, a wound-healing assay was performed, which is a standard in vitro technique used in small molecule screening for the discovery of drug candidates [61,62].

This experiment consisted in making a "wound" in a confluent monolayer of HCT-116 and MCF-7 cells, which were next treated with the test compounds at their IC_{50} concentrations. Then, the migration of cells was observed for 72 h in order to fill the formed gap (Figure 6). In the control, cell migration from the edges of the wound is visible, gradually filling the gap. After 72 h, the wounds are almost completely covered with cells. In the same way, cell migration is observed in healthy NHDF cells. On the other hand, a significantly slower migration of HCT-116 and MCF-7 cells was observed after treatment with the tested **A-1** and **A-2** glycoconjugates under experimental conditions. After 72 h, an open wound comparable to the initial one can be noticed.
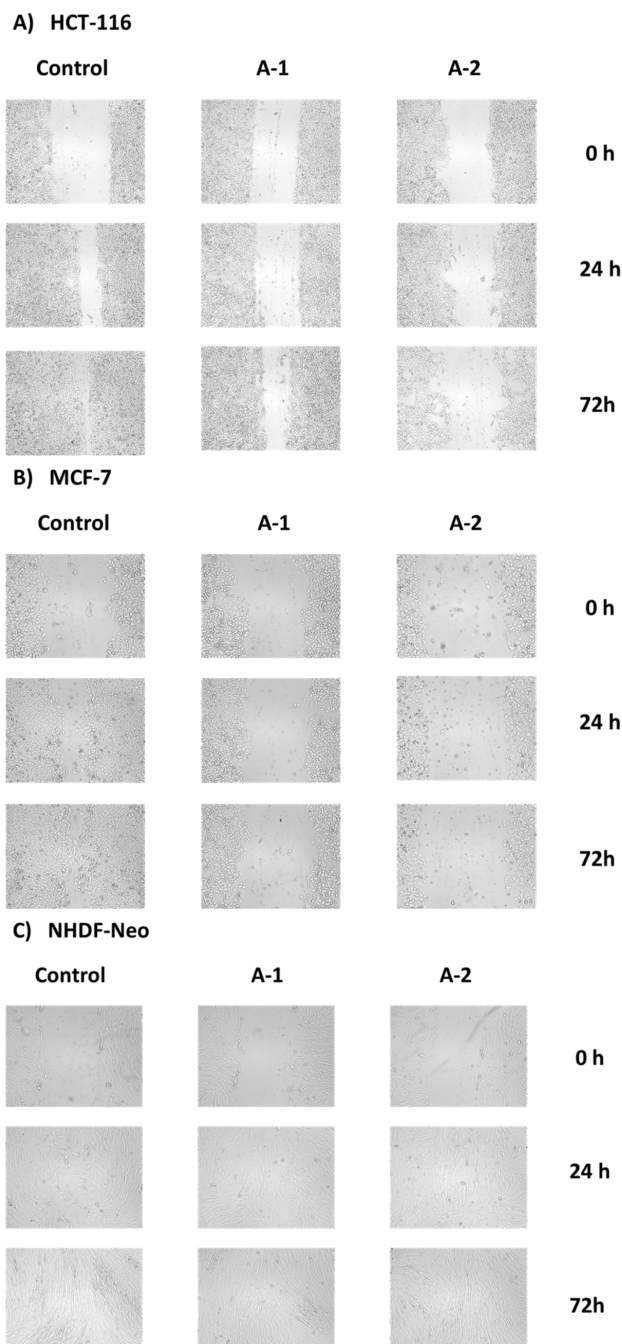
Figure 6. Representative images of: (**A**) HCT-116 cancer cells, (**B**) MCF-7 cancer cells, and (**C**) NHDF-Neo healthy cells, were acquired at time 0 and after 24 h and 72 h incubation with compounds **A-1** and **A-2** in wound healing assay. Better quality and larger images are included in Supplementary Materials (Figure S75).

2.2.5. Apoptosis and Cell Cycle Analyses by Flow Cytometry

After determining the cytotoxic activity of the tested compounds in the MTT test and calculating their IC_{50} parameters, cytometric measurements were started to determine what kind of cell death was caused by the most active compounds. This is important information from the point of view of drug design, as it provides detailed information on the cytotoxicity of a compound. Apoptosis is a natural biological process involving programmed cell death and plays an important role in maintaining correct homeostasis between cell proliferation and cell death. This is in contrast to necrosis, which is accompanied by acute inflammation, preceded by cell degradation due to the loss of the integrity of the cell membrane. It is possible to distinguish viable cells from apoptotic and necrotic cell fractions using Annexin V-FITC and Propidium Iodide (PI). Annexin V-FITC labels phosphatidylserine residues that, after the start of apoptosis, are located on the outer surface of the cell membrane, enabling the identification of cells in the early stages of apoptosis. PI binds stoichiometrically to intracellular DNA during late apoptosis and necrosis when the cell membrane has been damaged. This combination allows for the differentiation of early apoptotic (A+/P−), late apoptotic (A+/P+), necrosis (A−/P+), and normal (A−/P−) cells that can be quantified by flow cytometry. The experiments were performed on the HCT-116 and MCF-7 cancer cell lines and the NHDF-Neo healthy cell line. Cells were treated with compounds at concentrations equal to their previously calculated IC_{50} value and allowed to incubate for 24 h. The results of the level of apoptosis induction by the tested compounds are presented in Figure 7 and in the Supplementary Materials (Figure S73).
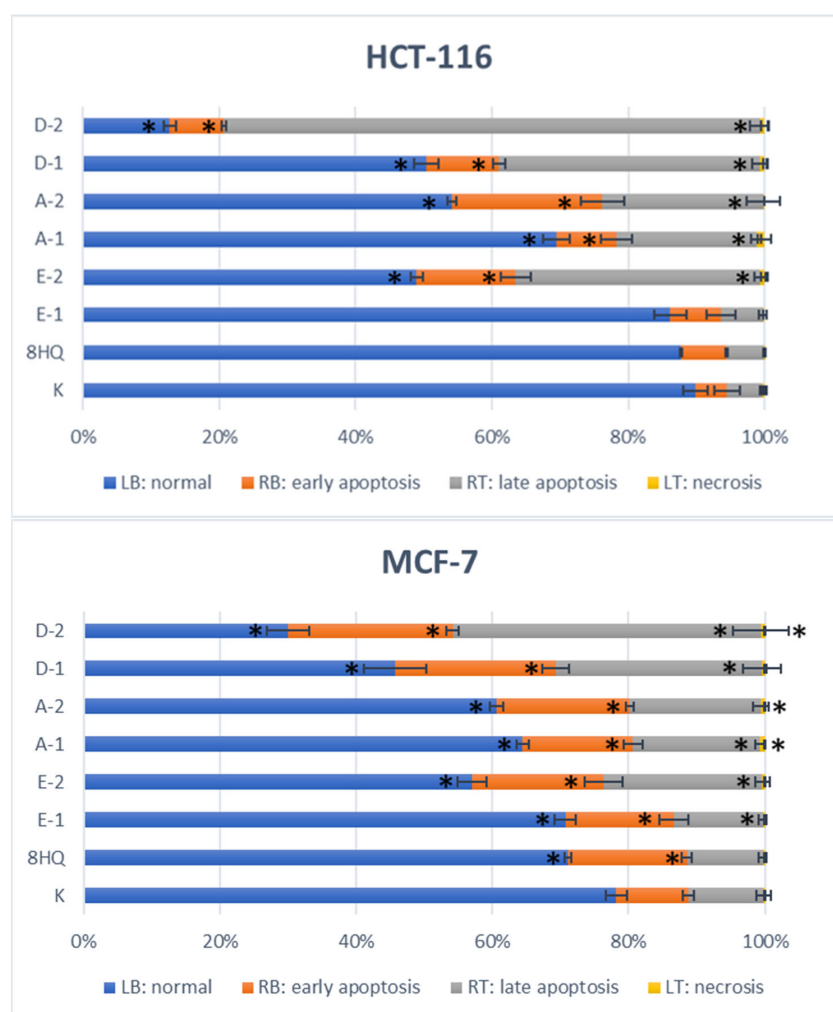
Figure 7. *Cont*.
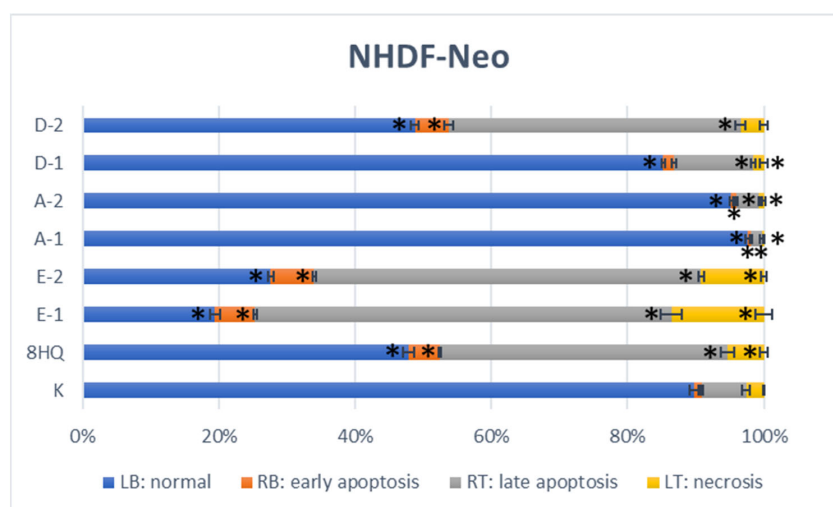
Figure 7. Flow cytometry analysis of HCT-116, MCF-7, and NHDF-Neo cell apoptosis after incubation for 24 h with test compounds used in their IC_{50} doses. The fractions of dead cells were detected by the FITC Annexin-V Apoptosis Detection Kit with PI. Means $\pm$ SD from three independent experiments. * *p*-value < 0.05, in comparison to the control.

After 24-h incubation of HCT-116 and MCF-7 cancer cells with test compounds, the appearance of a certain percentage of apoptotic cells was observed. However, fortunately, neither compound caused necrotic cell death. This means that the applied IC_{50} dose affects the entry of cells into the apoptotic pathway and does not cause uncontrolled pathological cell death as a result of mechanical damage. Induction of apoptosis as a result of DNA damage in precancerous lesions can remove potentially pathological cells, thus inhibiting tumor proliferation. Comparing the obtained results with the control fraction, a higher percentage of apoptotic cells was noted for the HCT-116 line, which confirms the previous conclusions about the high sensitivity of this cell line to the tested compounds. In the case of the MCF-7 cell line, a lower percentage of apoptotic cells was observed under the experimental conditions, which may be due to the short incubation time of the cells with the test drugs. A noticeably higher fraction of cells in early and late apoptosis was observed during the action of compounds without the protection of the hydroxyl groups in the sugar unit, compared to their acetylated counterparts. Moreover, the glycoconjugates induce both early and late apoptosis much more efficiently than the 8HQ aglycone, for which results were similar to the control fraction. The opposite is true for the healthy NHDF-Neo cell line, where most of the glycoconjugates showed less toxicity. After 24 h of incubation of cells with test compounds, the derivative of trehalose **D-2** showed the strongest pro-apoptotic properties (87% apoptotic cells for HCT-116 and 70% apoptotic cells for MCF-7). At the same time, this compound showed high toxicity also to healthy cells (51% of the dead cell fraction for NHDF-Neo). This indicates that under the influence of this compound, healthy cells were also damaged and entered the apoptotic pathway. The glycoconjugate **E-1** more strongly inhibited the proliferation of cancer cells in the MTT assay than the glycoconjugate **E-2**, but as it turned out, it did not induce apoptosis in the HCT-116 or MCF-7 cell lines. Interestingly, it was the deprotected derivative that was characterized by better proapoptotic properties than the protected compound. In addition, in the case of the NHDF-Neo cell line, for glycoconjugates *type E*, i.e., compounds with an aglycon attached through the anomeric position of the sugar, some necrotic cells (14% for **E-1** and 9% for **E-2**) and a very large number of cells in late apoptosis (61% and 57%) were noted. Finally, cells treated with derivatives **A-1** and **A-2** showed signs of apoptosis in HCT-116 (29% and 46% apoptotic cells, respectively) and MCF-7 (35% and 39% apoptotic cells, respectively). In contrast, in the case of the NHDF-Neo cell line, no increased percentage of dead cells for these compounds was observed compared to the control. After 24 h of incubation, 98% and 95% of normal cells remained for **A-1** and **A-2**, respectively. The remaining compounds

induced apoptosis in NHDF cells as compared to control. This confirms the higher safety of C-6 functionalized glycoconjugates previously noted in the MTT test compared to the glycoconjugates modified at the anomeric position.

After determining the type of cell death caused by the test compounds, the flow cytometry technique was used to study their influence on potential changes in the course of the cell cycle of the HCT-116, MCF-7, and NHDF-Neo lines. The cell cycle is the sequence of growth and division of cells, both normal and cancerous. This process begins from the resting phase (G0) through the active growth phases (G1, S, G2), leading to mitosis (M) in which the cell's nucleus divides. For experiments, cells were incubated with test compounds for 24 h at concentrations equal to their previously calculated IC_{50} value. After this time, cells were harvested and treated with a buffer to lysate the cells and isolate the cell nuclei. Propidium iodide was used to assess the amount of DNA in particular phases of the cell cycle. The results of the distribution of the cell cycle phases after exposure to test compounds are shown in Figure 8. Histograms of DNA content in cells are presented in the Supplementary Materials (Figure S74).
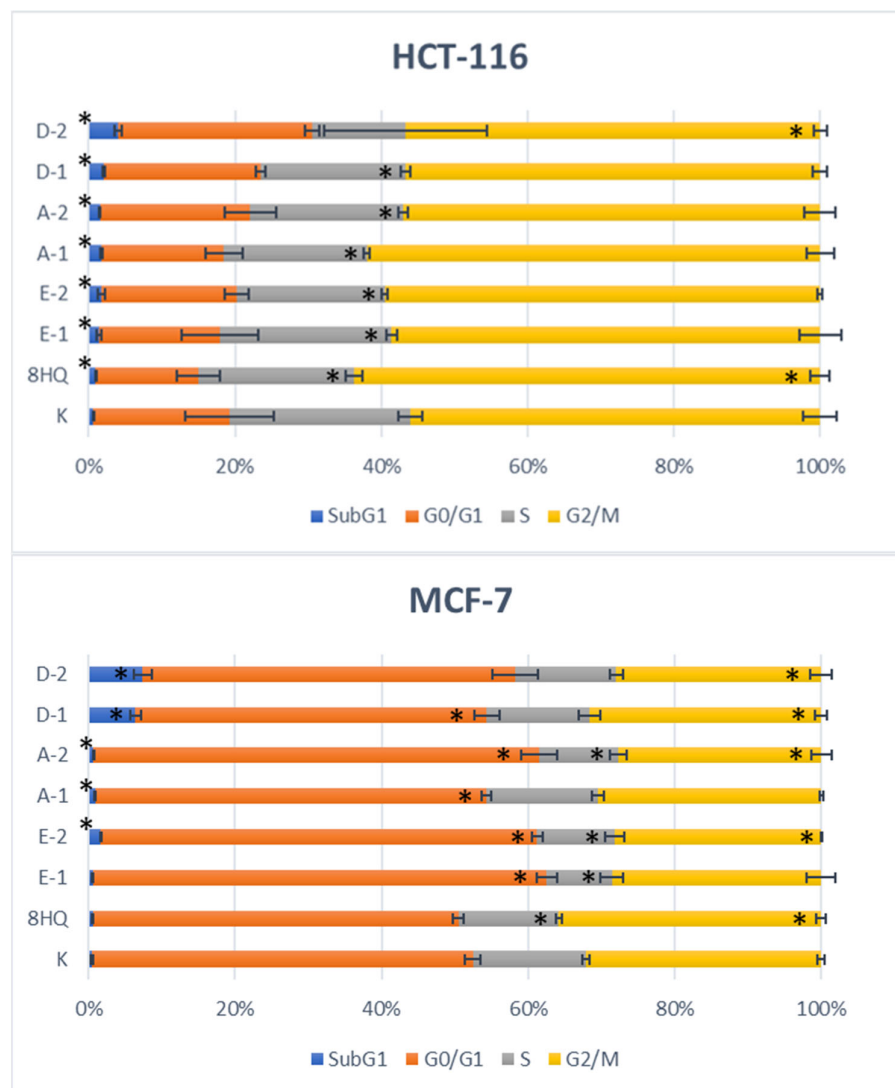
Figure 8. *Cont*.
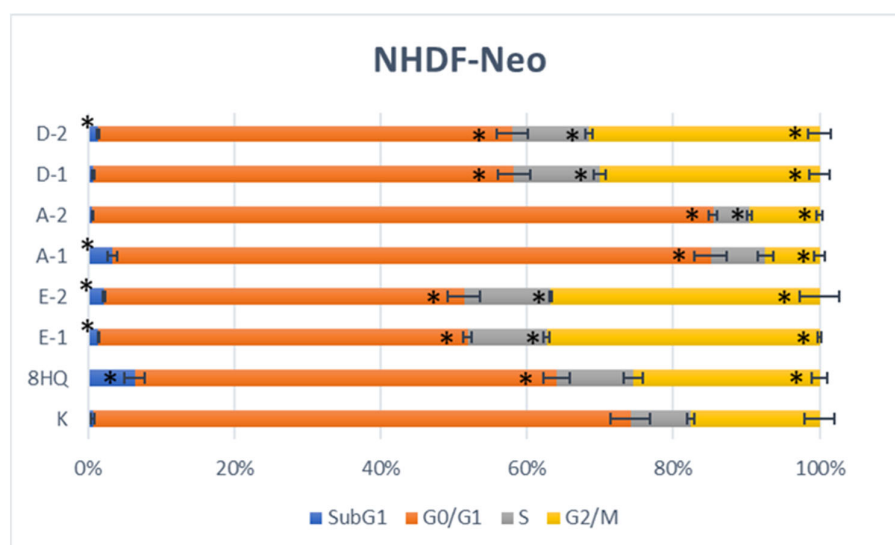
Figure 8. Flow cytometry analysis of HCT-116, MCF-7, and NHDF-Neo cell cycle distribution after incubation for 24 h with test compounds used in their IC$_{50}$ doses. Means $\pm$ SD from three independent experiments. * p-value < 0.05, in comparison to the control.

The cytometric evaluation showed that the tested compounds did not significantly alter the cell cycle phase distribution of the HCT-116 line as compared to populations of untreated control. It cannot be ruled out that the incubation time of cells with solutions of potential drugs turned out to be too short and the extension of the experiment time would change the course of the cell cycle. In the MCF-7 cell line, an increase in the cells of the subG1 fraction was noted for glycoconjugates *type D*. The increase of the subG1 phase corresponds to the apoptotic and necrotic cell fractions. These results are consistent with cytotoxicity and apoptosis studies, in which trehalose derivatives showed the highest cytotoxicity within this cell line. Whereas for glycoconjugates of *type A* and *type E*, an increase in the number of cells in the G0/G1 phase was observed, this also indicates the cytostatic potential of these compounds. In the case of the NHDF-Neo cell line, compounds **A-1** and **A-2** slightly decreased the number of cells in the G2/M phase with a simultaneous slight increase in the percentage of cells in the G0/G1 phase. The other compounds changed the progression of the cell cycle oppositely. Namely, an increased G2/M fraction and a decreased G0/G1 fraction were observed for them. It follows that, under the influence of the tested compounds, the cell cycle was arrested and cell division was inhibited. Changes in this phase of the cycle may also result from the initiation of repair processes of the damaged cell. Moreover, for the healthy cell line, cell's death and damage, presented as the subG1 phase increasing was noted for compound 8HQ, which is consistent with the results of the apoptosis assays.

2.2.6. Intercalation Study

Due to the steric and electron features, quinoline-based compounds are well-known DNA intercalating agents [63]. Therefore, the antiproliferative action of quinoline-related compounds can be related among others to intercalating between two adjacent base pairs of duplex DNA and inhibiting nucleic acid synthesis [64]. In order to evaluate the ability of DNA intercalation by synthesized glycoconjugates, we performed DNA-binding studies on the example of compounds **A-2** and **E-2**. The binding of the **A-2** and **E-2** to ctDNA has been characterized through absorption titration, which is an effective technique for DNA intercalation studies [65]. The experiments were carried out for a constant concentration of glycoconjugates with increasing concentrations of ctDNA. As shown in UV-Vis absorption spectrums (Figure 9) the glycoconjugates show the hypochromic and bathochromic effects that were observed upon binding to increasing concentrations of ctDNA. Both the hypochromic and bathochromic effects strongly suggest that synthesized glycoconjugates

intercalate DNA, due to a strong interaction between the electronic states of the 8HQ scaffold and those of the DNA bases [66]. Accordingly introducing a sugar unit with a triazole linker does not interfere DNA intercalation ability of the 8HQ scaffold.
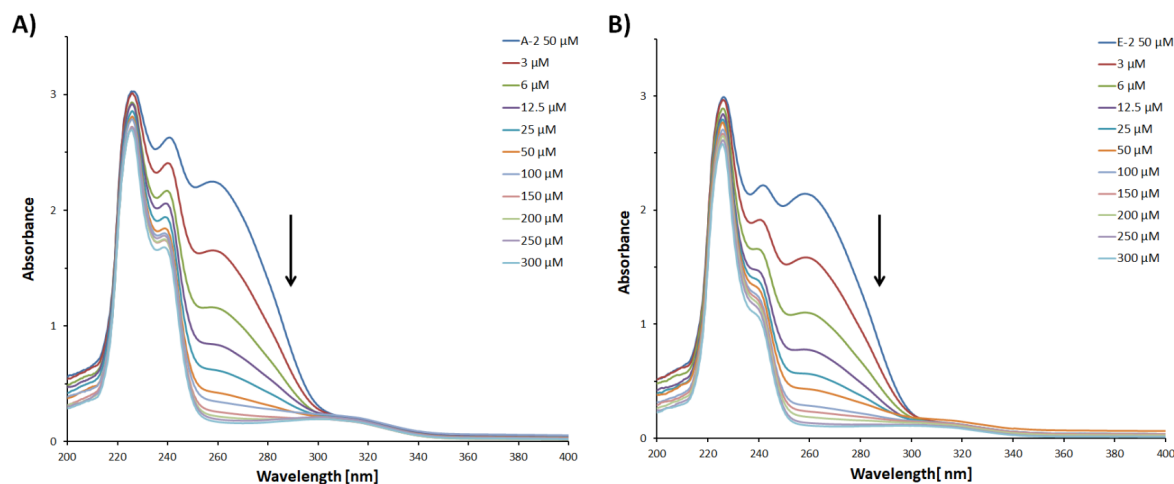
Figure 9. UV-Vis titrations of compounds: (**A**) **A-2** and (**B**) **E-2** with ctDNA.

3. Materials and Methods

3.1. General Information

All used reagents and solvents were purchased from Sigma-Aldrich (Saint Louis, MO, USA), ACROS Organics (Geel, Belgium), and Avantor Performance Materials (Gliwice, Poland) and were used without further purification. All evaporations were performed on a rotary evaporator under reduced pressure at 40 °C. Thin layer chromatography (TLC) was used to monitor the progress of the reaction. The TLC plates precoated of silica gel 60 F254 (Merck Millipore, Burlington, MA, USA) were visualized under UV light (λ = 254 nm) or by charring after spraying with 10% solution of sulfuric acid in ethanol. Column chromatography was carried out on Silica Gel 60 (70–230 mesh, Fluka, St. Louis, MI, USA). NMR spectra were recorded on an Agilent spectrometer at a frequency of 400 MHz using CDCl$_3$, DMSO-d6, or CD$_3$OD as the solvents and tetramethylsilane (TMS) as an internal standard, which were purchased from ACROS Organics (Geel, Belgium). The chemical shifts (δ) values were reported in ppm and the coupling constants (J) in Hz. The following abbreviations were used to explain the observed multiplicities: s: singlet, bs: broad singlet, d: doublet, dd: doublet of doublets, ddd: doublet of doublet of doublets, t: triplet, dd~t: doublet of doublets resembling a triplet (with similar values of coupling constants), q: quintet, m: multiplet. High-resolution mass spectra (HRMS) were recorded on a WATERS LCT Premier XE system using the electrospray ionization (ESI) technique. Optical rotations were measured on a JASCO P-2000 polarimeter using a sodium lamp (λ = 589.3 nm) at room temperature. Melting points were determined on an OptiMelt (MPA 100) Stanford Research Systems. The absorbance on the MTT assay was measured spectrophotometrically at the 570 nm wavelength using a plate reader (Epoch, BioTek, Winooski, VT, USA).

8-(2-Propyn-1-yloxy)quinoline **24** [34], 8-(2-azidoethoxy)quinoline **25** [35], 8-(3-azidopropoxy) quinoline **26** [35] and 2-azidoethanol **28** [67] were synthesized according to the respective published procedures. D-Glucose **1**, D-galactose **7**, D-glucuronic acid **13**, trehalose **17**, propargyl alcohol **27**, 8-hydroxyquinoline (8HQ), and 4,6-*O*-ethylidene-α-D-glucose (EDG) are commercially available (Sigma-Aldrich).

3.2. Chemistry

3.2.1. General Procedure for the Synthesis of Sugar Derivatives

Synthesis of 1,2,3,4-Tetra-O-acetyl-6-O-triphenylmethyl-D-glucopyranose **2**: D-Glucose **1** (1.507 g, 8.365 mmol) was dissolved in pyridine (8 mL), and then trityl chloride (2.350 g, 8.430 mmol) and DMAP (0.180 g, 1.473 mmol) were added. The reaction mixture was stirred for 24 h at room temperature. After this time, acetyl chloride (4 mL) was added in portions to the reaction mixture and stirred for 1 h at room temperature. Then, the reaction diluted with dichloromethane (100 mL) and washed with brine (3 × 30 mL). The organic layer was dried over anhydrous $MgSO_4$, filtered off, and the solvent was concentrated under reduced pressure. The crude product was purified by column chromatography (toluene/ethyl acetate; gradient 100:1 to 10:1) to give product **2** as a white solid (4.155 g, 84%); ratio of anomers (α:β = 1:1.3). ^{1}H NMR (400 MHz, CDCl$_3$): δ 1.73, 1.74, 2.00, 2.01, 2.03, 2.04, 2.15, 2.15 (8s, 24H, 4 × CH$_3$-α, 4 × CH$_3$-β), 3.02 (dd, 1H, *J* = 3.9 Hz, *J* = 10.7 Hz, H6a-α), 3.07 (dd, 1H, *J* = 4.2 Hz, *J* = 10.6 Hz, H6a-β), 3.32 (dd, 1H, *J* = 2.2 Hz, *J* = 10.7 Hz, H6b-α), 3.34 (dd, 1H, *J* = 2.5 Hz, *J* = 10.6 Hz, H6a-β), 3.69 (ddd, 1H, *J* = 2.5 Hz, *J* = 4.2 Hz, *J* = 9.8 Hz, H5-β), 4.02 (ddd, 1H, *J* = 2.2 Hz, *J* = 3.9 Hz, *J* = 10.2 Hz, H5-α), 5.14–5.29 (m, 4H, H2-α, H4-α, H2-β, H4-β), 5.31 (dd~t, 1H, *J* = 9.6 Hz, *J* = 10.1 Hz, H3-β), 5.41 (dd~t, 1H, *J* = 9.7 Hz, *J* = 10.0 Hz, H3-α), 5.72 (d, 1H, *J* = 8.0 Hz, H1-β), 6.44 (d, 1H, *J* = 3.7 Hz, H1-α), 7.12–7.46 (m, 30H, 3 × Ph-α, 3 × Ph-β); ^{13}C NMR (100 MHz, CDCl$_3$): δ 20.42, 20.45, 20.49, 20.60, 20.64, 20.74, 20.87, 20.93 (4 × CH$_3$-α, 4 × CH$_3$-β), 61.24, 61.69 (C6-α, C6-β), 68.29, 68.34, 69.50, 70.36, 70.56, 71.26, 73.19, 74.07 (C2-α, C3-α, C4-α, C5-α, C2-β, C3-β, C4-β, C5-β), 86.54, 86.66 (C-Ph$_3$-α, C-Ph$_3$-β), 89.36, 91.94 (C1-α, C1-β), 127.02, 127.02, 127.79, 127.81, 128.70, 128.72 (C2$_{Ph}$-α, C3$_{Ph}$-α, C4$_{Ph}$-α, C2$_{Ph}$-β, C3$_{Ph}$-β, C4$_{Ph}$-β), 143.46, 143.48 (C1$_{Ph}$-α, C1$_{Ph}$-β), 168.88, 168.89, 168.93, 168.97, 169.33, 169.76, 170.24, 170.43 (4 × CO-α, 4 × CO-β); HRMS (ESI-TOF): calcd for C$_{33}$H$_{34}$O$_{10}$Na ([M + Na]$^+$): *m/z* 613.2050; found: *m/z* 613.2050.

Synthesis of 1,2,3,4-Tetra-O-acetyl-D-glucopyranose **3**: Compound **2** (1.251 g, 2.116 mmol) was suspended in glacial acetic acid (10 mL). The solution was cooled to 0 °C and 33% solution of hydrogen bromide in acetic acid (0.370 mL, 6.494 mmol) was added. Stirring was continued at room temperature for 1 h. After completion, the reaction was diluted with chloroform (50 mL) and water (50 mL). The aqueous phase was washed with chloroform (2 × 30 mL), and the combined organic phases were washed with NaHCO$_3$ (2 × 50 mL) and brine (1 × 50 mL). Next, the organic layer was dried over anhydrous $MgSO_4$, filtered off, and the solvent was concentrated under reduced pressure. The crude product was purified by column chromatography (toluene/ethyl acetate; gradient 20:1 to 1:1) to give product **3** as a yellow oil (0.597 g, 81%); ratio of anomers (α:β = 1:3.3). ^{1}H NMR (400 MHz, CDCl$_3$): δ 2.02, 2.03, 2.03, 2.04, 2.07, 2.08, 2.11, 2.18 (8s, 24H, 4 × CH$_3$-α, 4 × CH$_3$-β), 3.54–3.62 (m, 2H, H6a-α, H6a-β), 3.65 (ddd, 1H, *J* = 2.2 Hz, *J* = 4.2 Hz, *J* = 9.9 Hz, H5-β), 3.69–3.81 (m, 2H, H6b-α, H6b-β), 3.93 (ddd, 1H, *J* = 2.3 Hz, *J* = 4.0 Hz, *J* = 10.2 Hz, H5-α), 5.04–5.15 (m, 4H, H2-α, H4-α, H2-β, H4-β), 5.31 (dd~t, 1H, *J* = 9.5 Hz, *J* = 9.5 Hz, H3-β), 5.53 (dd~t, 1H, *J* = 9.9 Hz, *J* = 10.0 Hz, H3-α), 5.73 (d, 1H, *J* = 8.3 Hz, H1-β), 6.35 (d, 1H, *J* = 3.7 Hz, H1-α); ^{13}C NMR (100 MHz, CDCl$_3$): δ 20.46, 20.56, 20.60, 20.63, 20.69, 20.81, 20.89, 21.33 (4 × CH$_3$-α, 4 × CH$_3$-β), 60.85, 62.44 (C6-α, C6-β), 68.20, 68.31, 69.38, 69.60, 70.43, 72.05, 72.64, 74.92 (C2-α, C3-α, C4-α, C5-α, C2-β, C3-β, C4-β, C5-β), 89.12, 91.74 (C1-α, C1-β), 168.89, 168.98, 169.06, 169.26, 169.66, 170.09, 170.19, 170.26 (4 × CO-α, 4 × CO-β); HRMS (ESI-TOF): calcd for C$_{14}$H$_{20}$O$_{10}$Na ([M + Na]$^+$): *m/z* 371.0954; found: *m/z* 371.0951.

Synthesis of 1,2,3,4-Tetra-O-acetyl-6-O-p-toluenesulfonyl-D-glucopyranose **4**: To a solution of **3** (0.338 g, 0.970 mmol) in pyridine (5 mL), *p*-toluenosulfonyl chloride (0.461 g, 2.418 mmol) and DMAP (23.8 mg, 0.195 mmol) were added. The reaction mixture was stirred at room temperature for 24 h. After completion, the reaction was diluted with water (50 mL) and washed with chloroform (3 × 50 mL). The organic layer was dried over anhydrous $MgSO_4$, filtered off, and the solvent was concentrated under reduced pressure. The crude product was purified by column chromatography (toluene/ethyl acetate; gradient 30:1 to 2:1) to give product **4** as a white solid (0.352 g, 72%); ratio of anomers (α:β = 1:4). ^{1}H NMR (400 MHz,

CDCl$_3$): δ 1.98, 1.99, 2.00, 2.01, 2.02, 2.02, 2.09, 2.16 (8s, 24H, 4 × CH$_3$-α, 4 × CH$_3$-β), 2.46 (s, 6H, Ar-CH$_3$-α, Ar-CH$_3$-β), 3.84 (m, 1H, H5-β), 4.04–5.25 (m, 5H, H5-α, H6a-α, H6b-α, H6a-β, H6b-β), 4.93–5.09 (m, 4H, H2-α, H4-α, H2-β, H4-β), 5.20 (dd~t, 1H, *J* = 9.4 Hz, *J* = 9.4 Hz, H3-β), 5.42 (dd~t, 1H, *J* = 9.6 Hz, *J* = 10.2 Hz, H3-α), 5.65 (d, 1H, *J* = 8.2 Hz, H1-β), 6.21 (d, 1H, *J* = 3.7 Hz, H1-α), 7.32–7.38 (m, 4H, Ar-H-α, Ar-H-β), 7.75–7.80 (m, 4H, Ar-H-α, Ar-H-β); ^{13}C NMR (100 MHz, CDCl$_3$): δ 20.40, 20.49, 20.52, 20.55, 20.58, 20.64, 20.74, 20.84 (4 × CH$_3$-α, 4 × CH$_3$-β), 21.68 (Ar-C̲H$_3$-α, Ar-C̲H$_3$-β), 66.74, 67.16, 67.95, 68.11, 69.00, 69.61, 70.05, 70.29, 72.17, 72.58 (C2-α, C3-α, C4-α, C5-α, C6-α, C2-β, C3-β, C4-β, C5-β, C6-β), 88.70, 91.53 (C1-α, C1-β), 128.16, 129.85, 132.43, 145.13 (Ar-α, Ar-β), 168.62, 168.74, 169.11, 169.26, 169.29, 169.55, 170.08, 170.20 (4 × CO-α, 4 × CO-β); HRMS (ESI-TOF): calcd for C$_{21}$H$_{26}$O$_{12}$SNa ([M + Na]$^+$): *m/z* 525.1043; found: *m/z* 525.1043.

Synthesis of 1,2,3,4-Tetra-O-acetyl-6-azido-6-deoxy-D-glucopyranose **5**: To a solution of **4** (0.319 g, 0.635 mmol) in dry DMF (5 mL), sodium azide (0.208 g, 3.200 mmol) was added. The reaction mixture was stirred at 80 °C for 2 h. After this time, the solution was diluted with chloroform (50 mL) and water (50 mL). The aqueous phase was washed with chloroform (2 × 30 mL), and the combined organic phases were washed with brine (2 × 30 mL). Next, the organic layer was dried over anhydrous MgSO$_4$, filtered off, and the solvent was concentrated at reduced pressure. The crude product was purified by column chromatography (toluene/ethyl acetate; gradient 30:1 to 10:1) to give product **5** as a white solid (0.216 g, 91%); ratio of anomers (α:β = 1.7:1). ^{1}H NMR (400 MHz, CDCl$_3$): δ 2.02, 2.02, 2.03, 2.04, 2.04, 2.05, 2.12, 2.19 (8s, 24H, 4 × CH$_3$-α, 4 × CH$_3$-β), 3.27–3.45 (m, 4H, H6a-α, H6b-α, H6a-β, H6b-β), 3.81 (ddd, 1H, *J* = 3.4 Hz, *J* = 5.2 Hz, *J* = 9.9 Hz, H5-β), 4.08 (ddd, 1H, *J* = 2.8 Hz, *J* = 5.5 Hz, *J* = 10.1 Hz, H5-α), 5.04–5.17 (m, 4H, H2-α, H4-α, H2-β, H4-β), 5.25 (dd~t, 1H, *J* = 9.4 Hz, *J* = 9.4 Hz, H3-β), 5.47 (dd~t, 1H, *J* = 9.7 Hz, *J* = 10.0 Hz, H3-α), 5.73 (d, 1H, *J* = 8.3 Hz, H1-β), 6.36 (d, 1H, *J* = 3.7 Hz, H1-α); ^{13}C NMR (100 MHz, CDCl$_3$): δ 20.44, 20.55, 20.57, 20.59, 20.66, 20.75, 20.82, 20.85 (4 × CH$_3$-α, 4 × CH$_3$-β), 50.65, 50.73 (C6-α, C6-β), 69.01, 69.07, 69.17, 69.68, 70.15, 70.92, 72.69, 73.84 (C2-α, C3-α, C4-α, C5-α, C2-β, C3-β, C4-β, C5-β), 88.88, 91.54 (C1-α, C1-β), 168.69, 168.93, 169.20, 169.42, 169.61, 169.93, 170.11, 170.24 (4 × CO-α, 4 × CO-β); HRMS (ESI-TOF): calcd for C$_{14}$H$_{19}$N$_3$O$_9$Na ([M + Na]$^+$): *m/z* 396.1019; found: *m/z* 396.1022.

Synthesis of 6-Azido-6-deoxy-D-glucopyranose **6**: Compound **5** (0.479 g, 1.283 mmol) was suspended in MeOH (10 mL), and then 1 M solution of MeONa in MeOH (1.3 mL, 1.3 mmol) was added. The reaction mixture was stirred for 0.5 h at room temperature. The reaction progress was monitored on TLC. After the reaction was complete, the mixture was neutralized with *Amberlyst*-15 ion exchange resin, filtered off, and the filtrate was concentrated under reduced pressure to give product **6** as a white solid (0.218 g, 83%); ratio of anomers (α:β = 1:1). ^{1}H NMR (400 MHz, DMSO): δ 2.93 (dd, 1H, *J* = 7.7 Hz, *J* = 8.9 Hz, H2-β), 2.99–3.05 (m, 2H, H4-α, H4-β), 3.10–3.17 (m, 2H, H2-α, H3-β), 3.23–3.31 (m, 2H, H3-α, H5-β), 3.32–3.42 (m, 2H, H6a-α, H6a-β), 3.43–3.52 (m, 2H, H6b-α, H6b-β), 3.74 (ddd, 1H, *J* = 2.4 Hz, *J* = 6.4 Hz, *J* = 9.3 Hz, H5-α), 4.31 (d, 1H, *J* = 7.7 Hz, H1-β), 4.93 (d, 1H, *J* = 3.6 Hz, H1-α); ^{13}C NMR (100 MHz, DMSO): δ51.60, 51.69 (C6-α, C6-β), 70.45, 70.93, 71.34, 72.22, 72.71, 74.60, 74.64, 76.34 (C2-α, C3-α, C4-α, C5-α, C2-β, C3-β, C4-β, C5-β), 92.43, 97.06 (C1-α, C1-β); HRMS (ESI-TOF): calcd for C$_6$H$_{11}$N$_3$O$_5$Na ([M + Na]$^+$): *m/z* 228.0596; found: *m/z* 228.0604.

Synthesis of 1,2:3,4-Di-O-isopropylidene-α-D-galactopyranose **8**: To a solution of D-galactose **7** (3.122 g, 17.329 mmol) in dry acetone (150 mL), iodine (0.923 g, 3.637 mmol) was added. The reaction mixture was stirred at room temperature for 24 h. After the completion reaction, 10% Na$_2$S$_2$O$_3$ aqueous solution (18 mL) was added to the reaction mixture and then the solvent was evaporated under reduced pressure. The residue was diluted with dichloromethane (150 mL) and washed with brine (2 × 50 mL). The organic layer was dried over anhydrous MgSO$_4$, filtered off, and the solvent was concentrated under reduced pressure. The crude product was purified by column chromatography (toluene/ethyl

acetate; gradient 44:1 to 2:1) to give product **8** as a yellow oil (4.150 g, 92%). $[\alpha]^{26}_D = -50.4$ (c = 1.0, CHCl$_3$); ^{1}H NMR (400 MHz, CDCl$_3$): δ 1.34, 1.34, 1.46, 1.54 (4s, 12H, 4 × CH$_3$), 3.75 (m, 1H, H5), 3.83–3.91 (m, 2H, H6a, H6b), 4.28 (dd, 1H, *J* = 1.7 Hz, *J* = 7.9 Hz, H4), 4.34 (dd, 1H, *J* = 2.4 Hz, *J* = 5.0 Hz, H2), 4.62 (dd, 1H, *J* = 2.4 Hz, *J* = 7.9 Hz, H3), 5.57 (d, 1H, *J* = 5.0 Hz, H1); ^{13}C NMR (100 MHz, CDCl$_3$): δ 24.45, 25.08, 26.07, 26.18 (4xCH$_3$), 62.49 (C6), 68.23, 70.73, 70.91, 71.76 (C2, C3, C4, C5), 96.44 (C1), 108.82, 109.62 (2 × $\underline{C}$(CH$_3$)$_2$); HRMS (ESI-TOF): calcd for C$_{12}$H$_{20}$O$_6$Na ([M + Na]$^+$): *m/z* 283.1158; found: *m/z* 283.1162.

Synthesis of 1,2:3,4-Di-O-isopropylidene-6-O-p-toluenesulfonyl-α-D-galactopyranose **9**: To a solution of compound **8** (1.324 g, 5.087 mmol) in pyridine (10 mL), *p*-toluenosulfonyl chloride (2.378 g, 12.473 mmol) and DMAP (0.120 g, 0.982 mmol) were added. The reaction mixture was stirred at room temperature for 24 h. After completion, the reaction was diluted with water (80 mL) and washed with chloroform (3 × 80 mL). The organic layer was dried over anhydrous MgSO$_4$, filtered off, and the solvent was concentrated under reduced pressure. The crude product was purified by column chromatography (toluene/ethyl acetate; gradient 100:1 to 5:1) to give product **9** as a yellow oil (1.886 g, 90%). $[\alpha]^{26}_D = -24.4$ (c = 1.0, CHCl$_3$); ^{1}H NMR (400 MHz, CDCl$_3$): δ 1.28, 1.32, 1.35, 1.50 (4s, 12H, 4 × CH$_3$), 2.44 (s, 3H, Ar-CH$_3$), 4.02–4.13 (m, 2H, H6a, H6b), 4.17–4.23 (m, 2H, H4, H5), 4.29 (dd, 1H, *J* = 2.5 Hz, *J* = 5.0 Hz, H2), 4.59 (dd, 1H, *J* = 2.5 Hz, *J* = 7.9 Hz, H3), 5.46 (d, 1H, *J* = 5.0 Hz, H1), 7.33 (d, 2H, *J* = 8.2 Hz, Ar-H), 7.81 (d, 2H, *J* = 8.2 Hz, Ar-H); ^{13}C NMR (100 MHz, CDCl$_3$): δ 21.63 (Ar-$\underline{C}$H$_3$), 24.36, 24.92, 25.82, 25.99 (4 × CH$_3$), 65.88 (C6), 68.20, 70.38, 70.42, 70.53 (C2, C3, C4, C5), 96.13 (C1), 108.95, 109.59 (2 × $\underline{C}$(CH$_3$)$_2$), 128.12, 129.74, 132.84, 144.75 (Ar); HRMS (ESI-TOF): calcd for C$_{19}$H$_{26}$O$_8$SNa ([M + Na]$^+$): *m/z* 437.1246; found: *m/z* 473.1248.

Synthesis of 1,2:3,4-Di-O-isopropylidene-6-azido-6-deoxy-α-D-galactopyranose **10**: To a solution of compound **9** (0.798 g, 1.925 mmol) in dry DMF (7 mL), sodium azide (0.507 g, 7.799 mmol) was added. The reaction mixture was stirred at 120 °C for 24 h. After this time, the reaction was diluted with chloroform (30 mL) and water (30 mL). The aqueous phase was washed with chloroform (2 × 30 mL), and the combined organic phases were washed with water (1 × 30 mL) and brine (1 × 30 mL). Next, the organic layer was dried over anhydrous MgSO$_4$, filtered off, and the solvent was concentrated under reduced pressure. The crude product was purified by column chromatography (toluene/ethyl acetate; gradient 30:1 to 10:1) to give product **10** as a colorless oil (0.432 g, 79%). $[\alpha]^{24}_D = -104.2$ (c = 1.0, CHCl$_3$); ^{1}H NMR (400 MHz, CDCl$_3$): δ 1.34, 1.35, 1.46, 1.55 (4s, 12H, 4 × CH$_3$), 3.37 (dd, 1H, *J* = 5.4 Hz, *J* = 12.7 Hz, H6a), 3.52 (dd, 1H, *J* = 7.8 Hz, *J* = 12.7 Hz, H6b), 3.92 (ddd, 1H, *J* = 2.0 Hz, *J* = 5.4 Hz, *J* = 7.8 Hz, H5), 4.20 (dd, 1H, *J* = 2.0 Hz, *J* = 7.9 Hz, H4), 4.34 (dd, 1H, *J* = 2.5 Hz, *J* = 5.0 Hz, H2), 4.63 (dd, 1H, *J* = 2.5 Hz, *J* = 7.9 Hz, H3), 5.55 (d, 1H, *J* = 5.0 Hz, H1); ^{13}C NMR (100 MHz, CDCl$_3$): δ 24.44, 24.89, 25.95, 26.03 (4 × CH$_3$), 50.68 (C6), 67.00, 70.40, 70.81, 71.17 (C2, C3, C4, C5), 96.35 (C1), 108.81, 109.63 (2 × $\underline{C}$(CH$_3$)$_2$); HRMS (ESI-TOF): calcd for C$_{12}$H$_{19}$N$_3$O$_5$Na ([M + Na]$^+$): *m/z* 308.1222; found: *m/z* 308.1224.

Synthesis of 6-Azido-6-deoxy-D-galactopyranose **11**: Compound **10** (0.410 g, 1.437 mmol) was suspended in water (0.9 mL). The solution was cooled to 0 °C and trifluoroacetic acid (3.5 mL) was added in portions. Stirring was continued at room temperature for 2 h. After completion, the reaction mixture was concentrated under reduced pressure with the addition of *i*-propanol. Next, the residue was purified by column chromatography (dry loading: chloroform/methanol; gradient 50:1 to 5:1) to give product **11** as a white solid (0.193 g, 65%); ratio of anomers (α:β = 6.3:1). ^{1}H NMR (400 MHz, DMSO): δ 3.17 (m, 1H, H6a-β), 3.28 (dd, 1H, *J* = 4.3 Hz, *J* = 12.7 Hz, H6a-α), 3.37–3.47 (m, 2H, H6b-α, H6b-β), 3.48–3.59 (m, 4H, H2-α, H2-β, H3-α, H3-β), 3.61 (m, 1H, H5-α), 3.68 (m, 1H, H5-β), 3.95 (dd, 1H, *J* = 4.2 Hz, *J* = 8.6 Hz, H4-α), 4.09 (dd, 1H, *J* = 5.2 Hz, *J* = 10.5 Hz, H4-β), 4.26 (t, 1H, *J* = 7.1 Hz, OH-β), 4.33 (d, 1H, *J* = 6.6 Hz, OH-α), 4.53 (d, 1H, *J* = 5.2 Hz, OH-α), 4.54 (d, 1H, *J* = 6.7 Hz, OH-α), 4.58 (d, 1H, *J* = 4.5 Hz, OH-β), 4.71 (d, 1H, *J* = 5.2 Hz, OH-β), 4.75 (d, 1H, *J* = 4.3 Hz, OH-β), 4.95 (t, 1H, *J* = 4.1 Hz, OH-α), 6.29 (d, 1H, *J* = 4.8 Hz, H1-α), 6.62 (d, 1H, *J* = 6.9 Hz, H1-β); ^{13}C NMR (100 MHz, DMSO): δ 51.36, 51.46 (C6-α, C6-β), 68.40, 68.83,

68.97, 69.60 (C2-α, C3-α, C4-α, C5-α), 71.72, 71.74, 72.97, 73.08 (C2-β, C3-β, C4-β, C5-β), 92.71 (C1-α), 97.42 (C1-β); HRMS (ESI-TOF): calcd for $C_6H_{11}N_3O_5Na$ ([M + Na]$^+$): *m/z* 228.0596; found: *m/z* 228.0595.

Synthesis of 1,2,3,4-Tetra-O-acetyl-6-azido-6-deoxy-D-galactopyranose **12**: Unprotected compound **11** (0.308 g, 1.501 mmol) was suspended in acetic anhydride (5 mL) and sodium acetate (0.286 g, 3.487 mmol) was added. The reaction mixture was heated to reflux for 1 h. After completion, the reaction was diluted with water (30 mL) and chloroform (30 mL). The aqueous phase was washed with chloroform (3 × 30 mL), and the combined organic phases were washed with NaHCO$_3$ (1 × 30 mL) and brine (1 × 30 mL). Next, the organic layer was dried over anhydrous MgSO$_4$, filtered off, and the solvent was concentrated under reduced pressure. The crude product was purified by column chromatography (toluene/ethyl acetate; gradient 30:1 to 10:1) to give product **12** as a colorless oil (0.377 g, 67%); ratio of anomers (α:β = 1:2.6). ^{1}H NMR (400 MHz, CDCl$_3$): δ 2.00, 2.05, 2.12, 2.19 (4s, 12H, 4xCH$_3$-β), 2.01, 2.02, 2.17, 2.18 (4s, 12H, 4 × CH$_3$-α), 3.22 (dd, 1H, *J* = 5.4 Hz, *J* = 12.8 Hz, H6a-β), 3.23 (dd, 1H, *J* = 5.5 Hz, *J* = 12.8 Hz, H6a-α), 3.45 (dd, 1H, *J* = 7.4 Hz, *J* = 12.8 Hz, H6b-α), 3.53 (dd, 1H, *J* = 7.4 Hz, *J* = 12.8 Hz, H6b-β), 3.95 (m, 1H, H5-β), 4.23 (m, 1H, H5-α), 5.08 (dd, 1H, *J* = 3.4 Hz, *J* = 10.4 Hz, H3-β), 5.30–5.37 (m, 3H, H2-β, H2-α, H3-α), 5.41 (dd, 1H, *J* = 1.1 Hz, *J* = 3.4 Hz, H4-β), 5.48 (m, 1H, H4-α), 5.72 (d, 1H, *J* = 8.3 Hz, H1-β), 6.40 (bs, 1H, H1-α); ^{13}C NMR (100 MHz, CDCl$_3$): δ 20.52, 20.53, 20.61, 20.63, 20.65, 20.68, 20.76, 20.88 (4 × CH$_3$-α, 4 × CH$_3$-β), 50.08, 50.32 (C6-α, C6-β), 66.36, 67.37, 67.52, 67.69, 68.14, 70.13, 70.83, 73.20 (C2-α, C3-α, C4-α, C5-α, C2-β, C3-β, C4-β, C5-β), 89.63, 92.13 (C1-α, C1-β), 168.86, 168.88, 169.36, 169.39, 169.87, 169.88, 170.05, 170.08 (4 × CO-α, 4 × CO-β); HRMS (ESI-TOF): calcd for $C_{14}H_{19}N_3O_9Na$ ([M + Na]$^+$): *m/z* 396.1019; found: *m/z* 396.1020.

Synthesis of 1,2,3,4-Tetra-O-acetyl-β-D-glucopyranuronic acetic anhydride **14**: D-Glucuronic acid **13** (2.003 g, 10.317 mmol) was suspended in acetic anhydride (30 mL). The solution was cooled to 0 °C and iodine (150.0 mg, 0.591 mmol) was added. Stirring was continued at 0 °C for 1 h and further at room temperature for 3 h. After the completion reaction, acetic anhydride was removed under reduced pressure, and the residue was diluted with dichloromethane (40 mL) and washed with 1M Na$_2$S$_2$O$_3$ (2 × 40 mL). The organic layer was dried over anhydrous MgSO$_4$, filtered off, and the solvent was concentrated under reduced pressure and recrystallized from dichloromethane/hexane to give product **14** as a white solid (3.511 g, 84%). ^{1}H NMR (400 MHz, CDCl$_3$): δ 2.04, 2.06, 2.07, 2.13, 2.28 (5s, 15H, 5 × CH$_3$), 4.34 (d, 1H, *J* = 9.2 Hz, H5), 5.13 (dd, 1H, *J* = 6.9 Hz, *J* = 8.6 Hz, H2), 5.30 (dd~t, 1H, *J* = 8.6 Hz, *J* = 9.1 Hz, H3), 5.38 (dd~t, 1H, *J* = 9.1 Hz, *J* = 9.2 Hz, H4), 5.82 (d, 1H, *J* = 6.9 Hz, H1); ^{13}C NMR (100 MHz, CDCl$_3$): δ 20.58, 20.64, 20.64, 20.81, 22.19 (5 × CH$_3$), 68.20, 70.19, 71.44, 73.13 (C2, C3, C4, C5), 91.49 (C1), 162.69 (C6), 164.87, 168.80, 169.33, 169.48, 169.97 (5 × <u>C</u>OCH$_3$); HRMS (ESI-TOF): calcd for $C_{16}H_{20}O_{12}Na$ ([M + Na]$^+$): *m/z* 427.0852; found: *m/z* 427.0851.

Synthesis of 1,2,3,4-Tetra-O-acetyl-N-(prop-2-yn-1-yl)-β-D-glucopyranuronic acid amide **15**: To a solution of anhydride **14** (1.7 g, 4.205 mmol) in dry dichloromethane (20 mL), propargyl amine (400 µL, 6.245 mmol) was added. The reaction mixture was stirred overnight at room temperature. Afterward, the solvent was evaporated under reduced pressure, and the residue was purified by column chromatography (toluene/ethyl acetate; gradient 50:1 to 5:1) to give product **15** as a white solid (0.745 g, 44%). ^{1}H NMR (400 MHz, CDCl$_3$): δ 2.03, 2.05, 2.08, 2.15 (4s, 12H, 4 × CH$_3$), 2.26 (t, 1H, *J* = 2.6 Hz, CCH), 4.03 (m, 2H, CH$_2$), 4.12 (d, 1H, *J* = 9.6 Hz, H5), 5.11 (dd, 1H, *J* = 7.9 Hz, *J* = 8.9 Hz, H2), 5.22 (dd~t, 1H, *J* = 9.2 Hz, *J* = 9.6 Hz, H4), 5.31 (dd~t, 1H, *J* = 8.9 Hz, *J* = 9.2 Hz, H3), 5.77 (d, 1H, *J* = 7.9 Hz, H1), 6.50 (t, 1H, *J* = 5.1 Hz, NH); ^{13}C NMR (100 MHz, CDCl$_3$): δ 20.54, 20.54, 20.68, 20.78 (4 × CH$_3$), 28.92 (CH$_2$), 68.75, 70.23, 71.94, 72.12 (C2, C3, C4, C5), 72.88 (C<u>C</u>H), 78.62 (<u>C</u>CH), 91.40 (C1), 165.71 (CONH), 168.78, 169.23, 169.61, 169.81 (4 × <u>C</u>OCH$_3$); HRMS (ESI-TOF): calcd for $C_{17}H_{21}NO_{10}Na$ ([M + Na]$^+$): *m/z* 422.1063; found: *m/z* 422.1064.

Synthesis of N-(prop-2-yn-1-yl)-D-glucopyranuronic acid amide **16**: Acetylated amide **15** (0.526 g, 1.317 mmol) was suspended in MeOH (20 mL), and then 1 M solution of MeONa in MeOH (1.3 mL, 1.3 mmol) was added. The reaction mixture was stirred for 0.5 h at room temperature. The reaction progress was monitored on TLC. After the reaction was complete, the mixture was neutralized with *Amberlyst*-15 ion exchange resin, filtered off, and the filtrate was concentrated under reduced pressure to give product **16** as a white solid (0.301 g, 99%); ratio of anomers (α:β = 1.3:1). ^{1}H NMR (400 MHz, CD$_3$OD): δ 2.55–2.60 (m, 2H, CCH-α, CCH-β), 3.18 (dd, 1H, *J* = 7.8 Hz, *J* = 9.2 Hz, H2-β), 3.36–3.52 (m, 4H, H2-α, H3-β, H4-α, H4-β), 3.69 (d, 1H, *J* = 9.7 Hz, H5-β), 3.72 (dd~t, 1H, *J* = 9.2 Hz, *J* = 9.6 Hz, H3-α), 3.98–4.02 (m, 4H, CH$_2$-α, CH$_2$-β), 4.18 (d, 1H, *J* = 9.9 Hz, H5-α), 4.53 (d, 1H, *J* = 7.8 Hz, H1-β), 5.18 (d, 1H, *J* = 3.7 Hz, H1-α), 8.52 (s, 2H, NH-α, NH-β); ^{13}C NMR (100 MHz, CD$_3$OD): δ 29.17, 29.24 (CH$_2$-α, CH$_2$-β), 71.91, 72.19, 73.30, 73.50, 73.98, 74.41, 75.80, 76.29 (C2-α, C3-α, C4-α, C5-α, C2-β, C3-β, C4-β, C5-β), 72.13, 72.33 (C$\underline{C}$H-α, C$\underline{C}$H-β), 80.32, 80.43 ($\underline{C}$CH-α, $\underline{C}$CH-β), 94.27, 98.52 (C1-α, C1-β), 169.97, 171.69 (CONH-α, CONH-β); HRMS (ESI-TOF): calcd for C$_9$H$_{13}$NO$_6$Na ([M + Na]$^+$): *m/z* 254.0641; found: *m/z* 254.0641.

Synthesis of 6,6′-Dibromo-6,6′-dideoxy-D-trehalose **18**: To a solution of D-trehalose **17** (1.008 g, 2.945 mmol) in dry DMF (10 mL), triphenylphosphine (3.325 g, 12.677 mmol) and NBS (2.268 g, 12.742 mmol) were added. The reaction mixture was stirred at room temperature for 72 h. Afterward, the solvent was evaporated under reduced pressure, and the residue was purified by column chromatography (chloroform/methanol; gradient 50:1 to 1:1) to give product **18** as a white solid (1.368 g, 99%). m.p.: 131–132 °C; [α]$^{24}_D$ = 109.0 (c = 1.0, DMSO); ^{1}H NMR (400 MHz, DMSO): δ 3.11 (dd~t, 2H, *J* = 9.1 Hz, *J* = 9.2 Hz, 2 × H4), 3.27 (dd, 2H, *J* = 3.6 Hz, *J* = 9.5 Hz, 2 × H2), 3.52–3.63 (m, 4H, 2 × H3, 2 × H6a), 3.69 (dd, 2H, *J* = 2.3 Hz, *J* = 10.8 Hz, 2 × H6b), 3.87 (ddd, 2H, *J* = 2.3 Hz, *J* = 5.5 Hz, *J* = 9.3 Hz, 2 × H5), 4.92 (d, 2H, *J* = 3.6 Hz, 2 × H1); ^{13}C NMR (100 MHz, DMSO): δ 35.57 (2 × C6), 70.35, 71.35, 72.02, 72.41 (2 × C2, 2 × C3, 2 × C4, 2 × C5), 93.40 (2 × C1); HRMS (ESI-TOF): calcd for C$_{12}$H$_{20}$Br$_2$O$_9$Na ([M + Na]$^+$): *m/z* 488.9372; found: *m/z* 488.9367.

Synthesis of 6,6′-Diiodo-6,6′-dideoxy-D-trehalose **19**: To a solution of D-trehalose **17** (1.018 g, 2.974 mmol) in dry DMF (10 mL), triphenylphosphine (3.281 g, 12.509 mmol) and iodine (3.224 g, 12.702 mmol) were added. The reaction mixture was stirred at room temperature for 72 h. Afterward, the solvent was evaporated under reduced pressure, and the residue was purified by column chromatography (chloroform/methanol; gradient 50:1 to 1:1) to give product **19** as a white solid (1.588 g, 95%). m.p.: 62–63 °C; [α]$^{24}_D$ = 95.0 (c = 1.0, DMSO); ^{1}H NMR (400 MHz, DMSO): δ 3.00 (m, 2H, 2 × H4), 3.26–3.35 (m, 4H, 2 × H2, 2 × H6a), 3.45–3.52 (m, 4H, 2 × H3, 2 × H6b), 3.59 (m, 2H, 2 × H5), 4.81 (d, 2H, *J* = 6.2 Hz, 2 × OH), 4.91 (m, 2H, 2 × OH), 4.96 (d, 2H, *J* = 3.7 Hz, 2 × H1), 5.16 (d, 2H, *J* = 5.4 Hz, 2 × OH); ^{13}C NMR (100 MHz, DMSO): δ 10.59 (2 × C6), 69.92, 71.39, 72.12, 73.96 (2 × C2, 2 × C3, 2 × C4, 2 × C5), 93.19 (2 × C1); HRMS (ESI-TOF): calcd for C$_{12}$H$_{20}$I$_2$O$_9$Na ([M + Na]$^+$): *m/z* 584.9094; found: *m/z* 584.9090.

Synthesis of 6,6′-Diazido-6,6′-dideoxy-D-trehalose **20** *(Procedure A)*: To a solution of **18** (1.234 g, 2.637 mmol) in dry DMF (20 mL), sodium azide (1.030 g, 15.844 mmol) was added. The reaction mixture was stirred at 60 °C for 24 h. After completion reaction, the residual salt was filtered off and the solvent was concentrated under reduced pressure. The residue was purified by column chromatography (chloroform/methanol; gradient 20:1 to 1:1) to give product **20** as a white solid (0.568 g, 55%).

Synthesis of 6,6′-Diazido-6,6′-dideoxy-D-trehalose **20** *(Procedure B)*: Compound **23** (0.202 g, 0.313 mmol) was suspended in MeOH (10 mL), and then 1 M solution of MeONa in MeOH (0.5 mL, 0.5 mmol) was added. The reaction mixture was stirred for 1 h at room temperature. The reaction progress was monitored on TLC. After the reaction was complete, the mixture was neutralized with *Amberlyst*-15 ion exchange resin, filtered off, and the filtrate was concentrated under reduced pressure to give product **20b** as a white solid (0.107 g, 87%). m.p.: 144 °C; [α]$^{24}_D$ = 47.0 (c = 1.0, DMSO); ^{1}H NMR (400 MHz, DMSO): δ 3.10 (m, 2H,

2 × H4), 3.29 (m, 2H, 2 × H2), 3.39 (m, 4H, 2 × H6a, 2 × H6b), 3.54 (m, 2H, 2 × H3), 3.95 (m, 2H, 2 × H5), 4.86–4.93 (m, 6H, 2 × H1, 4 × OH), 5.12 (d, 2H, J = 5.3 Hz, 2 × OH); ^{13}C NMR (100 MHz, DMSO): δ 51.26 (2 × C6), 70.95, 71.30, 71.37, 72.46 (2 × C2, 2 × C3, 2 × C4, 2 × C5), 93.91 (2 × C1); HRMS (ESI-TOF): calcd for $C_{12}H_{20}N_6O_9Na$ ([M + Na]$^+$): m/z 415.1189; found: m/z 415.1193.

Synthesis of 2,3,4,2′,3′,4′-Hexa-O-acetyl-6,6′-dibromo-6,6′-dideoxy-D-trehalose **21**: Compound **18** (1 g, 2.136 mmol) was dissolved in pyridine (3 mL), the solution was cooled to 0 °C and Ac$_2$O (3 mL) was added. Stirring was continued overnight at room temperature. After completion, the reaction solution was poured into ice water. The precipitated crystals are filtered off under reduced pressure and recrystallized from methanol to give product **21** as a white solid (1.072 g, 70%). m.p.: 161 °C; [α]$^{24}_D$ = 114.0 (c = 1.0, CHCl$_3$); ^{1}H NMR (400 MHz, CDCl$_3$): δ 2.03, 2.08, 2.13 (3s, 18H, 6 × CH$_3$), 3.32 (dd, 2H, J = 7.8 Hz, J = 11.2 Hz, 2 × H6a), 3.39 (dd, 2H, J = 2.6 Hz, J = 11.2 Hz, 2 × H6b), 4.12 (ddd, 2H, J = 2.6 Hz, J = 7.8 Hz, J = 10.1 Hz, 2 × H5), 4.97 (dd, 2H, J = 9.2 Hz, J = 10.1 Hz, 2 × H4), 5.16 (dd, 2H, J = 3.9 Hz, J = 10.2 Hz, 2 × H2), 5.38 (d, 2H, J = 3.9 Hz, 2 × H1), 5.49 (dd, 2H, J = 9.2 Hz, J = 10.2 Hz, 2 × H3); ^{13}C NMR (100 MHz, CDCl$_3$): δ 20.66, 20.68, 20.94 (6 × CH$_3$), 30.40 (2 × C6), 69.36, 69.80, 69.96, 71.23 (2 × C2, 2 × C3, 2 × C4, 2 × C5), 91.91 (2 × C1), 169.47, 169.57, 169.92 (6 × CO); HRMS (ESI-TOF): calcd for $C_{24}H_{32}Br_2O_{15}Na$ ([M + Na]$^+$): m/z 741.0006; found: m/z 741.0008.

Synthesis of 2,3,4,2′,3′,4′-Hexa-O-acetyl-6,6′-diiodo-6,6′-dideoxy-D-trehalose **22**: Compound **19** (1.646 g, 2.928 mmol) was dissolved in pyridine (5 mL), the solution was cooled to 0 °C and Ac$_2$O (5 mL) was added. Stirring was continued overnight at room temperature. After completion, the reaction solution was poured into ice water. The precipitated crystals are filtered off under reduced pressure and recrystallized from methanol to give product **22** as a white solid (1.788 g, 75%). m.p.: 190 °C; [α]$^{23}_D$ = 84.2 (c = 1.0, CHCl$_3$); ^{1}H NMR (400 MHz, CDCl$_3$): δ 2.02, 2.08, 2.15 (3s, 18H, 6 × CH$_3$), 3.07 (dd, 2H, J = 9.0 Hz, J = 10.9 Hz, 2 × H6a), 3.23 (dd, 2H, J = 2.5 Hz, J = 10.9 Hz, 2 × H6b), 3.96 (ddd, 2H, J = 2.5 Hz, J = 9.0 Hz, J = 9.8 Hz, 2 × H5), 4.90 (dd, 2H, J = 9.2 Hz, J = 9.8 Hz, 2 × H4), 5.20 (dd, 2H, J = 3.9 Hz, J = 10.2 Hz, 2 × H2), 5.42 (d, 2H, J = 3.9 Hz, 2 × H1), 5.48 (dd, 2H, J = 9.2 Hz, J = 10.2 Hz, 2 × H3); ^{13}C NMR (100 MHz, CDCl$_3$): δ 2.49 (2 × C6), 20.64, 20.70, 21.20 (6 × CH$_3$), 69.30, 69.75, 69.96, 72.34 (2 × C2, 2 × C3, 2 × C4, 2 × C5), 91.78 (2 × C1), 169.45, 169.58, 169.91 (6 × CO); HRMS (ESI-TOF): calcd for $C_{24}H_{32}I_2O_{15}Na$ ([M + Na]$^+$): m/z 836.9728; found: m/z 836.9733.

Synthesis of 2,3,4,2′,3′,4′-Hexa-O-acetyl-6,6′-diazido-6,6′-dideoxy-D-trehalose **23**: To a solution of **21** or **22** (0.484 g, 0.672 mmol) in dry DMF (10 mL), sodium azide (0.273 g, 4.199 mmol) was added. The reaction mixture was stirred at 60 °C for 24 h. After completion, the reaction was diluted with ethyl acetate (30 mL) and water (30 mL). The aqueous phase was washed with ethyl acetate (2 × 30 mL), and the combined organic phases were washed with water (1 × 30 mL) and brine (1 × 30 mL). Next, the organic layer was dried over anhydrous MgSO$_4$, filtered, and the solvent was concentrated under reduced pressure. The crude product was purified by column chromatography (toluene/ethyl acetate; gradient 20:1 to 1:1) to give product **23** as a white solid (0.425 g, 98%). m.p.: 150–151 °C; [α]$^{24}_D$ = 39.5 (c = 1.0, CHCl$_3$); ^{1}H NMR (400 MHz, CDCl$_3$): δ 2.03, 2.07, 2.13 (3s, 18H, 6 × CH$_3$), 3.17 (dd, 2H, J = 2.5 Hz, J = 13.3 Hz, 2 × H6a), 3.37 (dd, 2H, J = 7.3 Hz, J = 13.3 Hz, 2 × H6b), 4.09 (ddd, 2H, J = 2.5 Hz, J = 7.3 Hz, J = 10.2 Hz, 2 × H5), 5.00 (dd, 2H, J = 9.3 Hz, J = 10.2 Hz, 2 × H4), 5.09 (dd, 2H, J = 3.9 Hz, J = 10.3 Hz, 2 × H2), 5.34 (d, 2H, J = 3.9 Hz, 2 × H1), 5.48 (dd, 2H, J = 9.3 Hz, J = 10.3 Hz, 2 × H3); ^{13}C NMR (100 MHz, CDCl$_3$): δ 20.64, 20.66, 20.67 (6 × CH$_3$), 50.99 (2 × C6), 69.67, 69.72, 69.83, 69.92 (2 × C2, 2 × C3, 2 × C4, 2 × C5), 93.01 (2 × C1), 169.62, 169.65, 169.96 (6 × CO); HRMS (ESI-TOF): calcd for $C_{24}H_{32}N_6O_{15}Na$ ([M + Na]$^+$): m/z 667.1823; found: m/z 667.1819.

3.2.2. General Procedure for the Synthesis of Glycoconjugates

Synthesis of Glycoconjugates *Type A*

The 1,2,3,4-tetra-*O*-acetyl-6-azido-6-deoxy-D-glucopyranose **5** (0.118 g, 0.316 mmol) or 6-azido-6-deoxy-D-glucopyranose **6** (0.100 g, 0.487 mmol) and 8-(2-propyn-1-yloxy)quinoline **24** (1 equiv) were dissolved in *i*-PrOH (3 mL) and THF (3 mL). Then, sodium ascorbate (0.4 equiv) dissolved in H_2O (1.5 mL) and $CuSO_4 \cdot 5H_2O$ (0.2 equiv) dissolved in H_2O (1.5 mL), mixed together and added to the obtained solution. The reaction mixture was stirred overnight at room temperature. The reaction progress was monitored on TLC in an eluent system $CHCl_3$:MeOH (10:1 for protected or 2:1 for unprotected compounds). After completion of the reaction, the precipitate of inorganic salts was filtered off, and the filtrate was concentrated under reduced pressure. The crude product was purified by column chromatography (toluene:ethyl acetate, 2:1 and chloroform:methanol, 70:1 for fully protected glycoconjugates or chloroform:methanol, gradient: 50:1 to 10:1 for unprotected glycoconjugates).

- Glycoconjugate **A-1**

The product was obtained as a green solid (0.163 g, 93%); ratio of anomers (α:β = 1:1.4); ^{1}H NMR (400 MHz, $CDCl_3$): δ 1.99, 2.00, 2.01, 2.02, 2.04, 2.05, 2.09, 2.09 (8s, 24H, 4 × CH_3-α, 4 × CH_3-β), 4.00 (m, 1H, H5-β), 4.32 (m, 1H, H5-α), 4.36–4.44 (m, 2H, H6a-α, H6a-β), 4.51–4.64 (m, 2H, H6b-α, H6b-β), 4.82 (dd~t, 1H, *J* = 9.4 Hz, *J* = 10.0 Hz, H4-β), 4.83 (dd~t, 1H, *J* = 9.4 Hz, *J* = 10.1 Hz, H4-α), 4.99 (dd, 1H, *J* = 3.7 Hz, *J* = 10.2 Hz, H2-α), 5.06 (dd, 1H, *J* = 8.3 Hz, *J* = 9.5 Hz, H2-β), 5.23 (dd~t, 1H, *J* = 9.4 Hz, *J* = 9.5 Hz, H3-β), 5.45 (dd, 1H, *J* = 9.4 Hz, *J* = 10.2 Hz, H3-α), 5.56, 5.58 (2s, 4H, CH_2O-α, CH_2O-β), 5.59 (d, 1H, *J* = 8.3 Hz, H1-β), 6.24 (d, 1H, *J* = 3.7 Hz, H1-α), 7.28–7.35 (m, 2H, H7$_{quin}$-α, H7$_{quin}$-β), 7.37–7.48 (m, 6H, H3$_{quin}$-α, H5$_{quin}$-α, H6$_{quin}$-α, H3$_{quin}$-β, H5$_{quin}$-β, H6$_{quin}$-β), 7.81, 7.83 (2s, 2H, H5$_{triaz}$-α, H5$_{triaz}$-β), 8.10–8.16 (m, 2H, H4$_{quin}$-α, H4$_{quin}$-β), 8.91–8.96 (m, 2H, H2$_{quin}$-α, H2$_{quin}$-β); ^{13}C NMR (100 MHz, $CDCl_3$): δ 19.73, 20.39, 20.51, 20.52, 20.63, 20.70, 20.95, 21.05 (4 × CH_3-α, 4 × CH_3-β), 50.44, 50.55 (C6-α, C6-β), 62.78, 62.83 (CH_2O-α, CH_2O-β), 68.97, 69.04, 69.27, 69.51, 69.99, 70.27, 72.45, 73.15 (C2-α, C3-α, C4-α, C5-α, C2-β, C3-β, C4-β, C5-β), 88.62, 91.61 (C1-α, C1-β), 110.06, 110.06 (C7$_{quin}$-α, C7$_{quin}$-β), 120.16, 120.28 (C5$_{quin}$-α, C5$_{quin}$-β), 121.57, 121.64 (C3$_{quin}$-α, C3$_{quin}$-β), 124.68, 124.81 (C5$_{triaz}$-α, C5$_{triaz}$-β), 126.68, 126.79 (C6$_{quin}$-α, C6$_{quin}$-β), 129.49, 129.57 (C4a$_{quin}$-α, C4a$_{quin}$-β), 135.95, 136.49 (C4$_{quin}$-α, C4$_{quin}$-β), 140.39, 140.39 (C8a$_{quin}$-α, C8a$_{quin}$-β), 144.37, 144.50 (C4$_{triaz}$-α, C4$_{triaz}$-β), 149.29, 149.38 (C2$_{quin}$-α, C2$_{quin}$-β), 153.84, 153.85 (C8$_{quin}$-α, C8$_{quin}$-β), 168.46, 168.62, 169.10, 169.45, 169.49, 169.55, 169.96, 170.09 (4 × CO-α, 4 × CO-β); HRMS (ESI-TOF): calcd for $C_{26}H_{29}N_4O_{10}$ ([M + H]$^+$): *m/z* 557.1884; found: *m/z* 557.1887.

- Glycoconjugate **A-2**

The product was obtained as a brown solid (0.130 g, 69%); ratio of anomers (α:β = 1.3:1); ^{1}H NMR (400 MHz, DMSO): δ 2.91–3.08 (m, 3H, H2-β, H4-α, H4-β), 3.15–3.21 (m, 2H, H2-α, H3-β), 3.49 (m, 1H, H3-α), 3.63 (m, 1H, H5-β), 4.05 (m, 1H, H5-α), 4.30 (t, 1H, *J* = 6.3 Hz, OH-α), 4.38–4.48 (m, 2H, H6a-α, H6a-β), 4.52 (d, 1H, *J* = 4.8 Hz, OH-β), 4.57 (t, 1H, *J* = 6.5 Hz, OH-α), 4.73 (dd, 1H, *J* = 2.2 Hz, *J* = 9.0 Hz, H6b-α), 4.77 (dd, 1H, *J* = 2.2 Hz, *J* = 9.1 Hz, H6b-β), 4.83 (d, 1H, *J* = 4.0 Hz, OH-α), 4.90 (t, 1H, *J* = 4.2 Hz, OH-α), 4.95 (d, 1H, *J* = 4.6 Hz, OH-β), 5.03 (d, 1H, *J* = 4.4 Hz, OH-β), 5.31, 5.32 (2s, 4H, CH_2O-α, CH_2O-β), 5.37 (d, 1H, *J* = 5.5 Hz, OH-β), 6.55 (d, 1H, *J* = 4.9 Hz, H1-α), 6.89 (d, 1H, *J* = 6.3 Hz, H1-β), 7.40–7.46 (m, 2H, H7$_{quin}$-α, H7$_{quin}$-β), 7.50–7.58 (m, 6H, H3$_{quin}$-α, H5$_{quin}$-α, H6$_{quin}$-α, H3$_{quin}$-β, H5$_{quin}$-β, H6$_{quin}$-β), 8.23, 8.26 (2s, 2H, H5$_{triaz}$-α, H5$_{triaz}$-β), 8.30–8.34 (m, 2H, H4$_{quin}$-α, H4$_{quin}$-β), 8.79–8.83 (m, 2H, H2$_{quin}$-α, H2$_{quin}$-β); ^{13}C NMR (100 MHz, DMSO): δ 51.29, 51.41 (C6-α, C6-β), 61.68, 61.70 (CH_2O-α, CH_2O-β), 70.13, 71.53, 72.07, 72.61, 74.26, 74.53, 76.02, 76.13 (C2-α, C3-α, C4-α, C5-α, C2-β, C3-β, C4-β, C5-β), 92.34, 96.81 (C1-α, C1-β), 109.76, 109.81 (C7$_{quin}$-α, C7$_{quin}$-β), 119.94, 119.98 (C5$_{quin}$-α, C5$_{quin}$-β), 121.88, 121.92 (C3$_{quin}$-α, C3$_{quin}$-β), 125.89, 125.97 (C5$_{triaz}$-α, C5$_{triaz}$-β), 126.75, 126.78 (C6$_{quin}$-α, C6$_{quin}$-β), 129.05, 129.08 (C4a$_{quin}$-α, C4a$_{quin}$-β), 135.80, 135.84 (C4$_{quin}$-α, C4$_{quin}$-β), 139.60, 139.63 (C8a$_{quin}$-α, C8a$_{quin}$-β), 142.04, 142.16 (C4$_{triaz}$-α, C4$_{triaz}$-β), 148.93, 148.96 (C2$_{quin}$-α,

C2$_{quin}$-β), 153.90, 153.93 (C8$_{quin}$-α, C8$_{quin}$-β); HRMS (ESI-TOF): calcd for C$_{18}$H$_{21}$N$_4$O$_6$ ([M + H]$^+$): *m/z* 389.1461; found: *m/z* 389.1461.

Synthesis of Glycoconjugates *Type B*

The 1,2,3,4-tetra-*O*-acetyl-6-azido-6-deoxy-D-galactopyranose **12** (0.086 g, 0.230 mmol) or 6-azido-6-deoxy-D-galactopyranose **11** (0.106 g, 0.517 mmol) and 8-(2-propyn-1-yloxy) quinoline **24** (1 equiv) were dissolved in *i*-PrOH (3 mL) and THF (3 mL). Then, sodium ascorbate (0.4 equiv) dissolved in H$_2$O (1.5 mL) and CuSO$_4$·5H$_2$O (0.2 equiv) dissolved in H$_2$O (1.5 mL), mixed together and added to the obtained solution. The reaction mixture was stirred overnight at room temperature. The reaction progress was monitored on TLC in an eluent system CHCl$_3$:MeOH (10:1 for protected or 2:1 for unprotected compounds). After completion of the reaction, the precipitate of inorganic salts was filtered off, and the filtrate was concentrated under reduced pressure. The crude product was purified by column chromatography (toluene:ethyl acetate, 2:1 and chloroform:methanol, 70:1 for fully protected glycoconjugates or chloroform:methanol, gradient: 50:1 to 10:1 for unprotected glycoconjugates).

- Glycoconjugate **B-1**

The product was obtained as a brown solid (0.110 g, 86%); ratio of anomers (α:β = 1:2); ^{1}H NMR (400 MHz, CDCl$_3$): δ 1.98, 2.03, 2.05, 2.16 (4s, 12H, 4 × CH$_3$-β), 1.99, 2.01, 2.03, 2.16 (4s, 12H, 4 × CH$_3$-α), 4.22 (m, 1H, H5-β), 4.31–4.44 (m, 2H, H6a-α, H6a-β), 4.50 (dd, 1H, *J* = 4.2 Hz, *J* = 14.1 Hz, H6b-α), 4.55 (m, 1H, H5-α), 4.59 (dd, 1H, *J* = 3.9 Hz, *J* = 14.4 Hz, H6b-β), 5.07 (dd, 1H, *J* = 3.4 Hz, *J* = 10.4 Hz, H3-β), 5.28–5.36 (m, 3H, H2-α, H2-β, H3-α), 5.42 (m, 1H, H4-β), 5.49 (m, 1H, H4-α), 5.53–5.58 (m, 4H, CH$_2$O-α, CH$_2$O-β), 5.59 (d, 1H, *J* = 8.3 Hz, H1-β), 6.32 (bs, 1H, H1-α), 7.29–7.35 (m, 2H, H7$_{quin}$-α, H7$_{quin}$-β), 7.36–7.60 (m, 6H, H3$_{quin}$-α, H5$_{quin}$-α, H6$_{quin}$-α, H3$_{quin}$-β, H5$_{quin}$-β, H6$_{quin}$-β), 7.77 (s, 1H, H5$_{triaz}$-α), 7.79 (s, 1H, H5$_{triaz}$-β), 8.07–8.19 (m, 2H, H4$_{quin}$-α, H4$_{quin}$-β), 8.88–8.99 (m, 2H, H2$_{quin}$-α, H2$_{quin}$-β); ^{13}C NMR (100 MHz, CDCl$_3$): δ 20.48, 20.50, 20.58, 20.60, 20.62, 20.69, 20.75, 20.83 (4 × CH$_3$-α, 4 × CH$_3$-β), 50.06, 50.14 (C6-α, C6-β), 62.70, 62.77 (CH$_2$O-α, CH$_2$O-β), 66.22, 67.18, 67.51, 67.62, 68.16, 69.85, 70.56, 72.74 (C2-α, C3-α, C4-α, C5-α, C2-β, C3-β, C4-β, C5-β), 89.43 (C1-α), 92.09 (C1-β), 109.51, 109.99 (C7$_{quin}$-α, C7$_{quin}$-β), 120.12, 120.24 (C5$_{quin}$-α, C5$_{quin}$-β), 121.59, 121.61 (C3$_{quin}$-α, C3$_{quin}$-β), 124.45, 124.55 (C5$_{triaz}$-α, C5$_{triaz}$-β), 126.73, 126.81 (C6$_{quin}$-α, C6$_{quin}$-β), 129.48, 129.50 (C4a$_{quin}$-α, C4a$_{quin}$-β), 135.96, 136.03 (C4$_{quin}$-α, C4$_{quin}$-β), 140.34, 140.40 (C8a$_{quin}$-α, C8a$_{quin}$-β), 144.31, 144.44 (C4$_{triaz}$-α, C4$_{triaz}$-β), 149.27, 149.33 (C2$_{quin}$-α, C2$_{quin}$-β), 153.77, 153.80 (C8$_{quin}$-α, C8$_{quin}$-β), 168.62, 168.67, 169.33, 169.74, 169.84, 169.89, 169.92, 169.96 (4 × CO-α, 4 × CO-β); HRMS (ESI-TOF): calcd for C$_{26}$H$_{29}$N$_4$O$_{10}$ ([M + H]$^+$): *m/z* 557.1884; found: *m/z* 557.1885.

- Glycoconjugate **B-2**

The product was obtained as a brown solid (0.129 g, 64%); ratio of anomers (α:β = 1.4:1); ^{1}H NMR (400 MHz, DMSO): δ 3.17 (m, 1H, H6a-β), 3.28 (m, 1H, H6a-α), 3.53–3.66 (m, 2H, H2-α, H3-α), 3.68 (m, 1H, H5-β), 3.76 (m, 1H, H5-α), 3.97 (dd, 1H, *J* = 3.5 Hz, *J* = 8.9 Hz, H3-β), 4.23 (dd, 1H, *J* = 6.5 Hz, *J* = 7.2 Hz, H2-β), 4.29–4.39 (m, 3H, H4-α, H4-β, H6b-β), 4.47–4.61 (m, 4H, 3 × OH-β, H6b-α), 4.63 (m, 1H, OH-α), 4.74–4.82 (m, 3H, 2 × OH-α, OH-β), 4.93 (m, 1H, OH-α), 5.28–5.36 (m, 4H, CH$_2$O-α, CH$_2$O-β), 6.41 (d, 1H, *J* = 4.5 Hz, H1-α), 6.79 (d, 1H, *J* = 6.4 Hz, H1-β), 7.39–7.46 (m, 2H, H7$_{quin}$-α, H7$_{quin}$-β), 7.49–7.60 (m, 6H, H3$_{quin}$-α, H5$_{quin}$-α, H6$_{quin}$-α, H3$_{quin}$-β, H5$_{quin}$-β, H6$_{quin}$-β), 8.30–8.35 (m, 2H, H4$_{quin}$-α, H4$_{quin}$-β), 8.30 (s, 1H, H5$_{triaz}$-α), 8.31 (s, 1H, H5$_{triaz}$-β), 8.78–8.84 (m, 2H, H2$_{quin}$-α, H2$_{quin}$-β); ^{13}C NMR (100 MHz, DMSO): δ 51.23 (C6-α, C6-β), 61.73 (CH$_2$O-α, CH$_2$O-β), 68.32, 68.89, 68.92, 69.06, 69.69, 71.51, 72.86, 72.91 (C2-α, C3-α, C4-α, C5-α, C2-β, C3-β, C4-β, C5-β), 92.66 (C1-α), 97.25 (C1-β), 109.78, 109.81 (C7$_{quin}$-α, C7$_{quin}$-β), 119.97, 119.99 (C5$_{quin}$-α, C5$_{quin}$-β), 121.85, 121.88 (C3$_{quin}$-α, C3$_{quin}$-β), 125.68, 125.78 (C5$_{triaz}$-α, C5$_{triaz}$-β), 126.76, 126.79 (C6$_{quin}$-α, C6$_{quin}$-β), 129.03, 129.05 (C4a$_{quin}$-α, C4a$_{quin}$-β), 135.79, 135.84 (C4$_{quin}$-α, C4$_{quin}$-β), 139.62, 139.63 (C8a$_{quin}$-α, C8a$_{quin}$-β), 142.02, 142.15 (C4$_{triaz}$-α,

C4$_{triaz}$-β), 148.95, 148.97 (C2$_{quin}$-α, C2$_{quin}$-β), 153.90, 153.91 (C8$_{quin}$-α, C8$_{quin}$-β); HRMS (ESI-TOF): calcd for $C_{18}H_{21}N_4O_6$ ([M + H]$^+$): *m/z* 389.1464; found: *m/z* 389.1461.

Synthesis of Glycoconjugates *Type C*

The 1,2,3,4-tetra-*O*-acetyl-*N*-(prop-2-yn-1-yl)-β-D-glucopyranuronic acid amide **15** (0.085 g, 0.213 mmol) or *N*-(prop-2-yn-1-yl)-D-glucopyranuronic acid amide **16** (0.095 g, 0.411 mmol) and 8-(2-azidoethoxy)quinolone **25** (1 equiv) or 8-(3-azidopropoxy)quinolone **26** (1 equiv) were dissolved in *i*-PrOH (3 mL) and THF (3 mL). Then, sodium ascorbate (0.4 equiv) dissolved in H_2O (1.5 mL) and CuSO$_4$·5H$_2$O (0.2 equiv) dissolved in H_2O (1.5 mL), mixed together and added to the obtained solution. The reaction mixture was stirred overnight at room temperature. The reaction progress was monitored on TLC in an eluent system CHCl$_3$:MeOH (10:1 for protected or 2:1 for unprotected compounds). After completion of the reaction, the precipitate of inorganic salts was filtered off, and the filtrate was concentrated under reduced pressure. The crude product was purified by column chromatography (toluene:ethyl acetate, 2:1 and chloroform:methanol, 80:1 for fully protected glycoconjugates or chloroform:methanol, gradient: 50:1 to 5:1 for unprotected glycoconjugates).

- Glycoconjugate **C-1**

The product was obtained as a white solid (0.0989 g, 76%); ^{1}H NMR (400 MHz, CDCl$_3$): δ 2.01, 2.03, 2.04, 2.11 (4s, 12H, 4 × CH$_3$), 4.04 (d, 1H, *J* = 9.8 Hz, H5), 4.46 (dd, 1H, *J* = 5.3 Hz, *J* = 15.2 Hz, CH$_2$), 4.51 (dd, 1H, *J* = 5.6 Hz, *J* = 15.2 Hz, CH$_2$), 4.66 (m, 2H, CH$_2$), 4.97 (t, 2H, *J* = 5.2 Hz, CH$_2$), 5.08 (dd, 1H, *J* = 8.2 Hz, *J* = 9.2 Hz, H2), 5.14 (dd~t, 1H, *J* = 9.3 Hz, *J* = 9.8 Hz, H4), 5.28 (dd~t, 1H, *J* = 9.2 Hz, *J* = 9.3 Hz, H3), 5.73 (d, 1H, *J* = 8.2 Hz, H1), 6.89 (m, 1H, NH), 7.04 (d, 1H, *J* = 7.2 Hz, H7$_{quin}$), 7.41–7.50 (m, 3H, H3$_{quin}$, H5$_{quin}$, H6$_{quin}$), 8.12 (s, 1H, H5$_{triaz}$), 8.17 (d, 1H, *J* = 8.2 Hz, H4$_{quin}$), 8.98 (m, 1H, H2$_{quin}$); ^{13}C NMR (100 MHz, CDCl$_3$): δ 20.54, 20.54, 20.69, 20.75 (4 × CH$_3$), 34.59, 49.64, 67.56 (3 × CH$_2$), 68.93, 70.17, 72.01, 72.90 (C2, C3, C4, C5), 91.21 (C1), 109.99 (C7$_{quin}$), 121.03 (C5$_{quin}$), 121.91 (C3$_{quin}$), 124.14 (C5$_{triaz}$), 126.52 (C6$_{quin}$), 129.62 (C4a$_{quin}$), 136.05 (C4$_{quin}$), 140.32 (C8a$_{quin}$), 143.96 (C4$_{triaz}$), 149.64 (C2$_{quin}$), 153.78 (C8$_{quin}$), 165.86 (CONH), 168.75, 169.19, 169.60, 169.80 (4 × COCH$_3$); HRMS (ESI-TOF): calcd for $C_{28}H_{32}N_5O_{11}$ ([M + H]$^+$): *m/z* 614.2098; found: *m/z* 614.2091.

- Glycoconjugate **C-2**

The product was obtained as a white solid (0.101 g, 76%); ^{1}H NMR (400 MHz, CDCl$_3$): δ 2.01, 2.03, 2.04, 2.12 (4s, 12H, 4 × CH$_3$), 2.63 (q, 2H, *J* = 6.2 Hz, CH$_2$), 4.03 (d, 1H, *J* = 9.9 Hz, H5), 4.26 (m, 2H, CH$_2$), 4.43 (dd, 1H, *J* = 5.5 Hz, *J* = 15.2 Hz, CH$_2$), 4.53 (dd, 1H, *J* = 6.2 Hz, *J* = 15.2 Hz, CH$_2$), 4.72 (t, 2H, *J* = 6.6 Hz, CH$_2$), 5.09 (dd, 1H, *J* = 8.2 Hz, *J* = 9.3 Hz, H2), 5.14 (dd~t, 1H, *J* = 9.3 Hz, *J* = 9.9 Hz, H4), 5.29 (dd~t, 1H, *J* = 9.3 Hz, *J* = 9.3 Hz, H3), 5.73 (d, 1H, *J* = 8.2 Hz, H1), 6.90 (t, 1H, *J* = 5.5 Hz, NH), 7.05 (m, 1H, H7$_{quin}$), 7.41–7.48 (m, 3H, H3$_{quin}$, H5$_{quin}$, H6$_{quin}$), 7.70 (s, 1H, H5$_{triaz}$), 8.16 (m, 1H, H4$_{quin}$), 8.96 (m, 1H, H2$_{quin}$); ^{13}C NMR (100 MHz, CDCl$_3$): δ 20.53, 20.53, 20.70, 20.75 (4 × CH$_3$), 29.67, 34.53, 47.36, 65.37 (4 × CH$_2$), 68.93, 70.15, 71.98, 72.86 (C2, C3, C4, C5), 91.21 (C1), 109.47 (C7$_{quin}$), 120.26 (C5$_{quin}$), 121.71 (C3$_{quin}$), 123.22 (C5$_{triaz}$), 126.73 (C6$_{quin}$), 129.57 (C4a$_{quin}$), 136.16 (C4$_{quin}$), 140.21 (C8a$_{quin}$), 143.96 (C4$_{triaz}$), 149.33 (C2$_{quin}$), 154.24 (C8$_{quin}$), 165.93 (CONH), 168.77, 169.19, 169.64, 169.79 (4 × COCH$_3$); HRMS (ESI-TOF): calcd for $C_{29}H_{34}N_5O_{11}$ ([M + H]$^+$): *m/z* 628.2255; found: *m/z* 628.2252.

- Glycoconjugate **C-3**

The product was obtained as a white solid (0.127 g, 67%); ratio of anomers (α:β = 1:1.1); ^{1}H NMR (400 MHz, DMSO): δ 2.34–2.44 (m, 4H, CH$_2$-α, CH$_2$-β), 2.96 (m, 1H, H2-β), 3.14 (m, 1H, H4-β), 3.21 (m, 1H, H2-α), 3.29 (m, 1H, H4-α), 3.38 (m, 1H, H3-β), 3.44 (m, 1H, H3-α), 3.58 (d, 1H, *J* = 9.7 Hz, H5-β), 4.00 (d, 1H, *J* = 9.8 Hz, H5-α), 4.15–4.23 (m, 4H, CH$_2$-α, CH$_2$-β), 4.29–4.35 (m, 5H, CH$_2$-α, CH$_2$-β, OH), 4.56–4.64 (m, 5H, CH$_2$-α, CH$_2$-β, OH), 4.80 (m, 1H, OH), 4.93 (m, 1H, OH), 4.95 (m, 1H, OH), 4.97 (m, 1H, OH), 5.04 (m, 1H, OH), 5.09 (m,

1H, OH), 6.45 (d, 1H, J = 4.7 Hz, H1-α), 6.76 (d, 1H, J = 6.6 Hz, H1-β), 7.20 (m, 2H, H7$_{quin}$-α, H7$_{quin}$-β), 7.47–7.61 (m, 6H, H3$_{quin}$-α, H5$_{quin}$-α, H6$_{quin}$-α, H3$_{quin}$-β, H5$_{quin}$-β, H6$_{quin}$-β), 7.99, 8.02 (2s, 2H, H5$_{triaz}$-α, H5$_{triaz}$-β), 8.33 (m, 2H, H4$_{quin}$-α, H4$_{quin}$-β), 8.41 (m, 2H, NH-α, NH-β), 8.90 (bs, 2H, H2$_{quin}$-α, H2$_{quin}$-β); ^{13}C NMR (100 MHz, DMSO): δ 29.66, 29.66, 34.22, 34.22, 46.56, 46.56, 65.40, 65.40 (4 × CH$_2$-α, 4 × CH$_2$-β), 71.27, 71.48, 71.88, 72.20, 72.71, 74.46, 75.56, 76.32 (C2-α, C3-α, C4-α, C5-α, C2-β, C3-β, C4-β, C5-β), 92.77, 97.36 (C1-α, C1-β), 109.82, 109.88 (C7$_{quin}$-α, C7$_{quin}$-β), 119.86, 119.94 (C5$_{quin}$-α, C5$_{quin}$-β), 121.78, 121.87 (C3$_{quin}$-α, C3$_{quin}$-β), 122.97, 123.03 (C5$_{triaz}$-α, C5$_{triaz}$-β), 126.81, 126.89 (C6$_{quin}$-α, C6$_{quin}$-β), 129.04, 129.10 (C4a$_{quin}$-α, C4a$_{quin}$-β), 135.77, 135.86 (C4$_{quin}$-α, C4$_{quin}$-β), 139.77, 139.82 (C8a$_{quin}$-α, C8a$_{quin}$-β), 144.74, 144.92 (C4$_{triaz}$-α, C4$_{triaz}$-β), 149.01, 149.05 (C2$_{quin}$-α, C2$_{quin}$-β), 154.15, 154.21 (C8$_{quin}$-α, C8$_{quin}$-β), 168.78, 169.82 (CONH-α, CONH-β); HRMS (ESI-TOF): calcd for C$_{21}$H$_{26}$N$_5$O$_7$ ([M + H]$^+$): m/z 460.1832; found: m/z 460.1829.

Synthesis of Glycoconjugates *Type D*

The 2,3,4,2′,3′,4′-hexa-*O*-acetyl-6,6′-diazido-6,6′-dideoxy-D-trehalose **23** (0.095 g, 0.147 mmol) or 6,6′-diazido-6,6′-dideoxy-D-trehalose **20** (0.203 g, 0.517 mmol) and 8-(2-propyn-1-yloxy)quinoline **24** (2 equiv) were dissolved in *i*-PrOH (4 mL) and THF (4 mL). Then, sodium ascorbate (0.4 equiv) dissolved in H$_2$O (2 mL) and CuSO$_4$·5H$_2$O (0.2 equiv) dissolved in H$_2$O (2 mL), mixed together and added to the obtained solution. The reaction mixture was stirred overnight at room temperature. The reaction progress was monitored on TLC in an eluent system CHCl$_3$:MeOH (10:1 for protected or 1:1 for unprotected compounds). After completion of the reaction, the precipitate of inorganic salts was filtered off, and the filtrate was concentrated under reduced pressure. The crude product was purified by column chromatography (toluene:ethyl acetate, 2:1 and chloroform:methanol, 50:1 for fully protected glycoconjugates or chloroform:methanol, gradient: 50:1 to 5:1 for unprotected glycoconjugates).

- Glycoconjugate **D-1**

The product was obtained as a yellow solid (0.113 g, 76%); m.p.: 118 °C; [α]$^{23}_D$ = 15.8 (c = 1.0, CHCl$_3$); ^{1}H NMR (400 MHz, CDCl$_3$): δ 2.00, 2.03, 2.09 (3s, 18H, 6 × CH$_3$), 3.88 (dd, 2H, J = 9.4 Hz, J = 13.9 Hz, 2 × H6a), 3.99 (ddd, 2H, J = 1.3 Hz, J = 9.4 Hz, J = 10.0 Hz, 2 × H5), 4.32 (d, 2H, J = 3.8 Hz, 2 × H1), 4.44 (dd, 2H, J = 1.3 Hz, J = 13.9 Hz, 2 × H6b), 4.70 (dd~t, 2H, J = 9.7 Hz, J = 10.0 Hz, 2 × H4), 4.72 (dd, 2H, J = 3.8 Hz, J = 9.7 Hz, 2 × H2), 5.31 (dd~t, 2H, J = 9.7 Hz, J = 9.7 Hz, 2 × H3), 5.53 i 5.57 (qAB, 4H, J = 13.2 Hz, 2 × CH$_2$O), 7.32 (m, 2H, 2 × H7$_{quin}$), 7.39 (dd, 2H, J = 4.1 Hz, J = 8.3 Hz, 2 × H5$_{quin}$), 7.44 (m, 2H, 2 × H6$_{quin}$), 7.50 (t, 2H, J = 7.9 Hz, 2 × H3$_{quin}$), 7.64 (s, 2H, 2 × H5$_{triaz}$), 8.14 (dd, 2H, J = 1.2 Hz, J = 8.3 Hz, 2 × H4$_{quin}$), 8.88 (m, 2H, 2 × H2$_{quin}$); ^{13}C NMR (100 MHz, CDCl$_3$): δ 20.51, 20.59, 20.65 (6 × CH$_3$), 50.56 (2 × C6), 62.72 (2 × CH$_2$OH), 68.54, 68.83, 69.63, 69.73 (2 × C2, 2 × C3, 2 × C4, 2 × C5), 90.97 (2 × C1), 109.87 (2 × C7$_{quin}$), 120.10 (2 × C5$_{quin}$), 121.71 (2 × C3$_{quin}$), 124.78 (2 × C5$_{triaz}$), 127.07 (2 × C6$_{quin}$), 129.49 (2 × C4a$_{quin}$), 136.00 (2 × C4$_{quin}$), 140.38 (2 × C8a$_{quin}$), 144.48 (2 × C4$_{triaz}$), 149.30 (2 × C2$_{quin}$), 153.91 (2 × C8$_{quin}$), 169.24, 169.70, 169.81 (6 × CO); HRMS (ESI-TOF): calcd for C$_{48}$H$_{51}$N$_8$O$_{17}$ ([M + H]$^+$): m/z 1011.3372; found: m/z 1011.3370.

- Glycoconjugate **D-2**

The product was obtained as a brown solid (0.244 g, 62%); m.p.: 182–183 °C; [α]$^{24}_D$ = 40.0 (c = 1.0, DMSO); ^{1}H NMR (400 MHz, DMSO): δ 3.00 (m, 2H, 2 × H4), 3.22 (m, 2H, 2 × H2), 3.61 (m, 2H, 2 × H3), 4.25 (m, 2H, 2 × H5), 4.47 (dd, 2H, J = 8.2 Hz, J = 14.2 Hz, 2 × H6a), 4.62 (d, 2H, J = 3.6 Hz, 2 × H1), 4.65 (dd, 2H, J = 2.3 Hz, J = 14.2 Hz, 2 × H6b), 5.11 (bs, 2H, 2 × OH), 5.32 i 5.35 (qAB, 4H, J = 12.0 Hz, 2 × CH$_2$O), 5.36 (bs, 2H, 2 × OH), 5.44 (bs, 2H, 2 × OH), 7.38 (m, 2H, J = 2.7 Hz, J = 6.3 Hz, 2 × H7$_{quin}$), 7.47–7.56 (m, 6H, 2 × H3$_{quin}$, 2 × H5$_{quin}$, 2 × H6$_{quin}$), 8.27 (s, 2H, 2 × H5$_{triaz}$), 8.32 (dd, 2H, J = 1.7 Hz, J = 8.3 Hz, 2 × H4$_{quin}$), 8.89 (dd, 2H, J = 1.7 Hz, J = 4.2 Hz, 2 × H2$_{quin}$); ^{13}C NMR (100 MHz, DMSO): δ 50.80 (2 × C6), 62.17 (2 × CH$_2$OH), 69.75, 70.97, 71.34, 72.64 (2 × C2, 2 × C3, 2 × C4, 2 × C5), 94.57 (2 × C1), 109.94 (2 × C7$_{quin}$), 119.96 (2 × C5$_{quin}$), 121.78 (2 × C3$_{quin}$),

124.53 (2 × C5$_{triaz}$), 126.73 (2 × C6$_{quin}$), 129.05 (2 × C4a$_{quin}$), 136.01 (2 × C4$_{quin}$), 139.46 (2 × C8a$_{quin}$), 142.68 (2 × C4$_{triaz}$), 149.32 (2 × C2$_{quin}$), 153.70 (2 × C8$_{quin}$); HRMS (ESI-TOF): calcd for $C_{36}H_{39}N_8O_{11}$ ([M + H]$^+$): *m/z* 759.2738; found: *m/z* 759.2735.

3.2.3. General Procedure for the Synthesis of Metabolites of Glycoconjugates

The appropriate sugar derivatives **5**, **6**, **11**, **12**, **15**, **16**, **20**, or **23** (1 equiv) and propargyl alcohol **27** or 2-azidoethanol **28** (1 equiv) were dissolved in *i*-PrOH (4 mL) and THF (4 mL). Then, sodium ascorbate (0.4 equiv) dissolved in H_2O (2 mL) and CuSO$_4$·5H$_2$O (0.2 equiv) dissolved in H_2O (2 mL), mixed together and added to the obtained solution. The reaction mixture was stirred overnight at room temperature. The reaction progress was monitored on TLC in an eluent system CHCl$_3$:MeOH (10:1 for protected or 2:1 for unprotected compounds). After completion of the reaction, the precipitate of inorganic salts was filtered off, and the filtrate was concentrated under reduced pressure. The crude product was purified by column chromatography (toluene:ethyl acetate, 2:1 and chloroform:methanol, 20:1 for protected products or chloroform:methanol, gradient: 50:1 to 1:1 for unprotected products) to give metabolites **29–36**.

- Metabolite **29**

Starting from 1,2,3,4-tetra-*O*-acetyl-6-azido-6-deoxy-D-glucopyranose **5** (0.527 g, 1.412 mmol) and propargyl alcohol **27** (83 µL, 1.421 mmol). The product was obtained as a white solid (0.522 g, 86%); ratio of anomers (α:β = 1.5:1); ^{1}H NMR (400 MHz, DMSO): δ 1.93, 1.97, 1.98, 2.00, 2.00, 2.01, 2.05, 2.14 (8s, 24H, 4 × CH$_3$-α, 4 × CH$_3$-β), 4.40–4.48 (m, 2H, H5-α, H5-β), 4.50, 4.51 (2s, 4H, CH$_2$O-α, CH$_2$O-β), 4.52–4.63 (m, 4H, H6a-α, H6b-α, H6a-β, H6b-β), 4.82 (dd~t, 1H, *J* = 9.4 Hz, *J* = 9.5 Hz, H4-β), 4.91 (dd, 1H, *J* = 9.4 Hz, *J* = 10.1 Hz, H4-α), 4.92 (dd, 1H, *J* = 8.3 Hz, *J* = 9.8 Hz, H2-β), 4.99 (dd, 1H, *J* = 3.7 Hz, *J* = 10.3 Hz, H2-α), 5.15–5.19 (m, 2H, OH-α, OH-β), 5.32 (dd, 1H, *J* = 9.4 Hz, *J* = 10.3 Hz, H3-α), 5.42 (dd~t, 1H, *J* = 9.5 Hz, *J* = 9.8 Hz, H3-β), 5.93 (d, 1H, *J* = 8.3 Hz, H1-β), 6.14 (d, 1H, *J* = 3.7 Hz, H1-α), 7.80 (s, 1H, H5$_{triaz}$-β), 7.88 (s, 1H, H5$_{triaz}$-α); ^{13}C NMR (100 MHz, DMSO): δ 20.24, 20.25, 20.30, 20.33, 20.43, 20.45, 20.49, 20.52 (4 × CH$_3$-α, 4 × CH$_3$-β), 49.42, 49.54 (C6-α, C6-β), 54.95, 54.97 (CH$_2$OH-α, CH$_2$OH-β), 68.44, 68.80, 69.03, 69.28, 69.30, 69.80, 71.76, 71.78 (C2-α, C3-α, C4-α, C5-α, C2-β, C3-β, C4-β, C5-β), 88.02, 90.77 (C1-α, C1-β), 123.36, 123.47 (C5$_{triaz}$-α, C5$_{triaz}$-β), 147.95, 147.97 (C4$_{triaz}$-α, C4$_{triaz}$-β), 168.59, 168.81, 169.05, 169.08, 169.24, 169.48, 169.51, 169.68 (4 × CO-α, 4 × CO-β); HRMS (ESI-TOF): calcd for $C_{17}H_{24}N_3O_{10}$ ([M + H]$^+$): *m/z* 430.1462; found: *m/z* 430.1463.

- Metabolite **30**

Starting from 6-azido-6-deoxy-D-glucopyranose **6** (0.093 g, 0.453 mmol) and propargyl alcohol **27** (30 µL, 0.514 mmol). The product was obtained as a brown solid (0.82 g, 69%); ratio of anomers (α:β = 1:1); ^{1}H NMR (400 MHz, DMSO): δ 2.87–3.03 (m, 3H, H2-β, H4-α, H4-β), 3.09–3.15 (m, 2H, H2-α, H3-β), 3.19 (m, 1H, H3-α), 3.40–3.46 (m, 2H, H6a-α, H6a-β), 3.47–3.55 (m, 2H, H6b-α, H6b-β), 3.93 (ddd, 1H, *J* = 2.2 Hz, *J* = 8.4 Hz, *J* = 10.2 Hz, H5-α), 4.25 (d, 1H, *J* = 7.8 Hz, H1-β), 4.35 (ddd, 1H, *J* = 3.3 Hz, *J* = 8.3 Hz, *J* = 14.3 Hz, H5-β), 4.50, 4.51 (2s, 4H, CH$_2$O-α, CH$_2$O-β), 4.66 (m, 2H, OH-α, OH-β), 4.88 (d, 1H, *J* = 3.4 Hz, H1-α), 7.83, 7.87 (2s, 2H, H5$_{triaz}$-α, H5$_{triaz}$-β); ^{13}C NMR (100 MHz, DMSO): δ 50.92, 50.99 (C6-α, C6-β), 54.97, 54.98 (CH$_2$OH-α, CH$_2$OH-β), 70.01, 71.35, 71.82, 72.06, 72.62, 74.21, 74.54, 76.13 (C2-α, C3-α, C4-α, C5-α, C2-β, C3-β, C4-β, C5-β), 92.30, 96.84 (C1-α, C1-β), 123.45, 123.51 (C5$_{triaz}$-α, C5$_{triaz}$-β), 147.55, 147.64 (C4$_{triaz}$-α, C4$_{triaz}$-β); HRMS (ESI-TOF): calcd for $C_9H_{16}N_3O_6$ ([M + H]$^+$): *m/z* 262.1039; found: *m/z* 262.1040.

- Metabolite **31**

Starting from 1,2,3,4-tetra-*O*-acetylo-6-azido-6-deoxy-D-galactopyranose **12** (0.111 g, 0.297 mmol) and propargyl alcohol **27** (20 µL, 0.342 mmol). The product was obtained as a white solid (0.111 g, 87%); ratio of anomers (α:β = 1:2.5); ^{1}H NMR (400 MHz, DMSO): δ 1.91, 2.00, 2.05, 2.16 (4s, 12H, 4 × CH$_3$-β), 1.94, 2.00, 2.11, 2.15 (4s, 12H, 4 × CH$_3$-α), 4.45–4.52 (m, 6H, H6a-α, H6a-β, CH$_2$-α, CH$_2$-β), 4.53 (m, 1H, H6b-β), 4.57 (m, 1H, H6b-α), 4.65

(m, 1H, H5-β), 4.73 (m, 1H, H5-α), 5.06–5.14 (m, 2H, H2-α, H2-β), 5.15–5.22 (m, 4H, H4-α, H4-β, OH-α, OH-β), 5.26 (dd, 1H, J = 3.3 Hz, J = 10.9 Hz, H3-α), 5.32 (dd, 1H, J = 3.5 Hz, J = 10.5 Hz, H3-β), 5.86 (d, 1H, J = 8.3 Hz, H1-β), 6.21 (d, 1H, J = 3.7 Hz, H1-α), 7.87 (s, 1H, H5$_{triaz}$-β), 7.90 (s, 1H, H5$_{triaz}$-α); ^{13}C NMR (100 MHz, DMSO): δ 20.19, 20.21, 20.26, 20.29, 20.33, 20.35, 20.37, 20.42 (4 × CH$_3$-α, 4 × CH$_3$-β), 48.48, 48.68 (C6-α, C6-β), 54.86, 54.89 (CH$_2$OH-α, CH$_2$OH-β), 65.90, 66.77, 67.26, 67.34, 67.44, 69.09, 69.82, 71.69 (C2-α, C3-α, C4-α, C5-α, C2-β, C3-β, C4-β, C5-β), 88.53 (C1-α), 91.17 (C1-β), 123.04, 123.09 (C5$_{triaz}$-α, C5$_{triaz}$-β), 147.88, 147.97 (C4$_{triaz}$-α, C4$_{triaz}$-β), 168.57, 168.81, 169.11, 169.16, 169.30, 169.41, 169.67, 169.70 (4 × CO-α, 4 × CO-β); HRMS (ESI-TOF): calcd for C$_{17}$H$_{24}$N$_3$O$_{10}$ ([M + H]$^+$): *m/z* 430.1462; found: *m/z* 430.1461.

- Metabolite **32**

Starting from 6-azido-6-deoxy-D-galactopyranose **11** (0.126 g, 0.614 mmol) and propargyl alcohol **27** (36 µL, 0.616 mmol). The product was obtained as a brown solid (0.098 g, 61%); ratio of anomers (α:β = 2.2:1); ^{1}H NMR (400 MHz, DMSO): δ 3.17 (m, 1H, H6a-β), 3.28 (m, 1H, H6a-α), 3.50–3.59 (m, 4H, H2-α, H3-α, H2-β, H3-β), 3.67 (m, 1H, H5-α), 3.87 (m, 1H, H5-β), 4.19 (m, 1H, H4-β), 4.23 (m, 1H, H4-α), 4.35 (m, 1H, H6b-α), 4.40–4.53 (m, 9H, H6b-β, CH$_2$-α, CH$_2$-β, 4 × OH-β), 4.61 (d, 1H, J = 5.1 Hz, OH-α), 4.70–4.80 (m, 2H, 2 × OH-α), 4.90 (m, 1H, OH-α), 5.11–5.21 (m, 2H, CH$_2$<u>OH</u>-α, CH$_2$<u>OH</u>-β), 6.24 (d, 1H, J = 4.8 Hz, H1-α), 6.63 (d, 1H, J = 6.7 Hz, H1-β), 7.90 (s, 1H, H5$_{triaz}$-α), 7.92 (s, 1H, H5$_{triaz}$-β); ^{13}C NMR (100 MHz, DMSO): δ 50.81, 50.86 (C6-α, C6-β), 55.01, 55.06 (CH$_2$OH-α, CH$_2$OH-β), 68.34, 68.89, 68.91, 69.53 (C2-α, C3-α, C4-α, C5-α), 71.60, 71.66, 72.89, 72.94 (C2-β, C3-β, C4-β, C5-β), 92.66 (C1-α), 97.33 (C1-β), 123.32, 123.35 (C5$_{triaz}$-α, C5$_{triaz}$-β), 147.58, 147.67 (C4$_{triaz}$-α, C4$_{triaz}$-β); HRMS (ESI-TOF): calcd for C$_9$H$_{16}$N$_3$O$_6$ ([M + H]$^+$): *m/z* 262.1039; found: *m/z* 262.1039.

- Metabolite **33**

Starting from 1,2,3,4-tetra-*O*-acetyl-*N*-(prop-2-yn-1-yl)-β-D-glucopyranuronic acid amide **15** (0.104 g, 0.260 mmol) and 2-azidoethanol **28** (0.023 g, 0.264 mmol). The product was obtained as a white solid (0.092 g, 73%); ^{1}H NMR (400 MHz, CDCl$_3$): δ 2.00, 2.03, 2.06, 2.13 (4s, 12H, 4 × CH$_3$), 4.04 (d, 1H, J = 9.9 Hz, H5), 4.05 (m, 2H, CH$_2$), 4.30–4.45 (m, 2H, CH$_2$), 4.51–4.66 (m, 2H, CH$_2$), 5.06 (dd~t, 1H, J = 9.4 Hz, J = 9.9 Hz, H4), 5.09 (dd, 1H, J = 8.2 Hz, J = 9.4 Hz, H2), 5.30 (dd~t, 1H, J = 9.4 Hz, J = 9.4 Hz, H3), 5.74 (d, 1H, J = 8.2 Hz, H1), 7.10 (m, 1H, NH), 7.67 (s, 1H, H5$_{triaz}$); ^{13}C NMR (100 MHz, CDCl$_3$): δ 20.52, 20.52, 20.71, 20.75 (4 × CH$_3$), 34.31, 53.07, 61.23 (3 × CH$_2$), 69.15, 70.07, 71.76, 72.87 (C2, C3, C4, C5), 91.16 (C1), 123.77 (C5$_{triaz}$), 144.09 (C4$_{triaz}$), 166.04 (CONH), 168.85, 169.21, 169.75, 170.71 (4 × COCH$_3$); HRMS (ESI-TOF): calcd for C$_{19}$H$_{27}$N$_4$O$_{11}$ ([M + H]$^+$): *m/z* 487.1676; found: *m/z* 487.1672.

- Metabolite **34**

Starting from *N*-(prop-2-yn-1-yl)-D-glucopyranuronic acid amide **16** (0.318 g, 1.375 mmol) and 2-azidoethanol **28** (0.120 g, 1.378 mmol). The product was obtained as a brown solid (0.280 g, 64%); ratio of anomers (α:β = 1:1); ^{1}H NMR (400 MHz, DMSO): δ 2.95 (dd, 1H, J = 8.2 Hz, J = 9.0 Hz, H2-β), 3.14 (m, 1H, H4-β), 3.19 (dd, 1H, J = 3.6 Hz, J = 9.2 Hz, H2-α), 3.31 (m, 1H, H4-α), 3.36 (m, 1H, H3-β), 3.44 (dd~t, 1H, J = 9.0 Hz, J = 9.2 Hz, H3-α), 3.58 (d, 1H, J = 9.6 Hz, H5-β), 3.72–3.77 (m, 4H, CH$_2$-α, CH$_2$-β), 4.00 (d, 1H, J = 9.6 Hz, H5-α), 4.29–4.33 (m, 4H, CH$_2$-α, CH$_2$-β), 4.31 (d, 1H, J = 8.2 Hz, H1-β), 4.33–4.37 (m, 4H, CH$_2$-α, CH$_2$-β), 4.95 (d, 1H, J = 3.6 Hz, H1-α), 7.81, 7.84 (2s, 2H, H5$_{triaz}$-α, H5$_{triaz}$-β), 8.42 (m, 2H, NH-α, NH-β); ^{13}C NMR (100 MHz, DMSO): δ 34.04, 34.09, 51.97, 52.04, 59.71, 59.76 (3 × CH$_2$-α, 3 × CH$_2$-β), 71.17, 71.39, 71.78, 72.11, 72.62, 74.35, 75.46, 76.22 (C2-α, C3-α, C4-α, C5-α, C2-β, C3-β, C4-β, C5-β), 92.67, 97.26 (C1-α, C1-β), 123.07, 123.13 (C5$_{triaz}$-α, C5$_{triaz}$-β), 144.29, 144.49 (C4$_{triaz}$-α, C4$_{triaz}$-β), 168.67, 169.71 (CONH-α, CONH-β); HRMS (ESI-TOF): calcd for C$_{11}$H$_{18}$N$_4$O$_7$Na ([M + Na]$^+$): *m/z* 341.1073; found: *m/z* 341.1072.

- Metabolite **35**

Starting from 2,3,4,2′,3′,4′-hexa-*O*-acetyl-6,6′-diazido-6,6′-dideoxy-D-trehalose **23** (0.076 g, 0.118 mmol) and propargyl alcohol **27** (15 µL, 0.257 mmol). The product was obtained as

a yellow solid (0.081 g, 91%); m.p.: 92–93 °C; $[\alpha]^{23}_D$ = 72.9 (c = 0.27, CHCl₃); ¹H NMR (400 MHz, DMSO): δ 1.95, 2.00, 2.02 (3s, 18H, 6 × CH₃), 4.23 (ddd, 2H, J = 2.8 Hz, J = 7.8 Hz, J = 10.4 Hz, 2 × H5), 4.48 (d, 4H, J = 5.6 Hz, 2 × CH₂O), 4.50 (dd, 2H, J = 7.8 Hz, J = 14.4 Hz, 2 × H6a), 4.60 (dd, 2H, J = 2.8 Hz, J = 14.4 Hz, 2 × H6b), 4.85 (d, 2H, J = 3.6 Hz, 2 × H1), 4.95 (dd~t, 2H, J = 9.4 Hz, J = 10.4 Hz, 2 × H4), 5.01 (dd, 2H, J = 3.6 Hz, J = 10.3 Hz, 2 × H2), 5.12 (t, 2H, J = 5.6 Hz, 2 × OH), 5.27 (dd, 2H, J = 9.4 Hz, J = 10.3 Hz, 2 × H3), 7.84 (s, 2H, 2 × H5_triaz); ¹³C NMR (100 MHz, DMSO): δ 20.33, 20.36, 20.46 (6 × CH₃), 49.42 (2 × C6), 54.96 (2 × CH₂OH), 68.05, 68.43, 69.14, 69.53 (2 × C2, 2 × C3, 2 × C4, 2 × C5), 90.92 (2 × C1), 123.67 (2 × C5_triaz), 148.01 (2 × C4_triaz), 169.00, 169.30, 169.69 (6 × CO); HRMS (ESI-TOF): calcd for $C_{30}H_{41}N_6O_{17}$ ([M + H]⁺): *m/z* 757.2528; found: *m/z* 757.2526.

- Metabolite **36**

Starting from 6,6′-diazido-6,6′-dideoxy-D-trehalose **20** (0.097 g, 0.247 mmol) and propargyl alcohol **27** (30 μL, 0.514 mmol). The product was obtained as a yellow solid (0.102 g, 82%); m.p.: 118 °C; $[\alpha]^{24}_D$ = 102.0 (c = 1.0, DMSO); ¹H NMR (400 MHz, DMSO): δ 2.95 (dd~t, 2H, J = 9.1 Hz, J = 9.9 Hz, 2 × H4), 3.17 (dd, 2H, J = 3.6 Hz, J = 9.2 Hz, 2 × H2), 3.55 (dd~t, 2H, J = 9.1 Hz, J = 9.2 Hz, 2 × H3), 4.12 (ddd, 2H, J = 2.6 Hz, J = 7.2 Hz, J = 9.9 Hz, 2 × H5), 4.43 (dd, 2H, J = 7.2 Hz, J = 14.3 Hz, 2 × H6a), 4.49 (s, 4H, 2 × CH₂O), 4.56 (dd, 2H, J = 2.6 Hz, J = 14.3 Hz, 2 × H6b), 4.60 (d, 2H, J = 3.6 Hz, 2 × H1), 7.84 (s, 2H, 2 × H5_triaz); ¹³C NMR (100 MHz, DMSO): δ 50.46 (2 × C6), 54.97 (2 × CH₂OH), 69.77, 71.14, 71.19, 72.60 (2 × C2, 2 × C3, 2 × C4, 2 × C5), 93.74 (2 × C1), 123.13 (2 × C5_triaz), 147.76 (2 × C4_triaz); HRMS (ESI-TOF): calcd for $C_{18}H_{29}N_6O_{11}$ ([M + H]⁺): *m/z* 505.1894; found: *m/z* 505.1895.

3.3. Biological Evaluation

3.3.1. Cell Cultures

Three cell lines were used for biological assays. The human colon adenocarcinoma cell line (HCT-116) was purchased from the American Type Culture Collection (ATCC, Manassas, VA, USA). The human breast adenocarcinoma cell line (MCF-7) was obtained from the collection of the Maria Skłodowska-Curie Memorial Cancer Center and the National Institute of Oncology branch in Gliwice, Poland. The Normal Human Dermal Fibroblasts-Neonatal (NHDF-Neo) was purchased from Lonza (Cat. No. CC-2509, NHDF-Neo, Dermal Fibroblasts, Neonatal, Lonza, Warsaw, Poland). All cells were cultured as a monolayer in a complete medium under standard conditions in a humidified incubator with 5% CO₂ at 37 °C. The complete culture media consisted of RPMI 1640 or DMEM/F12 medium (HyClone Laboratories, Inc., Logan, UT, USA), supplemented with 10% of heat-inactivated fetal bovine serum (FBS; EURx, Gdańsk, Poland) and 1% of Antibiotic Antimycotic Solution: penicillin (10,000 U/mL) and streptomycin (10,000 μg/mL) (Sigma-Aldrich, Taufkirchen, Germany).

3.3.2. MTT Cytotoxicity Assay

The in vitro cytotoxicity of the test compounds was determined by the MTT (3-[4,5–dimethylthiazol-2-yl]-2,5-diphenyltetrazolium bromide) test (Sigma-Aldrich, Taufkirchen, Germany) according to the manufacturer's protocol [58]. At the beginning, for each cell line were determined the optimal seeding densities to ensure exponential growth throughout the experimental period. The confluent layer of cells were trypsinized, collected, and suspended in a growth medium. The cell suspension were then seeded into 96-well plates at a density of 1×10^4 or 2×10^3 (HCT-116) or 5×10^3 (MCF-7, NHDF-Neo) per well and incubated for 24 h under standard conditions (5% CO₂, 37 °C). Then, the culture medium was replaced with solutions of different concentrations of test compounds in a fresh medium. Stock solutions of test compounds were prepared in DMSO and diluted to final concentrations with appropriate volumes of the growth medium directly before the experiment. Cells suspended in a medium supplemented with 0.5% DMSO (the amount of DMSO necessary to dissolve the highest dose of the respective sample) were used as a control of the experiment. The final DMSO concentration did not affect cell viability. The compound-treated cells were incubated for a further 24–72 h. After that, the medium

was removed and the MTT solution (50 μL, 0.5 mg/mL in PBS) was added into each well and incubated for another 3 h under standard conditions (5% CO_2, 37 °C). After this time, the MTT dye was carefully removed, and the acquired formazan crystals were dissolved by DMSO (Chempur, Piekary Śląskie, Poland). The proliferation was evaluated by measuring the formazan product's absorbance at a wavelength of 570 nm with a microplate spectrophotometer (Epoch, BioTek, Winooski, VT, USA). All experiments were conducted in triplicate with four technical repeats for each tested concentration. Results were expressed as the percentage change in the viability of the test cells relative to the untreated control cells and calculated as the inhibitory concentration (IC_{50}). The IC_{50} values were defined as the drug concentration that was necessary to reduce cell proliferation to 50% of the untreated control and this parameter was calculated using CalcuSyn software (version 2.0, Biosoft, Cambridge, UK). The results are expressed as the average value ± standard deviation (SD).

3.3.3. Clonogenic Assay

To determine the number of colonies forming by cells after exposure to the test compounds, a clonogenic assay was performed as reported in the literature [60]. The cells were seeded into 6-well plates at a density of 1×10^5 (HCT-116) or 2×10^5 (MCF-7, NHDF-Neo) per well (3 mL) and allowed to attach for 24 h under standard conditions with 5% CO_2 at 37 °C. The following day, the medium was removed and cells were treated with solutions of test compounds in fresh medium at a dose equal to their IC_{50} values. Control cells were grown with fresh medium supplemented with 0.5% DMSO. After 72 h of incubation, the cells were collected by trypsinization and then reseeded into new 6-well plates at a density of 1000 cells/well/3 mL. The plates with cells were incubated for 10 days under standard conditions with 5% CO_2 at 37 °C. After this time, the medium was removed and the cells were washed with PBS, fixed with ice-cold ethanol (-20 °C) for 3 min, and washed again with PBS. Finally, cells were stained with crystal violet (0.01% in H_2O; Sigma-Aldrich, Taufkirchen, Germany) for 20 min. The plates were then washed with H_2O and allowed to air-dry.

3.3.4. Wound-Healing Assay

To analyze the migration properties of cells exposed to test compounds, a wound-healing assay was performed as reported in the literature [61,62]. The cells were seeded into 6-well plates at a density of 3×10^5 (HCT-116) or 4×10^5 (MCF-7, NHDF-Neo) per well (3 mL) and allowed to attach for 24 h under standard conditions with 5% CO_2 at 37 °C. After forming a confluent monolayer, a linear scratch in each sample with a 200 μL pipette tip was made and the first photo at time zero was taken. The cells were washed with PBS and then treated with solutions of test compounds in a fresh medium at a dose equal to their IC_{50} values. Control cells were grown with fresh medium supplemented with 0.5% DMSO. The cells were incubated and monitored for 72 h under standard conditions with 5% CO_2 at 37 °C. Cell monitoring and photos were taken using Live Cell Movie Analyzer, JuLI™ Br & FL (NanoEnTek Inc., Seoul, Korea).

3.3.5. Apoptosis and Cell Cycle Analyses by Flow Cytometry

The cell cycle and the type of cell death induced by the test compounds were measured by using flow cytometry according to the manufacturer's protocol. The cells were seeded into 6-well plates at a density of 3×10^5 (HCT-116) or 4×10^5 (MCF-7, NHDF-Neo) per well (3 mL) and allowed to attach for 24 h under standard conditions with 5% CO_2 at 37 °C. The following day, the medium was removed and cells were treated with solutions of test compounds in fresh medium at a dose equal to their IC_{50} values. Control cells were grown with fresh medium supplemented with 0.5% DMSO. After 24 h of incubation, the cells were collected by trypsinization. Then, samples were centrifuged (3 min, 2000 rpm, RT) and washed with PBS, after which the cells were centrifuged again (3 min, 2000 rpm, RT) and the supernatant was carefully removed. The resulting precipitate contained cells, which were used for flow cytometry experiments.

The fraction of dead cells after treatment with the test compounds were detected using the FITC Annexin-V Apoptosis Detection Kit with PI (BioLegend, San Diego, CA, USA). First, cells were suspended in 50 μL of cold Annexin-V Binding Buffer (BioLegend, San Diego, CA, USA) and incubated in the dark with 2.5 μL of antibody Annexin-V FITC and 10 μL of propidium iodide (PI) at 37 °C for 20 min. 250 μL of the Annexin-V Binding Buffer was then added and the samples were incubated in the dark on ice for 15 min. Cytometric analyses were performed using an Aria III flow cytometer (Becton Dickinson, Franklin Lakes, NJ, USA) with the FITC configuration (488 nm excitation; emission: LP mirror 503, BP filter 530/30) or PE configuration (547 nm excitation; emission: 585 nm) and at least 10,000 cells were counted.

For cell cycle analysis, the cells were suspended in 300 μL of hypotonic buffer (consisting of: sodium citrate dihydrate 1 g/L, propidium iodide (PI) 1 mg/mL, RNAse A 10 mg/mL (EURx, Gdańsk, Poland), Triton X-100 1:9), mixed gently and incubated in the dark at room temperature for 20–30 min. Cytometric analyses were performed immediately using an Aria III flow cytometer (Becton Dickinson, Franklin Lakes, NJ, USA), using at least 10,000 cells per sample. The cytofluorimetric configurations (PE) used are described above.

The experiment was conducted in three independent repetitions. The obtained results were analyzed using Flowing Software (Cell Imaging Core, Turku Center for Biotechnology, Turku, Finland).

3.3.6. Intercalation Study

For the DNA binding studies, all experiments were carried out in molecular biology grade Tris-HCl buffer at pH 7.5 (EURx, Poland). The purity of the calf thymus DNA (ctDNA) (Sigma-Aldrich, St. Louis, MO, USA) was determined by measuring the ratio of UV absorbance at 260 and 280 nm. Here, the ratio was in the range of 1.8–1.9, indicating the DNA was sufficiently free from protein. The concentration of ctDNA was determined from the absorbance at 260 nm and using a molar absorption coefficient $\varepsilon = 6600$ M^{-1} cm^{-1} [68]. The glycoconjugates **A-2** and **E-2** were dissolved in DMSO to a concentration of 10 mM, followed by diluting with Tris-HCl buffer to a concentration of 1 mM, which were used as the stock solutions, respectively. The absorption titration experiments were carried out by keeping the concentration of the glycoconjugates at a constant concentration of 50 μM while varying the ctDNA concentration from 3 to 300 μM. The samples were incubated for 2 h at 37 °C with gently shaking and the absorption spectra were measured using a UV–Vis-NIR spectrophotometer JASCO V-570 (Tokyo, Japan) in the range of 200–400 nm.

3.3.7. Statistical Analysis

For biological evaluation, at least three replicates were performed for every kind of experiment. The results were presented as means $\pm$ standard deviation (SD). The statistical analysis was based on a *t*-test, and a *p*-value less than 0.05 was considered statistically significant, indicated on the figures with an asterisk (*).

4. Conclusions

Focusing on the characteristic feature of cancer, which is increased demand for glucose, an anti-cancer treatment strategy based on the use of GLUT transporters for the targeted transport of drugs to the tumor cell has been developed. This strategy is a promising way to avoid the systemic toxicity of potential pharmaceuticals.

First, the synthesis pathways of sugar derivatives functionalized at the C-6 position were designed. D-Glucose, D-galactose, as well as glucuronic acid, and trehalose were used for this purpose. New glycoconjugates were prepared by the copper(I)-catalyzed 1,3-dipolar azide-alkyne cycloaddition between sugar derivatives and appropriately functionalized 8-hydroxyquinoline derivatives. The structures of all created products were confirmed using spectroscopy of nuclear magnetic resonance (^{1}H NMR and ^{13}C NMR) and high-resolution mass spectrometry (HRMS). Glycoconjugates were assessed in vitro for their cytotoxic activity against HCT-116 and MCF-7 cell lines, as well as against healthy NHDF-

Neo cells. The results show that the most active are glycoconjugates derivatives of D-glucose in which the triazole-quinoline was attached through the triazole nitrogen atom to the D-glucose unit directly to the carbon at the C-6 position. These glycoconjugates are more cytotoxic and selective than the analogous glycoconjugates formed by the C-1 anomeric position of D-glucose. Following the use of an EDG inhibitor and partial inhibition of GLUT activity, probably decreased compound uptake occurred, which resulted in less accumulation in cells and less anti-cancer activity. Additionally, glycoconjugates containing an unprotected glucose residue are more selective compared to the derivative with an acetylated sugar moiety. This proves the use of GLUT proteins in the transport of glycoconjugates to cancer cells. Compounds with acetyl protection in the sugar part are characterized by high lipophilicity, so this type of compound prefers passive transport across the cell membrane. This transport is non-selective, so these compounds also damage healthy cells. The results of the apoptosis and cell cycle analyses by flow cytometry confirmed the anticancer potential of the tested compounds. Experiments have shown that the new type of glycoconjugates shows pro-apoptotic properties, without causing inflammatory processes and without significantly affecting changes in the distribution of the cell cycle. The ability of glycoconjugates to interact with DNA by intercalation, which may subsequently induce damage to nucleic acids, was also confirmed. Moreover, glycoconjugates were able to reduce the clonogenic potential of cancer cells and inhibit their migration process.

In conclusion, the glycoconjugates formed through the C-6 position of D-glucose should be considered promising in therapy for the targeted transport of drugs into the tumor cell. It has been proven that the new type of glycoconjugates shows an increased affinity for GLUT, which means that they can be transported directly to tumor cells, avoiding systemic toxicity. The strategies for the synthesis of sugar derivatives using the C-6 position developed here may be used in the further design of new active sugar derivatives.

References

1. Srinivasarao, M.; Low, P.S. Ligand-Targeted Drug Delivery. *Chem. Rev.* **2017**, *117*, 12133–12164. [CrossRef] [PubMed]
2. Srinivasarao, M.; Galliford, C.V.; Low, P.S. Principles in the design of ligand-targeted cancer therapeutics and imaging agents. *Nat. Rev. Drug Discov.* **2015**, *14*, 203–219. [CrossRef] [PubMed]

3. Muro, S. Challenges in design and characterization of ligand-targeted drug delivery systems. *J. Control. Release* **2012**, *164*, 125–137. [CrossRef] [PubMed]

4. Tsimberidou, A.M. Targeted therapy in cancer. *Cancer Chemother. Pharmacol.* **2015**, *76*, 1113–1132. [CrossRef]

5. Pérez-Herrero, E.; Fernández-Medarde, A. Advanced targeted therapies in cancer: Drug nanocarriers, the future of chemotherapy. *Eur. J. Pharm. Biopharm.* **2015**, *93*, 52–79. [CrossRef]

6. Parker, N.; Turk, M.J.; Westrick, E.; Lewis, J.D.; Low, P.S.; Leamon, C.P. Folate receptor expression in carcinomas and normal tissues determined by a quantitative radioligand binding assay. *Anal. Biochem.* **2005**, *338*, 284–293. [CrossRef]

7. Nomura, N.; Pastorino, S.; Jiang, P.; Lambert, G.; Crawford, J.R.; Gymnopoulos, M.; Piccioni, D.; Juarez, T.; Pingle, S.C.; Makale, M.; et al. Prostate specific membrane antigen (PSMA) expression in primary gliomas and breast cancer brain metastases. *Cancer Cell Int.* **2014**, *14*, 26. [CrossRef]

8. Schmittgen, T.D.; Teske, S.; Vessella, R.L.; True, L.D.; Zakrajsek, B.A. Expression of prostate specific membrane antigen and three alternatively spliced variants of PSMA in prostate cancer patients. *Int. J. Cancer* **2003**, *107*, 323–329. [CrossRef]

9. Zhong, L.; Li, Y.; Xiong, L.; Wang, W.; Wu, M.; Yuan, T.; Yang, W.; Tian, C.; Miao, Z.; Wang, T.; et al. Small molecules in targeted cancer therapy: Advances, challenges, and future perspectives. *Sig. Transduct. Target. Ther.* **2021**, *6*, 201. [CrossRef]

10. Kratz, F.; Müller, I.A.; Ryppa, C.; Warnecke, A. Prodrug Strategies in Anticancer Chemotherapy. *Chem. Med. Chem.* **2008**, *3*, 20–53. [CrossRef]

11. Domiński, A.; Konieczny, T.; Duale, K.; Krawczyk, M.; Pastuch-Gawołek, G.; Kurcok, P. Stimuli-Responsive Aliphatic Polycarbonate Nanocarriers for Tumor-Targeted Drug Delivery. *Polymers* **2020**, *12*, 2890. [CrossRef]

12. Warburg, O. On the origin of cancer cells. *Science* **1956**, *123*, 309–314. [CrossRef]

13. DeBerardinis, R.J.; Chandel, N.S. We need to talk about the Warburg effect. *Nat. Metab.* **2020**, *2*, 127–129. [CrossRef]

14. Tanasova, M.; Fedie, J.R. Molecular Tools for Facilitative Carbohydrate Transporters (Gluts). *ChemBioChem* **2017**, *18*, 1774–1788. [CrossRef]

15. Barron, C.C.; Bilan, P.J.; Tsakiridis, T.; Tsiani, E. Facilitative glucose transporters: Implications for cancer detection, prognosis and treatment. *Metabolism* **2016**, *65*, 124–139. [CrossRef]

16. Szablewski, L. Expression of glucose transporters in cancers. *Biochim. Biophys. Acta* **2013**, *1835*, 164–169. [CrossRef]

17. Calvaresi, E.C.; Hergenrother, P.J. Glucose conjugation for the specific targeting and treatment of cancer. *Chem. Sci.* **2013**, *4*, 2319–2333. [CrossRef]

18. La Ferla, B.; Airoldi, C.; Zona, C.; Orsato, A.; Cardona, F.; Merlo, S.; Sironi, E.; D'Orazio, G.; Nicotra, F. Natural glycoconjugates with antitumor activity. *Nat. Prod. Rep.* **2011**, *28*, 630–648. [CrossRef]

19. Fu, J.; Yang, J.; Seeberger, P.H.; Yin, J. Glycoconjugates for glucose transporter-mediated cancer-specific targeting and treatment. *Carbohydr. Res.* **2020**, *498*, 108195. [CrossRef]

20. Pohl, J.; Bertram, B.; Hilgard, P.; Nowrousian, M.R.; Stüben, J.; Wießler, M. D-19575—A sugar-linked isophosphoramide mustard derivative exploiting transmembrane glucose transport. *Cancer Chemother. Pharmacol.* **1995**, *35*, 364–370. [CrossRef]

21. Shimizu, T.; Okamoto, I.; Tamura, K.; Satoh, T.; Miyazaki, M.; Akashi, Y.; Ozaki, T.; Fukuoka, M.; Nakagawa, K. Phase I clinical and pharmacokinetic study of the glucose-conjugated cytotoxic agent D-19575 (glufosfamide) in patients with solid tumors. *Cancer Chemother. Pharmacol.* **2010**, *65*, 243–250. [CrossRef]

22. Lacombe, D. Glufosfamide: Can We Improve the Process of Anticancer Agent Development? *Expert Opin. Investig. Drugs* **2012**, *21*, 749–754. [CrossRef]

23. Wu, M.; Li, H.; Liu, R.; Gao, X.; Zhang, M.; Liu, P.; Fu, Z.; Yang, J.; Zhang-Negrerie, D.; Gao, Q. Galactose conjugated platinum(II) complex targeting the Warburg effect for treatment of non-small cell lung cancer and colon cancer. *Eur. J. Med. Chem.* **2016**, *110*, 32–42. [CrossRef]

24. Halmos, T.; Santarromana, M.; Antonakis, K.; Scherman, D. Synthesis of glucose-chlorambucil derivatives and their recognition by the human GLUT1 glucose transporter. *Eur. J. Pharmacol.* **1996**, *318*, 477–484. [CrossRef]

25. Lin, Y.S.; Tungpradit, R.; Sinchaikul, S.; An, F.M.; Liu, D.Z.; Phutrakul, S.; Chen, S.T. Targeting the Delivery of Glycan-Based Paclitaxel Prodrugs to Cancer Cells via Glucose Transporters. *J. Med. Chem.* **2008**, *51*, 7428–7441. [CrossRef]

26. Cao, J.; Cui, S.; Li, S.; Du, C.; Tian, J.; Wan, S.; Qian, Z.; Gu, Y.; Chen, W.R.; Wang, G. Targeted Cancer Therapy with a 2-Deoxyglucose–Based Adriamycin Complex. *Cancer Res.* **2013**, *73*, 1362–1373. [CrossRef]

27. Kumar, P.; Shustov, G.; Liang, H.; Khlebnikov, V.; Zheng, W.; Yang, X.H.; Cheeseman, C.; Wiebe, L.I. Design, Synthesis, and Preliminary Biological Evaluation of 6-O-Glucose–Azomycin Adducts for Diagnosis and Therapy of Hypoxic Tumors. *J. Med. Chem.* **2012**, *55*, 6033–6046. [CrossRef]

28. Woźniak, M.; Pastuch-Gawołek, G.; Makuch, S.; Wiśniewski, J.; Krenács, T.; Hamar, P.; Gamian, A.; Szeja, W.; Szkudlarek, D.; Krawczyk, M.; et al. In Vitro and In Vivo Efficacy of a Novel Glucose–Methotrexate Conjugate in Targeted Cancer Treatment. *Int. J. Mol. Sci.* **2021**, *22*, 1748. [CrossRef]

29. Akam, E.A.; Tomat, E. Targeting Iron in Colon Cancer via Glycoconjugation of Thiosemicarbazone Prochelators. *Bioconjugate Chem.* **2016**, *27*, 1807–1812. [CrossRef]

30. Zhao, F.Q.; Keating, A.F. Functional Properties and Genomics of Glucose Transporters. *Curr. Genom.* **2007**, *8*, 113–128. [CrossRef]

31. Deng, D.; Xu, C.; Sun, P.; Wu, J.; Yan, C.; Hu, M.; Yan, N. Crystal structure of the human glucose transporter GLUT1. *Nature* **2014**, *510*, 121–133. [CrossRef] [PubMed]

32. Fernández, C.; Nieto, O.; Rivas, E.; Montenegro, G.; Fontenla, J.A.; Fernández-Mayoralas, A. Synthesis and biological studies of glycosyl dopamine derivatives as potential antiparkinsonian agents. *Carbohydr. Res.* **2000**, *327*, 353–365. [CrossRef]

33. Patra, M.; Johnstone, T.C.; Suntharalingam, K.; Lippard, S.J. A Potent Glucose–Platinum Conjugate Exploits Glucose Transporters and Preferentially Accumulates in Cancer Cells. *Angew. Chem. Int. Ed.* **2016**, *55*, 2550–2554. [CrossRef] [PubMed]

34. Krawczyk, M.; Pastuch-Gawolek, G.; Mrozek-Wilczkiewicz, A.; Kuczak, M.; Skonieczna, M.; Musiol, R. Synthesis of 8-hydroxyquinoline glycoconjugates and preliminary assay of their β1,4-GalT inhibitory and anti-cancer properties. *Bioorg. Chem.* **2019**, *84*, 326–338. [CrossRef] [PubMed]

35. Krawczyk, M.; Pastuch-Gawołek, G.; Pluta, A.; Erfurt, K.; Domiński, A.; Kurcok, P. 8-Hydroxyquinoline Glycoconjugates: Modifications in the Linker Structure and Their Effect on the Cytotoxicity of the Obtained Compounds. *Molecules* **2019**, *24*, 4181. [CrossRef] [PubMed]

36. Krawczyk, M.; Pastuch-Gawołek, G.; Hadasik, A.; Erfurt, K. 8-Hydroxyquinoline Glycoconjugates Containing Sulfur at the Sugar Anomeric Position—Synthesis and Preliminary Evaluation of Their Cytotoxicity. *Molecules* **2020**, *25*, 4174. [CrossRef]

37. Prachayasittikul, V.; Prachayasittikul, S.; Ruchirawat, S.; Prachayasittikul, V. 8-Hydroxyquinolines: A review of their metal chelating properties and medicinal applications. *Drug Des. Dev. Ther.* **2013**, *7*, 1157–1178. [CrossRef]

38. Song, Y.; Xu, H.; Chen, W.; Zhan, P.; Liu, X. 8-Hydroxyquinoline: A privileged structure with a broad-ranging pharmacological potential. *Med. Chem. Commun.* **2015**, *6*, 61–74. [CrossRef]

39. Oliveri, V.; Vecchio, G. 8-Hydroxyquinolines in medicinal chemistry: A structural perspective. *Eur. J. Med. Chem.* **2016**, *120*, 252–274. [CrossRef]

40. Santini, C.; Pellei, M.; Gandin, V.; Porchia, M.; Tisato, F.; Marzano, C. Advances in Copper Complexes as Anticancer Agents. *Chem. Rev.* **2014**, *114*, 815–862. [CrossRef]

41. Gupte, A.; Mumper, R.J. Elevated copper and oxidative stress in cancer cells as a target for cancer treatment. *Cancer Treat. Rev.* **2009**, *35*, 32–46. [CrossRef]

42. Gaur, K.; Vázquez-Salgado, A.M.; Duran-Camacho, G.; Dominguez-Martinez, I.; Benjamín-Rivera, J.A.; Fernández-Vega, L.; Carmona Sarabia, L.; Cruz García, A.; Pérez-Deliz, F.; Méndez Román, J.A.; et al. Iron and Copper Intracellular Chelation as an Anticancer Drug Strategy. *Inorganics* **2018**, *6*, 126. [CrossRef]

43. Nagelkerke, A.; Bussink, J.; Rowan, A.E.; Span, P.N. The mechanical microenvironment in cancer: How physics affects tumours. *Semin. Cancer Biol.* **2015**, *35*, 62–70. [CrossRef]

44. Dal Corso, A.; Pignataro, L.; Belvisi, L.; Gennari, C. Innovative Linker Strategies for Tumor-Targeted Drug Conjugates. *Chem. Eur. J.* **2019**, *25*, 14740–14757. [CrossRef]

45. Dheer, D.; Sing, V.; Shankar, R. Medicinal attributes of 1,2,3-triazoles: Current developments. *Bioorg. Chem.* **2017**, *71*, 30–54. [CrossRef]

46. Lei, Z.; Wang, J.; Mao, G.; Wen, Y.; Tian, Y.; Wu, H.; Li, Y.; Xu, H. Glucose Positions Affect the Phloem Mobility of Glucose–Fipronil Conjugates. *J. Agric. Food Chem.* **2014**, *62*, 6065–6071. [CrossRef]

47. Arai, M.A.; Yamaguchi, Y.; Ishibashi, M. Total synthesis of agalloside, isolated from Aquilaria agallocha, by the 5-*O*-glycosylation of flavan. *Org. Biomol. Chem.* **2017**, *15*, 5025–5032. [CrossRef]

48. Işılar, Ö.; Bulut, A.; Yaglioglu, A.S.; Demirtaş, İ.; Arat, E.; Türk, M. Synthesis and biological evaluation of novel urea, thiourea and squaramide diastereomers possessing sugar backbone. *Carbohydr. Res.* **2020**, *492*, 107991. [CrossRef]

49. Zemplén, G.; Pacsu, E. Über die Verseifung acetylierter Zucker und verwandter Substanzen. *Ber. Dtsch. Chem. Ges. (A B Ser.)* **1929**, *62*, 1613–1614. [CrossRef]

50. Campo, V.L.; Carvalho, I.; Da Silva, C.H.T.P.; Schenkman, S.; Hill, L.; Nepogodiev, S.A.; Field, R.A. Cyclooligomerisation of azido-alkyne-functionalised sugars: Synthesis of 1,6-linked cyclic *pseudo*-galactooligosaccharides and assessment of their sialylation by *Trypanosoma cruzi trans*-sialidase. *Chem. Sci.* **2010**, *1*, 507–514. [CrossRef]

51. Laurent, P.; Razafindralambo, H.; Wathelet, B.; Blecker, C.; Wathelet, J.P.; Paquot, M. Synthesis and Surface-Active Properties of Uronic Amide Derivatives, Surfactants from Renewable Organic Raw Materials. *J. Surfactants Deterg.* **2011**, *14*, 51–63. [CrossRef]

52. Menger, F.M.; Mbadugha, B.N.A. Gemini Surfactants with a Disaccharide Spacer. *J. Am. Chem. Soc.* **2001**, *123*, 875–885. [CrossRef]

53. Wang, M.; Xu, Z.; Tu, P.; Yu, X.; Xiao, S.; Yang, M. α,α-Trehalose derivatives bearing guanidino groups as inhibitors to HIV-1 Tat–TAR RNA interaction in human cells. *Bioorg. Med. Chem. Lett.* **2004**, *14*, 2585–2588. [CrossRef]

54. Srinivasachari, S.; Liu, Y.; Zhang, G.; Prevette, L.; Reineke, T.M. Trehalose Click Polymers Inhibit Nanoparticle Aggregation and Promote pDNA Delivery in Serum. *J. Am. Chem. Soc.* **2006**, *128*, 8176–8184. [CrossRef]

55. Kolb, H.C.; Finn, M.G.; Sharpless, K.B. Click Chemistry: Diverse Chemical Function from a Few Good Reactions. *Angew. Chem. Int. Ed.* **2001**, *40*, 2004–2021. [CrossRef]

56. Liang, L.; Astruc, D. The copper(I)-catalyzed alkyne-azide cycloaddition (CuAAC) "click" reaction and its applications. An overview. *Coord. Chem. Rev.* **2011**, *255*, 2933–2945. [CrossRef]

57. Domińska, M.; Pastuch-Gawołek, G.; Domiński, A.; Kurcok, P.; Erfurt, K. Synthesis and Preliminary Evaluation of the Cytotoxicity of Potential Metabolites of Quinoline Glycoconjugates. *Molecules* **2022**, *27*, 1040. [CrossRef]

58. Mosmann, T. Rapid colorimetric assay for cellular growth and survival: Application to proliferation and cytotoxicity assays. *J. Immunol. Methods* **1983**, *65*, 55–63. [CrossRef]

59. Deng, D.; Yan, N. GLUT, SGLT, and SWEET: Structural and mechanistic investigations of the glucose transporters. *Protein Sci.* **2016**, *25*, 546–558. [CrossRef]

60. Franken, N.; Rodermond, H.; Stap, J.; Haveman, J.; van Bree, C. Clonogenic assay of cells in vitro. *Nat. Protoc.* **2006**, *1*, 2315–2319. [CrossRef]
61. Cory, G. Scratch-wound assay. *Methods Mol. Biol.* **2011**, *769*, 25–30. [CrossRef] [PubMed]
62. Hulkower, K.I.; Herber, R.L. Cell Migration and Invasion Assays as Tools for Drug Discovery. *Pharmaceutics* **2011**, *3*, 107–124. [CrossRef] [PubMed]
63. Lauria, A.; La Monica, G.; Bono, A.; Martorana, A. Quinoline anticancer agents active on DNA and DNA-interacting proteins: From classical to emerging therapeutic targets. *Eur. J. Med. Chem.* **2021**, *220*, 113555. [CrossRef] [PubMed]
64. Perin, N.; Nhili, R.; Cindric, M.; Bertosa, B.; Vusak, D.; Martin-Kleiner, I.; Laine, W.; Karminski-Zamola, G.; Kralj, M.; David-Cordonnier, M.H.; et al. Amino substituted benzimidazo [1,2-a]quinolines: Antiproliferative potency, 3D QSAR study and DNA binding properties. *Eur. J. Med. Chem.* **2016**, *122*, 530–545. [CrossRef]
65. Loganathan, R.; Ramakrishnan, S.; Suresh, E.; Riyasdeen, A.; Akbarsha, M.A.; Palaniandavar, M. Mixed Ligand Copper(II) Complexes of N,N-Bis(benzimidazol-2-ylmethyl)amine (BBA) with Diimine Co-Ligands: Efficient Chemical Nuclease and Protease Activities and Cytotoxicity. *Inorg. Chem.* **2012**, *51*, 5512–5532. [CrossRef]
66. Ma, T.; Xu, J.; Wang, Y.; Yu, H.; Yang, Y.; Liu, Y.; Ding, W.; Zhu, W.; Chen, R.; Ge, Z.; et al. Ternary copper(II) complexes with amino acid chains and heterocyclic bases: DNA binding, cytotoxic and cell apoptosis induction properties. *J. Inorg. Biochem.* **2015**, *144*, 38–46. [CrossRef]
67. Semenov, S.N.; Belding, L.; Cafferty, B.J.; Mousavi, M.P.S.; Finogenova, A.M.; Cruz, R.S.; Skorb, E.V.; Whitesides, G.M. Autocatalytic Cycles in a Copper-Catalyzed Azide–Alkyne Cycloaddition Reaction. *J. Am. Chem. Soc.* **2018**, *140*, 10221–10232. [CrossRef]
68. Da Silva, C.M.; Silva, M.M.; Reis, F.S.; Ruiz, A.L.T.G.; de Carvalho, J.E.; Santos, J.C.C.; Figueiredo, I.M.; Alves, R.B.; Modolo, L.V.; de Fatima, A. Studies on free radical scavenging, cancer cell antiproliferation, and calf thymus DNA interaction of Schiff bases. *J. Photochem. Photobiol. B Biol.* **2017**, *172*, 129–138. [CrossRef]

Publikacja P.5

Synthesis and Preliminary Evaluation of the Cytotoxicity
of Potential Metabolites of Quinoline Glycoconjugates

M. Domińska[*], G. Pastuch-Gawołek[*], A. Domiński, P. Kurcok, K. Erfurt

Materiały uzupełniające do publikacji znajdują się w dołączonej płycie CD

Article

Synthesis and Preliminary Evaluation of the Cytotoxicity of Potential Metabolites of Quinoline Glycoconjugates

Monika Domińska [1,2,*], Gabriela Pastuch-Gawołek [1,2,*], Adrian Domiński [3], Piotr Kurcok [3] and Karol Erfurt [4]

1   Department of Organic Chemistry, Bioorganic Chemistry and Biotechnology,
    Silesian University of Technology, B. Krzywoustego 4, 44-100 Gliwice, Poland
2   Biotechnology Centre, Silesian University of Technology, B. Krzywoustego 8, 44-100 Gliwice, Poland
3   Centre of Polymer and Carbon Materials, Polish Academy of Sciences, M. Curie-Skłodowskiej 34,
    41-819 Zabrze, Poland; adrian.dominski@cmpw-pan.edu.pl (A.D.); piotr.kurcok@cmpw-pan.edu.pl (P.K.)
4   Department of Chemical Organic Technology and Petrochemistry, Silesian University of Technology,
    B. Krzywoustego 4, 44-100 Gliwice, Poland; karol.erfurt@polsl.pl
*   Correspondence: monika.krawczyk@polsl.pl (M.D.); gabriela.pastuch@polsl.pl (G.P.-G.)

Abstract: The design of prodrugs is one of the important strategies for selective anti-cancer therapies. When designing prodrugs, attention is paid to the possibility of their targeting tumor-specific markers such as proteins responsible for glucose uptake. That is why glycoconjugation of biologically active compounds is a frequently used strategy. Glycoconjugates consisting of three basic building blocks: a sugar unit, a linker containing a 1,2,3-triazole ring, and an 8-hydroxyquinoline fragment was described earlier. It is not known whether their cytotoxicity is due to whole glycoconjugates action or their metabolites. To check the biological activity of products that can be released from glycoconjugates under the action of hydrolytic enzymes, the synthetically obtained potential metabolites were tested in vitro for the inhibition of proliferation of HCT-116, MCF-7, and NHDF-Neo cell lines using the MTT assay. Research shows that for the full activity of glycoconjugates, the presence of all three building blocks in the structure of a potential drug is necessary. For selected derivatives, additional tests of targeted drug delivery to tumor cells were carried out using polymer nanocarriers in which they are encapsulated. This approach significantly lowered the determined IC$_{50}$ values of the tested compounds and improved their selectivity and effectiveness.

Keywords: quinoline glycoconjugates; metabolites; cytotoxicity; anticancer activity; click chemistry

1. Introduction

Designing anticancer drugs is one of the greatest challenges in medicinal chemistry in the XXI century. There are many therapeutic strategies for the treatment of cancer, such as surgery, radiation therapy, and chemotherapy. However, most of the available anti-cancer therapies are characterized by narrow therapeutic windows, which are mainly due to their high systemic toxicity, caused by a lack of tumor-specific selectivity. Therefore, it is necessary to search for new, effective drugs for the treatment of cancer. An important element of this search is the increasingly better understanding of the mechanisms of action of potential drugs, which may result in the implementation of safer, more selective therapies.

One of the many directions offered by medical chemistry is the concept of designing prodrugs, i.e., substances that become active only as a result of their metabolism inside the body. According to the definition proposed 60 years ago, prodrugs are inactive derivatives of drugs that undergo biotransformation in vivo to release active molecules, allowing specific drug delivery and triggering a therapeutic effect. The prodrug strategy minimizes drug deactivation before achieving the expected molecular goal and is the starting point for research into mechanisms that determine the bioavailability of potential drugs [1–3].

Most prodrugs are designed to improve the physicochemical, biopharmaceutical, or pharmacokinetic properties of a compound. The main aim is to improve the solubility and bioavailability of the drug and to increase its penetration into the cell. In most cases, prodrugs are simple chemical derivatives that require only one to two chemical or enzymatic transformation steps to yield the active parent drug. In some cases, a prodrug may consist of two pharmacologically active drugs that are coupled together into a single molecule so that each drug acts as a promoiety for the other such derivatives, called co-drugs [4]. A significant amount of the conventional chemotherapeutic agents have poor pharmacokinetic profiles and are distributed non-specifically in the body, leading to systemic toxicity with serious side effects. When designing prodrugs, attention is paid to the possibility of targeting tumor-specific markers. The microenvironment of tumors differs significantly from normal tissues. Compared to healthy counterparts, cancer tissues are characterized by unique pathophysiological markers such as hypoxia or a reducing microenvironment, high intracellular glutathione level, low pH, specific proteins overexpression, and elevated level of reactive oxygen species. All of these factors can act as promoters of prodrugs activation to induce a pharmacological effect without damaging normal tissues [5,6].

Cancer cells are characterized by changed energy metabolism compared to healthy cells. This fact contributes to the Warburg effect and is one of the most common features of cancer. Cancer cells produce their energy through glycolysis followed by lactic acid fermentation, characteristic of hypoxic conditions, and its level is much higher (over a hundred times) than in healthy cells, for which mitochondrial oxidative phosphorylation is the main source of energy [7,8]. The high rate of glycolysis consumes large amounts of glucose, hence the cells of some neoplasms are characterized by overexpression of proteins responsible for glucose uptake into their interior, the so-called GLUT transporters [9–11]. This fact can be exploited for the selective delivery of drugs by glycoconjugation of biologically active compounds [12,13]. The glycoconjugate prodrugs aim to reduce the systemic toxicity of the drug by targeted transport to cancer cells via GLUT transporters and the release of the active form of the drug in the intracellular microenvironment.

It is also known that cancer cells have an increased need for metal ions such as zinc, calcium, iron, and copper. They are involved in basic cellular processes, therefore their chelation effect plays an important role in drug design [14–16]. The elevated amount of copper in cancerous tissues, combined with the fact that copper promotes angiogenesis, cancer growth, and metastasis, has led to attempts to obtain copper-complexing compounds and use them in anti-cancer therapy [17–19]. An example of such a compound is 8-hydroxyquinoline, the derivatives of which constitute one of the important groups of metal-chelating compounds necessary for the growth and angiogenesis of neoplastic cells [20–23]. The conducted experiments proved that the conjugation of metallodrugs with a molecule of sugar is able to deliver prodrugs to a specific tumor tissue due to the overexpression of glucose receptors in neoplastic cells, which provides better antitumor activity and reduction in systemic toxicity [24,25].

Considering the above, our research group conducted a series of experiments on the glycoconjugation of 8-hydroxyquinoline (8-HQ) derivatives [26–28]. We assumed that due to the addition of a sugar derivative to the active 8-HQ fragment, the obtained molecules would be able to selectively enter a tumor cell using the Warburg effect. Moreover, the addition of the 1,2,3-triazole fragment to the structure of glycoconjugates improved their cytotoxic activity and had a positive effect on the ability to form complexes with metal ions. Several of the designed glycoconjugates derivatives of 8-HQ have shown significant cytotoxicity at the micromolar level against the variety of cell lines tested, compared to their parent compounds. The designed bonds linking sugar and quinoline are stable in the extracellular space. However, after entering the cell, these compounds can be degraded under the action of hydrolytic enzymes, releasing the active form of the drug, which is able to induce cytotoxicity (Figure 1). Except for the cytotoxicity assessment of the glycoconjugates themselves, it seems advisable to check the biological activity of products that can be released in the tumor cell from glycoconjugates by the action of hydrolytic

enzymes. Comprehensive research should focus on assessing the activity of each of the possible metabolites of a given prodrug to determine exactly what role individual fragments of the molecule play, as well as which of their structural elements are responsible for the antitumor effect and whether these compounds are not toxic to healthy cells.
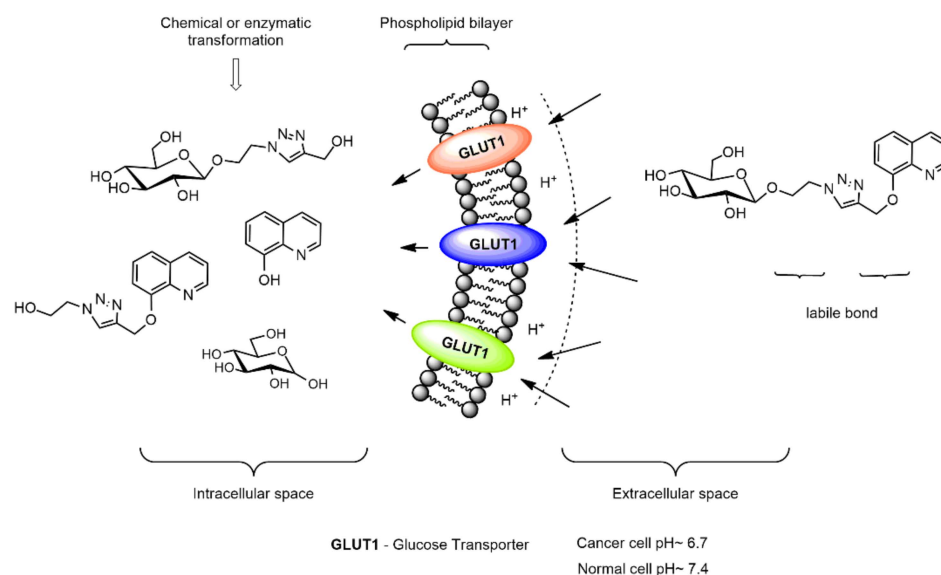
Figure 1. Interaction at the micro-environment. Targeted prodrug delivery.

2. Results and Discussion

2.1. Synthesis

The aim of the research was to obtain and evaluate the biological activity of potential metabolites that may be formed in biological systems by the degradation of anti-cancer prodrugs based on glycoconjugates derivatives of 8-hydroxyquinoline described in recent works [26–28]. This will allow answering the question of which fragment of the molecule is responsible for the obtained biological activity.

The designed compounds consist of an 8-hydroxyquinoline fragment linked by an aliphatic chain of various lengths to a 1,2,3-triazole ring. The second type of metabolites are D-glucose derivatives containing anomeric oxygen, nitrogen, or sulfur atom and also connect to the 1,2,3-triazole ring by various linkers. Due to the stability of triazoles in typical physiological conditions, the 1,2,3-triazole linker is present in glycoconjugates and all metabolite structures. Studies have shown that the 1,2,3-triazole ring is an important system that influences anti-cancer activity. Furthermore, their tendency to form hydrogen bonds increases the solubility of such molecules in biological systems, which favor binding to biomolecular targets, thus allowing in vivo administration [29].

The desired metabolites were prepared by the copper(I)-catalyzed 1,3-dipolar azide-alkyne cycloaddition (CuAAC), in the variant used for the synthesis of biologically active compounds belonging to the group of the so-called *click-chemistry* reactions developed by Sharples [29–32]. This type of reaction allows for the quick and efficient synthesis of new compounds and combinatorial libraries. This process is characterized by high yields, stereospecificity, mild reaction conditions, the absence of by-products, and the simplicity of product purification. The CuAAC reaction was carried out between the appropriate azide or propargyl quinoline derivatives **3–10** or sugar derivatives **11–24** and 2-azidoethanol **1** or propargyl alcohol **2**. A general procedure for the synthesis of metabolites is shown in Schemes 1 and 2. Used for the reaction, quinoline substrates functionalized in the 8-OH position (Figure 2) and sugar derivatives substituted at the anomeric position (Figure 3) were prepared according to the previously published procedures [26–28]. Propargyl alcohol **2** is a commercially available reagent, whereas 2-azidoethanol **1** was obtained by substituting 2-bromoethanol with sodium azide in DMF [33]. Confirmation of bromine atom exchange

to the azide moiety was the appearance in the ^{13}C-NMR spectra of the signal of CH_2N_3 carbon with a shift of about 53.5 ppm.
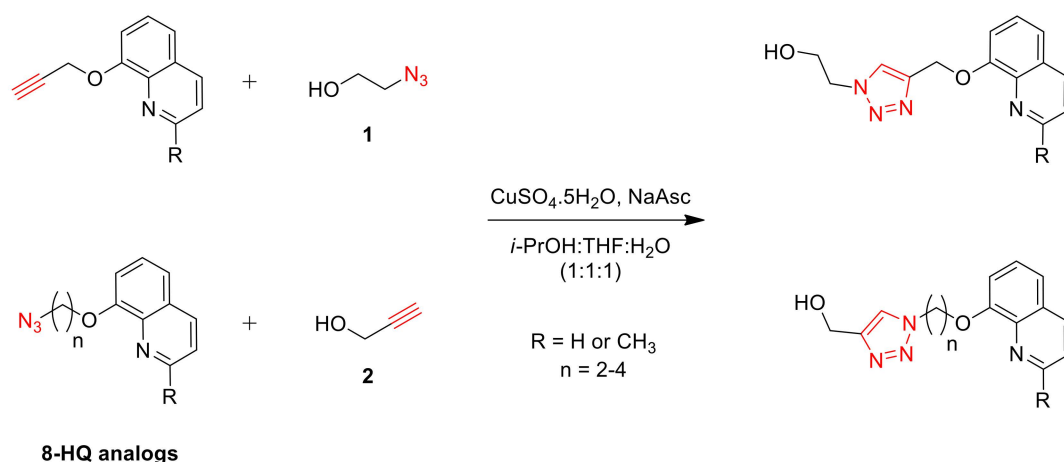
Scheme 1. Strategies for the synthesis of metabolites of 8-hydroxyquinoline derivatives.
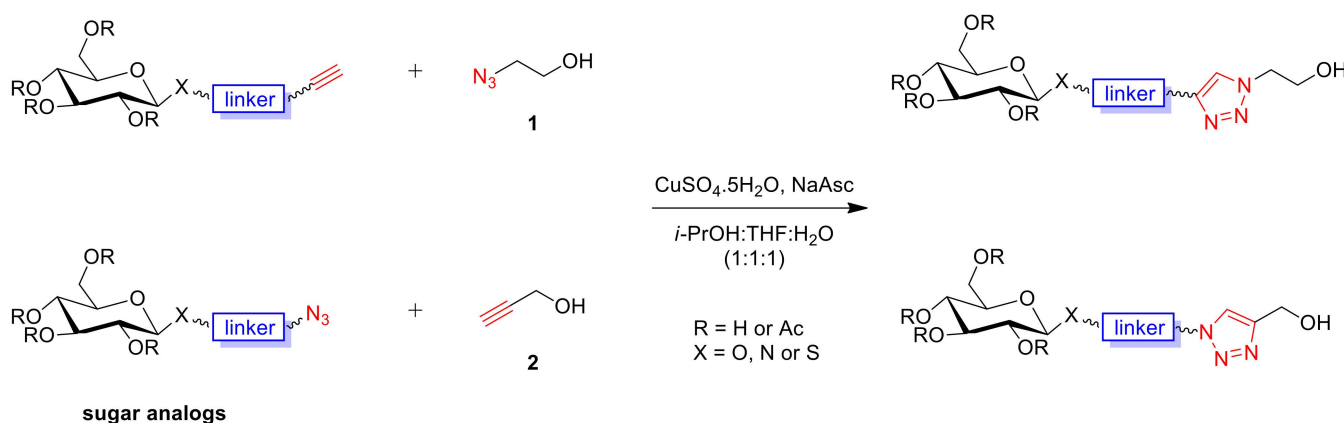
Scheme 2. Strategies for the synthesis of metabolites of sugar derivatives.
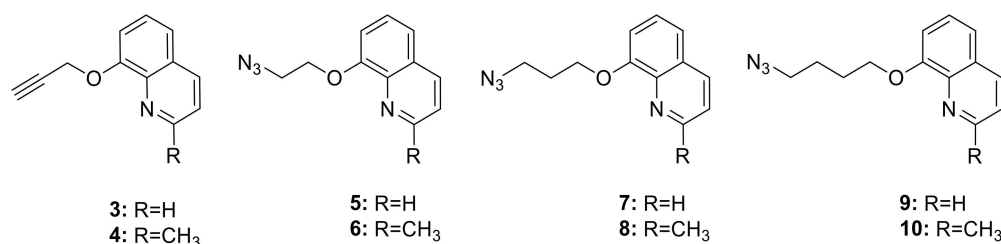
Figure 2. Structures of substrates derivatives of 8-hydroxyquinoline.

The reaction for the synthesis of metabolites was carried out by dissolving the mentioned reagents in an equimolar ratio in the THF/*i*-PrOH solvent system, followed by adding the CuSO$_4$·5H$_2$O/NaAsc aqueous catalyst system to the reaction mixture. CuSO$_4$ was used as the source of copper ions. Meanwhile, sodium ascorbate was a reducing agent of Cu(II) to Cu(I) in situ and avoided the formation of oxidation byproducts. The reaction was carried out for 24 h at room temperature. Pure products were isolated by column chromatography in good or very good yields. As a result of the reaction, structures containing only a 1,4-disubstituted 1,2,3-triazole ring in the linker were obtained. The structures of all synthesized metabolites, as well as the standard glycoconjugates, are presented in Tables 1 and 2. The new structures were confirmed using NMR and HRMS spectroscopy methods. The presence of characteristic signals in the NMR spectra originating from the

1,2,3-triazole ring indicated the formation of the desired product. These are signal a singlet at about δ = 7.9 ppm from the H-C(5) proton triazole ring in ^{1}H-NMR spectra and two characteristic carbon signals at about 123 ppm and 144 ppm for C(4) and C(5) from triazole ring in the ^{13}C-NMR spectra. The NMR spectra of all synthesized products are presented in the Supplementary Materials. The physicochemical properties, such as melting point and optical rotation, were also determined.
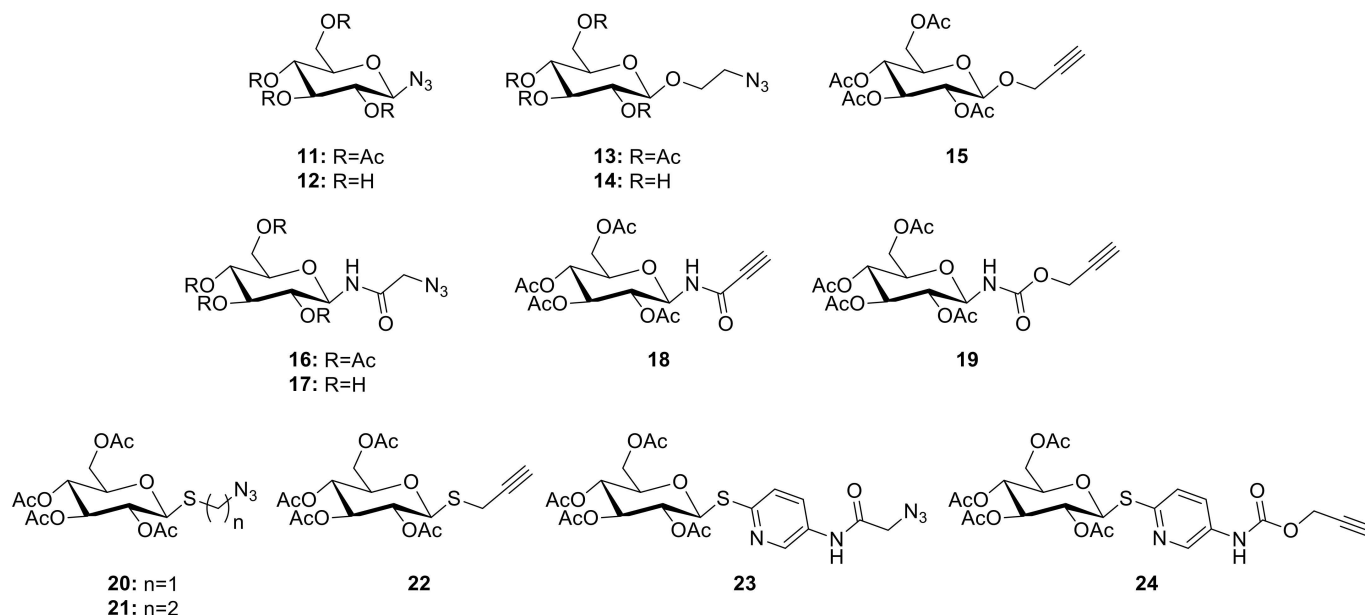
Figure 3. Structures of substrates derivatives of sugar.

2.2. Cytotoxicity Studies

The obtained compounds were tested in vitro for the inhibition of the proliferation of several tumor cell lines. Cell lines were selected for the experiments, on which glycoconjugates from which described metabolites could arise were previously tested. HCT-116 (colorectal carcinoma cell line) and MCF-7 (human breast adenocarcinoma cell line) are characterized by a high demand for glucose and overexpression of the GLUT transporters [34,35]. In addition, an excess of copper ions was observed near the above-mentioned lines [36,37]. NHDF-Neo (Normal Human Dermal Fibroblasts-Neonatal) is a healthy cell line and is a reference point to evaluate the selectivity of compounds. Screening of cell viability after exposure to the compounds was performed using the MTT assay. It is used to measure cellular metabolic activity as an indicator of cell viability, proliferation, and cytotoxicity. The basis of the MTT method is the ability of mitochondrial dehydrogenase present in the mitochondria of metabolically active cells to convert the yellow tetrazolium salt (MTT) into purple formazan crystals. MTT assay was carried out according to the protocol (MTT, Sigma-Aldrich, Taufkirchen, Germany) [38]. Cells were treated with various concentrations of test compounds for 24–72 h. The activity of test compounds is expressed by IC$_{50}$ values, defined as 50% inhibition of cell growth compared to the untreated control. The results are presented in Tables 1 and 2 and compared with the activity of glycoconjugates, which could theoretically form the tested potential metabolites.

Table 1. Biological activity of the obtained compounds (metabolites of 8-hydroxyquinoline derivatives and glycoconjugates from which they could arise).

R[1]:   R[2]:   R[3]:   R[4]:

* binding site

Compound Number	Structure	Activity IC$_{50}$ [μM] [a]			Glycoconjugate Structure [d]	Activity IC$_{50}$ [μM]		
		HCT-116 [b]	MCF-7 [c]	NHDF [b]		HCT-116	MCF-7	NHDF
M1		>800	>800	-		239.95 ± 2.27	105.91 ± 4.06	216.12 ± 9.68
M2		>800	>800	-		290.62 ± 7.02	135.97 ± 1.47	715.16 ± 10.63
M3		>800	>800	-		216.95 ± 4.73	196.49 ± 1.91	405.85 ± 5.73
M4		>800	750.45 ± 1.07	-		229.56 ± 2.59	375.58 ± 8.34	-
M5		>800	602.95 ± 1.95	-		142.98 ± 2.30	200.60 ± 1.10	214.75 ± 6.43
M6		469.82 ± 8.61	194.13 ± 0.18	202.02 ± 3.29		135.07 ± 6.98	221.11 ± 2.40	426.80 ± 3.80
M7		196.18 ± 3.55	155.96 ± 0.45	131.99 ± 1.00		328.75 ± 9.02	254.81 ± 3.63	-
M8		564.85 ± 3.59	286.01± 1.42	-		294.74 ± 1.79	214.83 ± 1.65	>800

[a] Cytotoxicity was evaluated using the MTT assay; [b] Incubation time 24 h; [c] Incubation time 72 h; [d] The synthesis and biological activity of the presented glycoconjugates are described in publications [26–28]. Data are presented as the mean ± standard deviation (*n* = 3).

Table 2. Biological activity of the obtained compounds (metabolites of sugar derivatives and glycoconjugates from which they could arise).

R[1]:   R[2]:   R[3]:   R[4]:

* binding site

Compound Number	Structure	Activity IC$_{50}$ [μM] [a]			Glycoconjugate Structure [d]	Activity IC$_{50}$ [μM]		
		HCT-116 [b]	MCF-7 [c]	NHDF [b]		HCT-116	MCF-7	NHDF
M9		>800	>800	-		69.00 ± 2.53	57.69 ± 3.32	57.37 ± 3.19
M10		>800	>800	-		212.00 ± 7.71	185.34 ± 2.21	247.24 ± 11.64
M11		>800	>800	-		239.95 ± 2.27	105.91 ± 4.06	216.12 ± 9.68
M12		>800	>800	-		>800	>800	-
M13		>800	>800	-		216.95 ± 4.73	196.49 ± 1.91	405.85 ± 5.73
M14		258.32 ± 2.06	428.66 ± 2.11	101.15 ± 4.98		246.24 ± 6.19	192.66 ± 3.71	219.14 ± 2.40
M15		747.66 ± 8.29	>800	-		112.79 ± 1.58	87.89 ± 4.11	94.69 ± 0.46
M16		>800	>800	-		239.05 ± 2.97	203.78 ± 3.55	382.61 ± 2.42
M17		>800	>800	-		246.23 ± 1.31	176.40 ± 1.81	696.74 ± 1.60
M18		107.24 ± 2.17	248.77 ± 1.58	89.07 ± 8.63		106.71 ± 4.10	59.12 ± 1.46	54.62 ± 0.74
M19		>800	792.99 ± 1.30	-		127.05 ± 1.75	76.30 ± 1.33	105.32 ± 3.40

Table 2. *Cont.*

R[1]:   R[2]:   R[3]:   R[4]:

* binding site

Compound Number	Structure	Activity IC$_{50}$ [μM] [a]			Glycoconjugate Structure [d]	Activity IC$_{50}$ [μM]		
		HCT-116 [b]	MCF-7 [c]	NHDF [b]		HCT-116	MCF-7	NHDF
M20		>800	>800	-		172.83 ± 3.48	153.34 ± 0.25	229.12 ± 2.06
M21		>800	>800	-		146.16 ± 3.49	69.72 ± 3.50	71.81 ± 6.70
M22		>800	>800	-		63.49 ± 2.37	67.50 ± 1.58	64.00 ± 5.34

[a] Cytotoxicity was evaluated using the MTT assay; [b] Incubation time 24 h; [c] Incubation time 72 h; [d] The synthesis and biological activity of the presented glycoconjugates are described in publications [26–28]. Data are presented as the mean ± standard deviation (*n* = 3).

The motivation for obtaining the metabolites **M1**–**M8** presented in Table 1 was to check whether the addition of a sugar unit is necessary to improve the biological properties of 8-HQ or whether the introduction of the linker containing the 1,2,3-triazole ring alone would be sufficient. In contrast to the glycoconjugates, which were mostly able to inhibit cell proliferation in the concentration range studied, most of the resulting 8-HQ derivative metabolites did not show interesting activity. Considering the influence of the length of the alkyl chain between the quinoline fragment and the 1,2,3-triazole ring, the most active turned out to be metabolites with three or four carbon atoms in the linker. It is probably related to the possibility of the compound penetrating the phospholipid membrane into the cells. The compound with the longest alkyl chain and the 1,2,3-triazole ring is characterized by the highest lipophilicity, which may help in its transport across cell membranes. The observed lower activity of the analogous glycoconjugate than the most active metabolite **M7** probably indicates incomplete hydrolysis of the glycosidic bond in the cell by β-glycosidases, leading to the release of active aglycone, which is able to complex copper(II) ions.
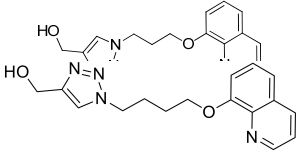
The obtained metabolites containing a sugar part and a linker with a 1,2,3-triazole ring in the structure were also weakly active or completely inactive against the tested tumor cell lines (Table 2). This confirms that the quinoline fragment is responsible for showing antiproliferative activity. On the other hand, sugar molecules are also an additional source of energy, allowing the proliferation of cells. The exceptions are the compounds **M14** and **M18**. Probably the combination of the 1,2,3-triazole ring with an amide moiety, as in the case of the **M14** compound, improves the ability to complex Cu^{2+} ions, thus inhibiting the proliferation of neoplastic cells by eliminating an important factor of their growth. It is worth adding that the sugar derivative **16** without the 1,2,3-triazole ring was completely inactive against the tested cell lines. Due to the presence of acetyl protecting groups in the sugar part, which improve the lipophilicity of the molecule, the metabolite **M14** may be able to cross biological barriers and enter cells by passive diffusion. The analogous metabolite **M15** with the unprotected sugar fragment showed no antiproliferative activity. The deprotected derivatives apparently do not have sufficient affinity for GLUT transporters. Cytotoxic activity was also demonstrated by the metabolite **M18** containing a sulfur atom in the anomeric position of the sugar. Probably the compounds with the *S*-glycosidic bond do not undergo premature enzymatic degradation before entering the cell and therefore the sulfur atom together with the 1,2,3-triazole ring is able to complex copper ions. It was observed that the extension of the alkyl chain in the metabolite **M19** did not improve the cytotoxicity. On the other hand, the spatial orientation of the 1,2,3-triazole ring with the linker turned out to be important. For comparison, in order to create a 1,2,3-triazole system in the structure of the metabolite **M20**, a derivative of 1-thiosugar with an anomeric propargyl moiety was used. This reaction created an "inverted" system of 1,2,3-triazole in relation to that in the **M18** metabolite. This compound did not show any antiproliferative activity. It can be assumed that not only the hydrolytic stability is important for biological activity, but also the mutual spatial orientation of the atom in the anomeric position of the sugar and the 1,2,3-triazole ring. In view of the above results, the lack of activity of the **M21** and **M22** derivatives is surprising. Quite unexpectedly, no beneficial effect was found to introduce an additional pyridine fragment together with an amide or carbamate bond into the linker structure between the 1-thiosugar moiety and the 1,2,3 triazole ring. This additional fragment was supposed to increase the ability of metabolites to complex copper ions, which are needed for the growth of cancer cells. Perhaps additional cytotoxicity studies on an extended panel of tumor cell lines are worth carrying out for these molecules.

Compounds showing activity against the tested tumor cell lines turned out to be toxic to healthy cells at the same time. This is because passive transport, which allows them to enter the cell, is not preferred for designed prodrugs and does not guarantee selectivity. As a result, the tested compounds damage both cancer cells and healthy cells. Experiments should be extended in the direction allowing for better matching of compounds to the structure of GLUT transporters, which should ultimately improve their selectivity.

The above experiments do not explain whether the low cytotoxic activity of the obtained metabolites results from the real lack of activity of the structures or because of the difficulties crossing of biological membranes by 8-HQ derivatives. To investigate this issue in detail, additional targeted drug delivery experiments to tumor cells were required. One of the strategies to increase the bioavailability and selectivity of drugs is the use of polymeric carriers in which they are encapsulated. Their action is based on the controlled release of encapsulated drugs under the influence of appropriate intracellular stimuli (e.g., temperature, pH), thus improving the drug's ability to target cancer cells [39,40]. It is known that in the microenvironment of neoplastic tissues there is a mildly acidic environment, which results from excessive glycolysis in tumors [41]. Therefore, for the targeted transport of selected, previously tested, metabolites **M5** and **M7**, specially developed biodegradable pH-sensitive polymer nanocarriers were used, which decompose with the release of the drug under the influence of pH changes [42]. Herein, pH-responsive micelles consisting of poly(ethylene glycol)-*b*-poly(acetal-functionalized aliphatic carbonate)-*b*-oligo([R]-3-hydroxybutyrate) triblock copolymer were used as nanocarriers for metabolites. Recent studies have shown that the encapsulation of 8-HQ derivative glycoconjugates in pH-sensitive nanocarriers significantly improved their effectiveness by avoiding systemic side effects and reducing the doses of administered prodrugs [42].

The in vitro cytotoxic activity of free drugs (**M5** and **M7**) and drug-loaded pH-responsive micelles (**M5**-micelles and **M7**-micelles) was determined by the MTT test. Cells were incubated with the appropriate compounds for 72 h in a concentration range oscillating within the IC_{50} activity of the above-mentioned compounds. The polymeric material can be safely used in research because it is not toxic to the cell lines tested [42]. The relationship between cell viability and the concentration of free drugs and drug-loaded micelles is shown in Figure 4. The IC_{50} value was also determined for each case and is summarized in Table 3. The results demonstrate that the drug-loaded micelles showed a much stronger cytotoxic effect against all tested cell lines as compared to the free drugs. **M5** and **M7** loaded into micelles achieve much lower IC_{50} values compared to their free counterparts. It is worth noting that the inhibitory effect of micelles loaded with metabolites on the proliferation of healthy NHDF-Neo cells, in comparison to free drugs, is not as great as in case wherein they are applied to neoplastic cells. As a result, metabolites-loaded micelles showed a higher selectivity index compared to free metabolites, which may be due to the specific microenvironment of tumor cells. It can be assumed that the use of micelles facilitates the active transport of compounds directly to the cancer cell, thus increasing the accumulation of the drug in cancer cells and its effectiveness. The lower cytotoxic activity of free metabolites as well as of free glycoconjugates is probably due to their difficult penetration into the cell through phospholipid membranes. The low activity of analogous glycoconjugates may also be caused by too early hydrolysis of the glycosidic linkage and therefore difficult crossing of biological membranes, or by an incompatibility between the sugar derivatives and GLUT transporters. However, no mechanism of action can be ruled out at this stage.

Table 3. Biological activity of the free metabolites and metabolites loaded into micelles.

Compound Number	Structure	Activity IC_{50} [μM] [a]		
		HCT-116 [b]	MCF-7 [b]	NHDF [b]
M5		>800	602.95 ± 1.95	509.52 ± 3.26
M5-micelles		23.59 ± 1.44	33.04 ± 1.73	59.54 ± 2.81
M7		169.19 ± 3.90	155.96 ± 0.45	85.14 ± 4.16
M7-micelles		12.41 ± 0.41	4.46 ± 0.36	45.76 ± 1.78

[a] Cytotoxicity was evaluated using the MTT assay; [b] Incubation time 72 h. Data are presented as the mean ± standard deviation (*n* = 3).
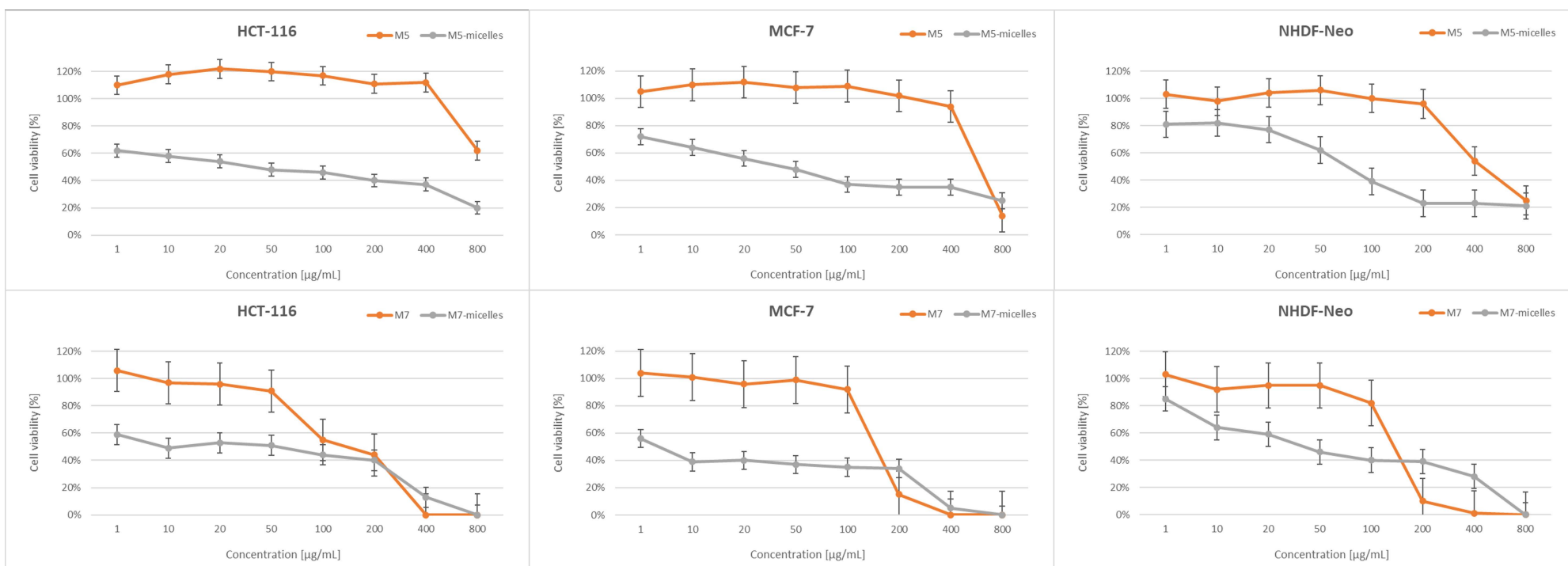
Figure 4. The cell viability of free metabolites and metabolites loaded into micelles for HCT-116, MCF-7, and NHDF-Neo cells after 72 h of incubation. Data are presented as the mean ± standard deviation (*n* = 3).

3. Materials and Methods

3.1. General Information

NMR spectra were recorded with an Agilent spectrometer at a frequency of 400 MHz or Varian spectrometer at a frequency of 600 MHz using tetramethylsilane (TMS) as the internal standard and $CDCl_3$ or DMSO-d6 as the solvents, which were purchased from ACROS Organics (Geel, Belgium). Chemical shifts (δ) were reported in ppm and the coupling constants (*J*) in Hz. The following abbreviations were used to explain the observed multiplicities: s: singlet, d: doublet, dd: doublet of doublets, ddd: doublet of doublet of doublets, t: triplet, dd~t: doublet of doublets resembling a triplet (with similar values of coupling constants), m: multiplet, b: broad. High-resolution mass spectra (HRMS) were recorded with a WATERS LCT Premier XE system using the electrospray-ionization (ESI) technique. Optical rotations were measured with a JASCO P-2000 polarimeter using a sodium lamp (589.3 nm) at room temperature. Melting point measurements were performed on OptiMelt (MPA 100) Stanford Research Systems. Reactions were monitored by thin-layer chromatography (TLC) on precoated plates of silica gel 60 F254 (Merck Millipore, Burlington, MA, USA). The TLC plates were visualized under UV light (λ = 254 nm) or by charring after spraying with 10% solution of sulfuric acid in ethanol. Crude products were purified using column chromatography performed on Silica Gel 60 (70–230 mesh, Fluka, St. Louis, MI, USA), developed with toluene:EtOAc or $CHCl_3$:MeOH as solvent systems. Organic solvents were evaporated on a rotary evaporator under diminished pressure at 40 °C. The absorbance on the MTT assay was measured spectrophotometrically at the 570 nm wavelength using a plate reader (Epoch, BioTek, Winooski, VT, USA).

All used chemicals and solvents were purchased from Sigma-Aldrich (Saint Louis, MO, USA), ACROS Organics (Geel, Belgium), and Avantor Performance Materials (Gliwice, Poland) and were used without further purification. D-Glucose, 8-hydroxyquinoline, 8-hydroxyquinaldine, and propargyl alcohol **2** are commercially available (Sigma-Aldrich). 2-Azidoethanol **1**, 8-Hydroxyquinoline derivatives **3**–**10** and sugar derivatives **11**–**24** were prepared according to the respective published procedures [26–28,33].

3.2. Chemistry

3.2.1. General Procedure for the Synthesis of Metabolites **M1**–**M22**

The appropriate 8-hydroxyquinoline derivative **3**–**10** or sugar derivative **11**–**24** (1 eq.) was dissolved in dry THF (2 mL) and *i*-PrOH (2 mL) and then 2-azidoethanol **1** or propargyl alcohol **2** (1 eq.) was added. The solutions of sodium ascorbate (0.4 eq.) in H_2O (1 mL) and $CuSO_4 \cdot 5H_2O$ (0.2 eq.) in H_2O (1 mL) were mixed and immediately added to the reaction mixture. The reaction was stirred at room temperature for 24 h. The reaction progress was monitored by TLC in an eluents system $CHCl_3$:MeOH (20:1 or 2:1). After completion of the reaction, the catalyst systems were filtered off and solvents were concentrated under reduced pressure. The crude residues were purified using column chromatography (toluene:AcOEt, 2:1 and $CHCl_3$:MeOH, 100:1 for fully protected glycoconjugates and analogs of 8-HQ or gradient of $CHCl_3$:MeOH from 50:1 to 2:1 for products with unprotected sugar part).

1-Hydroxyethyl-4-(8-quinolinyloxymethyl)-*1H*-1,2,3-triazol **M1**: Starting from 8-(prop-2-yn-1-yloxy)quinoline **3** and 2-azidoethanol **1**, the product was obtained as a brown solid (81% yield); m.p.: 126–128 °C; $[\alpha]^{25}_D$ = −0.6 (c = 1.0, $CHCl_3$); ^1H NMR (400 MHz, $CDCl_3$): δ 4.01 (t, 2H, *J* = 5.0 Hz, CH_2), 4.45 (t, 2H, *J* = 5.0 Hz, CH_2), 5.46 (s, 2H, CH_2O_{Quin}), 7.28 (dd, 1H, *J* = 1.4 Hz, *J* = 8.2 Hz, H-7$_{Quin}$), 7.35–7.48 (m, 3H, H-3$_{Quin}$, H-5$_{Quin}$, H-6$_{Quin}$), 7.94 (s, 1H, H-5$_{Triaz}$), 8.12 (d, 1H, *J* = 8.3 Hz, H-4$_{Quin}$), 8.83 (bs, 1H, H-2$_{Quin}$); ^{13}C NMR (100 MHz, $CDCl_3$): δ 52.82 (CH_2N), 61.02 (CH_2O), 62.75 (CH_2O), 109.78 (C-7$_{Quin}$), 120.19 (C-5$_{Quin}$), 121.68 (C-3$_{Quin}$), 124.65 (C-5$_{Triaz}$), 126.82 (C-6$_{Quin}$), 129.50 (C-4a$_{Quin}$), 136.19 (C-4$_{Quin}$), 140.00 (C-8a$_{Quin}$), 143.72 (C-4$_{Triaz}$), 149.12 (C-2$_{Quin}$), 153.76 (C-8$_{Quin}$); HRMS (ESI-TOF): calcd for $C_{14}H_{15}N_4O_2$ ([M + H]$^+$): *m/z* 271.1195; found: *m/z* 271.1199.

1-Hydroxyethyl-4-(2-methyl-8-quinolinyloxymethyl)-1*H*-1,2,3-triazol **M2**: Starting from 2-methyl-8-(prop-2-yn-1-yloxy)quinoline **4** and 2-azidoethanol **1**, the product was ob-

tained as a brown solid (80% yield); m.p.: 109–111 °C; $[\alpha]^{25}_D$ = 0.2 (c = 1.0, CHCl$_3$); ^{1}H-NMR (600 MHz, CDCl$_3$): δ 2.73 (s, 3H, CH$_3$), 3.99 (t, 2H, *J* = 5.0 Hz, CH$_2$), 4.44 (t, 2H, *J* = 5.0 Hz, CH$_2$), 5.46 (s, 2H, CH$_2$O$_{Quin}$), 7.24 (m, 1H, H-7$_{Quin}$), 7.29 (d, 1H, *J* = 8.4 Hz, H-3$_{Quin}$), 7.34–7.38 (m, 2H, H-5$_{chin}$, H-6$_{Quin}$), 7.90 (s, 1H, H-5$_{Triaz}$), 8.00 (d, 1H, *J* = 8.4 Hz, H-4$_{Quin}$); ^{13}C-NMR (150 MHz, CDCl$_3$): δ 25.40 (CH$_3$), 52.76 (CH$_2$N), 61.01 (CH$_2$O), 63.01 (CH$_2$O), 110.24 (C-7$_{Quin}$), 120.16 (C-5$_{Quin}$), 122.67 (C-3$_{Quin}$), 124.52 (C-5$_{Triaz}$), 125.74 (C-6$_{Quin}$), 127.73 (C-4a$_{Quin}$), 136.28 (C-4$_{Quin}$), 139.65 (C-8a$_{Quin}$), 144.00 (C-4$_{Triaz}$), 153.30 (C-2$_{Quin}$), 158.20 (C-8$_{Quin}$); HRMS (ESI-TOF): calcd for C$_{15}$H$_{17}$N$_4$O$_2$ ([M + H]$^+$): *m/z* 285.1352; found: *m/z* 285.1357.

4-Hydroxymethyl-1-(8-quinolinyloxyethyl)-1*H*-1,2,3-triazol **M3**: Starting from 8-(2-azidoethoxy)quinoline **5** and propargyl alcohol **2**, the product was obtained as a brown solid (91% yield); m.p.: 116–119 °C; $[\alpha]^{25}_D$ = 23.0 (c = 1.0, CHCl$_3$); ^{1}H-NMR (400 MHz, DMSO): δ 4.51 (s, 2H, CH$_2$OH), 4.61 (t, 2H, *J* = 5.1 Hz, CH$_2$), 4.89 (t, 2H, *J* = 5.1 Hz, CH$_2$), 7.25 (dd, 1H, *J* = 1.5 Hz, *J* = 7.5 Hz, H-7$_{Quin}$), 7.47–7.58 (m, 3H, H-3$_{Quin}$, H-5$_{Quin}$, H-6$_{Quin}$), 8.25 (s, 1H, H-5$_{Triaz}$), 8.33 (dd, 1H, *J* = 1.9 Hz, *J* = 8.6 Hz, H-4$_{Quin}$), 8.89 (dd, 1H, *J* = 1.7 Hz, *J* = 4.1 Hz, H-2$_{Quin}$); ^{13}C-NMR (100 MHz, DMSO): δ 49.02 (CH$_2$N), 55.04 (CH$_2$O), 67.37 (CH$_2$O), 110.39 (C-7$_{Quin}$), 120.43 (C-5$_{Quin}$), 121.90 (C-3$_{Quin}$), 123.32 (C-5$_{Triaz}$), 126.70 (C-6$_{Quin}$), 129.07 (C-4a$_{Quin}$), 135.82 (C-4$_{Quin}$), 139.70 (C-8a$_{Quin}$), 148.07 (C-4$_{Triaz}$), 149.21 (C-2$_{Quin}$), 153.71 (C-8$_{Quin}$); HRMS (ESI-TOF): calcd for C$_{14}$H$_{15}$N$_4$O$_2$ ([M + H]$^+$): *m/z* 271.1195; found: *m/z* 271.1197.

4-Hydroxymethyl-1-(2-methyl-8-quinolinyloxyethyl)-1*H*-1,2,3-triazol **M4**: Starting from 2-methyl-8-(2-azidoethoxy)quinoline **6** and propargyl alcohol **2**, the product was obtained as a beige solid (83% yield); m.p.: 150–152 °C; $[\alpha]^{25}_D$ = −27.0 (c = 1.0, CHCl$_3$); ^{1}H-NMR (400 MHz, DMSO): δ 2.69 (s, 3H, CH$_3$), 4.53 (d, 2H, *J* = 4.2 Hz, CH$_2$OH), 4.57 (t, 2H, *J* = 5.1 Hz, CH$_2$), 4.88 (t, 2H, *J* = 5.1 Hz, CH$_2$), 5.15 (bs, 1H, OH), 7.20 (dd, 1H, *J* = 1.3 Hz, *J* = 7.7 Hz, H-7$_{Quin}$), 7.39–7.46 (m, 2H, H-3$_{Quin}$, H-6$_{Quin}$), 7.50 (dd, 1H, *J* = 1.2 Hz, *J* = 8.2 Hz, H-5$_{Quin}$), 8.20 (d, 1H, *J* = 8.4 Hz, H-4$_{Quin}$); 8.46 (s, 1H, H-5$_{Triaz}$), ^{13}C-NMR (100 MHz, DMSO): δ 25.02 (CH$_3$), 49.02 (CH$_2$N), 55.12 (CH$_2$O), 67.54 (CH$_2$O), 110.88 (C-7$_{Quin}$), 120.33 (C-5$_{Quin}$), 122.52 (C-3$_{Quin}$), 123.71 (C-5$_{Triaz}$), 125.66 (C-6$_{Quin}$), 127.33 (C-4a$_{Quin}$), 135.99 (C-4$_{Quin}$), 139.26 (C-8a$_{Quin}$), 148.08 (C-4$_{Triaz}$), 153.23 (C-2$_{Quin}$), 157.55 (C-8$_{Quin}$); HRMS (ESI-TOF): calcd for C$_{15}$H$_{17}$N$_4$O$_2$ ([M + H]$^+$): *m/z* 285.1352; found: *m/z* 285.1353.

4-Hydroxymethyl-1-(8-quinolinyloxypropyl)-1*H*-1,2,3-triazol **M5**: Starting from 8-(3-azidopropoxy)quinoline **7** and propargyl alcohol **2**, the product was obtained as a brown solid (86% yield); m.p.: 126–127 °C; $[\alpha]^{25}_D$ = 19.0 (c = 1.0, CHCl$_3$); ^{1}H-NMR (400 MHz, DMSO): δ 2.41 (p, 2H, *J* = 6.5 Hz, CH$_2$), 4.19 (t, 2H, *J* = 6.1 Hz, CH$_2$), 4.51 (s, 2H, CH$_2$OH), 4.62 (t, 2H, *J* = 6.9 Hz, CH$_2$), 7.19 (dd, 1H, *J* = 2.0 Hz, *J* = 7.0 Hz, H-7$_{Quin}$), 7.47–7.59 (m, 3H, H-3$_{Quin}$, H-5$_{Quin}$, H-6$_{Quin}$), 8.10 (s, 1H, H-5$_{Triaz}$), 8.32 (dd, 1H, *J* = 1.6 Hz, *J* = 8.2 Hz, H-4$_{Quin}$), 8.89 (bs, 1H, H-2$_{Quin}$); ^{13}C-NMR (100 MHz, DMSO): δ 29.56 (CH$_2$), 46.37 (CH$_2$N), 54.97 (CH$_2$O), 65.31 (CH$_2$O), 109.76 (C-7$_{Quin}$), 119.83 (C-5$_{Quin}$), 121.76 (C-3$_{Quin}$), 122.76 (C-5$_{Triaz}$), 126.70 (C-6$_{Quin}$), 128.97 (C-4a$_{Quin}$), 135.71 (C-4$_{Quin}$), 139.70 (C-8a$_{Quin}$), 147.96 (C-4$_{Triaz}$), 148.95 (C-2$_{Quin}$), 154.13 (C-8$_{Quin}$); HRMS (ESI-TOF): calcd for C$_{15}$H$_{17}$N$_4$O$_2$ ([M + H]$^+$): *m/z* 285.1352; found: *m/z* 285.1354.

4-Hydroxymethyl-1-(2-methyl-8-quinolinyloxypropyl)-1*H*-1,2,3-triazol **M6**: Starting from 2-methyl-8-(3-azidopropoxy)quinoline **8** and propargyl alcohol **2**, the product was obtained as a brown oil (79% yield); $[\alpha]^{25}_D$ = 3.0 (c = 1.0, CHCl$_3$); ^{1}H-NMR (400 MHz, DMSO): δ 2.41 (m, 2H, CH$_2$), 2.68 (s, 3H, CH$_3$), 4.19 (m, 2H, CH$_2$), 4.51 (s, 2H, CH$_2$OH), 4.63 (m, 2H, CH$_2$), 7.18 (m, 1H, H-7$_{Quin}$), 7.36–7.56 (m, 3H, H-3$_{Quin}$, H-5$_{Quin}$, H-6$_{Quin}$), 8.12 (s, 1H, H-5$_{Triaz}$), 8.22 (m, 1H, H-4$_{Quin}$); ^{13}C-NMR (100 MHz, DMSO): δ 24.96 (CH$_3$), 29.56 (CH$_2$), 46.43 (CH$_2$N), 55.03 (CH$_2$O), 65.58 (CH$_2$O), 110.40 (C-7$_{Quin}$), 119.87 (C-5$_{Quin}$), 122.53 (C-3$_{Quin}$), 122.94 (C-5$_{Triaz}$), 125.80 (C-6$_{Quin}$), 128.93 (C-4a$_{Quin}$), 136.05 (C-4$_{Quin}$), 139.10 (C-8a$_{Quin}$), 148.10 (C-4$_{Triaz}$), 153.34 (C-2$_{Quin}$), 158.93 (C-8$_{Quin}$); HRMS (ESI-TOF): calcd for C$_{16}$H$_{19}$N$_4$O$_2$ ([M + H]$^+$): *m/z* 299.1508; found: *m/z* 299.1509.

4-Hydroxymethyl-1-(8-quinolinyloxybutyl)-1*H*-1,2,3-triazol **M7**: Starting from 8-(4-azidobutoxy)quinoline **9** and propargyl alcohol **2**, the product was obtained as a brown oil

(80% yield); $[\alpha]^{25}_D = 1.0$ (c = 1.0, CHCl$_3$); ^{1}H-NMR (400 MHz, DMSO): δ 1.82 (m, 2H, CH$_2$), 2.07 (m, 2H, CH$_2$), 4.21 (t, 2H, *J* = 5.6 Hz, CH$_2$), 4.51 (t, 2H, *J* = 5.6 Hz, CH$_2$), 4.52 (s, 2H, CH$_2$OH), 7.20 (m, 1H, H-7$_{Quin}$), 7.40–7.66 (m, 3H, H-3$_{Quin}$, H-5$_{Quin}$, H-6$_{Quin}$), 8.12 (s, 1H, H-5$_{Triaz}$), 8.32 (m, 1H, H-4$_{Quin}$), 8.87 (bs, 1H, H-2$_{Quin}$); ^{13}C-NMR (100 MHz, DMSO): δ 25.57 (CH$_2$), 27.01 (CH$_2$), 48.93 (CH$_2$N), 55.08 (CH$_2$O), 67.85 (CH$_2$O), 109.36 (C-7$_{Quin}$), 119.63 (C-5$_{Quin}$), 121.84 (C-3$_{Quin}$), 122.91 (C-5$_{Triaz}$), 126.84 (C-6$_{Quin}$), 128.85 (C-4a$_{Quin}$), 135.75 (C-4$_{Quin}$), 139.75 (C-8a$_{Quin}$), 147.92 (C-4$_{Triaz}$), 148.89 (C-2$_{Quin}$), 154.50 (C-8$_{Quin}$); HRMS (ESI-TOF): calcd for C$_{16}$H$_{19}$N$_4$O$_2$ ([M + H]$^+$): *m/z* 299.1508; found: *m/z* 299.1509.

4-Hydroxymethyl-1-(2-methyl-8-quinolinyloxybutyl)-1*H*-1,2,3-triazol **M8**: Starting from 2-methyl-8-(4-azidobutoxy)quinoline **10** and propargyl alcohol **2**, the product was obtained as a brown oil (76% yield); $[\alpha]^{24}_D = -2.0$ (c = 0.9, CHCl$_3$); ^{1}H-NMR (400 MHz, DMSO): δ 1.80 (m, 2H, CH$_2$), 2.07 (m, 2H, CH$_2$), 2.64 (s, 3H, CH$_3$), 4.20 (m, 2H, CH$_2$), 4.48–4.60 (m, 4H, CH$_2$, CH$_2$OH), 7.16 (m, 1H, H-7$_{Quin}$), 7.34–7.50 (m, 3H, H-3$_{Quin}$, H-5$_{Quin}$, H-6$_{Quin}$), 8.18 (m, 1H, H-4$_{Quin}$); 8.19 (s, 1H, H-5$_{Triaz}$), ^{13}C-NMR (100 MHz, DMSO): δ 24.97 (CH$_3$), 25.30 (CH$_2$), 27.19 (CH$_2$), 48.93 (CH$_2$N), 55.07 (CH$_2$O), 68.11 (CH$_2$O), 109.60 (C-7$_{Quin}$), 119.40 (C-5$_{Quin}$), 122.42 (C-3$_{Quin}$), 123.15 (C-5$_{Triaz}$), 125.74 (C-6$_{Quin}$), 127.22 (C-4a$_{Quin}$), 135.94 (C-4$_{Quin}$), 139.16 (C-8a$_{Quin}$), 147.95 (C-4$_{Triaz}$), 153.88 (C-2$_{Quin}$), 157.19 (C-8$_{Quin}$); HRMS (ESI-TOF): calcd for C$_{17}$H$_{21}$N$_4$O$_2$ ([M + H]$^+$): *m/z* 313.1665; found: *m/z* 313.1664.

4-Hydroxymethyl-1-*N*-(2,3,4,6-tetra-*O*-acetyl-β-D-glucopyranosyl)-1*H*-1,2,3-triazol **M9**: Starting from 2,3,4,6-tetra-*O*-acetyl-β-D-glucopyranosyl azide **11** and propargyl alcohol **2**, the product was obtained as a white solid (91% yield); m.p.: 165–166 °C; $[\alpha]^{24}_D = -15.8$ (c = 1.0, CHCl$_3$); ^{1}H-NMR (400 MHz, CDCl$_3$): δ 1.88, 2.03, 2.07, 2.08 (4s, 12H, CH$_3$CO), 4.01 (ddd, 1H, *J* = 2.2 Hz, *J* = 5.0 Hz, *J* = 10.1 Hz, H-5$_{Glu}$), 4.15 (dd, 1H, *J* = 2.2 Hz, *J* = 12.6 Hz, H-6a$_{Glu}$), 4.30 (dd, 1H, *J* = 5.0 Hz, *J* = 12.6 Hz, H-6b$_{Glu}$), 4.81 (bs, 2H, CH$_2$OH), 5.25 (dd~t, 1H, *J* = 9.5 Hz, *J* = 10.1 Hz, H-4$_{Glu}$), 5.39–4.49 (m, 2H, H-2$_{Glu}$, H-3$_{Glu}$), 5.89 (d, 1H, *J* = 9.3 Hz, H-1$_{Glu}$), 7.79 (s, 1H, H-5$_{Triaz}$); ^{13}C-NMR (100 MHz, CDCl$_3$): δ 20.19, 20.51, 20.54, 20.67 (CH$_3$CO), 56.61 (CH$_2$OH), 61.56 (C-6$_{Glu}$), 67.73, 70.35, 72.67, 75.14 (C-2$_{Glu}$, C-3$_{Glu}$, C-4$_{Glu}$, C-5$_{Glu}$), 85.76 (C-1$_{Glu}$), 120.04 (C-5$_{Triaz}$), 148.42 (C-4$_{Triaz}$), 169.00, 169.36, 169.90, 170.48 (CH$_3$CO); HRMS (ESI-TOF): calcd for C$_{17}$H$_{24}$N$_3$O$_{10}$ ([M + H]$^+$): *m/z* 430.1462; found: *m/z* 430.1457.

4-Hydroxymethyl-1-*N*-(β-D-glucopyranosyl)-1*H*-1,2,3-triazol **M10**: Starting from β-D-glucopyranosyl azide **12** and propargyl alcohol **2**, the product was obtained as a brown solid (90% yield); m.p.: 142–145 °C; $[\alpha]^{24}_D = 3.0$ (c = 1.0, CH$_3$OH); ^{1}H-NMR (400 MHz, DMSO): δ 3.23 (m, 1H, H-2$_{Glu}$), 3.34–3.48 (m, 3H, H-3$_{Glu}$, H-4$_{Glu}$, H-5$_{Glu}$), 3.64–3.80 (m, 2H, H-6a$_{Glu}$, H-6b$_{Glu}$), 4.53 (m, 2H, CH$_2$OH), 4.60 (m, 1H, OH), 5.12 (d, 1H, *J* = 4.9 Hz, OH), 5.18 (t, 1H, *J* = 4.3 Hz, 6-OH), 5.24 (d, 1H, *J* = 3.9 Hz, OH), 5.33 (d, 1H, *J* = 5.8 Hz, OH), 5.50 (d, 1H, *J* = 9.3 Hz, H-1$_{Glu}$), 8.11 (s, 1H, H-5$_{Triaz}$); ^{13}C-NMR (100 MHz, DMSO): δ 54.91 (CH$_2$OH), 60.77 (C-6$_{Glu}$), 69.58, 72.04, 77.01, 79.87 (C-2$_{Glu}$, C-3$_{Glu}$, C-4$_{Glu}$, C-5$_{Glu}$), 87.37 (C-1$_{Glu}$), 121.87 (C-5$_{Triaz}$), 147.74 (C-4$_{Triaz}$); HRMS (ESI-TOF): calcd for C$_9$H$_{16}$N$_3$O$_6$ ([M + H]$^+$): *m/z* 262.1039; found: *m/z* 262.1037.

4-Hydroxymethyl-1-(2-(2,3,4,6-tetra-*O*-acetyl-β-D-glucopyranosyloxy)ethyl)-1*H*-1,2,3-triazol **M11**: Starting from 2-azidoethyl 2,3,4,6-tetra-*O*-acetyl-β-D-glucopyranoside **13** and propargyl alcohol **2**, the product was obtained as a white solid (79% yield), m.p.: 151–152 °C; $[\alpha]^{24}_D = -5.6$ (c = 1.0, CHCl$_3$); ^{1}H-NMR (400 MHz, CDCl$_3$): δ 1.96, 2.00, 2.02, 2.08 (4s, 12H, CH$_3$CO), 3.71 (ddd, 1H, *J* = 2.4 Hz, *J* = 4.7 Hz, *J* = 9.9 Hz, H-5$_{Glu}$), 3.92 (m, 1H, CH$_2$O), 4.13 (dd, 1H, *J* = 2.4 Hz, *J* = 12.4 Hz, H-6a$_{Glu}$), 4.23 (m, 1H, CH$_2$O), 4.25 (dd, 1H, *J* = 4.7 Hz, *J* = 12.4 Hz, H-6b$_{Glu}$), 4.48 (d, 1H, *J* = 7.8 Hz, H-1$_{Glu}$), 4.50–4.67 (m, 2H, CH$_2$N), 4.79 (s, 2H, CH$_2$OH), 4.98 (dd, 1H, *J* = 7.8 Hz, *J* = 9.4 Hz H-2$_{glu}$), 5.07 (dd~t, 1H, *J* = 9.4 Hz, *J* = 9.9 Hz, H-4$_{glu}$), 5.17 (dd~t, 1H, *J* = 9.4 Hz, *J* = 9.4 Hz, H-3$_{glu}$), 7.61 (s, 1H, H-5$_{Triaz}$); ^{13}C-NMR (100 MHz, CDCl$_3$): δ 20.57, 20.57, 20.60, 20.72 (CH$_3$CO), 49.97 (CH$_2$N), 56.65 (CH$_2$OH), 61.74 (C-6$_{Glu}$), 67.86, 68.22, 71.12, 71.98, 72.46 (C-2$_{Glu}$, C-3$_{Glu}$, C-4$_{Glu}$, C-5$_{Glu}$, CH$_2$O), 100.43 (C-1$_{Glu}$), 123.36 (C-5$_{Triaz}$), 147.67 (C-4$_{Triaz}$), 169.47, 169.67, 170.09, 170.63 (CH$_3$CO); HRMS (ESI-TOF): calcd for C$_{19}$H$_{28}$N$_3$O$_{11}$ ([M + H]$^+$): *m/z* 474.1724; found: *m/z* 474.1725.

4-Hydroxymethyl-1-(2-(β-D-glucopyranosyloxy)ethyl)-1*H*-1,2,3-triazol **M12**: Starting from 2-azidoethyl β-D-glucopyranoside **14** and propargyl alcohol **2**, the product was obtained as a white solid (96% yield); m.p.: 60–63 °C; [α]^{22}$_D$ = −5.0 (c = 1.0, DMSO); ^{1}H-NMR (400 MHz, DMSO): δ 2.96 (m, 1H, H-2$_{Glu}$), 3.04 (m, 1H, H-4$_{Glu}$), 3.09–3.16 (m, 2H, H-3$_{Glu}$, H-5$_{Glu}$), 3.43 (m, 1H, H-6a$_{Glu}$), 3.67 (m, 1H, H-6b$_{Glu}$), 3.90 (m, 1H, CH$_2$O), 4.00–4.14 (m, 3H, CH$_2$O, CH$_2$N), 4.23 (d, 1H, *J* = 7.8 Hz, H-1$_{Glu}$), 4.51 (d, 2H, *J* = 5.4 Hz, CH$_2$OH), 4.55 (t, 1H, *J* = 5.4 Hz, OH), 4.92 (d, 1H, *J* = 5.2 Hz, OH), 4.95 (d, 1H, *J* = 4.8 Hz, OH), 5.06 (d, 1H, *J* = 4.9 Hz, OH), 5.14 (t, 1H, *J* = 5.6 Hz, 6-OH), 8.01 (s, 1H, H-5$_{triaz}$); ^{13}C-NMR (100 MHz, DMSO): δ 49.57 (CH$_2$N), 55.02 (CH$_2$OH), 61.07 (C-6$_{Glu}$), 67.44, 70.02, 73.33, 76.62, 77.00 (C-2$_{Glu}$, C-3$_{Glu}$, C-4$_{Glu}$, C-5$_{Glu}$, CH$_2$O), 102.96 (C-1$_{Glu}$), 123.48 (C-5$_{Triaz}$), 147.70 (C-4$_{Triaz}$); HRMS (ESI-TOF): calcd for C$_{11}$H$_{20}$N$_3$O$_7$ ([M + H]$^+$): *m/z* 306.1301; found: *m/z* 306.1300.

1-Hydroxyethyl-4-((2,3,4,6-tetra-*O*-acetyl-β-D-glucopyranosyloxy)methyl)-1*H*-1,2,3-triazol **M13**: Starting from propargyl 2,3,4,6-tetra-*O*-acetyl-β-D-glucopyranoside **15** and 2-azidoethanol **1**, the product was obtained as a colorless oil (76% yield); [α]^{25}$_D$ = −24.0 (c = 1.0, CHCl$_3$); ^{1}H-NMR (400 MHz, CDCl$_3$): δ 2.00, 2.00, 2.03, 2.09 (4s, 12H, CH$_3$CO), 3.73 (ddd, 1H, *J* = 2.4 Hz, *J* = 4.7 Hz, *J* = 10.0 Hz, H-5$_{Glu}$), 4.03–4.10 (m, 2H, CH$_2$OH), 4.16 (dd, 1H, *J* = 2.4 Hz, *J* = 12.3 Hz, H-6a$_{Glu}$), 4.25 (dd, 1H, *J* = 4.7 Hz, *J* = 12.3 Hz, H-6b$_{Glu}$), 4.42–4.56 (m, 2H, CH$_2$N), 4.70 (d, 1H, *J* = 7.9 Hz, H-1$_{Glu}$), 4.84 and 4.92 (qAB, 2H, *J* = 12.7 Hz, CH$_2$C), 4.98 (dd, 1H, *J* = 7.9 Hz, *J* = 9.5 Hz H-2$_{Glu}$), 5.09 (dd~t, 1H, *J* = 9.4 Hz, *J* = 10.0 Hz, H-4$_{Glu}$), 5.21 (dd~t, 1H, *J* = 9.4 Hz, *J* = 9.5 Hz, H-3$_{Glu}$), 7.67 (s, 1H, H-5$_{Triaz}$); ^{13}C-NMR (100 MHz, CDCl$_3$): δ 20.60, 20.69, 20.78 (<u>C</u>H$_3$CO), 52.72 (CH$_2$N), 61.15, 61.82, 63.10 (CH$_2$OH, CH$_2$O, C-6$_{Glu}$), 68.36, 71.42, 71.94, 72.73 (C-2$_{Glu}$, C-3$_{Glu}$, C-4$_{Glu}$, C-5$_{Glu}$), 99.98 (C-1$_{Glu}$), 124.10 (C-5$_{Triaz}$), 144.09 (C-4$_{Triaz}$), 169.43, 169.55, 170.20, 170.79 (CH$_3$<u>C</u>O); HRMS (ESI-TOF): calcd for C$_{19}$H$_{28}$N$_3$O$_{11}$ ([M + H]$^+$): *m/z* 474.1724; found: *m/z* 474.1726.

2-(4-(Hydroxymethyl)-1*H*-1,2,3-triazol-1-yl)-*N*-(2,3,4,6-tetra-*O*-acetyl-β-D-glucopyranosyl)acetamide **M14**: Starting from 2,3,4,6-tetra-*O*-acetyl-*N*-(β-D-glucopyranosyl)azidoacetamide **16** and propargyl alcohol **2**, the product was obtained as a white solid (92% yield); m.p.: 173–174 °C; [α]^{24}$_D$ = 4.8 (c = 1.0, CHCl$_3$); ^{1}H-NMR (400 MHz, CDCl$_3$): δ 2.00, 2.03, 2.03, 2.08 (4s, 12H, CH$_3$CO), 3.82 (ddd, 1H, *J* = 2.2 Hz, *J* = 4.4 Hz, *J* = 10.0 Hz, H-5$_{Glu}$), 4.10 (dd, 1H, *J* = 2.2 Hz, *J* = 12.5 Hz, H-6a$_{Glu}$), 4.27 (dd, 1H, *J* = 4.4 Hz, *J* = 12.5 Hz, H-6b$_{Glu}$), 4.82 (s, 2H, CH$_2$OH), 4.87 (dd~t, 1H, *J* = 9.5 Hz, *J* = 9.5 Hz, H-2$_{Glu}$), 5.03 and 5.14 (qAB, 2H, *J* = 16.6 Hz, CH$_2$N), 5.04 (dd~t, 1H, *J* = 9.5 Hz, *J* = 10.0 Hz H-4$_{Glu}$), 5.20 (dd~t, 1H, *J* = 9.1 Hz, *J* = 9.5 Hz, H-1$_{Glu}$), 5.28 (dd~t, 1H, *J* = 9.5 Hz, *J* = 9.5 Hz, H-3$_{Glu}$), 6.92 (d, 1H, *J* = 9.1 Hz, NH), 7.66 (s, 1H, H-5$_{Triaz}$); ^{13}C-NMR (100 MHz, CDCl$_3$): δ 20.53, 20.56, 20.59, 20.72 (<u>C</u>H$_3$CO), 52.74 (CH$_2$N), 56.44 (CH$_2$OH), 61.54 (C-6$_{Glu}$), 68.01, 70.39, 72.54, 73.81 (C-2$_{Glu}$, C-3$_{Glu}$, C-4$_{Glu}$, C-5$_{Glu}$), 78.36 (C-1$_{Glu}$), 123.38 (C-5$_{Triaz}$), 148.62 (C-4$_{Triaz}$), 165.90 (C=O), 169.49, 169.83, 170.62, 171.16 (CH$_3$<u>C</u>O); HRMS (ESI-TOF): calcd for C$_{19}$H$_{27}$N$_4$O$_{11}$ ([M + H]$^+$): *m/z* 487.1676; found: *m/z* 487.1676.

2-(4-(Hydroxymethyl)-1*H*-1,2,3-triazol-1-yl)-*N*-(β-D-glucopyranosyl)acetamide **M15**: Starting from *N*-(β-D-glucopyranosyl)azidoacetamide **17** and propargyl alcohol **2**, the product was obtained as a yellow solid (86% yield); m.p.: 155–158 °C; [α]^{23}$_D$ = 14.0 (c = 1.0, DMSO); ^{1}H-NMR (400 MHz, DMSO): δ 3.03–3.15 (m, 3H, H-2$_{Glu}$, H-4$_{Glu}$, H-5$_{Glu}$), 3.19 (m, 1H, H-3$_{Glu}$), 3.42 (m, 1H, H-6a$_{Glu}$), 3.64 (m, 1H, H-6b$_{Glu}$), 4.52 (s, 2H, CH$_2$OH), 4.71 (dd~t, 1H, *J* = 8.9 Hz, *J* = 9.0 Hz, H-1$_{Glu}$), 5.08 and 5.13 (qAB, 2H, *J* = 16.4 Hz, CH$_2$N), 7.91 (s, 1H, H-5$_{Triaz}$), 8.94 (d, 1H, *J* = 9.0 Hz, NH); ^{13}C-NMR (100 MHz, DMSO): δ 51.47 (CH$_2$N), 55.02 (CH$_2$OH), 60.82 (C-6$_{Glu}$), 69.86, 72.61, 77.33, 78.73 (C-2$_{Glu}$, C-3$_{Glu}$, C-4$_{Glu}$, C-5$_{Glu}$), 79.67 (C-1$_{Glu}$), 124.31 (C-5$_{Triaz}$), 147.70 (C-4$_{Triaz}$), 165.95 (C=O), HRMS (ESI-TOF): calcd for C$_{11}$H$_{19}$N$_4$O$_7$ ([M + H]$^+$): *m/z* 319.1254; found: *m/z* 319.1251.

1-(2-Hydroxyethyl)-*N*-(2,3,4,6-tetra-*O*-acetyl-β-D-glucopyranosyl)-1*H*-1,2,3-triazole-4-carboxamide **M16**: Starting from 2,3,4,6-tetra-*O*-acetyl-*N*-(β-D-glucopyranosyl)propiolamide **18** and 2-azidoethanol **1**, the product was obtained as a white solid (88% yield); m.p.: 194–196 °C; [α]^{23}$_D$ = −15.6 (c = 1.0, CHCl$_3$); ^{1}H-NMR (600 MHz, CDCl$_3$): δ 1.99, 2.03, 2.05, 2.07 (4s, 12H, CH$_3$CO), 3.91 (ddd, 1H, *J* = 2.2 Hz, *J* = 4.3 Hz, *J* = 10.0 Hz, H-5$_{Glu}$), 4.06–4.11 (m, 2H, CH$_2$OH), 4.10 (dd, 1H, *J* = 2.2 Hz, *J* = 12.5 Hz, H-6a$_{Glu}$), 4.27 (dd, 1H, *J* = 4.3 Hz,

J = 12.5 Hz, H-6b$_{Glu}$), 4.51–4.59 (m, 2H, CH$_2$N), 5.13 (dd~t, 1H, *J* = 9.6 Hz, *J* = 10.0 Hz, H-4$_{Glu}$), 5.15 (dd~t, 1H, *J* = 9.5 Hz, *J* = 9.5 Hz H-2$_{glu}$), 5.35 (dd~t, 1H, *J* = 9.5 Hz, *J* = 9.5 Hz, H-1$_{glu}$), 5.47 (dd~t, 1H, *J* = 9.5 Hz, *J* = 9.6 Hz, H-3$_{Glu}$), 7.93 (d, 1H, *J* = 9.6 Hz, NH), 8.27 (s, 1H, H-5$_{Triaz}$); ^{13}C-NMR (150 MHz, CDCl$_3$): δ 20.58, 20.61, 20.73 (CH$_3$CO), 52.97 (CH$_2$N), 60.86 (CH$_2$OH), 61.68 (C-6$_{Glu}$), 68.16, 70.43, 73.07, 73.63 (C-2$_{Glu}$, C-3$_{Glu}$, C-4$_{Glu}$, C-5$_{Glu}$), 77.84 (C-1$_{Glu}$), 127.38 (C-5$_{Triaz}$), 141.85 (C-4$_{Triaz}$), 160.53 (C=O), 169.55, 170.06, 170.30, 170.71 (CH$_3$CO); HRMS (ESI-TOF): calcd for C$_{19}$H$_{27}$N$_4$O$_{11}$ ([M + H]$^+$): *m/z* 487.1676; found: *m/z* 487.1678.

(1-(2-Hydroxyethyl)-1*H*-1,2,3-triazol-4-yl)methyl (2,3,4,6-tetra-*O*-acetyl-β-D-glucopyranosyl)carbamate **M17**: Starting from 2,3,4,6-tetra-*O*-acetyl-*N*-(β-D-glucopyranosyl)-*O*-propargyl carbamate **19** and 2-azidoethanol **1**, the product was obtained as a white solid (83% yield); m.p.: 93–95 °C; [α]$^{23}_D$ = 0.8 (c = 1.0, CHCl$_3$); ^{1}H-NMR (400 MHz, CDCl$_3$): δ 2.01, 2.03, 2.07 (4s, 12H, CH$_3$CO), 3.83 (m, 1H, H-5$_{Glu}$), 4.00–4.08 (m, 2H, CH$_2$OH), 4.13 (m, 1H, H-6a$_{Glu}$), 4.29 (m, 1H, H-6b$_{Glu}$), 4.40–4.58 (m, 2H, CH$_2$N), 4.94 (m, 1H, H-1$_{Glu}$), 4.99–5.19 (m, 3H, CH$_2$O, H-2$_{Glu}$), 5.20–5.35 (m, 2H, H-3$_{Glu}$, H-4$_{Glu}$), 6.06 (m, 1H, NH), 7.75 (s, 1H, H-5$_{Triaz}$); ^{13}C NMR (100 MHz, CDCl$_3$): δ 20.57, 20.58, 20.66, 20.73 (CH$_3$CO), 52.74 (CH$_2$N), 58.64, 61.00, 61.58 (CH$_2$OH, CH$_2$O, C-6$_{Glu}$), 68.07, 70.18, 72.93, 73.32 (C-2$_{Glu}$, C-3$_{Glu}$, C-4$_{Glu}$, C-5$_{Glu}$), 80.78 (C-1$_{Glu}$), 125.01 (C-5$_{Triaz}$), 142.36 (C-4$_{Triaz}$), 155.49 (C=O), 169.53, 169.95, 170.56, 170.64 (CH$_3$CO); HRMS (ESI-TOF): calcd for C$_{20}$H$_{29}$N$_4$O$_{12}$ ([M + H]$^+$): *m/z* 517.1782; found: *m/z* 517.1780.

4-Hydroxymethyl-1-((2,3,4,6-tetra-*O*-acetyl-β-D-glucopyranosyl)thiomethyl)-1*H*-1,2,3-triazol **M18**: Starting from azidomethyl 2,3,4,6-tetra-*O*-acetyl-1-thio-β-D-glucopyranoside **20** and propargyl alcohol **2**, the product was obtained as a white solid (78% yield); m.p.: 135–137 °C; [α]$^{25}_D$ = −33.0 (c = 1.0, CHCl$_3$); ^{1}H NMR (400 MHz, CDCl$_3$): δ 2.00, 2.03, 2.05, 2.10 (4s, 12H, CH$_3$CO), 3.69 (ddd, 1H, *J* = 2.5 Hz, *J* = 4.2 Hz, *J* = 10.0 Hz, H-5$_{Glu}$), 4.12 (dd, 1H, *J* = 4.2 Hz, *J* = 12.5 Hz, H-6a$_{Glu}$), 4.17 (dd, 1H, *J* = 2.5 Hz, *J* = 12.5 Hz, H-6b$_{Glu}$), 4.64 (d, 1H, *J* = 10.1 Hz, H-1$_{Glu}$), 4.81 (bs, 2H, CH$_2$OH), 5.03 (dd~t, 1H, *J* = 9.3 Hz, *J* = 10.1 Hz, H-2$_{Glu}$), 5.09 (dd~t, 1H, *J* = 9.4 Hz, *J* = 10.0 Hz, H-4$_{Glu}$), 5.20 (dd~t, 1H, *J* = 9.3 Hz, *J* = 9.4 Hz, H-3$_{Glu}$), 5.39 i 5.67 (qAB, 2H, *J* = 14.7 Hz, CH$_2$N), 7.77 (s, 1H, H-5$_{Triaz}$); ^{13}C-NMR (100 MHz, CDCl$_3$): δ 20.56, 20.58, 20.61, 20.82 (CH$_3$CO), 48.61 (CH$_2$N), 56.78 (CH$_2$OH), 61.52 (C-6$_{Glu}$), 67.92, 69.58, 73.57, 76.21 (C-2$_{Glu}$, C-3$_{Glu}$, C-4$_{Glu}$, C-5$_{Glu}$), 82.37 (C-1$_{Glu}$), 121.69 (C-5$_{Triaz}$), 148.96 (C-4$_{Triaz}$), 169.33, 169.45, 170.02, 170.83 (CH$_3$CO); HRMS (ESI-TOF): calcd for C$_{18}$H$_{26}$N$_3$O$_{10}$S ([M + H]$^+$): *m/z* 476.1339; found: *m/z* 476.1339.

4-Hydroxymethyl-1-((2,3,4,6-tetra-*O*-acetyl-β-D-glucopyranosyl)thioethyl)-1*H*-1,2,3-triazol **M19**: Starting from 2-azidoethyl 2,3,4,6-tetra-*O*-acetyl-1-thio-β-D-glucopyranoside **21** and propargyl alcohol **2**, the product was obtained as a white solid (86% yield); m.p.: 150 °C; [α]$^{24}_D$ = −31.8 (c = 1.0, CHCl$_3$); ^{1}H-NMR (400 MHz, CDCl$_3$): δ 2.01, 2.04, 2.06, 2.08 (4s, 12H, CH$_3$CO), 3.06 (m, 1H, CHS), 3.27 (m, 1H, CHS), 3.73 (ddd, 1H, *J* = 3.1 Hz, *J* = 4.3 Hz, *J* = 10.1 Hz, H-5$_{Glu}$), 4.19 (dd, 1H, *J* = 3.1 Hz, *J* = 12.5 Hz, H-6a$_{Glu}$), 4.23 (dd, 1H, *J* = 4.3 Hz, *J* = 12.5 Hz, H-6b$_{Glu}$), 4.44 (d, 1H, *J* = 10.0 Hz, H-1$_{Glu}$), 4.53–4.69 (m, 2H, CH$_2$N), 4.81 (s, 2H, CH$_2$OH), 5.04 (dd~t, 1H, *J* = 9.4 Hz, *J* = 10.0 Hz, H-2$_{Glu}$), 5.08 (dd~t, 1H, *J* = 9.4 Hz, *J* = 10.1 Hz, H-4$_{Glu}$), 5.22 (dd~t, 1H, *J* = 9.4 Hz, *J* = 9.4 Hz, H-3$_{Glu}$), 7.68 (s, 1H, H-5$_{Triaz}$); ^{13}C-NMR (100 MHz, CDCl$_3$): δ 20.57, 20.58, 20.66, 20.75 (CH$_3$CO), 30.34 (CH$_2$S), 50.50 (CH$_2$N), 56.61 (CH$_2$OH), 61.92 (C-6$_{Glu}$), 68.12, 69.48, 73.54, 76.23 (C-2$_{Glu}$, C-3$_{Glu}$, C-4$_{Glu}$, C-5$_{Glu}$), 83.63 (C-1$_{Glu}$), 122.77 (C-5$_{Triaz}$), 147.63 (C-4$_{Triaz}$), 169.40, 169.46, 170.08, 170.62 (CH$_3$CO); HRMS (ESI-TOF): calcd for C$_{19}$H$_{28}$N$_3$O$_{10}$S ([M + H]$^+$): *m/z* 490.1495; found: *m/z* 490.1497.

1-Hydroxyethyl-4-((2,3,4,6-tetra-*O*-acetyl-β-D-glucopyranosyl)thiomethyl)-1*H*-1,2,3-triazol **M20**: Starting from propargyl 2,3,4,6-tetra-*O*-acetyl-1-thio-β-D-glycopyranosides **22** and 2-azidoethanol **1**, the product was obtained as a colorless oil (73% yield); [α]$^{25}_D$ = −24.4 (c = 0.5, CHCl$_3$); ^{1}H-NMR (600 MHz, CDCl$_3$): δ 2.00, 2.02, 2.03, 2.09 (4s, 12H, CH$_3$CO), 3.73 (ddd, 1H, *J* = 2.4 Hz, *J* = 4.5 Hz, *J* = 10.1 Hz, H-5$_{Glu}$), 3.93 and 4.03 (qAB, 2H, *J* = 14.8 Hz, CH$_2$S), 4.03–4.09 (m, 2H, CH$_2$OH), 4.15 (dd, 1H, *J* = 2.4 Hz, *J* = 12.4 Hz, H-6a$_{Glu}$), 4.21 (dd, 1H, *J* = 4.5 Hz, *J* = 12.4 Hz, H-6b$_{Glu}$), 4.43–4.52 (m, 2H, CH$_2$N), 4.62 (d, 1H, *J* = 10.1 Hz, H-1$_{Glu}$), 4.99 (dd, 1H, *J* = 9.3 Hz, *J* = 10.1 Hz H-4$_{Glu}$), 5.10 (dd~t, 1H, *J* = 9.4 Hz, *J* = 10.1 Hz,

H-2$_{Glu}$), 5.20 (dd~t, 1H, *J* = 9.3 Hz, *J* = 9.4 Hz, H-3$_{Glu}$), 7.65 (s, 1H, H-5$_{Triaz}$); ^{13}C-NMR (150 MHz, CDCl$_3$): δ 20.58, 20.69, 20.79 (<u>C</u>H$_3$CO), 24.23 (CH$_2$S), 52.80 (CH$_2$N), 61.12, 61.96 (CH$_2$OH, C-6$_{Glu}$), 68.29, 70.08, 73.84, 75.88 (C-2$_{Glu}$, C-3$_{Glu}$, C-4$_{Glu}$, C-5$_{Glu}$), 82.72 (C-1$_{Glu}$), 123.49 (C-5$_{Triaz}$), 144.79 (C-4$_{Triaz}$), 169.43, 169.64, 170.14, 170.82 (CH$_3$CO); HRMS (ESI-TOF): calcd for C$_{19}$H$_{28}$N$_3$O$_{10}$S ([M + H]$^+$): *m/z* 490.1495; found: *m/z* 490.1493.

2-(4-(Hydroxymethyl)-1*H*-1,2,3-triazol-1-yl)-*N*-(6-((2,3,4,6-tetra-*O*-acetyl-β-D-glucopyranosyl)thio)pyridin-3-yl)acetamide **M21**: Starting from (5-azidoacetamide-2-pyridyl) 2,3,4,6-tetra-*O*-acetyl-1-thio-β-D-glucopyranoside **23** and propargyl alcohol **2**, the product was obtained as a white solid (83% yield); m.p.: 171–174 °C; [α]$^{25}_D$ = −7.8 (c = 0.9, CHCl$_3$); ^{1}H-NMR (400 MHz, DMSO): δ 1.96, 1.98, 1.98, 2.00 (4s, 12H, CH$_3$CO), 4.02 (m, 1H, H-5$_{Glu}$), 4.10–4.20 (m, 2H, H-6a$_{Glu}$, H-6b$_{Glu}$), 4.55 (d, 2H, *J* = 5.6 Hz, CH$_2$OH), 4.93–5.04 (m, 2H, H-2$_{Glu}$, H-4$_{Glu}$), 5.20 (t, 1H, *J* = 5.6 Hz, OH), 5.34 (s, 2H, CH$_2$N), 5.42 (dd~t, 1H, *J* = 9.4 Hz, *J* = 9.4 Hz, H-3$_{Glu}$), 5.73 (d, 1H, *J* = 10.3 Hz, H-1$_{Glu}$), 7.42 (d, 1H, *J* = 8.7 Hz, H-3$_{Pyr}$), 7.97 (dd, 1H, *J* = 2.6 Hz, *J* = 8.7 Hz, H-4$_{Pyr}$), 7.99 (s, 1H, H-5$_{Triaz}$), 8.67 (d, 1H, *J* = 2.1 Hz, H-6$_{Pyr}$), 10.72 (s, 1H, NH); ^{13}C-NMR (100 MHz, DMSO): δ 20.27, 20.32, 20.37, 20.45 (<u>C</u>H$_3$CO), 51.95 (CH$_2$N), 55.01 (CH$_2$OH), 61.83 (C-6$_{Glu}$), 68.02, 69.39, 72.96, 74.51 (C-2$_{Glu}$, C-3$_{Glu}$, C-4$_{Glu}$, C-5$_{Glu}$), 81.15 (C-1$_{Glu}$), 122.92 (C-5$_{Triaz}$), 124.36 (C$_{Pyr}$), 127.82 (C$_{Pyr}$), 133.21 (C$_{Pyr}$), 140.55 (C$_{Pyr}$), 147.86 (C-4$_{Triaz}$), 149.66 (C$_{Pyr}$), 164.94 (C=O), 169.08, 169.27, 169.47, 169.88 (CH$_3$<u>C</u>O); HRMS (ESI-TOF): calcd for C$_{24}$H$_{30}$N$_5$O$_{11}$S ([M + H]$^+$): *m/z* 596.1663; found: *m/z* 596.1662.

(1-(2-Hydroxyethyl)-1*H*-1,2,3-triazol-4-yl)methyl (6-((2,3,4,6-tetra-*O*-acetyl-β-D-glucopyranosyl)thio)pyridin-3-yl)carbamate **M22**: Starting from (5-(((prop-2-yn-1-yloxy)carbonyl)amino)-2-pyridyl) 2,3,4,6-tetra-*O*-acetyl-1-thio-β-D-glucopyranoside **24** and 2-azidoethanol **1**, the product was obtained as a white solid (86% yield); m.p.: 124–126 °C; [α]$^{24}_D$ = −4.2 (c = 1.0, CHCl$_3$); ^{1}H-NMR (400 MHz, DMSO): δ 1.95, 1.97, 1.98, 2.00 (4s, 12H, CH$_3$CO), 3.73–3.82 (m, 2H, CH$_2$OH), 4.02 (m, 1H, H-5$_{Glu}$), 4.09–4.19 (m, 2H, H-6a$_{Glu}$, H-6b$_{Glu}$), 4.41 (d, 2H, *J* = 5.4 Hz, CH$_2$N), 4.93–5.06 (m, 2H, H-2$_{Glu}$, H-4$_{Glu}$), 5.22 (s, 2H, CH$_2$O), 5.41 (dd~t, 1H, *J* = 9.4 Hz, *J* = 9.4 Hz, H-3$_{Glu}$), 5.69 (d, 1H, *J* = 10.3 Hz, H-1$_{Glu}$), 7.38 (d, 1H, *J* = 8.7 Hz, H-3$_{Pyr}$), 7.84 (dd, 1H, *J* = 2.1 Hz, *J* = 8.7 Hz, H-4$_{Pyr}$), 8.15 (s, 1H, H-5$_{Triaz}$), 8.54 (d, 1H, *J* = 2.1 Hz, H-6$_{Pyr}$), 10.02 (s, 1H, NH); ^{13}C-NMR (100 MHz, DMSO): δ 20.18, 20.23, 20.28, 20.34 (<u>C</u>H$_3$CO), 52.08 (CH$_2$N), 57.67 (CH$_2$O), 59.71 (CH$_2$OH), 61.73 (C-6$_{Glu}$), 67.93, 69.33, 72.90, 74.40 (C-2$_{Glu}$, C-3$_{Glu}$, C-4$_{Glu}$, C-5$_{Glu}$), 81.26 (C-1$_{Glu}$), 123.05 (C-5$_{Triaz}$), 125.17 (C$_{Pyr}$), 126.59 (C$_{Pyr}$), 133.84 (C$_{Pyr}$), 139.68 (C$_{Pyr}$), 141.52 (C-4$_{Triaz}$), 148.02 (C$_{Pyr}$), 153.12 (C=O), 168.98, 169.17, 169.38, 169.80 (CH$_3$<u>C</u>O); HRMS (ESI-TOF): calcd for C$_{25}$H$_{32}$N$_5$O$_{12}$S ([M + H]$^+$): *m/z* 626.1768; found: *m/z* 626.1769.

3.2.2. Preparation and Characterization of Micelles

Micelles were prepared by standard solvent evaporation method from pH-responsive amphiphilic poly(ethylene glycol)-*b*-polycarbonate-*b*-oligo([R]-3-hydroxybutyrate) copolymer which was synthesized by PEG/organocatalyst-initiated ring-opening polymerization of ketal-protected six-membered cyclic carbonate and subsequent esterification with natural oligo([R]-3-hydroxybutyrate) as described in our previous study [42]. The size and morphology of micelles were determined by dynamic light scattering (DLS) measurements using a Brookhaven BI-200 goniometer equipped with a Brookhaven BI-9000 AT (Brookhaven Instruments Corp., Holtsville, NY, USA) and cryo-TEM (Tecnai F20 X TWIN mi-croscope (FEI Company, Hillsboro, OR, USA), respectively. The DLS and cryo-TEM measurement of the drug free micelles showed a relatively small hydrodynamic size of ~25.5 nm with a spherical shape [42] (Figure S45a,b). Meanwhile, metabolite-loaded mi-celles revealed particles size of around ~34 nm and ~36 nm for **M5**-micelles and **M7**-micelles, respectively (Figure S45c,d). Furthermore, the drug loading efficiency (DLE) and the drug loading content (DLC) were determined according to standard formulas. The encapsulation properties of pH-sensitive micelles were evaluated at the feed drug ratio of the copolymer was 1:10. The DLC and DLE values for micelles loaded with **M5** were 5.4% ± 0.1 and 49.9% ± 1.6 and with **M7** 5.2% ± 0.2 and 46.8% ± 2.9, respectively. No significant differences in encapsulation properties were observed between metabolites, which is probably related to the

small difference in chemical structure. Detailed information on copolymer synthesis and physicochemical characterization of micelles has been provided in our former studies [42].

3.3. Biological Evaluation

3.3.1. Cell Cultures

The human colon adenocarcinoma cell line (HCT-116) was purchased from the American Type Culture Collection (ATCC, Manassas, VA, USA). The human breast adenocarcinoma cell line (MCF-7) was obtained from collections at the Maria Sklodowska-Curie Memorial Cancer Center and National Institute of Oncology (Gliwice, Poland). The Normal Human Dermal Fibroblasts-Neonatal (NHDF-Neo) was purchased from LONZA (Cat. No. CC-2509, NHDF-Neo, Dermal Fibroblasts, Neonatal, Lonza, Poland). Cells were grown in a culture medium in a humidified atmosphere at 5% CO_2 and 37 °C. The culture media consisted of RPMI 1640 or DMEM+F12 (HyClone), supplemented with 10% of heat-inactivated fetal bovine serum (FBS, EURx, Poland) and 1% of Antibiotic Antimycotic Solution, 100 U/mL penicillin, and 10 mg/mL streptomycin (Sigma-Aldrich, Taufkirchen, Germany).

3.3.2. MTT Assay

Cells viability was assessed by the MTT (3-[4,5–dimethylthiazol-2-yl]-2,5-diphenyltetrazolium bromide) test (Sigma-Aldrich, Taufkirchen, Germany) according to the manufacturer's protocol. Stock solutions of tested compounds were prepared in DMSO and diluted to the desired concentrations with the appropriate volumes of the growth medium directly before the experiment (DMSO content in the highest concentration did not exceed 0.5%). The cells were seeded into 96-well plates at concentration 1×10^4 (HCT-116, NHDF-Neo) or 5×10^3 (MCF-7) per well and incubated for 24 h at 37 °C in a humidified atmosphere of 5% CO_2. Then, the culture medium was removed, replaced with the solution of the tested compounds in a fresh medium with varying concentrations. As a control in the cytotoxicity studies, cells suspended in a medium supplemented with 0.5% DMSO were used. It was the amount of DMSO necessary to dissolve the highest concentration of a given sample. Then, cells were incubated for a further 24 h or 72 h. After this time, the medium was removed, and the MTT solution (50 μL, 0.5 mg/mL in PBS) was added into each well. After 3 h of incubation, the MTT solution was carefully removed, and the acquired formazan crystals were dissolved in DMSO. The absorbance was measured spectrophotometrically at the 570 nm wavelength using a multi-well plate reader (Epoch, BioTek, Winooski, VT, USA). The experiment was conducted in at least three independent repetitions with four technical repetitions for each tested concentration, and the results were expressed as the survival fraction (%) of the control. The IC_{50} values were calculated using CalcuSyn software (version 2.0, Biosoft, Cambridge, UK). The IC_{50} parameter was defined as the concentration of drug that was necessary to reduce the proliferation of cells to 50% of the untreated control. The results are shown as the average value $\pm$ SD.

4. Conclusions

As part of the research, the ability to inhibit the proliferation of cancer cells by glycoconjugates derivatives of 8-hydroxyquinoline and their metabolites, which theoretically may be released in biological systems under the action of hydrolytic enzymes, were compared. For the study, compounds were selected consisting of an 8-hydroxyquinoline fragment linked by an aliphatic chain of various lengths to a 1,2,3-triazole ring as well as D-glucose derivatives containing anomeric oxygen, nitrogen, or sulfur atom also connected to the 1,2,3-triazole ring by various linkers. The applied CuAAC reaction allowed for a quick and efficient synthesis of metabolites, which in the next stage were subjected to MTT cytotoxicity screening tests.

The performed studies prove that the presence of all three building blocks is necessary for the full cytotoxic activity of glycoconjugates: the sugar unit, the linker containing a 1,2,3-triazole ring, and the 8-hydroxyquinoline fragment. The sugar fragment improves

the pharmacokinetic properties of potential drugs. On the other hand, a heteroaromatic fragment increases the cytotoxicity of glycoconjugates, probably by improving the chelating capacity of metal ions, thus inhibiting the growth of neoplastic cells. The toxic effect of metabolites on normal cells indicates that further studies are necessary to improve the transport of prodrugs directly to the tumor cells. Therefore, it is worth continuing the idea of adding a sugar unit to 8-HQ, however, by using a position other than the anomeric position that participates in binding to GLUT transporters, so that the obtained derivatives will have sufficient affinity for these transporters.

The high IC_{50} values of the metabolites do not clearly indicate their lack of anticancer activity. Perhaps these compounds cannot reach the target site of action. The encapsulation of selected metabolites in micelles significantly improved their cytotoxic effect through the possibility of using a much lower therapeutic dose of the drug. The use of pH-sensitive micelles allows the drug to be released close to the tumor cell, preventing early release of the drug into the systemic circulation, thus reducing its side effects.

Supplementary Materials: The following supporting information can be downloaded online. Figures S1–S44: ^{1}H and ^{13}C-NMR spectra of all obtained compounds; Figure S45: Characterization of micelles.

Author Contributions: Conceptualization, M.D. and G.P.-G.; methodology, M.D., G.P.-G. and A.D.; validation, M.D. and G.P.-G.; formal analysis, M.D.; investigation, M.D; synthesis of chemical compounds, M.D.; synthesis of polymer nanocarriers, A.D.; cytotoxicity tests, M.D.; mass spectra, K.E.; writing—original draft preparation, M.D.; writing—review and editing, M.D., G.P.-G., A.D. and P.K.; visualization, M.D.; supervision, G.P.-G. and P.K.; funding acquisition, M.D. and G.P.-G.; All authors have read and agreed to the published version of the manuscript.

Institutional Review Board Statement: Not applicable.

Informed Consent Statement: Not applicable.

Data Availability Statement: Data are contained within the article.

Conflicts of Interest: The authors declare no conflict of interest.

Sample Availability: Samples of the compounds **M1**–**M22** are available from the authors.

References

1. Rautio, J.; Kumpulainen, H.; Heimbach, T.; Oliyai, R.; Oh, D.; Järvinen, T.; Savolainen, J. Prodrugs: Design and clinical appli-cations. *Nat. Rev. Drug Discov.* **2008**, *7*, 255–270. [CrossRef] [PubMed]
2. Kratz, F.; Müller, I.A.; Ryppa, C.; Warnecke, A. Prodrug Strategies in Anticancer Chemotherapy. *ChemMedChem* **2008**, *3*, 20–53. [CrossRef] [PubMed]
3. Markovic, M.; Ben-Shabat, S.; Dahan, A. Prodrugs for Improved Drug Delivery: Lessons Learned from Recently Developed and Marketed Products. *Pharmaceutics* **2020**, *12*, 1031. [CrossRef] [PubMed]
4. Arpicco, S.; Dosio, F.; Stella, B.; Cattel, L. Anticancer prodrugs: An overview of major strategies and recent developments. *Curr. Top. Med. Chem.* **2011**, *11*, 2346–2381. [CrossRef]
5. Mura, S.; Nicolas, J.; Couvreur, P. Stimuli-responsive nanocarriers for drug delivery. *Nat. Mater.* **2013**, *12*, 991–1003. [CrossRef]
6. Danhier, F.; Feron, O.; Préat, V. To Exploit the Tumor Microenvironment: Passive and Active Tumor Targeting of Nanocarri-ers for Anti-cancer Drug Delivery. *J. Control. Release* **2010**, *148*, 135–146. [CrossRef]
7. Warburg, O. On the Origin of Cancer Cells. *Science* **1956**, *123*, 309–314. [CrossRef]
8. Vander Heiden, M.G.; Cantley, L.C.; Thompson, C. Understanding the Warburg Effect: The Metabolic Requirements of Cell Proliferation. *Science* **2009**, *324*, 1029–1033. [CrossRef]
9. Barron, C.C.; Bilan, P.J.; Tsakiridis, T.; Tsiani, E. Facilitative glucose transporters: Implications for cancer detection, prognosis and treatment. *Metabolism* **2016**, *65*, 124–139. [CrossRef]
10. Tanasova, M.; Fedie, J.R. Molecular Tools for Facilitative Carbohydrate Transporters (Gluts). *ChemBioChem* **2017**, *18*, 1774–1788. [CrossRef]
11. Szablewski, L. Expression of glucose transporters in cancers. *Biochim. Biophys. Acta* **2013**, *1835*, 164–169. [CrossRef]
12. Calvaresi, E.C.; Hergenrother, P.J. Glucose conjugation for the specific targeting and treatment of cancer. *Chem. Sci.* **2013**, *4*, 2319–2333. [CrossRef]

13. Granchi, C.; Fortunato, S.; Minutolo, F. Anticancer agents interacting with membrane glucose transporters. *MedChemComm* **2016**, *7*, 1716–1729. [CrossRef]

14. Ding, W.Q.; Lind, S.E. Metal Ionophores—An Emerging Class of Anticancer Drugs. *IUBMB Life* **2009**, *61*, 1013–1018. [CrossRef]

15. Santini, C.; Pellei, M.; Gandin, V.; Porchia, M.; Tisato, F.; Marzano, C. Advances in Copper Complexes as Anticancer Agents. *Chem. Rev.* **2014**, *114*, 815–862. [CrossRef]

16. Wang, X.; Wang, X.; Jin, S.; Muhammad, N.; Guo, Z. Stimuli-Responsive Therapeutic Metallodrugs. *Chem. Rev.* **2019**, *119*, 1138–1192. [CrossRef]

17. Gupte, A.; Mumper, R.J. Elevated copper and oxidative stress in cancer cells as a target for cancer treatment. *Cancer Treat. Rev.* **2009**, *35*, 32–46. [CrossRef]

18. Gaur, K.; Vázquez-Salgado, A.M.; Duran-Camacho, G.; Dominguez-Martinez, I.; Benjamín-Rivera, J.A.; Fernández-Vega, L.; Carmona Sarabia, L.; Cruz García, A.; Pérez-Deliz, F.; Méndez Román, J.A.; et al. Iron and Copper Intracellular Chelation as an Anticancer Drug Strategy. *Inorganics* **2018**, *6*, 126. [CrossRef]

19. Denoyer, D.; Masaldan, S.; La Fontaine, S.; Cater, M.A. Targeting copper in cancer therapy: "Copper That Cancer". *Metallomics* **2015**, *7*, 1459–1476. [CrossRef]

20. Song, Y.; Xu, H.; Chen, W.; Zhan, P.; Liu, X. 8-Hydroxyquinoline: A privileged structure with a broad-ranging pharmacolog-ical potential. *Med. Chem. Commun.* **2015**, *6*, 61–74. [CrossRef]

21. Prachayasittikul, V.; Prachayasittikul, S.; Ruchirawat, S. 8-Hydroxyquinolines: A review of their metal chelating properties and medicinal applications. *Drug Des. Dev. Ther.* **2013**, *7*, 1157–1178. [CrossRef]

22. Savić-Gajić, I.M.; Savic, I.M. Drug design strategies with metal-hydroxyquinoline complexes. *Expert Opin. Drug Discov.* **2020**, *15*, 383–390. [CrossRef]

23. Oliveri, V.; Vecchio, G. 8-Hydroxyquinolines in medicinal chemistry: A structural perspective. *Eur. J. Med. Chem.* **2016**, *120*, 252–274. [CrossRef]

24. Ma, J.; Yang, X.; Hao, W.; Huang, Z.; Wang, X.; Wang, P.G. Mono-functionalized glycosylated platinum(IV) complexes possessed both pH and redox dual-responsive properties: Exhibited enhanced safety and preferentially accumulated in cancer cells in vitro and in vivo. *Eur. J. Med. Chem.* **2017**, *128*, 45–55. [CrossRef] [PubMed]

25. Patra, M.; Johnstone, T.C.; Suntharalingam, K.; Lippard, S.J. A Potent Glucose−Platinum Conjugate Exploits Glucose Trans-porters and Preferentially Accumulates in Cancer Cells. Angew. *Chem. Int. Ed.* **2016**, *55*, 2550–2554. [CrossRef] [PubMed]

26. Krawczyk, M.; Pastuch-Gawolek, G.; Mrozek-Wilczkiewicz, A.; Kuczak, M.; Skonieczna, M.; Musiol, R. Synthesis of 8-hydroxyquinoline glycoconjugates and preliminary assay of their β1,4-GalT inhibitory and anti-cancer properties. *Bioorg. Chem.* **2019**, *84*, 326–338. [CrossRef] [PubMed]

27. Krawczyk, M.; Pastuch-Gawołek, G.; Pluta, A.; Erfurt, K.; Domiński, A.; Kurcok, P. 8-Hydroxyquinoline Glycoconjugates: Modifications in the Linker Structure and Their Effect on the Cytotoxicity of the Obtained Compounds. *Molecules* **2019**, *24*, 4181. [CrossRef] [PubMed]

28. Krawczyk, M.; Pastuch-Gawołek, G.; Hadasik, A.; Erfurt, K. 8-Hydroxyquinoline Glycoconjugates Containing Sulfur at the Sugar Anomeric Position—Synthesis and Preliminary Evaluation of Their Cytotoxicity. *Molecules* **2020**, *25*, 4174. [CrossRef]

29. Dheer, D.; Singh, V.; Shankar, R. Medicinal attributes of 1,2,3-triazoles: Current developments. *Bioorganic Chem.* **2017**, *71*, 30–54. [CrossRef]

30. Liang, L.; Astruc, D. The copper(I)-catalyzed alkyne-azide cycloaddition (CuAAC) "click" reaction and its applications. *An overview. Coord. Chem. Rev.* **2011**, *255*, 2933–2945. [CrossRef]

31. Kolb, H.C.; Finn, M.G.; Sharpless, K.B. Click Chemistry: Diverse Chemical Function from a Few Good Reactions. *Angew. Chem. Int. Ed.* **2001**, *40*, 2004–2021. [CrossRef]

32. Tiwari, V.K.; Mishra, B.B.; Mishra, K.B.; Mishra, N.; Singh, A.S.; Chen, X. Cu-Catalyzed Click Reaction in Carbohydrate Chemistry. *Chem. Rev.* **2016**, *116*, 3086–3240. [CrossRef]

33. Semenov, S.N.; Belding, L.; Cafferty, B.J.; Mousavi, M.P.S.; Finogenova, A.M.; Cruz, R.S.; Skorb, E.V.; Whitesides, G.M. Autocatalytic Cycles in a Copper-Catalyzed Azide–Alkyne Cycloaddition Reaction. *J. Am. Chem. Soc.* **2018**, *140*, 10221–10232. [CrossRef]

34. Haber, R.S.; Rathan, A.; Weiser, K.R.; Pritsker, A.; Itzkowitz, S.H.; Bodian, C.; Slater, G.; Weiss, A.; Burstein, D.E. GLUT1 Glucose Transporter Expression in Colorectal Carcinoma: A marker for poor prognosis. *Cancer* **1998**, *83*, 34–40. [CrossRef]

35. Brown, R.S.; Wahl, R.L. Overexpression of Glut-1 Glucose Transporter in Human Breast Cancer. *Cancer* **1993**, *72*, 2979–2985. [CrossRef]

36. Gupta, S.K.; Shukla, V.K.; Vaidya, M.P.; Roy, S.K.; Gupta, S. Serum and tissue trace elements in colorectal cancer. *J. Surg. Oncol.* **1993**, *52*, 172–175. [CrossRef]

37. Kuo, H.W.; Chen, S.F.; Wu, C.C.; Chen, D.R.; Lee, J.H. Serum and Tissue Trace Elements in Patients with Breast Cancer in Taiwan. *Biol. Trace Element Res.* **2002**, *89*, 1–11. [CrossRef]

38. Mosmann, T. Rapid colorimetric assay for cellular growth and survival: Application to proliferation and cytotoxicity assays. *J. Immunol. Methods* **1983**, *65*, 55–63. [CrossRef]

39. Domiński, A.; Konieczny, T.; Duale, K.; Krawczyk, M.; Pastuch-Gawołek, G.; Kurcok, P. Stimuli-Responsive Aliphatic Poly-carbonate Nanocarriers for Tumor-Targeted Drug Delivery. *Polymers* **2020**, *12*, 2890. [CrossRef]

40. Kamaly, K.; Yameen, B.; Wu, J.; Farokhzad, O.C. Degradable Controlled-Release Polymers and Polymeric Nanoparticles: Mechanisms of Controlling Drug Release. *Chem. Rev.* **2016**, *116*, 2602–2663. [CrossRef]

41. Kato, Y.; Ozawa, S.; Miyamoto, C.; Maehata, Y.; Suzuki, A.; Maeda, T.; Baba, Y. Acidic extracellular microenvironment and cancer. *Cancer Cell Int.* **2013**, *13*, 89. [CrossRef] [PubMed]

42. Domiński, A.; Krawczyk, M.; Konieczny, T.; Kasprów, M.; Foryś, A.; Pastuch-Gawołek, G.; Kurcok, P. Biodegradable pH-responsive micelles loaded with 8-hydroxyquinoline glycoconjugates for Warburg effect based tumor targeting. *Eur. J. Pharm. Biopharm.* **2020**, *154*, 317–329. [CrossRef] [PubMed]

Publikacja P.6

Biodegradable pH-Responsive Micelles Loaded with
8-Hydroxyquinoline Glycoconjugates for Warburg Effect Based
Tumor Targeting

A. Domiński, **M. Krawczyk**, T. Konieczny, M. Kasprów, A. Foryś,
G. Pastuch-Gawołek, P. Kurcok[*]

Materiały uzupełniające do publikacji znajdują się w dołączonej płycie CD

Biodegradable pH-responsive micelles loaded with 8-hydroxyquinoline glycoconjugates for Warburg effect based tumor targeting

Adrian Domiński[a], Monika Krawczyk[b,c], Tomasz Konieczny[a], Maciej Kasprów[a], Aleksander Foryś[a], Gabriela Pastuch-Gawołek[b,c], Piotr Kurcok[a,*]

[a] Centre of Polymer and Carbon Materials, Polish Academy of Sciences, 34, M. Curie-Skłodowskiej St, 41-819 Zabrze, Poland
[b] Department of Organic Chemistry, Bioorganic Chemistry and Biotechnology, Faculty of Chemistry, Silesian University of Technology, Krzywoustego 4, 44-100 Gliwice, Poland
[c] Biotechnology Centre, Silesian University of Technology, Krzywoustego 8, 44-100 Gliwice, Poland

ARTICLE INFO

ABSTRACT

Biodegradable triblock copolymer poly(ethylene glycol)-b-polycarbonate-b-oligo([R]-3-hydroxybutyrate) was prepared *via* metal-free ring-opening polymerization of ketal protected six-membered cyclic carbonate followed by esterification with bacterial oligo([R]-3-hydroxybutyrate) (oPHB). Amphiphilic triblock copolymer self-organizes into micelles with a diameter of ~25 nm. Acid-triggered hydrolysis of ketal groups to two hydroxyl groups causes an increase in hydrophilicity of the hydrophobic micelle core, resulting in the micelles swell and drug release. oPHB was added as core-forming block to increase the stability of prepared micelles in all pH (7.4, 6.4, 5.5) studied. Doxorubicin and 8-hydroxyquinoline glucose- and galactose conjugates were loaded in the micelles. *In vitro* drug release profiles in PBS buffers with different pH showed that a small amount of loaded drug was released in PBS at pH 7.4, while the drug was released much faster at pH 5.5. MTT assay showed that the blank micelles were non-toxic to different cell lines, while glycoconjugates-loaded micelles, showed significantly increased ability to inhibit the proliferation of MCF-7 and HCT-116 cells compared to free glycoconjugates. The glycoconjugation of anti-cancer drugs and pH-responsive nanocarriers have separately shown great potential to increase the tumor-targeted drug delivery efficiency. The combination of drug glycoconjugation and the use of pH-responsive nanocarrier opens up new possibilities to develop novel strategies for efficient tumor therapy.

1. Introduction

Nowadays, cancer is one of the biggest problems in modern society, remaining the top three leading risks factor for global mortality [1]. Conventional chemotherapy is currently one of the most important strategies in treating cancer. However, the high toxicity of anti-cancer drugs, in combination with the growing multi-drug resistance of cancer cells to a significant number of clinical pharmaceutics is a major obstacle to obtaining effective anti-cancer therapy results [2,3]. When designing new cancer treatments, it is vital to distinguish and take advantage of the differences between cancer cells and normal cells. One such difference is the specific metabolism of glucose by tumor tissues. Tumors consume tremendous amounts of glucose compared to healthy tissues due to a high rate of glycolysis, to obtain the energy needed to increase proliferation [4–7]. This relationship between the high rate of glucose uptake and increased cell proliferation with simultaneous acidification of the tumor microenvironment due to lactate secretion is known as the Warburg effect [8] and resulting from tumors mitochondrial metabolic changes [9]. Tumor tissues present a very fast rate of glycolysis leading to lactic acid fermentation which is characteristic of hypoxic conditions [10–12]. The increased glycolysis is associated with the overexpression of glucose transporters (GLUT). GLUTs are special transmembrane proteins that facilitate concentration-dependent glucose uptake inside the cell [13,14]. This persistent high lactate production by cancer cells provides intrinsic acidity of the tumor microenvironment [4,11,15]. Due to this, scientists are exploiting the Warburg effect in many drug delivery applications to achieve higher tumor-targeting efficacy and local drug concentrations, as well as to minimize systemic exposure [16–21].

It has been broadly reported that conjugation of anti-cancer drugs with the sugar units (especially glucose) can significantly enhance bioavailability, water solubility as well as facilitate intermembrane

---

transport and reduce toxicity of anti-cancer drugs [22–25]. Because of the overexpression of GLUT in cancer cells, compared to normal cells, the conjugation of therapeutics with sugar derivatives is a widely used technique for designing anti-cancer therapeutic agents based on already used anti-cancer drugs, such as glufosfamide [26], oxaliplatin [27], paclitaxel [28], natural compounds [29], e.g., flavonoids or polyphenols or small-molecule compounds [30,31]. The addition of a sugar unit into the therapeutic structure significantly improves drug absorption into highly glycolytic cancer cells, among others through active transport by GLUT transporters, capable of transporting sugars such as glucose, galactose, mannose and glucosamine [32], while not showing toxicity to healthy tissues [23]. However, conventional or conjugated therapeutics showed a series of problems, such as limited stability or nonspecific toxicity [29]. Moreover, the tumor is heterogeneous and the levels of GLUT transporters overexpression are different from cell to cell in the tumor [33]. To overcome these challenges, tumor-targeted drug delivery nanoparticles, e.g., micelles, polymersomes, etc. have been developed, that may revolutionize conventional chemotherapy. Due to the pH gradient in the internal and external microenvironment of cancer cells (the physiological pH value is 7.4; in the tumor, the extracellular pH value is ~6.0–7.0, while inside cancer cells the pH value is ~5.0–6.0 in endosomes and ~4.0–5.0 in lysosomes [34,35]), pH-sensitive polymeric nanoconstructs have attracted great attention in therapeutics delivery applications [36–38].

Micelles can be used to encapsulate fragile anti-cancer therapeutics, but they can also be designed to respond to changes in pH by incorporating into a polymer structure acid-labile groups (acetal/ketal, hydrazone, orthoester, etc. [39–43]). Because of these incorporated acid-sensitive chemical groups, micelles can respond to the acidic microenvironment of cancer cells, by disassembling, changing micelle size, shape or surface charge [44–47]. This leads to the release of the encapsulated drugs in a controlled manner and improving the ability of the drug to target the tumor cells. Particularly, it is interesting to introduce the pH-sensitive groups to the polymeric nanocarriers based on PEGylated biodegradable polymers such as: aliphatic polyesters (polylactide [48], poly(3-hydroxybutyrate) [49], poly(ε-caprolactone) [50]) or aliphatic polycarbonates [51], which are all approved by the American Food and Drug Administration (FDA).

The aliphatic polycarbonates deserve a special attention here, because of their easily-tuned functionality to achieve excellent tumor targeting performance. Various biodegradable pH-sensitive micelles based on aliphatic polycarbonate with different acid-sensitive groups, e.g., acetal [52–54], hydrazone [55,56], Schiff-base linkage [57], tertiary amine [35,58,59] have been developed. In particular, an acetal is an attractive group due to its unique characteristics, such as its stability at physiological pH and susceptibility to hydrolysis at acidic pH. Furthermore, various pH-responsive micelles based on acetal group have been reported and their physico-chemical properties and pH-triggered hydrolysis behavior were characterized in detail [60,61]. However, the major obstacle of the acetal-based polymeric micelles is the acid-triggered hydrolysis of the acetal group into two hydroxyl groups, which causes an increase in hydrophilicity of the hydrophobic micelle core. That is why obtaining stable micelles is not an easy task. To overcome these challenges, various pH-responsive core crosslinked micelles showing improved stability against dilution and prolonged circulation time have been developed [34,62–67]. The crosslinking of micelles may also unfavorably influence drug release in the tumor, leading to the worse therapeutic outcome [60–62]. Tuning of the share of individual blocks in the copolymer is also a feasible method to control the stability, size or drug encapsulation efficiency of micelles [49]. It is well documented that the high crystallinity hydrophobic core-forming blocks (i.e. poly([R]-3-hydroxybutyrate) [49] or poly(L-lactide) [68,69] enhancing the colloidal stability of micelles in an aqueous medium but a high degree of crystallinity significantly decreases the drug loading efficiency [70,71]. However, addition of a short highly hydrophobic crystalline biodegradable core-forming block into amphiphilic

copolymer might create a superior balance between stability and drug release efficiency of acetal-base pH-responsive micelles.

The polymeric micelles that are designed to respond to only one stimulus have shown limited success in clinical trials [37,38]. Therefore, multi-stimuli polymeric micelles, that are sensitive to two or more stimuli, have gained a broad interest in recent years [72,73]. The conjugation of various tumor targeting ligands on the surface of micelles to obtain the specific recognition by the overexpression of the corresponding receptors in the tumor to enhancing the therapeutic effect was also studied [74,75].

The 8-hydroxyquinoline (8-HQ) is a promising biological activity scaffold, in which its derivatives were successfully applied to design therapeutics used in the treatment of neurodegenerative diseases, anti-HIV, and a wide spectrum of solid tumors [76–78]. 8-HQ displays an anti-cancer effect due to its interaction with metal ions (Cu, Zn, Fe etc.) which tumor tissues have increased demand [79]. However, the 8-HQ scaffold has poor bioavailability, solubility and pharmacokinetic parameters. For this reason, 8-HQ derivatives have been modified by the conjugation with a sugar unit to facilitate intermembrane transport. [80–82]. Besides, the encapsulation of such 8-HQ prodrugs in nanocarriers should significantly improve their efficacy by avoiding systemic side effects and reducing the doses of prodrugs administered.

The glycoconjugation of anti-cancer drugs and pH-responsive micelles have separately shown great potential to increase the tumor targeted drug delivery efficiency. On the other hand, a joint action between glycoconjugation and pH-responsive nanocarrier system seems to be a rationally designed synergistic anticancer therapy to significantly improve selectivity in tumor-targeting drug delivery. Herein, we develop 8-hydroxyquinoline glycoconjugates-loaded biodegradable and non-toxic pH-responsive poly(ethylene glycol)-b-polycarbonate-b-poly[R]-3-hydroxybutyrate micelles by functionalizing polycarbonate repeating units with acetal groups. Acid-triggered hydrolysis of the acetal group to two hydroxyl groups causes an increase in hydrophilicity of the hydrophobic micelle core, causing the micelles to swell and initiates prodrugs release. The addition of biodegradable and biocompatible hydrophobic bacterial poly([R]-3-hydroxybutyrate) as core-forming unit was used to increase the stability of micelles, as well as to prolong circulation time and drug release. The synthesis of copolymers, preparation and characterization of micelles, pH-triggered degradation and *in vitro* drug release profile were studied. Additionally, the cytotoxicity of blank micelles and *in vitro* activity of drug- and prodrugs-loaded micelles were investigated against both healthy cells and cancer cells by using MTT assay.

2. Experimental section

2.1. Materials

Pentaerythritol (99%, Sigma-Aldrich), *p*-toluenesulfonic acid monohydrate (99%, Sigma-Aldrich), 2,2-dimethoxypropane (99%, Sigma-Aldrich) were used as received. DOWEX-MARATHON and Dowex 50WX8 (both Sigma-Aldrich) were washed with dry THF before use. Methoxy poly(ethylene glycol) (mPEG$_{5000}$, Sigma-Aldrich, M_n = 5.0 kg mol^{-1}) was dried by two azeotropic distillations using anhydrous toluene. 1,5,7-Triazabicyclo-[4.4.0]dec-5-ene (TBD) (98%, Sigma-Aldrich) was dried under vacuum at 60 °C for 24 h. 1,8-Diazabicyclo[5.4.0]undec-7-ene (DBU) (98%, Sigma-Aldrich) was distilled under reduced pressure over BaO. Poly([R]-3-hydroxybutyrate) (nPHB) (Mw = 430,000 Đ = 2.99; ICI product - PHB G08) was used as received. Ethyl chloroformate (97%, Sigma-Aldrich), oxalyl chloride (98%, Sigma-Aldrich) were used as received. Triethylamine (NEt$_3$) and *N,N*-diisopropylethylamine (both 99%, Sigma-Aldrich), dichloromethane (DCM) and *N,N*-dimethylformamide (DMF) (both POCH) were dried over CaH$_2$ and distilled under reduced pressure prior to use THF (POCH) was distilled over a sodium-potassium alloy. Petroleum ether (VWR Chemicals), diethyl ether (99%, VWR

Chemicals), NaHCO₃ (POCH), pyrene (+98%, Acros Organics), HCl$_{aq}$ (35–38%, POCH), CHCl₃ (98%, POCH), n-hexane (95%, POCH) were all used as received. Doxorubicin hydrochloride (DOX·HCl) was purchased from LC Laboratories (Woburn, MA).

Model glycoconjugates used for *in vitro* cytotoxicity tests: 8-((1-(2,3,4,6-tetra-O-acetyl-β-D-glucopyranosyl)-1H-1,2,3-triazol-4-yl) methoxy)quinoline (8HQ-glucose conjugate – 8HQ-Glu) and 8-((1-(2,3,4,6-tetra-O-acetyl-β-D-galactopyranosyl)-1H-1,2,3-triazol-4-yl) methoxy)quinoline (8HQ-galactose conjugate – 8HQ-Gal) were synthesized according to literature protocol [80]. Structure of glycoconjugates is presented in Fig. S1.

Cell Lines

The human colon adenocarcinoma cell line HCT-116 was obtained from American Type Culture Collection (ATCC, Manassas, VA, USA). The human cell line MCF-7 was obtained from collections at the Maria Sklodowska-Curie Memorial Cancer Center and Institute of Oncology, branch in Gliwice, Poland, as a kind gift from Monika Pietrowska and prof. Wiesława Widłak. The Normal Human Dermal Fibroblasts-Neonatal, NHDF-Neo were purchased from LONZA (Cat. No. CC-2509, NHDF-Neo, Dermal Fibroblasts, Neonatal, Lonza, Poland). The culture media consisted of RPMI 1640 or DMEM + F12 medium, supplemented with 10% fetal bovine serum and 5% antibiotics (penicillin and streptomycin). The culture media were purchased from HyClone. Fetal bovine serum (FBS) was delivered by Eurx, Poland and Antibiotic Antimycotic Solution (100×) by Sigma-Aldrich, Germany.

2.2. Synthesis of the cyclic carbonate of 2,2-dimethyl-5,5 bis (hydroxymethyl)-1,3-dioxane (KPC)

The cyclic carbonate monomer functionalized with ketal-protected hydroxymethyl groups (KPC) (9,9-dimethyl-2,4,8,10-tetraoxaspiro[5.5] undecan-3-one) was synthesized according to literature protocol [83]. Briefly, pentaerythritol (25 g, 0.184 mol, 1.0 eq.) and p-toluenesulfonic acid monohydrate (0.3 g, 1.577 mmol) were dissolved in 300 mL of DMF at 80 °C, then the reaction mixture was cooled to 40 °C and 2,2-dimethoxypropane (22.6 mL, 19.12 g, 0.184 mol, 1.0 eq.) was added and the reaction was carried out overnight at room temperature. Then, 5 g of DOWEX-MARATHON were added and stirred for 1 h, and the reaction mixture was filtered. Next, the solvent was stripped-off under reduced pressure, the dry product was extracted using Soxhlet apparatus with petroleum ether for 6 h and then twice with diethyl ether for 6 h. The residual solid (2,2-dimethyl-5,5-bis(hydroxymethyl)-1,3-dioxane) was dried under vacuum to constant weight. Yield: 65%. ¹H NMR (600 MHz, CDCl₃, δ): 1.42 ppm (s, 6H, CH₃), 3.73 ppm (s, 4H, CH₂-OH), 3.77 ppm (s, 4H, CH₂-O). Next, under the nitrogen flow, into a reaction mixture composed of (2,2-dimethyl-5,5-bis(hydroxymethyl)-1,3-dioxane (10 g, 0.057 mol, 1 eq.) and ethyl chloroformate (13.51 mL, 15.40 g, 0.142 mol, 2.5 eq.) in 500 mL of anhydrous THF and thermostated at 0 °C, solution of triethylamine (19.75 mL, 14.36 g, 0.142 mol, 2.5 eq.) in 50 mL dry THF was added dropwise. The reaction mixture was stirred for 2 h at 0 °C. Then the cooling bath was taken out and the mixture was stirred for another 1 h at room temperature. Next, the precipitated triethylammonium chloride was filtered off, THF stripped off and the residue was twice recrystallized from THF. The white crystals of cyclic carbonate of 2,2-dimethyl-5,5-bis(hydroxymethyl)-1,3-dioxane were obtained with 51% yield. ¹H NMR (600 MHz, CDCl₃, δ): 1.44 ppm (s, 6H, CH₃), 3.80 ppm (s, 4H, CH₂-O), 4.30 ppm (s, 4H, CH₂-O-C(O)-O).

2.3. Synthesis of PEG-PKPC diblock copolymer

The polymerizations were performed in an anhydrous atmosphere (glove-box, H₂O < 1 ppm, O₂ < 1 ppm). The diblock copolymer was synthesized by ring-opening polymerization (ROP) of KPC using PEG as

an initiator and TBD as catalysts in dry THF at room temperature. Typically, vial equipped with a stirring bar was charged with a solution of KPC (0.0607 g, 0.3 mmol, 15 eq.) in 1.5 mL of dry THF. In another vial, a solution of initiator mPEG-OH (M$_n$ = 5000 g mol⁻¹, 0.1 g, 0.02 mmol, 1 eq.) and TBD (0.0014 g, 0.01 mmol, 0.5 eq.) in 1.5 mL of dry THF was prepared in next vial. Then, the initiator–catalyst solution was added to the monomer solution. The conversion of the monomer was monitored by using ¹H NMR. The polymerization reaction was quenched by acidification with Dowex 50WX8. The obtained copolymer was precipitated in 20-fold cold diethyl ether twice and dried under vacuum to constant weight. ¹H NMR (600 MHz, CDCl₃, δ): 1.42 ppm (s, 6nH, CH₃), 3.37 ppm (s, 3H, CH₃-O), 3.66 ppm (s, 4mH CH₂-CH₂-O), 3.76 ppm (s, 4nH, CH₂-O), 4.2 ppm (s, 4nH, CH₂-O-C(O)-O). SEC: (CHCl₃, PS standards): M$_n$ = 7300 g mol⁻¹, Đ = 1.42.

2.4. Synthesis of oligo([R]-3-hydroxybutyrate) via anionically controlled temperature degradation of nPHB

The oligo([R]-3-hydroxybutyrate) (oPHB) was synthesized *via* reactive extrusion degradation of the commercially available nPHB according to our previously reported procedure [84]. Briefly, nPHB was mixed with NaHCO₃ then thermally treated in single screw extruder with three heating zones (i), (ii) and (iii) each 8 cm length, respectively applying temperatures: (i) 110 °C, (ii) 175 °C and (iii) 175 °C, 80 rpm (polymer was in the extruder about 2 min). Obtained oligo([R]-3-hydroxybutyrate) were dissolved in 500 mL of CHCl₃ and was washed three times with 1 M HCl$_{aq}$ followed by ten washings with distilled water. Next, the polymer was isolated by precipitation in cold n-hexane and dried under vacuum at rt. to constant weight. ¹H NMR (600 MHz, CDCl₃, δ): 1.28 ppm (d, 3nH, CH₃), 2.5 ppm (m, 2nH, CH₂), 5.25 ppm (m, 1nH, CH), 1.86 ppm (d, 3H, CH₃-CH), 5.8 ppm (d, 1H, CH₃CH = CH), 6.95 ppm (m, 1H, CH₃-CH =). SEC: (CHCl₃, PS standards): M$_n$ = 1000 g mol⁻¹, Đ = 1.8.

2.5. Synthesis of PEG-PKPC-oPHB triblock copolymer

The solution of oPHB (0.08 g, 0.08 mmol, 1.2 eq.) in 20 mL of dry DCM with 2 drops of dry DMF was thermostated in 0 °C. Next, a solution of oxalyl chloride (0.008 mL, 0.012 g, 0.093 mmol, 1.4 eq.) in 10 mL of dry DCM was slowly added dropwise. The reaction was stirred for 20 min at 0 °C, then the cooling bath was taken out and the mixture was stirred for another 2 h at rt. Then, volatiles was stripped-off under vacuum and the obtained acyl chloride was dissolved in 15 mL of dry DCM and added dropwise into a solution of PEG-PKPC (0.5 g, 0.067 mmol, 1 eq.) and triethylamine (0.093 mL, 0.0675 g 0.667 mmol, 10 eq.) in 20 mL of anhydrous DCM thermostated in 0 °C. The reaction was stirred for 20 min at 0 °C, then the cooling bath was removed and the reaction was carried out for 3 h at rt. Next, volatiles were stripped-off under vacuum and to the residue 20 mL THF was added. The precipitated triethylammonium chloride and oPHB excess were filtered off through an aluminum oxide bed, which then was washed with an additional 20 mL of THF. The obtained PEG-PKPC-oPHB copolymer was isolated by precipitation in cold n-hexane and dried under vacuum at rt. to constant weight. ¹H NMR (600 MHz, CDCl₃, δ): 1.42 ppm (s, 6nH, CH₃), 3.37 ppm (s, 3H, CH₃-O), 3.66 ppm (s, 4mH CH₂-CH₂-O), 3.76 ppm (s, 4nH, CH₂-O), 4.2 ppm (s, 4nH, CH₂-O-C(O)-O), 1.28 ppm (d, 3nH, CH₃), 2.5 ppm (m, 2nH, CH₂), 5.25 ppm (m, 1nH, CH), 1.86 (d, 3H, CH₃-CH), 5.8 (d, 1H, CH₃CH = CH), 6.95 ppm (m, 1H, CH₃-CH =). SEC: (CHCl₃, PS standards): M$_n$ = 8300 g mol⁻¹, Đ = 1.57.

2.6. Characterization of synthetic copolymers

¹H NMR spectra were recorded at Bruker-Avance II 600 MHz (Fremont, CA, USA) in CDCl₃ with tetramethylsilane (TMS) as an internal standard. Size exclusion chromatography (SEC) was performed in CHCl₃ at 35 °C with a flow rate of 1 mL min⁻¹, using a Spectra-Physic

8800 gel permeation chromatograph (Santa Clara, CA, USA), equipped with a PL-gel 5 mm MIXED-E ultra-high efficiency column and Shodex SE 61 differential refractive index detector with polystyrene standards for calibration.

2.7. Preparation of micelles and self-assembly behavior characterization

Blank micelles were prepared by a solvent evaporation method as follows: the respective copolymers were dissolved in DCM and then the solvent was stripped-off to get a thin film at the bottom of the vial. After removing the traces of organic solvent, the formed thin film was dispersed by the addition of 10 mL of deionized water to obtain a concentration of 1 mg mL^{-1}. Then, the mixture was vigorously stirred for 60 min at rt. and treated for 30 min with sonicator in an ice cold bath. The obtained solution (1 mg mL^{-1}) was filtered through a syringe filter (0.2 μm, Sartorius) to break up larger aggregates. The final concentration of the solution was *ca.* 1 mg mL^{-1} and obtained micelle solutions were used for other characterization studies without any further purification.

The critical micelle concentration (CMC) of the copolymers was determined by a fluorescence method using pyrene as a probe. A predetermined amount of pyrene (1 · 10^{-6} mol L^{-1}) in acetone was added into a brown glass flask and acetone was evaporated completely in dark. Then, 5 mL of each micelle solutions at different concentrations (ranging from 1 · 10^{-5} to 1.0 mg mL^{-1}) prepared by serial dilution method were added to vials. The samples were then incubated overnight at rt. in dark and characterized. The fluorescence spectra were recorded on a Hitachi F-2500 Spectrometer (Tokyo, Japan). The scanning range was from 300 to 360 nm and the excitation wavelength was 391 nm. The ratios of fluorescence intensities at 337 nm over 333 nm (I_{337}/I_{333}) were plotted against the logarithm of polymer concentration. The value of the intersection of two tangents was determined as the critical micelle concentration.

The hydrodynamic size of micelles was determined by dynamic light scattering (DLS) measurements using a Brookhaven BI-200 goniometer equipped with a Brookhaven BI-9000 AT (New York, USA) digital autocorrelator and a 35 mW laser with vertically polarized light with wavelength λ = 637 nm. DLS measurements were carried out at a constant temperature of 25 or 37 °C. The correlation curve was developed using the CONTIN algorithm. Simultaneously, in order to investigate the stability and acid-triggered degradation of micelles at different pH 5 mg of freeze-dried micelles were incubated at 37 °C in 5 mL PBS buffer with different pH 7.4, 6.4 and 5.5 respectively. At predetermined time intervals, the change of micelles size was measured.

The morphologies of the micelles were observed using Cryogenic Transmission Electron Microscopy (cryo-TEM). Images were obtained using a Tecnai F20 X TWIN microscope (FEI Company, Hillsboro, Oregon, USA) equipped with field emission gun, operating at an acceleration voltage of 200 kV. Images were recorded on the Gatan Rio 16 CMOS 4k camera (Gatan Inc., Pleasanton, California, USA) and processed with Gatan Microscopy Suite (GMS) software (Gatan Inc., Pleasanton, California, USA). Specimen preparation was done by vitrification of the aqueous solutions on grids with holey carbon film (Quantifoil R 2/2; Quantifoil Micro Tools GmbH, Großlöbichau, Germany). Prior to use, the grids were activated for 15 s in oxygen plasma using a Femto plasma cleaner (Diener Electronic, Ebhausen, Germany). Cryo-samples were prepared by applying a droplet (3 μL) of the suspension to the grid, blotting with filter paper and immediate freezing in liquid ethane using a fully automated blotting device Vitrobot Mark IV (Thermo Fisher Scientific, Waltham, Massachusetts, USA). After preparation, the vitrified specimens were kept under liquid nitrogen until they were inserted into a cryo-TEM-holder Gatan 626 (Gatan Inc., Pleasanton, USA) and analyzed in the TEM at −178 °C.

2.8. Drug loading and in vitro release studies

Drug-loaded micelles were prepared using a procedure similar to the preparation of the blank micelles. Briefly, 10 mg of the copolymer and 1 mg of the drug, deprotonated doxorubicin or 8-hydroxyquinoline glycoconjugates respectively, were dissolved in DCM, followed by solvent evaporation, water addition, stirring and sonication. Then, solution was centrifuged at 3000 rpm for 5 min to eliminate the unloaded drug. The supernatant was recovered and filtered through syringe filter, lyophilized and kept in freeze-dried storage. The predetermined amount of lyophilized drug-loaded micelles was redissolved in DMSO. The drug concentration was measured by detecting the UV absorbance at 481 nm for DOX and 260 nm for 8HQ-glycoconjugates using a two-beam UV–Vis-NIR spectrophotometer JASCO V-570 (Tokyo, Japan) and determined according to a calibration curve. The drug loading efficiency (DLE) and drug loading content (DLC) were calculated according to the following equations:

$$Drug\ loading\ efficiency\ (DLE\%)$$
$$= \frac{weight\ of\ drug\ in\ micelles}{weight\ of\ drug\ in\ feed} \times 100\%$$

$$Drug\ loading\ content\ (DLC\%)$$
$$= \frac{weight\ of\ drug\ in\ micelles}{weight\ of\ drug\ loaded\ micelles} \times 100\%$$

The *in vitro* drug release from micelles was performed at 37 °C in PBS at pH 7.4, 6.4 and 5.5 by a dialysis method. Typically, 3 mL of drug-loaded micelles with known drug concentration was introduced into a 3 mL Float-A-Lyzer G2 dialysis device (MWCO 7000; Spectra/Por). Each device was placed in 150 mL of corresponding PBS buffer at 37 °C with stirring at 100 rpm. At predetermined time intervals, a sample of 50 μL was drawn and replaced with equal amount of fresh buffer. Quantitative assessment of released drug was performed by measuring the UV absorption at 481 nm for DOX and 260 nm for 8HQ-glycoconjugates based on a calibration curve. The release experiments were conducted in triplicate. The results presented are the average data.

2.9. MTT assay

A lifespan of the cells was assessed with an MTT (3-[4–di-methylthiazol-2-yl]-2,5-diphenyltetrazolium bromide) assay (Sigma-Aldrich). Stock solutions of DOX or glycoconjugates were prepared in DMSO and diluted with the appropriate volumes of the growth medium directly before the experiment. Free micelles and drug-loaded micelles were diluted with the appropriate volumes of the growth medium directly before the experiment. The cells were seeded into 96-well plates at concentration 2 · 10^3 (HCT-116) or 5 · 10^3 (MCF-7, NHDF-Neo) per well. The cell cultures were incubated for 24 h at 37 °C in a humidified atmosphere of 5% CO$_2$. Then the culture medium was removed, replaced with a solution of the tested compounds in medium with varying concentrations and incubated further for 24 h, 48 h or 72 h. After that, the medium was removed and the MTT solution (50 μL, 0.5 mg mL^{-1} in PBS) was added. After 3 h of incubation, the MTT solution was removed and the precipitated formazan was dissolved in DMSO. Finally, the absorbance at the 570 nm wavelength was measured spectrophotometrically with the plate reader (Epoch, BioTek, USA). The experiment was conducted in at least three independent iterations with four technical repetitions. The IC$_{50}$ values were calculated using CalcuSyn software. The IC$_{50}$ parameter was defined as the compound concentration that was necessary to reduce the proliferation of cells to 50% of the untreated control.
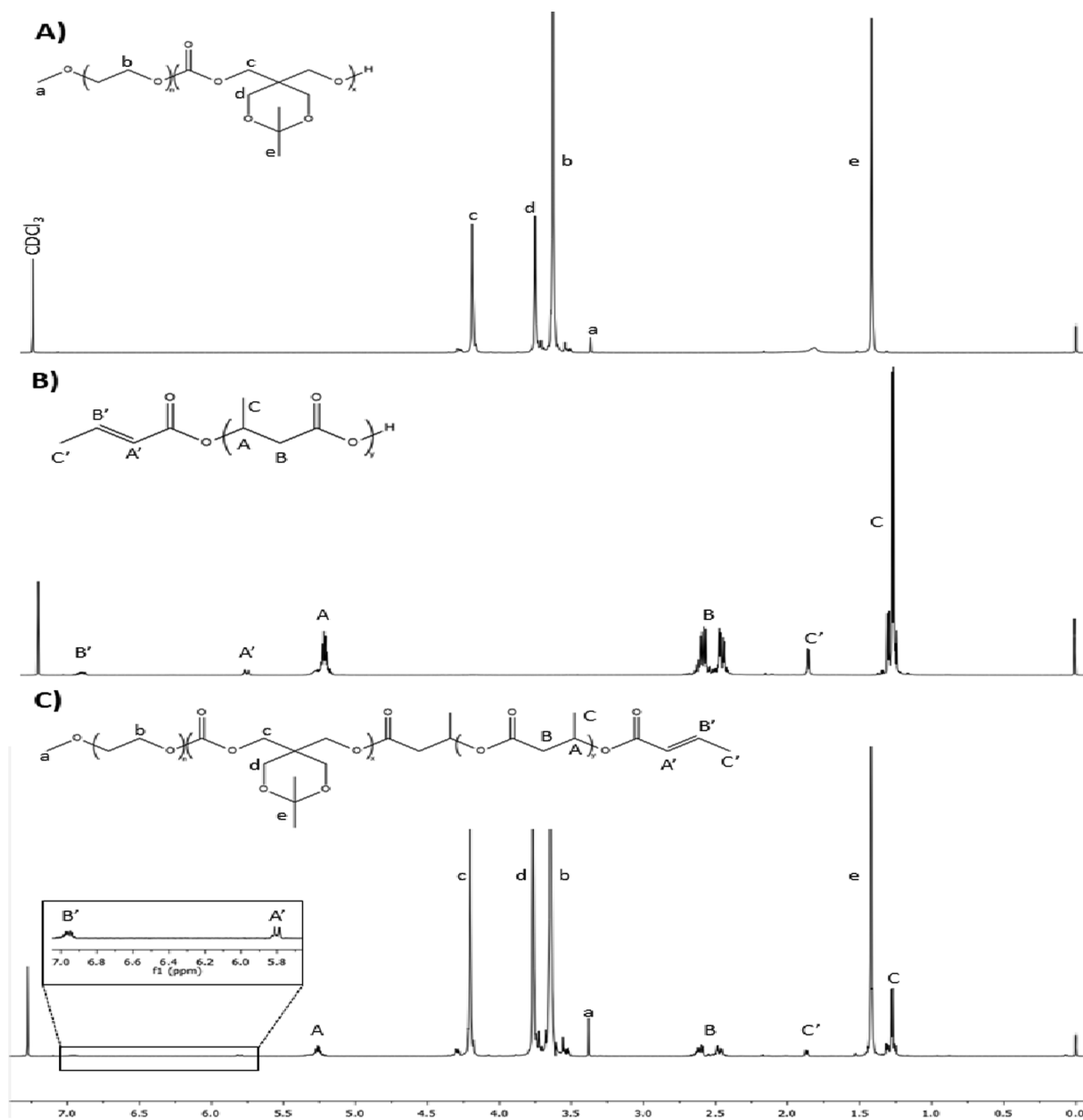
Fig. 1. ^{1}H NMR spectrum (CDCl$_3$, 600 MHz) of: (A) mPEG-PKPC, (B) oligo([R]-3-hydroxybutyrate) and (C) mPEG-PKPC-oPHB.

3. Results and discussion

3.1. Synthesis and characterization of PEG-PKPC and PEG-PKPC-oPHB copolymers

This work aims to develop biodegradable micelles for pH-triggered release of anti-cancer 8-hydroxyquinoline gluco- and galactoconjugate prodrugs, for which amphiphilic copolymer containing acid-responsive ketal groups and bacterial oligo([R]-3-hydroxybutyrate) (oPHB) block was designed. The acid-labile ketal groups were crucial to rapid drug release in the acidic tumor microenvironment, whereas hydrophobic oPHB core-forming block was hypothesized to offer increased micelles stability, preventing premature drug release. The PEGylated ketal-functionalized polycarbonate block copolymer (PEG-PKPC) was synthesized by methoxy poly(ethylene glycol) (mPEG) initiated metal-free ring-opening polymerization (ROP) of a six-membered cyclic carbonate modified with a pH-responsive ketal group and the triblock copolymer PEG-PKPC-oPHB was synthesized by the conjugation of oPHB with the

PEG-PKPC backbone in a simple esterification reaction. The ketal-functionalized six-membered cyclic carbonate monomer (9,9-dimethyl-2,4,8,10-tetraoxaspiro[5.5]undecan-3-one) was synthesized and its chemical structure was confirmed by ^{1}H NMR (Fig. S2). The ability to controlled ROP of such acetal-functionalized monomer using organo-catalyst was studied in the presence of 1,8-diazabicyclo[5.4.0]undec-7-ene (DBU) or 1,5,7-triazabicyclo-[4.4.0]dec-5-ene (TBD). All poly-merizations were performed at rt. in THF using mPEG$_{5000}$-OH as an initiator. Both catalytic systems enable to reach relatively high monomer conversions (> 90%). However, in case DBU was used as a catalyst, the polymerization proceeded slow, and monomer conversion of < 5% in 24 h and 90% in 14 days was observed. Moreover, large difference between theoretical and experimental molar mass was ob-served, probably due to the side reactions occurring. However, much better result i.e., monomer conversion > 90%, was reached in 24 h using a more basic TBD as a catalyst. Obtained copolymer had a molar mass matching the theoretical value and dispersity of Đ = 1.42.

Amphiphilic copolymers can self-organizing into micelles and this is

primarily determined by the hydrophilic weight fraction (f), its molar mass, and the interaction parameter of the hydrophobic block with water [49]. The change in the hydrophilic weight fraction (f) affects the hydrophobic interactions and the size of the self-organized system, therefore micelles are mainly formed at the hydrophilic weight fraction (f) of 45–70% [53]. Here, the average degree of polymerization of KPC units was aimed to be 15 in order to keep the hydrophilic weight fraction of f_{PEG} at 60%. The ^{1}H NMR spectrum of PEG-PKPC showed the characteristic signals of both: mPEG units at δ = 3.38 and 3.64 ppm and KPC units at δ = 1.42, 3.77 and 4.2 ppm, respectively. The average degree of polymerization of KPC block was calculated to 12, from the NMR spectrum basing on the integration of peaks areas at δ = 3.38 ppm and δ = 4.2 ppm corresponding to the protons of the mPEG methoxy group protons and PKPC methylene main chain signal, respectively. Therefore, the molar mass of diblock copolymer determined by using ^{1}H NMR was $7.6 \cdot 10^3$ g mol^{-1} (f_{PEG} = 68%), and correlates with the number average molar mass determined by SEC. To prepare PEG-PKPC-oPHB triblock copolymer, oligo[R]-3-hydroxybutyrate was firstly synthesized *via* anionically controlled temperature degradation of high molar mass bacterial nPHB. The commercially available nPHB was mixed with NaHCO$_3$ in weight ratio 10:1 and thermally treated in a laboratory single screw extruder to obtain oligomers of nPHB. ^{1}H NMR spectrum of low molar mass nPHB obtained in reactive extrusion degradation shows besides of oPHB polymer chain characteristic signals at δ = 1.28 (CH$_3$), 2.5 (CH$_2$) and 5.25 (CH) ppm and also signals corresponding to crotonate end group: CH$_3$ at 1.86 ppm and peaks at δ = 5.8 and 6.95 ppm assigned respectively to the CH$_3$-CH = and = CH-C(O)- protons of crotonate end group. The average molar mass of oPHB was determined to be 1000 g mol^{-1}. SEC measurements revealed that obtained polymer has a Mn = 1000 g mol^{-1} with an acceptable level of dispersity ($Đ$ = 1.8) confirming controlled manner of degradation. Prepared oPHB was further reacted with PEG-PKPC to obtain PEG-PKPC-oPHB triblock copolymer, wherein oPHB carboxylic end group was esterified with hydroxyl end group from PEG-PKPC. The ability to obtain quantitative esterification of PEG-PKPC with oPHB was studied in presence of DCC/DMAP as typical catalytic system in Steglich esterification. However, the yield of this reaction was *ca.* 70% after 5 days. Moreover, so long reaction time lead to partial deacetalization reaction. It turned out that the most effective method to quantitative esterification is application of oPHB in the form of its acyl chloride (α-crotonate-ω-acyl chloride-oPHB) in the presence of triethylamine excess. The structure of PEG-PKPC-oPHB triblock copolymer was verified by ^{1}H NMR as shown in Fig. 1. All of the main characteristic peaks of mPEG units (δ = 3.64 and 3.38 ppm), PKPC units (δ = 1.42, 3.77, 4.2 ppm) and oPHB units (δ = 1.28, 2.5, 5.25 ppm) are clearly detected. Furthermore, the intensity ratio of two different end groups, at δ = 1.86 ppm corresponding to crotonate CH$_3$ protons and δ = 3.38 ppm from CH$_3$-O-PEG was close to 1:1 (1:0.98, Fig. S3) which might indicate the successful quantitative conjugation of PEG-KPC with oPHB. It is worth mentioning that low intensity peak at δ = 2.18 ppm in ^{1}H NMR of crude post reaction mixture was ascribed to the protons of acetone, which is the result of the deketalization reaction that is proceeding during conjugation. However, quantitative assessment based on ^{1}H NMR revealed that only less than 5% of acetal groups has been hydrolyzed. Moreover, the SEC analysis proves the triblock copolymer formation (Fig. S4; Table 1).

3.2. Preparation and characterization of micelles

The synthesized amphiphilic copolymers tend to self-organize into core-shell micelles in aqueous solution. The hydrophobic copolymer chain blocks self-assemble to form the core of the micelle, while the outward shell consists of hydrophilic PEG. The structure of PEG-PKPC and PEG-PKPC-oPHB micelles were determined by ^{1}H NMR spectroscopy (Fig. S5). ^{1}H NMR spectrum of PEG-PKPC-oPHB after micellization shows that the peaks corresponding to polycarbonate block are

Table 1
Characteristics of copolymers.

Copolymer[a]	Mn,$_{NMR}$[b,c] [g mol^{-1}]	Mn,$_{SEC}$ [g mol^{-1}]	$Đ$	f_{PEG}[d] [%]	CMC [mg mL^{-1}]
PEG-PKCP	7600	7300	1.42	68	0.0056
PEG-PKCP-oPHB	8500	8300	1.57	61	0.0027

[a] mPEG block had Mn = 5200 and $Đ$ = 1.24, (determined by SEC).
[b] Estimated form ^{1}H NMR from equation: Mn$_{NMR\ PEG-PKPC}$ = Mn $_{PEG}$ + [I (PKPC) CH$_2$/(ImPEGCH$_3$-O/3)]/4 · 202, where 202 is molar mass of KPC repeating unit.
[c] Mn $_{NMR\ PEG-PKPC-oPHB}$ = Mn $_{NMR\ PEG-PKPC}$ + Mn $_{NMR\ oPHB}$ = Mn $_{PEG}$ + [I (PKPC) CH$_2$/(ImPEGCH$_3$-O/3)]/4 · 202 + [Ipolym (oPHB) CH/(ImPEGCH$_3$-O/3)] · 86, where 86 is molar mass of HB repeating unit.
[d] f_{PEG} content in copolymer.

barely visible and the oligo-3-hydroxybutyrate peaks are not detected. Furthermore, peaks corresponding to the PEG chains are clearly visible after self-assembly. These results showed that hydrophobic PKPC-oPHB blocks are located in the core after micellization to limit their interaction with the aqueous media. Moreover, oPHB is the block that forms the central core of the micelle, while the hydrophilic PEG chains are located outside in a mobile state. Similar results were observed for PEG-PKPC micelles (Fig. S5).

The critical micelle concentration (CMC) of synthesized copolymers were determined using pyrene as a fluorescence probe and calculated from the plot of the excitation intensity ratio as a function of the copolymer concentration (Fig. S6). The CMC value of micelles intended for controlled release of drugs is a crucial parameter to determine the stability of micelles. Hence, the lowering CMC value is highly desired for increasing stability of the micelles in the *in vivo* bloodstream. The calculated value of the CMC for the PEG-PKPC-oPHB was 0.0027 mg ml^{-1} and it was twice lower than that of PEG-PKPC which was 0.0056 mg mL^{-1} (Table 1). This phenomenon is the effect of the addition of the highly hydrophobic oPHB, which significantly increases the hydrophobic interactions in the core of micelles.

The obtained micelles were characterized by DLS and cryo-TEM. The DLS results for blank micelles showed that the average size of PEG-PKPC and PEG-PKPC-oPHB micelles were 19.3 nm and 25.5 nm with a narrow size distribution of 0.14 and 0.16, respectively. This results indicated that the incorporation of short and highly hydrophobic oPHB as core-forming block does not substantially affect the hydrodynamic size and polydispersity index (PDI) of obtained micelles (Table 2). The drug-loaded micelles were also analyzed by DLS. Obtained results revealed that the average size of 8HQ-Glu-loaded PEG-PKPC micelles was increased to 27.7 nm, and for the PEG-PKPC-oPHB, the average size was also increased to 30 nm. These results indicate that the drug loading did not substantially affect the size of micelles, however, it affects the polydispersity index, which increased from 0.14 and 0.16 to 0.23 and 0.22 for PEG-PKPC and PEG-PKPC-oPHB respectively (see supplementary Fig. S7). The morphology of the micelles was also studied by cryo-TEM. The images presented in Fig. 2, showed the obtained micelles had a spherical structure and the approximate size of the micelles with homogeneous size distribution corresponds to the one determined in DLS measurements.

3.3. Stability and acid-triggered degradation of micelles

The stability and size changes of the PEG-PKPC and PEG-PKPC-oPHB micelles were studied by DLS as a function of exposure time in PBS buffers (pH 7.4, 6.4 and 5.5) at 37 °C as shown in Fig. 3. It can be seen that the size of the PEG-PKPC micelles was substantially unchanged and was about 25 nm after 8 h of incubation in PBS at pH 7.4. However, after 24 h PEG-PKPC micelles tend to increase the size and after 72 h micelles are disintegrating. These results may be attributed to

Table 2
Characterization of blank and drug-loaded micelles.

Copolymer	Blank micelle		8HQ-Glu-/8HQ-Gal-loaded micelle				DOX-loaded micelle			
	Size [nm]	PDI	Size[a] [nm]	PDI[a]	DLE [%]	DLC [%]	Size [nm]	PDI	DLE [%]	DLC [%]
PEG-PKPC	19.3 ± 0.6	0.14 ± 0.03	27.7 ± 2.1	0.23 ± 0.02	45.1 ± 2.9/43.9 ± 3.3	4.7 ± 0.2/4.6 ± 0.3	36.4 ± 1.9	0.18 ± 0.04	48.2 ± 3.5	5.4 ± 0.3
PEG-PKPC-oPHB	25.5 ± 1.1	0.16 ± 0.02	30.0 ± 2.8	0.22 ± 0.02	49.0 ± 4.1/48.4 ± 3.0	5.2 ± 0.2/5.2 ± 0.2	37.6 ± 3.7	0.21 ± 0.03	53.8 ± 4.4	6.0 ± 0.3

[a] Size and PDI was determined for 8HQ-Glu-loaded micelles; Data are presented as the mean ± standard deviation (n = 3).

the spontaneous hydrolysis of ketal groups resulting in formation of two hydroxyl groups, as their presence increasing the hydrophilicity of micelle core (according to [62], polycarbonate functionalized with two hydroxyl groups is highly hydrophilic but not water-soluble). The formation of carbonate units with hydroxyl groups causes the micelles to become unstable and the process of reorganization with the formation of large aggregates is observed. PEG-PKPC-oPHB micelles size at pH 7.4 remained nearly unchanged up to 24 h, then after 48 h micelles start to reorganize. In more acidic buffer (pH 6.4), it was observed that PEG-PKPC micelles swell immediately and after 4 h start to form large aggregates. At pH 5.5 PEG-PKPC micelles swell and become unstable much faster than in buffers with pH 7.4 and 6.4 respectively. Their complete disintegration can be observed after 8 h at pH 5.5, which is due to the accelerated hydrolysis of ketal groups in an acidic environment. However, micelles containing oPHB block as core-forming units are relatively more stable. In a slightly acidic environment, at pH 6.4, micelles rapidly swell and as a result of reorganization begin to form larger aggregates after 24 h. Equally, at pH 5.5 PEG-PKPC-oPHB micelles swell instantly and form larger aggregates after 8 h. These results establish that the addition of biodegradable highly hydrophobic oligo [R]-3-hydroxybutyrate block as core-forming unit increasing the stability of prepared micelles at all pH values studied.

3.4. Drug loading and in vitro release studies

The drug-loading and release properties of micelles were studied using the UV–Vis spectroscopy. Hydrophobic drugs: DOX, 8HQ-Glu and 8HQ-Gal were successfully loaded into micelles, where the feed drug ratio to copolymer was 1/10. The drug-loading properties (drug loading content - DLC) and (drug loading efficiency - DLE) were determined using equations presented in experimental part. The DLC and DLE of 8HQ-Glu-loaded PEG-PKPC micelles were 45.1% and 4.7%, while the values for DOX-loaded PEG-PKPC micelles were 48.2% and 5.4%. At the same feed drug dose, DLC and DLE for PEG-PKPC-oPHB micelles loaded with 8HQ-Glu were 49% and 5.2% and with DOX-loading 53.8% and 6%, respectively. No significant differences in loading properties were observed between 8HQ-Glu and 8HQ-Gal which is related to the slight difference in chemical structure. PEG-PKPC-oPHB micelles showed higher DLC than PEG-PKPC counterparts, due to a stronger interaction between hydrophobic drugs with longer hydrophobic segments. In general, increasing the length of the hydrophobic copolymer block leads to an increase in the content of the encapsulated drug. However, a slight increase in DLE and DLC in the investigated triblock copolymer micelles can be attributed to the presence of PHB in the copolymer structure, since the crystallinity of the blocks forming the micelles core does not favor drug loading [70,71]. The in vitro drug release profiles of drug-loaded micelles were carried out in PBS buffer solutions at different pH, i.e. 7.4, 6.4 and 5.5 respectively (Fig. 4).

The results indicate that at the pH 7.4 both studied micelles (diblock and triblock) displayed a slow and sustained drug release and fairly similar amount of drug i.e. after 72 h, 41% were released from PEG-PKPC micelles and 46% from PEG-PKPC-oPHB micelles. Under a mild acidic environment (pH 6.4) the much faster drug release was observed. In fact, 67% and 60% drug release were observed for PEG-PKPC and PEG-PKPC-oPHB in 24 h. The complete release of drug from PEG-PKPC micelles was observed after 72 h, while 82% of encapsulated drug was released after the same time from PEG-PKPC-oPHB micelles. Results obtained in buffer with pH 5.5 showed that the drug was released fastest. The release profile of the drug showed that 66% and 53% of the drug were released within 8 h and 85% and 77% after 24 h from PEG-PKPC and PEG-PKPC-oPHB micelles, respectively. For comparison, less than 33% and 32% of drug were released at pH 7.4 after 24 h. As a reference, the free drug release was also studied. The cumulative release of free drug showed a release of 82% within 8 h independently of buffer pH. The above results indicate that encapsulated drug release was faster under acidic environment as a result of accelerated acid
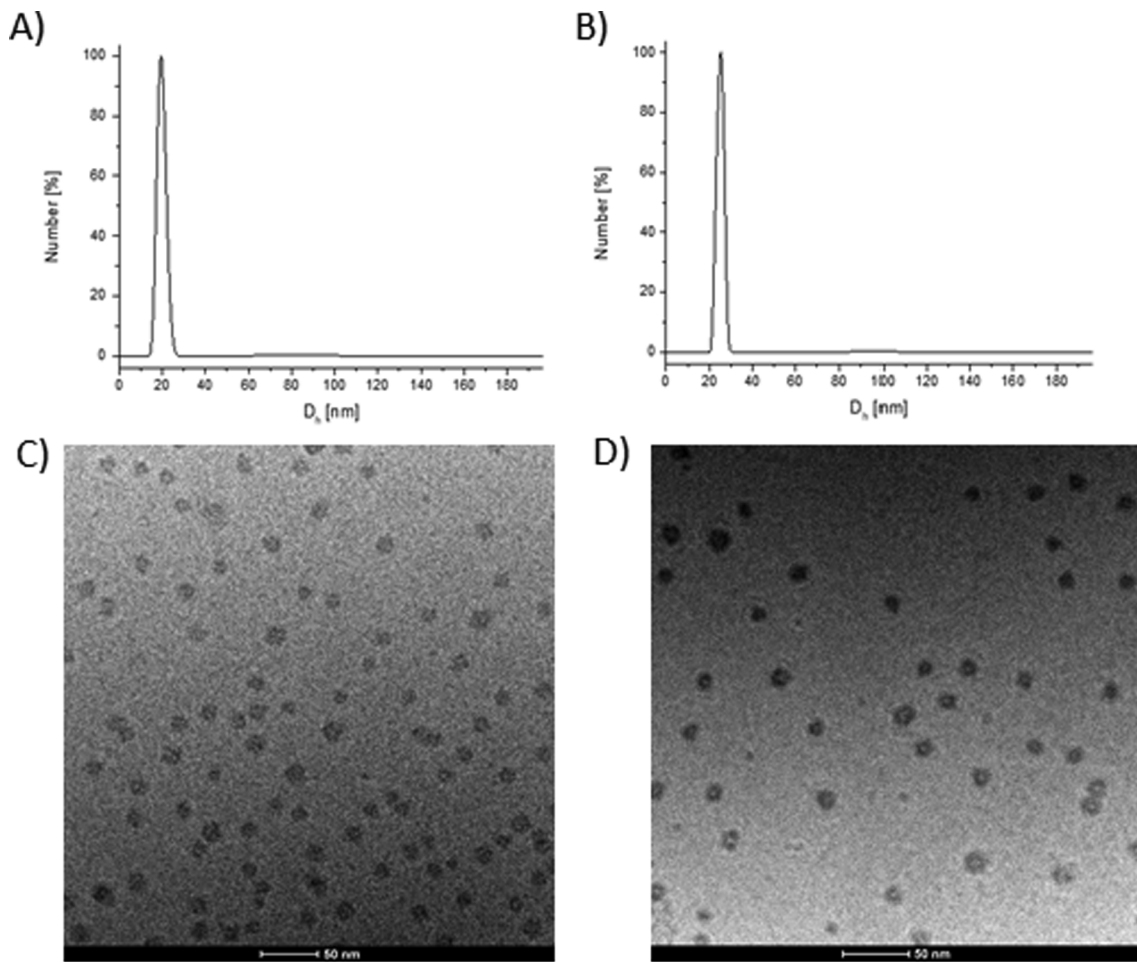
Fig. 2. The size distribution and cryo-TEM images of PEG-PKPC (A and C) and PEG-PKPC-oPHB (B and D) micelles.
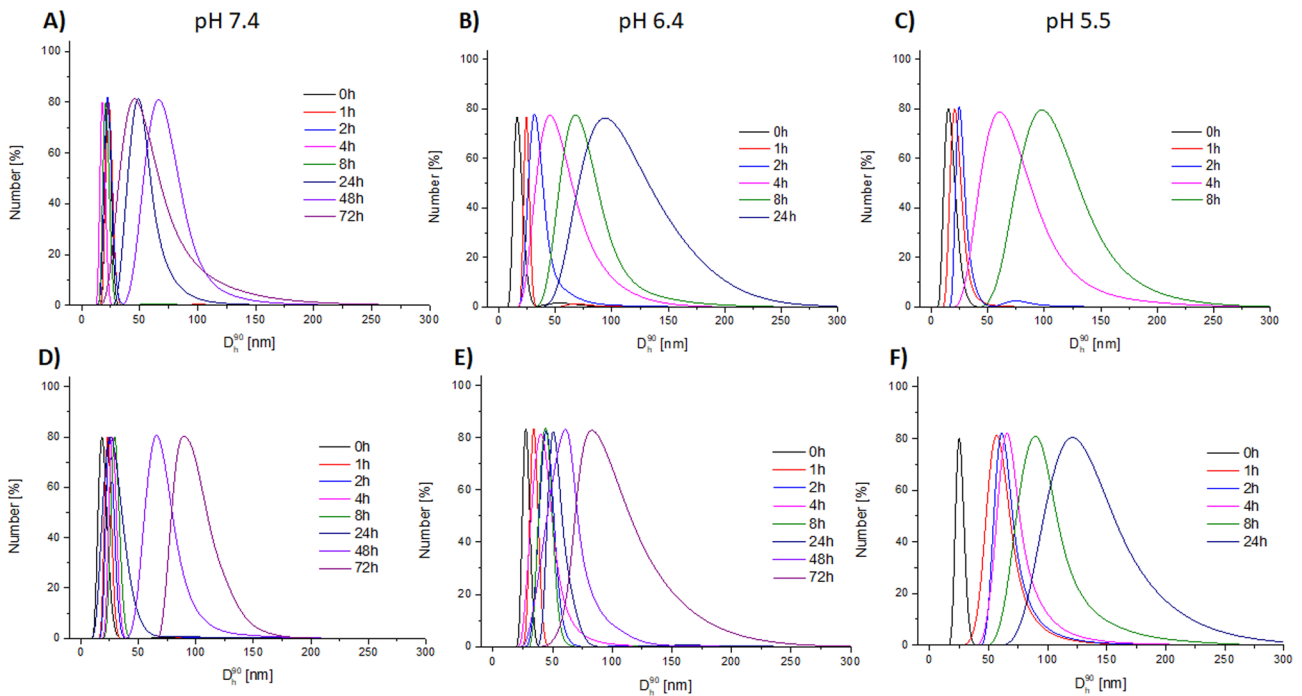
Fig. 3. Change in hydrodynamic diameter (*d*, nm) of PEG-PKPC (A–C) and PEG-PKPC-oPHB (D–F) micelles in PBS buffers at different pH monitored by DLS.
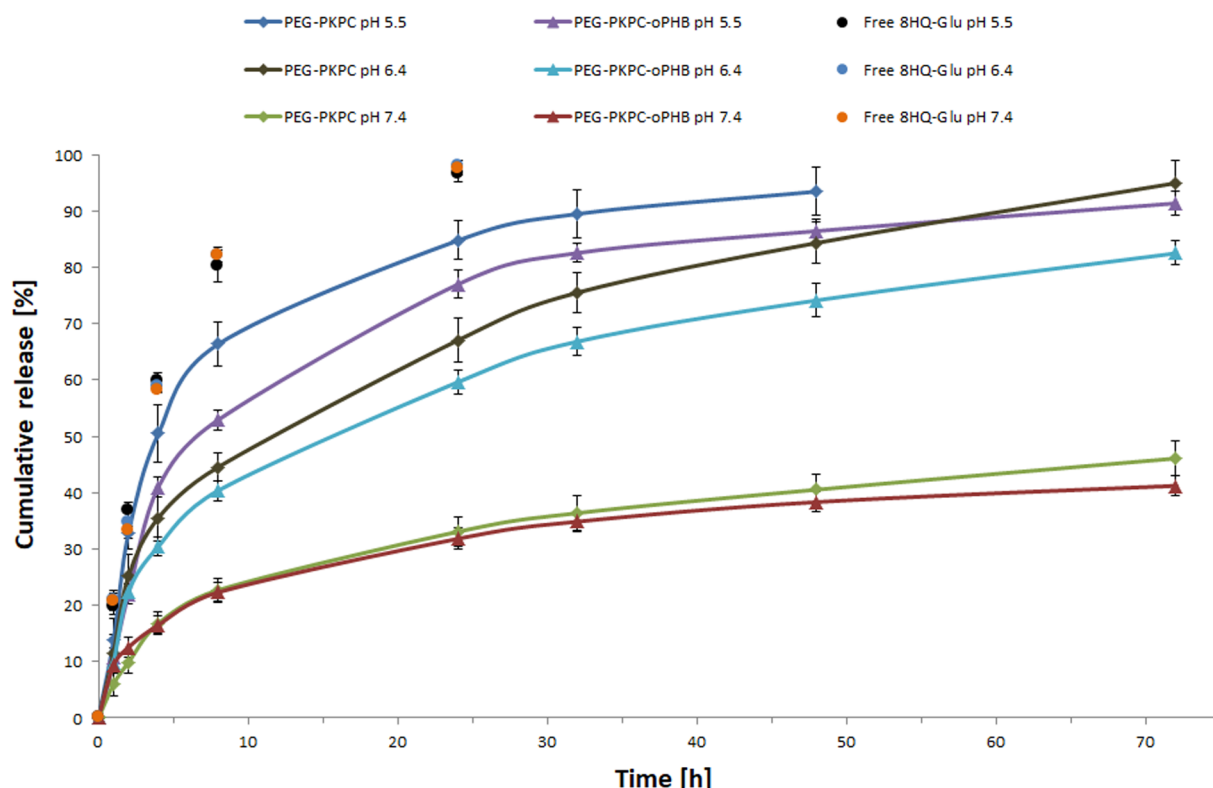
Fig. 4. pH-dependent drug release profiles for free 8HQ-Glu, PEG-PKPC and PEG-PKPC-oPHB micelles in PBS buffers at 37 °C. Data are presented as the mean ± standard deviation (n = 3).

hydrolysis of ketal groups. The addition of oPHB as core-forming segment increased stability and resulted in prolonged drug release. The results correlate with earlier DLS micelles behavior measurements.

3.5. Cytotoxicity of blank and drug-loaded micelles

The cytotoxic activity *in vitro* of PEG-PKPC-oPHB blank micelles, free drugs (DOX, 8HQ-Glu, 8HQ-Gal) and drug-loaded micelles was determined by MTT assay. Tests were conducted on cell lines: HCT-116 (colorectal carcinoma cell line) and MCF-7 (human breast adenocarcinoma cell line). In these cell lines, a slightly acidic microenvironment was observed [85]. The selectivity of compounds was tested on Normal Human Dermal Fibroblasts-Neonatal (NHDF-Neo). The use of micelles as the carriers should facilitate the transport of drugs and their release only directly into cancer tissues. Cells were incubated with the appropriate compounds for 24, 48 and 72 h in a concentration range oscillating within the IC$_{50}$ activity of the above-mentioned drugs.

In the beginning, the effect of blank micelles on cell viability was assessed (Fig. 5.). Free micelles were analyzed at concentrations corresponding to drug-loaded micelles. It turned out, that even the highest dose used was not toxic to the tested cell lines. The proliferation of cells

incubated with free micelles was maintained above 90% for 72 h of the experiment, which indicates that the PEG-PKPC-oPHB micelles are biocompatible with tested healthy cells NHDF-Neo and cancer cell lines MCF-7 or HCT-116.

The relationship between cell proliferation and the concentration of free drugs and drug-loaded micelles is shown in Fig. 6 for DOX as a model drug commonly used for the studies of tumor-targeting drug delivery systems, while Figs. 7 and 8 for 8HQ-Gal and 8HQ-Glu used as model glycoconjugate, respectively. All compounds showed dose-dependent inhibition of cell proliferation. Some deviations between the effects of individual compounds were observed. This phenomenon is probably related to the different mechanisms of action of compounds released near the cancer cells. Doxorubicin is a commonly used cytostatic in cancer therapies. However, its use is limited due to its non-selectivity and numerous side effects, especially cardiotoxicity [86]. It was decided to use the above-mentioned nanocarriers to improve the selectivity of its action, through targeted delivery to tumor cells. As shown in Fig. 6, free DOX has a strong cytotoxic effect on the MCF-7 and HCT-116 cell lines after 24, 48 and 72 h incubation. During the incubation of cancer cells with drugs, DOX-loaded micelles showed comparable cytotoxicity to the cells tested, as free drug. Interestingly, at
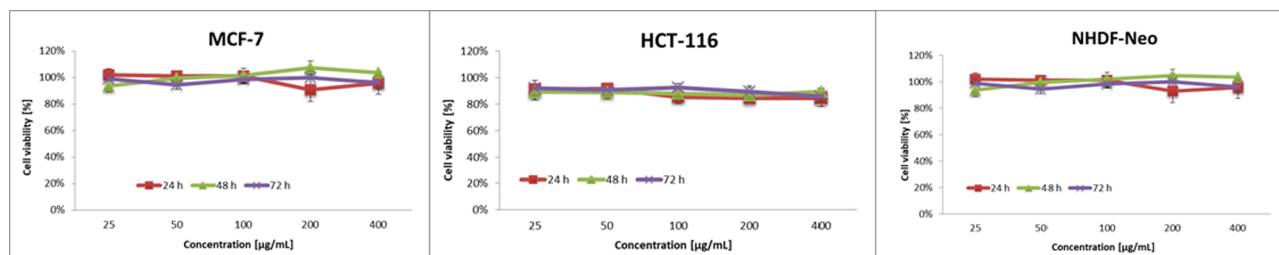
Fig. 5. Cytotoxicity of blank micelles (PEG-PKPC-oPHB) on cells: (a) MCF-7, (b) HCT-116, (c) NHDF-Neo. Data are presented as the mean ± standard deviation (n = 3).
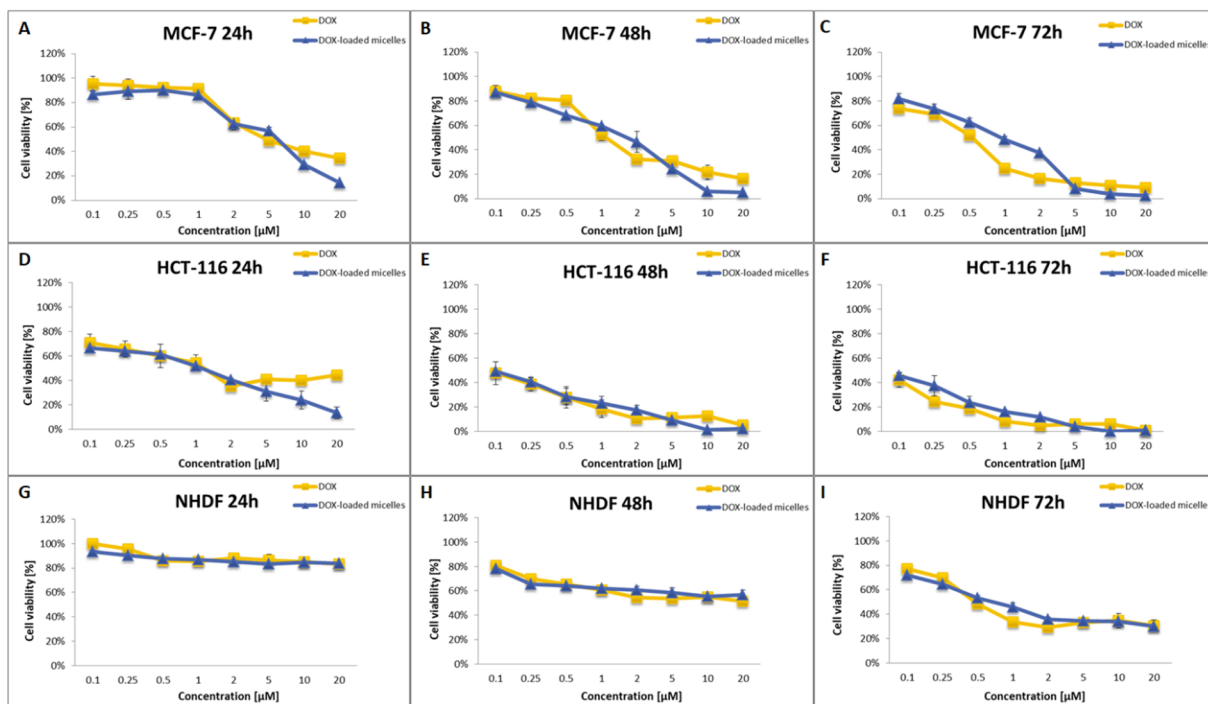
Fig. 6. The cell viability of free DOX and DOX-loaded micelles for MCF-7, HCT-116 and NHDF-Neo cells after 24 h (A, D, G, respectively), 48 h (B, E, H, respectively) and 72 h (C, F, I, respectively). Data are presented as the mean ± standard deviation (n = 3).

a concentration above 5 μM, the cytotoxic activity of drug-loaded micelles was higher compared to free DOX. Importantly, this effect was not seen in case of healthy cells. At higher doses of the drug DOX-loaded micelles showed increased antitumor activity while maintaining unchanged, relative to the free DOX, toxicity to healthy cells.

MTT tests showed a higher ability to inhibit cell proliferation by glycoconjugates-loaded micelles compared to free prodrugs (Figs. 7 and 8). It can be assumed that the use of micelles facilitates active transport

of the glycoconjugate directly into the cancer cell, thereby increasing the accumulation of the drug in the cancer cells and its effectiveness. The lower cytotoxic activity of free glycoconjugates is probably due to their hindered penetration into the cell through the phospholipid membranes. Moreover, the toxicity of the free glycoconjugate persists over time, the effect did not increase with increasing incubation time (Table 3). In contrast, the cytotoxicity of glycoconjugate loaded in micelles increases over time. This suggests that this effect is achieved by
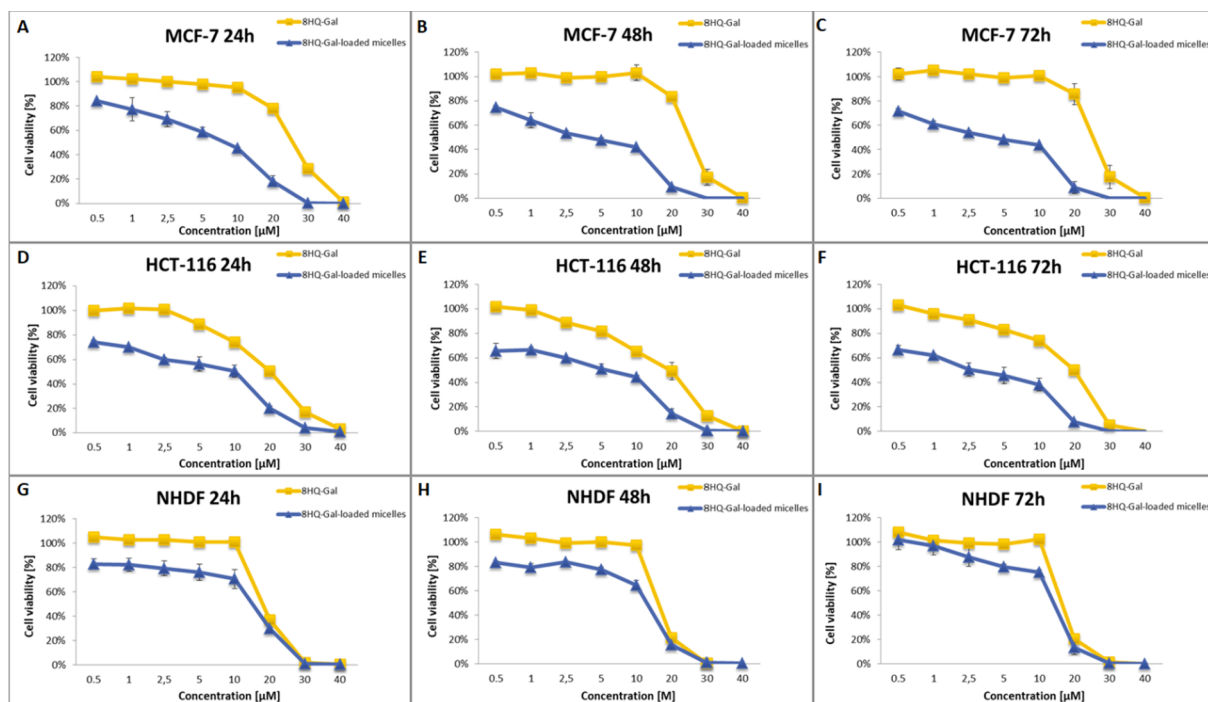
Fig. 7. The cell viability of free 8HQ-Gal and 8HQ-Gal-loaded micelles for MCF-7, HCT-116 and NHDF-Neo cells after 24 h (A, D, G, respectively), 48 h (B, E, H, respectively) and 72 h (C, F, I, respectively). Data are presented as the mean ± standard deviation (n = 3).
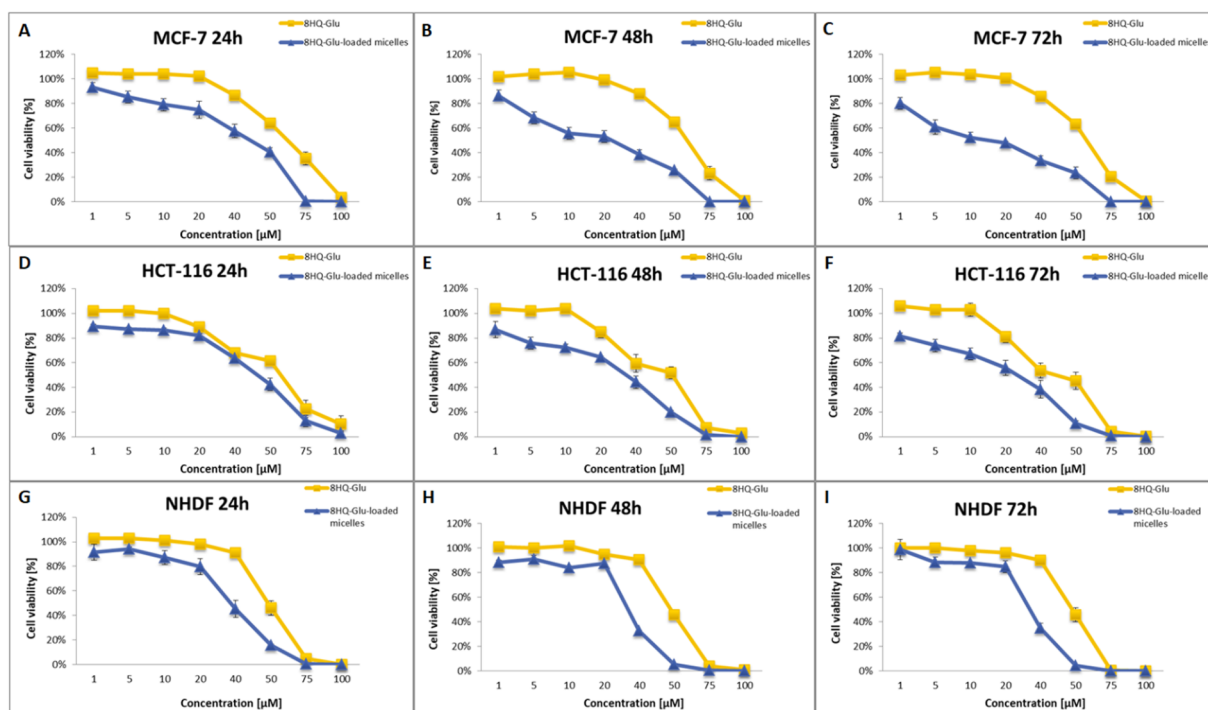
Fig. 8. The cell viability of free 8HQ-Glu and 8HQ-Glu loaded micelles for MCF-7, HCT-116 and NHDF-Neo cells after 24 h (A, D, G, respectively), 48 h (B, E, H, respectively) and 72 h (C, F, I, respectively). Data are presented as the mean ± standard deviation (n = 3).

Table 3

Screening of cytotoxicity of tested compounds against MCF-7, HCT-116 and NHDF-Neo cells for 24, 48 and 72 h incubation time.

Compound	Activity IC$_{50}$ [µM][a] MCF-7		
	24 h	48 h	72 h
DOX	5.19 ± 0.09	1.65 ± 0.04	0.52 ± 0.01
DOX-micelles	5.86 ± 0.12	1.07 ± 0.05	0.68 ± 0.01
8HQ-Glu	58.73 ± 2.53	56.93 ± 2.68	56.17 ± 3.10
8HQ-Glu-mic[b]	45.09 ± 2.32	23.09 ± 0.95	13.48 ± 0.52
8HQ-Gal	25.28 ± 1.08	24.58 ± 1.23	24.86 ± 1.09
8HQ-Gal-mic[c]	5.38 ± 0.03	2.69 ± 0.01	2.50 ± 0.01

Compound	Activity IC$_{50}$ [µM][a] HCT-116		
	24 h	48 h	72 h
DOX	1.85 ± 0.04	0.098 ± 0.01	0.102 ± 0.01
DOX-micelles	1.12 ± 0.02	0.072 ± 0.01	0.089 ± 0.01
8HQ-Glu	61.70 ± 2.84	53.94 ± 3.37	43.77 ± 2.51
8HQ-Glu-mic[b]	46.24 ± 1.38	33.05 ± 0.89	25.62 ± 1.02
8HQ-Gal	20.07 ± 0.52	19.86 ± 0.65	20.03 ± 0.20
8HQ-Gal-mic[c]	10.10 ± 0.11	5.62 ± 0.25	2.60 ± 0.09

Compound	Activity IC$_{50}$ [µM][a] NHDF-Neo		
	24 h	48 h	72 h
DOX	> 20	> 20	0.49 ± 0.01
DOX-micelles	> 20	> 20	0.62 ± 0.01
8HQ-Glu	47.27 ± 1.38	48.40 ± 1.09	48.98 ± 0.96
8HQ-Glu-mic[b]	32.45 ± 0.55	30.55 ± 0.98	29.82 ± 1.12
8HQ-Gal	19.26 ± 0.21	16.58 ± 0.25	18.29 ± 0.85
8HQ-Gal-mic[c]	14.24 ± 1.02	11.96 ± 0.62	12.90 ± 0.55

[a] Cytotoxicity was evaluated using the MTT assay.
[b] 8HQ-Glu-loaded micelles.
[c] 8HQ-Gal-loaded micelles. Data are presented as the mean ± standard deviation (n = 3).

transporting the glycoconjugate into the cells and their extended-release. Glycoconjugate-loaded micelles achieve significantly lower IC$_{50}$ values than free glycoconjugates (Table 3). For example, for galacto-conjugate, the dose resulting 50% cell growth inhibition compared to the untreated control (IC$_{50}$ activity) was calculated to be 24.86 ± 1.09 µM for MCF-7 and 20.03 ± 0.20 µM for HCT-116 after 72 h incubation. While the encapsulation of the drug in micelles allowed to reduce this activity to 2.50 ± 0.01 µM for MCF-7 and 2.60 ± 0.09 µM for HCT-116, respectively. Therefore, the use of pH-sensitive micelles allows the application of a much smaller dose of the drug to kill the same amount of cancer cells as free drug. By using this drug delivery system, the therapeutic dose of the drug can be significantly reduced, thereby reducing its side effects.

4. Conclusions

In this study, biodegradable and biocompatible pH-responsive amphiphilic poly(ethylene glycol)-b-polycarbonate-b-oligo([R]-3-hydroxybutyrate) was synthesized by PEG/organocatalyst initiated ring-opening polymerization of acetal-functionalized six-membered cyclic carbonate and subsequent esterification with bacterial oPHB. The chemical structure of the copolymer was confirmed by both ^{1}H NMR and SEC. Synthesized amphiphilic copolymers self-organize into a core-shell structure spherical micelle with an average hydrodynamic diameter of 20–30 nm. Acid-triggered hydrolysis of the acetal group to two hydroxyl groups increases the hydrophilicity of the hydrophobic micelles core, causing swelling of the micelles and the release of encapsulated therapeutic agents. Addition of hydrophobic bacterial oligo([R]-3-hydroxybutyrate) as core-forming block significantly increases the stability of micelles, whereby micelles gain additional advantages such as enhanced stability against dilution, prolonged circulation time and drug release. An anti-cancer DOX, 8HQ-Glu, and 8HQ-Gal were encapsulated into micelles, to improve the metabolic stability and delivery of glycoconjugated prodrugs in cancer cells for efficient tumor therapy. MTT assay results show that the blank micelles were non-toxic to the tested cell lines, while the therapeutics-loaded micelles showed noticeable anticancer efficacy and confirmed the pH-dependent, controlled release

of drugs from micelles. This can significantly reduce the systemic toxicity of the anticancer drugs used and it also confirms that the obtained pH-responsive micelles can be used as non-toxic tumor-targeting drug carriers for chemotherapy. Furthermore, glycoconjugates-loaded micelles showed a significantly increased ability to inhibit the proliferation of cancer cells compared to free glycoconjugates. This is due to enhanced uptake and pH-triggered release of prodrugs, while free glycoconjugates only showed passive diffusion through the lipid barriers of cancer cells. The glycoconjugation of anti-cancer drugs and pH-responsive nanocarriers have separately shown great potential to increase the tumor targeted drug delivery efficiency. The combination of drug glycoconjugation and the use of pH-responsive micelles opens up new possibilities to develop novel strategies for efficient tumor therapy.

Declaration of Competing Interest

The authors declare that they have no known competing financial interests or personal relationships that could have appeared to influence the work reported in this paper.

Acknowledgments

Appendix A. Supplementary material

Supplementary data to this article can be found online at https://doi.org/10.1016/j.ejpb.2020.07.019.

References

[1] R.L. Siegel, K.D. Miller, A. Jemal, Cancer Statistics, 2019, CA Cancer J. Clin. 69 (2019) 7–34, https://doi.org/10.3322/caac.21551.

[2] R. Krishna, L.D. Mayer, Multidrug resistance (MDR) in cancer Mechanisms, reversal using modulators of MDR and the role of MDR modulators in influencing the pharmacokinetics of anticancer drugs, Eur. J. Pharm. Sci. 11 (4) (2000) 265–283, https://doi.org/10.1016/S0928-0987(00)00114-7.

[3] M. Majidinia, M. Mirza-Aghazadeh-Attari, M. Rahimi, A. Mihanfar, A. Karimian, A. Safa, B. Yousefi, Overcoming multidrug resistance in cancer: Recent progress in nanotechnology and new horizons, IUBMB Life (2020) 1–17, https://doi.org/10.1002/iub.2215.

[4] R.J. DeBerardinis, N.S. Chandel, We need to talk about the Warburg effect, Nat. Metab. 2 (2020) 127–129, https://doi.org/10.1038/s42255-020-0172-2.

[5] P. Vaupel, H. Schmidberger, A. Mayer, The Warburg effect: essential part of metabolic reprogramming and central contributor to cancer progression, Int. J. Radiat. Biol. 95 (7) (2019) 912–919, https://doi.org/10.1080/09553002.2019.1589653.

[6] R. Cairns, I. Harris, T. Mak, Regulation of cancer cell metabolism, Nat. Rev. Cancer 11 (2011) 85–95, https://doi.org/10.1038/nrc2981.

[7] S. Schuster, D. Boley, P. Möller, H. Stark, C. Kaleta, Mathematical models for explaining the Warburg effect: a review focused on ATP and biomass production, Biochem. Soc. Trans. 43 (6) (2015) 1187–1194, https://doi.org/10.1042/BST20150153.

[8] O. Warburg, On the origin of cancer cells, Science 123 (3191) (1956) 309–314 https://www.jstor.org/stable/1750066.

[9] J. Lu, M. Tan, Q. Cai, The Warburg effect in tumor progression: mitochondrial oxidative metabolism as an anti-metastasis mechanism, Cancer Letters 356 (2) (2015) 156–164, https://doi.org/10.1016/j.canlet.2014.04.001.

[10] M.G. Vander Heiden, L.C. Cantley, C.B. Thompson, Understanding the Warburg effect: the metabolic requirements of cell proliferation, Science 324 (5930) (2009) 1029–1033, https://doi.org/10.1126/science:1160809.

[11] S.K. Parks, W. Mueller-Klieser, J. Pouysségur, Lactate and acidity in the cancer microenvironment, Annu. Rev. Cancer Biol. 4 (1) (2020) 141–158, https://doi.org/10.1146/annurev-cancerbio-030419-033556.

[12] N.Y. Spencer, R.C. Stanton, The Warburg effect, lactate, and nearly a century of trying to cure cancer, Semin. Nephrol. 39 (4) (2019) 380–393, https://doi.org/10.1016/j.semnephrol.2019.04.007.

[13] C.C. Barron, P.J. Bilan, T. Tsakiridis, E. Tsiani, Facilitative glucose transporters: implications for cancer detection, prognosis and treatment, Metabolism 65 (2016) 124–139, https://doi.org/10.1016/j.metabol.2015.10.007.

[14] L. Szablewski, Expression of glucose transporters in cancers, Biochim. Biophys. Acta 1835 (2) (2013) 164–169, https://doi.org/10.1016/j.bbcan.2012.12.004.

[15] Y. Kato, S. Ozawa, C. Miyamoto, Y. Maehata, A. Suzuki, T. Maeda, Y. Baba, Acidic extracellular microenvironment and cancer, Cancer Cell Int. 13 (2013) 89, https://doi.org/10.1186/1475-2867-13-89.

[16] C. Roma-Rodrigues, R. Mendes, P.V. Baptista, A.R. Fernandes, Targeting tumor microenvironment for cancer therapy, Int. J. Mol. Sci. 20 (4) (2019) 840, https://doi.org/10.3390/ijms20040840.

[17] B. Bhattacharya, M.F. Mohd Omar, R. Soong, The Warburg effect and drug resistance: the Warburg effect and drug resistance, British J. Pharmacol. 173 (6) (2016) 970–979, https://doi.org/10.1111/bph.v173.610.1111/bph.13422.

[18] A. Glenister, M.I. Simone, T.W. Hambley, A Warburg effect targeting vector designed to increase the uptake of compounds by cancer cells demonstrates glucose and hypoxia dependent uptake, PLoS ONE 14 (7) (2019) e0217712, , https://doi.org/10.1371/journal.pone.0217712.

[19] L. Schwartz, T. Seyfried, K.O. Alfarouk, J. Da Veiga Moreira, S. Fais, Out of Warburg effect: an effective cancer treatment targeting the tumor specific metabolism and dysregulated pH, Semin. Cancer Biol. 43 (2017) 134–138, https://doi.org/10.1016/j.semcancer.2017.01.005.

[20] C. Roma-Rodrigues, I. Pombo, L. Raposo, P. Pedrosa, A.R. Fernandes, P.V. Baptista, Nanotheranostics targeting the tumor microenvironment, Front. Bioeng. Biotechnol. 7 (2019) 197, https://doi.org/10.3389/fbioe.2019.00197.

[21] C. Granchi, F. Minutolo, Anti-cancer agents counteracting tumor glycolysis, Chem. Med. Chem. 7 (2012) 1318–1350, https://doi.org/10.1002/cmdc.201200176.

[22] C. Reily, T.J. Stewart, M.B. Renfrow, J. Nowak, Glycosylation in health and disease, Nat. Rev. Nephrol. 15 (2019) 346–366, https://doi.org/10.1038/s41581-019-0129-4.

[23] E.C. Calvaresi, P.J. Hergenrother, Glucose conjugation for the specific targeting and treatment of cancer, Chem. Sci. 4 (2013) 2319–2333, https://doi.org/10.1039/C3SC22205E.

[24] R.K. Tekade, X. Sun, The Warburg effect and glucose-derived cancer theranostics, Drug Discov. Today 22 (11) (2017) 1637–1653, https://doi.org/10.1016/j.drudis.2017.08.003.

[25] V. Oliveri, M. Viale, C. Aiello, G. Vecchio, New 8-hydroxyquinoline Galactosides. The role of the sugar in the antiproliferative activity of copper(II) ionophores, J. Inorg. Biochem. 142 (2015) 101–108, https://doi.org/10.1016/j.jinorgbio.2014.09.017.

[26] D. Lacombe, Glufosfamide: can we improve the process of anticancer agent development? Expert Opin. Investig. Drugs 21 (5) (2012) 749–754, https://doi.org/10.1517/13543784.2012.670218.

[27] M.E. Cucciolito, F. De Luca Bossa, R. Esposito, G. Ferraro, A. Iadonisi, G. Petruk, L. D'Elia, C. Romanetti, S. Traboni, A. Tuzi, D.M. Monti, A. Merlino, F. Ruffo, C-Glycosylation in platinum-based agents: a viable strategy to improve cytotoxicity and selectivity, Inorg. Chem. Front. 5 (2018) 2921–2933, https://doi.org/10.1039/C8QI00664D.

[28] Y.-S. Lin, R. Tungpradit, S. Sinchaikul, F.-M. An, D.-Z. Liu, S. Phutrakul, S.-T. Chen, Targeting the delivery of glycan-based paclitaxel prodrugs to cancer cells via glucose transporters, J. Med. Chem. 51 (23) (2008) 7428–7441, https://doi.org/10.1021/jm8006257.

[29] C. Granchi, S. Fortunato, F. Minutolo, Anticancer agents interacting with membrane glucose transporters, Med. Chem. Commun. 7 (2016) 1716–1729, https://doi.org/10.1039/C6MD00287K.

[30] S. Makuch, M. Woźniak, M. Krawczyk, G. Pastuch-Gawołek, W. Szeja, S. Agrawal, Glycoconjugation as a promising treatment strategy for psoriasis, JPET 373 (2) (2020) 204–212, https://doi.org/10.1124/jpet.119.263657.

[31] G. Pastuch-Gawołek, K. Malarz, A. Mrozek-Wilczkiewicz, M. Musioł, M. Serda, B. Czaplińska, R. Musioł, Small molecule glycoconjugates with anticancer activity, Eur. J. Med. Chem. 112 (2016) 130–144, https://doi.org/10.1016/j.ejmech.2016.01.061.

[32] F.-Q. Zhao, A.F. Keating, Functional properties and genomics of glucose transporters, Curr. Genom. 8 (2) (2007) 113–128, https://doi.org/10.2174/138920207780368187.

[33] M. Junttila, F. de Sauvage, Influence of tumour micro-environment heterogeneity on therapeutic response, Nature 501 (2013) 346–354, https://doi.org/10.1038/nature12626.

[34] J. Hu, J. He, M. Zhang, P. Ni, Precise modular synthesis and a structure–property study of acid-cleavable star-block copolymers for pH-triggered drug delivery, Polym. Chem. 6 (2015) 1553–1566, https://doi.org/10.1039/C4PY01391C.

[35] L. Yu, C. Lin, Z. Zheng, Z. Li, X. Wang, Self-assembly of pH-responsive biodegradable mixed micelles based on anionic and cationic polycarbonates for doxorubicin delivery, Colloids Surf. B 145 (2016) 392–400, https://doi.org/10.1016/j.colsurfb.2016.05.029.

[36] S. Thakkar, D. Sharma, K. Kalia, R.K. Tekade, Tumor microenvironment targeted nanotherapeutics for cancer therapy and diagnosis: a review, Acta Biomater. 101 (2020) 43–68, https://doi.org/10.1016/j.actbio.2019.09.009.

[37] L. Feng, Z. Dong, D. Tao, Y. Zhang, Z. Liu, The acidic tumor microenvironment: a target for smart cancer nanotheranostics, Nat. Sci. Rev. 5 (2) (2018) 269–286, https://doi.org/10.1093/nsr/nwx062.

[38] J. Du, L.A. Lane, S. Nie, Stimuli-responsive nanoparticles for targeting the tumor microenvironment, J. Control. Release 219 (2015) 205–214, https://doi.org/10.1016/j.jconrel.2015.08.050.

[39] X. Pang, Y. Jiang, Q. Xiao, A.W. Leung, H. Hua, C. Xu, pH-responsive polymer–drug conjugates: design and progress, J. Control. Release 222 (2016) 116–129, https://doi.org/10.1016/j.jconrel.2015.12.024.

[40] X. He, J. Li, S. An, C. Jiang, pH-sensitive drug-delivery systems for tumor targeting, Ther. Deliv. 4 (12) (2013) 1499–1510, https://doi.org/10.4155/tde.13.120.

[41] S.J. Sonawane, R.S. Kalhapure, T. Govender, Hydrazone linkages in pH responsive drug delivery systems, Eur. J. Pharm. Sci. 99 (2017) 45–65, https://doi.org/10.1016/j.ejps.2016.12.011.

[42] F. Meng, Y. Zhong, R. Cheng, C. Deng, Z. Zhong, pH-sensitive polymeric nanoparticles for tumor-targeting doxorubicin delivery: concept and recent advances,

Nanomedicine 9 (3) (2014) 487–499, https://doi.org/10.2217/nnm.13.212.

[43] W. Gao, J.M. Chan, O.C. Farokhzad, pH-responsive nanoparticles for drug delivery, Mol. Pharm. 7 (6) (2010) 1913–1920, https://doi.org/10.1021/mp100253e.

[44] N. Deirram, C. Zhang, S.S. Kermaniyan, A.P.R. Johnston, G.K. Such, pH-responsive polymer nanoparticles for drug delivery, Macromol. Rapid Commun. 40 (2019) 1800917, https://doi.org/10.1002/marc.201800917.

[45] M. Kanamala, W.R. Wilson, M. Yang, B.D. Palmer, Z. Wu, Mechanisms and biomaterials in pH-responsive tumour targeted drug delivery: a review, Biomaterials 85 (2016) 152–167, https://doi.org/10.1016/j.biomaterials.2016.01.061.

[46] R. Cheng, F. Meng, C. Deng, Z. Zhong, Bioresponsive polymeric nanotherapeutics for targeted cancer chemotherapy, Nanotoday 10 (5) (2015) 656–670, https://doi.org/10.1016/j.nantod.2015.09.005.

[47] Z. Wang, X. Deng, J. Ding, W. Zhou, X. Zheng, G. Tang, Mechanisms of drug release in pH-sensitive micelles for tumour targeted drug delivery system: a review, Int. J. Pharm. 535 (1–2) (2018) 253–260, https://doi.org/10.1016/j.ijpharm.2017.11.003.

[48] B. Tyler, D. Gullotti, A. Mangraviti, T. Utsuki, H. Brem, Polylactic acid (PLA) controlled delivery carriers for biomedical applications, Adv. Drug Deliv. Rev. 107 (2016) 163–175, https://doi.org/10.1016/j.addr.2016.06.018.

[49] G. Barouti, C.G. Jaffredo, S.M. Guillaume, Advances in drug delivery systems based on synthetic poly(hydroxyalkanoate) (co)polymers, Prog. Polym. Sci. 73 (2017) 1–31, https://doi.org/10.1016/j.progpolymsci.2017.05.002.

[50] P. Grossen, D. Witzigmann, S. Sieber, J. Huwyler, PEG-PCL-based nanomedicines: a biodegradable drug delivery system and its application, J. Control. Release 260 (2017) 46–60, https://doi.org/10.1016/j.jconrel.2017.05.028.

[51] Y. Dai, X. Zhang, Recent development of functional aliphatic polycarbonates in the construction of amphiphilic polymers, Polym. Chem. 8 (2017) 7429–7437, https://doi.org/10.1039/C7PY01815K.

[52] W. Chen, F. Meng, F. Li, S.-J. Ji, Z. Zhong, pH-responsive biodegradable micelles based on acid-labile polycarbonate hydrophobe: synthesis and triggered drug release, Biomacromolecules 10 (7) (2009) 1727–1735, https://doi.org/10.1021/bm900074d.

[53] W. Chen, F. Meng, R. Cheng, Z. Zhong, pH-Sensitive degradable polymersomes for triggered release of anticancer drugs: a comparative study with micelles, J. Control. Release 142 (2010) 40–46, https://doi.org/10.1016/j.jconrel.2009.09.023.

[54] Y. Gu, Y. Zhong, F. Meng, R. Cheng, C. Deng, Z. Zhong, Acetal-linked paclitaxel prodrug micellar nanoparticles as a versatile and potent platform for cancer therapy, Biomacromolecules 14 (8) (2013) 2772–2780, https://doi.org/10.1021/bm400615n.

[55] T. Jiang, Y.-M. Li, Y. Lv, Y.-J. Cheng, F. He, R.-X. Zhuo, Amphiphilic polycarbonate conjugates of doxorubicin with pH-sensitive hydrazone linker for controlled release, Colloid Surf. B 111 (2013) 542–548, https://doi.org/10.1016/j.colsurfb.2013.06.054.

[56] M.N. Ganivada, P. Kumar, P. Kanjilal, H. Dinda, J. Sarma, R. Shunmugam, Polycarbonate based biodegradable copolymers for stimuli responsive targeted drug delivery, Polym. Chem. 7 (2016) 4237–4245, https://doi.org/10.1039/C6PY00615A.

[57] X. Ke, D.J. Coady, C. Yang, A.C. Engler, J.L. Hedrick, Y.Y. Yang, pH-sensitive polycarbonate micelles for enhanced intracellular release of anticancer drugs: a strategy to circumvent multidrug resistance, Polym. Chem. 5 (2014) 2621–2628, https://doi.org/10.1039/C3PY01784B.

[58] Y. Zhang, Y. Xu, C. Wei, C. Sun, B. Yan, J. Hu, W. Lu, One-shot synthesis and solution properties of ROS/pH responsive methoxy poly(ethylene glycol)-b-polycarbonate, Polym. Chem. 10 (2019) 2143–2151, https://doi.org/10.1039/C9PY00060G.

[59] X.-L. Yang, J. Li, W.-X. Wu, Y.-H. Liu, N. Wang, X.-Q. Yu, Preparation of fluorophore-tagged polymeric drug delivery vehicles with multiple biological stimuli-triggered drug release, Mater. Sci. Eng. C 108 (2020) 110358, , https://doi.org/10.1016/j.msec.2019.110358.

[60] Y. Li, K. Xiao, W. Zhu, W. Denga, K.S. Lam, Stimuli-responsive cross-linked micelles for on-demand drug delivery against cancers, Adv. Drug Deliv. Rev. 66 (2014) 58–73, https://doi.org/10.1016/j.addr.2013.09.008.

[61] W. Chen, F. Meng, R. Cheng, C. Deng, J. Feijen, Z. Zhong, Facile construction of dual-bioresponsive biodegradable micelles with superior extracellular stability and activated intracellular drug release, J. Control. Release 210 (2015) 125–133, https://doi.org/10.1016/j.jconrel.2015.05.273.

[62] Y. Wu, W. Chen, F. Meng, Z. Wang, R. Cheng, C. Deng, H. Liu, Z. Zhong, Core-crosslinked pH-sensitive degradable micelles: a promising approach to resolve the extracellular stability versus intracellular drug release dilemma, J. Control. Release 164 (3) (2012) 338–345, https://doi.org/10.1016/j.jconrel.2012.07.011.

[63] Y. Xia, N. Wang, Z. Qina, J. Wua, F. Wanga, L. Zhanga, X. Xia, J. Li, Y. Lu, Polycarbonate-based core-crosslinked redox-responsive nanoparticles for targeted delivery of anticancer drug, J. Mater. Chem. B 6 (2018) 3348–3357, https://doi.org/10.1039/C8TB00346G.

[64] X. Zhang, H. Dong, S. Fu, Z. Zhong, R. Zhuo, Redox-responsive micelles with cores crosslinked via click chemistry, Macromol. Rapid Commun. 37 (12) (2016) 993–997, https://doi.org/10.1002/marc.201600049.

[65] X. Yi, D. Zhao, Q. Zhang, J. Xu, G. Yuan, R. Zhuo, F. Li, A co-delivery system based

on reduction-sensitive polymeric prodrug capable of loading hydrophilic and hydrophobic drugs for combination chemotherapy, Polym. Chem. 7 (2016) 5966–5977, https://doi.org/10.1039/C6PY00900J.

[66] X.-Q. Yi, Q. Zhang, D. Zhao, J.-Q. Xu, Z.-L. Zhong, R.-X. Zhuo, F. Li, Preparation of pH and redox dual-sensitive core crosslinked micelles for overcoming drug resistance of DOX, Polym. Chem. 7 (2016) 1719–1729, https://doi.org/10.1039/C5PY01783A.

[67] J. He, Y. Xia, Y. Niu, D. Hu, X. Xia, Y. Lu, W. Xu, pH-responsive core crosslinked polycarbonate micelles via thiol-acrylate Michael addition reaction, J. Appl. Polym. Sci. 134 (5) (2017) 44421, https://doi.org/10.1002/app.44421.

[68] E.V. Razuvaeva, A.I. Kulebyakina, D.R. Streltsov, A.V. Bakirov, R.A. Kamyshinsky, N.M. Kuznetsov, S.N. Chvalun, E.V. Shtykova, Effect of composition and molecular structure of poly(L–lactic acid)/poly(ethylene oxide) block copolymers on Micellar morphology in aqueous solution, Langmuir 34 (50) (2018) 15470–15482, https://doi.org/10.1021/acs.langmuir.8b03379.

[69] C. Ma, P. Pan, G. Shan, Y. Bao, M. Fujita, M. Maeda, Core−shell structure, biodegradation, and drug release behavior of poly(lactic acid)/poly(ethylene glycol) block copolymer micelles tuned by macromolecular stereostructure, Langmuir 31 (4) (2015) 1527–1536, https://doi.org/10.1021/la503869d.

[70] A. Kowalczuk, R. Trzcinska, B. Trzebicka, A.H.E. Müller, A. Dworak, C.B. Tsvetanov, Loading of polymer nanocarriers: factors, mechanisms and applications, Prog. Polym. Sci. 39 (1) (2014) 43–86, https://doi.org/10.1016/j.progpolymsci.2013.10.004.

[71] Z.L. Tyrrell, Y. Shena, M. Radosz, Fabrication of micellar nanoparticles for drug delivery through the self-assembly of block copolymers, Prog. Polym. Sci. 35 (9) (2010) 1128–1143, https://doi.org/10.1016/j.progpolymsci.2010.06.003.

[72] M. Karimi, A. Ghasemi, P.S. Zangaba, R. Rahighi, S.M.M. Basri, H. Mirshekari, M. Amiri, Z.S. Pishabad, A. Aslani, M. Bozorgomid, D. Ghosh, A. Beyzavi, A. Vaseghi, A.R. Aref, L. Haghani, S. Bahramia, M.R. Hamblin, Smart micro/nanoparticles in stimulus-responsive drug/gene delivery systems, Chem. Soc. Rev. 45 (2016) 1457–1501, https://doi.org/10.1039/C5CS00798D.

[73] S. Guragain, B.P. Bastakoti, V. Malgras, K. Nakashima, Y. Yamauchi, Multi-stimuli-responsive polymeric materials, Chem. Eur. J. 21 (38) (2015) 13164–13174, https://doi.org/10.1002/chem.201501101.

[74] K.C. Tjandra, P. Thordarson, Multivalency in drug delivery−when is it too much of a good thing? Bioconjugate Chem. 30 (3) (2019) 503–514, https://doi.org/10.1021/acs.bioconjchem.8b00804.

[75] S.D. Steichen, M. Caldorera-Moore, N.A. Peppas, A review of current nanoparticle and targeting moieties for the delivery of cancer therapeutics, Eur. J. Pharm. Sci. 48 (2013) 416–427, https://doi.org/10.1016/j.ejps.2012.12.006.

[76] V. Oliveri, G. Vecchio, 8-Hydroxyquinolines in medicinal chemistry: a structural perspective, Eur. J. Med. Chem. 120 (2016) 252–274, https://doi.org/10.1016/j.ejmech.2016.05.007.

[77] Y. Song, H. Xu, W. Chen, P. Zhan, X. Liu, 8-Hydroxyquinoline: a privileged structure with a broad-ranging pharmacological potential, Med. Chem. Commun. 6 (2015) 61–74, https://doi.org/10.1039/C4MD00284A.

[78] R. Musiol, An overview of quinoline as a privileged scaffold in cancer drug discovery, Expert Opin. Drug Discov. 12 (6) (2017) 583–597, https://doi.org/10.1080/17460441.2017.1319357.

[79] W.-Q. Ding, S.E. Lind, Metal ionophores – an emerging class of anticancer drugs, IUBMB Life 61 (11) (2009) 1013–1018, https://doi.org/10.1002/iub.253.

[80] M. Krawczyk, G. Pastuch-Gawolek, A. Mrozek-Wilczkiewicz, M. Kuczak, M. Skonieczna, R. Musiol, Synthesis of 8-hydroxyquinoline glycoconjugates and preliminary assay of their β1,4-GalT inhibitory and anti-cancer properties, Bioorg. Chem. 84 (2019) 326–338, https://doi.org/10.1016/j.bioorg.2018.11.047.

[81] M. Krawczyk, G. Pastuch-Gawołek, A. Pluta, K. Erfurt, A. Domiński, P. Kurcok, 8-Hydroxyquinoline glycoconjugates: modifications in the linker structure and their effect on the cytotoxicity of the obtained compounds, Molecules 24 (22) (2019) 4181, https://doi.org/10.3390/molecules24224181.

[82] I.M. Savić-Gajić, I.M. Savić, Drug design strategies with metalhydroxyquinoline complexes, Expert Opin. Drug Discov. 15 (3) (2020) 383–390, https://doi.org/10.1080/17460441.2020.1702964.

[83] E.J. Vandenberg, D. Tian, A. New, Crystalline high melting bis(hydroxymethyl) polycarbonate and its acetone ketal for biomaterial applications, Macromolecules 32 (11) (1999) 3613–3619, https://doi.org/10.1021/ma9816822.

[84] M. Kawalec, M. Sobota, M. Scandola, M. Kowalczuk, P. Kurcok, A Convenient route to PHB macromonomers via anionically controlled moderate-temperature degradation of PHB, J. Polym. Sci.: Part A Polym. Chem. 48 (23) (2010) 5490–5497, https://doi.org/10.1002/pola.24357.

[85] M. Schindler, S. Grabski, E. Hoff, S.M. Simon, Defective pH regulation of acidic compartments in human breast cancer cells (MCF-7) is normalized in adriamycin-resistant cells (MCF-7adr), Biochemistry 35 (9) (1996) 2811–2817, https://doi.org/10.1021/bi952234e.

[86] S. Xiong, Z. Wang, J. Liu, X. Deng, R. Xiong, X. Cao, Z. Xie, X. Lei, Y. Chen, G. Tang, A pH-sensitive prodrug strategy to co-deliver DOX and TOS in TPGS nanomicelles for tumor therapy, Colloids Surf. B: Biointerfaces 173 (2019) 346–355, https://doi.org/10.1016/j.colsurfb.2018.10.012.

Publikacja P.7

Shell-Sheddable Micelles Based on Poly(ethylene glycol)-hydrazone-poly[R,S]-3-hydroxybutyrate Copolymer Loaded with 8-Hydroxyquinoline Glycoconjugates as a Dual Tumor-Targeting Drug Delivery System

A. Domiński[*], **M. Domińska**, M. Skonieczna, G. Pastuch-Gawołek, P. Kurcok[*]

Materiały uzupełniające do publikacji znajdują się w dołączonej płycie CD

pharmaceutics

Article

Shell-Sheddable Micelles Based on Poly(ethylene glycol)-hydrazone-poly[R,S]-3-hydroxybutyrate Copolymer Loaded with 8-Hydroxyquinoline Glycoconjugates as a Dual Tumor-Targeting Drug Delivery System

Adrian Domiński [1,*][ID], Monika Domińska [2,3][ID], Magdalena Skonieczna [3,4][ID], Gabriela Pastuch-Gawołek [2,3][ID] and Piotr Kurcok [1,*][ID]

1 Centre of Polymer and Carbon Materials, Polish Academy of Sciences, 34, M. Curie-Skłodowskiej St., 41-819 Zabrze, Poland
2 Department of Organic Chemistry, Bioorganic Chemistry and Biotechnology, Faculty of Chemistry, Silesian University of Technology, Krzywoustego 4, 44-100 Gliwice, Poland; monika.krawczyk@polsl.pl (M.D.); gabriela.pastuch@polsl.pl (G.P.-G.)
3 Biotechnology Centre, Silesian University of Technology, Krzywoustego 8, 44-100 Gliwice, Poland; Magdalena.Skonieczna@polsl.pl
4 Department of Systems Biology and Engineering, Faculty of Automatic Control, Electronics and Computer Science, Silesian University of Technology, 44-100 Gliwice, Poland
* Correspondence: adrian.dominski@cmpw-pan.edu.pl (A.D.); piotr.kurcok@cmpw-pan.edu.pl (P.K.)

Abstract: The development of selective delivery of anticancer drugs into tumor tissues to avoid systemic toxicity is a crucial challenge in cancer therapy. In this context, we evaluated the efficacy of a combination of nanocarrier pH-sensitivity and glycoconjugation of encapsulated drugs, since both vectors take advantage of the tumor-specific Warburg effect. Herein, we synthesized biodegradable diblock copolymer, a poly(ethylene glycol)-hydrazone linkage-poly[R,S]-3-hydroxybutyrate, which could further self-assemble into micelles with a diameter of ~55 nm. The hydrazone bond was incorporated between two copolymer blocks under an acidic pH, causing the shell-shedding of micelles which results in the drug's release. The micelles were stable at pH 7.4, but decompose in acidic pH, as stated by DLS studies. The copolymer was used as a nanocarrier for 8-hydroxyquinoline glucose and galactose conjugates as well as doxorubicin, and exhibited pH-dependent drug release behavior. In vitro cytotoxicity, apoptosis, and life cycle assays studies of blank and drug-loaded micelles were performed on Normal Human Dermal Fibroblasts-Neonatal (NHDF-Neo), colon carcinoma (HCT-116), and breast cancer (MCF-7) for 24, 48, and 72 h. A lack of toxicity of blank micelles was demonstrated, whereas the glycoconjugates-loaded micelles revealed enhanced selectivity to inhibit the proliferation of cancer cells. The strategy of combining pH-responsive nanocarriers with glycoconjugation of the drug molecule provides an alternative to the *modus operandi* of designing multi-stimuli nanocarriers to increase the selectivity of anticancer therapy.

Keywords: micelles; pH-responsive; biodegradable; drug release; quinoline glycoconjugates; Warburg effect

1. Introduction

Stimuli-responsive polymeric micelles based on amphiphilic well-defined block copolymers have gained great attention over the past decade in the field of anticancer drug delivery [1,2]. Self-assembled nanostructures generally have a hydrophilic outer shell and hydrophobic core. The hydrophilic shell of the micelle prevents steric recognition by the immune system and its removal by the macrophage system from the bloodstream. In contrast, the hydrophobic core can encapsulate fragile hydrophobic anticancer therapeutics [3]. The encapsulation of anticancer drugs in nanocarriers enhances drug accumulation in the

tumor tissues through enhanced permeability and the retention effect. Thus, the therapeutic dose of the drug can be reduced, thereby minimizing its side effects [4]. In particular, polymeric nanoparticles derived from biodegradable and biocompatible polyesters such as polylactide [5], poly(ε-caprolactone) [6], poly(3-hydroxybutyrate) [7] or aliphatic polycarbonates [8] are broadly used as drug carriers. Among these, poly(3-hydroxybutyrate) (PHB) is considered to be a future "green" material for biomedical or drug delivery applications [9]. To further its applications in drug delivery systems, it is crucial to obtain PHB in a highly controlled manner with the desired stereochemistry, which is essential for its physicochemical properties [10,11]. Therefore, extensive studies have focused on the ring-opening polymerization of β-lactones to obtain the polymer with the desired molar mass, low dispersity, microstructure, and reduced side reactions [12–16]. The isotactic poly ([R]-3-hydroxybutyrate) is synthesized both biotechnologically through bacterial fermentation and chemically by the polymerization of β-butyrolactone (β-BL) [17]. Both anionic and coordination ring-opening polymerization of β-butyrolactone enable the obtaining of "tailor-made" poly (3-hydroxybutyrate), and its microstructure significantly depends on both the absolute configuration of β-BL and the type of catalyst used [13]. However, the anionic ring-opening polymerization of racemic β-BL—atactic poly([R,S]-3-hydroxybutyrate) (aPHB) is most often synthesized, due to the presence of a chiral C4 carbon in the β-butyrolactone molecule. OligoPHB has been used for drug conjugation to increase metabolic stability, bioavailability, and avoid multi-drug resistance [18,19]. Additionally, poly(3-hydroxybutyrate) is degraded and further resorbs in vivo, meaning that their degradation by-products are eliminated via natural pathways, both during the filtration and after metabolization without causing cytotoxicity. Due to this, PHB has great potential as a building material for anticancer drug delivery systems. However, the non-stimuli-responsive PHB-based micelles have some drawbacks, i.e., the slow drug release from nanocarriers, which significantly lowers the efficiency of therapeutic outcome [20]. Understanding the differences between tumors and healthy tissues is very important when designing new anti-cancer drug carriers. One such difference is the unique metabolism of sugar derivatives by tumor tissues. During the progression, cancer cells significantly increase the glycolysis rate other than mitochondrial oxidative phosphorylation to increase their proliferation [21]. As a consequence, the accumulated pyruvate is mainly converted into lactic acid, which makes the microenvironment of neoplastic tissues slightly acidic (pH 6.5–6.8) [22]. The increased sugar uptake of tumor tissues is related to the overexpression of glucose transporters, which are membrane proteins that facilitate concentration-dependent glucose and galactose uptake inside the cell [23]. This atypical relationship between increased proliferation, the high uptake of sugar derivatives, and the decrease in the extracellular pH of tumor tissues caused by lactate production is known as the Warburg effect [24]. This effect has been found in almost all types of tumors [25]. Therefore, many studies use the Warburg effect in drug delivery applications to improve cancer targeting and selectivity, e.g., by incorporating a sugar unit into the drug structure (glycoconjugation) [26,27] or using pH-sensitive drug carriers [28,29]. Recently, our group reported that a combination of pH-responsive nanocarriers loaded with glycoconjugates significantly improves their selectivity to inhibit the proliferation of cancer cells [30]. In the construction of the pH-responsive nanocarriers, acetal, imine, oxime, vinyl ether, hydrazone or orthoester are typical acid-sensitive chemical linkages, which are stable at physiological pH, but are rapidly hydrolyzed in an acidic environment [31]. The hydrazone linkage has attracted considerable attention in anticancer drug delivery systems, due to its stability at physiological pH and fast hydrolysis in a mildly acidic environment [32]. Moreover, hydrazone-based doxorubicin prodrugs NC-6300 and INNO-206 were reported to be under Phase I and II of clinical trials, respectively [33,34]. In both cases, data revealed that hydrazone-based prodrugs showed significantly higher anticancer activity and reduced side-effects compared to free drugs, an effect which is related to the release of the drug in the tumor tissues. The incorporating acid-labile bonds into the polymer structure, so nanocarriers can be designed to respond in the acidic tumor microenvironment by disas-

sembling, changing their size, shape, surface charge, etc. [35]. As a result, the encapsulated drugs are released in a controlled manner with the ability to target tumor tissues. It is well-known that PEGylation is effective in forming the "stealth" surface of the micelles to avoid non-specific interactions with proteins and prolong the circulation time of nanocarriers in the bloodstream [36]. However, it is also known that PEGylation reduces the cellular uptake of nanoparticles by cancer cells, leading to decreased therapeutic outcomes [37]. Therefore, nanocarriers for cancer treatment should be "stealth" protected with a PEG shell layer, with the capability due to the shell-shedding effect at the tumor site to increase internalization by cancer cells [38]. The unique pathophysiological markers of tumor tissues, i.e., lower pH in the microenvironment of cancer cells, the higher level of reactive oxygen species, high intracellular glutathione levels, hypoxic conditions, or the overexpression of various specific enzymes can act as an endogenous trigger to promote the shell-shedding effect in nanocarriers. As a result, the drug is released in a controlled manner and the ability of the drug to target the tumor tissues is improved. Yang et al. [39] reported a pH-responsive shell-sheddable nanocarrier based on a copolymer of poly(ethylene glycol) and polylactide with an acid-labile acetal linkage bridge for tumor-targeted paclitaxel delivery. The PEG shedding was triggered by tumor's acidic microenvironment, resulting in prolonged circulation time, enhanced cellular uptake, and an improved in vivo tumor inhibition rate. Manna et al. [40] reported that a four-arm star amphiphilic block copolymer based on [star-(poly(D,L-lactide)-b-poly(N-vinylpyrrolidone)$_4$] loaded with methotrexate showed pH-dependent drug release and excellent antitumor efficacy against methotrexate-resistant Dalton lymphoma and Raji cells, whereas a free drug was ineffective. Moreover, the treatment of Dalton lymphoma tumor-bearing mice revealed the prolonged survival of mice with active disease and the generation of CD8+ T-cell-mediated cytolytic responses against the tumor, which was significantly reduced in untreated tumor-bearing mice. Yang et al. [41] prepared dual pH-sensitive polymeric nanoparticles based on a diblock copolymer, consisting of acetal-linked poly(ethylene glycol) and catechol-functionalized aliphatic polycarbonate for anticancer drug delivery. The bortezomib was conjugated to the copolymer through a pH-sensitive boronate ester bond between catechol groups and a drug-derived phenylboronic acid group. The nanocarrier rapidly released bortezomib in response to the acidic tumor microenvironment. Furthermore, the conjugation of paclitaxel via acetal bonding to the poly(ethylene glycol)-b-poly(acrylic acid) copolymer was reported by Zhong and coauthors as a pH-sensitive micellar prodrug with potent antitumor activity against multi-drug-resistant cancer cells [42]. Zhong et al. [43] developed reduction-responsive shell-sheddable micelles from a poly(ethylene glycol)-disulfide linker-poly(ε-caprolactone) copolymer for paclitaxel delivery.

In this work, we report biodegradable copolymer comprising poly(ethylene glycol) and poly([R,S]-3-hydroxybutyrate) blocks linked via hydrazone bond. The resulting amphiphilic copolymer can self-assemble into nanosized shell-sheddable micelles for pH-triggered delivery of encapsulated anticancer agents (8-hydroxyquinoline glycoconjugates and doxorubicin). The hydrazone bond incorporated between two copolymer blocks is broken under the acidic media, causing the shedding of PEG shells, which results in the decomposition of micelles and subsequent drug release. The synthesis of the copolymers, characterization of micelles, pH-dependent degradation of nanocarriers, and drug release profiles were investigated. Moreover, in vitro cytotoxicity of the blank micelles and the activity of drug-loaded mPEG-hyd-aPHB micelles were studied using an MTT (3-[4,5–dimethylthiazol-2-yl]-2,5-diphenyltetrazolium bromide) assay combined with apoptosis and cell cycle assays against healthy cells (NHDF-Neo) and cancer cells (HCT-116 and MCF-7).

2. Materials and Methods

2.1. Materials

Poly(ethylene glycol) monomethyl ether (mPEG, M_n = 5000 g mol^{-1}, Sigma-Aldrich, Steinheim, Germany) was dried by azeotropic distillation from anhydrous toluene. Tri-

ethylamine (99%, Sigma-Aldrich, Steinheim, Germany), dichloromethane (DCM) (99%, VWR Chemicals, Fontenary-Sous-Bois, France) were dried over CaH$_2$ and distilled before use. In addition, 4-Nitrophenyl chloroformate (*p*-NPC 99%, TCI Chemicals, Belgium), hydrazine monohydrate (64–65%, Sigma-Aldrich, Steinheim, Germany) (>98%, Sigma-Aldrich, Steinheim, Germany), levulinic acid (>98%, Alfa Aesar, Haverhill, MA, USA), trifluoroacetic acid (TFA, >99%, Sigma-Aldrich, Steinheim, Germany), pyrene (+98%, Acros Organics, Acros Organics, Geel, Belgium), methanol (MeOH), ethanol, and diethyl ether (all 99%, VWR Chemicals, Fontenary-Sous-Bois, France) were used as received. DMSO (99%, VWR Chemicals, Fontenary-Sous-Bois, France) was distilled under reduced pressure over CaH$_2$ and two subsequent reduced pressure distillations over BaO. β-Butyrolactone (>98% Sigma-Aldrich, Steinheim, Germany) was purified as described in [44]. Doxorubicin hydrochloride (DOX·HCl) was purchased from LC Laboratories. The mPEG-COONa was prepared as described in [45]. Model glycoconjugates (see Figure S1) for in vitro cytotoxicity studies, i.e., 8-((1-(2,3,4,6-tetra-*O*-acetyl-β-D-glucopyranosyl)-1H-1,2,3-triazol-4-yl)methoxy)quinoline (8HQ-glucose conjugate–8HQ-Glu) and 8-((1-(2,3,4,6-tetra-*O*-acetyl-β-D-galactopyranosyl)-1H-1,2,3-triazol-4-yl)methoxy)quinoline (8HQ-galactose conjugate—8HQ-Gal) were synthesized as described earlier in [46].

Cell Cultures

The Normal Human Dermal Fibroblasts-Neonatal, NHDF-Neo were purchased from LONZA (Cat. No. CC-2509, NHDF-Neo, Dermal Fibroblasts, Neonatal, Lonza, Poland). The human breast adenocarcinoma cell line MCF-7 was obtained from the collection at the Maria Sklodowska-Curie Memorial Cancer Center and National Institute of Oncology (Gliwice, Poland). The human colon adenocarcinoma cell line HCT-116 was obtained from an American Type Culture Collection (ATCC, Manassas, VA, USA). Cells were grown in a humidified atmosphere with 5% CO$_2$ and at 37 °C in a culture medium. The culture media consisted of RPMI 1640 (HyClone laboratories, Inc.) or DMEM+F12 (HyClone laboratories, Inc.), supplemented with 10% heat-inactivated fetal bovine serum (FBS) (Eurx, Gdańsk, Poland) and 5% Antibiotic Antimycotic Solution, 100 U/mL penicillin, and 10 mg/mL streptomycin (Sigma-Aldrich, Steinheim, Germany).

2.2. Synthesis of mPEG-hyd-LEV Macroinitiator

Under a dry nitrogen atmosphere, the solution of mPEG (5 g, 1.0 mmol, 1.0 eq.) and triethylamine (0.21 mL, 1.5 mmol, 1.5 eq.) in 50 mL of dry DCM was thermostated in 0 °C. Next, a solution of *p*-nitrophenyl chloroformate (*p*-NPC) (2.02 g, 10 mmol, 10 eq.) in 25 mL of dry DCM was introduced dropwise. The reaction mixture was stirred for 30 min at 0 °C. Next, the temperature was increased to room temperature (rt) and the reaction was carried out for 48 h. The DCM was evaporated, excess methanol was added and stirred for 1 h to remove unreacted *p*-NPC. Then, the volatiles were stripped off under reduced pressure, the product was redissolved in DCM, washed three times with brine, and precipitated in cold diethyl ether. The residual solid mPEG-NPC was dried under vacuum to a constant weight. Yield: 85%. ^{1}H NMR (600 MHz, CDCl$_3$, Figure S2a) δ: 3.38 (3H, CH$_3$-O), 3.65 (4mH, CH$_2$-CH$_2$-O), 4.44 (2H, CH$_2$-O-C(O)), 7.4 (2H, Ar H), 8.28 (2H, Ar H). Next, the PEG-NPC (3 g, 0.58 mmol, 1.0 eq.) was dissolved in 50 mL of DCM and slowly added dropwise into hydrazine monohydrate (1.13 mL, 23.23 mmol, ~40 eq.) solution in 50 mL of DCM thermostated at 0 °C. The reaction mixture was stirred for 30 min at 0 °C, and then at rt for 24 h. Then, volatiles were stripped off under vacuum, and the obtained solid was dissolved in deionized water, dialyzed against water (MWCO 1000) at rt for 48 h and lyophilized to obtain mPEG-NH-NH$_2$. Yield: 68%. ^{1}H NMR (600 MHz, CDCl$_3$, Figure S2b) δ: 3.38 (3H, CH$_3$-O), 3.65 (4mH, CH$_2$-CH$_2$-O), 4.27 (2H, CH$_2$-O-C(O)). The solution of mPEG-NH-NH$_2$ (1 g, 0.2 mmol, 1 eq.) and levulinic acid potassium salt (0.03 g, 0.26 mmol, 1.3 eq.) in 20 mL of dry methanol with 2 drops of TFA was stirred for 48 h at 50 °C. Next, the reaction solution was dialyzed (MWCO 1000) against KOH ethanol solution for 24 h, and against ethanol for 24 h, followed by drying under vacuum at rt to a constant weight.

The mPEG-hyd-LEV macroinitiator was stored at −4 °C in glovebox. Yield: 57%. ^{1}H NMR (600 MHz, CDCl$_3$, Figure S2c) δ: 1.99 (3H, CH$_3$-C=N), 2.47 (4H, C-CH$_2$-CH$_2$-C(O)), 3.38 (3H, CH$_3$-O), 3.65 (4mH, CH$_2$-CH$_2$-O), 4.33 (2H, CH$_2$-O-C(O)).

2.3. Synthesis of mPEG-hyd-aPHB

The polymerizations were performed in the glovebox (H$_2$O < 1 ppm, O$_2$ < 5 ppm). The ring-opening of β-butyrolactone initiated with hydrazone bond-containing mPEG-hyd-LEV macroinitiator was carried out in dry DMSO at a monomer concentration of 1 mol L^{-1} at rt. Briefly, mPEG-hyd-LEV (0.3 g, 0.05 mmol, 1 eq.) were dissolved in DMSO, after which complete macroinitiator solubilization of the β-butyrolactone (187.9 μL, 2.31 mmol, 40 eq.) was added. Conversion of the monomer was measured by ^{1}H NMR spectroscopy, based on the disappearance of the signals derived from the β-butyrolactone. After quantitative monomer conversion, the resulting copolymer was lyophilized and stored at −4 °C in the glovebox. ^{1}H NMR (600 MHz, CDCl$_3$) δ: 1.28 ppm (3nH, CH$_3$), 2.02 (3H, CH$_3$-C=N), 2.54 ppm (2nH, CH$_2$), 3.38 (3H, CH$_3$-O), 3.65 (4mH, CH$_2$-CH$_2$-O), 4.2 (2H, CH$_2$-O-C(O)), 5.25 ppm (1nH, CH). SEC: (DMF, PEG standards): M$_n$ = 8200 g mol^{-1}, Đ = 1.14.

The mPEG-*b*-aPHB diblock copolymer was synthesized in similar conditions using mPEG-COONa as the macroinitiator. ^{1}H NMR (600 MHz, CDCl$_3$, Figure S3) δ: 1.28 ppm (3nH, CH$_3$), 2.54 ppm (2nH, CH$_2$), 3.38 ppm (3H, CH$_3$-O), 3.65 ppm (4mH, CH$_2$-CH$_2$-O), 4.2 ppm (2H, CH$_2$-O-C(O)), 5.25 ppm (1nH, C**H**-CH$_2$). SEC: (DMF, PEG standards): M$_n$ = 7900 g mol^{-1}, Đ = 1.08.

2.4. Characterization of Synthetic Copolymers

The ^{1}H NMR spectra were recorded on the Bruker-Avance II 600 MHz with Ultrashield Plus Magnets (Fremont, CA, USA) at room temperature in CDCl$_3$ with tetramethylsilane (TMS) as an internal standard. Size exclusion chromatography (SEC) measurements were performed at 45 °C in DMF with the addition of 5 mmol L^{-1} LiBr at a nominal flow rate of 1 mL min^{-1}. The chromatography system contained a multiangle light scattering detector (DAWN HELEOS, Wyatt Technology, λ = 658 nm), a refractive index detector (Dn-2010 RI, WGE Dr Bures), and a column system (PSS gel GRAM guard and three columns PSS GRAM 100 Å, 1000 Å and 3000 Å). The molar mass and dispersity were evaluated using ASTRA 5.3.4.10 software from Wyatt Technologies. Poly(ethylene glycol) standards with a low dispersity mass distribution (M$_n$ values ranging from 1010 to 29,600 g mol^{-1}, Polymer Laboratories) were used to generate a calibration curve.

2.5. Micelles Preparation and Characterization

The solvent evaporation method was used to prepare mPEG-hyd-aPHB and mPEG-*b*-aPHB micelles. Briefly, 10 mg of the copolymer was dissolved in dry DCM. Next, after the solvent evaporation, a thin film at the bottom of the vial was formed. After removing the traces of organic solvent, the film was dispersed in PBS buffer (10 mL; copolymer concentration was equal to 1 mg · mL^{-1}). Next, the mixture was stirred for 60 min at room temperature and sonicated for 30 min in an ice-cold bath. Then, the micelle suspension was filtered using a syringe filter (0.2 μm, Sartorius). The obtained micelle solution was lyophilized and stored at −4 °C in the glovebox. The critical micelle concentration (CMC) was determined using pyrene as a fluorescence probe. A predetermined amount of pyrene (6 × 10^{-6} mol · L^{-1}) in acetone was added to micelle solutions of different concentrations (ranging from 1 × 10^{-5} to 1.0 mg · mL^{-1}) in phosphate buffer. The samples were incubated overnight at rt in the dark. The fluorescence spectra were recorded on a Hitachi F-2500 Spectrometer (Tokyo, Japan) from 300 to 360 nm with the emission wavelength at 391 nm. The intensity ratio of pyrene at 336 over 333 nm was plotted against the logarithm of copolymer concentration to determine the critical micelle concentration. The hydrodynamic diameter and size distribution of micelles were determined by dynamic light scattering (DLS) measurements using a Zetasizer Nano ZS90 (Malvern Instruments). To examine the stability and acid-triggered degradation of micelles at various pH levels, the 10 mg of freeze-dried

micelles was dispersed in 10 mL of PBS buffer with pH 7.4, 6.4, and 5.5 respectively. The mixture was incubated at 37 °C, and at predetermined time intervals, the hydrodynamic diameter of the micelles was measured. The morphologies of the micelles were observed using Cryogenic Transmission Electron Microscopy (cryo-TEM). Images were obtained using a Tecnai F20 X TWIN microscope (FEI Company, Hillsboro, OR, USA) equipped with a field emission gun, operating at an acceleration voltage of 200 kV. Images were recorded on the Gatan Rio 16 CMOS 4k camera (Gatan Inc., Pleasanton, CA, USA) and processed with Gatan Microscopy Suite (GMS) software (Gatan Inc., Pleasanton, CA, USA). Specimen preparation was carried out by vitrification of the aqueous solutions on grids with holey carbon film (Quantifoil R 2/2; Quantifoil Micro Tools GmbH, Großlöbichau, Germany). Before use, the grids were activated for 15 s in oxygen plasma using a Femto plasma cleaner (Diener Electronic, Ebhausen, Germany). Cryo-samples were prepared by applying a droplet (3 μL) of the suspension to the grid, blotting with filter paper and immediate freezing in liquid ethane using a fully automated blotting device Vitrobot Mark IV (Thermo Fisher Scientific, Waltham, MA, USA). After preparation, the vitrified specimens were kept under liquid nitrogen until they were inserted into a cryo-TEM-holder Gatan 626 (Gatan Inc., Pleasanton, CA, USA) and analyzed in the TEM at −178 °C.

2.6. In Vitro Drug Loading and Release Studies

Drug loaded micelles were prepared identically to blank micelles using 10 mg of copolymer, 1 mg of drug and 10 mL of DCM. Next, the unloaded drug was eliminated by filtration through a syringe filter (0.2 μm, Sartorius), the drug-loaded micelles solution was lyophilized, and then stored at −4 °C in the glovebox. To determine the drug loading efficiency (DLE) and drug loading content (DLC) the lyophilized drug-loaded micelles were redissolved in DMSO and analyzed with a UV-Vis-NIR spectrophotometer JASCO V-570 (Tokyo, Japan) using a standard curve method. The DLE and DLC were calculated according to the following equations:

$$\text{Drug loading efficiency (DLE\%)} = \frac{\text{weight of drug in micelles}}{\text{weight of drug in feed}} \times 100\%$$

$$\text{Drug loading content (DLC\%)} = \frac{\text{weight of drug in micelles}}{\text{weight of drug loaded micelles}} \times 100\%$$

In vitro drug release from micelles was carried out in PBS at pH 7.4, 6.4, and 5.5 at 37 °C via a dialysis method. Typically, 3 mL (1 mg · mL^{-1}) of drug-loaded micelles were transferred into a Float-A-Lyzer G2 dialysis device (MWCO 7000). Each dialysis device was immersed into 150 mL of corresponding buffer at 37 °C, stirring at 100 rpm. At predetermined time intervals, 50 μL of the solution was withdrawn from the dialysis device and replaced with an equal amount of fresh buffer. Quantitative assessment of the released drugs was carried out by UV-Vis spectroscopy. The release experiments were conducted in triplicate, and the results presented are the average of the data.

2.7. MTT Assay

Cell viability was assessed by the MTT assay (Merck, Darmstadt, Germany). Stock solutions of used compounds (glycoconjugates or DOX) were prepared in DMSO (DMSO content in the highest concentration did not exceed 0.5%) and diluted to the desired concentrations with the culture medium directly before the experiment. Blank micelles and drug-loaded micelle solutions were also diluted to the desired concentrations with the culture medium directly before the experiment. The cells were seeded into 96-well plates at concentrations of 5×10^3 (MCF-7, NHDF-Neo) or 2×10^3 (HCT-116) per well and incubated for 24 h in a humidified atmosphere of 5% CO$_2$ at 37 °C. Next, the culture medium was removed and replaced with a solution of the tested compounds in a medium with varying concentrations. Cells treated with DMSO in the fresh medium (0.5%) were used as controls. Then cells were incubated with compounds for a further 24 h, 48 h, or

72 h. After that, the solutions were removed and the MTT solution (50 μL, 0.5 mg · mL^{-1} in PBS) was added into each well. After 3 h of incubation, the MTT solution was removed and the precipitated formazan crystals were dissolved in DMSO. The absorbance was measured spectrophotometrically at a 570 nm wavelength using the plate reader (Epoch, BioTek, Winooski, VT, USA). The experiment was conducted in at least three independent repetitions with four technical repeats for each tested concentration. The results were expressed as the survival fraction (%) of the control. The IC$_{50}$ values were calculated using CalcuSyn software (version 2.0, Biosoft, Cambridge, UK). The IC$_{50}$ parameter was defined as the concentration of the drug that was necessary to reduce the proliferation of cells to 50% of the untreated control. The results are shown as the average value $\pm$ standard deviation (SD).

2.8. Apoptosis and Cell Cycle Analyses

The cell cycle and the type of cell death induced by the test compounds were measured by using flow cytometry. The cells were seeded into 6-well plates at concentrations of 3×10^5 (HCT-116) or 4×10^5 (MCF-7, NHDF-Neo) per well and incubated for 24 h in a humidified atmosphere of 5% CO$_2$ at 37 °C. Then, the culture medium was removed and replaced with a solution of the tested compounds at a concentration equal to the IC$_{50}$ value. Cells treated with blank micelle were also tested. The untreated cells with fresh medium were used as the control. After 24 h of incubation, the solutions were removed and the cells were collected by trypsinization. Then cells were centrifuged (3 min, 2000 rpm, RT) and washed with PBS. Then the cells were centrifuged again (3 min, 2000 rpm, RT) and the supernatant was removed. The resulting pellet contained cells, which were used for flow cytometric experiments. The fraction of dead cells after treatment with the test compounds were detected using the Annexin-V apoptosis assay (BioLegend, San Diego, CA, USA) and propidium iodide (PI) solution (100 μg/mL (Merck, Darmstadt, Germany)) uptake test. Cells were suspended in 50 μL of cold Annexin-V binding buffer and incubated in the dark with 2.5 μL of antibody Annexin-V FITC and 10 μL of PI solution (3 mg/mL) for 20 min at 37 °C. After this time, 250 μL of the Annexin-V binding buffer was added and the samples were incubated in the dark on ice for 15 min. Cytometric analyses were performed immediately using an Aria III flow cytometer (Becton Dickinson, Franklin Lakes, NJ, USA) with the FITC configuration (488 nm excitation; emission: LP mirror 503, BP filter 530/30) or PE configuration (547 nm excitation; emission: 585 nm) and at least 10,000 cells were counted.

For cell cycle analysis, the cells were suspended in 250 μL of hypotonic buffer (consisting of: sodium citrate dihydrate 1 g/L, propidium iodide (PI) 1 mg/mL, RNAse A 10 mg/mL, Triton X-100 1:9) and incubated in the dark at rt for 20 min. Measurement was performed using an Aria III flow cytometer (Becton Dickinson, USA), using at least 10,000 cells per sample. The cytofluorimetric configurations used are described above. The obtained data were analyzed using Flowing Software (Cell Imaging Core, Turku Center for Biotechnology, Turku, Finland).

2.9. Cell Microscopy Imaging

Microscopic imaging of cells was performed using fluorescence microscopy (Olympus FV1000 microscope). The cells were seeded into 35 mm Glass Bottom Dishes (MatTek Corporation) at a concentration of 5×10^4 (HCT-116, MCF-7, NHDF-Neo) in 2 mL of medium and incubated for 24 h in a humidified atmosphere of 5% CO$_2$ at 37 °C. Then, the culture medium was removed and replaced with a solution of the free DOX or DOX-loaded micelles in a medium at a dose of 1 μM (concentration equal to the previously calculated IC$_{50}$ value). The untreated cells with the fresh medium were used as controls. After 24 h of incubation, 2 μL of Hoechst 33342 dye was added to the medium and incubated in the dark for 20 min at 37 °C. Then, the solutions were removed and the cells were washed with PBS. To each dish, 500 μL of PBS was introduced, then the cells were covered with a coverslip and observed using a fluorescence microscope. All imaging conditions, including

laser power, photomultiplier tube, and offset settings, were aligned with the fluorescence intensity of the sample. Images were analyzed using free software ImageJ 1.47v (Wayne Rasband, National Institute of Health, Bethesda, MD, USA).

2.10. Statistical Analysis

For biological evaluation, at least three replicates were performed for every kind of experiment. The results were presented as the mean value $+/-$ SD. The statistical analysis was based on a *t*-test, and a *p*-value less than 0.05 was considered statistically significant, indicated on the figures with an asterisk.

3. Results and Discussion

3.1. Copolymer Synthesis and Characterization

The synthetic route of mPEG-hyd-aPHB is shown in Figure 1a. The essential issue in the design of shell-shedding micelles was the location of the pH-sensitive linkage between the hydrophilic and hydrophobic blocks. Herein, an acid-labile hydrazone bond was incorporated into the macroinitiator structure as described below. Namely, the amine-terminated monomethoxy poly(ethylene glycol) ($M_n = 5000$ g mol^{-1}) (mPEG-NH-NH$_2$) was first synthesized in two steps. Then, mPEG-NH-NH$_2$ was reacted with levulinic acid potassium salt to obtain a hydrazone-containing macroinitiator. Subsequently, chain extension via anionic ring-opening polymerization of β-butyrolactone afforded the desired amphiphilic copolymer.
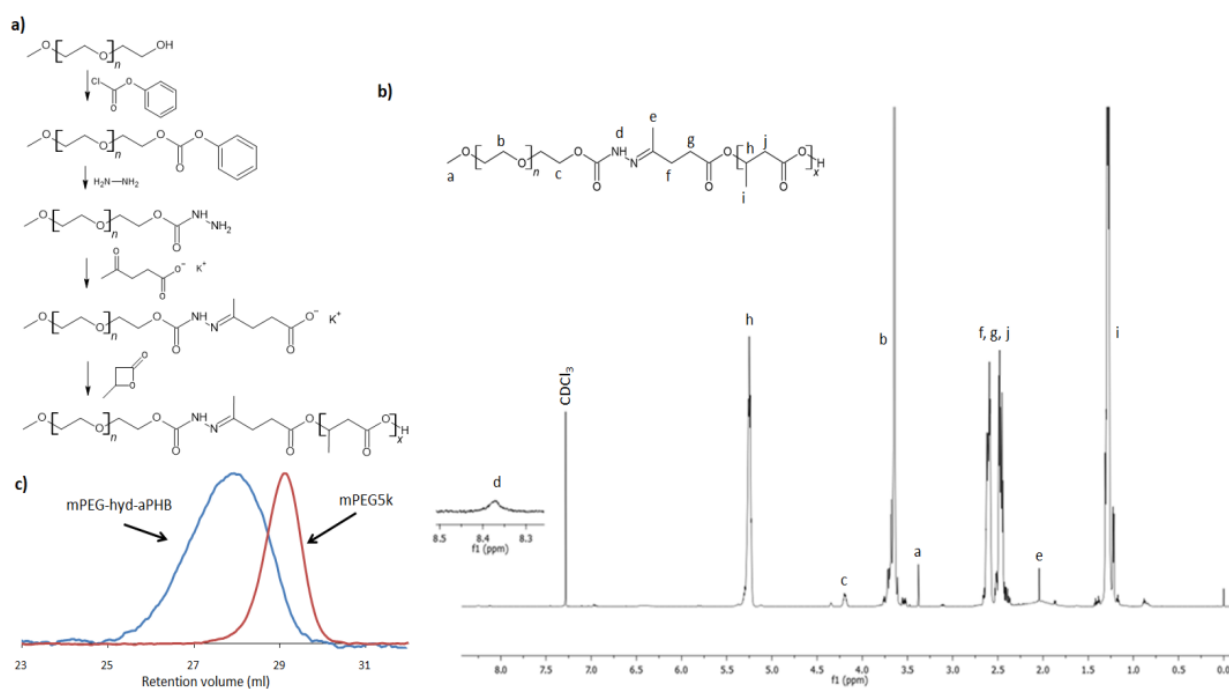
Figure 1. (**a**) The synthetic route for the mPEG-hyd-aPHB copolymer; (**b**) ^{1}H NMR spectrum (CDCl$_3$, 600 MHz) of mPEG-hyd-aPHB; (**c**) SEC traces of mPEG$_{5000}$ and mPEG-hyd-aPHB.

Firstly, the hydroxyl end group of mPEG was activated through a reaction with *p*-nitrophenyl chloroformate to obtain mPEG-NPC. Upon activation of the mPEG hydroxyl end group with p-NPC, the ^{1}H NMR spectrum (Figure S2a) revealed signals of the mPEG chain (3.65 and 3.38 ppm) and derived signals at δ = 7.4 and 8.28 ppm from aromatic protons of the *p*-nitrophenyl group, as well as a peak at 4.44 ppm attributed to substitution of mPEG with the NPC terminal methylene group. Then, the mPEG-NPC was reacted with hydrazine to obtain mPEG-NH-NH$_2$. The disappearance of the aromatic *p*-NPC signals and the shifting of the signal of a methylene group from δ = 4.44 ppm to 4.27 ppm, observed in

^{1}H NMR spectrum of amine-terminated mPEG (Figure S2b), confirms the mPEG-NH-NH$_2$ formation. Subsequently, amino-terminated mPEG was further reacted with levulinic acid potassium salt. In a facile amine-ketone coupling reaction, a hydrazone bond containing potassium carboxylate macroninitiator was formed. The chemical structure of the macroinitiator (mPEG-hyd-LEV) was verified by ^{1}H NMR, which is shown in Figure S2c. The presence of characteristic signals derived from incorporated levulinic acid potassium salt was observed. Importantly, the signal of the methyl group of potassium levulinic acid salt (see inset in Figure S2c) shifted from $\delta = 2.20$ ppm to 1.99 ppm, indicating hydrazone bond formation. The same effect was observed for the signals ascribed to levulinic acid methylene groups (triplets at $\delta = 2.62$ and 2.76 ppm) that overlapped after the formation of the hydrazone bond and were observed as a multiplet at $\delta = 2.47$ ppm. Finally, the pH-responsive amphiphilic poly(ethylene glycol)-hyd-poly([R,S]-3-hydroxybutyrate) copolymer (mPEG-hyd-aPHB) was synthesized by anionic ring-opening polymerization of β-butyrolactone initiated with obtained hydrazone linkage-containing macroinitiator. In aqueous media, the amphiphilic block copolymers, depending on the copolymer hydrophilic block weight fraction (*f*), molar mass, and the interactions of the hydrophobic copolymer block with water may self-organize into micelles [20]. The hydrophilic block weight fraction usually affects the hydrophobic interactions and size of self-assembled structures and, if *f* is in the range of 45–75%, micelles are usually formed [47]. Therefore, the molar mass of poly([R,S]-3-hydroxybutyrate) block was planned to be 3500 g · mol^{-1} to keep the mPEG, i.e., hydrophilic block weight fraction, at the level of 60%. In β-butyrolactone anionic ring-opening polymerization, the initiation reaction by a weak nucleophile, e.g., carboxylic acid salt, the initiator attacks the C4 carbon of the β-butyrolactone ring by breaking the alkyloxygen bonds. As a result, the carboxylate ions formed in this reaction are the propagation centers. The activity of the initiator and the propagation species in such polymerization strongly depend on counter-ion size, cation-anion interactions, and solvent polarity [48]. Playing with the counterion size and solvent polarity, the activity of the initiating system and the reaction kinetics can be easily adjusted. For the sake of simplicity and efficiency, a reaction system containing a potassium counter-ion and DMSO as a solvent was chosen to obtain the appropriate polymerization conditions. The DMSO as a high-polar solvent activates the carboxylate species by strong solvation of the cation, resulting in significant increases in the reactivity of the system. As a result, the kinetics of the reaction allow for a controlled polymerization process on carboxylate growing species. The ^{1}H NMR spectrum of mPEG-hyd-aPHB is shown in Figure 1b. All of the main characteristic signals assigned to mPEG ($\delta = 3.38$ and 3.65 ppm) and methylene group of hydrazone-functionalized levulinic acid at $\delta = 2.02$ ppm and aPHB at $\delta = 1.28, 2.54, 5.25$ ppm) were observed. Using integral ratio with the molar mass of the mPEG block (5000 g mol^{-1}), the molar mass of mPEG-hyd-aPHB was determined to be 8600 g mol^{-1}. This value correlates with the theoretical one, 8600 g mol^{-1}. SEC analysis, shown in Figure 1c, revealed that the obtained copolymer had a molar mass of 8200 g mol^{-1} with a dispersity value Đ = 1.14. It is worth mentioning that very low-intensity signals at $\delta = 1.86, 5.8$ and 6.95 ppm in the ^{1}H NMR spectrum of the copolymer were ascribed to the crotonate protons, which are a result of the abstraction of an acidic proton either from β-butyrolactone or aPHB (Figure S4) [13]. However, the amount is deemed to be negligible. The mPEG-*b*-aPHB diblock copolymer with a similar composition was also synthesized (Figure S3) and used as a pH-insensitive control in further studies. The results of the ^{1}H NMR and SEC analyses for the synthesized copolymers are summarized in Table 1.

Table 1. Characteristics of copolymers.

Block Copolymer	Mn,NMR [a] [g mol^{-1}]	Mn,SEC [b] [g mol^{-1}]	Đ	f_{PEG} [%]	CMC [c] [μg mL^{-1}]
mPEG-hyd-aPHB	8600	8200	1.14	58	3.6
mPEG-*b*-aPHB	8100	7900	1.08	62	2.2

[a] The mPEG block had M_n = 5000 and Đ = 1.01 (determined by SEC). [b] Determined by SEC with DMF as solvent and poly(ethylene glycol) standards. [c] Determined using pyrene as a fluorescence probe.

3.2. Self-Assembly of the Copolymers

The synthesized amphiphilic copolymers spontaneously aggregated into core-shell structured micelles in an aqueous solution. Herein, the corresponding copolymers self-assembled into micelles, in which a core consists of hydrophobic aPHB blocks and an outer shell containing hydrophilic PEG chains. The structures of pH-responsive mPEG-hyd-aPHB and non-pH-responsive mPEG-*b*-aPHB micelles were confirmed using ^{1}H NMR spectroscopy. Figure S5 shows the ^{1}H NMR spectra corresponding to the lyophilized micelles that were resuspended in D$_2$O. After micellization, the signals ascribed to aPHB blocks are barely visible, indicating that aPHB chains are located in the core of the micelles. Moreover, peaks corresponding to PEG protons are visible after self-organizing because poly(ethylene glycol) chains are in an outer mobile state. Similar results were observed for both mPEG-hyd-aPHB and mPEG-*b*-aPHB micelles. The critical micelle concentration was determined, using pyrene as a probe, from the plot of the excitation intensity ratio as a function of the copolymer concentration (Figure S6). The CMC values of mPEG-hyd-aPHB and mPEG-b-aPHB were determined to be 3.6 μg mL^{-1} and 2.2 μg mL^{-1}, respectively (Table 1). The obtained micelles were characterized by DLS and cryo-TEM. As shown in Figure 2, the mPEG-hyd-aPHB formed micelles with a hydrodynamic diameter of ~55 nm and with a narrow size distribution (PDI = 0.14). In contrast, the hydrodynamic diameter for DOX-loaded mPEG-hyd-aPHB increased to ~86 nm, with a simultaneous increase in the PDI value up to 0.22. This increase in the hydrodynamic diameter of the micelles could be caused by drug encapsulation in the core. Additionally, it significantly increases the PDI values for drug-loaded micelles (Table 2). Next, cryo-TEM studies were used to observe the morphology of the micelles, revealing that the micelles had regular spherical shapes. The mean hydrodynamic diameters of nanoparticles determined by cryo-TEM were slightly lower compared with the values revealed by DLS, since the diameter obtained from DLS studies shows the hydrodynamic diameters in a hydrated state in the solution, while the diameter observed by cryo-TEM indicates the same for dried micelles [49].
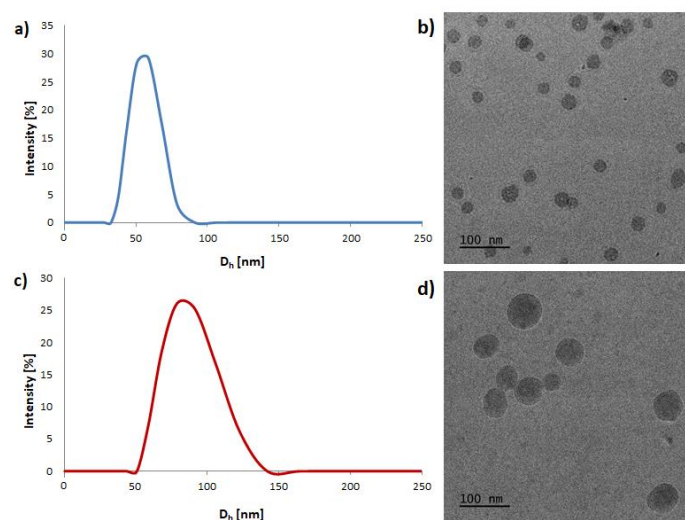
Figure 2. The size distribution and cryo-TEM images of mPEG-hyd-aPHB micelles (**a**,**b**) and 8HQ-loaded mPEG-hyd-aPHB micelles (**c**,**d**).

Table 2. Characterization of blank and drug-loaded micelles.

Sample	mPEG-hyd-aPHB				mPEG-*b*-aPHB			
	Size [nm]	PDI	DLC [%]	DLE [%]	Size [nm]	PDI	DLC [%]	DLE [%]
Blank micelles	55.3 ± 2.8	0.14 ± 0.01	_	_	49.5 ± 4.1	0.18 ± 0.02	_	_
DOX-loaded micelles	85.7 ± 5.1	0.22 ± 0.03	5.3 ± 0.4	48.6 ± 3.1	82.8 ± 6.2	0.2 ± 0.01	5.7 ± 0.2	54.1 ± 3.8
8HQ-loaded micelles	77.7 ± 3.8	0.19 ± 0.02	6.0 ± 0.1	55.1 ± 1.9	87.9 ± 2.9	0.15 ± 0.02	5.8 ± 0.4	55.3 ± 2.3
8HQ-Glu-loaded micelles	104.9 ± 4.5	0.25 ± 0.03	5.2 ± 0.2	45.6 ± 2.2	100.8 ± 3.1	0.28 ± 0.04	5.1 ± 0.3	47.1 ± 2.6
8HQ-Gal-loaded micelles	92.5 ± 4.2	0.22 ± 0.02	5.3 ± 0.3	46.4 ± 2.5	99.9 ± 5.4	0.19 ± 0.02	5.3 ± 0.3	48.1 ± 3.2

3.3. Drug Loading and In Vitro Release Studies

To examine the pH-triggered degradation of mPEG-hyd-aPHB micelles, the DLS technique was used to monitor the size changes in the micelles under various acidic conditions (PBS buffers with pH 7.4, 6.4, and 5.5) at 37 °C. In addition, non-pH-sensitive mPEG-*b*-aPHB micelles were also studied as a control. As shown in Figure 3, at physiological pH (7.4) the mPEG-hyd-aPHB micelles remained stable up to 24 h. After this, micelles slowly start forming larger aggregates, probably due to very slow hydrolysis of hydrazone linkage followed by reorganization. Under a mildly acidic environment (pH 6.4) mPEG-hyd-aPHB micelles started reorganizing into larger structures after 2 h, and larger micelles with hydrodynamic diameters of ~150 nm were formed over 48 h. Furthermore, as shown in Figure 3f, hydrazone bond-containing micelles immediately after dispersion in pH 5.5 buffer become unstable and form >200 nm particles (it took about 15 min to disperse the freeze-dried micelles in the corresponding buffer for measurement—which corresponds to sample "0 h" in the graph in all cases). Within 2 h, the hydrodynamic diameter increased up to >300 nm. After 24 h, populations from 100 to 800 nm were observed, meaning that the destruction of the particles had occurred. The observed phenomenon may be attributed to the hydrolysis of the hydrazone linkage, which leads to shedding of the hydrophilic PEG chains from the micelle and subsequent aggregation of hydrophobic core-forming chains into larger agglomerates [50]. In the case of control studies using non-pH-sensitive mPEG-*b*-aPHB micelles, no significant changes in the hydrodynamic diameters were observed. The obtained results indicate that mPEG-hyd-aPHB micelles are stable in the physiological environment and possess pH-responsive properties.

The drug-loading and in vitro release studies were carried out to evaluate the feasibility of using mPEG-hyd-aPHB nanocarriers as a pH-responsive anticancer drug delivery system. It is well-known that the hydrophobic core of micelles can encapsulate hydrophobic drugs. In this work, 8-hydroxyquinoline (8HQ), 8-hydroxyquinoline glucose conjugate (8HQ-Glu), 8-hydroxyquinoline galactose conjugate (8HQ-Gal), and doxorubicin (DOX) were used as hydrophobic model drugs to evaluate drug-loading properties and in vitro pH-dependent release behaviors from mPEG-hyd-aPHB and mPEG-*b*-aPHB micelles. The drug to copolymer ratio was 1:10. The drug loading efficiency (DLE) and drug loading content (DLC) are listed in Table 2. It shows that, in the case of loading doxorubicin or both glycoconjugates, the DLC and DLE values show no significant differences. The DLC and DLE values of DOX-loaded mPEG-hyd-aPHB micelles were 5.3% and 48.6%, while the values for 8HQ-Glu and 8HQ-Gal were 5.2%, 45.6%, and 5.3%, 46.4% respectively. Nevertheless, the DLC and DLE of 8HQ are slightly higher at 6% and 55.1% respectively. This discrepancy may be due to the fact that highly hydrophobic low-molecular weight compounds generally show better loading properties [51].
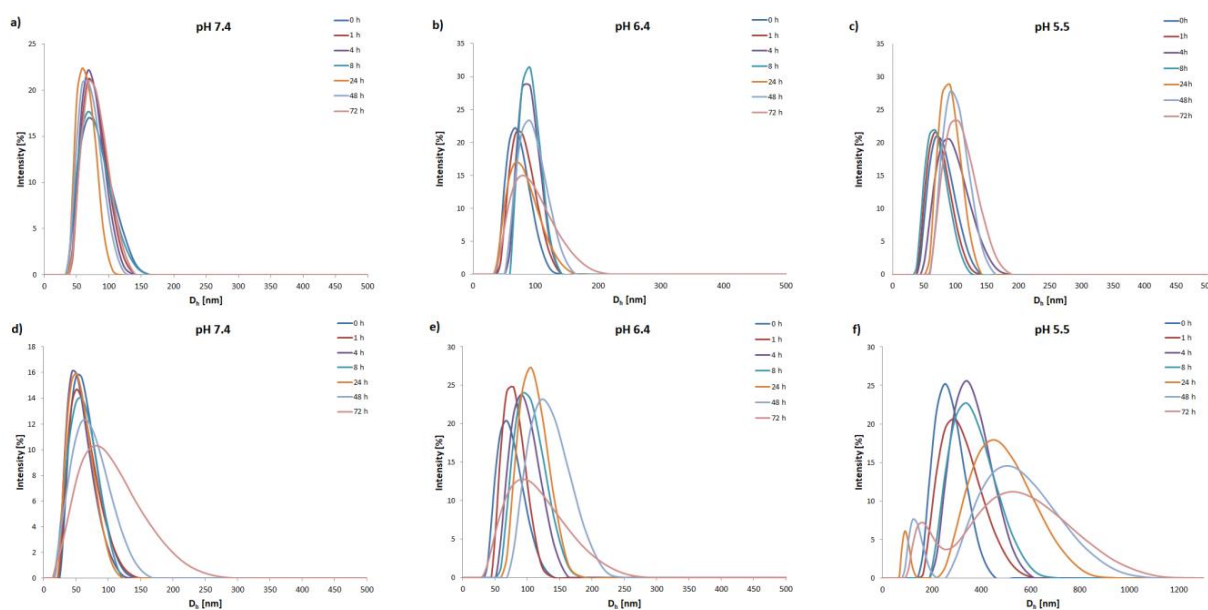
Figure 3. Changes in hydrodynamic diameter (d, nm) of mPEG-b-aPHB micelles (**a–c**) and mPEG-hyd-aPHB micelles (**d–f**) in PBS buffers at different pHs determined by DLS.

The in vitro drug release profiles of mPEG-hyd-aPHB and mPEG-*b*-aPHB micelles were studied under three different buffer solutions of pH 7.4, 6.4, and 5.5, respectively, at 37 °C. Figure 4 shows the doxorubicin release profiles for the pH-responsive and control micelles at different pH values. These profiles showed that, at the physiological pH, encapsulated DOX was released from mPEG-hyd-aPHB micelles at levels of 21% and 40% after 8 h and 32 h, respectively. Under mildly acidic conditions (pH 6.4) corresponding to the extracellular pH of tumor tissues, the drug was released faster, i.e., 37% and 51% after 8 and 24 h, respectively. However, at pH 5.5 (the endo-lysosomal pH in cancer cells) the burst release of DOX was observed with 47% of the drug released after 8 h. The complete release of DOX from mPEG-hyd-aPHB micelles was observed after 48 h, whereas 79% of the drug was released. The control mPEG-*b*-aPHB micelles displayed a slower sustained release profile under all studied pH conditions. Less than ~36% of the DOX was released over 48 h in all pH values. The slight differences in the released DOX for mPEG-*b*-aPHB are most likely due to the hydrophobic DOX solubility increases with lowered pH [52]. For comparison, the effect of the matrix was also examined, the cumulative release of the free drug showed a release of 70% and 94%, within 4 and 8 h separately from pH conditions. The above results demonstrate that encapsulated drug release from mPEG-hyd-aPHB was significantly faster in acidic conditions as a result of accelerated hydrolysis of hydrazone linkage.

3.4. In Vitro Cytotoxicity Assay

It has been well-reported that tumor tissues have an increased demand for metal ions such as copper, iron, zinc, etc., since these microelements are involved in many cellular processes. Therefore, ion binding agents acting as ionophores are considered a promising therapeutic strategy in clinical practice [53,54]. Especially, the 8-hydroxyquinoline (8-HQ) scaffold is a privileged structure used in designing new active agents with therapeutic potential because of its ability of chelating metals [55]. On the other hand, the 8-HQ scaffold possesses poor solubility, bioavailability, and pharmacokinetic parameters [56]. The major challenge in the development of novel anticancer compounds is their selectivity towards tumor tissues. Therefore, it seems rational to use all abnormalities of cancer cells to increase the selectivity of anticancer therapies. Taking advantage of the Warburg effect, the 8-HQ derivatives have been successfully modified by conjugation with different sugar units to improve intramembrane transport and selectivity in drug targeting [57,58]. On the other

hand, it has been widely described in the literature that tumor tissues are heterogeneous, and the levels of overexpression in GLUT transporters are different from cell to cell [59]. Therefore, the combination of glycoconjugation with pH-responsive nanocarriers to exploit the tumor-specific Warburg effect should improve the selectivity of anticancer therapy.
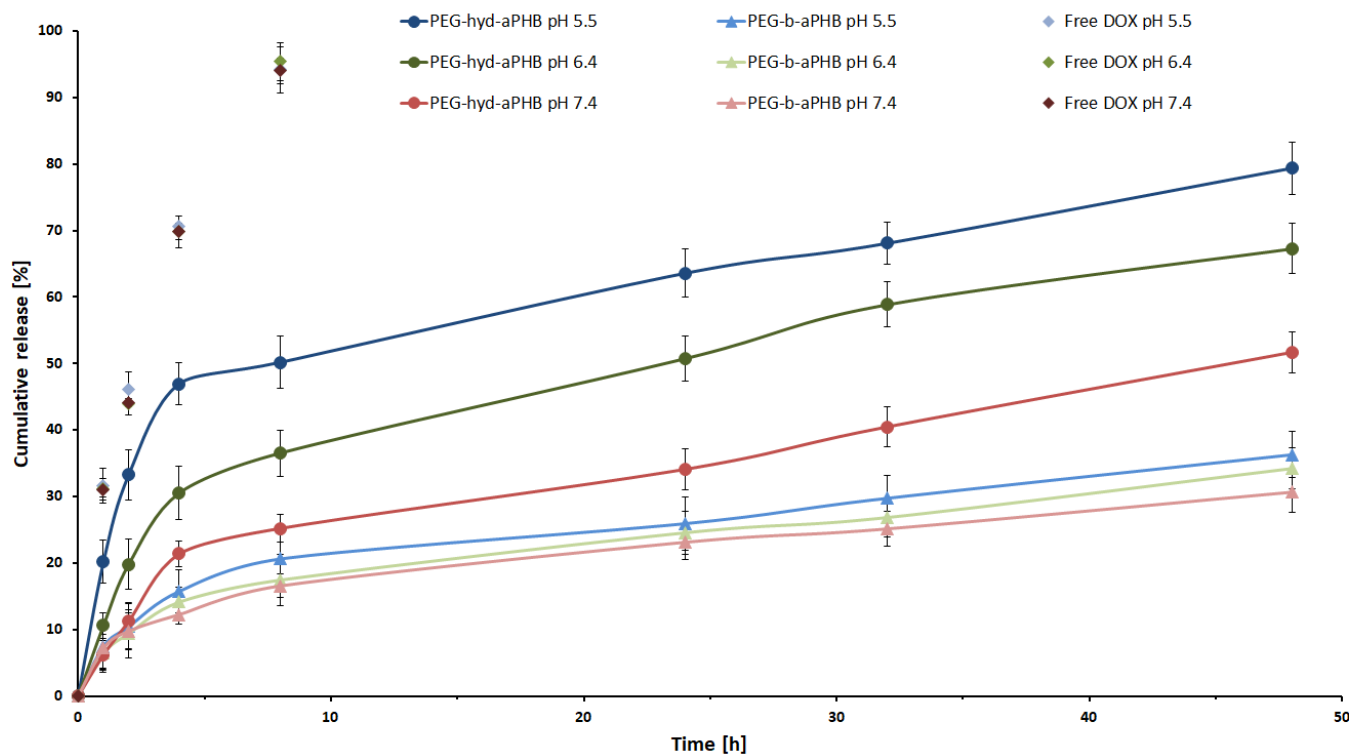
Figure 4. In vitro release profiles for DOX from mPEG-hyd-aPHB micelles, mPEG-b-aPHB micelles and free DOX in PBS buffers at 37 °C. Data are presented as the mean ± SD (*n* = 3).

In the present studies, the cytotoxic activity in vitro of mPEG-hyd-aPHB blank micelles as well as model drugs, i.e., 8-hydroxyquinoline (8HQ), glucose-conjugate 8-hydroxyquinoline (8HQ-Glu), galactose-conjugate 8-hydroxyquinoline (8HQ-Gal), doxorubicin (DOX), and drug-loaded micelles (DOX-micelles, 8HQ-mic, 8HQ-Glu-mic, and 8HQ-Gal-mic) was evaluated by MTT assay. The selectivity of compounds was tested on two cancer cell lines: HCT-116 (colorectal carcinoma cell line) and MCF-7 (human breast adenocarcinoma cell line), as well as, for comparison, on a healthy cell line—Normal Human Dermal Fibroblasts-Neonatal (NHDF-Neo). Overexpression of GLUT transporters as well as a slightly acidic microenvironment have been observed in these cell lines [60–62]. Cells were incubated with the appropriate free drugs or drug-loaded micelles for 24, 48, and 72 h in a concentration range oscillating within their IC$_{50}$ activity.

In the beginning, the effect of blank micelles on cell viability was investigated (Figure 5). The results of the cytotoxicity assay indicate that the blank micelles in the concentration range tested were non-toxic to the tested cell lines, and therefore are not able to inhibit the proliferation of cancer as well as normal cells. This confirms that these nanocarriers could be safely used for research on the drug delivery system targeting cancer. The viability of NHDF cells during incubation with the blank micelles remained in the range of 92–103% at all of the tested concentrations, even after 72 h of the experiment.
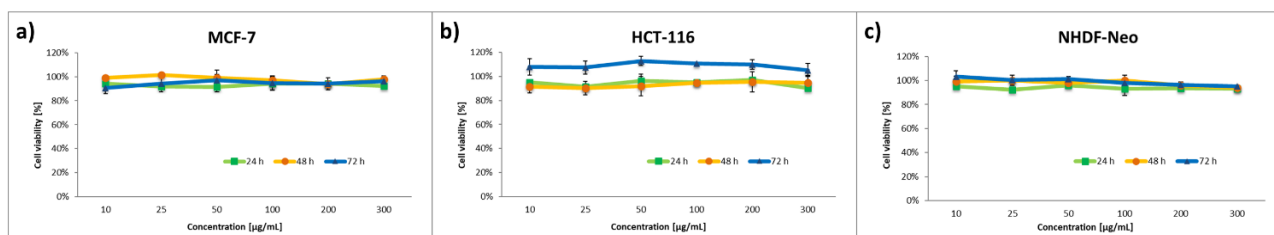
Figure 5. Cytotoxicity of the blank micelles on corresponding cells: (**a**) MCF-7, (**b**) HCT-116, (**c**) NHDF-Neo. Data are presented as the mean ± SD (*n* = 3).

The effect of the nanocarriers was assessed by comparing the cytotoxic activity of free drugs and drug-loaded micelles. The dose-dependent cytotoxic effect of each of the tested compounds is shown in Figures 6–9. Results of the screening tests were used to determine the IC_{50} value, defined as 50% cell growth inhibition in comparison to the untreated control, and are summarized in Table 3. The results showed that free 8HQ-Glu and 8HQ-Gal exhibit constant activity over time against all cell lines tested. The IC_{50} values obtained for free glycoconjugates are mostly higher than for their micelle form (Table 3). The lower cytotoxic activity of free glycoconjugates is probably caused by their hindered penetration through the cell membranes. In the case of drug-loaded micelles, the cell viability decreases with incubation time, which is not noticeable when free glycoconjugates are incubated. This is due to the gradual slow release of the drug from the micelles. The cytotoxicity of the glycoconjugate will increase with the degree of release of the drug from the polymeric carriers. The closure of glycoconjugates in micelles significantly improved their cytotoxic activity—the compound exhibited a strong effect at low doses.
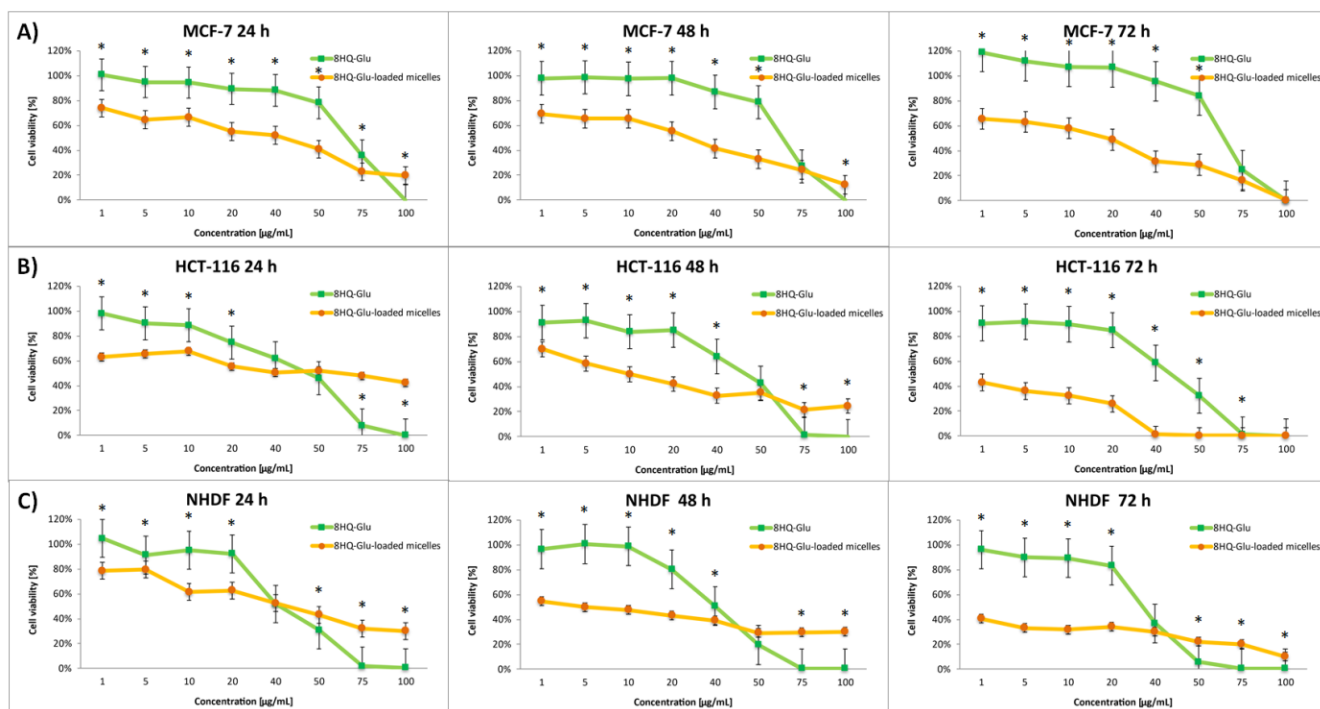
Figure 6. Cytotoxicity of different doses of free 8HQ-Glu and 8HQ-Glu-loaded micelles for MCF-7 (**A**), HCT-116 (**B**), and NHDF-Neo (**C**) cells after 24 h, 48 h, and 72 h of incubation. Data are presented as the mean ± SD (*n* = 3). The statistical significance between compounds was calculated with a *t*-test with *p*-value < 0.05, and indicated by an asterisk.
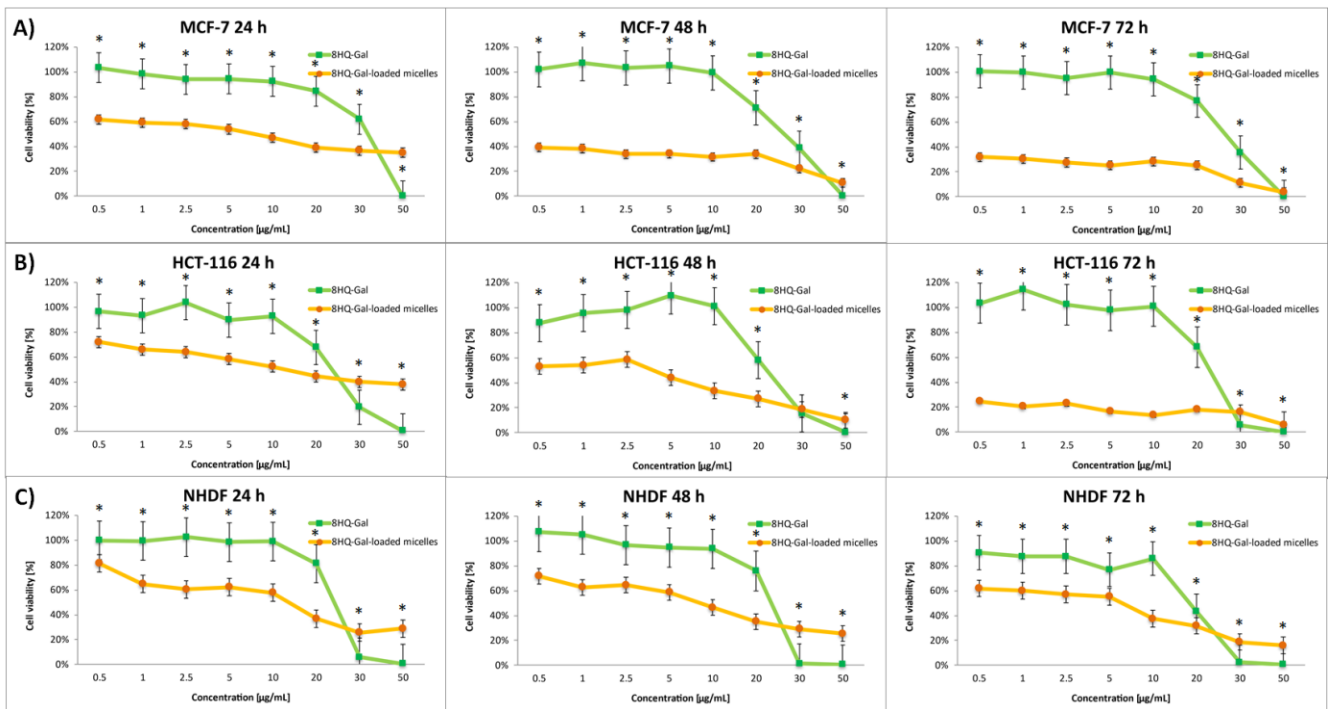
Figure 7. Cytotoxicity of different doses of free 8HQ-Gal and 8HQ-Gal-loaded micelles for MCF-7 (**A**), HCT-116 (**B**), and NHDF-Neo (**C**) cells after 24 h, 48 h, and 72 h of incubation. Data are presented as the mean $\pm$ SD (n = 3). The statistical significance between compounds was calculated with a *t*-test with *p*-value < 0.05, and indicated by an asterisk.
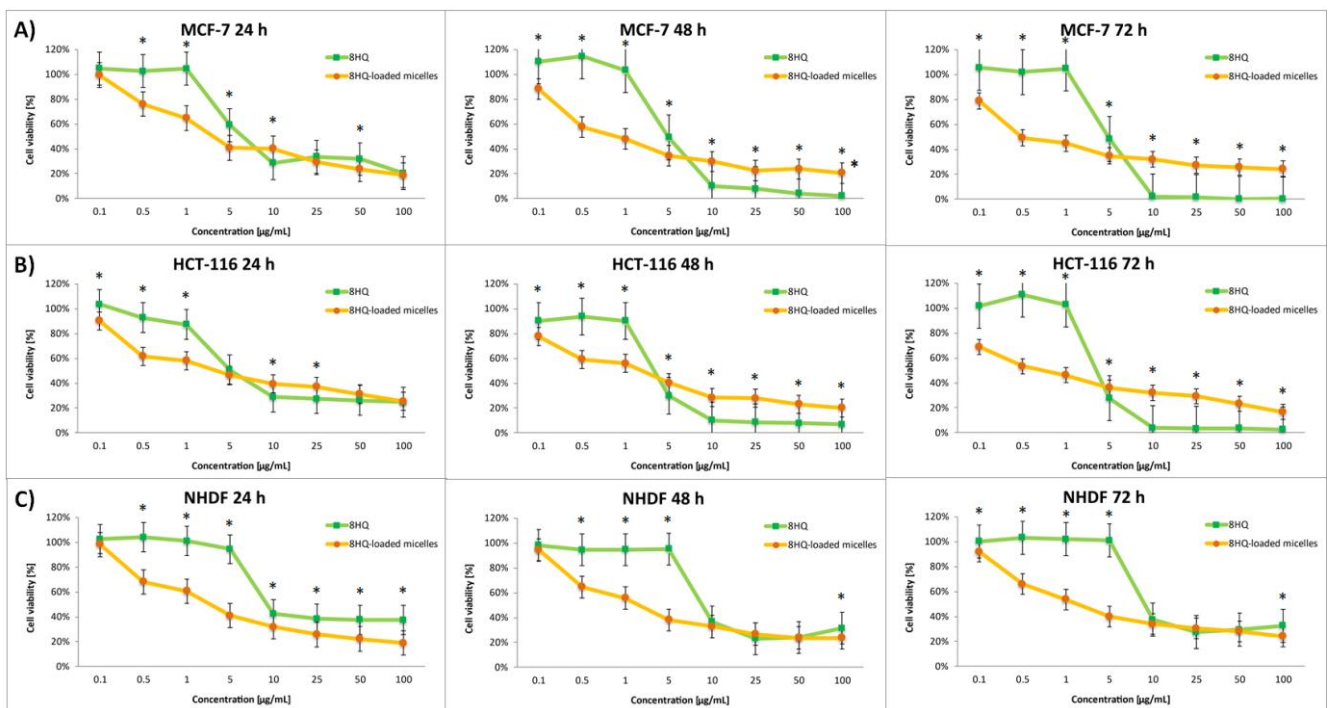
Figure 8. Cytotoxicity of different doses of free 8HQ and 8HQ-loaded micelles for MCF-7 (**A**), HCT-116 (**B**), and NHDF-Neo (**C**) cells after 24 h, 48 h, and 72 h of incubation. Data are presented as the mean $\pm$ SD (n = 3). The statistical significance between compounds was calculated with a *t*-test with *p*-value < 0.05, and indicated by an asterisk.
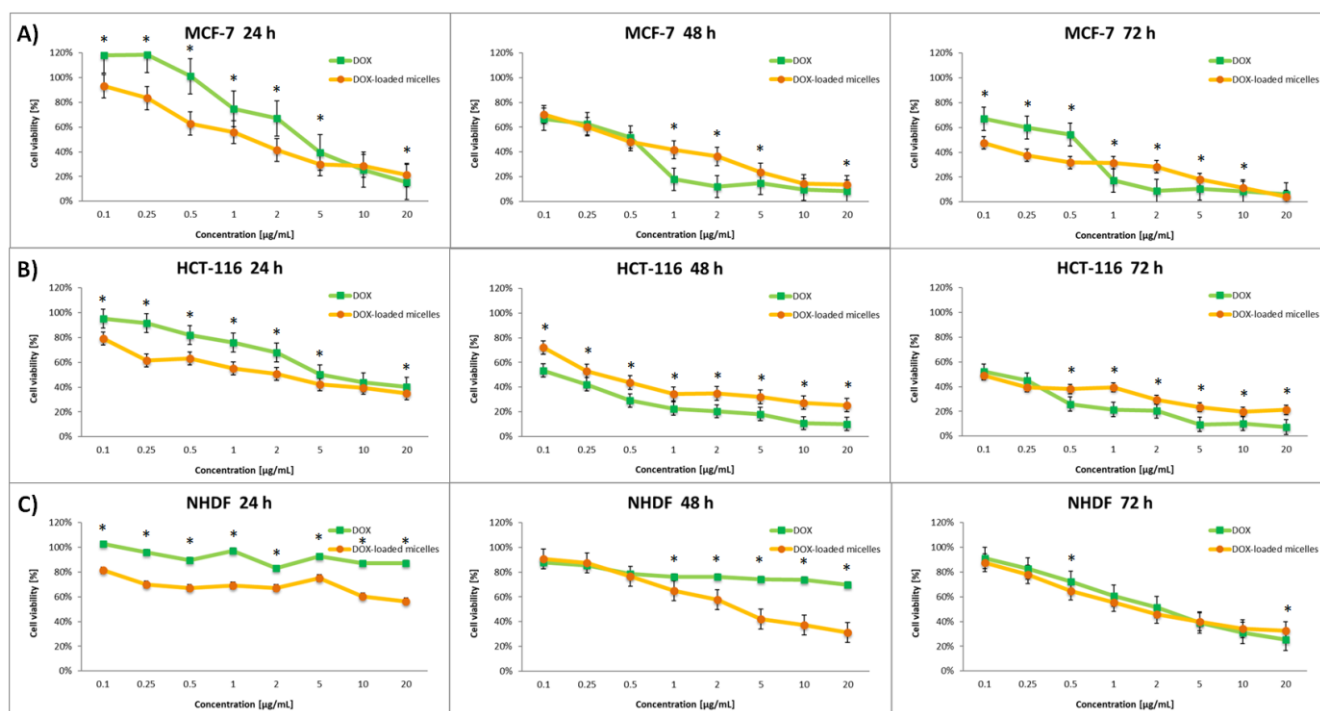
Figure 9. Cytotoxicity of different doses of free DOX and DOX-loaded micelles for MCF-7 (**A**), HCT-116 (**B**), and NHDF-Neo (**C**) cells after 24 h, 48 h, and 72 h of incubation. Data are presented as the mean $\pm$ SD (n = 3). The statistical significance between compounds was calculated with a *t*-test with *p*-value < 0.05, and indicated by an asterisk.

Table 3. Screening of cytotoxicity of tested compounds against MCF-7, HCT-116, and NHDF-Neo cells for 24, 48, and 72 h incubation time.

Compound	Activity IC$_{50}$ [µM] [a]		
	MCF-7		
	24 h	**48 h**	**72 h**
DOX	3.42 $\pm$ 0.03	0.58 $\pm$ 0.02	0.57 $\pm$ 0.02
DOX-micelles	1.96 $\pm$ 0.01	0.52 $\pm$ 0.02	0.13 $\pm$ 0.01
8HQ	7.17 $\pm$ 0.21	2.86 $\pm$ 0.09	3.01 $\pm$ 0.05
8HQ-mic [b]	4.82 $\pm$ 0.17	2.11 $\pm$ 0.11	0.75 $\pm$ 0.04
8HQ-Glu	65.86 $\pm$ 2.22	62.07 $\pm$ 1.84	63.57 $\pm$ 2.01
8HQ-Glu-mic [c]	37.57 $\pm$ 0.92	3.85 $\pm$ 0.19	0.59 $\pm$ 0.02
8HQ-Gal	26.39 $\pm$ 1.28	23.15 $\pm$ 0.99	24.60 $\pm$ 0.52
8HQ-Gal-mic [d]	5.59 $\pm$ 0.14	0.21 $\pm$ 0.01	0.19 $\pm$ 0.01

Compound	Activity IC$_{50}$ [µM] [a]		
	HCT-116		
	24 h	**48 h**	**72 h**
DOX	6.94 $\pm$ 0.33	0.095 $\pm$ 0.01	0.105 $\pm$ 0.01
DOX-micelles	2.36 $\pm$ 0.08	0.45 $\pm$ 0.01	0.078 $\pm$ 0.01
8HQ	9.33 $\pm$ 0.22	4.12 $\pm$ 0.12	4.40 $\pm$ 0.08
8HQ-mic [b]	4.95 $\pm$ 0.16	1.80 $\pm$ 0.05	0.91 $\pm$ 0.04
8HQ-Glu	49.67 $\pm$ 1.32	47.20 $\pm$ 1.14	45.73 $\pm$ 1.81
8HQ-Glu-mic [c]	49.60 $\pm$ 2.11	8.46 $\pm$ 0.12	0.38 $\pm$ 0.02
8HQ-Gal	22.10 $\pm$ 0.84	23.09 $\pm$ 0.92	22.52 $\pm$ 1.02
8HQ-Gal-mic [d]	10.83 $\pm$ 0.33	2.64 $\pm$ 0.12	0.017 $\pm$ 0.01

Table 3. *Cont.*

Compound	Activity IC$_{50}$ [µM] [a]		
	NHDF-Neo		
	24 h	48 h	72 h
DOX	>20	>20	2.71 ± 0.08
DOX-micelles	>20	3.93 ± 0.12	2.50 ± 0.06
8HQ	9.34 ± 0.25	8.97 ± 0.19	9.64 ± 0.32
8HQ-mic [b]	5.18 ± 0.26	3.96 ± 0.12	3.97 ± 0.09
8HQ-Glu	41.00 ± 2.01	41.11 ± 1.73	30.02 ± 0.94
8HQ-Glu-mic [c]	41.70 ± 1.42	22.53 ± 0.65	13.38 ± 0.39
8HQ-Gal	20.14 ± 0.75	21.77 ± 0.89	18.30 ± 0.74
8HQ-Gal-mic [d]	7.47 ± 0.17	5.55 ± 0.17	2.79 ± 0.13

[a] Cytotoxicity was evaluated using the MTT assay; [b] 8HQ-loaded micelles; [c] 8HQ-Glu-loaded micelles; [d] 8HQ-Gal-loaded micelles. Data are presented as the mean ± SD (*n* = 3).

The main challenge in the development of new pharmaceuticals is their selectivity. The optimal drug should target only cancer cells and save healthy ones. Unfortunately, the tested glycoconjugates (8HQ-Glu and 8HQ-Gal) turned out to be toxic also to healthy cells (NHDF-Neo). The lack of selectivity is probably due to the mechanism by which the drug penetrates the cell. Table 4 presents the selectivity index of the tested compounds after 72 h of incubation. The selectivity index (SI) was calculated as a ratio of the IC$_{50}$ value determined for normal cells to the IC$_{50}$ value determined for cancer cells. The higher the SI, the safer and more selective the test compound is. It is worth noting that 8HQ-Glu-mic and 8HQ-Gal-mic showed high selectivity towards HCT-116 cells (SI = 35.21 and 164.12, respectively) and slightly lower selectivity towards MCF-7 cells (SI = 22.68 and 14.68, respectively).

Table 4. Selectivity index (SI) of tested compounds after 72 h incubation time.

Compound	Selectivity Index (SI) [a]	
	MCF-7	HCT-116
DOX	4.75	25.81
DOX-micelles	19.23	32.05
8HQ	3.20	2.19
8HQ-mic [b]	5.29	4.36
8HQ-Glu	0.47	1.39
8HQ-Glu-mic [c]	22.68	35.21
8HQ-Gal	0.74	0.81
8HQ-Gal-mic [d]	14.68	164.12

[a] Selectivity index (SI) was calculated as a ratio of the IC50 value for healthy cells (NHDF-Neo) and the IC50 value for cancer cells (MCF-7 or HCT-116); [b] 8HQ-loaded micelles; [c] 8HQ-Glu-loaded micelles; [d] 8HQ-Gal-loaded micelles.

The above results suggest a different kind of drug-loaded micelle interactions with normal cells compared to colon and breast cancer cells. The difference may be due to the environment surrounding the cells. The use of micelles allows the release of the drug in a low-pH environment, thereby increasing drug accumulation in the tumor and preventing early drug release into systemic circulation. Thus, hydrazone linkage could maintain stability in normal cells, but by taking advantage of the acidic environment near the tumor cells, the micelles can release the drug already near the tumor cell. On the other hand, the non-polar nature of the released glycoconjugates should facilitate the process of crossing the phospholipid bilayer through passive diffusion and cell penetration, where intracellular hydrolytic enzymes are then able to remove acetyl groups in sugar units. Due to the nature of the micelles, it is necessary to load them with hydrophobic compounds such as glycoconjugates with acetyl protection of the hydroxyl groups. One

of the future possibilities to improve the selectivity even more is to develop a material that allows the closure of hydrophilic glycoconjugates with free OH groups in the sugar unit. Such compounds have the potential to penetrate the tumor cell by active transport through GLUT transporters. Another possibility is for micelles to enter the neoplastic cell by endocytosis. Then, there will be a gradual degradation of pH-sensitive micelles already in the tumor cell and the gradual release of cytotoxic drugs. In healthy tissue, the drug is released less or not at all, due to the less favorable environment not leading to the degradation of the nanocarriers.

To approximate the mechanism of compound penetration cells, experiments were performed with 8HQ. This compound shows poor bioavailability, so when released from micelles near the cancer cell, it should show a similar effect to free 8HQ due to the impeded ability of the compound to cross into the cell. The experiments showed that 8HQ-loaded micelles exhibited higher proliferation inhibition compared to free 8HQ toward HCT-116 and MCF-7 cells in the concentration range tested. In addition, the maximum cytotoxic dose of free 8HQ can be observed already after 48 h. In contrast, in the case of 8HQ-mic, the drug is released over time and causes the gradual death of tumor cells for 72 h of the experiment. Therefore, we are probably dealing with the penetration of micelles by endocytosis into the tumor cell and the slow release of the loaded 8HQ inside the cell. However, no mechanism of action can be excluded at this step. Additionally, more detailed studies are needed to determine the penetration mechanism and treatment options. It should be noted that, in the case of 8HQ and 8HQ-mic, there was only a slight improvement in the selectivity index. This suggests that both the micelles and the sugar fragment are needed to improve the activity of free 8HQ. Most of all, the addition of a sugar unit allowed improvement of the selectivity of the tested compounds (as can be noticed from the examples of the compounds 8HQ-Glu-mic and 8HQ-Gal-mic). Thus, the synergistic action of pH-responsive nanocarriers and glycoconjugation could exhibit better efficacy through higher toxicity and lower side effects.

Experiments have also been carried out on the standard drug used as an anticancer agent—doxorubicin. As with glycoconjugates, it has been found that the DOX is released gradually from the micelles. Finally, after 72 h of the experiment in vitro, DOX-loaded micelles showed comparable antiproliferative activity compared to unmodified free DOX against various cancer cell lines and a higher selectivity index in comparison to free DOX. The entrapment of the drug in the carriers enhances the therapeutic effect by protecting the drug from early degradation and prolongs the release of the reduced dose of the drug locally, not systemically.

3.5. Apoptosis and Cell Cycle Analyses by Flow Cytometry

After completing the MTT cytotoxicity test and determining the IC_{50} parameters for compounds, a test using Annexin V-FITC and Propidium Iodide (PI) was performed, aimed at determining what type of cell death is caused by the tested compounds. The compounds were selected at concentrations equal to their previously calculated IC_{50} value. The experiments were carried out for the MCF-7 and HCT-116 tumor cell line and the NHDF-Neo healthy cell line, for the one-time test of 24 h cell incubation with compound solutions. The results of the apoptosis analysis using the flow cytometry method are shown in Figures 10 and S7. Apoptosis is a natural biological process involving programmed or suicidal cell death, which plays an important role in maintaining the correct homeostasis between proliferation and cell death. The test carried out allows the distinguishing of live cells from apoptotic and necrotic cell subpopulations, which is a source of important information on the cytotoxicity of chemicals. Annexin V-FITC labels the phosphatidylserine sites that, after the start of apoptosis, are located on an outer layer of the cell membrane, enabling the detection of early apoptosis. PI labels intracellular DNA (PI binds stoichiometrically to DNA) in cells during late apoptosis and necrosis, where the cell membrane has been disturbed. This combination allows for the differentiation of early apoptotic (A+/P−), late

apoptotic (A+/P+), necrotic (A−/P+), and viable cells (A−/P−), which can be quantified by flow cytometry.
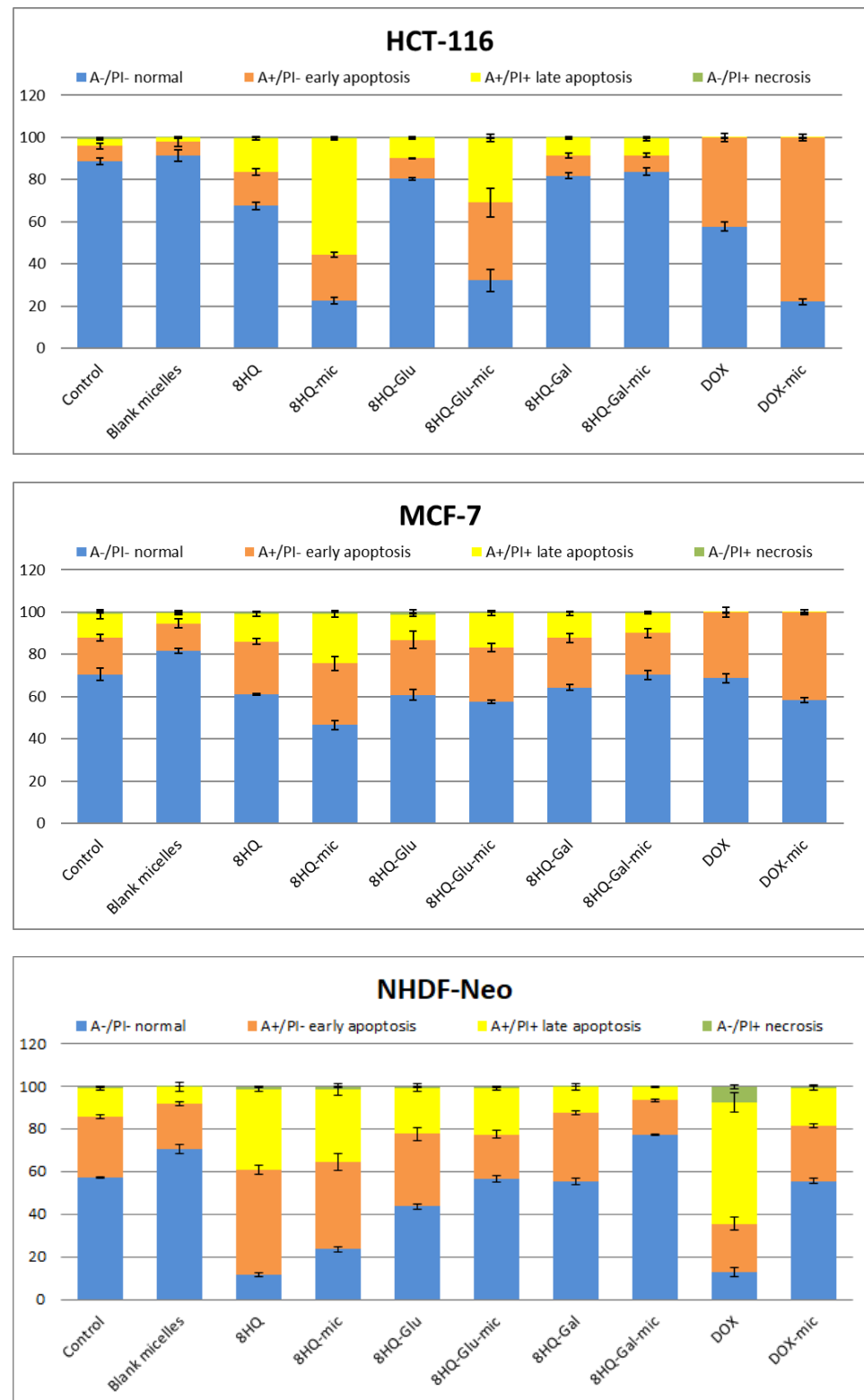
Figure 10. Flow cytometry analysis of HCT-116, MCF-7, and NHDF-Neo cell apoptosis induced by tested compounds at a dose equal to the previously calculated IC_{50} value after incubation for 24 h. Apoptotic effects as determined by Annexin V-FITC and PI assays. Data are presented as mean $\pm$ SD ($n = 3$).

Figure 10 shows the level of induction of apoptosis by the tested compound. After 24 h of incubation, no necrotic conditions were detected in any of the cell lines used. On the other hand, the percentage of cells in both early and late apoptosis was observed. This means that the applied IC_{50} dose affects the entry of cells into the apoptosis pathway and does not cause uncontrolled pathological cell death as a result of mechanical damage. As can be seen, blank micelles, comparable to the untreated control group, show no apoptosis characteristics after 24 h of incubation. Thus, the results of the apoptosis test confirmed the negligible toxic effect of the nanocarriers on the cells tested. On the other hand, entrapment of drugs in carriers, in almost every case, increased the rate of apoptosis of tumor cells compared to free drugs. The highest rate of apoptosis in both cancer cell lines was recorded for 8HQ-mic (79% for HCT-116 and 52% for MCF-7, respectively), which was much higher than for free 8HQ (33% for HCT-116 and 40% for MCF-7). At the same time, this compound showed high toxicity also to healthy cells (76% for NHDF-Neo). These results are in agreement with the MTT cytotoxicity assays described previously. A high share of dead cells was also observed for the compounds 8HQ-Glu-mic (69% for HCT-116 and 42% for MCF-7) and DOX-mic (78% for HCT-116 and 42% for MCF-7). Moreover, 8HQ-Glu-mic and DOX-mic induce both early and late apoptosis much more effectively than free 8HQ-Glu (20% for HCT-116 and 41% for MCF-7) and free DOX (45% for HCT-116 and 34% for MCF-7). The opposite is true for the NHDF-Neo healthy cell line, where the entrapment of drugs in micelles resulted in lower toxicity to these cells. The percentage of apoptotic cells is higher after treating healthy cells with free drugs than with drug-loaded micelles. The results of the measurements performed do not show clear apoptotic changes for 8HQ-Gal and 8HQ-Gal-mic, which may be due to the short incubation time. Extending the incubation time to 72 h would probably give better results, which would be reflected in the results of the MTT cytotoxicity tests. A higher percentage of apoptotic cells was observed in the HCT-116 cell line, which is also consistent with the results of the MTT cytotoxicity assays. This suggests that the cells of the colon cancer line are particularly sensitive to the compounds tested. The insensitivity of MCF-7 cells can be explained by the short incubation time of cells with test drugs.

After analyzing the type of cell death that is induced by the tested compounds, their influence on the progression of the cell cycle was investigated using the flow cytometry technique. The method of cell lysis and isolation of cell nuclei was used for the study. Namely, the collected cells were treated with a hypotonic buffer with a lysis effect, containing propidium iodide, which can bind to DNA by intercalation. It is known that cancer cells are characterized by uncontrolled cell proliferation. The cell cycle consists of the sequence of cell growth and division. The results of the analysis of the cell cycle distribution induced by tested drugs at a dose equal to the previously calculated IC_{50} value after incubation of 24 h are shown in Figure 11. Untreated cells were considered as controls. For the HCT-116 cell line, an increased Sub-G1 cellular fraction was observed after 24 h of incubation with the IC_{50} doses of 8HQ-mic as well as DOX and DOX-mic, which may suggest an increased sensitivity of the cells of this line to the tested prodrugs and the cytostatic potential of active substances released from the carriers. Cells in the sub-G1 phase correspond to apoptotic cells, so the results are in agreement with the results of the cell apoptosis analysis. Interestingly, the percentage of cells arrested in the Sub-G1 phase after treatment with 8HQ-loaded micelles is higher than for free 8HQ. The remaining compounds tested did not significantly affect the change of cell cycle phases as compared to the control. Cytometric evaluation for the MCF-7 cell line indicated that the effect of the tested compounds after 24 h of incubation did not significantly change the cell cycle phase distribution in comparison to the untreated control populations. The results are in agreement with the apoptosis and cytotoxicity studies performed previously. Perhaps this is caused by insufficient incubation time of the cells with the tested compounds. The results of tests performed on the healthy NHDF-Neo cell line showed cell cycle arrest in the Sub-G1 phase for the compounds 8HQ and 8HQ-mic, as well as DOX and DOX-mic. At the same time, the analyzes confirmed that neither the glycoconjugates nor the drug-loaded micelles

caused any detectable cytotoxic effects. Taking into account the fact that the drugs at the IC_{50} dose were used in the research, inhibition of the NHDF-Neo cell cycle in the G2/M phase, which controls mitosis, was noticed. In general, cells are able to repair damage caused by drug doses. This reflects an increase in the G2/M phase, which does not result in the cell cycle arrest and inhibition of cell division, but a delay in the progression of the cell cycle due to mechanism repair processes that block the entry of cells into mitosis. It is worth emphasizing that the distribution of the cell cycle for the used carriers did not differ from the control data, which confirms the safety of their use in drug delivery systems. These experiments have shown that the developed micelles are safe, which is consistent with the earlier results of the MTT and Annexin V assays.
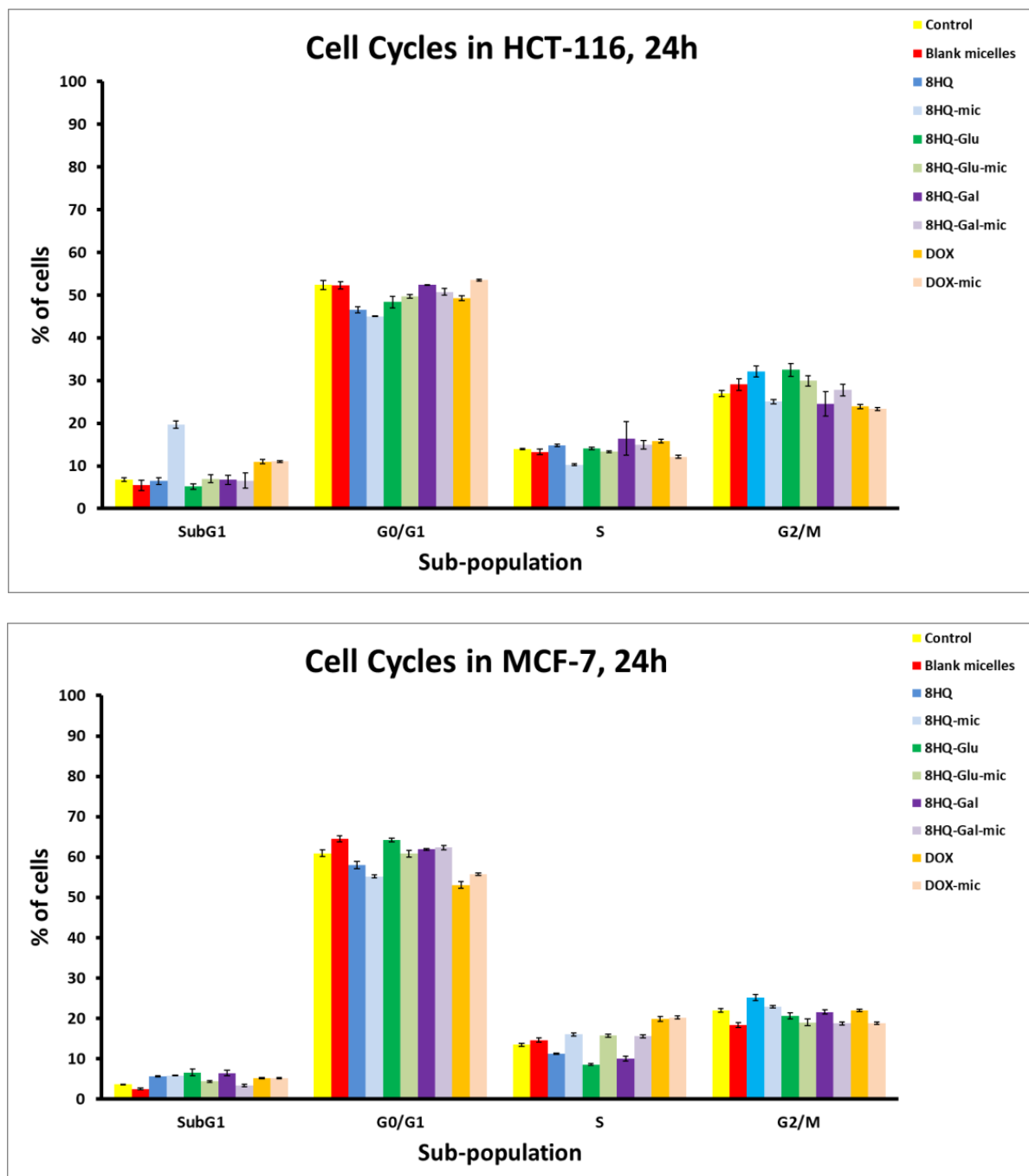
Figure 11. *Cont.*
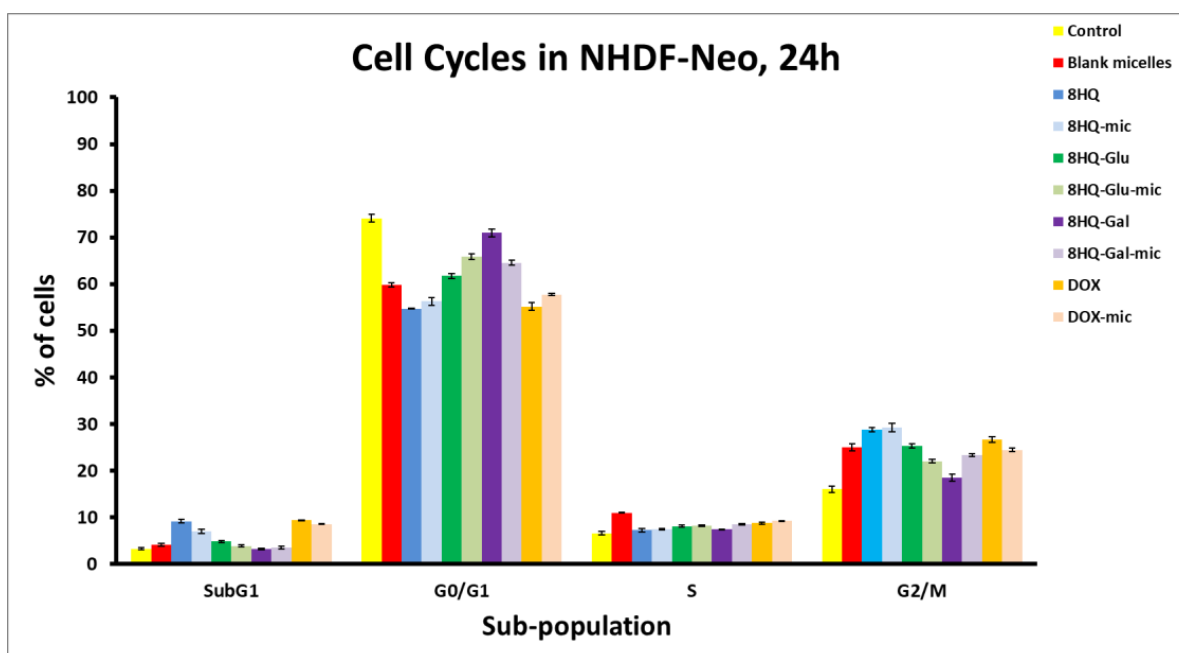
Figure 11. Flow cytometry analysis of HCT-116, MCF-7, and NHDF-NEO cell cycle distribution induced by tested drugs at a dose equal to the previously calculated IC$_{50}$ value after incubation of 24 h. Data are presented as mean $\pm$ SD (n = 3).

The results of the apoptosis and cell cycle analyses by flow cytometry confirmed the anticancer activity of the tested compounds and showed that they exhibit pro-apoptotic properties, without pro-inflammatory processes, and without affecting changes in the cell cycle distribution. The above results confirm that the use of nanocarriers increased the effectiveness of the compounds in the selective destruction of tumor cells, which can be attributed to the increased cellular uptake of carriers and the intracellular controlled release of the active molecules triggered by pH changes.

3.6. Cellular Uptake and Intracellular Drug Release

Whether nanoparticles enter cells is an important factor in cancer therapy. The intracellular localization of DOX-loaded mPEG-hyd-aPHB micelles was investigated in both healthy cells (NHDF-Neo) and cancer cells (HCT116 and MCF-7) using fluorescence microscopy. Cells were incubated with DOX or DOX-loaded micelles for 24 h at a concentration of 1 μM (concentration equal to the previously calculated IC$_{50}$ value). After incubation, the morphological characteristics of the cell nuclei were assessed by staining the cells with Hoechst 33342 dye, which passes through intact cell membranes and intercalates into DNA, then emits blue fluorescence. On the other hand, DOX, as a fluorescent compound, is visible in the red fluorescence channel. As shown in Figure 12, the free doxorubicin was found in the nuclei of all cell lines studied, as evidenced by a co-localization with the blue fluorescence of Hoechst 33342. However, DOX-loaded micelles were observed in the cytoplasm and nuclei. This can be attributed to the different cellular uptake mechanisms of free drugs and drug-loaded micelles. Free DOX was brought immediately into the cells through a passive diffusion mechanism, while nanosized DOX-loaded micelles were mostly internalized via an endocytosis process. Controlled release of the drug from the micelles, under the influence of pH, then delayed the delivery of DOX to the nucleus. However, the tumor's acidic microenvironment could cause the breaking of the hydrazone linkage which could release the drug extracellularly. Because DOX itself is a fluorescent molecule, the intensity of red fluorescence in the cells should be equal to the amount of DOX uptake by cancer cells. The tested cancer cells (MCF-7 and HCT-116) treated with DOX-loaded mPEG-hyd-aPHB micelles revealed a higher intensity of red fluorescence in

the nuclei compared to healthy NHDF-Neo cells, in which most of the DOX was observed in the cytoplasm. The observation could be attributed to the exhibition of intracellular drug-release behavior by the pH-responsive mPEG-hyd-aPHB micelles after they were internalized into cells. This is probably due to the faster release of DOX from micelles at acidic endo-lysosomal pH in cancer cells and the self-quenching effect of doxorubicin encapsulated in nanocarriers before release [63]. The acidic endo-lysosomal pH allows the cleavage of hydrazone bonds in mPEG-hyd-aPHB micelles, thus leading to prompt intracellular drug release from nanocarriers. The performed microscopic imaging confirmed that mPEG-hyd-aPHB nanocarriers could efficiently deliver DOX to tumor cells. The fluorescence intensity quantization method from the row images is presented in Supplementary File Figure S8. The signal intensity was measured, then followed by the digital quantization procedure presented previously [64].
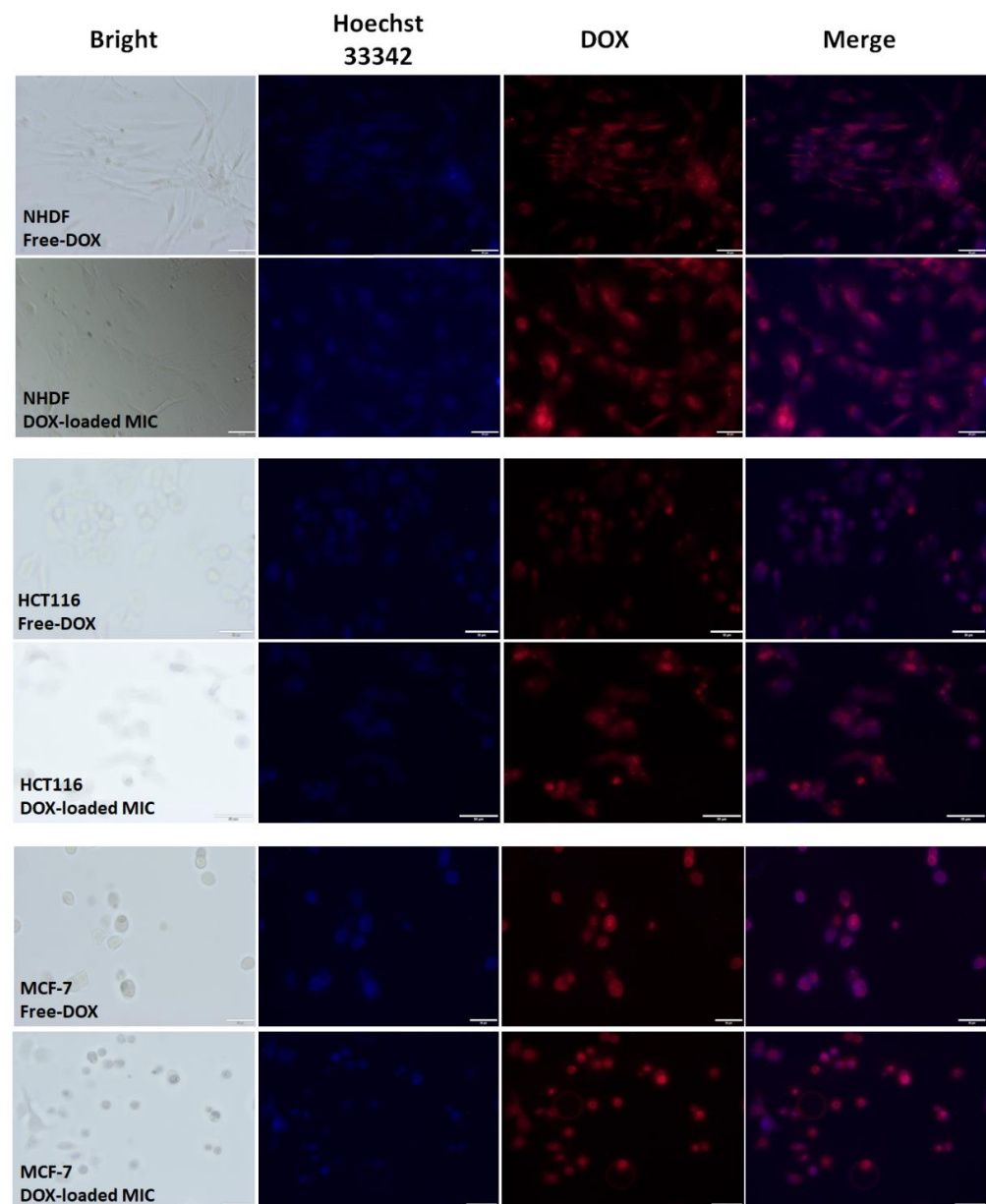
Figure 12. Microscopic images of MCF-7, HCT-116, and NHDF-Neo cells after 24 h of incubation with DOX and DOX-loaded mPEG-hyd-aPHB micelles (DOX dose: 1 μM). Images from left to right show cell nuclei stained by Hoechst 33342 (blue), DOX fluorescence in cells (red), and overlays of blue and red images. Scale bar: 50 μm.

4. Conclusions

In summary, biodegradable poly(ethylene glycol)-hyd-poly([R,S]-3-hydroxybutyrate) was synthesized via the anionic ring-opening polymerization of β-butyrolactone initiated by a hydrazone-functionalized PEG macroinitiator. The amphiphilic diblock copolymer could readily self-organize to form core-shell structured micelles (~70 nm determined by DLS and TEM) in an aqueous medium. The micelles were stable in physiological conditions (pH 7.4), while acid-triggered destruction of the hydrazone linkage caused shedding of the PEG chains, resulting in the release of the drug. In vitro drug release studies revealed that after 8 h, 21%, 37%, and 47% of the drug were released under pH 7.4, 6.4, and 5.5, respectively, demonstrating pH-dependent drug release behavior. The anticancer agents 8HQ, 8HQ-Glu, 8HQ-Gal, and DOX were effectively loaded into micelles to improve the metabolic stability and selectivity of tumor therapy. Red fluorescence signals, from the row images obtained after 24 h of incubation with micelles loaded with doxorubicin, were higher. The computational image preprocessing, as a quantization method, confirms better bioavailability of the novel anticancer agents. The in vitro cytotoxicity studies confirmed that blank mPEG-hyd-aPHB micelles are non-toxic towards HCT-116 and MCF-7 cells as well as, most importantly, towards healthy cell lines NHDF-Neo. Moreover, MTT assay results revealed that drug-loaded micelles efficiently inhibit cancer cell proliferation and promote the apoptosis of tumor cells. In some cases, especially after 72 h of incubation, 8HQ-glycoconjugates, which are still being investigated as potential anti-neoplastic agents, exhibit cytotoxicity comparable to the known drug DOX. However, even more importantly, the loading of drugs into micelles significantly increases their selectivity. This is particularly evident in the case of 8-HQ-glycoconjugates, for which the selectivity index in comparison to free drugs has increased, at best by up to two hundred times, and in other cases in the range of 19 to 48 times. The enhanced selectivity and antitumor efficacy of 8HQ-glycoconjugate-loaded micelles over free 8HQ are attributed to the joint effects of several factors, including taking advantage of the Warburg effect, i.e., the pH-triggered drug release, facilitated intermembrane transport of glycoconjugates, and prolonged circulation time or enhanced cellular internalization of nanocarriers by tumor cells. The strategy of a combination of pH-sensitive nanocarriers with glycoconjugation of the drug molecule provides an alternative for the design of sophisticated multi-stimuli nanocarriers to increase the selectivity of anticancer therapy. These promising in vitro results encourage the expansion of the panel of micelle loaded compounds, in which a sugar moiety has been attached to the drug in order to improve its selectivity. If subsequent results confirm the observations made so far, it will be advisable to select the best candidates for the next stage of in vivo tests.

Supplementary Materials: The following supporting information can be downloaded at: https://www.mdpi.com/article/10.3390/pharmaceutics14020290/s1, Figure S1: Structure of glycoconjugates (A) 8-((1-(2,3,4,6-tetra-O-acetyl-β-D-glucopyranosyl)-1H-1,2,3-triazol-4-yl)methoxy)quinoline (8HQ-glucose conjugate–8HQ-Glu) and (B) 8-((1-(2,3,4,6-tetra-O-acetyl-β-D-galactopyranosyl)-1H-1,2,3-triazol-4-yl)methoxy)quinoline (8HQ-galactose conjugate–8HQ-Gal); Figure S2: 1H NMR spectrum (CDCl3, 600 MHz) of PEG-NPC, PEG-NH-NH2 and PEG-hyd-LEV; Figure S3: (a) 1H NMR spectrum (CDCl3, 600 MHz) and (b) SEC traces of mPEG-b-aPHB; Figure S4: The possible routes of crotonate end-groups forming i.e. (i) abstraction of the acidic proton of a monomer methylene group with formation of lactone enolate, followed by elimination reaction to form a crotonate anion, which initiates further polymerization anionic ring-opening polymerization of β-butyrolactone; (ii) chain transfer to the copolymer according to the E1cB mechanism; Figure S5: 1H NMR (D2O, 600MHz) spectrum of (a) mPEG-hyd-aPHB micelles, (b) mPEG-hyd-aPHB micelles using water suppression technique; (c) mPEG-b-aPHB micelles and (d) mPEG-b-aPHB micelles (water suppression); Figure S6: CMC of (a) mPEG-hyd-aPHB and (b) mPEG-b-aPHB; Figure S7: Typical graphs of Annexin V/PI double staining apoptosis assay; Figure S8: Image processing method for a fluorescence intensity measurements, based on the Figure 12.

References

1. Sun, H.; Zhong, Z. 100th Anniversary of Macromolecular Science Viewpoint: Biological Stimuli-Sensitive Polymer Prodrugs and Nanoparticles for Tumor-Specific Drug Delivery. *ACS Macro Lett.* **2020**, *9*, 1292–1302. [CrossRef]
2. Kamaly, N.; Yameen, B.; Wu, J.; Farokhzad, O.C. Degradable Controlled-Release Polymers and Polymeric Nanoparticles: Mechanisms of Controlling Drug Release. *Chem. Rev.* **2016**, *116*, 2602–2663. [CrossRef] [PubMed]
3. Sun, Q.; Zhou, Z.; Qiu, N.; Shen, Y. Rational Design of Cancer Nanomedicine: Nanoproperty Integration and Synchronization. *Adv. Mater.* **2017**, *29*. [CrossRef] [PubMed]
4. Blanco, E.; Shen, H.; Ferrari, M. Principles of nanoparticle design for overcoming biological barriers to drug delivery. *Nat. Biotechnol.* **2015**, *33*, 941–951. [CrossRef]
5. Tyler, B.; Gullotti, D.; Mangraviti, A.; Utsuki, T.; Brem, H. Polylactic acid (PLA) controlled delivery carriers for biomedical applications. *Adv. Drug Deliv. Rev.* **2016**, *107*, 163–175. [CrossRef]
6. Grossen, P.; Witzigmann, D.; Sieber, S.; Huwyler, J. PEG-PCL-based nanomedicines: A biodegradable drug delivery system and its application. *J. Control. Release* **2017**, *260*, 46–60. [CrossRef]
7. Michalak, M.; Kurcok, P.; Hakkarainen, M. Polyhydroxyalkanoate-based drug delivery systems. *Polym. Int.* **2016**, *66*, 617–622. [CrossRef]
8. Domiński, A.; Konieczny, T.; Duale, K.; Krawczyk, M.; Pastuch-Gawołek, G.; Kurcok, P. Stimuli-Responsive Aliphatic Polycarbonate Nanocarriers for Tumor-Targeted Drug Delivery. *Polymers* **2020**, *12*, 2890. [CrossRef]
9. Luo, Z.; Wu, Y.; Li, Z.; Loh, X.J. Recent Progress in Polyhydroxyalkanoates-Based Copolymers for Biomedical Applications. *Biotechnol. J.* **2019**, *14*, e1900283. [CrossRef]
10. Jedliński, Z.; Kurcok, P.; Lenz, R.W. First Facile Synthesis of Biomimetic Poly-(R)-3-hydroxybutyrate via Regioselective Anionic Polymerization of (S)-β-Butyrolactone. *Macromolecules* **1998**, *31*, 6718–6720. [CrossRef]
11. Kurcok, P.; Dubois, P.; Jerome, R. Polymerization of β-butyrolactone initiated with Al(OiPr)3. *Polym. Int.* **1996**, *41*, 479–485. [CrossRef]
12. Khalil, A.; Cammas-Marion, S.; Coulembier, O. Organocatalysis applied to the ring-opening polymerization of β-lactones: A brief overview. *J. Polym. Sci. Part A Polym. Chem.* **2019**, *57*, 657–672. [CrossRef]
13. Domiński, A.; Konieczny, T.; Zięba, M.; Klim, M.; Kurcok, P. Anionic Polymerization of β-Butyrolactone Initiated with Sodium Phenoxides. The Effect of the Initiator Basicity/Nucleophilicity on the ROP Mechanism. *Polymers* **2019**, *11*, 1221. [CrossRef] [PubMed]
14. Kurcok, P.; Jedlinski, Z.; Kowalczuk, M. Reactions of β-lactones with potassium alkoxides and their complexes with 18-crown-6 in aprotic solvents. *J. Org. Chem.* **1993**, *58*, 4219–4220. [CrossRef]
15. Dong, X.; Robinson, J.R. The role of neutral donor ligands in the isoselective ring-opening polymerization of rac-β-butyrolactone. *Chem. Sci.* **2020**, *11*, 8184–8195. [CrossRef]
16. Tang, X.; Chen, E.Y.-X. Chemical synthesis of perfectly isotactic and high melting bacterial poly(3-hydroxybutyrate) from bio-sourced racemic cyclic diolide. *Nat. Commun.* **2018**, *9*, 2345. [CrossRef]
17. Jiang, G.; Hill, D.J.; Kowalczuk, M.; Johnston, B.; Adamus, G.; Irorere, V.; Radecka, I. Carbon Sources for Polyhydroxyalkanoates and an Integrated Biorefinery. *Int. J. Mol. Sci.* **2016**, *17*, 1157. [CrossRef]
18. Zawidlak-Węgrzyńska, B.; Kawalec, M.; Bosek, I.; Łuczyk-Juzwa, M.; Adamus, G.; Rusin, A.; Filipczak, P.; Głowala-Kosińska, M.; Wolańska, K.; Krawczyk, Z.; et al. Synthesis and antiproliferative properties of ibuprofen–oligo(3-hydroxybutyrate) conjugates. *Eur. J. Med. Chem.* **2010**, *45*, 1833–1842. [CrossRef]

19. Elustondo, P.A.; Angelova, P.R.; Kawalec, M.; Michalak, M.; Kurcok, P.; Abramov, A.Y.; Pavlov, E.V. Polyhydroxybutyrate Targets Mammalian Mitochondria and Increases Permeability of Plasmalemmal and Mitochondrial Membranes. *PLoS ONE* **2013**, *8*, e75812. [CrossRef]

20. Barouti, G.; Jaffredo, C.G.; Guillaume, S.M. Advances in drug delivery systems based on synthetic poly(hydroxybutyrate) (co)polymers. *Prog. Polym. Sci.* **2017**, *73*, 1–31. [CrossRef]

21. DeBerardinis, R.J.; Chandel, N.S. We need to talk about the Warburg effect. *Nat. Metab.* **2020**, *2*, 127–129. [CrossRef] [PubMed]

22. Kato, Y.; Ozawa, S.; Miyamoto, C.; Maehata, Y.; Suzuki, A.; Maeda, T.; Baba, Y. Acidic extracellular microenvironment and cancer. *Cancer Cell Int.* **2013**, *13*, 89. [CrossRef] [PubMed]

23. Barron, C.C.; Bilan, P.J.; Tsakiridis, T.; Tsiani, E. Facilitative glucose transporters: Implications for cancer detection, prognosis and treatment. *Metabolism* **2015**, *65*, 124–139. [CrossRef]

24. Warburg, O. On the origin of cancer cells. *Science* **1956**, *123*, 309–314. [CrossRef] [PubMed]

25. Tekade, R.K.; Sun, X. The Warburg effect and glucose-derived cancer theranostics. *Drug Discov. Today* **2017**, *22*, 1637–1653. [CrossRef] [PubMed]

26. Krawczyk, M.; Pastuch-Gawołek, G.; Pluta, A.; Erfurt, K.; Domiński, A.; Kurcok, P. 8-Hydroxyquinoline Glycoconjugates: Modifications in the Linker Structure and Their Effect on the Cytotoxicity of the Obtained Compounds. *Molecules* **2019**, *24*, 4181. [CrossRef]

27. Calvaresi, E.; Hergenrother, P.J. Glucose conjugation for the specific targeting and treatment of cancer. *Chem. Sci.* **2013**, *4*, 2319–2333. [CrossRef]

28. Deirram, N.; Zhang, C.; Kermaniyan, S.S.; Johnston, A.P.R.; Such, G.K. pH-Responsive Polymer Nanoparticles for Drug Delivery. *Macromol. Rapid Commun.* **2019**, *40*, e1800917. [CrossRef]

29. Kanamala, M.; Wilson, W.R.; Yang, M.; Palmer, B.D.; Wu, Z. Mechanisms and biomaterials in pH-responsive tumour targeted drug delivery: A review. *Biomaterials* **2016**, *85*, 152–167. [CrossRef]

30. Domiński, A.; Krawczyk, M.; Konieczny, T.; Kasprów, M.; Foryś, A.; Pastuch-Gawołek, G.; Kurcok, P. Biodegradable pH-responsive micelles loaded with 8-hydroxyquinoline glycoconjugates for Warburg effect-based tumor targeting. *Eur. J. Pharm. Biopharm.* **2020**, *154*, 317–329. [CrossRef]

31. Gao, W.; Chan, J.M.; Farokhzad, O.C. pH-Responsive Nanoparticles for Drug Delivery. *Mol. Pharm.* **2010**, *7*, 1913–1920. [CrossRef] [PubMed]

32. Sonawane, S.J.; Kalhapure, R.S.; Govender, T. Hydrazone linkages in pH responsive drug delivery systems. *Eur. J. Pharm. Sci.* **2017**, *99*, 45–65. [CrossRef] [PubMed]

33. Takahashi, A.; Yamamoto, Y.; Yasunaga, M.; Koga, Y.; Kuroda, J.; Takigahira, M.; Harada, M.; Saito, H.; Hayashi, T.; Kato, Y.; et al. NC-6300, an epirubicin-incorporating micelle, extends the antitumor effect and reduces the cardiotoxicity of epirubicin. *Cancer Sci.* **2013**, *104*, 920–925. [CrossRef] [PubMed]

34. Kratz, F. INNO-206 (DOXO-EMCH), an Albumin-Binding Prodrug of Doxorubicin Under Development for Phase II Studies. *Curr. Bioact. Compd.* **2011**, *7*, 33–38. [CrossRef]

35. Wang, Z.; Deng, X.; Ding, J.; Zhou, W.; Zheng, X.; Tang, G. Mechanisms of drug release in pH-sensitive micelles for tumour targeted drug delivery system: A review. *Int. J. Pharm.* **2018**, *535*, 253–260. [CrossRef]

36. Jin, Q.; Deng, Y.; Chen, X.; Ji, J. Rational Design of Cancer Nanomedicine for Simultaneous Stealth Surface and Enhanced Cellular Uptake. *ACS Nano* **2019**, *13*, 954–977. [CrossRef]

37. Hatakeyama, H.; Akita, H.; Harashima, H. The Polyethyleneglycol Dilemma: Advantage and Disadvantage of PEGylation of Liposomes for Systemic Genes and Nucleic Acids Delivery to Tumors. *Biol. Pharm. Bull.* **2013**, *36*, 892–899. [CrossRef]

38. Kong, L.; Campbell, F.; Kros, A. DePEGylation strategies to increase cancer nanomedicine efficacy. *Nanoscale Horiz.* **2018**, *4*, 378–387. [CrossRef]

39. Xiao, L.; Huang, L.; Moingeon, F.; Gauthier, M.; Yang, G. pH-Responsive Poly(Ethylene Glycol)-block-Polylactide Micelles for Tumor-Targeted Drug Delivery. *Biomacromolecules* **2017**, *18*, 2711–2722. [CrossRef]

40. Hira, S.K.; Ramesh, K.; Gupta, U.; Mitra, K.; Misra, N.; Ray, B.; Manna, P.P. Methotrexate-Loaded Four-Arm Star Amphiphilic Block Copolymer Elicits CD8+ T Cell Response against a Highly Aggressive and Metastatic Experimental Lymphoma. *ACS Appl. Mater. Interfaces* **2015**, *7*, 20021–20033. [CrossRef]

41. Liu, S.; Ono, R.J.; Yang, C.; Gao, S.; Tan, J.Y.M.; Hedrick, J.L.; Yang, Y.Y. Dual pH-Responsive Shell-Cleavable Polycarbonate Micellar Nanoparticles for in Vivo Anticancer Drug Delivery. *ACS Appl. Mater. Interfaces* **2018**, *10*, 19355–19364. [CrossRef] [PubMed]

42. Gu, Y.; Zhong, Y.; Meng, F.; Cheng, R.; Deng, C.; Zhong, Z. Acetal-Linked Paclitaxel Prodrug Micellar Nanoparticles as a Versatile and Potent Platform for Cancer Therapy. *Biomacromolecules* **2013**, *14*, 2772–2780. [CrossRef] [PubMed]

43. Zhu, Y.; Wang, X.; Zhang, J.; Meng, F.; Deng, C.; Cheng, R.; Feijen, J.; Zhong, Z. Exogenous vitamin C boosts the antitumor efficacy of paclitaxel containing reduction-sensitive shell-sheddable micelles in vivo. *J. Control. Release* **2017**, *250*, 9–19. [CrossRef] [PubMed]

44. Kawalec, M.; Coulembier, O.; Gerbaux, P.; Sobota, M.; De Winter, J.; Dubois, P.; Kowalczuk, M.; Kurcok, P. Traces do matter—Purity of 4-methyl-2-oxetanone and its effect on anionic ring-opening polymerization as evidenced by phosphazene superbase catalysis. *React. Funct. Polym.* **2012**, *72*, 509–520. [CrossRef]

45. Liu, K.L.; Goh, S.H.; Li, J. Controlled synthesis and characterizations of amphiphilic poly[(R,S)-3-hydroxybutyrate]-poly(ethylene glycol)-poly[(R,S)-3-hydroxybutyrate] triblock copolymers. *Polymers* **2007**, *49*, 732–741. [CrossRef]

46. Krawczyk, M.; Pastuch-Gawolek, G.; Mrozek-Wilczkiewicz, A.; Kuczak, M.; Skonieczna, M.; Musiol, R. Synthesis of 8-hydroxyquinoline glycoconjugates and preliminary assay of their β1,4-GalT inhibitory and anti-cancer properties. *Bioorg. Chem.* **2018**, *84*, 326–338. [CrossRef]

47. Won, Y.-Y.; Brannan, A.K.; Davis, H.T.; Bates, F.S. Cryogenic Transmission Electron Microscopy (Cryo-TEM) of Micelles and Vesicles Formed in Water by Poly(ethylene oxide)-Based Block Copolymers. *J. Phys. Chem. B* **2002**, *106*, 3354–3364. [CrossRef]

48. Kawalec, M.; Śmiga-Matuszowicz, M.; Kurcok, P. Counterion and solvent effects on the anionic polymerization of β-butyrolactone initiated with acetic acid salts. *Eur. Polym. J.* **2008**, *44*, 3556–3563. [CrossRef]

49. Cui, C.; Yu, P.; Wu, M.; Zhang, Y.; Liu, L.; Wu, B.; Wang, C.-X.; Zhuo, R.-X.; Huang, S.-W. Reduction-sensitive micelles with sheddable PEG shells self-assembled from a Y-shaped amphiphilic polymer for intracellular doxorubicine release. *Colloids Surf. B Biointerfaces* **2015**, *129*, 137–145. [CrossRef]

50. Wang, D.; Su, Y.; Jin, C.; Zhu, B.; Pang, Y.; Zhu, L.; Liu, J.; Tu, C.; Yan, D.; Zhu, X. Supramolecular Copolymer Micelles Based on the Complementary Multiple Hydrogen Bonds of Nucleobases for Drug Delivery. *Biomacromolecules* **2011**, *12*, 1370–1379. [CrossRef]

51. Wang, N.; Cheng, X.; Li, N.; Wang, H.; Chen, H. Nanocarriers and Their Loading Strategies. *Adv. Health Mater.* **2018**, *8*, e1801002. [CrossRef] [PubMed]

52. Cao, H.; Chen, C.; Xie, D.; Chen, X.; Wang, P.; Wang, Y.; Song, H.; Wang, W. A hyperbranched amphiphilic acetal polymer for pH-sensitive drug delivery. *Polym. Chem.* **2017**, *9*, 169–177. [CrossRef]

53. Santini, C.; Pellei, M.; Gandin, V.; Porchia, M.; Tisato, F.; Marzano, C. Advances in Copper Complexes as Anticancer Agents. *Chem. Rev.* **2013**, *114*, 815–862. [CrossRef] [PubMed]

54. Gaur, K.; Vázquez-Salgado, A.M.; Duran-Camacho, G.; Dominguez-Martinez, I.; Benjamín-Rivera, J.A.; Fernández-Vega, L.; Sarabia, L.C.; García, A.C.; Pérez-Deliz, F.; Román, J.A.M.; et al. Iron and Copper Intracellular Chelation as an Anticancer Drug Strategy. *Inorganics* **2018**, *6*, 126. [CrossRef]

55. Prachayasittikul, V.; Prachayasittikul, V.; Prachayasittikul, S.; Ruchirawat, S. 8-Hydroxyquinolines: A review of their metal chelating properties and medicinal applications. *Drug Des. Dev. Ther.* **2013**, *7*, 1157–1178. [CrossRef]

56. Song, Y.; Xu, H.; Chen, W.; Zhan, P.; Liu, X. 8-Hydroxyquinoline: A privileged structure with a broad-ranging pharmacological potential. *MedChemComm* **2014**, *6*, 61–74. [CrossRef]

57. Pastuch-Gawołek, G.; Malarz, K.; Mrozek-Wilczkiewicz, A.; Musioł, M.; Serda, M.; Czaplińska, B.; Musioł, R. Small molecule glycoconjugates with anticancer activity. *Eur. J. Med. Chem.* **2016**, *112*, 130–144. [CrossRef]

58. Oliveri, V. Glycoconjugates of Quinolines: Application in Medicinal Chemistry. *Mini-Rev. Med. Chem.* **2016**, *16*, 1185–1194. [CrossRef]

59. Cabral, H.; Miyata, K.; Osada, K.; Kataoka, K. Block Copolymer Micelles in Nanomedicine Applications. *Chem. Rev.* **2018**, *118*, 6844–6892. [CrossRef]

60. Brown, R.S.; Wahl, R.L. Overexpression of Glut-1 Glucose Transporter in Human Breast Cancer. *Cancer* **1993**, *72*, 2979–2985. [CrossRef]

61. Haber, R.S.; Rathan, A.; Weiser, K.R.; Pritsker, A.; Itzkowitz, S.H.; Bodian, C.; Slater, G.; Weiss, A.; Burstein, D.E. GLUT1 Glucose Transporter Expression in Colorectal Carcinoma: A marker for poor prognosis. *Cancer* **1998**, *83*, 34–40. [CrossRef]

62. Schindler, M.; Grabski, S.; Hoff, E.; Simon, S.M. Defective pH Regulation of Acidic Compartments in Human Breast Cancer Cells (MCF-7) Is Normalized in Adriamycin-Resistant Cells (MCF-7adr). *Biochemistry* **1996**, *35*, 2811–2817. [CrossRef] [PubMed]

63. Bae, Y.; Fukushima, S.; Harada, A.; Kataoka, K. Design of Environment-Sensitive Supramolecular Assemblies for Intracellular Drug Delivery: Polymeric Micelles that are Responsive to Intracellular pH Change. *Angew. Chem.* **2003**, *115*, 4788–4791. [CrossRef]

64. Skonieczna, M.; Hudy, D.; Poterala-Hejmo, A.; Hejmo, T.; Buldak, R.J.; Dziedzic, A. Effects of Resveratrol, Berberine and Their Combinations on Reactive Oxygen Species, Survival and Apoptosis in Human Squamous Carcinoma (SCC-25) Cells. *Anti-Cancer Agents Med. Chem.* **2019**, *19*, 1161–1171. [CrossRef]

Publikacja P.8

Overcoming Hypoxia-Induced Chemoresistance in Cancer Using
a Novel Glycoconjugate of Methotrexate

M. Woźniak, G. Pastuch-Gawołek, S. Makuch, J. Wiśniewski, P. Ziółkowski, W. Szeja,
M. Krawczyk[*], S. Agrawal[*]

Materiały uzupełniające do publikacji znajdują się w dołączonej płycie CD

Article

Overcoming Hypoxia-Induced Chemoresistance in Cancer Using a Novel Glycoconjugate of Methotrexate

Marta Woźniak [1], Gabriela Pastuch-Gawołek [2,3], Sebastian Makuch [1], Jerzy Wiśniewski [4], Piotr Ziółkowski [1], Wiesław Szeja [2], Monika Krawczyk [2,3,*] and Siddarth Agrawal [1,5,*]

[1] Department of Pathology, Wrocław Medical University, Marcinkowskiego 1, 50-368 Wrocław, Poland; marta.wozniak@umed.wroc.pl (M.W.); sebastian.mk21@gmail.com (S.M.); piotr.ziolkowski@umed.wroc.pl (P.Z.)

[2] Department of Organic Chemistry, Bioorganic Chemistry and Biotechnology, Faculty of Chemistry, Silesian University of Technology, Krzywoustego 4, 44-100 Gliwice, Poland; gabriela.pastuch@polsl.pl (G.P.-G.); wieslaw.szeja@adres.pl (W.S.)

[3] Biotechnology Centre, Silesian University of Technology, Krzywoustego 4, 44-100 Gliwice, Poland

[4] Department of Medical Biochemistry, Wroclaw Medical University, Marcinkowskiego 1, 50-368 Wrocław, Poland; jerzy.wisniewski@umed.wroc.pl

[5] Department and Clinic of Internal Medicine, Occupational Diseases, Hypertension and Clinical Oncology, Wroclaw Medical University, Marcinkowskiego 1, 50-368 Wrocław, Poland

* Correspondence: monika.krawczyk@polsl.pl (M.K.); siddarth@agrawal.pl (S.A.)

Abstract: The oxygen and nutrient-deprived tumor microenvironment is considered a key mechanism responsible for cancer resistance to chemotherapy. Methotrexate (MTX) is a widely incorporated chemotherapeutic agent employed in the treatment of several malignancies. However, drug resistance and systemic toxicity limit the curative effect in most cases. The present work aimed to design, synthesize, and biologically evaluate a novel glucose-methotrexate conjugate (Glu-MTX). Our study showed that Glu-MTX exerts an increased cytotoxic effect on cancer cells in comparison to MTX in hypoxia (1% O_2) and glucose starvation conditions. Furthermore, Glu-MTX was found to inhibit the proliferation and migration of cancer cells more effectively than MTX does. Our results demonstrate that the conjugation of MTX to glucose led to an increase in potency against malignant cells under oxygen and nutrient stress. The observations shed light on a potential therapeutic approach to overcome chemoresistance in cancer.

Keywords: glycoconjugates; tumor microenvironment; methotrexate conjugate; hypoxia; cancer

1. Introduction

Chemotherapy is the leading treatment modality in oncological care and is commonly applied in combination with surgery or radiotherapy, depending on tumor advancement. During cancer progression, the tumor increases in size and triggers a series of events, including hypoxia and a nutrient-deficient environment [1]. These responses arise from the increase in oxygen and nutrient consumption due to significant growth of malignant proliferation, as well as an inadequate supply of substrates to the cells due to the formation of an irregular tumor microvasculature with leaky vessels [2]. An oxygen- and nutrient-deprived tumor microenvironment is considered a key mechanism responsible for cancer resistance to current treatment modalities, including chemotherapy, radiotherapy, and photodynamic therapy [3]. The critical role of hypoxia in chemotherapy resistance is well-documented and involves several pathways, predominantly the upregulation of hypoxia-inducible factor-1α (HIF-1α). The HIF-1α mediates the angiogenesis, invasion, metastasis of malignant cells; induces glucose transporters (GLUT) to increase glucose import; and contributes to chemotherapy resistance by enhancing the expression of membrane efflux pump P-glycoprotein (P-gp), which identifies chemotherapeutic drugs and removes them from cells [4]. These events are among the primary contributors to multidrug resistance,

which often results in cancer relapse and higher mortality [5]. Thus, breaking hypoxia-induced drug resistance is necessary to elevate the efficacy of cancer chemotherapy and increase the patient's lifespan.

To survive in an oxygen- and nutrient-deprived environment and address the energy demands resulting from rapid proliferation, tumor cells significantly increase glucose uptake and the flux of metabolites through glycolysis [6]. This metabolic shift, termed "the Warburg effect", is one of cancer's most common traits and provides clinically corroborated strategies for cancer diagnostics and treatment.

Chemotherapy is the leading treatment modality in oncological care and is commonly applied in combination with surgery or radiotherapy, depending on tumor advancement. The modification of biologically active compounds with polymers is one way to alter and control their pharmacokinetics, biodistribution, and often toxicity [7]. The primary underlying mechanism proposed for nanomedicine-based cancer therapy is passive targeting associated with enhanced permeability and retention [8]. To be most effective, anticancer drugs must penetrate tissue efficiently, reaching all the cancer cells that comprise the target population in a concentration sufficient to exert a therapeutic effect. The therapeutic effect of conjugates of biologically active compounds with polymers is reduced because of limited penetration [9].

Based on the overexpression of specific receptors on tumor cells, ligand-targeted drug delivery has been developed with the ability to efficiently deliver imaging agents in the tumor area or drugs into tumor cells via receptor-mediated endocytosis [10]. As mentioned above, elevated glucose intake and GLUT overexpression frequently occur in neoplasms and provide clinically corroborated strategies for cancer treatment [11–13]. Therefore, glycoconjugation, in which known cytotoxins or targeted anticancer therapeutics have been linked to glucose to improve cancer targeting and cellular selectivity, has become an appealing strategy for the targeted delivery of anticancer drugs [14,15]. These strategies employ the use of conjugates of D-glucose and bioactive molecule methotrexate (MTX) to improve efficacy and lower toxicity. MTX has been successfully used for many years in the treatment of patients with cancer and as an anti-inflammatory drug for the treatment of inflammatory diseases, such as rheumatoid arthritis.

There are many novel delivery systems that have been developed to improve the pitfalls of MTX therapy, ranging from polymeric conjugates, such as human serum albumin, liposomes, microspheres, solid lipid nanoparticles, polymeric nanoparticles, dendrimers, polymeric micelles, in situ forming hydrogels, and carrier erythrocyte, to nanotechnology-based vehicles such as carbon nanotubes, magnetic nanoparticles, and gold nanoparticles. Some of them are further modified with targeting ligands for active targeting purposes [16]. The pharmacokinetic properties of MTX polymeric conjugates are unsatisfactory because of their low penetration into cancer cells.

In the present work, we designed, synthesized, and biologically evaluated a novel glucose-methotrexate conjugate (Glu-MTX). Here, we investigated whether Glu-MTX could overcome MTX chemoresistance in oxygen and glucose-deprived cancer cells and the relative molecular mechanisms. This research aimed to assess the possibility of overcoming tumor microenvironment-induced drug resistance by conjugating a chemotherapeutic agent to glucose.

2. Results

2.1. Chemistry

When designing the synthesis of glycoconjugate derivatives of MTX, the following assumptions were made: glycoconjugate is selectively transferred to the cancer cell by GLUT proteins responsible for the transfer of D-glucose to tumor cells. To increase the water solubility of the prodrug and increase the affinity for GLUT transmembrane proteins, the conjugate contains two sugar units. The designed construct contains D-glucose linked via a linker to MTX. The key bonds connecting both molecules are susceptible to the action of hydrolytic enzymes, which allows the release of MTX, D-glucose, and the linker in the

cell. D-glucose is connected to the linker via a β-glycosidic bond that is susceptible to hydrolysis catalyzed by glycoside hydrolases. On the other hand, MTX is connected to the linker by a carbamate bond formed with the participation of amino groups. The cleavable linkage allows the release of the cytotoxic payload inside the malignant cells, possibly through enzymatic hydrolysis. The critical step of connecting the D-glucose derivative to MTX is accomplished in the 1,3-dipolar cycloaddition of the azide to a terminal alkyne bond in a variant developed by Sharpless [17], which is a method widely used in the synthesis of biologically active compounds [18].

The ability of substituted glucose analogs to be substrates for GLUT-1 has been investigated [19,20]. Kinetic and computational modeling studies using glucose analogs suggest that the hydroxyl groups at positions 1 and 3 and the pyran oxygen in the D-glucose most thermodynamically stable conformation are involved in stabilizing hydrogen bonding interactions with amino acid residues within the transporter. The loss of hydrogen bond acceptors at these positions makes glucose analogs poor substrates for GLUT-1. Thus, these data suggest that for glucose conjugates to remain substrates for GLUT-1, compounds with hydrogen bond acceptors such as nitrogen or oxygen must be retained proximal to carbons 1 and 3, and substitutions at the C1 position may retain a higher affinity for GLUT-1 if they are present in an equatorial conformation. A large number of known glucose conjugates are conjugated to the anticancer agent at position 1, with the C1 oxygen intact and locked into the equatorial β-D-position [21,22].

Based on literature data, a synthesis of glycoconjugate was designed in which D-glucose via a linker is associated with the cytotoxic compound methotrexate (Figure 1).
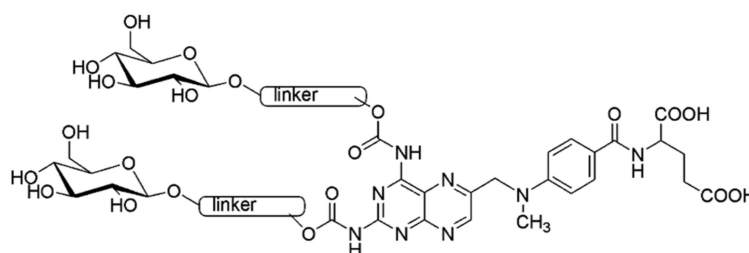
Figure 1. Structure of the MTX glycoconjugate (methotrexate glycoconjugate).

The sugar unit occurring in the most thermodynamically stable $^4C_1$ conformation is connected by the β-*O*-glycosyl bond with the spacer because, as is evident from the literature studies, such an orientation is preferred by the GLUT-1 transporting protein. The next fragment of the spacer contains the 1,2,3-triazine system because, as can be expected from the literature studies, the introduction of a functional group capable of hydrogen bonding increases the affinity of the compound to the transporting protein. The methotrexate is connected to the linker by forming a carbamate bond. After the introduction into the cell, the designed conjugate is susceptible to hydrolysis catalyzed by hydrolytic enzymes (glucosidases, peptidases) overexpressed in cancer cells following the release of a cytotoxic substance in the cancer target.

The coupling of two molecular components with different properties promises to generate a new conjugate with unprecedented biological activity, as different molecular segments can act together [23]. This perspective is a new, practically simple, and very reliable fast-growing approach for the development of pharmaceutically important drug-like molecules that can accelerate drug discovery research for human use. Sharpless et al. [17] discussed the Cu(I)-catalyzed azide−alkyne 1,3-dipolar cycloaddition ("click chemistry"), a set of powerful, selective, and reliable reactions for coupling molecular fragments under mild reaction conditions. The option to combine bioconjugation with click chemistry has emerged as a versatile tool with a wide range of applications. Effectively, the 1,2,3-triazole ring results in an ideal linker in bioconjugation, as (a) it presents a good water solubility, thus allowing in vivo administration; (b) it is analogous to an amide function for its electronic properties but is resistant to hydrolysis; (c) it is sufficiently stable in

biological systems; and, finally, (d) it is a rigid linker, which allows internal interaction between the two linked moieties to be avoided. The unique features of click chemistry provide a toolbox for efficient coupling methodologies for the synthesis of a variety of conjugates [18,24]. Of the click reactions that have been developed, the most widely applied is the copper-catalyzed azide−alkyne cycloaddition reaction (CuAAC). Considering the advantages of this solution in our glycoconjugate synthesis project, a sugar unit containing a terminal azide group was combined with a propargyl carbamate-derived methotrexate. This convenient approach enables the rapid synthesis of carbohydrate conjugates in which the heterocyclic triazole ring serves as a shackle for joining the carbohydrate moiety to the biomolecule. When we move toward carbohydrate chemistry, the sugar moiety can be easily furnished with an azide functionality with routine synthetic protocols [25,26]. One of the substrates in the synthesis of glycoconjugate was the 2-azidoethyl β-D-glucopyranoside **1**. It was obtained as β-glucoside in a coupling reaction between 2-bromoethanol and 1,2,3,4,6-penta-*O*-acetyl-β-D-glucose in the presence of boron trifluoride diethyl etherate (BF₃·Et₂O) as a catalyst [26]. An azido function was introduced via the S_N2 displacement of the bromine, using sodium azide in *N,N*-dimethylformamide (DMF) [25]. The last step was deprotection of the *O*-acetyl-protected glucoside under Zemplén conditions by the use of sodium methoxide in MeOH [25,27].

The second intermediate substrate is a derivative of methotrexate bearing a terminal acetylenic group. This synthesis was much more challenging. Such a group can be attached to methotrexate via an amide or a carbamate bond. Methotrexate is an unstable compound that is practically insoluble in organic solvents applied in the amidation reaction. A more convenient way to prepare amides could be the direct condensation of carboxylic acids and amines. Nevertheless, it is known that such an "ideal" amidation process needs very harsh conditions (temperature above 100 °C) to circumvent unreactive carboxylate-ammonium salts formation toward the desired amide bond formation [28]. This is adverse because other sensitive functionalities are present within coupled compounds. Therefore, the activation of carboxylic acid seems to be necessary [28]. The results of the conducted experiments associated with the selection of activation conditions are presented in Table 1.

Table 1. Adjusting the condensation reaction conditions.

Procedure	Substrate 1	Substrate 2	Reagents	Solvent	Reaction Time [h]	Yield [%]
A	MTX	Propiolic acid	DCC DCC/DMAP DCC/DMAP	DMF DMF DMF/CH₂Cl₂	48	traces 12 18
B	MTX	Propargyl chloroformate	Pyridine Triethylamine DMAP Imidazole	DMF/CH₂Cl₂	24	22 inseparable reaction mixture
C	MTX	Propargyl chloroformate	*N*-Methylimidazole	CHCl₃ THF CH₃CN DMF/CH₂Cl₂ CH₂Cl₂	24	- 8 4 21 32
			NMI/Hünigs base	CH₂Cl₂		42

There are numerous commercially available coupling reagents for constructing an amide bond, including carbodiimides alone or plus additives such as HOBt or DMAP [29]. The carbodiimide reacts with the carboxylic acid to form *O*-acylisourea mixed anhydride, which can react directly with an amine to yield the desired amide. We applied the DCC/DMAP condensing system for coupling propiolic acid with methotrexate. The reaction was carried out at room temperature for 48 h in different solvents. Unfortunately, the complex reaction mixture was formed, and the desired product was isolated in a poor

yield. The low yield of the desired product induced us to search for another method of MTX functionalization. The reaction of acyl halides with an amino group is, in principle, the simplest approach to amide bond synthesis. Propargyl acid chlorides are unstable, and we choose the commercially available propargyl chloroformate. Such a reaction requires the presence of a tertiary amine in the reaction medium. A range of tertiary amines was tested; however, the reaction of MTX with propargyl chloroformate in the presence of a variety of organic bases such as pyridine, Et$_3$N, DMAP, and imidazole in several different solvents gave MTX derivatives in very low yields. The treatment of methotrexate with two equivalents of propargyl chloroformate and tertiary amine in DMF/CH$_2$Cl$_2$ at room temperature gave the mixed anhydrides [29], which were condensed with amine groups of MTX, and an inseparable reaction mixture was obtained. An extremely effective acylating agent, 1-carboxybenzyl 3-ethylimidazol triethyloxonium tetrafluoroborate, was applied in the synthesis of nucleoside carbamates [30]. Assuming that an analogous acylating agent can be formed in a reaction of propargyl chloroformate **2** and *N*-methylimidazole, this compound was selected in subsequent reactions. When *N*-methylimidazole (NMI) was used, the yield of the desired carbamate derivative of MTX **4** was significantly improved depending on the solvent (DMF, CH$_2$Cl$_2$, CH$_3$CN, THF, CHCl$_3$). The optimal yield of **4** was obtained in the reaction with four molar equivalents of compound **2** in the presence of eight molar equivalents of NMI and tertiary amine (*N,N*-diisopropylethylamine) in methylene chloride, which was carried out for 24 h at room temperature (Scheme 1).
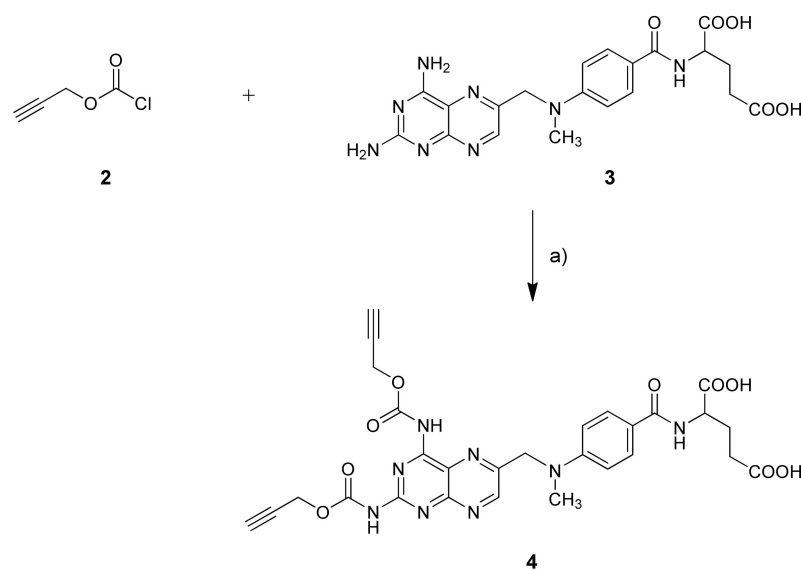
a) *N*-Methylimidazole, *N,N*-diisopropylethylamine, methylene chloride, r.t., 24 h

Scheme 1. Functionalization of methotrexate.

The structure of the obtained product **4** was elucidated by ^{1}H and ^{13}C NMR data. This product was assigned as the propargyl carbamate. According to ^{13}C NMR spectra, the acetylene carbon (77.73, 78.47 ppm) and carbamate carbon signals (165.61 ppm) were still present, indicating that the acylation of amines took place. This compound has been used as a scaffold for the synthesis of multivalent carbohydrate conjugates (Scheme 2).

Methotrexate intermediate derivative **4** is an unstable compound that is practically insoluble in water and typical solvents applied in the copper-catalyzed azide−alkyne cycloaddition reaction (CuAAC) [17,18,24]. For this reason, a series of experiments adjusting the CuAAC reaction conditions were performed (Table 2).
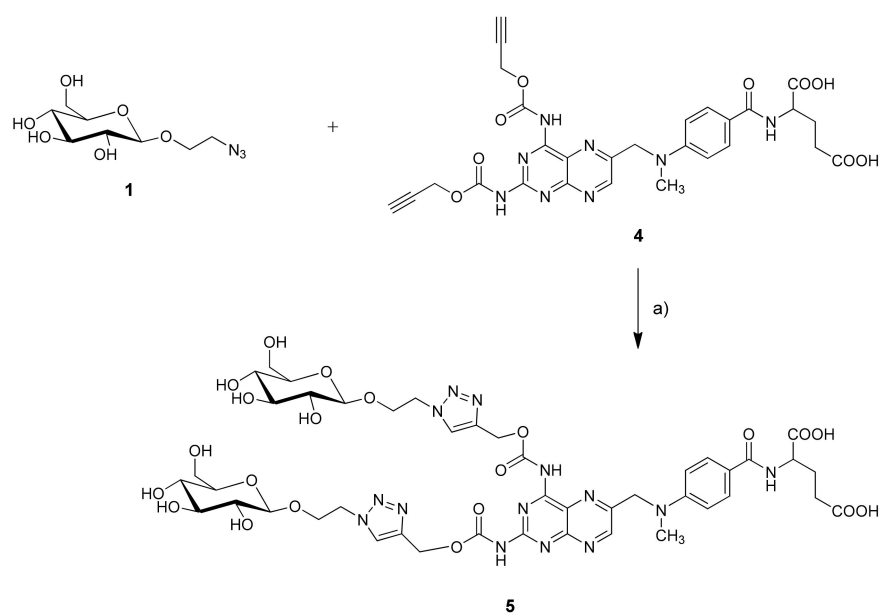
a) CuSO₄·5H₂O, sodium ascorbate, H₂O / THF / *i*-PrOH / *N,N*-diisopropylethylamine, r.t., 24 h

Scheme 2. Synthesis of glycoconjugate Glu-MTX.

Table 2. Adjusting the CuAAC reaction conditions (copper catalyzed azido-alkyne cycloaddition).

Procedure	Substrate 1	Substrate 2	Catalyst	Solvent	Reaction Time [h]	Yield [%]
A	1	4	NaAsc/CuSO₄·5H₂O	THF/*i*-PrOH/H₂O	24	11
B	1	4	NaAsc/CuSO₄·5H₂O	THF/*i*-PrOH/H₂O NaOH	24	43
C	1	4	NaAsc/CuSO₄·5H₂O	THF/*i*-PrOH/H₂O Hünig's base	24	77

The conventional Cu(I)-catalyzed coupling of **4** with glucosyl azide **1** afforded the desired product in low yields (11%). The low yield of glycoconjugate induced us to search for a better procedure of conjugation. As it turned out, copper(I)-catalyzed cycloaddition exclusively transformed substrates into the 1,2,3-triazole conjugate with the best yield (77%) by the treatment of sugar azide **1** with a solution of MTX carbamate **4** in the mixture of THF/*i*-PrOH/H₂O with the addition of *N,N*-diisopropylethylamine under sonification (Scheme 2).

Glycoconjugate **5** was purified by column chromatography, and its structure was elucidated by ¹H and ¹³C NMR data and mass spectrometry analysis. The NMR analyses were in full agreement with the expected structure (see the Supporting Information). ¹H NMR and coupling constants unambiguously confirmed β-configurations at the anomeric centers of the pyranose units. The remarkably well-resolved NMR peaks indicated that the glycoconjugate exhibited only marginal aggregation behavior in the DMSO solution.

Additionally, we have performed a mass spectrometry analysis, which indicated that within 4 h after the administration of the conjugate to the culture medium, the compound did not undergo degradation and entered the cells and released the cytotoxic payload (MTX) (Figure S1). However, we did not find other high molecular weight products (such as triazole or the linker) in the intracellular compartment, which suggests that the sugar moiety of the conjugate is quickly degraded after the internalization of the compound.

2.2. Biology Experiments

2.2.1. Glu-MTX Compared to MTX Exerted More Potent Cytotoxic Activity on MCF-7 and SW480 Cancer Cell Lines in Hypoxia and Glucose-Deprived Microenvironment

To investigate the effect of hypoxia on the MTX chemotherapy sensitivity, MCF-7 and SW480 cells in a controlled normoxia environment and a controlled hypoxia environment were relatively exposed to the various concentrations of MTX (5~20 μM) for 48 h. Compared with MCF-7/normoxia, the cell viability (%) in MCF-7/hypoxia decreases by 30% at the MTX dosage of 20 μM (Figure 2A). The same was observed for SW480 cells, where the viability (%) in normoxic cells was 29% lower than in hypoxic cells (Figure 2B). These findings indicate that hypoxia induces MTX chemoresistance. To investigate whether glucose and methotrexate conjugation could overcome hypoxia-induced drug resistance, we treated MCF-7 and SW480 cells in a controlled hypoxia environment with Glu-MTX for 48 h. Glu-MTX exerted a significantly stronger cytotoxic effect compared to MTX in hypoxic conditions. The IC_{50} of Glu-MTX was ~10 μM in both cell lines (Figure 2A,B). Compared to MTX, Glu-MTX at a dose of 20 μM exerted a 2.3 times greater cytotoxic effect on cancer cells in a hypoxic microenvironment.

To assess the effect of Glu-MTX in glucose-deprived cells, which were slightly more resistant to MTX than regular cells, we treated MCF-7 and SW480 cells in a controlled glucose-deprived environment with MTX and Glu-MTX for 48 h. The effect of glucose starvation on the MTX chemotherapy sensitivity was assessed in MCF-7 and SW480 cells in a controlled glucose-rich environment and controlled glucose-deprived environment. The cells were exposed to various concentrations of MTX (5~20 μM) for 48 h. Compared with MCF-7 cultured with glucose medium, the cell viability (%) of MCF-7 without glucose decreases by 17% at the Glu-MTX dosage of 20 μM (Figure 2C), whereas in SW480 cells, the viability (%) in glucose-rich cells was nearly 24% higher than in glucose-deprived cells at the Glu-MTX dosage of 20 μM (Figure 2D). These findings prove that glucose starvation affects the susceptibility of cancer cells to Glu-MTX and indicate the greater efficacy of Glu-MTX compared to MTX in glucose-deprived conditions.

To examine the effect of Glu-MTX in the tumor microenvironment, which comprises hypoxia and glucose-deprived medium, we treated MCF-7 and SW480 cells in the controlled hypoxia and glucose-deprived environment with MTX and Glu-MTX for 48 h. Both cancer cell lines were resistant to MTX (cell viability 74% for MCF-7 and 80% for SW480) even at a high dose of 20 μM, whereas, at the same dose, the cytotoxic effect of Glu-MTX was significantly higher (cell viability 33% for MCF-7 and 23% for SW480). The IC_{50} of Glu-MTX in the tumor microenvironment was in the range of 4~4.5 μM for both cell lines (Figure 2E).

2.2.2. Glu-MTX Inhibits the Wound Healing Process

Since the hypoxic breast and colon cancer cells could have altered migration behavior in response to different cytotoxic agents, we furthermore examined the effect of MTX and Glu-MTX on these parameters using in vitro wound-healing assay. The assay examines the migration of cells by evaluating the closure of a standard scratch in time. In both cancer cell lines, we found that Glu-MTX-treated cells had significantly slower migration than MTX-treated cells. At 48 h, the wound was unclosed in Glu-MTX-treated cells, whereas in MTX-treated cells, the gap was considerably smaller (Figure 3A,B).

2.2.3. Glu-MTX Induces Apoptosis by Increasing the Expression of Caspase-3 and Bax

The expression of proapoptotic proteins—caspase 3 and Bax in SW480/hypoxia cells—was analyzed by immunocytochemistry (Figure 4). We detected high levels of proapoptotic proteins (bax and caspase-3) in cells treated with Glu-MTX and MTX compared to the control. The intensity and percentage positivity of staining were similar or slightly elevated in Glu-MTX-treated cells compared to in MTX-treated cells.
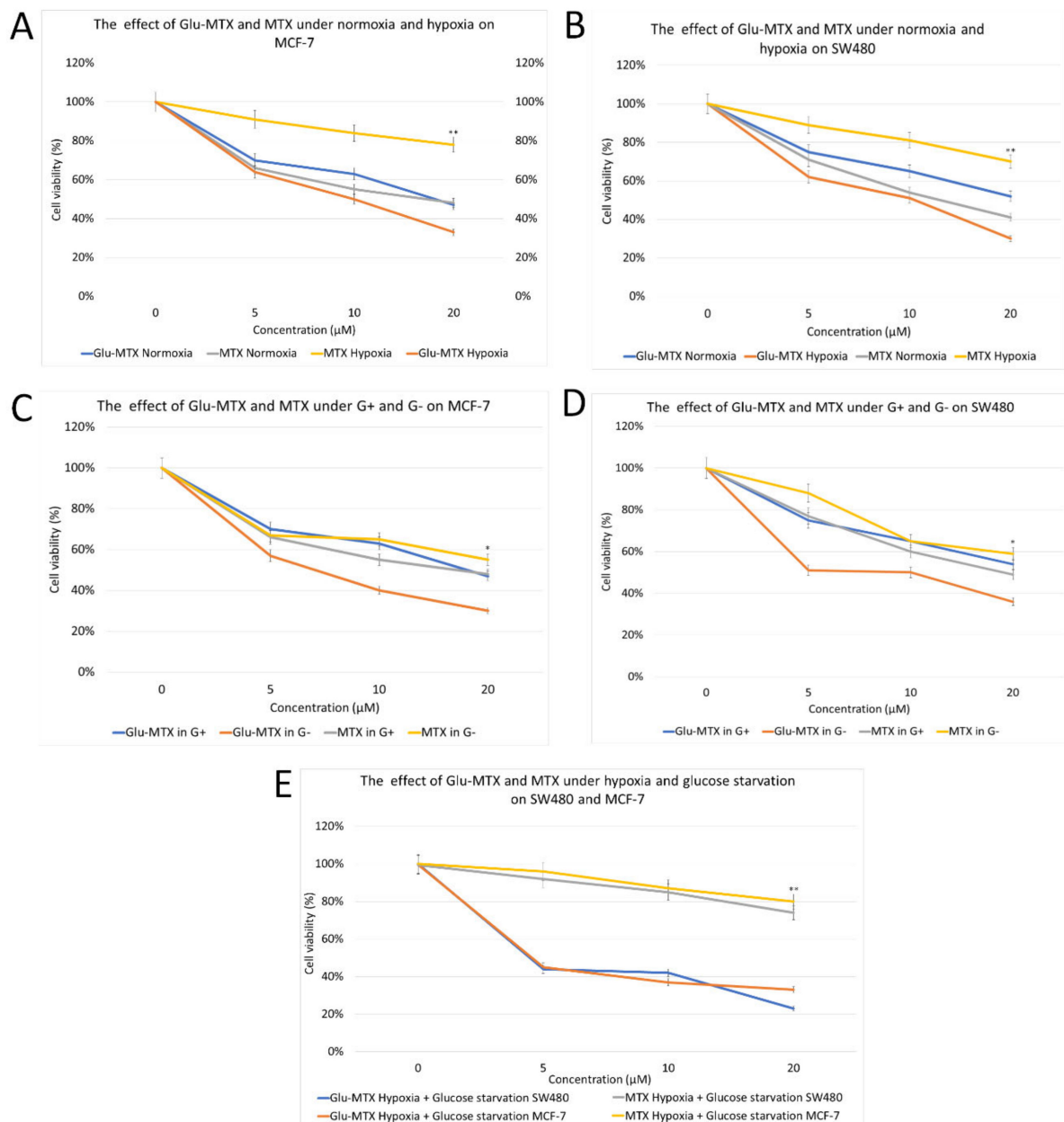
Figure 2. Results of cell viability after 48 h of incubation with 0, 5, 10, 20 µM of MTX and Glu-MTX evaluated by MTT assay. (**A**) Dose-dependency curves for MCF-7 cells in normoxic (21% of oxygen, 5% CO_2) and hypoxic (1% of oxygen, 5% CO_2) conditions. (**B**) Dose-dependency curves for SW480 cells in normoxic (21% of oxygen, 5% CO_2) and hypoxic (1% of oxygen, 5% CO_2) conditions. (**C**) Dose-dependency curves for MCF-7 cells cultured in medium with glucose (G+) and glucose-free medium (G−). (**D**) Dose-dependency curves for SW480 cells cultured in medium with glucose (G+) and glucose-free medium (G−). (**E**) Dose-dependency curves for MCF-7 and SW480 cells in normal culture conditions (21% of oxygen, 5% CO_2, G+) and in hypoxic (1% of oxygen, 5% CO_2) with glucose starvation conditions (G−). Data are expressed as mean ± SD from triplicates. * $p < 0.05$, ** $p < 0.01$, comparing Glu-MTX with MTX in hypoxia and/or glucose starvation conditions.

The flow cytometry analysis results are shown in Figure 5. The flow cytometry analysis results are shown in Figure 5. In comparison to the SW80 cells treated with MTX, Glu-MTX in hypoxic conditions presents increased late apoptosis after the proposed treatment. We have observed increased effectiveness of early and late apoptosis induction in almost 25% of cells after treatment with Glu-MTX (44%) in comparison to free MTX (19%). Control cells and MTX-treated cells demonstrate a similar rate of apoptosis induction and reveal decreased MTX potency in hypoxia.
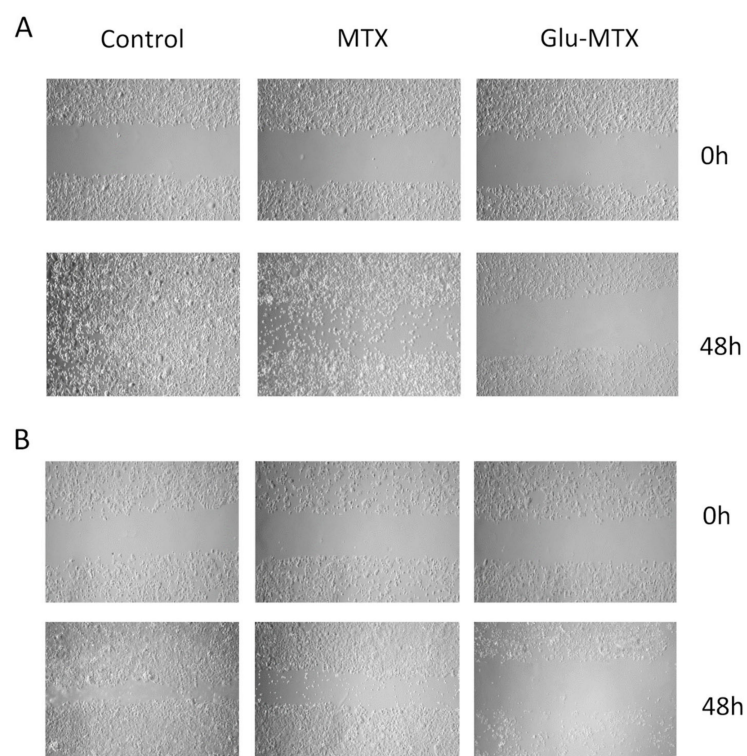
Figure 3. Wound-healing assay at time point 0 and after 48 h of incubation with 10 µM of MTX and Glu-MTX. Results show that after 48 h, the scrap in control cells is fully coated by cells, whereas in MTX-treated samples, the scrap is smaller compared to samples incubated with Glu-MTX, where no migration of cells is observed. (**A**) Representative images of SW480 cells. (**B**) Representative images of MCF-7 cells. 10× objectives were used to capture the photographs.
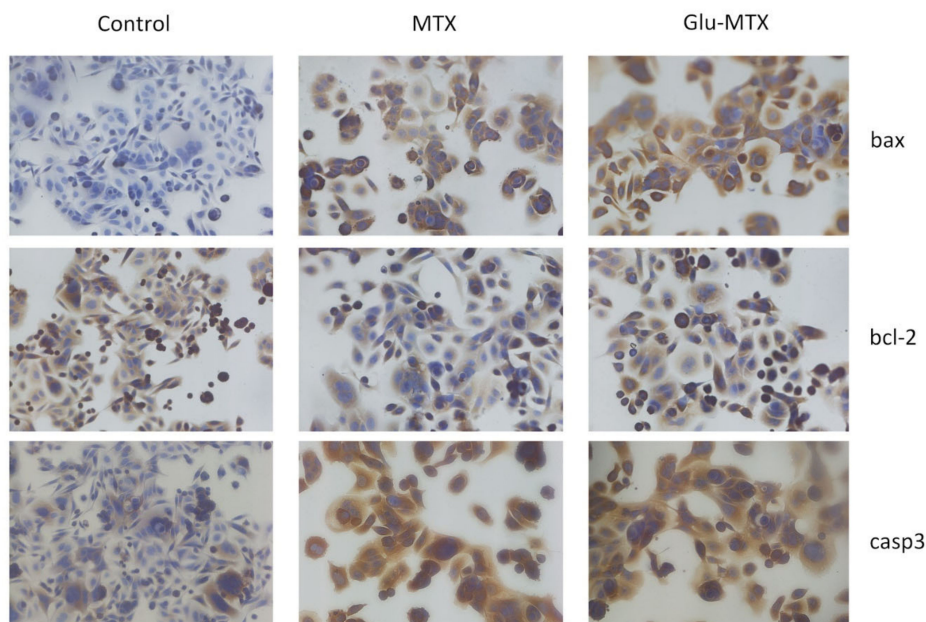
Figure 4. Representative images of the immunocytochemical analysis of bax, bcl-2, and caspase 3 apoptosis-related proteins in the SW480 cell line in control, treated with 10 µM of MTX and Glu-MTX samples after 48 h. 20× and 40× objectives were used to capture the photographs.
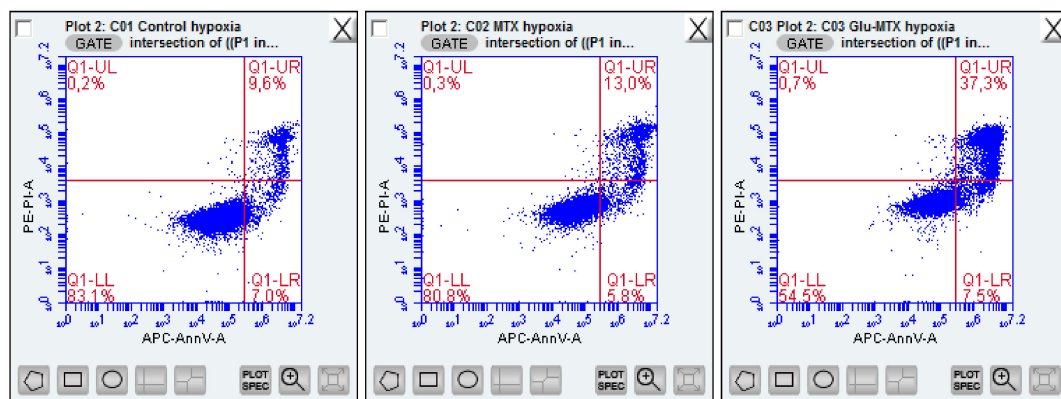
Figure 5. Results demonstrate representative images of flow cytometry analysis of viable (LL-lower left), early (LR-lower right), late (UR-upper right) apoptotic, and dead (UL-upper left) MCF-7 cells after incubation with 10 μM of MTX and Glu-MTX for 48 h in the tumor microenvironment in comparison to the control group without any treatment. All the samples were prepared using an Annexin V-FITC and PI Apoptosis Detection Kit (Abcam) and analyzed using a FACS Calibur flow cytometer (Beckton Dickinson, NJ, USA).

3. Discussion

Cancer cells' ability to evade or to handle the presence of chemotherapeutic agents is a fundamental challenge that oncology research aims to elucidate and overcome. Chemoresistance and malignant progression are closely linked with the tumor microenvironment, contributing to tumors' response to different therapeutic modalities [31,32]. The cancer microenvironment comprises many components, including extracellular matrix proteins, cancer-associated cells, and an aberrant vasculature. These physical elements give rise to the distinctive environmental properties of hypoxia and nutrient stress that inhibit the effect of cancer treatments [32]. The undesirable impact of hypoxia on malignancies relative to radio- and chemotherapy effectiveness has been established for several decades, and the survival rate of cancer patients with severely hypoxic tumors is shorter than that of patients with normoxic tumors [33].

Our study used a controlled hypoxia condition to assess the effectiveness of methotrexate on breast and colon cancer cells. We found that hypoxic cells were significantly more resistant to methotrexate than normoxic cells. These findings are consistent with previously published studies that found that hypoxia increased the resistance to methotrexate in various cancer types, including breast cancer, melanoma, and leukemia [34–36]. A study by Li et al. indicated that the HIF-1α-mediated pathway played a critical role in the susceptibility of MCF-7 breast cancer cells to methotrexate [34]. Due to the increasing evidence suggesting the role of nutrient stress, particularly glucose deprivation, in tumor cell survival, angiogenesis, and drug resistance, we assessed the effectiveness of methotrexate on glucose-deprived cancer cells [37–39]. We found that glucose-deficient cells were marginally less susceptible to methotrexate than regular cells.

We hypothesized that the linking of methotrexate to glucose could overcome the hypoxia- and/or nutrient stress-induced chemoresistance. The novel glycoconjugate of glucose and methotrexate exerted a strong and dose-dependent cytotoxic effect on hypoxic breast and colon cancer cells, which was nearly nine-fold more potent than MTX. Similarly, in a controlled glucose-deficient state, Glu-MTX displayed up to a three-fold enhanced cytotoxic effect in both cancer cell lines compared to MTX. As cancer cells consume glucose rampantly and given that glycolysis generates energy inefficiently, we hypothesize that Glu-MTX treatment under glucose starvation resulted in the potentiated cellular accumulation of the drug and thus resulted in an enhancement of cytotoxicity in tumor cells.

We cannot unequivocally state that the conjugate enters the cell specifically via the GLUT 1 transporter; however, given that the glycoconjugates are highly hydrophilic, they are unlikely to be internalized via passive diffusion through the lipid cell membrane. The accumulating evidence suggests that the cellular uptake of glycoconjugates must

be mediated by transmembrane transporters. GLUTs are the most frequent transporters facilitating the recognition and internalization of glycoconjugates. However, we must emphasize that the transport capability of GLUTs can be slightly influenced by complex factors, such as the structure and the substitution position of the carbohydrate, the length and steric hindrance of linkers, and the property of the payload. The past evidence suggests that the cellular uptake of some glycoconjugates is not mediated solely by GLUT but also by other receptors such as OCT2 [40]. Moreover, the potential role of other transporters such as SGLT, SWEET, and ASGPR (asialoglycoprotein receptor) should also be considered [41].

In the present study, we found an intriguing fact that in the tumor microenvironment, comprising hypoxia and glucose deprivation, MTX did not exert a cytotoxic effect on cancer cells. However, the conjugation of glucose to methotrexate allowed us to overcome the resistance and to achieve a potent, dose-dependent anticancer effect. Moreover, our studies revealed that the Glu-MTX inhibited hypoxic cells' cell migration process more effectively than MTX did. The results confirmed that Glu-MTX-treated cells expressed high levels of antiapoptotic proteins and underwent apoptosis.

Mounting evidence suggests that the expression of GLUTs is upregulated in many cancers under hypoxia and nutrient stress by key pro-survival pathways, including the HIF and AMP-activated protein kinase (AMPK) pathways [42,43]. This may explain our findings that Glu-MTX was significantly more potent in a hypoxic and/or glucose-deprived environment than MTX.

4. Materials and Methods

4.1. Chemistry

NMR spectra were recorded on an Agilent spectrometer 400 MHz (Agilent Technologies, Santa Clara, CA, USA) using TMS as an internal standard and $CDCl_3$ or DMSO as a solvent. NMR solvents were purchased from ACROS Organics (Geel, Belgium). Chemical shifts (δ) are expressed in ppm and coupling constants (J) in Hz. Optical rotations were measured with a JASCO 2000 polarimeter (JASCO Corporation, Tokyo, Japan) using a sodium lamp (589.3 nm) at room temperature. Melting point measurements were performed on a Stanford Research Systems OptiMelt (MPA 100) (Stanford Research System, Sunnyvale, CA, USA). Electrospray-ionization mass spectrometry was performed on a Xevo G2 Q-TOF mass spectrometer (Waters Chromatography, Etten-Leur, The Netherlands). Reactions were monitored by TLC on precoated plates of silica gel 60 F254 (Merck, Darmstadt, Deutschland). TLC plates were inspected under UV light (λ = 254 nm) or charring after spraying with 10% sulfuric acid in ethanol. Crude products were purified using column chromatography performed on silica gel 60 (Fluka, Honeywell, NJ, USA) developed with toluene/EtOAc and $CHCl_3$/MeOH as solvent systems. Organic solvents were evaporated on a rotary evaporator under diminished pressure at 40 °C.

All of the chemicals used in the experiments were purchased from Sigma-Aldrich (Saint Louis, MO, USA), ACROS Organics (Geel, Belgium), and Avantor Performance Materials Poland S.A (Gliwice, Poland) and were used without purification. Methotrexate **3**, propargyl chloroformate **2**, 2-bromoethanol, and D-glucose are commercially available. 1,2,3,4,6-Penta-*O*-acetyl-β-D-glucopyranose [44], 2-bromoethyl 2,3,4,6-tetra-*O*-acetyl-β-D-glucopyranoside [26], 2-azidoethyl 2,3,4,6-tetra-*O*-acetyl-β-D-glucopyranoside [25], and 2-azidoethyl β-D-glucopyranoside **1** [25,27] were prepared according to the respective published procedures.

4.1.1. Synthesis of Carbamate **4**

Methotrexate **3** (227 mg, 0.5 mmol), *N*-methylimidazole (320 μL, 4 mmol), and *N,N*-diisopropylethylamine (165 μL, 1 mmol) were sonicated for 30 min. The mixture was cooled in ice water, and the solution of propargyl chloroformate **2** (195 μL, 2 mmol) in methylene chloride (1 mL) was added. The reaction mixture was stirred for 24 h at ambient temperature and then poured into ice water. The crude product was precipitated with acetic acid, filtered, washed with water, and drying under reduced pressure left a residue

that was column chromatographed to yield bis-propargyl carbamate **4** (130 mg, 42% yield): m.p. 174–176 °C; $[\alpha]_D^{23} = -2$ (*c* = 1.0, DMSO).

^{1}H NMR (400 MHz, DMSO-d6): δ 1.85–2.16 (m, 2H, 2xCHMTX), 2.32 (m, 1H, CHMTX), 2.45 (m, 1H, CHMTX), 3.21 (s, 3H, CH$_3$MTX), 3.52 (m, 2H, 2xCH), 3.71 (s, 2H, CH$_2$), 4.35 (m, 1H, CHMTX), 4.62–4.72 (m, 2H, CH$_2$), 4.80 (s, 2H, CH$_2$MTX), 6.80–6.85 (m, 2H, H-PhMTX), 7.12 (s, 1H, NH), 7.28 (s, 1H, NH), 7.68–7.76 (m, 2H, H-PhMTX), 8.60 (m, 1H, NHMTX), 8.61 (s, 1H, H-7MTX).

^{13}C NMR (100 MHz, DMSO-d6): δ 25.31, 29.39, 32.88, 50.89, 50.97, 51.03, 54.14, 76.93, 77.73, 78.47, 110.36, 120.41, 120.46, 128.23, 146.26, 148.39, 150.20, 152.65, 160.80, 161.99, 165.61, 165.64, 170.95, 173.01, 173.18.

4.1.2. Synthesis of Glycoconjugate **5**

Carbamate **4** (62 mg, 0.1 mmol) and azidoethyl glucoside **1** (50 mg, 0.2 mmol) were dissolved in dry *i*-PrOH (2 mL), THF (2 mL) and *N,N*-diisopropylethylamine (60 μL, 0.36 mmol). The solutions of sodium ascorbate (8 mg, 0.04 mmol) in water (1 mL) and CuSO$_4$·5H$_2$O (5 mg, 0.02 mmol) in water (2 mL) were mixed and added to the reaction mixture and next stirred for 24 h at room temperature. The reaction mixture was filtered, the precipitate was washed with methyl alcohol, the combined filtrate was treated with acetic acid, and the crude product was separated by filtration, then washed, dried, and purified by column chromatography to yield glycoconjugate **5** (86 mg, 77% yield): m.p. 175–177 °C; $[\alpha]_D^{22} = -20$ (*c* = 1.0, DMSO).

^{1}H NMR (400 MHz, DMSO-d$_6$): δ 1.71–2.10 (m, 2H, 2xCHMTX), 2.19–2.39 (m, 2H, 2xCHMTX), 2.96 (dd, 2H, *J* = 7.8 Hz, *J* = 8.6 Hz, H-2$_{Glu}$), 3.03 (dd, 2H, *J* = 9.0 Hz, *J* = 9.4 Hz, H4$_{Glu}$), 3.09–3.55 (m, 9H, CH$_3$MTX, H-3$_{Glu}$, H-5$_{Glu}$, H-6a$_{Glu}$), 3.63–3.79 (m, 4H, 4xCCH), 3.68 (dd, 2H, *J* = 1.6 Hz, *J* = 11.4 Hz, H-6b$_{Glu}$), 3.86–3.95 (m, 2H, 2xCH), 4.01–4.12 (m, 2H, 2xCH),4.22 (d, 2H, *J* = 7.8 Hz, H-1$_{Glu}$), 4.29 (m, 1H, CHMTX), 4.55–4.61 (m, 4H, 2xCH$_2$), 4.79 (bs, 2H, OH), 5.21 (s, 2H, CH$_2$MTX), 6.80–6.87 (m, 2H, H-PhMTX), 7.66–7.72 (m, 2H, H-PhMTX), 7.95 (d, 1H, *J* = 7.0 Hz, NHMTX), 8.25 (s, 2H, H-5$_{triaz}$), 8.61 (s, 1H, H-7MTX).

^{13}C NMR (100 MHz, DMSO-d$_6$): δ 24.62, 30.33, 31.64, 48.55, 49.72, 54.87, 60.62, 61.05, 67.19, 69.99, 73.26, 76.54, 76.95, 102.87, 111.09, 121.49, 125.84, 128.62, 140.91, 146.75, 149.15, 150.83, 154.04, 163.78, 165.39, 165.56, 173.56, 174.26.

HRMS (ESI-TOF): calcd for C$_{44}$H$_{55}$N$_{14}$O$_{21}$Na$_2$ ([M+H]$^+$): *m/z* 1161.3462; found *m/z* 1161.3710.

4.1.3. LC/MS Analysis

UPLC analysis was performed on a Waters HSS T3 column (1.7 μm, 1 × 50 mm) using an Acquity UPLC system (Waters, Milford, MA, USA). The mobile phase consisted of 0.1% formic acid in water (mobile phase A) and 0.1% formic acid in methanol (mobile phase B). A gradient elution at a flow of 200 μL/min was performed according to the following: 0.5 min—5% B, 2.5 min—35% B, 3.5 min—90% B, 4.5 min—90% B, 4.55 min—5% B. The total run time was 6 min. The column temperature and the autosampler temperature were kept at 45 °C and 5 °C, respectively.

Mass spectral ionization and acquisition parameters were optimized on the Xevo G2 Q-TOF MS using electrospray ionization (ESI) in the positive ionization mode. The spray voltage, source temperature, and desolvation temperature were set at 0.5 kV, 120 °C, and 450 °C, respectively. Nitrogen was used as a desolvation and nebulizer gas. The desolvation gas flow was set at 800 L/h, and the cone gas flow was 70 L/h. Data were acquired using the Masslynx software (version 4.0, Waters, Milford, MA, USA).

4.2. Biology

4.2.1. Cell Culture

The cell line, human colon adenocarcinoma SW40 and human breast carcinoma MCF-7 obtained from the Leibniz Institute DSMZ-German Collection of Microorganisms and Cell Cultures (DSMZ, Germany), were grown in RPMI 1640 medium and supplemented

with 10% fetal bovine serum (FBS), 100 U/mL penicillin, 100 lg/mL streptomycin in a humidified incubator with 5% CO_2 at 37 °C. The culture medium was renewed every 2–3 days. Cell culture media, trypsin, FBS, and antibiotics were purchased from Gibco (Thermo Fisher Scientific Inc., Waltham, MA, USA).

4.2.2. Experiment Conditions and Cell Viability MTT Assay

Following MTT experiments, control cells were maintained in normoxia (21% O_2, 5% CO_2) and cultured in a complete medium with glucose. Hypoxic conditions were achieved by incubating cells in 1% O_2, 5% CO_2 incubator (New Brunswick Galaxy 48R, Eppendorf, Hamburg, Germany) and cultured in medium without glucose (RPMI 1640, no glucose, cat. no. 11879020).

For experiments with methotrexate and glucose conjugated MTX, cells were seeded in 96-well plates (8×10^3 cells/well). The next day, the cells were treated with culture medium (control) and different doses of the compounds (5, 10, 20 μM) for 48 h.

Following incubation, an MTT assay was performed. Cell viability was determined by the ability of the mitochondrial enzyme succinate dehydrogenase to convert the yellow tetrazolium salt (MTT) into violet formazan crystals in active cells. After 4 h of incubation, the medium was removed, and the water-insoluble dye was dissolved by dimethyl sulfoxide (Sigma Aldrich, Munich, Germany), generating the color, whose intensity is directly proportional to the number of viable cells. The absorbance was measured at 570 nm using the Bio-TekBioTek ELX800 multi-well reader (BioTek, Winooski, VT, USA). The percentage of viable cells (VC) was calculated as VC (100%) = (A of experimental group/A of the control group) $\times$ 100%. MTT experiments were repeated three times, and the figures represent the mean. For further experiments, the concentration of 10 μM MTX and Glu-MTX was used to evaluate the motility ability and apoptosis by flow cytometry and immunocytochemistry.

4.2.3. Wound-Healing Assay

To analyze the migration properties of MCF-7 and SW480 cells, a wound-healing assay was performed. Cells were seeded on 6-well plates in 1×10^6/well density to form a confluent monolayer. With a 200 μL pipette tip, a linear scratch was made in each sample. The first photograph in time point 0 was taken. Then, the cells were incubated with a dose of 10 μM MTX and Glu-MTX for 48 h. After incubation, the second photograph was taken when the scratch was closed in the control cell samples without any treatment. The experiment was repeated three times.

4.2.4. Flow Cytometry-Apoptosis Assay

To evaluate the apoptosis rate of cells in the tumor microenvironment, SW480 cells were seeded at a density of 3.5×10^5/well in a 6-well culture plate. The next day, cells were treated with MTX or Glu-MTX at a dose of 10 μM for 48 h. After treatment, cells were washed with PBS solution, detached by using 0.25% trypsin in EDTA, centrifuged, and prepared according to the manufacturer's instructions from Annexin V-FITC PI Apoptosis Detection Kit (Abcam, Cambridge, UK). First, cells were suspended in 500 μL of 1× Binding Buffer. Afterward, 5 μL of Annexin V (Annexin V-FITC) and 1 μL of propidium iodide (PI, 50 μg/mL) were added to each sample. The samples were incubated for 20 min in darkness at room temperature. For the evaluation of apoptosis, a BD Accuri C6 flow cytometer (Becton Dickinson, Franklin Lakes, NJ, USA) was used. Control cells, MTX, and Glu-MTX-treated samples were measured in triplicate. The obtained results were analyzed using the BD Accuri 6 Plus Software (Becton, Dickinson, NJ, USA).

4.2.5. ICC Staining for Apoptosis Detection

For the immunocytochemical analysis, the apoptotic proteins (Caspase-3, Bax, Bcl-2) were evaluated. MCF-7 cells were seeded on 8 Chamber Eppendorf Cell Imaging Slides (Eppendorf, Germany) at a density of 8×10^4/well. The following day, 10 μM Glu-MTX

and MTX were added to the wells for 48 h of incubation. Next, the cells were washed twice in PBS and fixed in 4% formaldehyde (Polysciences, Warrington, PA, USA) for 10 min at RT. After PBS washing, cells were permeabilized and incubated in a blocking solution containing 5% Normal Donkey Serum (Abcam, Bristol, UK), 3% Bovine Serum Albumin (Sigma Aldrich, Germany), 0.05% Tween 20 (Sigma Aldrich, Germany), 0.2% Triton X-100 (Sigma Aldrich, Germany), in PBS for 1 h at 4 °C. Then the primary antibodies: anti-Bax, anti-Bcl-2, and anti-Caspase 3 (Abcam, UK), in dilution 1:100, were applied, and the cells were incubated overnight at 4 °C. The next day, after PBS washing, the cells were incubated with a secondary anti-rabbit antibody (Sigma Aldrich, Germany) at RT for 1 h. After PBS washing, sections were stained with 3,3′-diaminobenzidine in chromogen solution (Dako EnVision+ Dual Link System-HRP, Agilent, USA) and counterstained with Mayer's hematoxylin for nucleus counterstaining.

The control sample was performed following the above instructions but without incubation with the compounds.

The light microscopy fitted with a digital camera (Nikon, Poland) with dry objectives 20× and 40× was used to take the photos.

5. Conclusions

The exploration of glycoconjugates for GLUT1-targeted cancer therapy began 25 years ago with the discovery of glufosfamide. Since then, numerous preclinical and clinical trials have been conducted on glucose conjugates in the treatment of various malignancies.

To our knowledge, this is the first time that an evaluation of the biological activity of glucose-conjugate in the tumor microenvironment has been performed. As hypoxia and nutrient stress are known to upregulate GLUT expression on the cancer cell surface and given that GLUTs confer the tumor selectivity of Glu-MTX, the results of our study confirm the viability of the strategy to combat tumor microenvironment-induced drug resistance in solid malignancies through linking of anticancer compounds with glucose. It is of paramount importance to validate anticancer agents' activity in models closer to their "native" microenvironment to improve the dismal success rates in transitioning anticancer agents from the laboratory to the clinic [45].

In summary, this work showed that the conjugation of methotrexate to glucose led to an increase in potency against malignant cells under hypoxia and nutrient stress. Although the finding has been confined to in vitro studies, our observations shed light on a potential therapeutic approach to overcome chemoresistance in cancer.

References

1. Roma-Rodrigues, C.; Mendes, R.; Baptista, P.; Fernandes, A. Targeting tumor microenvironment for cancer therapy. *Int. J. Mol. Sci.* **2019**, *20*, 840. [CrossRef] [PubMed]
2. Trédan, O.; Galmarini, C.M.; Patel, K.; Tannock, I.F. Drug resistance and the solid tumor microenvironment. *J. Natl. Cancer Inst.* **2007**, *99*, 1441–1454. [CrossRef] [PubMed]
3. Correia, A.L.; Bissell, M.J. The tumor microenvironment is a dominant force in multidrug resistance. *Drug Resist. Updat.* **2012**, *15*, 39–49. [CrossRef] [PubMed]
4. Nagao, A.; Kobayashi, M.; Koyasu, S.; Chow, C.C.T.; Harada, H. HIF-1-Dependent reprogramming of glucose metabolic pathway of cancer cells and its therapeutic significance. *Int. J. Mol. Sci.* **2019**, *20*, 238. [CrossRef] [PubMed]
5. Woźniak, M.; Makuch, S.; Winograd, K.; Wiśniewski, J.; Ziółkowski, P.; Agrawal, S. 6-Shogaol enhances the anticancer effect of 5-fluorouracil, oxaliplatin, and irinotecan via increase of apoptosis and autophagy in colon cancer cells in hypoxic/aglycemic conditions. *BMC Complement. Med. Ther.* **2020**, *20*, 141. [CrossRef] [PubMed]
6. Kato, Y.; Maeda, T.; Suzuki, A.; Baba, Y. Cancer metabolism: New insights into classic characteristics. *Jpn. Dent. Sci. Rev.* **2018**, *54*, 8–21. [CrossRef]
7. Gocheva, G.; Ivanova, A. A look at receptor ligand pairs for active-targeting drug delivery from crystallographic and molecular dynamics perspectives. *Mol. Pharm.* **2019**, *16*, 3293–3321. [CrossRef]
8. Zhu, Y.; Feijen, J.; Zhong, Z. Dual-targeted nanomedicines for enhanced tumor treatment. *Nano Today* **2018**, *18*, 65–85. [CrossRef]
9. Minchinton, A.I.; Tannock, I.F. Drug penetration in solid tumours. *Nat. Rev. Cancer* **2006**, *6*, 583–592. [CrossRef]
10. Srinivasarao, M.; Low, P.S. LiganD-targeted drug delivery. *Chem. Rev.* **2017**, *117*, 12133–12164. [CrossRef]
11. Cantor, J.R.; Sabatini, D.M. Cancer cell metabolism: One hallmark, many faces. *Cancer Discov.* **2012**, *2*, 881–898. [CrossRef] [PubMed]
12. Series, C.; Review, L. F-18 FDG PET/CT for detection of malignant involvement of peripheral nerves. *Clin. Nucl. Med.* **2011**, *36*, 96–100.
13. Heiden, M.G. Vander targeting cancer metabolism: A therapeutic window opens. *Nat. Rev. Drug Discov.* **2011**, *10*, 671–684. [CrossRef] [PubMed]
14. Calvaresi, E.C.; Hergenrother, P.J. Glucose conjugation for the specific targeting and treatment of cancer. *Chem. Sci.* **2013**, *4*, 2319. [CrossRef]
15. Srinivasarao, M.; Galliford, C.V.; Low, P.S. Principles in the design of liganD-targeted cancer therapeutics and imaging agents. *Nat. Rev. Drug Discov.* **2015**, *14*, 203–219. [CrossRef]
16. Abolmaali, S.S.; Tamaddon, A.M.; Dinarvand, R. A review of therapeutic challenges and achievements of methotrexate delivery systems for treatment of cancer and rheumatoid arthritis. *Cancer Chemother. Pharmacol.* **2013**, *71*, 1115–1130. [CrossRef]
17. Kolb, H.C.; Finn, M.G.; Sharpless, K.B. Click chemistry: Diverse chemical function from a few good reactions. *Angew. Chem. Int. Ed.* **2001**, *40*, 2004–2021. [CrossRef]
18. Thirumurugan, P.; Matosiuk, D.; Jozwiak, K. Click chemistry for drug development and diverse chemical-biology applications. *Chem. Rev.* **2013**, *113*, 4905–4979. [CrossRef]
19. Pohl, J.; Bertram, B.; Hilgard, P.; Nowrousian, M.R.; Stüben, J.; Wießler, M. D-19575—A sugar-linked isophosphoramide mustard derivative exploiting transmembrane glucose transport. *Cancer Chemother. Pharmacol.* **1995**, *35*, 364–370. [CrossRef]
20. Granchi, C.; Fortunato, S.; Minutolo, F. Anticancer agents interacting with membrane glucose transporters. *Med. Chem. Commun.* **2016**, *7*, 1716–1729. [CrossRef]
21. Barnett, J.E.G.; Holman, G.D.; Munday, K.A. Structural requirements for binding to the sugar-transport system of the human erythrocyte. *Biochem. J.* **1973**, *131*, 211–221. [CrossRef] [PubMed]
22. Mueckler, M.; Makepeace, C. Model of the exofacial substrate-binding site and helical folding of the human Glut1 glucose transporter based on scanning mutagenesis. *Biochemistry* **2009**, *48*, 5934–5942. [CrossRef] [PubMed]
23. Agarwal, P.; Bertozzi, C.R. Site-specific antibody-drug conjugates: The nexus of bioorthogonal chemistry, protein engineering, and drug development. *Bioconjug. Chem.* **2015**, *26*, 176–192. [CrossRef] [PubMed]
24. Tiwari, V.K.; Mishra, B.B.; Mishra, K.B.; Mishra, N.; Singh, A.S.; Chen, X. Cu-catalyzed click reaction in carbohydrate chemistry. *Chem. Rev.* **2016**, *116*, 3086–3240. [CrossRef]
25. Krawczyk, M.; Pastuch-Gawołek, G.; Pluta, A.; Erfurt, K.; Domiński, A.; Kurcok, P. 8-Hydroxyquinoline glycoconjugates: Modifications in the linker structure and their effect on the cytotoxicity of the obtained compounds. *Molecules* **2019**, *24*, 4181. [CrossRef]
26. Le Roux, A.; Meunier, S.; Le Gall, T.; Denis, J.M.; Bischoff, P.; Wagner, A. Synthesis and radioprotective properties of pulvinic acid derivatives. *Chem. Med. Chem.* **2011**, *6*, 561–569. [CrossRef]
27. Zemplén, G.; Pacsu, E. Über die Verseifung acetylierter Zucker und verwandter Substanzen. *Ber. Dtsch. Chem. Ges.* **1929**, *62*, 1613–1614. [CrossRef]
28. De Figueiredo, R.M.; Suppo, J.S.; Campagne, J.M. Nonclassical routes for amide bond formation. *Chem. Rev.* **2016**, *116*, 12029–12122. [CrossRef]
29. Kim, S.; Lee, J.I.; Kim, Y.C. A simple and mild esterification method for carboxylic acids using mixed carboxylic-carbonic anhydrides. *J. Org. Chem.* **1985**, *50*, 561–565. [CrossRef]

30. Watkins, B.E.; Kiely, J.S.; Rapoport, H. Synthesis of oligodeoxyribonucleotides using *N*-benzyloxycarbonyl-blocked nucleosides. *J. Am. Chem. Soc.* **1982**, *104*, 5702–5708. [CrossRef]

31. Pandey, M.; Prasad, S.; Tyagi, A.; Deb, L.; Huang, J.; Karelia, D.; Amin, S.; Aggarwal, B. Targeting cell survival proteins for cancer cell death. *Pharmaceuticals* **2016**, *9*, 11. [CrossRef] [PubMed]

32. Wang, M.; Zhao, J.; Zhang, L.; Wei, F.; Lian, Y.; Wu, Y.; Gong, Z.; Zhang, S.; Zhou, J.; Cao, K.; et al. Role of tumor microenvironment in tumorigenesis. *J. Cancer* **2017**, *8*, 761–773. [CrossRef] [PubMed]

33. Doktorova, H.; Hrabeta, J.; Khalil, M.A.; Eckschlager, T. Hypoxia-induced chemoresistance in cancer cells: The role of not only HIF-1. *Biomed. Pap.* **2015**, *159*, 166–177. [CrossRef] [PubMed]

34. Li, J.; Shi, M.; Cao, Y.; Yuan, W.; Pang, T.; Li, B.; Sun, Z.; Chen, L.; Zhao, R.C. Knockdown of hypoxia-inducible factor-1α in breast carcinoma MCF-7 cells results in reduced tumor growth and increased sensitivity to methotrexate. *Biochem. Biophys. Res. Commun.* **2006**, *342*, 1341–1351. [CrossRef] [PubMed]

35. Sanna, K.; Rofstad, E.K. Hypoxia-induced resistance to doxorubicin and methotrexate in human melanoma cell lines in vitro. *Int. J. Cancer* **1994**, *58*, 258–262. [CrossRef] [PubMed]

36. Petit, C.; Gouel, F.; Dubus, I.; Heuclin, C.; Roget, K.; Vannier, J.P. Hypoxia promotes chemoresistance in acute lymphoblastic leukemia cell lines by modulating death signaling pathways. *BMC Cancer* **2016**, *16*, 746. [CrossRef]

37. Nishimoto, A.; Kugimiya, N.; Hosoyama, T.; Enoki, T.; Li, T.-S.; Hamano, K. HIF-1 activation under glucose deprivation plays a central role in the acquisition of anti-apoptosis in human colon cancer cells. *Int. J. Oncol.* **2014**, *44*, 2077–2084. [CrossRef]

38. Mathews, E.H.; Stander, B.A.; Joubert, A.M.; Liebenberg, L. Tumor cell culture survival following glucose and glutamine deprivation at typical physiological concentrations. *Nutrition* **2014**, *30*, 218–227. [CrossRef]

39. Hu, Y.L.; Yin, Y.; Liu, H.Y.; Feng, Y.Y.; Bian, Z.H.; Zhou, L.Y.; Zhang, J.W.; Fei, B.J.; Wang, Y.G.; Huang, Z.H. Glucose deprivation induces chemoresistance in colorectal cancer cells by increasing ATF4 expression. *World J. Gastroenterol.* **2016**, *22*, 6235–6245. [CrossRef]

40. Fu, J.; Yang, J.; Seeberger, P.H.; Yin, J. Glycoconjugates for glucose transporter-mediated cancer-specific targeting and treatment. *Carbohydr. Res.* **2020**, *498*, 108195. [CrossRef]

41. Deng, D.; Yan, N. GLUT, SGLT, and SWEET: Structural and mechanistic investigations of the glucose transporters. *Protein Sci.* **2016**, *25*, 546–558. [CrossRef] [PubMed]

42. Barron, C.C.; Bilan, P.J.; Tsakiridis, T.; Tsiani, E. Facilitative glucose transporters: Implications for cancer detection, prognosis and treatment. *Metabolism* **2016**, *65*, 124–139. [CrossRef]

43. Parks, S.K.; Cormerais, Y.; Marchiq, I.; Pouyssegur, J. Hypoxia optimises tumour growth by controlling nutrient import and acidic metabolite export. *Mol. Aspects Med.* **2016**, *47*, 3–14. [CrossRef]

44. Yang, Q.R.; Qiao, W.H.; Zhang, S.M.; Qu, J.P.; Liu, D.L. Synthesis and characterization of a new cationic galactolipid with carbamate for gene delivery. *Tenside Surf. Det.* **2010**, *5*, 294–299. [CrossRef]

45. Bhattacharya, B.; Omar, M.F.M.; Soong, R. The Warburg effect and drug resistance. *Br. J. Pharmacol.* **2016**, *173*, 970–979. [CrossRef] [PubMed]

Publikacja P.9

The Effect of a New Glucose–Methotrexate Conjugate on Acute Lymphoblastic Leukemia and Non-Hodgkin's Lymphoma Cell Lines

M. Woźniak, S. Makuch, G. Pastuch-Gawołek, J. Wiśniewski, W. Szeja, M. Nowak, **M. Krawczyk**[*], S. Agrawal[*]

MDPI

Article

The Effect of a New Glucose–Methotrexate Conjugate on Acute Lymphoblastic Leukemia and Non-Hodgkin's Lymphoma Cell Lines

Marta Woźniak [1], Sebastian Makuch [1], Gabriela Pastuch-Gawołek [2,3], Jerzy Wiśniewski [4], Wiesław Szeja [2], Martyna Nowak [1], Monika Krawczyk [2,3,*] and Siddarth Agrawal [1,5,*]

[1] Department of Pathology, Wroclaw Medical University, 50-367 Wroclaw, Poland; marta.wozniak@umed.wroc.pl (M.W.); sebastian.mk21@gmail.com (S.M.); martyna.nowak96@o2.pl (M.N.)
[2] Department of Organic Chemistry, Bioorganic Chemistry and Biotechnology, Faculty of Chemistry, Silesian University of Technology, 44-100 Gliwice, Poland; gabriela.pastuch@polsl.pl (G.P.-G.); wieslaw.szeja@adres.pl (W.S.)
[3] Biotechnology Centre, Silesian University of Technology, 44-100 Gliwice, Poland
[4] Central Laboratory of Instrumental Analysis, Wroclaw University of Science and Technology, 50-370 Wroclaw, Poland; jerzy.wisniewski@pwr.edu.pl
[5] Department and Clinic of Internal Medicine, Occupational Diseases, Hypertension and Clinical Oncology, Wroclaw Medical University, 50-556 Wroclaw, Poland
* Correspondence: monika.krawczyk@polsl.pl (M.K.); siddarth@agrawal.pl (S.A.)

Abstract: Patients with hematologic malignancies require intensive therapies, including high-dose chemotherapy. Antimetabolite–methotrexate (MTX) has been used for many years in the treatment of leukemia and in lymphoma patients. However, the lack of MTX specificity causes a significant risk of morbidity, mortality, and severe side effects that impairs the quality of patients' life. Therefore, novel targeted therapies based on the malignant cells' common traits have become an essential treatment strategy. Glucose transporters have been found to be overexpressed in neoplastic cells, including hematologic malignancies. In this study, we biologically evaluated a novel glucose–methotrexate conjugate (Glu–MTX) in comparison to a free MTX. The research aimed to assess the effectiveness of Glu–MTX on chosen human lymphoma and leukemia cell lines. Cell cytotoxicity was verified by MTT viability test and flow cytometry. Moreover, the cell cycle and cellular uptake of Glu–MTX were evaluated. Our study reveals that conjugation of methotrexate with glucose significantly increases drug uptake and results in similar cytotoxicity of the synthesized compound. Although the finding has been confined to in vitro studies, our observations shed light on a potential therapeutic approach that increases the selectivity of chemotherapeutics and can improve leukemia and lymphoma patients' outcomes.

Keywords: warburg effect; anticancer drugs; hematologic malignancies; drug design and discovery; glucose metabolism; glycoconjugates; methotrexate; targeted therapy

1. Introduction

Chemotherapeutic agents have remained the mainstay of hematologic malignancies therapy for decades, and in combination with radiotherapy (RT), these modalities continue to be the first-line option for most entities [1]. The treatment yields high cure rates in many diseases such as lymphoblastic leukemias or Hodgkin lymphomas; however, dose-dependent severe side effects resulting from lack of selectivity remain a significant drawback of the therapy [2]. The foremost reason for the cessation of conventional chemotherapy is not the lack of efficacy but the resulting toxicity. Well-recognized acute side effects include pancytopenia that leads to severe bleeding, incurable infections, and organ damage. Cardiovascular complications and second malignancies are among the most frequent and potentially life-limiting late effects. Other long-term adverse outcomes,

particularly impaired organ function, infertility, fatigue, and pulmonary complications, are growing reasons for prolonged morbidity and mortality after effective first-line therapy in hematologic cancers.

The adverse outcomes limit the curative potential of conventional therapeutic modalities. Although young and fit cancer patients generally qualify for these treatments, the increasing number of elderly and frail individuals, as well as patients with multimorbidities, are commonly excluded from these therapeutic approaches. These facts emphasize the unmet need for potent yet safe treatments.

Methotrexate (MTX) is a cytostatic drug that is widely used to treat a wide variety of hematological cancers, either alone or in combination with other anticancer agents [3]. This compound competitively inhibits dihydrofolate reductase (DHFR), a crucial enzyme that produces tetrahydrofolate cofactors essential for DNA synthesis [4]. Despite its efficacy, this compound is characterized by low specificity and high toxicity to healthy cells.

In the last decades, notable advances in our understanding of disease-specific biologic and genetic features, courtesy of basic science research, have profoundly transformed the treatment landscape for hematologic malignancies with the introduction of targeted therapies. The accumulating evidence implies that we will observe a further shift from conventional chemo- and radiotherapy to preferred targeted therapies [2]. In an effort to improve the selectivity of methotrexate, MTX–AuNP (gold nanoparticles) and MTX–HA (hyaluronic acid) and their conjugates have been developed and studied [5,6]. The studies proved that the conjugation of MTX with a macromolecule or nanoparticles can be used as an invaluable tool in targeted cancer treatment.

To keep up with the fast multiplication and high-energy requirement, tumor cells significantly intensify their glucose dependence and metabolism [7,8]. Remarkably, malignant cells shift their metabolism from aerobic oxidation to anaerobic glycolysis, regardless of the oxygen concentrations. A direct implication of this metabolic transformation is lower energy production, resulting in an increase in facilitative glucose transporters (GLUT, gene family SLC2) on the cellular membrane [9]. Since GLUTs are overexpressed in numerous cancers, including hematologic malignancies [7,10], they provide a selective mechanism to target neoplastic cells. Noteworthy, targeted therapy is less toxic toward normal cells, compared to systemic therapy. Based on this information, one of the possible ways to reduce the toxicity of chemotherapy drugs is to use the differences between healthy and cancer cells to design prodrugs that will reduce drug toxicity before reaching the target cell, facilitate its transport into cancer cells through overexpressed proteins whose task is the transport of specific structural elements, and release the active form of the drug in the intracellular microenvironment.

The proposed solution focuses on improving the bioavailability and selectivity of methotrexate by attaching a sugar fragment to its structure. In the tested glucose–methotrexate conjugate (Glu–MTX), the sugar fragment facilitating the targeted uptake of the therapeutic agent is connected with the therapeutic agent such as methotrexate (MTX) via a linker characterized by lability under the action of intracellular hydrolytic enzymes. The mentioned linker is attached to the sugar unit via a glycosidic bond susceptible to degradation in the presence of intracellular glycosylhydrolases, and, contrastingly, it binds methotrexate via an easily hydrolyzed carbamate bond [8]. Such a designed structure of the tested compound allows for the assumption that after penetrating into the cell, Glu–MTX undergoes degradation with the release of the active form of the drug (MTX) and metabolites such as carbon dioxide and the 1,2,3-triazole derivative of glucose **3**, and the latter one may degrade further over time (Figure 1). An additional advantage of this conjugate is the fact that the glucose derivative **3**, containing the 1,2,3-triazole unit, released in the cell as a result of enzymatic hydrolysis, also has a slight cytotoxic activity [11]. Glycoconjugate Glu–MTX may be prepared in an efficient manner using one of the so-called click-chemistry reaction, the copper-catalyzed 1,3-dipolar cycloaddition of the azide to a terminal alkyne bond (CuAAC) in a variant developed by Sharpless and used for the synthesis of a wide range of biologically active compounds [12–15].
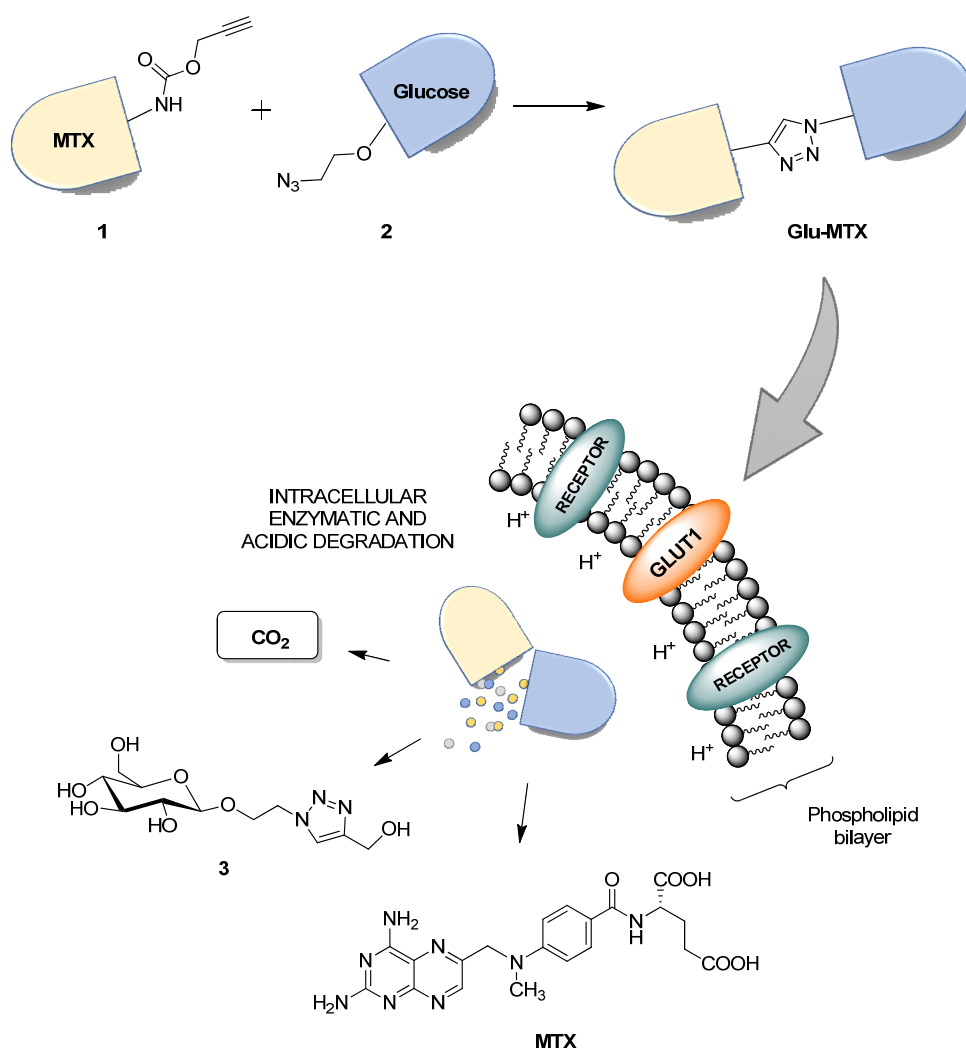
Figure 1. Scheme of Glu–MTX synthesis via copper-catalyzed 1,3-dipolar azide–alkyne cycloaddition (CuAAC), its transport into the cancer cell through the overexpressed GLUT1 transporters, and intracellular enzymatic and acidic degradation leading to the controlled release of biologically active metabolites (MTX and compound **3**).

In the current work, we have examined a Glu–MTX conjugate targeting GLUT1 in hematologic malignancies, namely, acute lymphoblastic leukemia and non-Hodgkin's lymphoma, and compared its effect with methotrexate, a chemotherapeutic agent widely applied in the treatment of leukemia and lymphoma.

2. Results

2.1. Glu–MTX Exerts a Similar Cytotoxic Effect on Lymphoma and Leukemia Cell Lines Compared to MTX

To evaluate the cytotoxic effect of Glu–MTX and compare it with free MTX, the MTT assay was performed on four hematologic cancer cell lines. The results showed that the Glu–MTX compound is cytotoxic in vitro. The comparative results of a survival evaluation of cells (IC50) are shown (Figures 2 and 3) for different hematological tumor cell lines

treated with methotrexate or glucose–methotrexate derivative (Glu–MTX). The cytotoxic effect of the glucose–methotrexate conjugate is similar to that of unmodified methotrexate.
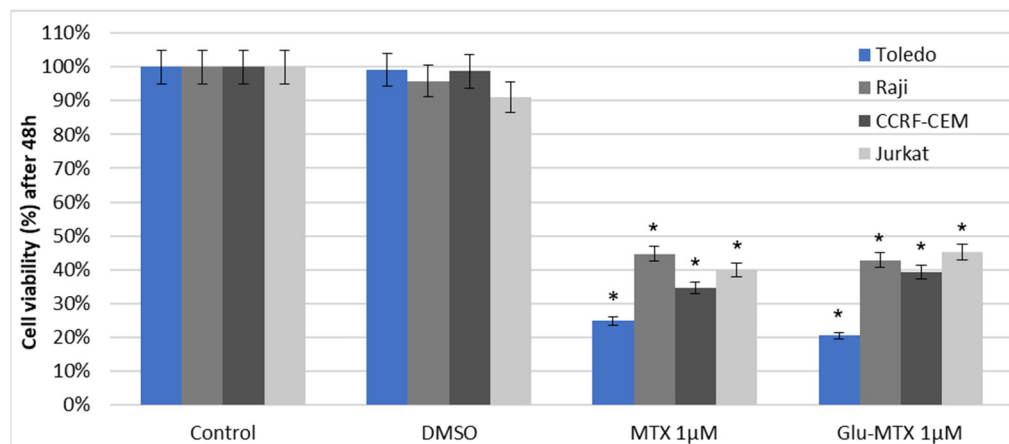
Figure 2. Cell viability after 48 h of incubation with 1 μM of MTX and Glu–MTX measured by MTT assay. DMSO was used as a vehicle. The statistical analysis of differences between control and treated sample was performed using an independent samples *t*-test. * $p < 0.05$ was indicated as statistical significance, comparing the viability of control cells with MTX and Glu–MTX-treated cells. Data are expressed as the mean $\pm$ S.D of three separate experiments.
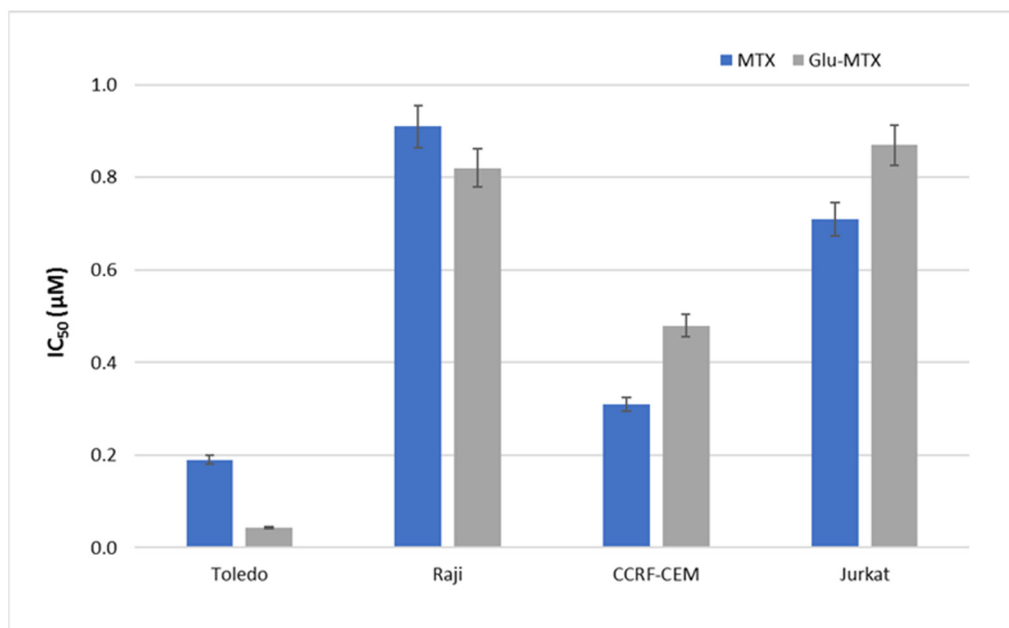
Figure 3. Comparison of IC_{50} activity of MTX and Glu–MTX. Incubation time 48 h.

2.2. Glu–MTX Induces Early and Late Apoptosis in Lymphoma and Leukemia Cell Lines and Displays a Similar Apoptotic Effect to Free MTX

The apoptosis rate of Glu–MTX-treated cells was compared with MTX-treated cells and analyzed by flow cytometry. The sum of early and late apoptosis varied at 24.5% for Raji, 35.5% for Jurkat, 47.7% for CCRF–CEM, and 59.2% for Toledo cell line, after the treatment with Glu–MTX for 48 h (Figures 4 and 5). Compared to free MTX (40.8%), the Glu–MTX induced apoptosis by 47.7% in the acute lymphoblastic leukemia CCRF–CEM cell line.
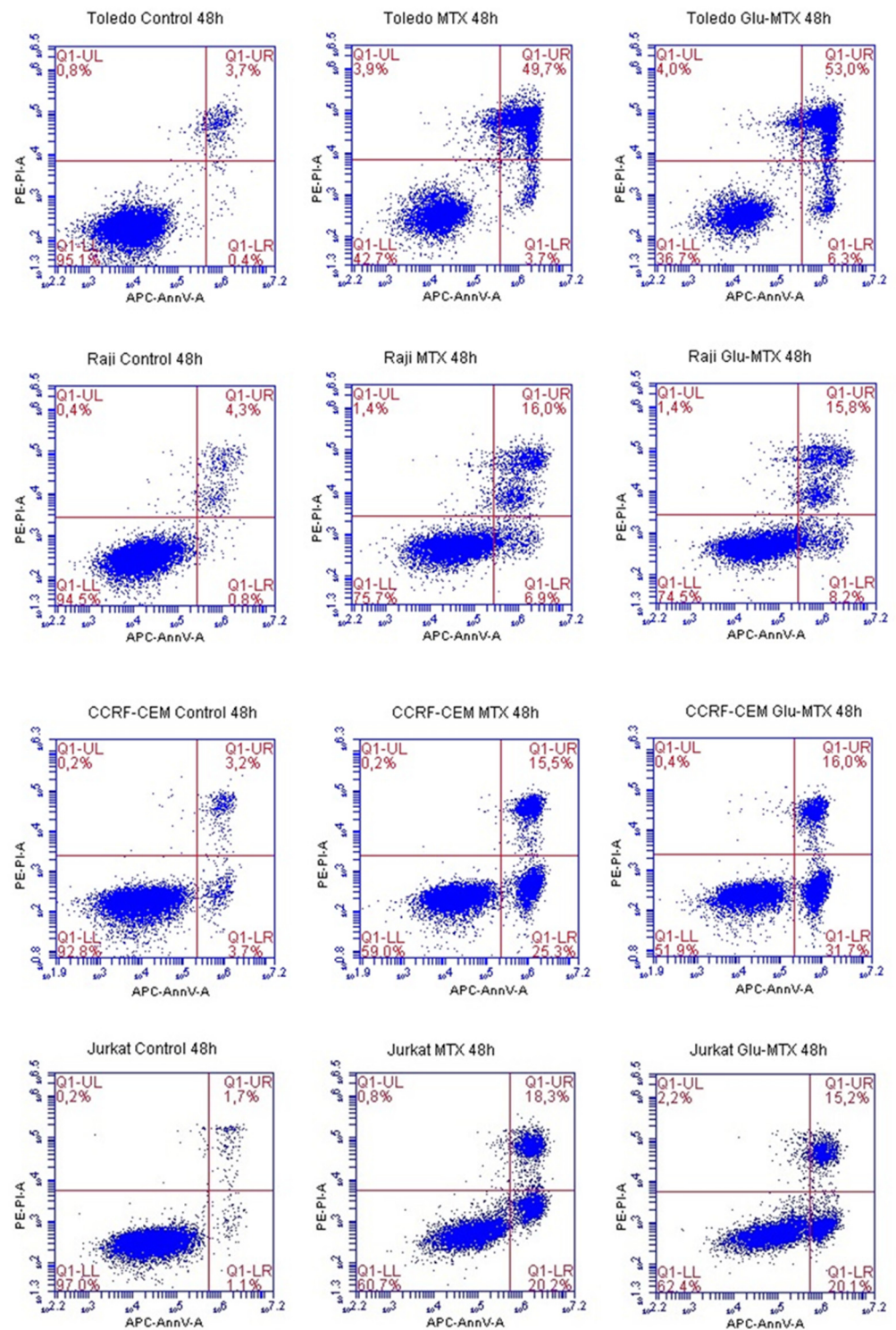
Figure 4. Representative images of flow cytometry analysis of alive (LL, lower left), early apoptotic (LR, lower right), late apoptotic (UR, upper right), and dead (UL, upper left) Toledo, Raji, CCRF–CEM, and Jurkat cells after incubation with 0.1 µM of MTX and Glu–MTX for 48 h.
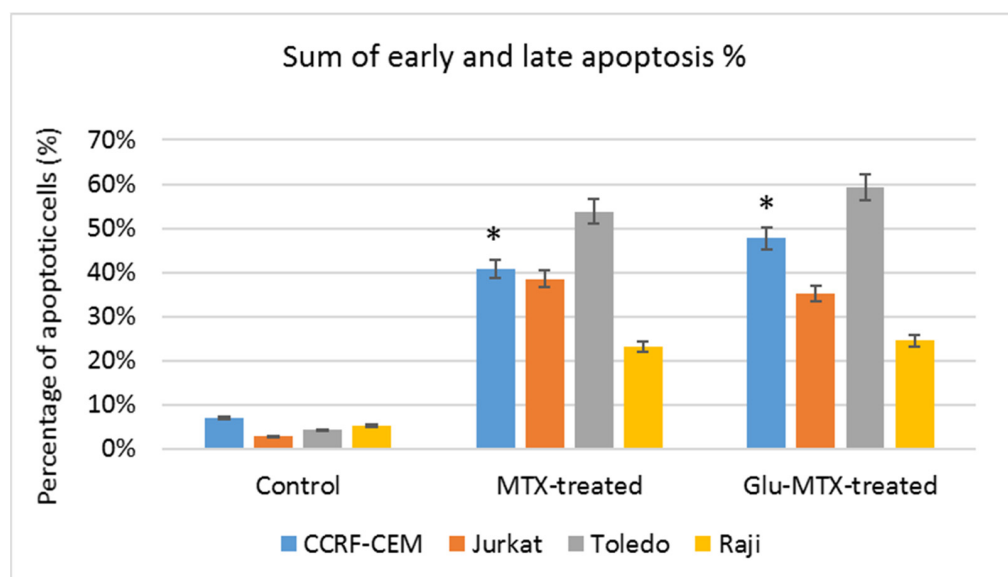
Figure 5. The percentage of early and late apoptotic cells after treatment with MTX and Glu–MTX. The statistical analysis of differences between control and treated sample was performed using an independent samples *t*-test. $* p < 0.05$ was indicated as statistical significance, comparing MTX-treated cells with Glu–MTX-treated.

2.3. Glu–MTX Displays a Similar to MTX Mechanism of Action and Inhibits DNA Synthesis in the S Phase of the Cell Cycle

To determine whether Glu–MTX displays the same mechanisms of action as MTX, its effect on cell cycle progression was examined on leukemia CCRF–CEM and Jurkat cell lines. The analysis showed that the 24 h treatment with Glu–MTX results in an S-phase arrested cell population (Figures 6 and 7). This result indicates that both compounds affect the cell cycle by arresting the cells in the S phase and display a similar mechanism of action. The most plausible explanation of this phenomenon could be that the cleavage of Glu–MTX and the release of free MTX occurs in the intracellular compartment. The results from lymphoma cell lines (Raji and Toledo) showed no changes in the cell cycle after the treatment with MTX and Glu–MTX.

2.4. The Cellular Uptake of Glu–MTX Is Significantly Higher in CCRF–CEM Acute Lymphoblastic Leukemia Cells Compared to Free MTX

To investigate the cellular transport of Glu–MTX and answer the question of whether the conjugation of glucose improves the accumulation of the compound in the intracellular compartment, a mass spectrometry analysis was performed. The results showed that the Glu–MTX is approximately 63 times more preferentially accumulated in the intracellular compartment of CCRF–CEM cells (which were characterized by increased apoptotic rate), compared to MTX (Figure 8). This result supports the hypothesis that glucose conjugates exploit the Warburg's effect and preferentially accumulate in cancer cells, contradistinctively to well-established nonconjugated agents that lack target specificity.
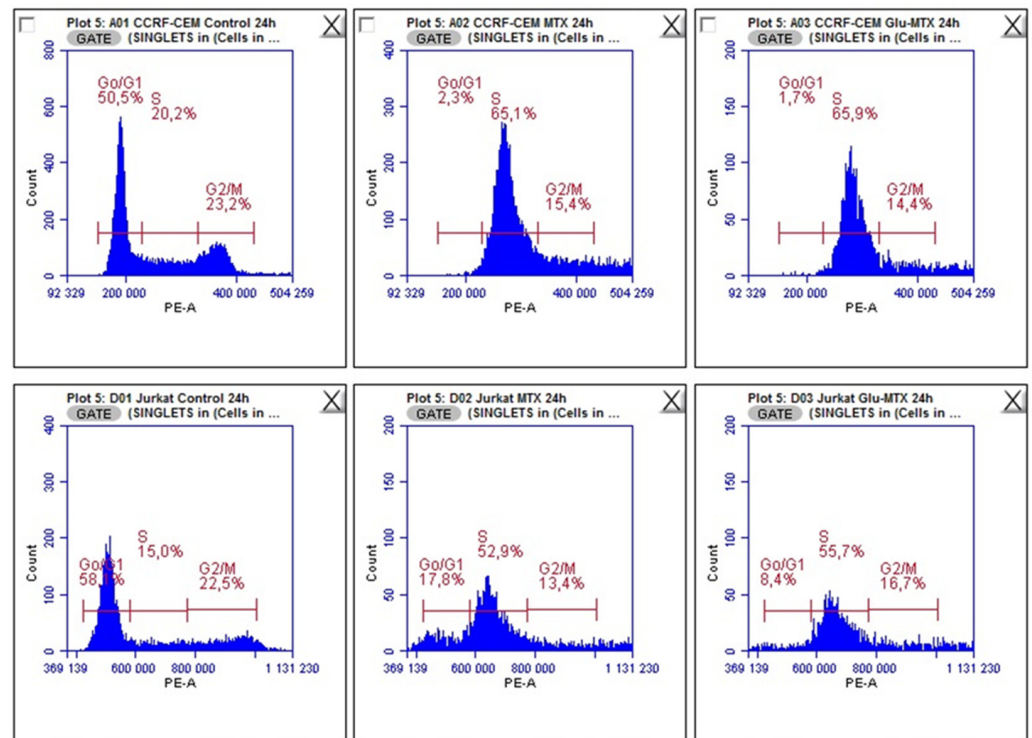
Figure 6. Cell cycle analysis of CCRF–CEM and Jurkat cells after treatment with 0.1 μM MTX and Glu–MTX for 24 h. For leukemia cells, cell cycle arrest in the S phase is characterized by the action of both the Glu–MTX conjugate and free methotrexate.
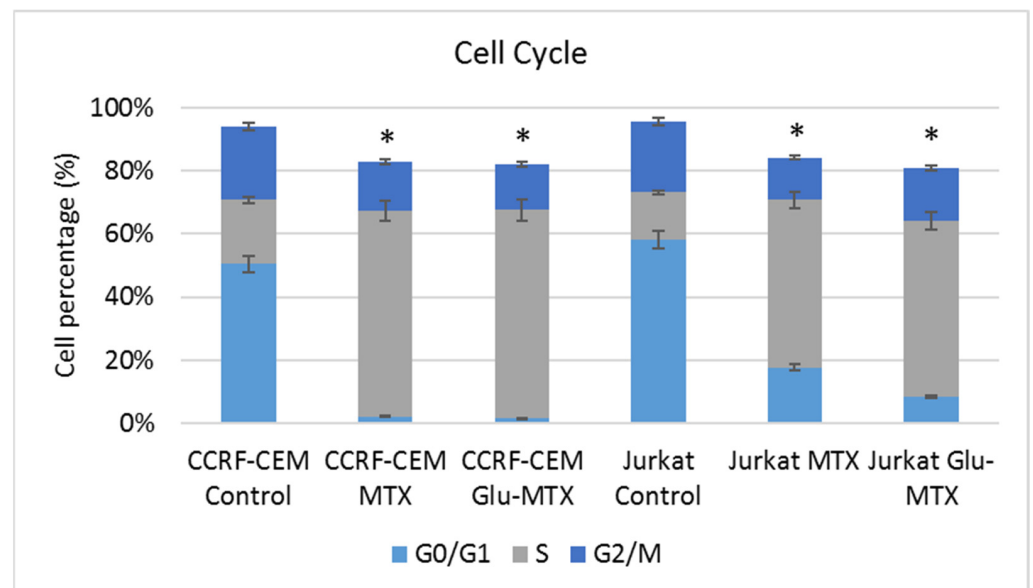
Figure 7. Comparative analysis between MTX and Glu–MTX-treated CCRF–CEM and Jurkat cells G0/G1, S, and G2/M phases. The statistical analysis of differences between control and treated samples was performed using ANOVA Kruskal–Wallis test. * $p < 0.05$ was indicated as statistical significance, comparing MTX and Glu–MTX-treated cells with control.
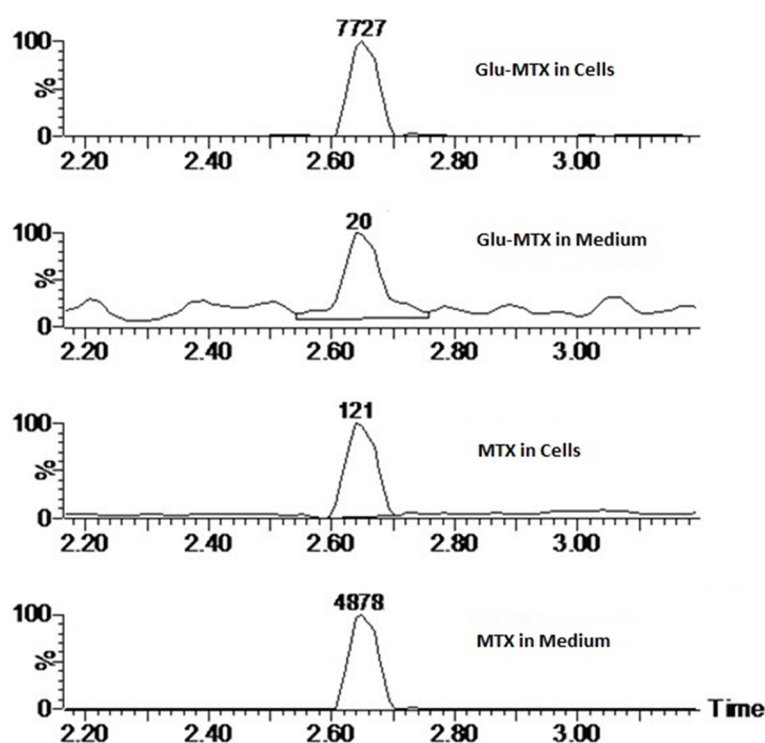
Figure 8. Extracted ion chromatograms of MTX (455.18 *m/z*) in cell extracts and culture medium. The peak area was shown above the peaks.

3. Discussion

The use of chemotherapy and autologous stem cell transplantation and the introduction of therapeutic agents, including proteasome, kinase, and histone deacetylase inhibitors, as well as immunomodulatory drugs, have enhanced clinical outcomes in patients with hematologic malignancies. However, a large portion of patients will discontinue the therapy due to adverse outcomes and/or eventually relapse, highlighting the urgent need for potent and safe therapeutic alternatives [16]. The bulk of these agents have significant toxicities that limit their dosing and potential for use in combination therapy. Although the introduction of targeted therapies has significantly enhanced outcomes for patients with hematologic malignancies, the unmet medical need remains. The burden of adverse effects resulting from systemic chemotherapy is heavy; hence, it would be desirable to develop a novel class of therapeutics that could combine conventional chemotherapeutic agents' high efficacy and versatility with low systemic toxicity. Our goal was to build upon glucose derivatives' success story by developing a novel carbohydrate conjugate that could exploit glucose transporters to target a range of hematologic malignancies selectively [17]. Here, we describe the generation and in vitro characterization of a glucose-methotrexate conjugate, a glucose transporter targeting agent with a unique combination of antitumor activities.

This study showed that the ability of Glu–MTX to induce apoptosis in vitro was slightly more prominent than MTX's in acute lymphoblastic leukemia CCRF–CEM cell line. Moreover, the compound exhibited potent activity in low doses, comparable to free MTX. However, increased uptake of Glu–MTX apparently did not translate into a significantly higher cytotoxic and apoptotic effect, which serves as an indication that the conjugate is less cytotoxic, compared to free MTX, which in turn supports the results of our previous study [11]. Another possible explanation for this could be the fact that the drug uptake was measured after 6 h, while the apoptotic effect was evaluated after 48 h, which suggests that efflux of free MTX originated from Glu–MTX to the outside of the cells could have occurred. Additionally, Glu–MTX affected the cell cycle by arresting the cells in the S phase, which indicates that the release of free MTX disassembled from Glu–MTX occurs in the intracellular compartment. Moreover, the uptake of Glu–MTX in leukemia cells was

63 times more efficient, compared to free MTX after 6 h of incubation. This result proves conclusively that the conjugation of glucose to MTX improves its selectivity and transport in leukemia cancer cells.

Nevertheless, our study bears several limitations. Firstly, the effect of Glu–MTX was not evaluated on primary malignant cells and normal hematopoietic cells. Moreover, because hematological malignancies are a heterogeneous group of neoplastic disorders, a larger panel of cell lines would be more desirable. Furthermore, since MTX affects folic acid metabolism, it can affect erythrocytes or some other healthy cells that express folate receptors. It would be valuable to measure the uptake of Glu–MTX by different healthy cells in different time points, as well as MTX's metabolites (e.g., folate–polyglutamate molecule levels) after the treatment. Yamauchi et al. [18] indicated that time-dependent change in MTX efflux in human leukemia cells corresponds with MTX activity. Moreover, according to the investigations of Walton et al. [19], circadian oscillations impact cancer cell metabolism and change the GLUT transporters' expression. Therefore, the above-mentioned findings may be important factors affecting Glu–MTX mechanism.

Lastly, further investigation is needed to determine whether the GLUT1 expression correlates with the increased drug uptake in leukemia and lymphoma cell lines. Notwithstanding the significantly higher cellular uptake of Glu-MTX, we cannot state that the transport of the conjugate is mediated exclusively by GLUT transporters. Previous studies have highlighted a potential role of sodium-driven glucose symporters (SGLTs), organic cation transporter 2 (OCT2), and SWEET transporters in the cellular transport of glycoconjugates [20,21]. In future research, it would be eligible to include studies of cell sensitization with insulin prior to Glu–MTX incubation to check whether insulin can promote GLUT transporters overexpression in lymphoma and leukemia cells to increase the cellular uptake of the conjugate. These investigations are well-known in different cancers, such as breast cancer [22,23]. Drawing on the example of several successful conjugates of glucose utilized in hematologic cancer treatment [24–26], with their favorable pharmacokinetic and safety profile, a functional Glu–MTX conjugate could offer the prospect of highly successful therapy in GLUT-abundant hematologic malignancies that might also be used readily in combination with other modalities to improve clinical outcomes. On the basis of the reported findings, Glu–MTX has shown potent in vitro activity in acute lymphoblastic leukemia and non-Hodgkin's lymphoma cell line models. Therefore, it presents an exciting opportunity for a novel class of compounds that could combine the high efficacy and versatility of conventional chemotherapeutic agents with low systemic toxicity.

4. Materials and Methods

4.1. Cell Culture

The human Diffuse large B-cell lymphoma (DLBCL) cell lines were obtained from the Leibniz Institute DSMZ-German Collection of Microorganisms and Cell Cultures (DSMZ, Braunschweig, Germany) (Raji) and the American Type Culture Collection ATCC (Toledo), while the human leukemia cell lines (CCRF–CEM, Jurkat) were kindly provided by Elzbieta Wojdat, Institute of Immunology and Experimental Therapy, the Polish Academy of Sciences, Poland. Cells were grown in RPMI 1640 medium (4.5 g/L D-glucose) supplemented with glutamine, 10% fetal bovine serum (FBS), penicillin, and streptomycin in a humidified incubator with 5% CO_2 at 37 °C. The culture medium was renewed every three days. Cell culture media, FBS, and antibiotics were purchased from Gibco (Thermo Fisher Scientific Inc., Waltham, MA, USA).

4.2. Cell Viability

To measure the metabolic activity and IC_{50} values, we used a colorimetric assay based on viable cells' ability to convert the yellow 3-(4,5-dimethylthiazol-2-yl)-2,5-diphenyl-tetrazolium bromide (MTT) dye to purple formazan crystals. Cells were cultured at 1×10^4 in 48-well plates and treated with MTX or Glu–MTX at a dose of 1μM for 48 h. Following incubation, MTT solution was added to the wells at a final concentration of 1 mg/mL

for 4 h. Subsequently, the plate was centrifuged to attach the cells, the supernatant was discarded and 100 µL of DMSO was added to the cell pellet/each well. The absorbance was measured at 570 nm using the Bio-TekBioTek ELX800 multiwell reader (BioTek, Winooski, VT, USA). The experiment was conducted in triplicate and the results were expressed as the mean ± S.D. The IC50 values were calculated using CalcuSyn software (version 2.0, Biosoft, Cambridge, UK) based on concentrations 0.05–5 µM and 48 h incubation time.

4.3. Annexin V–FITC Assay–Flow Cytometry

The percentage of alive, early, late apoptotic, and dead cells was measured by flow cytometry. Fluorochrome-labeled Annexin V was used to identify apoptotic cells. To distinguish the necrotic and early from late apoptotic cells we used propidium iodide (PI). Early apoptotic cells exclude PI, while late apoptotic cells and necrotic cells stain positively due to the passage of PI into the nucleus. For the experiment, cells were cultured at 5×10^5 in 12-well culture plates and treated with a dose of 0.1 µM MTX or Glu–MTX for 48 h. Control cells were cultured with DMSO at a final concentration of 100 nM. After 48 h, the cells were collected, centrifuged, and washed with PBS. The cell pellet of each sample was resuspended in 500 µL of 1X Binding Buffer. Then, 100 µL of each sample was mixed with 5 µL of APC fluorochrome-conjugated Annexin V and 5 µL of propidium iodide staining solution, accordingly to the staining protocol (ThermoFisher Scientific Inc., Waltham, MA, USA). After 20 min of incubation in darkness, the samples were vortexed and analyzed by a BD Accuri C6 flow cytometer (BD Biosciences, San Jose, CA, USA). The obtained results were evaluated using BD Accuri C6 plus software (version 1.0.23.1, BD Biosciences, San Jose, CA, USA).

4.4. Cell Cycle Analysis—Flow Cytometry

To investigate in which phase of the cell cycle, MTX and Glu–MTX arrest hematological lymphoma CCRF–CEM and Jurkat cells, cell cycle analysis with propidium iodide was performed. Propidium iodide was used as a fluorescent dye that binds to DNA. When excited by 488 nm laser light, DNA content in cell cycle analysis can be detected within the PE channel with a bandpass filter 610/10. Cells were cultured in 12-well plates in the count of 5×10^5 cells per well and incubated with media containing MTX or Glu–MTX at a dose of 0.1 µM for 24 h. After incubation, the cells were collected and washed with PBS solution. After centrifugation, the cell pellet was resuspended in 500 µL of cold PBS supplemented with 2.5 µL of PerFix-nc Buffer to fix the cells (BD Biosciences, San Jose, CA, USA). After 15 min, the cells were centrifuged again. The pellet was resuspended in a solution of 0.1% (*v/v*) Tritox X-100, 10 mL PBS and 0.4 mL 500 µg/mL propidium iodide (PI) and incubated in the dark in protection from light. The excitation wavelength was 488 nm, and the emitted wavelength was 630 nm. Flow cytometry was performed using BD Accuri™ C6 and analyzed using dedicated software (BD Biosciences, San Jose, CA, USA).

4.5. Cellular Uptake—Mass Spectrometry

To measure the cellular uptake of free MTX and the MTX originated from the conjugate, liquid chromatography/electrospray ionization tandem mass spectroscopy was used. CCRF–CEM cells were seeded in density 10^6 cells/well on a 6-well plate. Then, Glu–MTX and methotrexate were added in dose 0.1 µM for 6 h of incubation. To measure differences in cellular uptake, the cells were collected to the Eppendorf tube, centrifuged, and the medium was stored immediately at −80 °C. Next, the cell pellet was washed with 500 µL ice-cold methanol: H_2O (3:1). The collected supernatant was again centrifuged and stored at −80 °C until the analysis.

4.6. Conditions of LC–ESI–MS Analysis

The Waters LC–MS system comprised an Acquity UPLC and a Xevo-G2 mass spectrometer (Milford, MA, USA). Sample compounds separation was performed on an Acquity

UPLC BEH Shield column (2.1 × 50 mm, 1.7 μm). The column temperature and the autosampler temperature were kept at 40 °C and 6 °C, respectively. The mobile phase consisted of 0.1% formic acid (FA) in water was used as a mobile phase A and 0.1% FA in methanol as mobile phase B. Sample injection volume was 2 μL and the total run time of a gradient method was 6.5 min. The chromatographic method was as follows: 0.5 min—5% B, 2.0 min—40% B, 3.0 min—90% B, 4.5 min—90% B, 4.51 min—5% B. Mass spectral ionization and acquisition parameters were optimized on the Q-TOF mass spectrometer equipped with an ESI ion source in the positive ion mode. Nitrogen was used as the nebulizing and drying gas. The ion source temperature and the desolvation temperature were maintained at 120 and 400 °C. The desolvation gas flow was set at 850 L/h and the cone gas flow was 50 L/h. The capillary voltage was set at 0.5 kV. The MassLynx software (version 4.0, Waters, Milford, MA, USA) was used for data acquisition and processing.

4.7. Statistical Analysis

The results were presented as means from experiments performed in triplicate ± standard deviation (SD), and the statistical analysis of differences between control and treated sample was performed using an independent samples *t*-test or ANOVA Kruskal–Wallis test in the PQStat Software program (PQStat Software, Poland) The differences between groups were considered significant at $p < 0.05$.

5. Conclusions

In order to fulfill the hematologic malignances targeted therapies niche, we have examined the potential of glucose–methotrexate conjugate by targeting transporters that are upregulated in malignant cells. The conjugation of an antifolate metabolite with glucose seems to be a promising approach for the treatment of leukemia and lymphoma. Nevertheless, additional studies are needed to determine the therapeutic options and to overcome the limitations of the proposed therapy.

6. Patents

The authors are inventors on submitted patent applications (serial number P.426731).

Author Contributions: Conceptualization, M.W. and S.A.; methodology, M.W., G.P.-G., J.W., and M.K.; validation, G.P.-G.; formal analysis, S.M. and W.S.; investigation, M.W., S.M., and M.K.; writing—original draft preparation, M.W., G.P.-G., and S.A.; writing—review and editing, S.M., M.W., M.N., and M.K.; supervision, W.S.; project administration, S.A.; funding acquisition, S.A. All authors have read and agreed to the published version of the manuscript.

Institutional Review Board Statement: Not applicable.

Informed Consent Statement: Not applicable.

Data Availability Statement: Data are contained within the article.

Conflicts of Interest: The authors declare no conflict of interest.

Sample Availability: Samples of the compounds are not available from the authors.

References

1. Noh, J.Y.; Seo, H.; Lee, J.; Jung, H. Immunotherapy in hematologic malignancies: Emerging therapies and novel approaches. *Int. J. Mol. Sci.* **2020**, *21*, 8000. [CrossRef]
2. Simon, F.; Garcia Borrega, J.; Bröckelmann, P.J. *Toxicities of Novel Therapies for Hematologic Malignancies*; Taylor & Francis: London, UK, 2020; Volume 13.
3. Koźmiński, P.; Halik, P.K.; Chesori, R.; Gniazdowska, E. Overview of dual-acting drug methotrexate in different neurological diseases, autoimmune pathologies and cancers. *Int. J. Mol. Sci.* **2020**, *21*, 3483. [CrossRef] [PubMed]
4. Hagner, N.; Joerger, M. Cancer chemotherapy: Targeting folic acid synthesis. *Cancer Manag. Res.* **2010**, *2*, 293–301. [PubMed]

5. Shin, J.M.; Kim, S.H.; Thambi, T.; You, D.G.; Jeon, J.; Lee, J.O.; Chung, B.Y.; Jo, D.G.; Park, J.H. A hyaluronic acid–methotrexate conjugate for targeted therapy of rheumatoid arthritis. *Chem. Commun.* **2014**, *50*, 7632–7635. [CrossRef] [PubMed]

6. Chen, Y.H.; Tsai, C.Y.; Huang, P.Y.; Chang, M.Y.; Cheng, P.C.; Chou, C.H.; Chen, D.H.; Wang, C.R.; Shiau, A.L.; Wu, C.L. Methotrexate conjugated to gold nanoparticles inhibits tumor growth in a syngeneic lung tumor model. *Mol. Pharm.* **2007**, *4*, 713–722. [CrossRef]

7. Ancey, P.B.; Contat, C.; Meylan, E. Glucose transporters in cancer—From tumor cells to the tumor microenvironment. *FEBS J.* **2018**, *285*, 2926–2943. [CrossRef]

8. Woźniak, M.; Pastuch-Gawołek, G.; Makuch, S.; Wiśniewski, J.; Ziółkowski, P.; Szeja, W.; Krawczyk, M.; Agrawal, S. Overcoming hypoxia-induced chemoresistance in cancer using a novel glycoconjugate of methotrexate. *Pharmaceuticals* **2021**, *14*, 1–16.

9. Heiden, M.G.V.; Cantley, L.C.; Thompson, C.B. Understanding the warburg effect: The metabolic requirements of cell proliferation. *Science* **2009**, *324*, 1029–1033. [CrossRef]

10. Adekola, K.; Rosen, S.T.; Shanmugam, M. Glucose transporters in cancer metabolism. *Curr. Opin. Oncol.* **2012**, *24*, 650–654. [CrossRef]

11. Woźniak, M.; Pastuch-Gawołek, G.; Makuch, S.; Wiśniewski, J.; Krenács, T.; Hamar, P.; Gamian, A.; Szeja, W.; Szkudlarek, D.; Krawczyk, M.; et al. In vitro and in vivo efficacy of a novel glucose–methotrexate conjugate in targeted cancer treatment. *Int. J. Mol. Sci.* **2021**, *22*, 1748. [CrossRef]

12. Kolb, H.C.; Sharpless, K.B. The growing impact of click chemistry on drug discovery. *Drug Discov. Today* **2003**, *8*, 1128–1137. [CrossRef]

13. Ma, N.; Wang, Y.; Zhao, B.X.; Ye, W.C.; Jiang, S. The application of click chemistry in the synthesis of agents with anticancer activity. *Drug Des. Dev. Ther.* **2015**, *9*, 1585–1599.

14. Jiang, X.; Hao, X.; Jing, L.; Wu, G.; Kang, D.; Liu, X.; Zhan, P. Recent applications of click chemistry in drug discovery. *Expert Opin. Drug Discov.* **2019**, *14*, 779–789. [CrossRef]

15. Thirumurugan, P.; Matosiuk, D.; Jozwiak, K. Click chemistry for drug development and diverse chemical-biology applications. *Chem. Rev.* **2013**, *113*, 4905–4979. [CrossRef]

16. Klener, P., Jr.; Etrych, T.; Klener, P. Biological Therapy of Hematologic Malignancies: Toward a Chemotherapy-free Era. *Curr. Med. Chem.* **2017**, *26*, 1002–1018. [CrossRef] [PubMed]

17. Hossain, F.; Andreana, P.R. Developments in carbohydrate-based cancer therapeutics. *Pharmaceuticals* **2019**, *12*, 84. [CrossRef]

18. Yamauchi, A.; Ichimiya, T.; Inoue, K.; Taguchi, Y.; Matsunaga, N.; Koyanagi, S.; Fukagawa, T.; Aramaki, H.; Higuchi, S.; Ohdo, S. Cell-cycle-dependent pharmacology of methotrexate in HL-60. *J. Pharmacol. Sci.* **2005**, *99*, 335–341. [CrossRef] [PubMed]

19. Walton, Z.E.; Patel, C.H.; Brooks, R.C.; Yu, Y.; Ibrahim-Hashim, A.; Riddle, M.; Porcu, A.; Jiang, T.; Ecker, B.L.; Tameire, F.; et al. Acid Suspends the Circadian Clock in Hypoxia through Inhibition of mTOR. *Cell* **2018**, *174*, 72–87.e32. [CrossRef]

20. Deng, D.; Yan, N. GLUT, SGLT, and SWEET: Structural and mechanistic investigations of the glucose transporters. *Protein Sci.* **2016**, *25*, 546–558. [CrossRef] [PubMed]

21. Fu, J.; Yang, J.; Seeberger, P.H.; Yin, J. Glycoconjugates for glucose transporter-mediated cancer-specific targeting and treatment. *Carbohydr. Res.* **2020**, *498*, 108195. [CrossRef] [PubMed]

22. Agrawal, S.; Łuc, M.; Ziółkowski, P.; Agrawal, A.K.; Pielka, E.; Walaszek, K.; Zduniak, K.; Woźniak, M. Insulin-induced enhancement of MCF-7 breast cancer cell response to 5-fluorouracil and cyclophosphamide. *Tumor Biol.* **2017**, *39*. [CrossRef] [PubMed]

23. Barbosa, A.M.; Martel, F. Targeting glucose transporters for breast cancer therapy: The effect of natural and synthetic compounds. *Cancers* **2020**, *12*, 154. [CrossRef]

24. Li, H.; Gao, X.; Liu, R.; Wang, Y.; Zhang, M.; Fu, Z.; Mi, Y.; Wang, Y.; Yao, Z.; Gao, Q. Glucose conjugated platinum(II) complex: Antitumor superiority to oxaliplatin, combination effect and mechanism of action. *Eur. J. Med. Chem.* **2015**, *101*, 400–408. [CrossRef] [PubMed]

25. Mikuni, K.; Nakanishi, K.; Hara, K.; Hara, K.; Iwatani, W.; Amano, T.; Nakamura, K.; Tsuchiya, Y.; Okumoto, H.; Mandai, T. In vivo antitumor activity of novel water-soluble taxoids. *Biol. Pharm. Bull.* **2008**, *31*, 1155–1158. [CrossRef] [PubMed]

26. Liu, R.; Fu, Z.; Zhao, M.; Gao, X.; Li, H.; Mi, Q.; Liu, P.; Yang, J.; Yao, Z.; Gao, Q. GLUT1-mediated selective tumor targeting with fluorine containing platinum(II) glycoconjugates. *Oncotarget* **2017**, *8*, 39476–39496. [CrossRef]

Publikacja P.10

In Vitro and In Vivo Efficacy of a Novel Glucose–Methotrexate
Conjugate in Targeted Cancer Treatment

M. Woźniak, G. Pastuch-Gawołek, S. Makuch, J. Wiśniewski, T. Krenács, P. Hamar,
A. Gamian, W. Szeja, D. Szkudlarek, **M. Krawczyk**[*], S. Agrawal[*]

In Vitro and In Vivo Efficacy of a Novel Glucose–Methotrexate Conjugate in Targeted Cancer Treatment

Marta Woźniak [1], Gabriela Pastuch-Gawołek [2,3], Sebastian Makuch [1], Jerzy Wiśniewski [4,5], Tibor Krenács [6], Peter Hamar [7], Andrzej Gamian [5], Wiesław Szeja [2], Danuta Szkudlarek [1], Monika Krawczyk [2,3,*] and Siddarth Agrawal [1,8,*]

[1] Department of Pathology, Wroclaw Medical University, 50-367 Wroclaw, Poland; marta.wozniak@umed.wroc.pl (M.W.); sebastian.makuch@student.umed.wroc.pl (S.M.); danuta.szkudlarek@umed.wroc.pl (D.S.)
[2] Department of Organic Chemistry, Bioorganic Chemistry and Biotechnology, Faculty of Chemistry, 44-100 Gliwice, Poland; gabriela.pastuch-gawołek@polsl.pl (G.P.-G.); wieslaw.szeja@polsl.pl (W.S.)
[3] Biotechnology Centre, Silesian University of Technology, 44-100 Gliwice, Poland
[4] Department of Medical Biochemistry, Wroclaw Medical University, 50-367 Wroclaw, Poland; jerzy.wisniewski@hirszweld.pl
[5] Department of Immunology of Infectious Diseases, Hirszfeld Institute of Immunology and Experimental Therapy, Polish Academy of Sciences, 53-114 Wroclaw, Poland; andrzej.gamian@hirszfeld.pl
[6] Department of Pathology and Experimental Cancer Research, Semmelweis University, 1085 Budapest, Hungary; krenacst@gmail.com
[7] Institute of Translational Medicine, Semmelweis University, 1085 Budapest, Hungary; hamar.peter@med.semmelweis-univ.hu
[8] Department and Clinic of Internal Medicine, Occupational Diseases, Hypertension and Clinical Oncology, Wroclaw Medical University, 50-367 Wroclaw, Poland
*   Correspondence: monika.krawczyk@polsl.pl (M.K.); siddarth@agrawal.pl (S.A.)

Abstract: Methotrexate (MTX) is a commonly used antimetabolite, which inhibits folate and DNA synthesis to be effective in the treatment of various malignancies. However, MTX therapy is hindered by the lack of target tumor selectivity. We have designed, synthesized and evaluated a novel glucose–methotrexate conjugate (GLU–MTX) both in vitro and in vivo, in which a cleavable linkage allows intracellular MTX release after selective uptake through glucose transporter−1 (GLUT1). GLU–MTX inhibited the growth of colorectal (DLD-1), breast (MCF-7) and lung (A427) adenocarcinomas, squamous cell carcinoma (SCC-25), osteosarcoma (MG63) cell lines, but not in WI-38 healthy fibroblasts. In tumor cells, GLU–MTX uptake increased 17-fold compared to unconjugated MTX. 4,6-O-ethylidene-α-D-glucose (EDG), a GLUT1 inhibitor, significantly interfered with GLU–MTX induced growth inhibition, suggesting a glucose-mediated drug uptake. Glu-MTX also caused significant tumor growth delay in vivo in breast cancer-bearing mice. These results show that our GLUT-MTX conjugate can be selectively uptake by a range of tumor cells to cause their significant growth inhibition in vitro, which was also confirmed in a breast cancer model in vivo. GLUT1 inhibitor EDG interfered with these effects verifying the selective drug uptake. Accordingly, GLU–MTX offers a considerable tumor selectivity and may offer cancer growth inhibition at reduced toxicity.

Keywords: glycoconjugates; methotrexate; cancer treatment; glucose metabolism; drug design and discovery; anticancer drugs; targeted therapy; Warburg effect

1. Introduction

Methotrexate (MTX) is among the most widely applied and effective therapeutic agents available to treat various cancers, including breast cancer, lung cancer, bladder carcinoma, and osteogenic sarcoma, as well as autoimmune diseases [1]. However, MTX has a number of deficiencies that arise from a lack of tumor selectivity [2,3]. The pharmacokinetic parameters of MTX are unsatisfactory and frequently result in an insufficient

clinical response. Increasing the dose of MTX may result in higher therapeutic efficacy, but it also leads to a greater risk of side effects [4]. In general, the principal reason for the discontinuation of MTX is not the lack of efficacy but life-threatening toxicity. We addressed these limitations by designing a next-generation tumor-targeting MTX delivery system for improved safety and efficacy.

One of the attractive strategies to achieve the desired specificity is to connect a therapeutic agent with a ligand that selectively interacts with the pathological cell. To increase the safety and efficacy of the therapy, the synthesis of a prodrug in which the chemotherapeutic is bound to a ligand with a high-affinity for diseased cells is required. To achieve this, the diseased cells must overexpress the ligand-specific receptor that could facilitate the targeted uptake of the therapeutic agent. Examples of such prodrugs include peptide-drug, antibody–drug, aptamer-drug, and folic acid–drug conjugates [5].

In order to sustain the growth and proliferation, malignant cells significantly increase glucose uptake and the flux of substrates through glycolysis even under oxidative conditions. This abnormality, termed "the Warburg effect," originates from mitochondrial metabolic changes and is one of cancer's most common traits [6]. The elevated glucose intake requires the overexpression of glucose transporters (GLUTs), which is frequent in neo-plasms and provide clinical targets for therapy [7,8]. Therefore, glycoconjugation, in which cytotoxic agents or targeted anticancer therapeutics have been linked to glucose, can improve the selective uptake of anticancer drugs [9–14]. Since the introduction of glufosfamide [15], the potential of this strategy in diagnosis and therapy has already been realized, yet there is tremendous scope for improvement [7].

These ligand-targeting drugs (LTD) are constructed by conjugating a cleavable linker to the payload. The efficacy of such conjugate is primarily determined by the therapeutic agent activity, while the safety of the conjugate is dictated by the ligand specificity on the tumor cell. Separating the diseased cell selectivity and therapeutic drug activity is the most critical step which can be independently optimized. Therefore, we first focused on determining the optimal structure of the glucoside, through which the sugar is locked to the linker, then the transfer of the conjugate to tumor cells and its uptake mediated by GLUT1 protein. Based on these considerations, we designed, synthesized, and biologically evaluated a novel glucose–methotrexate conjugate (GLU–MTX), in which MTX, D-Glucose, and the linker are connected via a cleavable linkage susceptible to the action of hydrolytic enzymes. To the best of our knowledge, no one has previously synthesized or evaluated the conjugation of glucose to MTX. In our recent study, we showed that GLU–MTX exerts a strong cytotoxic effect on breast and colon cancer cells and displays an increased selectivity in the tumor microenvironment [16]. These findings conclusively prove the potential of glycoconjugation for the selective destruction of cancer cells by MTX. In view of this, the objective of this study was to further evaluate the efficacy of GLU–MTX on a wide variety of cancer cell lines as well as in vivo and examine the mechanisms underlying the cellular transport of glucose–methotrexate conjugate. The present study revealed that GLU–MTX is a potent therapeutic agent that preferentially accumulates in and annihilates cancer cells at reduced toxicity in the noncancerous tissues (Figure 1).
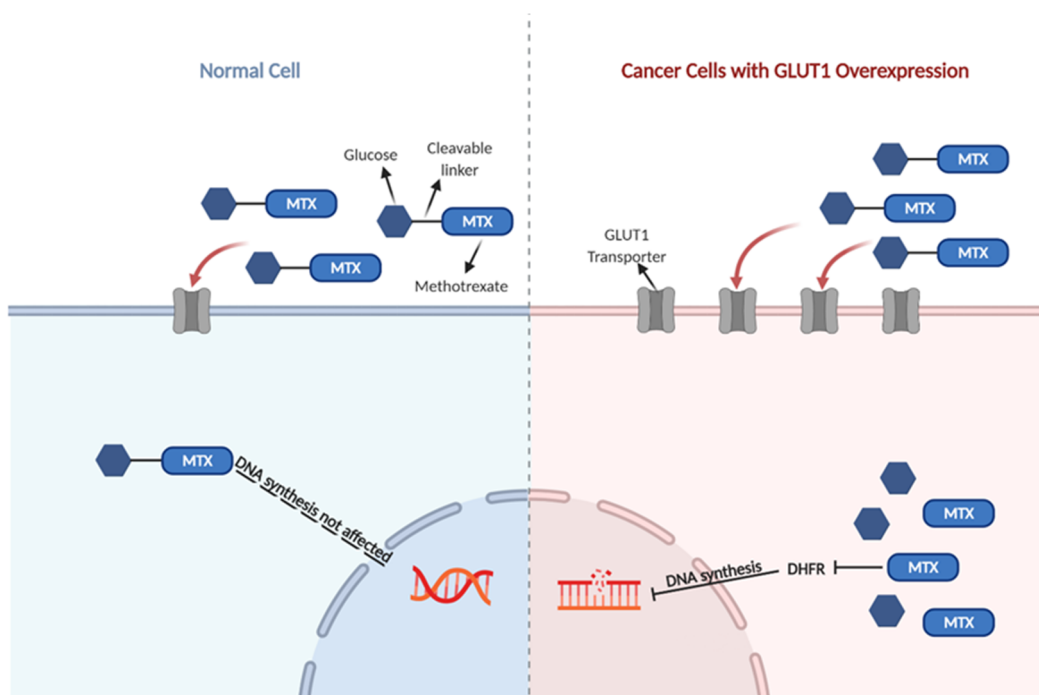
Figure 1. Cellular transport of glucose–methotrexate conjugate (GLU–MTX) in healthy and cancer cells with GLUT1 overexpression. The intracellular cleavage of acid-labile bonds in the acidic environment of cancer cells results in controlled release of MTX, which inhibits dihydrofolate reductase (DHFR) and leads to cell death. In healthy cells, no major effect in DNA synthesis is observed.

2. Results

2.1. Synthesis of Sugar Derivative Emerging from GLU–MTX Conjugate Hydrolysis in Tumor Cells

The initial stage of the research was the synthesis of a glucoconjugate **1** containing a D-glucose- unit linked via a glycosidic bond with a linker (Scheme 1). The conjugate 1 was prepared by the 1,3-dipolar cycloaddition reaction of 2-azidoethyl β-D-*O*-glucopyranoside and propargyl alcohol. As indicated in the experimental section, the results suggest that the uptake of the glucoconjugate **1** is mediated by the GLUT1 transporter. During these studies, it was also noticed that this compound has a weak cytotoxic effect. Based on the encouraging result that glucoconjugate **1** was transferred into the tumor cells, we synthesized prodrug GLU–MTX in the cycloaddition reaction according to the method developed by Sharpless. The substrates for this reaction were 2-azidoethyl β-D-*O*-glucopyranoside and MTX di-propargylcarbamide derivatives, obtained by reacting the propargyl chloroformate with an antibiotic (MTX) in the presence of *N*-methylimidazole (NMI) and tertiary amine such as *N*,*N*-diisopropylethylamine in methylene chloride as a solvent [16].
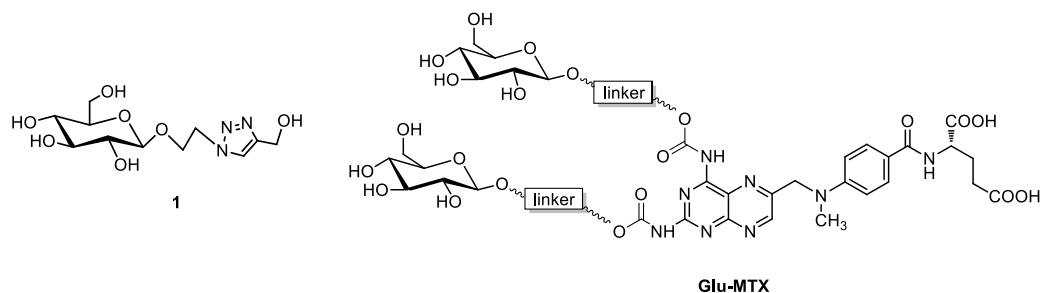
Scheme 1. Structures of the glucoconjugate **1** and GLU–MTX glycoconjugate.

GLU–MTX exhibits comparable antiproliferative activity to MTX against different cancer cell lines and has higher selectivity for cancer cells over normal cells in vitro.

GLU–MTX and MTX were first tested for their in vitro cytotoxicity with the use of the MTT assay. Six cell lines representing five types of human malignancies (breast, colon, skin, lung, bone) were cultured with test compounds at concentrations in the range of 10 to 50 μM for 48 h; then, cell viability was determined. The findings demonstrated that GLU–MTX had a similar cytotoxic effect compared to MTX on the SCC-25 skin cancer cell line (Figure 2A). Cell viability of the other MTX-treated cell lines was slightly lower (16–19% depending on the cell line) (Figure 2B–E than the viability of the same dose of GLU–MTX-treated cells. We compared the selectivity of GLU–MTX and MTX using various cancer cell lines to match the results with a healthy fibroblast WI38 cell line. As shown in Figure 2F, we found that the cellular viability of WI-38 was significantly higher in GLU–MTX-treated cells compared to MTX-treated cells. This result indicates that GLU–MTX is less cytotoxic to healthy cells than MTX.
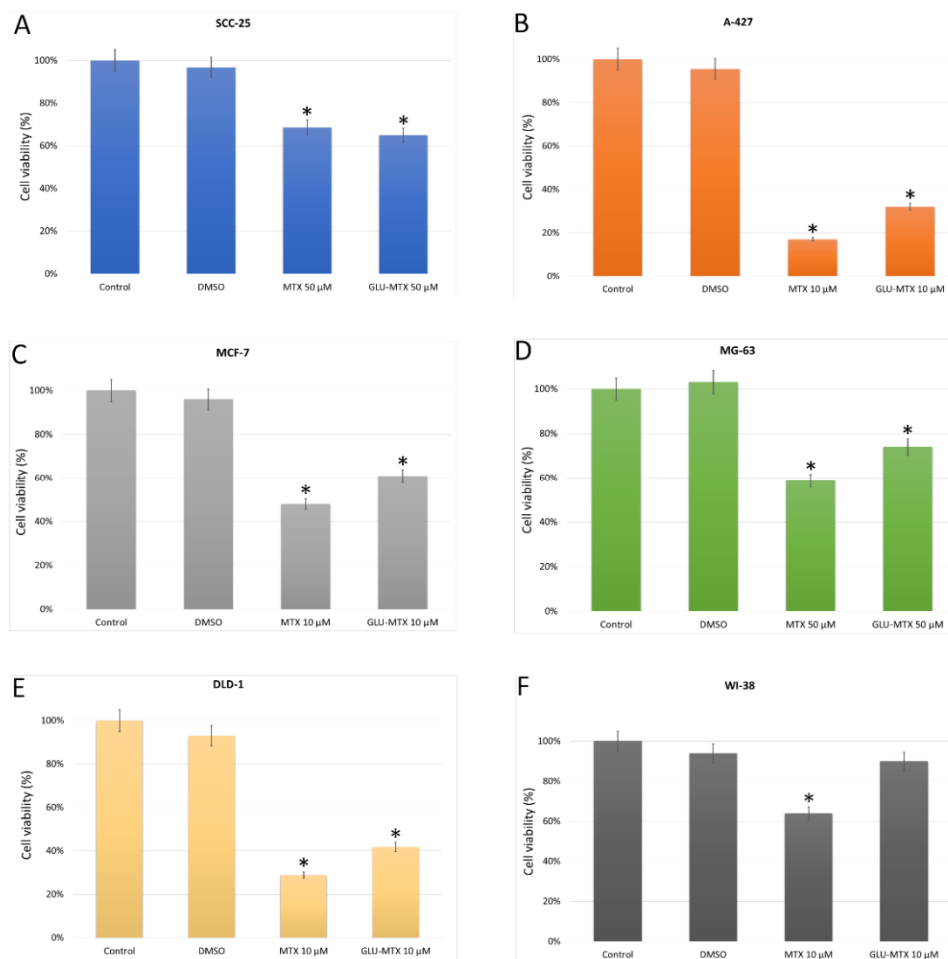
Figure 2. Cell viability of various human cancer cell lines: squamous cell carcinoma SCC-25, lung carcinoma A-427, human colon adenocarcinoma DLD-1, breast carcinoma MCF-7, osteosarcoma MG-63 (**A–E**) and normal human fibroblast WI-38 (**F**) after MTX and GLU–MTX treatment for 48 h at doses 10–50 μM. Results are presented as means ± standard deviations from three independent experiments. * $p < 0.05$ vs. control.

2.2. The Cytotoxic Effect of GLU–MTX Is Reversed by GLUT1 Inhibitor

The cytotoxicity assay was carried out in the absence and presence of an exofacial GLUT1 competitive inhibitor 4,6-O-ethylidene-α-D-glucose (EDG). Cells preincubated with EDG and then with conjugated MTX had a lower cell death ratio in comparison to cells incubated with free MTX in both cell lines. MCF-7 and A-427 cells viability after EDG + MTX treatment was 35% and 15%, respectively, whereas following EDG + GLU–MTX was 70% and 50%, respectively (Figure 3). The MTT assay results support the hypothesis that glucose transporter GLUT1 is involved in the cellular uptake of glucose conjugate MTX.
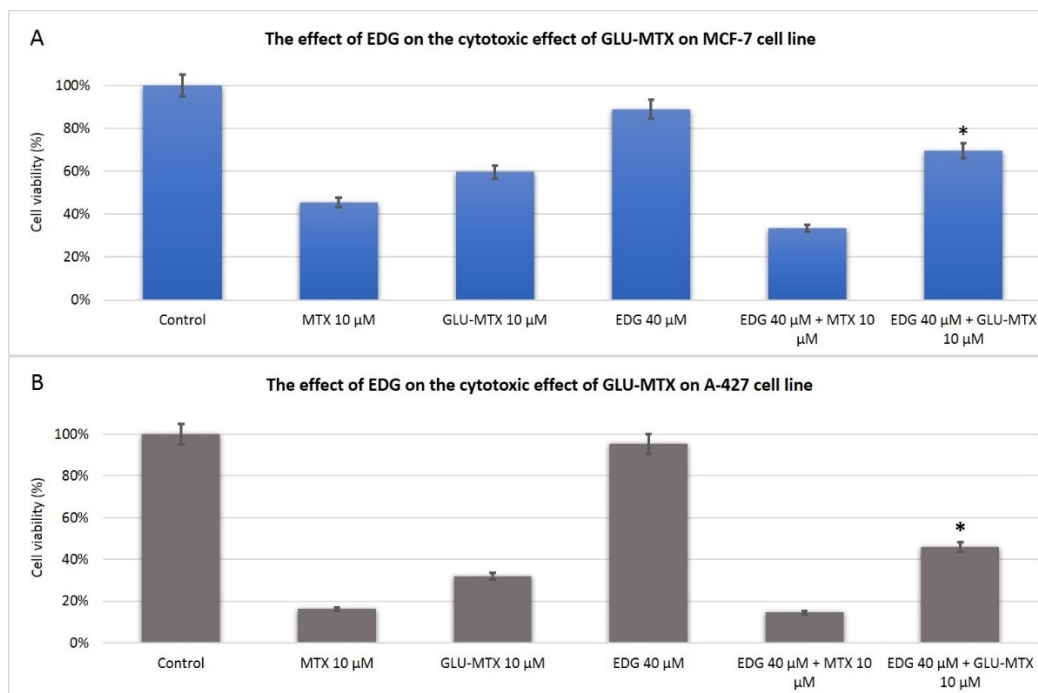
Figure 3. The effect of glucose transporter-1 (GLUT1) inhibitor 4,6-O-ethylidene-α-D-glucose (EDG) on the efficacy of free MTX and GLU–MTX treatment of (**A**) breast cancer cell line MCF-7 and (**B**) lung cancer cell line A-427. Cells were preincubated with EDG for 4 h and then incubated for 48 h with MTX or GLU–MTX. Results are presented as means $\pm$ standard deviations from two independent experiments. * $p < 0.05$ vs. GLU–MTX 10 µM.

2.3. Cellular Uptake of GLU–MTX Is Significantly Higher in SW-480 Colon Cancer Cells Compared to Free MTX

GLU–MTX is transported by facilitated diffusion exploiting overexpressed GLUT1 transporters [17] and is approximately 17-times more preferentially accumulated in cancer cells compared to free MTX (Figure 4). In the intracellular compartment, the cleavage of acid-labile bonds occurs, which results in the controlled release of free MTX.

2.4. Both MTX and GLU–MTX Lead to Cell Cycle Arrest in S Phase

To investigate whether MTX and GLU–MTX display the same mode of action, their effect on cell cycle progression was examined on the MCF-7 cell line. The results showed that cell populations in the S phase were significantly higher in MTX and GLU–MTX-treated cells after 24 h, in contradistinction with untreated cells (Figure 5, Table 1). This result proves that both compounds affect the cell cycle in a similar way, indicating the presence of free MTX originated from GLU–MTX in the intracellular compartment.
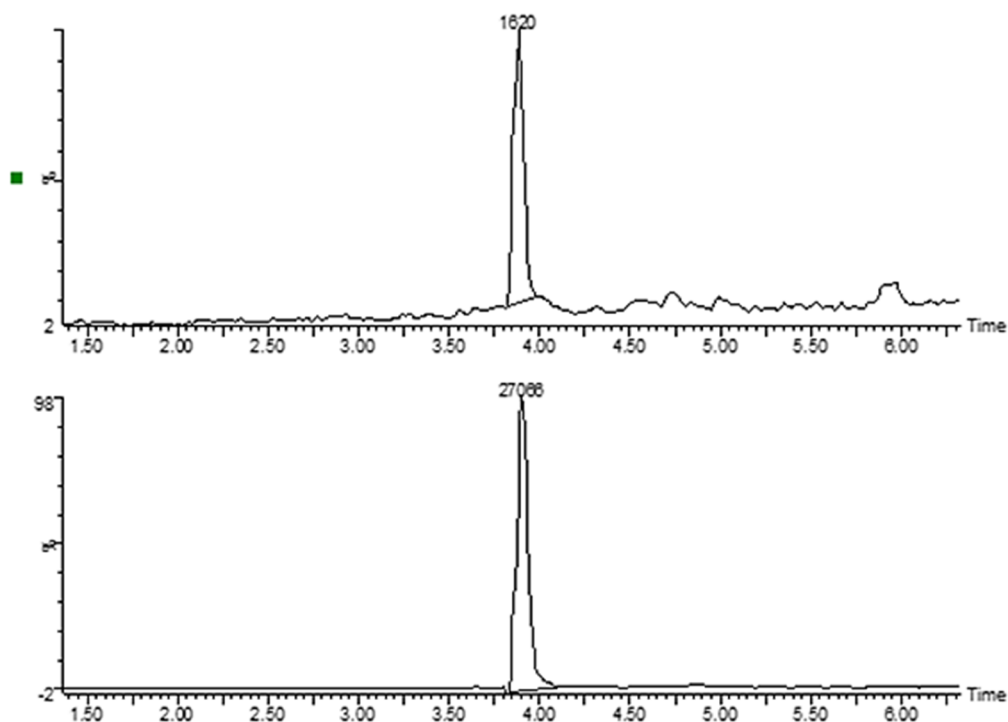
Figure 4. Mass chromatograms for m/z 455.18 ions in extracts from colon cancer SW-480 cell line—upper chromatogram MTX, lower GLU–MTX.
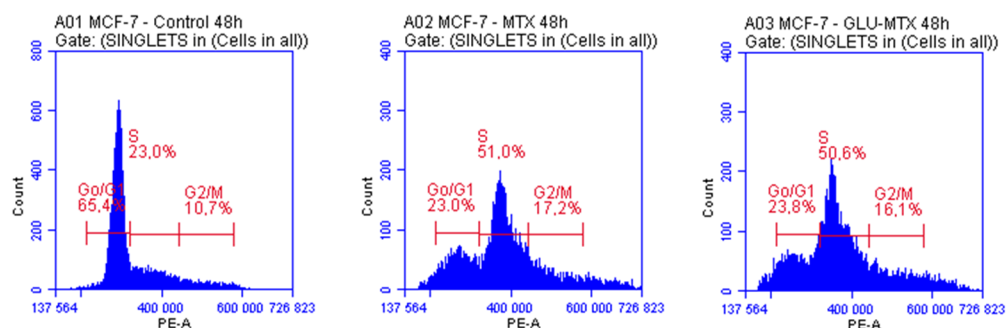

Figure 5. The effect of MTX and GLU–MTX on MFC-7 cell cycle progression.

Table 1. Cell cycle progression data presented as mean $\pm$ standard deviation (SD).

	G0/G1	S	G2/M
Control	65.4 ± 2.1	22.99 ± 0.8	10.7 ± 0.6
MTX	23.05 ± 1.4	50.97 ± 2.3	17.17 ± 1.3
GLU–MTX	23.83 ± 1.7	50.61 ± 1.9	16.11 ± 1.8

2.5. In Vivo Efficacy of GLU–MTX

After our observations of its potent in vitro effects, GLU–MTX and MTX were evaluated on 4T1 breast tumor-bearing mice, which are characterized by GLUT1 overexpression [18]. The compounds were injected i.v. in a single dose (day 0). MTX was given at 120 mg/kg, and GLU–MTX was given at a corresponding dose of 300 mg/kg. GLU–MTX significantly inhibited 4T1 allograft tumor growth by about 74.4% on day 18 ($p < 0.01$), whereas MTX led to tumor growth inhibition by 16.2% (Figure 6A). There was no significant loss of body weight in neither of the treatment groups (Figure 6B).
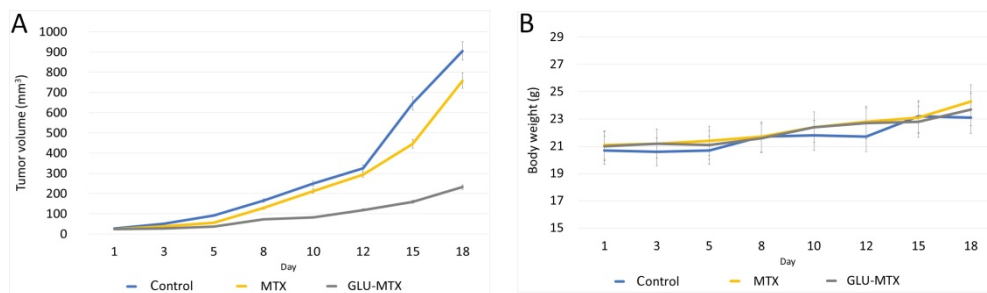
Figure 6. Results of the in vivo study. (**A**) The average tumor volume after 18 days in 3 groups (1—control, 2—MTX-treated and 3—GLU–MTX treated). In group 3, the tumor volume was significantly lower compared to other groups, as analyzed by one-way ANOVA followed by Bartlett's test ($p < 0.001$). (**B**) The effect of the therapy on body weight. No significant loss of body weight has been observed.

Histopathological analyses of the liver and lungs excised from MTX and GLU–MTX-treated mice showed differences in tissue morphology (Figure 7). Liver sections after MTX-treatment indicate visible periportal inflammation, while lung sections show lymphocytic and plasmacytic infiltration. Livers and lungs from GLU–MTX treated mice were without any morphological changes. Thus, the results indicate that GLU–MTX significantly inhibited tumor growth without affection of livers and lungs compared to free MTX.
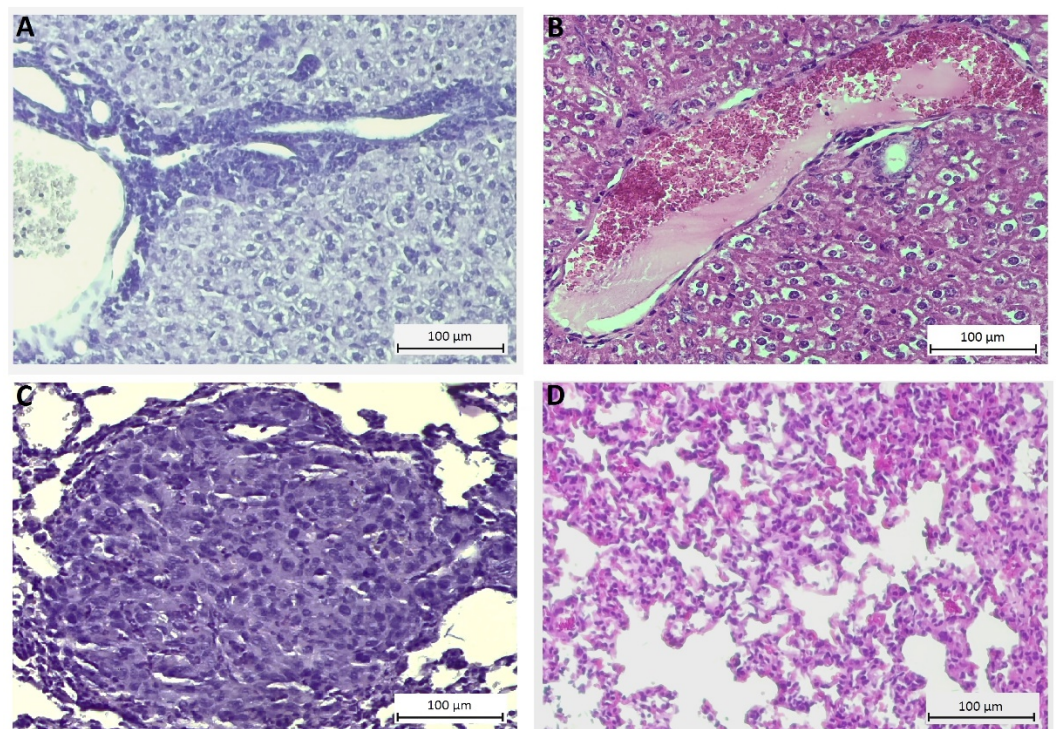
Figure 7. Representative images of liver and lung sections stained with hematoxylin–eosin (HE) to evaluate the cytotoxic impact of the MTX and GLU–MTX on the mice tissues. (**A**) Liver with typical for MTX therapy periportal inflammation. (**B**) The liver without pathological changes after GLU–MTX treatment. (**C**) The lung section shows lymphocytic and plasmacytic infiltration in mice treated with MTX. (**D**) Lung section without significant changes in the morphology from mice after treatment of GLU–MTX. Optical magnification: 200×. Scale bars 100 μm.

3. Discussion

The "Warburg effect," the increased aerobic glycolysis in many malignancies, has been extensively scrutinized and is now suggested to be the reason for most of the hallmarks of cancer [19,20]. Metabolic differences between normal and cancer provide an environment that often results in drug resistance. However, these characteristic features may also provide an opportunity to design appropriately tailored molecular targeted oncotherapy interventions.

This study represents the first attempt to systematically evaluate the anticancer activities of a novel glucose–methotrexate conjugate in vitro and in vivo. We have shown several essential characteristics of this drug: (a) GLU–MTX exhibits potent anticancer activity against a range of solid tumor cell lines with IC50 values similar to free MTX; (b) GLU–MTX preferentially annihilates cancer cells while showing low toxicity in noncancerous cells in vitro; (c) cellular uptake of GLU–MTX is glucose-transporter-specific; (d) the uptake of GLU-MTX in cancer cells is 17 times more efficient than that of MTX; (e) Glu-MTX caused significant tumor growth delay in breast tumor-bearing mice compared to MTX-treated and control mice.

Our results indicate that GLU–MTX may be used against a broad spectrum of cancers. Glu- MTX cytotoxicity consistently had IC50 values in the μmol/L range. The compound exerted higher selectivity for cancer cells over normal cells. The translocation efficiency and subsequent cellular accumulation were significantly higher in GLU–MTX-treated cells than in MTX. Notably, our results indicate that glucose transporter GLUT1 is involved in the cellular uptake of glucose conjugates. The viability of MTX-treated cells did not change significantly in the presence of an exofacial GLUT1 inhibitor. However, the GLUT1 inhibitor decreased the activity of GLU–MTX, which suggests that the reduced uptake of the compound resulted in lower cellular accumulation and weaker anticancer action. We cannot univocally state that the cellular transport of glucose conjugate is facilitated solely via the GLUT1 transporter. However, knowing that the glycoconjugates are highly hydrophilic, it is rather unlikely that their transport occurs via passive diffusion. Evidence has been found that the cellular uptake of some glycoconjugates may also be mediated by other receptors such as OCT2, SGLT, SWEET, and asialoglycoprotein receptor (ASGPR) [21,22]. These findings are corroborated by other studies showing that glucose conjugates exploit glucose transporters of cancer cells [9,17]. The uptake analysis showed that in the intracellular compartment, the payload was quickly detached from the conjugate. This suggests that the cleavable linkage allows the release of the cytotoxic payload inside the malignant cells, possibly through enzymatic hydrolysis. This finding is particularly significant as the spacer arm must be designed in such a way as to ensure its stability in the extracellular compartment while also allowing the action of the active cytotoxic payload addressed to tumor cells. The nature of the spacer thus influences how favorable drug delivery is and its outcome. Over-stable linkers can curb the activity of the associated pharmacophore, resulting in a low-potency compound. Conversely, an understable spacer can provoke poor target specificity and high systemic toxicity [23].

Our study bears several limitations. First, the synthesis is multi-staged and requires more delicate control of the experimental parameters. Hence, a limited amount of the compound was obtained for biological assays. Second, we were able to perform in vitro and in vivo analysis only on selected cancer cell models; hence the results may not be generalizable. Third, the in vivo study did not include multiple administrations of the tested compounds. Further analyses are required to examine these effects on an animal model.

4. Materials and Methods

4.1. Chemistry

NMR spectra were recorded with an Agilent spectrometer 400 MHz using TMS as internal standard and CDCl$_3$ or DMSO-d6 as a solvent. NMR solvents were purchased from ACROS Organics (Geel, Belgium). Chemical shifts (δ) were expressed in ppm and coupling constants (J) in Hz. Optical rotations were measured with a JASCO *P*-2000 polarimeter

using a sodium lamp (589.3 nm) at room temperature. Melting point measurements were performed on a Stanford Research Systems OptiMelt (MPA 100). Electrospray ionization mass spectrometry was performed on the Xevo G2 Q-TOF mass spectrometer. Reactions were monitored by TLC on precoated plates of silica gel 60 F254 (Merck Millipore, Burlington, MA, USA). The TLC plates were inspected under UV light (λ = 254 nm) or charring after spraying with 10% sulfuric acid in ethanol. Crude products were purified using column chromatography performed on silica gel 60 (70–230 mesh, Fluka, St. Louis, MI, USA) developed with toluene/EtOAc and $CHCl_3$/MeOH as solvent systems. Organic solvents were evaporated on a rotary evaporator under diminished pressure at 40 °C. All of the chemicals used in the experiments were purchased from Sig-ma-Aldrich (Saint Louis, Missouri, USA), ACROS Organics (Geel, Belgium), and Avantor Performance Materials Poland S.A (Gliwice, Poland) and were used without purification. Methotrexate, propargyl chloroformate, propargyl alcohol, and D-glucose are commercially available. 2-Azidoethyl β-D-O-glucopyranoside [24,25] and GLU–MTX [16] was prepared according to the respective published procedures.

Synthesis of Glycoconjugate

2-Azidoethyl β-D-O-glucopyranoside (82 mg, 0.33 mmol) and propargyl alcohol (20 µL, 0.33 mmol) were dissolved in a dry solvent system: THF (3 mL) and *i*-PrOH (3 mL). The solutions of sodium ascorbate (27 mg, 0.13 mmol) in H_2O (1.5 mL) and $CuSO_4 \cdot 5H2O$ (16 mg, 0.06 mmol) in H_2O (1.5 mL), mixed and immediately added to the reaction mixture. The reaction mixture was stirred for 24 h at room temperature. Then, the solvents were evaporated in vacuo, and the crude products were purified by column chromatography (dry loading: $CHCl_3$:MeOH, gradient: 50:1 to 2:1) to give products **1** (69 mg, 70% yield): m.p. 60–63 °C; $[\alpha]_D^{22}$ = −5 (c = 1.0, DMSO).

^{1}H NMR (400 MHz, DMSO-d6): δ 2.97 (m, 1H, H-2$_{Glu}$), 3.04 (m, 1H, H-4$_{Glu}$), 3.09–3.16 (m, 2H, H-3$_{Glu}$, H-5$_{Glu}$), 3.43 (m, 1H, H-6a$_{Glu}$), 3.68 (m, 1H, H-6bGlu), 3.89 (m, 1H, CH), 4.07 (m, 1H, CH), 4.23 (d, 1H, J = 7.8 Hz, H-1$_{Glu}$), 4.47–4.58 (m, 5H, 2xCH2, OH), 4.91 (d, 1H, J = 5.1 Hz, OH), 4.95 (d, 1H, J = 4.7 Hz, OH), 5.06 (d, 1H, J = 5.1 Hz, OH), 5.15 (dd, 1H, J = 5.5 Hz, J = 5.9 Hz, OH), 8.01 (s, 1H, H-5$_{triaz}$).

13C NMR (100 MHz, DMSO-d6): δ 49.54, 54.99, 61.05, 67.41, 69.99, 73.29, 76.60, 76.97, 102.93, 123.45, 147.68.

HRMS (ESI-TOF): calcd for $C_{11}H_{20}N_3O_7$ ($[M + H]^+$): m/z 306.1301; found m/z 306.1300.

4.2. Cell Culture

The panel of different human cell lines was used to evaluate the effectiveness of the novel compound, human colon adenocarcinoma SW-480 and DLD-1, breast carcinoma MCF-7, squamous cell carcinoma SCC-25 purchased from the Leibniz Institute DSMZ-German Collection of Microorganisms and Cell Cultures, (DSMZ, Braunschweig, Germany), lung carcinoma A427, osteosarcoma MG63, normal fibroblasts WI-38 kindly provided by Institute of Immunology and Experimental Therapy, the Polish Academy of Sciences, Poland, and obtained from American Type Culture Collection. Cell lines A427, MG63, WI-38 cells were maintained in Eagle's minimum essential medium, MCF-7, DLD-1 in RPMI 1640, SCC-25 in DMEM/F12 medium. To make the complete growth medium, fetal bovine serum (FBS) to a final concentration of 10% and 100 U/mL penicillin, 100lg/mL streptomycin were added. Cells were grown in a humidified incubator with 5% CO_2 at 37 °C. The fresh culture medium was changed every 2–3 days. Cell culture media, FBS, trypsin, and antibiotics were used from Gibco (Thermo Fisher Scientific Inc., Waltham, MA, USA).

4.3. In Vitro Cytotoxicity of MTX and GLU–MTX

For MTT experiments, cell lines were seeded in 96-well plates ($5-8 \times 10^3$ cells/well). The following day cells were treated with an appropriate complete culture medium (control) and different doses of methotrexate and glucose conjugated MTX (10, 50 μM) for 48 h.

After the incubation, an MTT assay was performed. Cell viability was evaluated by the conversion of the yellow tetrazolium salt (MTT) into violet formazan insoluble crystals in mitochondria of active cells. Following 4 h, the medium was removed, and the dye was dissolved by dimethyl sulfoxide (DMSO, Sigma-Aldrich, Munich Germany), creating the color, which intensity is proportional to the viable cells. The absorbance rate was measured at 490 nm, and the reference wavelength was 570 nm (Bio-TekBioTek ELX800 multi-well reader, BioTek, Winooski, VT, USA). The viable cells (VC) were calculated as VC (100%) = (absorbance of experimental group/absorbance of the control group) $\times$ 100%. MTT experiments were repeated, and figures represent the mean with standard deviation.

4.4. Measurement of Cellular Uptake of MTX and GLU–MTX by Mass Spectrometry

To measure differences in cellular uptake of Glu-Met and methotrexate, MCF-7 and SW480 cells were seeded in density 3×10^5/well on 6 well plates. When cells reached 80% confluence, the medium was replaced with 1 mL/well fresh medium with or without tested compounds in dose 50 μM. Following 6 h of incubation, the medium was centrifuged, collected and stored immediately at -80 °C. Then adherent cells were washed once with 1 mL PBS at room temperature (RT). Next, the plate was placed on ice and washed with 500 ul ice-cold methanol: H2O (3:1) twice. The collected supernatant was centrifuged and stored at -80 °C until the analysis.

4.5. LC/MS Analysis
4.5.1. Equipment

The UPLC system consisted of the Acquity UPLC binary pump, cooled sample manager and column oven (Waters, Milford, MA, USA). The mass spectrometer was a Xevo G2 Q-TOF MS equipped with an electrospray ionization interface (Waters, Milford, MA, USA). The data were acquired by using MassLynx software (version 4.0, Waters, Milford, MA, USA).

4.5.2. LC Conditions

Chromatographic separation was performed using a Waters BEH Shield (1.7 μm, 2.1 × 100 mm) analytical column. The oven temperature was set at 45 °C. The mobile phases containing 0.1% formic acid in water (mobile phase A) and 0.1% formic acid in methanol (mobile phase B) were used at a flow rate of 0.2 mL/min. Gradient elution was performed according to the following steps: 1.0 min—5% B, 5.0 min—40% B, 7.5 min—65% B, 10 min—90% B, 11 min—90% B, 11.1 min—5% B, 13 min—5% B. The autosampler temperature was kept at 5 °C.

4.5.3. MS Conditions

A mass spectrometer was interfaced with an electrospray ionization (ESI) probe. Mass spectra acquisition parameters were optimized using electrospray ionization (ESI) in the positive ionization mode. The temperatures were maintained at 120 °C and 450 °C for the source and desolvation line, respectively. The voltages were set at 0.5 kV and 40 V for the capillary and sampling cone, respectively. The desolvation gas and the cone gas (N2) flow rate was set at 800 L/h and 80 L/h, respectively.

4.6. Cell Cycle Analysis

After treatment, control cells, MTX and GLU–MTX-treated cells were harvested, collected and washed in PBS. Then, the cells were resuspended at $1-2 \times 10^6$ cells/mL, and 5 mL of cold 70% ethanol was carefully added. Afterward, the cells were fixed for at least 1 h at 4 °C. Following washing twice in PBS, 0.5 mL of FxCycle™ PI/RNase staining

solution (Life Technologies, Carlsbad, USA) to cell pellet was added and mixed well. The samples were incubated for 15–30 min at room temperature, protected from light and then analyzed by flow cytometry to determine the cell cycle profile.

4.7. Mouse Allograft Model of Human Breast Cancer

The animal use and care protocol were approved by the local ethical committee for animal experiments. The female BALB/c mice with a weight of 17–20 g (6–8 weeks old) were provided and maintained on free access to food and water. Then female BALB/c mice were injected subcutaneously with 4T1 breast cancer cell. The cells were suspended in 50 µL of Hanks' solution: Matrigel (9:1) and implanted in the second right mammary gland (10^5–10^6 cells per mouse).

All animals were monitored for activity, physical condition, body weight, and tumor growth. Tumor size was determined every other day by caliper measurement of two perpendicular diameters of the implant. Tumor weight (in grams) was calculated by the formula $TV = 1/2 \times a2 \times b$, in which a is the long diameter, and b is the short diameter (in millimeters).

4.8. In Vivo Chemotherapy

The animals bearing breast cancer allograft tumors were randomly divided into two treatment groups and a control group (5–7 mice per group). Test animals received a single i.v. injection via the tail vein of GLU–MTX and MTX at a dose of 300 mg/kg, and 120 mg/kg, respectively. The treatment was started one day after the transplantation of tumor cells. The control animals received an injection of 0.2 mL of the vehicle only. The tumor volume and weight of each mouse were measured over a period of 18 days. The body weights of 4T1 tumor-bearing mice treated with GLU–MTX, MTX, and vehicle (DMSO) only were recorded simultaneously every 2 to 3 days during the study. No mice were lost during the experiment.

4.9. Histological Evaluation of Toxicity

Formalin-fixed and paraffin-embedded tissue sections of livers and lungs were stained with hematoxylin–eosin (HE) to evaluate the impact of the therapeutics on the tissues and 4T1 cells metastasis.

4.10. Statistical Analysis

In vivo data were analyzed by one-way analysis of variance (ANOVA). $p < 0.05$ was considered statistically significant. Data from in vitro experiments were expressed as means ± standard deviation (SD), and the statistical analysis was performed using Mann–Whitney U test in the PAST 4.03 program. The differences between groups were considered significant at $p < 0.05$.

5. Conclusions

In conclusion, we have synthesized a novel GLU–MTX conjugate and have shown that it has broad-spectrum anticancer activity. The compound preferentially accumulates in and annihilates malignant cells while showing reduced accumulation and low toxicity in normal fibroblasts. These results collectively represent a critical step forward in developing molecular tumor-targeting properties into established therapeutic drugs for improved safety and efficacy of anticancer therapies. These studies are essential for further preclinical and clinical development of a glucose-based class of compounds.

6. Patents

The authors are inventors on submitted patent applications (serial number P.426731).

References

1. Khan, Z.A.; Tripathi, R.; Mishra, B. Methotrexate: A detailed review on drug delivery and clinical aspects. *Expert Opin. Drug Deliv.* **2012**, *9*, 151–169. [CrossRef]
2. Howard, S.C.; McCormick, J.; Pui, C.; Buddington, R.K.; Harvey, R.D. Preventing and Managing Toxicities of High-Dose Methotrexate. *Oncologist* **2016**, *21*, 1471–1482. [CrossRef] [PubMed]
3. Świerkot, J. Toxicity of low dose methotrexate in rheumatoid arthritis. *Adv. Clin. Exp. Med.* **2007**, *16*, 287–295.
4. Abolmaali, S.S.; Tamaddon, A.M.; Dinarvand, R. A review of therapeutic challenges and achievements of methotrexate delivery systems for treatment of cancer and rheumatoid arthritis. *Cancer Chemother. Pharmacol.* **2013**, *71*, 1115–1130. [CrossRef] [PubMed]
5. Mahato, R.; Tai, W.; Cheng, K. Prodrugs for improving tumor targetability and efficiency. *Adv. Drug Deliv. Rev.* **2011**, *63*, 659–670. [CrossRef]
6. Liberti, M.V.; Locasale, J.W. The Warburg Effect: How Does it Benefit Cancer Cells? *Trends Biochem. Sci.* **2016**, *41*, 211–218. [CrossRef]
7. Calvaresi, E.C.; Hergenrother, P.J. Glucose conjugation for the specific targeting and treatment of cancer. *Chem. Sci.* **2013**, *4*, 2319–2333. [CrossRef]
8. Makuch, S.; Wozniak, M.; Krawczyk, M.; Pastuch-Gawołek, G.; Szeja, W.; Agrawal, S. Glycoconjugation as a promising treatment strategy for psoriasis. *J. Pharmacol. Exp. Ther.* **2020**, *373*, 204–212. [CrossRef]
9. Patra, M.; Awuah, S.G.; Lippard, S.J. Chemical Approach to Positional Isomers of Glucose-Platinum Conjugates Reveals Specific Cancer Targeting through Glucose-Transporter-Mediated Uptake in Vitro and in Vivo. *J. Am. Chem. Soc.* **2016**, *138*, 12541–12551. [CrossRef]
10. Agrawal, S.; Wozniak, M.; Luc, M.; Walaszek, K.; Pielka, E.; Szeja, W.; Pastuch-Gawolek, G.; Gamian, A.; Ziolkowski, P. Insulin and novel thioglycosides exert suppressive effect on human breast and colon carcinoma cells. *Oncotarget* **2017**, *8*, 114173–114182. [CrossRef]
11. Ma, Y.; Wang, W.; Idowu, M.O.; Oh, U.; Wang, X.Y.; Temkin, S.M.; Fang, X. Ovarian cancer relies on glucose transporter 1 to fuel glycolysis and growth: Anti-tumor activity of BAY-876. *Cancers* **2019**, *11*, 33. [CrossRef] [PubMed]
12. Dyshlovoy, S.A.; Pelageev, D.N.; Hauschild, J.; Borisova, K.L.; Kaune, M.; Krisp, C.; Venz, S.; Sabutskii, Y.E.; Khmelevskaya, E.A.; Busenbender, T.; et al. Successful targeting of thewarburg effect in prostate cancer by glucose-conjugated 1,4-naphthoquinones. *Cancers* **2019**, *11*, 1609. [CrossRef] [PubMed]
13. Barbosa, A.M.; Martel, F. Targeting glucose transporters for breast cancer therapy: The effect of natural and synthetic compounds. *Cancers* **2020**, *12*, 154. [CrossRef] [PubMed]
14. Tomaszowski, K.-H.; Hellmann, N.; Ponath, V.; Takatsu, H.; Shin, H.-W.; Kaina, B. Uptake of glucose-conjugated MGMT inhibitors in cancer cells: Role of flippases and type IV P-type ATPases. *Sci. Rep.* **2017**, *7*, 13925. [CrossRef]
15. Pohl, J.; Bertram, B.; Hilgard, P.; Nowrousian, M.R.; Stüben, J.; Wießler, M. D-19575-a sugar-linked isophosphoramide mustard derivative exploiting transmembrane glucose transport. *Cancer Chemother. Pharmacol.* **1995**, *35*, 364–370. [CrossRef] [PubMed]
16. Woźniak, M.; Pastuch-Gawołek, G.; Makuch, S.; Wiśniewski, J.; Ziółkowski, P.; Szeja, W.; Krawczyk, M.; Agrawal, S. Overcoming hypoxia-induced chemoresistance in cancer using a novel glycoconjugate of methotrexate. *Pharmaceuticals* **2021**, *14*, 13. [CrossRef]
17. Patra, M.; Johnstone, T.C.; Suntharalingam, K.; Lippard, S.J. A Potent Glucose-Platinum Conjugate Exploits Glucose Transporters and Preferentially Accumulates in Cancer Cells. *Angew. Chem. Int. Ed.* **2016**, *55*, 2550–2554. [CrossRef]
18. Young, C.D.; Lewis, A.S.; Rudolph, M.C.; Ruehle, M.D.; Jackman, M.R.; Yun, U.J.; Ilkun, O.; Pereira, R.; Abel, E.D.; Anderson, S.M. Modulation of glucose transporter 1 (GLUT1) expression levels alters mouse mammary tumor cell growth in vitro and in vivo. *PLoS ONE* **2011**, *6*, e23205. [CrossRef] [PubMed]

19. Schwartz, L.; Supuran, C.; Alfarouk, K. The Warburg Effect and the Hallmarks of Cancer. *Anticancer Agents Med. Chem.* **2017**, *17*, 164–170. [CrossRef]

20. Hanahan, D.; Weinberg, R.A. Hallmarks of cancer: The next generation. *Cell* **2011**, *144*, 646–674. [CrossRef] [PubMed]

21. Fu, J.; Yang, J.; Seeberger, P.H.; Yin, J. Glycoconjugates for glucose transporter-mediated cancer-specific targeting and treatment. *Carbohydr. Res.* **2020**, *498*, 108195. [CrossRef] [PubMed]

22. Deng, D.; Yan, N. GLUT, SGLT, and SWEET: Structural and mechanistic investigations of the glucose transporters. *Protein Sci.* **2016**, *25*, 546–558. [CrossRef] [PubMed]

23. El Hilali, M.; Reux, B.; Debiton, E.; Leal, F.; Galmier, M.J.; Vivier, M.; Chezal, J.M.; Miot-Noirault, E.; Coudert, P.; Weber, V. Linker structure-activity relationships in fluorodeoxyglucose chlorambucil conjugates for tumor-targeted chemotherapy. *Bioorg. Med. Chem.* **2017**, *25*, 5692–5708. [CrossRef] [PubMed]

24. Krawczyk, M.; Pastuch-Gawołek, G.; Pluta, A.; Erfurt, K.; Domiński, A.; Kurcok, P. 8-hydroxyquinoline glycoconjugates: Modifications in the linker structure and their effect on the cytotoxicity of the obtained compounds. *Molecules* **2019**, *24*, 4181. [CrossRef] [PubMed]

25. Zemplén, G.; Pacsu, E. Über die Verseifung acetylierter Zucker und verwandter Substanzen. *Ber. Dtsch. Chem. Ges. (A B Ser.)* **1929**, *62*, 1613–1614. [CrossRef]